ROYAL HOLLOWAY UNIVERSITY OF LONDON

EARTH SCIENCES DEPARTMENT

Tectono-Stratigraphic evolution of the Barremian-Aptian Continental Rift Carbonates in Southern Campos Basin, Brazil

Thesis submitted as requirement for award of PhD degree

Student: MOISES CALAZANS MUNIZ
Supervisors: PROF. DAN BOSENCE
PROF. CHRIS ELDERS
Adviser: DR. GARY NICHOLS

Sponsor: PETROBRAS

TABLE OF CONTENTS

CHAPTER 10 - TECTONO – STRATIGRAPHIC MODELS AND DISCUSSION OF MAJOR RESULTS

CHAPTER 11 – CONCLUSIONS

ACKNOWLEDGMENTS

I gratefully acknowledge all those who in any way contributed to the completion of my PhD studies. The completion of this project would not have been possible without financial support from PETROBRAS and permission to use their data. Also I thank the assistance and encouragement of the colleagues and support of the Petrobras London staff.

I wish to address special thanks to the colleagues Dr. Carlos Monnerat, Dr. Luciano Magnavita, Dr Nivaldo Destro, Dra. Cecilia Lana, Dra. Sylvia Anjos, Jeanine Grillo and Dr. Joel Moura for their assistance and discussions.

I am pleased to thank the geophysicists Carlos Barcelos, Claudir Francisco and Vera Sales for the technical support and my managers Desidério Pires, Jonilton Pessoa, Dr. Mario Carminatti and Dr. Guilherme Estrella to allow the realisation of this project.

I could not forget to thank Lucila Reis, Cristiane, Eliane and Juarez the administrative support the Petrobras staff in the Macaé rock laboratory for the core logging work.

I thank the inestimable and effective supervising and help of Professor Dan Bosence and Professor Chris Elders for discussions and thesis editing. Also I thank Dr. Paul Wright and Dr. James Hendry for discussions on issues concerning non-marine carbonate rocks.

I also wish to mention the invaluable friendship and support from the RHUL Earth Sciences Department, the PhD students and staff, in special I would like to thank Kevin D'Souza, Frank Lehane, Nicola Scarselli and James Gardner.

To my darling wife Keila, who where my partner in this project, for her inestimable help, my children Karoline and Matheus for their friendship and comprehension of my absence on all the periods I have been in the UK. I thank my lovely mother Nilza and sister Mirian for their encouragement and unrestricted support. Finally I thank God for one more challenge fulfilled.

I declare that the work presented in this thesis is my own except where otherwise referenced.

Signed. …….

Moises Calazans Muniz

ABSTRACT

The southern Campos Basin comprises syn- and post-rift strata characterised by thick and extensive units of non-marine limestones. These carbonate platforms are scientifically significant due to their unusual palaeoenvironmental setting, and the complexity of the factors controlling their accumulation. They are of economic importance due to discoveries of giant hydrocarbon accumulations in these non-marine carbonate rocks.

3D seismic interpretations show an oblique extensional rifting system that formed a series of graben, half-graben, accommodation zones and horsts oriented NE-SW to NNE-SSW. The area is subdivided into three tectonic domains based on structural style, stretching factors and subsidence rates. The structural template of the syn-rift exerts a strong influence on depositional patterns.

Core logging and thin-section work together with FMI and sidewall core data indicate proximal to more distal lacustrine carbonate deposits with fluvio-deltaic clastics in marginal areas. The dominant carbonate facies are molluscan rudstones and floatstones and a taphonomic analysis (taphofacies) of the cored intervals and exposure surfaces indicate accumulation in shallowing-upward cycles in response to changes in lake level. Microbialite facies, Aptian in age, appear to occur in the most distal locations in restricted palaeoenvironmental conditions. Facies models are presented for the skeletal, mollusc-rich deposits of the Barremian Coqueiros Formation and the overlying microbialite-rich Aptian Macabu Formation.

The deposits are stacked in a hierarchical arrangement of four levels of cyclicity ranging from the entire rift basin fill to metre-scale cycles. Controls on formation of these cycles include structural setting, climate and lacustrine margin progradation.

Different types of carbonate platform form in the different basinal settings and include footwall areas of fault-blocks, accommodation zones and buried horst blocks.

The southern Campos Basin evolves from an initial alkali lake (Barremian) to a main phase of syn-rift, brackish lake conditions. The post-rift succession (Aptian) is characterised by both brackish and hypersaline conditions.

LIST OF ILLUSTRATIONS

CHAPTER 1 – INTRODUCTION

1.1. Primary considerations and justification

The discovery of large carbonate platform studies in continental rifts presents a challenge because existing facies and sequence stratigraphic models for such structures are based on marine carbonate systems and models for non-marine systems have not been established in published literature. The Campos Basin examples differ from marine carbonate platforms in that they are dominated by carbonate producing communities that are endemic mollusc- and ostracod-rich in the Barremian and by microbialites Aptian strata. These limestones form extensive hydrocarbon reservoirs in the pre-salt stratigraphy (Cretaceous) of the Campos Basin.

This PhD project is therefore justified for its scientific and also its economic importance and also because of scarcity of publications on non-marine carbonate platforms. For these reasons, and due to the complexity of the controls on the formation of carbonate platforms in continental rifts, a multidisciplinary approach is needed in order to erect tectono-stratigraphic models.

1.2. Aims

The major aim of this research is, therefore, to erect facies and tectono-stratigraphic models for non-marine carbonate platforms using an integrated multidisciplinary approach. This is to be achieved through a combination of 3D seismic interpretation, analysis of subsurface cores and datasets of gamma and FMI logs from the Early Cretaceous of the Campos Basin, Brazil, together with outcrop analogues from the Miocene of the Gulf of Suez and Jurassic of the Wessex Basin UK.

1.3. Research questions and hypotheses

In order to establish facies and tectono-stratigraphic models for these non-marine carbonates, the following questions are addressed:

- What are the syn-sedimentary tectonic controls on the depositional geometries and facies distribution of the carbonate rocks from Barremian-Aptian of the Campos Basin?

- Can the strata be analysed, subdivided and correlated using sequence stratigraphic principles to organize and understand the sedimentological framework and are these the same or different from standard sequence stratigraphic models based on marine successions?
- What was the environmental setting of these Early Cretaceous non-marine carbonates? Fresh-water, brackish or hypersaline?

1.4. Methodology

This research project involves analysis of sub-surface datasets (3D seismic and well data) from the Campos Basin. The project is focused on the sedimentology and stratigraphy of the carbonate successions; however, other datasets were also used to support the construction of the facies models. Furthermore, in order to complement the research, the results are compared to the outcrops from the Miocene of the Gulf of Suez, Egypt, which appear to have similar tectonic settings and stratigraphic geometries even though the facies differ from the Campos Basin examples by the composition and magnitude of the processes.

Thus, to reach the research goals and also answer the scientific questions outlined above, several parameters such as palaeogeography, tectonics, climate, biodiversity, sedimentology and carbonate rocks had to be investigated. For this purpose, 7500 km^2 of 3D seismic reflection were interpreted (5 seismic horizons were mapped in a dense mesh), 8 wells were studied in detail and a further 12 were used to tie the seismic to electrical logs, 400 m of core were logged (1:20 scale), 600 m of FMI log were interpreted (1:10 scale) and more than 200 thin sections were studied. In addition, as an analogue for the proposed models, a field trip to the Gulf of Suez, Egypt (5 days) was undertaken to study tectonic styles, spatial and temporal relationships of facies (even though they are different to Campus Basin!) and the geometries of the Miocene, Abu Shaar carbonate platform sequences. A short visit was also made to outcrops of the non-marine Purbeck strata in Dorset (2 days) in the south of England, to study Mesozoic non-marine microbialites; their facies, pore systems and depositional environments. Figure 1.1 shows the workflow adopted for achieving the objectives of the research and Figure 1.2 shows how the analyses were carried out and what softwares were used.

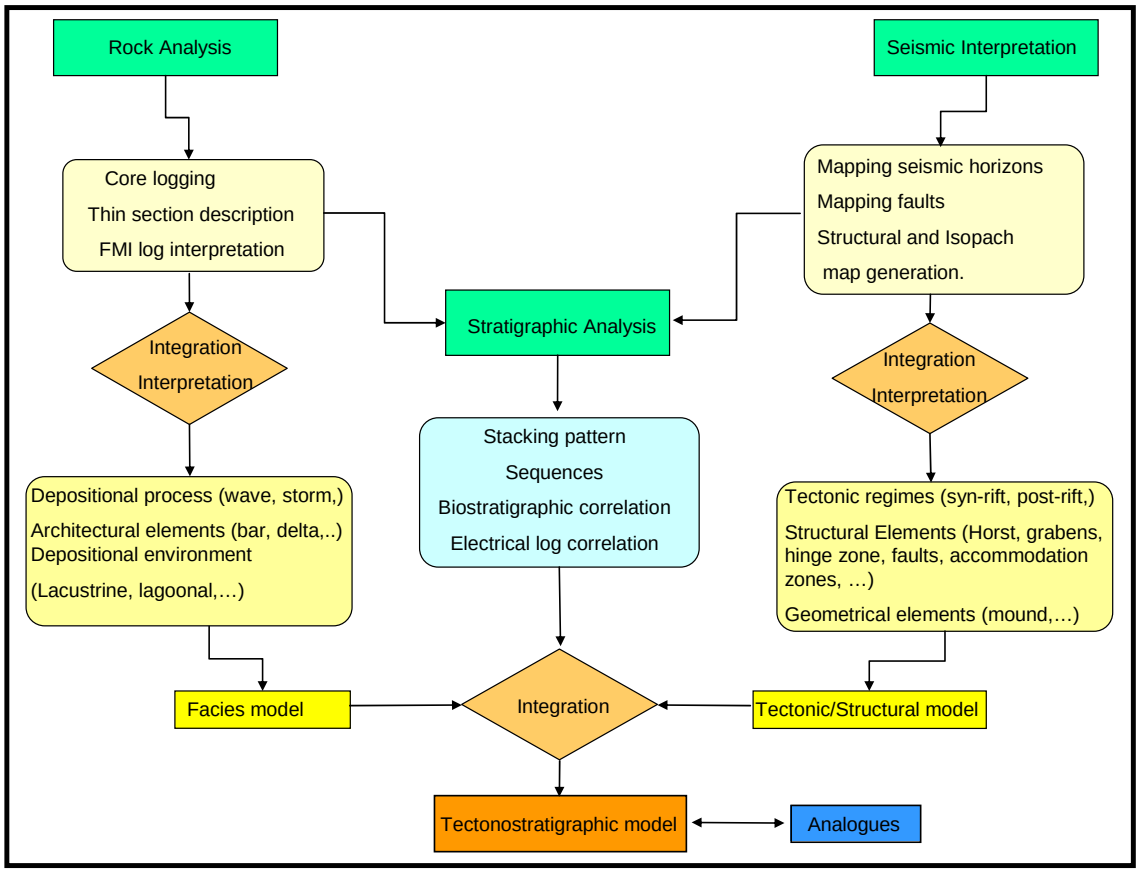

Figure 1.1 - Workflow undertaken to address the aims proposed on the PhD. project.

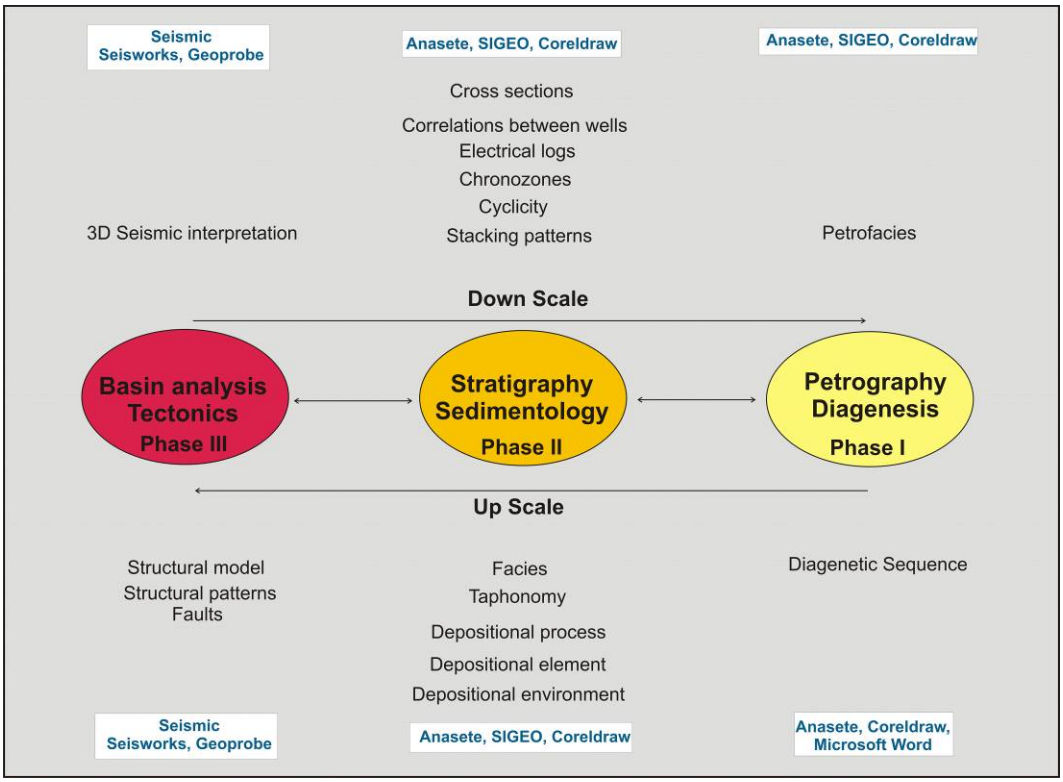

Figure 1.2 – Methods and software used to analyse display and aid in interpretation of the data.

1.5. Major Findings

As a result of the 3D seismic interpretation, three distinct tectonic domains were identified; with different strain rates (different beta values) and therefore expected different rates of subsidence. These different domains have peculiar tectonic styles and different carbonate platforms based on their morphology, and sedimentary geometries.

The first platform type occurs in the Pampo, Badejo, Linguado and Trilha oil fields area (Figure 2.1), in an unusual series of half-graben. These are also rich in clastic terrigenous sediments as they are close to the rift border faults. Clastic sediments predominate in the hangingwall depocentres whereas carbonates occupy the footwall areas as examples of fault-block carbonate platforms.

The second platform type occurs in the region of Espadarte oil field (Figure 2.1) where synthetic and antithetic half-graben form and are divided by accommodation or transfer zones. The geometries of the carbonate platforms are aggradational on interbasinal highs and clinoforms are seen prograding toward half-graben depocentres.

The third region, offshore, has the highest degree of stretching and asymmetric half-graben are linked to form a large symmetrical graben with some relict horsts that and forming highs and the template for unattached carbonate platforms. Progradation of carbonates is observed at the margins of these platforms followed by onlap of the subsequent basinal successions.

The standard sequence stratigraphic models that have been applied to marine carbonate successions are assessed to see how they might apply to non-marine carbonates with a strong tectonic control on their formation. The strata are most suitably subdivided using the transgressive-regressive (T-R) two systems tract model. The seismic stratigraphy facies analysis and the biostratigraphic data allow a subdivision of the entire basin fill into three T-R sequences. In addition a hierarchy of four orders of cyclicity is recognized from elementary and 4^{th} order cycles in the cores and FMI up to the three main T-R cycles mentioned above.

Likewise, the core logging, thin section analysis and also the palaeoecological data, including taphonomy, suggests a progressive change in the lake hydrology, from alkaline in the lower sequences, to fresh water, to brackish waters and hypersaline in the upper successions of the Aptian salts.

1.6. Organisation of the thesis

This thesis is composed of 11 chapters including this introduction. Following this introduction, Chapter 2 is a brief review of the published work on the regional geology of the Early Cretaceous of the Campos Basin, Brazil. Special attention is given to the pre-salt succession which is the main focus of this research.

Chapter 3 is a review of the tectonic development of rift basins which was undertaken to provide a background understanding prior to the erection of tectonic-stratigraphic models presented later in the thesis (Chapter 10).

Chapter 4 describes and discusses the structural settings of the pre-salt carbonates from the 3-D seismic interpretations and regional gravity data analysis. Five seismic horizons are mapped through the area and tied to the stratigraphy with 20 wells located mainly in the proximal areas. Three different tectonic domains are recognized based on their tectonic style and stratigraphic architecture.

Chapter 5 describes and interprets the sedimentary facies and presents facies models based on the examination of the cores. This covers both carbonate and siliclastic facies and a facies classification is presented. This chapter also contains a brief review of facies concepts, classification, and depositional process in lacustrine environments.

Chapter 6 begins with a brief review of taphonomic concepts and outlines the nature and relations between biostratinomic and diagenetic studies. Taphofacies are erected for abundant the mollusc-rich bioclastic carbonates described in the cores and these are related to varying amounts of within habitat and out of habitat reworking by storms and waves. The diagenesis of the carbonate facies is also briefly described and illustrated from thin section and cathodo-luminescence study. Both near- surface meteoric and burial diagenetic environments are identified and the origins of the pore types are described.

Chapter 7 describes the logged cores from 7 wells and FMI logging (plus sidewall cores) from one offshore well where no cores have been obtained. The core logs are presented in Appendix A in the back pocket of the thesis (or volume 2). The interpretation of the FMI log is presented separately as this involves the identification of FMI facies which are classified differently to the core-based facies because they contain less lithological information. The FMI facies in this more offshore well is the only sampling of large thicknesses of microbialite facies in the Aptian strata.

Chapter 8 presents the sequence stratigraphic analysis of the studied succession based on the core logging and the wireline data of the preceding chapter. A review of

different sequence stratigraphic methods is undertaken to assess which are most appropriate for application to non-marine carbonates with evidence of syndepositional tectonic controls on accommodation space. Transgressive-regressive cycles are identified on four orders of magnitude, each of which is considered to have a different control on cycle formation.

Chapter 9 outlines the seismostratigraphy, from the analysis of stacking patterns and stratigraphic geometries integrated with the tectonic setting of the syn- and post-rift strata of the Campos Basin undertaken in Chapter 4.

Chapter 10 is the main discussion chapter of the thesis and presents three tectono-stratigraphic models based on the different structural domains discussed in chapters 4 and 9. In addition the sedimentary evolution of the pre-salt of the Campos Basin is discussed in terms of its tectonic evolution, its palaeohydrology and palaeoclimatic settings.

Chapter 11 summarizes the main findings of this research and suggests areas for further study.

The Appendices comprise the sedimentological logs of the cored intervals (Appendix A in back pocket of thesis), the single FMI log (Appendix B in back pocket) and the two outcrop analogue studies are presented are in Appendix C.

CHAPTER 2 - REGIONAL GEOLOGY

2.1. Campos Basin

2.1.1. Location, economic importance, geographic limits area.

The Campos Basin is today the most prolific hydrocarbon basin in Brazil. Currently it accounts for two-thirds of the national hydrocarbon production (ANP, 2012). It is located on the continental platform offshore from the states of Rio the Janeiro and Espirito Santo; between the geographic coordinates 21º and 23º 30'S and comprising an approximately area of 100.000 km^2 (Figure 2.1). It is bounded to the north by the lineament of the Vitória volcanic high, which marks the frontier with Espirito Santo Basin and to the south by the lineament of Cabo Frio volcanic high, which delineates the boundary with the Santos Basin. Towards the east it is limited by the 3400 m isobath and to the west it extends 15 km onshore (Figure 2.1).

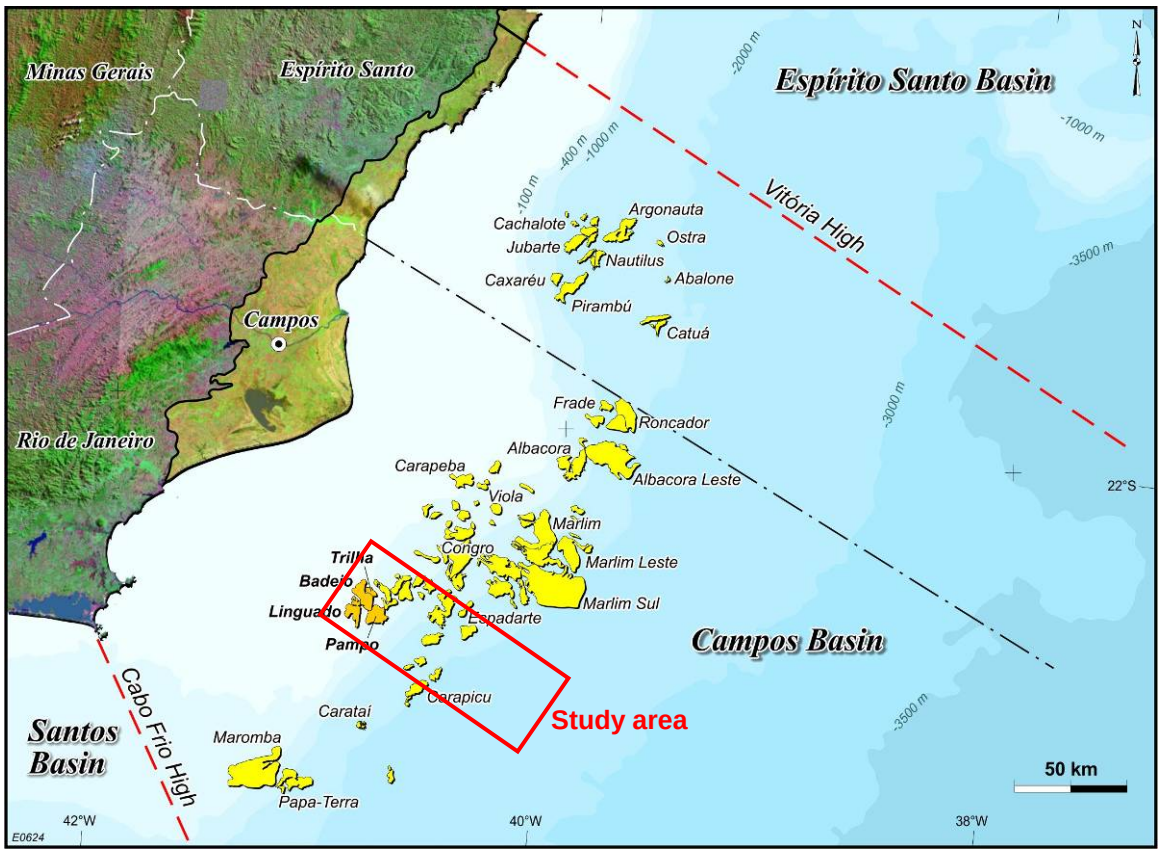

Figure 2.1 - Location map with the main oil fields in the Campos Basin – Red rectangle delineates the area of this study (Courtesy Petrobras). Orange colours are carbonate oil fields.

2.2. Tectonic and structural settings

The Campos Basin is a passive margin basin type (Klemme, 1980) formed as a result of the break-up of Gondwana in the Early Cretaceous (Guardado *et al.* 2000). It is located in the west side of the South Atlantic and it has the Lower Congo and Kwanza basins as its counterparts in the east (Figure 2.2).

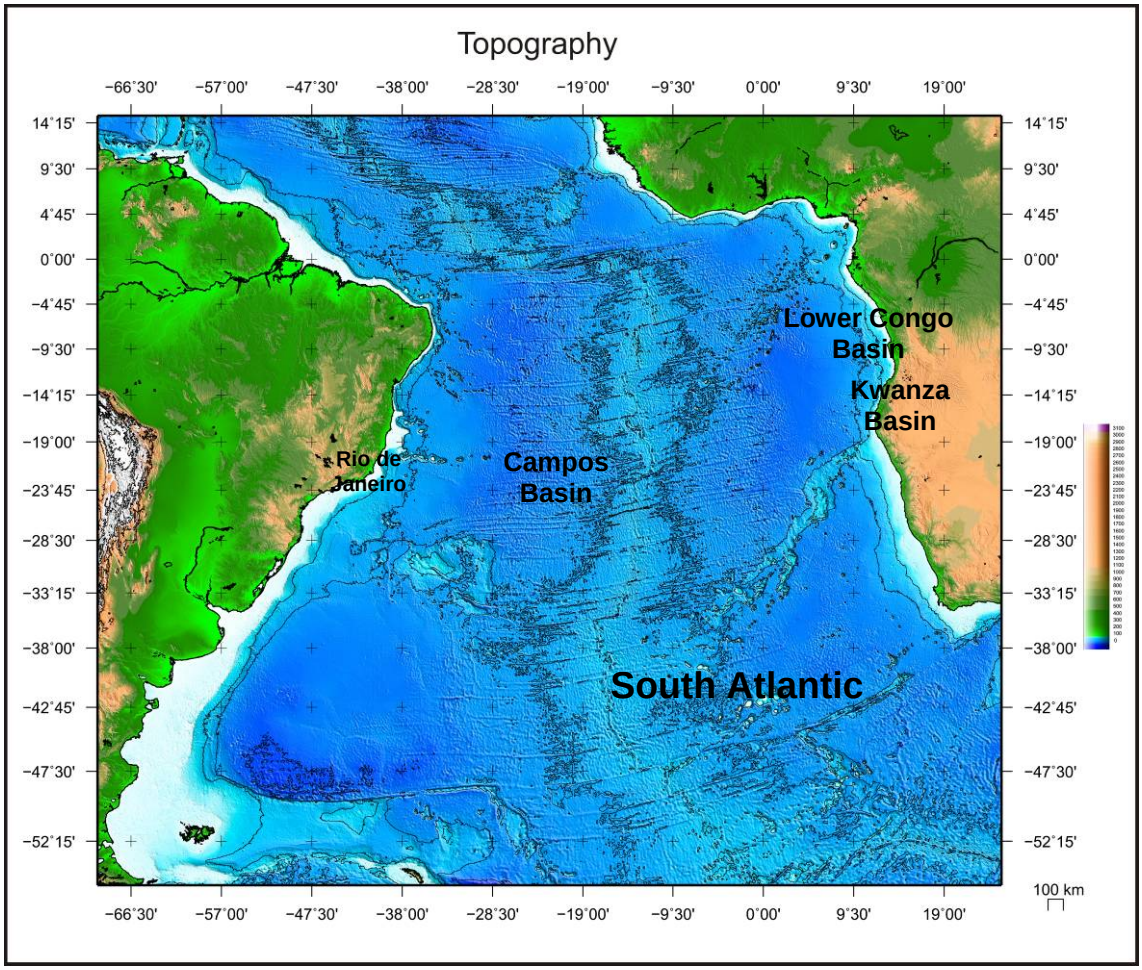

Figure 2.2 – Topography map with tectonic context of the Campos Basin (Source - http://topex.ucsd.edu/WWW_html/mar_topo.html).

The evolution of the South Atlantic starts with stretching and thinning of the continental crust to form a continental rift and subsequently evolving into oceanic spreading. Although the rifting commenced in the south (Argentina) during the Jurassic and evolved towards the equatorial segment (Mohriak *et al.* 2008), the Campos Basin rifting commenced later, in the Hauterivian (Rangel, 1994 *in* Davison, 1999). Subsidence of the stretched continental crust in the east commenced after the Aptian. Asmus (1975) and Barros (1980) defined three main tectonic phases to characterise the evolution of the

Campos Basin: Syn-Rift continental (early and late,) Post-Rift transitional and Post-Rift marine (transgressive and regressive).

By comparison McHargue (1990) divided the stratigraphy of the Congo Basin, on the subsiding West Africa passive margin, into two main intervals: the *pre-salt* section with continental rift sedimentation and the *post-salt* section with marine sedimentation. These major successions are separated by the Aptian Salt. In turn, in that basin, the pre-salt rift sequences were divided into *early rift* and *late rift* stages.

Within this tectonic context, in the Campos and Santos Basins, specific structural provinces, such as rifted margin, rift basins and transfer zones have been defined by some workers (e.g. Meisling *et al.* 2001; Mohriak *et al.* 1990; Mohriak & Dewey, 1987) using Bouguer gravity anomalies, regional seismic and deep seismic lines. The main elements interpreted by Meisling *et al.* (2001) from the residual Bouguer gravity anomalies, are: nearshore Moho uplift; failed spreading ridge; transfer zones and ancient ocean ridge transform faults (Figure 2.3).

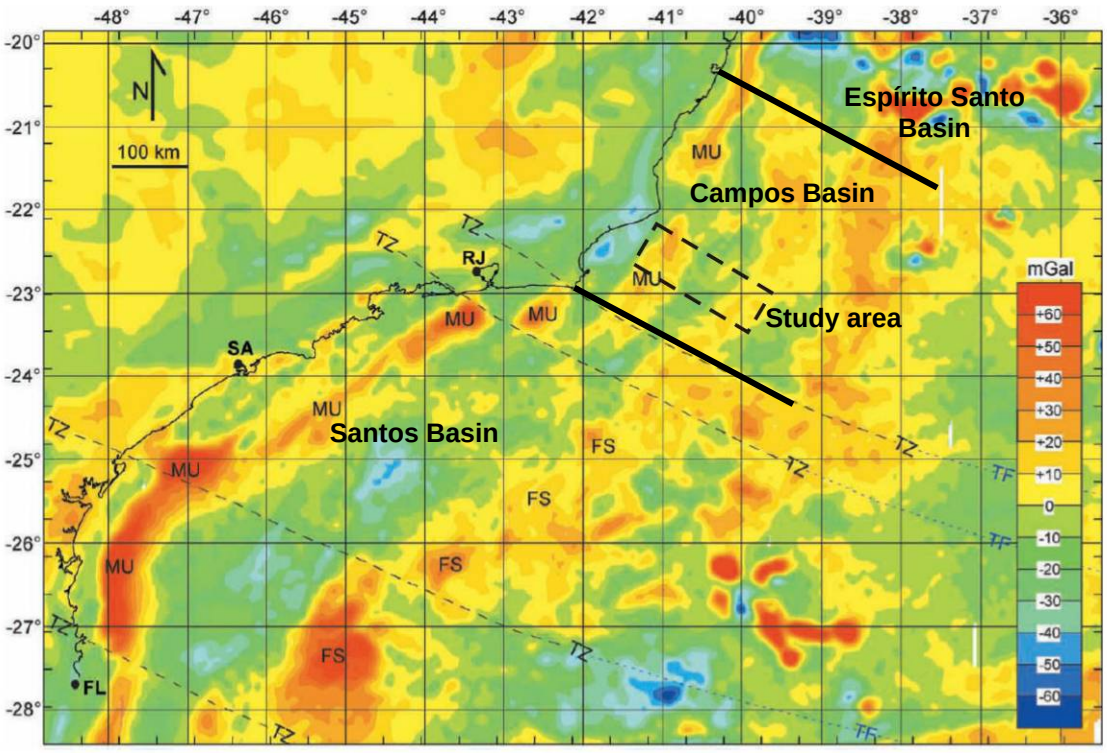

Figure 2.3 Map of gravity anomalies, Campos and Santos basins. The colour bar shows residual anomaly values in mGal. Onshore localities are: Florianópolis (FL), Santos (SA), and Rio de Janeiro (RJ). The main elements interpreted are: Moho uplift (MU), failed spreading ridge (FS) transfer zones (TZ) and transform faults (TF). Modified from Meisling *et al.* (2001).

The Moho uplift (MU) is a nearshore positive gravity anomaly (up to 80 mGal) orientated northeast-southwest. This gravity anomaly fits well with features of the lower crust (Moho) interpreted by Meisling *et al.* (2001), from a deep seismic reflector in the regional seismic lines (Figure 2.4). The footwalls of Neocomian extensional faults, associated with half-graben overlie these features and are related to uplift processes during the Early Cretaceous crustal extension and rifting.

Failed spreading ridge phenomena (Figure 2.3) represent several offshore positive gravity anomalies, up to 70 mGal, trending northeast-southwest. These offshore positive gravity anomalies were also interpreted by Demercian (1996), and coincide with zones that were interpreted by Meisling *et al.* (2001), based on seismic facies of regional seismic lines, as a pre-salt ridge of eroded volcanic and basement highs.

Negative gravity anomalies between the MU and FS strips are wide (~ 300 km) northeast-southwest trending, and match well with the interpretation of half graben seen in deep seismic lines (Mohriak & Dewey, 1987), which parallel the rift system axis. Meisling *et al.* (2001) interpreted the offset across the gravity anomalies as transfer zones (Figure 2.3). These zones lie in a west-northwest to east-southeast orientation, and according to Mohriak *et al.* (1995), are synchronous with extensional faulting during the Neocomian rifting.

According Nurnberg & Muller (1991), the plate tectonic reconstruction of the early Hauterivian stage of the Atlantic opening in the Campos and Santos Basins, shows an east-west extension direction. However, the transfer zones seen today are oblique to this direction. Prior fabric and structures of the South Atlantic rifting system played a major role in rift architecture. Meisling *et al.* (2001) postulate that the inherited basement structures trending northwest-southeast and the extension are at about 45º degrees to each other and can therefore be described as oblique (Figure 2.4).

2.3. Tectonic and stratigraphic evolution

In the Campos Basin the pre-rift is represented by a Precambrian crystalline basement. The early syn-rift, Neocomian, is characterized by volcanic sediments, seismically recognized as the deepest reflector mappable regionally, and clastic sediments recognized in subsurface well data and seismic, limited at its top by the stratigraphic marker LF-20 (Baumgarten, 1983). The late syn-rift section, Barremian-Aptian, is characterized by a succession of talc and stevensite-rich succession, followed

upwar by a clastic and carbonate rich succession, which is limited at its top by the stratigraphic marker LF-35. The stratigraphic marker is defined as a rock unit of depositional nature formed by lithofacies with physical attributes that are laterally extensive, recognized by subsurface log patterns that are seismically mappable regionally (Baumgarten, 1983; Rangel, 2000). This succession underlies a considerable thickness of bioclastic limestone (coquina). In its turn, the coquina is bounded at its top by a post-rift unconformity. The post-rift transition stage is limited by the post-rift regional unconformity and the base salt unconformity (Figure 2.5). Both are seismically mappable regionally. The post-rift sag phase succession is characterized by clastic sediments nearshore and microbial carbonates basinward, overlain by a thick layer of evaporites (Dias *et al.* 1987).

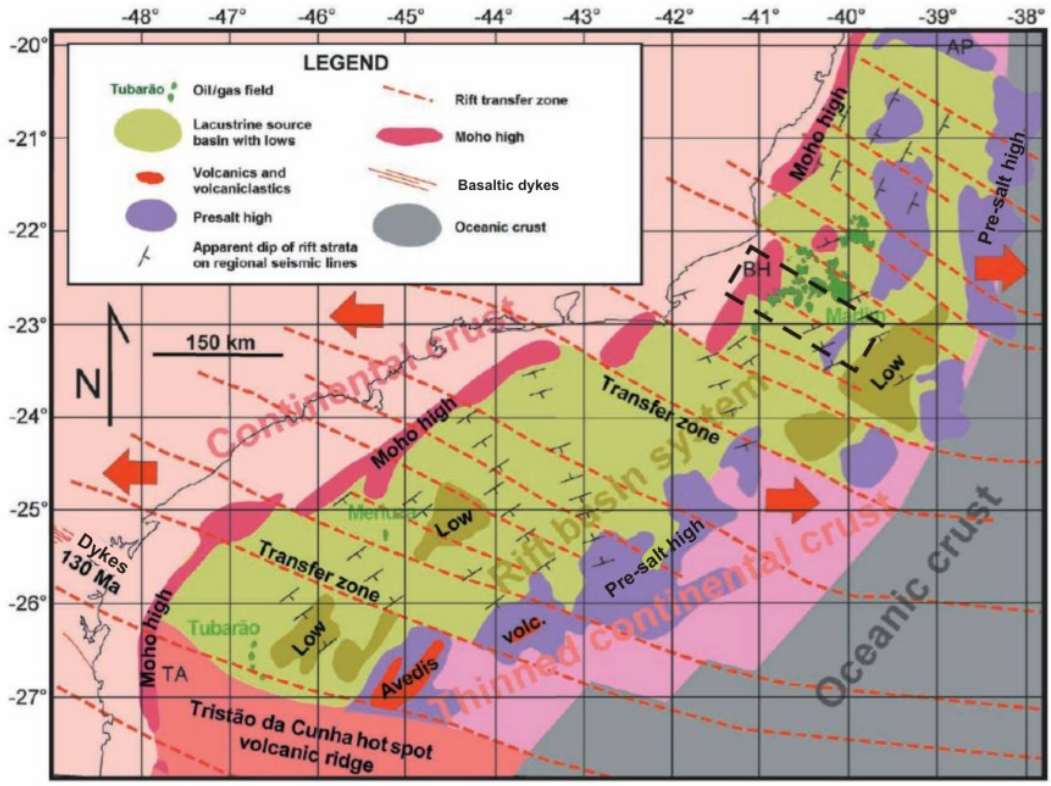

Figure 2.4 Map of main rift-related structural provinces, Campos and Santos basins. (TA) Torres Arch; (BH) Badejo High; (AP) Abrolhos Plateau. Modified from Meisling *et al.* (2001). Dashed black rectangle delineates the area of this study. (- minus signal) Longitude W, Latitude S.

After the evaporite section, the post-rift marine transgression took place in the Late Cretaceous with deposition of shallow-water carbonate platforms in the Albian covered by a pelagic and hemipelagic shale succession and also turbidities. Finally, the Cenozoic marine regressive succession is characterized by pelagic and hemipelagic prograding sediments and turbidite deposits (Figure 2.6).

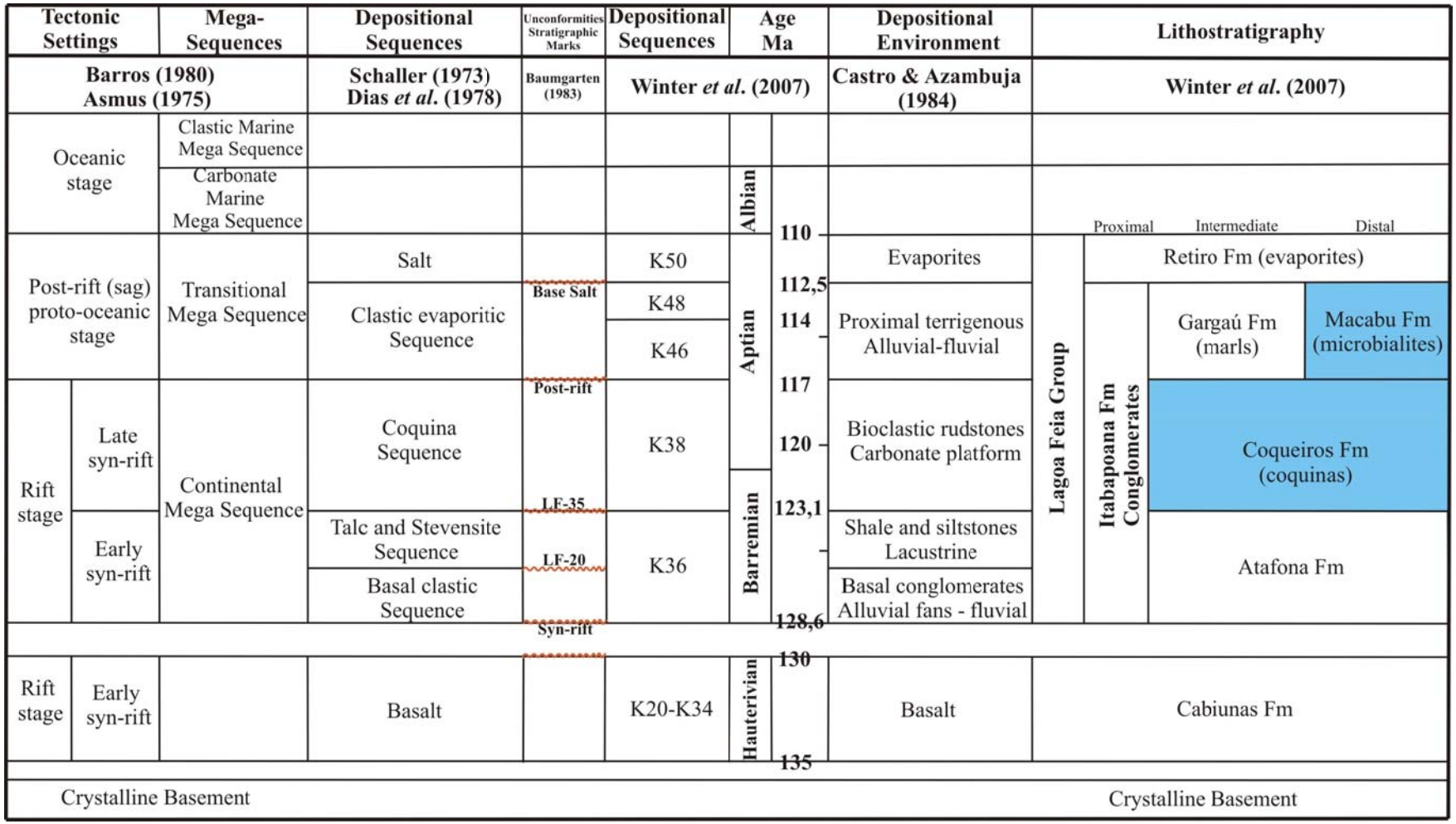

Figure 2.5 – Summary of the tectono-stratigraphic settings according various authors. The carbonate rocks of the Macabu and Coqueiros Formations (blue area), are this study.

A topographic barrier to the south the Wavis – Rio Grande ridge created the restriction necessary for deposition of non-marine carbonates followed by an extensive evaporite deposition at the top of post-rift transitional succession (Asmus, 1975; Abraão & Warne, 1990). No typical marine fossils are recorded in any of the pre-salt succession (Bertani, 1983), for this reason it is therefore referred to non-marine by the abundance of non-marine ostracod fauna (Silva Telles, 1992), but sporadically with possible some marine incursions, evidenced by very rare forams and marine ostracods, reported in Silva Telles, (1992).

Hessel & Mello (1987), state that the first signs of marine incursions in the Campos Basin are evidenced by the occurrence of typical bivalves, *Angelsina* and *Remondia*, the mass mortality of bivalves and Cyanobacteria bloom (blue-green algae). These phenomena occur in the graben system formed by rifting during the Aptian. A regional post-rift unconformity is recognized in seismic and can be seen in all the Campos Basin (Dias *et al.* 1987). Relative tectonic quiescence as gentle thermal subsidence, took place followed with little clastic influx. This subsidence took shallow marine, Early Cretaceous sediments to depths of tens to hundreds of meters in the east of the study area.

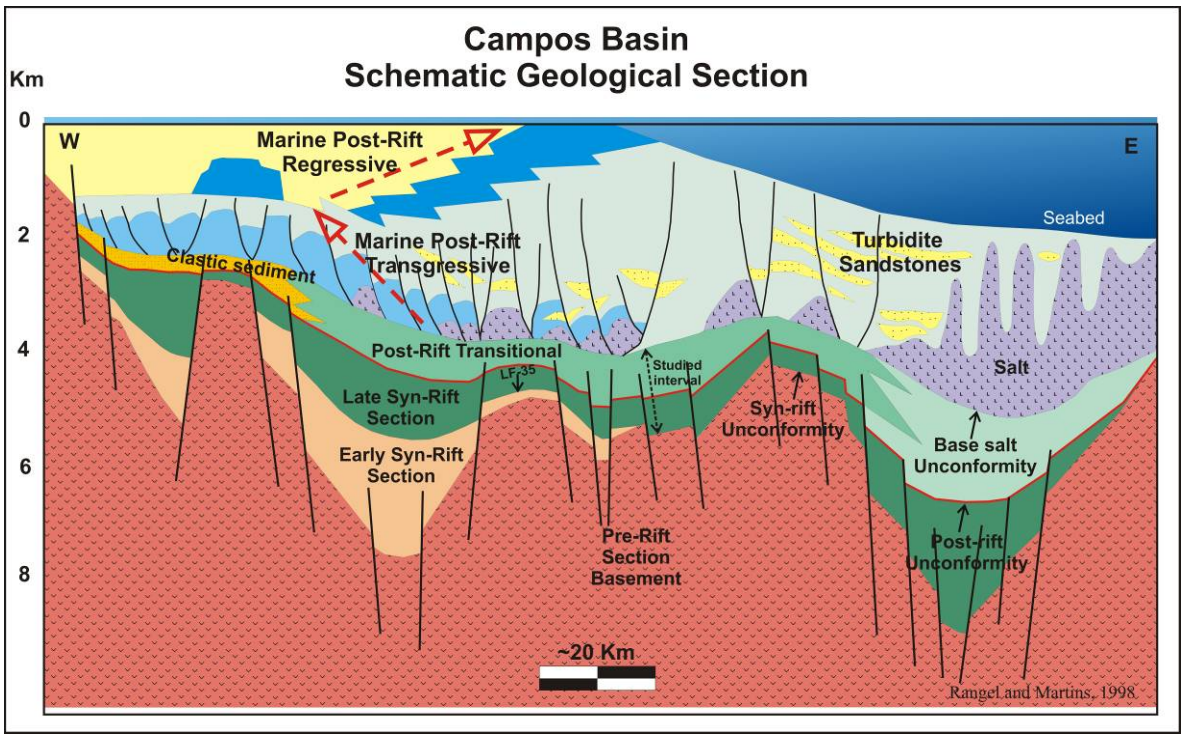

Figure 2.6 - Schematic Geologic Section showing the tectonic stratigraphic subdivisions of the Campos Basin (After Rangel & Martins, 1998).

2.4. Lithostratigraphy

Schaller (1973) initially defined the Lagoa Feia Formation as the entire sedimentary package up to the top of the evaporites. Since then several authors have contributed to the understanding of these successions (Castro & Azambuja Filho, 1980; Bertani & Carozzi, 1985a, 1985b; Dias *et al.* 1987; Rangel *et al.* 1994). However, Winter *et al.* (2007) raised the status of the Lagoa Feia Formation to a Group, as well as raising some Members to Formation status (Figure 2.5) as described below.

Lagoa Feia Group

The Lagoa Feia Group is currently regarded as being subdivided into the following Formations: Coqueiros and Retiro (defined by Rangel *et al.* 1994), Itabapoana, Atafona, Gargaú and Macabu (defined by Winter *et al.* 2007).

Itabapoana Formation

This formation is characterized by polymictic conglomerates, lithic sandstones, siltstones and shales (Rangel *et al.* 1994), associated with the western, basin border faults. The maximum thickness of sediments reaches 5000 m. These rocks lie unconformably on the basalts of Cabiúnas Formation and are interpreted to form from fan deltas and alluvial fans, on the margins of a lacustrine palaeoenvironments. The upper contact is expressed by angular unconformity with the Atafona Formation and more distally it passes to the Coqueiros Formation. The Itabapoana Formation grades laterally to shaly facies of the Atafona Formation or carbonates of the Coqueiros Formation. Locally, near the top of the formation it grades laterally into marls and shales of the Gargaú Formation and locally grade to the Macabu Formation carbonates.

Atafona Formation

The Atafona Formation is represented mostly by sandstones, siltstones and shales with interbedded thin carbonate layers (Rangel *et al.* 1994). The siltstones and sandstones are rich in talc and stevensite minerals, formed by chemical precipitation associated with hydrothermal activity in alkaline volcanic lakes (Bertani & Carozzi, 1985). The formation lies unconformably on basalts of the Cabiúnas Formation or laterally grades into the Coqueiros Formation. The upper contact is also unconformably

with the muddy sediments. According to palynological and ostracod dating, these sediments were deposited during the Barremian (Winter *et al.* 2007).

Gargaú Formation

This formation is represented by shales, siltstones, marls and sandstones. Commonly this formation occurs interbedded with mudstones, which grade distally into microbial carbonates of the Macabu Formation. These sediments were deposited in shallow lake palaeoenvironments, with some contributions of siliciclastic sand and, more rarely, conglomerates. The unit lies unconformably on carbonate rocks of the Coqueiros Formation. The upper contact is also unconformable, with evaporitic rocks of the Retiro Formation. Distally, the Gargaú Formation grades laterally into carbonate facies of the Macabu Formation and proximally it grades to sandy conglomeratic facies of the Itabapoana Formation. Based on palynological and ostracod dating, it is assigned an Aptian age (Winter *et al.* 2007).

Coqueiros Formation

The Coqueiros Formation is represented by interbedded layers of lacustrine shales and carbonates composed predominantly of molluscs (Rangel *et al.* 1994). These shelly deposits form hundreds of metres thick porous molluscan rudstones and floatstones (coquina). The packages of coquina were deposited in high-energy lacustrine palaeoenvironments, generally as reworked deposits, and are the major topic of this thesis.

Macabu Formation

The Macabu Formation is represented by microbial carbonates (Rangel *et al.* 1994). These are interpreted to have been deposited in an arid climate, in shallow and restricted water palaeoenvironments (Winter *et al.* 2007). This formation occurs in more distal areas of the Campos Basin and lies unconformably above clastic sediments of the Coqueiros Formation, more rarely on the basalt of the Cabiúnas Fm. The upper contact is unconformable with the Retiro Formation evaporites. Based on palynological and ostracod dating, these sediments are considered to be deposited during the late Aptian.

Retiro Formation.

This formation is characterized by evaporites, mainly halite and anhydrite. In the depocenters, marine sourced evaporite cycles can be seen with other more soluble minerals such as carnallite and sylvite (Winter *et al.* 2007).

2.5. Biostratigraphy

2.5.1. Biochronostratigraphic Framework

The eleven biostratigraphic units defined by Moura (1987) for the Lagoa Feia Group are based on non-marine ostracods. The boundaries of the biozones take into account the origin and extinction of ostracod faunas, due to abrupt changes and palaeoenvironmental conditions, and also the abundance of the species. This zoning was reviewed by Silva-Telles (1992) for the Coqueiros Formation and later was presented more completely in Carvalho *et al.* (1995). The method used follows the principles used to define biozones, known as "interval zones" according to Article nº 50 of the North American Commission on Stratigraphic Nomenclature (1983).

Carvalho *et al.* (1995) formalised biochronostratigraphic intervals as an additional tool for stratigraphic correlation, using biostratigraphic data combined with electrical logs beyond the areas sampled by of cored intervals. These biochronozones have a chronostratigraphic value as outlined in Article 75 of the North American Stratigraphic Code (1983).

Following the above method, the bottom of the Coqueiros Formation is identified as Subzone *Salvadoriella*? *pusilla* and labelled OS-930 or NRT-009.3; defined by the extinction of the species *Salvadoriella*? *pusilla Krömmelbein* & *Weber* (1971). The zone is characterized by the species *Petrobrasia diversicostata Krömmelbein* (1965). The biochronozone determined is labelled as C-930 or C 009.3 (Figure 2.7).

Continuing upward in the stratigraphy, just above is the Reconcavona? batake Zone (OS-1010); defined by the species Reconcavona? batake Grosdidier (1967). C-1000 is the corresponding biochronozone. This biozone can be subdivided into two subzones: the Reconcavona? retrosculpturata nomen nudum (nn) (OS-1010) at the base, whose corresponding biochronozone is the C-1010, and the Subzone Hourcqia african africana (0S-1020) on top, defined by the species Hourcqia africana africana Krömmelbein (1965), corresponding to biochronozone C-1020.

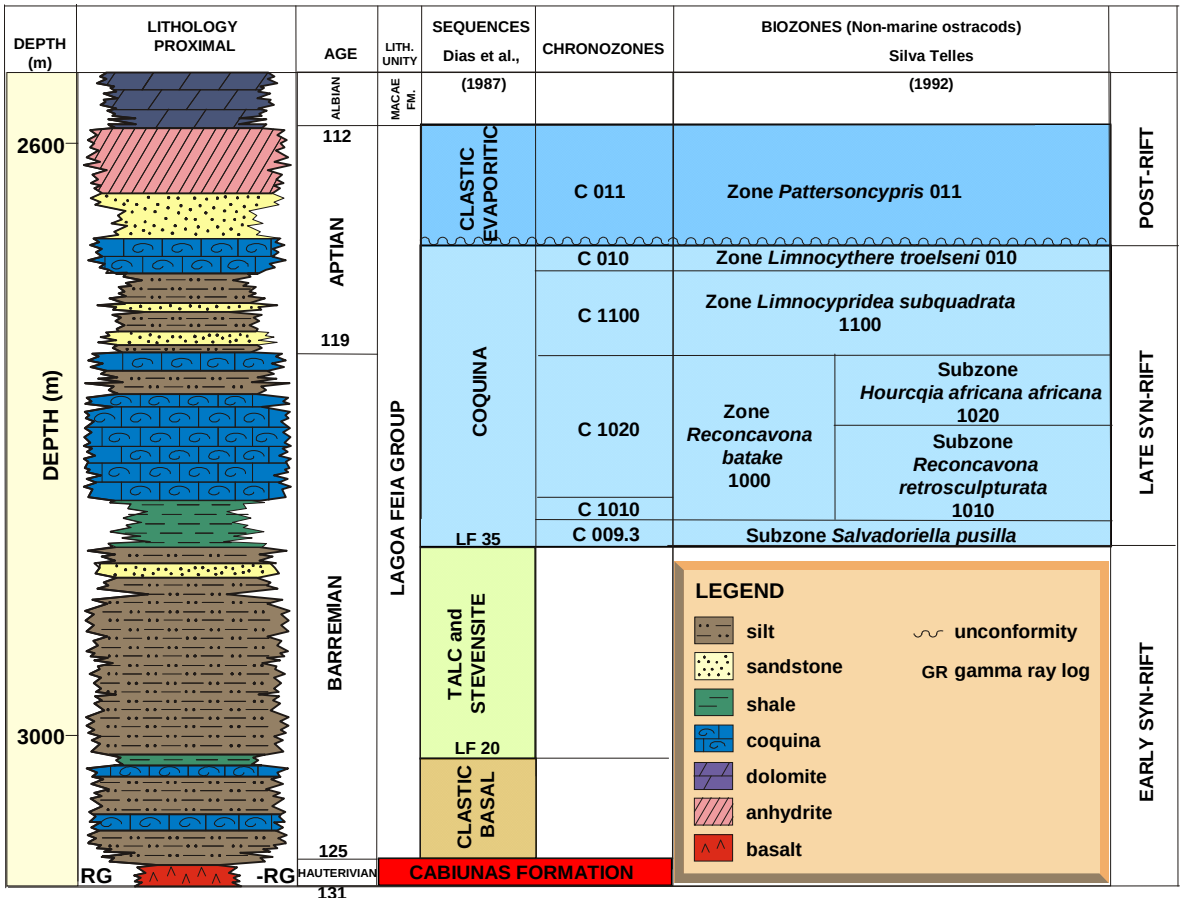

Figure 2.7 – Biochronostratigraphy for Domain I, framework of the Lagoa Feia Group, modified from Carvalho *et al.* (2000).

The following interval is the Limnocypridea Zone? subquadrata n.n. (0S-1100), whose species has defining smooth and knotted morphotypes. The corresponding biochronozone is the C-1100. At the top of the Coqueiros Formation occurs the Limnocythere? Zone troelseni (0S-1200 or NRT-010), characterized by specific mono fauna of this species. The biochronozone is the corresponding C-1200 or C-010 (NRT-010). The top of the Lagoa Feia Group is identified by the Pattersoncypris Zone (NRT-011). C-011 is its corresponding biochronozone (Figure 2.7).

2.6 Stratigraphic Framework of the Lagoa Feia Group, Campos Basin

As mentioned in the section 2.2, the tectonic and stratigraphic evolutionary history of the Campos Basin is related to the crustal rupture of Gondwana and the evolution of rifting that resulted in the establishment of the South Atlantic Ocean in the Early Cretaceous. Prior to this break, an extensive basaltic volcanic province existed between 135 to 130 Ma (Cordani *et al.* 1972). The sedimentary deposits in turn, started

from the Hauterivian age, and are marked by three stages of the basin evolution, which comprise these depositional mega-sequences (Asmus, 1975; Barros, 1980; Guazelli & Asmus, 1981 and Asmus, 1982): Rift stage (continental mega-sequence); Proto-oceanic or Gulf stage (transitional mega-sequence) and Ocean stage (clastic marine and carbonate marine mega-sequences) (Figure 2.5).

The lithological framework that comprises the continental and transitional mega-sequences is the subject of this thesis. These were classified by Schaller (1973) as the Lagoa Feia Formation, being defined as a non-marine sequence of terrigenous, carbonate and evaporites of the initial stages of sedimentation in the Campos Basin.

Dias *et al.* (1987), subdivided the Lagoa Feia Formation into four depositional sequences (*sensus* Mitchum Jr., *et al.* 1977): basal clastic sequence, talc and stevensite sequence, coquina sequence which correspond to the continental mega-sequence of Barros (1980) and Asmus (1975) and evaporitic clastic sequence, corresponding to the transitional mega-sequence of these authors. Rangel *et al.* (1994) have classified three depositional sequences within Lagoa Feia Formation, K30, K40 and K50 which Winter *et al.* (2007), split into K36, K38, K46, K48 and K50 (Figures 2.5 and 2.6).

2.6.1. Continental mega-sequence

The basal clastic sequence (lower K36) corresponds to the lower part of the Lagoa Feia Group, comprising the beginning of the sedimentary syn-rift fill. The rocks that compose this sequence, lie unconformably on basalts of the Cabiúnas Formation, and are bounded at its top by the stratigraphic marker LF-20. The clastic sequence comprises the conglomerates and sandstones of the Itabapoana Formation in proximal sites and the Atafona Formation in the distal areas and is made up of sandstones, siltstones and shales stevensite rich with 120 m thickness. It was deposited during the Barremian, from 128 Ma to 123 Ma (Figure 2.7).

The talc and stevensite sequence (upper K36) is characterized by lacustrine shales and siltstones with stevensite. It is bounded at the base by the stratigraphic marker LF-20, and at the top by the stratigraphic marker LF-35, which corresponds to a regional unconformity of 125.8 Ma (Winter *et al.* 2007). This seismic horizon marks the base of Coquina sequence, which is seismically traceable throughout the area. This sequence develops significant thicknesses in the depositional lows and locally non-deposition in the structural highs (Dias *et al.* 1987). It comprises the Itabapoana

Formation in the proximal areas and Atafona Formation in the distal sites, which sediments were deposited during the Barremian age.

The Coquina sequence (K38) corresponds to the intermediate portion of the Lagoa Feia Group, comprising the Itabapoana and Coqueiros formations, deposited during an interval ranging from the late Barremian to the early Aptian. It is bounded at the base by the stratigraphic marker LF-35, and its upper limit by a regional erosive event, occurring between 120 Ma and 123.1 Ma, and easily identified on seismic sections. The Coqueiros Formation contains considerable reservoirs and the main source rock of the basin.

2.6.2. Transitional mega-sequence

The clastic-evaporitic sequence (K46, K48 and K50) corresponds to the upper part of the Lagoa Feia Group, and accumulated during the post-rift sag phase of basin evolution. A great expansion of the basin and transition from continental to marine environments took place during the development of this succession. It comprises conglomeratic alluvial fans of the Itabapoana Formation in the proximal area, and marl and shale of the Gargaú Formation in the intermediate sites and microbial carbonates of the Macabu Formation in the most distal areas (Winter *et al.* 2007). Overlying the Gargaú and Macabu is a thick sequence of evaporite (marine sourced), halite and anhydrite, of the Retiro Formation (K50). The lower limit for this sequence is the post-rift unconformity (break up?) at 117 Ma and the upper limit, the top salt. There is a strong unconformity at the base of the evaporites separating carbonate-clastic sequences (K46, K48) from evaporites (K50), halite and anhydrite.

2.7 Conclusions

The break up of the Gondwana and continuous rifting and formation of the South Atlantic passive margin basins, involved three main evolutionary stages: continental rifting, gulf or proto-oceanic stage and finally marine stage. This project focuses on carbonate platforms formed in the continental lacustrine environment, in the Campos Basin, Brazil.

Few publications are available on non-marine carbonate platforms, especially those formed in rift basins. So, the tectonic settings and structural patterns in the Campos Basin, as well as all the depositional sequences previously defined by its

sequence boundary in the Barremian to Aptian interval, form the background for this research. The published lithostratigraphic and biochronostratigraphic frameworks form the basis for all sedimentological and stratigraphic studies of this thesis. The interval of study comprises the carbonate rocks of the Coqueiros and Macabu Formations, bounded by the stratigraphic marker LF-35 and the base salt unconformity.

CHAPTER 3 - RIFT BASINS AND PASSIVE MARGIN REVIEW

To provide a better understanding for the following chapters, a brief review of the concepts of the tectonics and structural styles in rift and passive margin basins is required.

3.1. Causes of lithospheric extension and basin formation

The topographic relief on the surface of the earth is a product of processes involving thermo-mechanical properties of the continental lithosphere and underlying asthenosphere (Ebinger *et al.* 2002). To commence the rifting process, the upwelling of heat from convection in the mantle, results in doming, thinning and lateral changes to the density and rheology of the continental lithosphere. Consequently, tectonic plates of the upper crustal lithosphere, which have a brittle behaviour, undergo extension which results in lateral stretching, rifting, subsidence and uplift (Figure 3.1). This deformation is the cause of formation and evolution of rift basins (Ebinger *et al.* 2002; Ingersoll, 1988).

The Campos Basin is an Atlantic passive margin basin type (Klemme, 1980), that resulted from a continuous rifting process within the supercontinent of Pangea (140 Ma) culminating via oceanic spreading (divergent plate boundaries) in the formation of the South Atlantic Sea (Chang *et al.* 1992) due to lithospheric stretching and plume activity.

3.2. Rift and Passive margin basin models

A rift is defined as an elongated depression bounded by normal faults that converge at its centre. Rifts are generated by deformational processes that in most cases put the whole lithosphere under extension (Neuman & Ramberg; 1978; Burchfiel, 1980). Several models for the rift initiation have been proposed. One of them relates to heat flow, caused by the convection of the mantle (Morgan 1972; Van der Pluijm & Marshak, 1997). This model postulates that the upwelling of the mantle produces deformation on the lithosphere and crust, resulting in rift basins and uplifted flanks. Subsequent cooling of the heated lithosphere returns it to its original thickness producing the post-rift thermal subsidence and forming a sag basin (McKenzie, 1978).

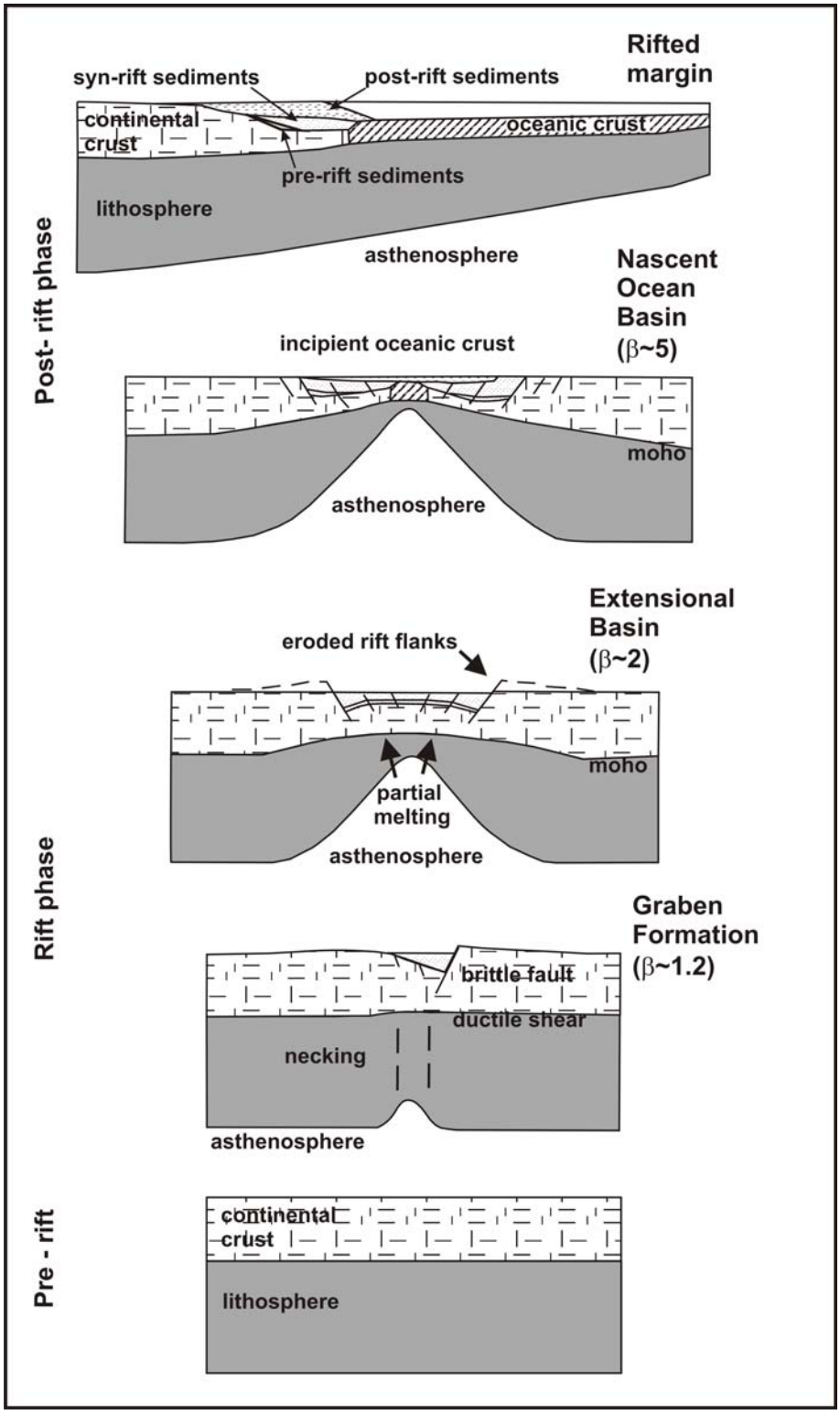

Figure 3.1 Summary of rift evolution (after Salvesen, 1978; from Ebinger *et al*. 2002).

3.2.1 Passive and active rifting

Two models of rifting are postulated: active and passive rifting models. In the active rifting model, convective upwelling results in regional uplift that drives extension, and syn-rift volcanism. This can occur due to mantle plume emplacement

(e.g. White & McKenzie, 1989), whereas passive rifts are formed in response to lithospheric extension caused by a regional stress field. In this case little or no volcanism occurs during the syn-rift stage (Sengor & Burke, 1978) and the extension generated by plate movements external to the rift basin leads the passive input of asthenospheric material.

3.2.2 Pure shear, simple shear

Rift basins can also be classified according to the mechanism of rifting; crustal stretching as passive pure shear, simple shear and heterogeneous stretching models (Sengor & Burke, 1978).

McKenzie (1978) proposed the passive pure shear model that is based on the upwelling of the hot asthenosphere, uniform mechanical stretching, extension and faulting in the brittle upper crust and ductile deformation in the lower crust forming a symmetric rift basin with conjugated border faults (Figure 3.2a). Allen & Allen (1990) argue that pure shear mechanism produce a uniform extension in the crust with no solid body rotation. Deformation is only the result of shear strain. After cooling of the lithosphere and associated thermal subsidence and sediment infill, the post-rift stage, will be symmetrically arranged in relation to the main rift axis (Figure 3.2d; Bosence, 1998).

On the other hand, the Wernicke (1985) passive, simple shear model, states that asymmetric lithospheric extension through a translithospheric gently dipping detachment zone of shearing (Figure 3.2b). In this model the lithosphere may be extended laterally and asymmetrically from a zone of brittle upper crustal stretching, that is mechanically rifted, to a zone of ductile, lower crust and mantle lithospheric stretching. This results in distal, thermally influenced subsidence basin (Buck *et al.* 1988; Kusnir & Egan, 1990). In this sense, the simple shear model has a solid body rotation, forming an asymmetric rift (Allen & Allen, 1990), where conjugate borders have different structures and thermal histories. In the distal region the thinning of the lithospheric mantle, uplift and erosion of the crust is followed by thermal subsidence (Figure 3.2b).

Alternatively, the Coward & Ries (1986) model combines heterogeneous and patchy lithospheric stretching (Figure 3.2c). They assume that the lower crust stretches and thins in a narrow zone, whereas the upper crust extension is spread over a large area involving faults which propagate away from the main rift border (outer zone) on a low-

angle lithospheric detachment, thus forming a basin. After local inversion, uplift and erosion can occur, followed by thermal subsidence in the inner zone, just above the zone of lower crustal and mantle thinning (Figure 3.3c). As a consequence a thermal basin is developed in the inner axis of the rift.

In many rift basins, magmatic activity is present due to the rise of mantle plumes beneath a stretched and thinned lithosphere (Storey *et al.* 1992). This mantle-plume related model proposed by White & McKenzie (1989) postulate that a new continental split can occur where thermal anomalies in the mantle due to plumes, produce enormous quantities of pre and syn-rift igneous rock (Figure 3.2d). The mantle plume is formed when temperature rises a little above normal (e.g. 100 to 200º C), generating a thermal anomaly and decompression melting of asthenospheric mantle. In their studies, they concluded that to maintain isostatic equilibrium, more than 2 km of subsidence is created when the stretching value is approximately 5 (β=5). Moreover, a considerable increment in subsidence takes place when a large amount of flood basalt is added. The basin formed subsides thermally after the rifting and magmatic processes as the asthenosphere cools (Bosence, 1998).

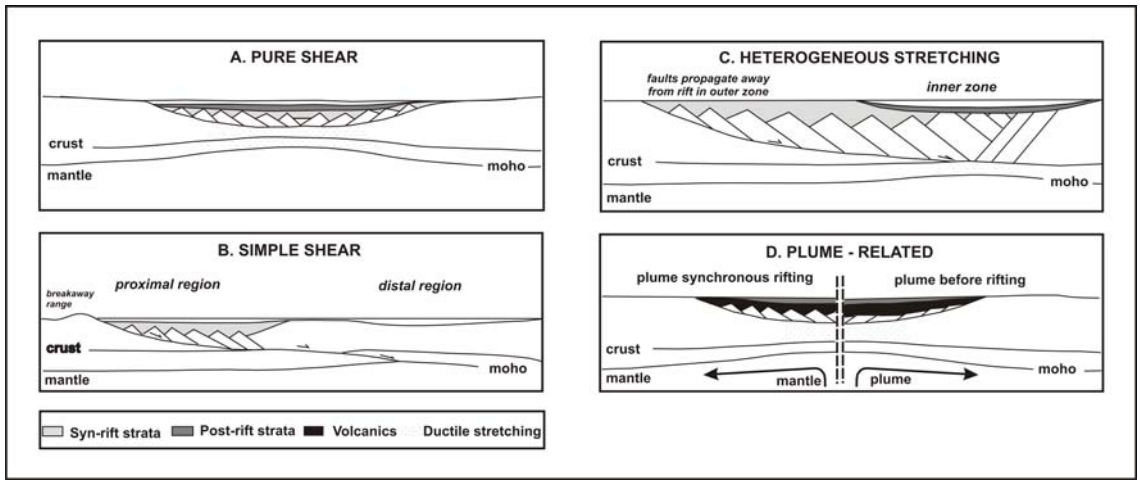

Figure 3.2 Models of rift basins formation. (a) Pure shear model (after McKenzie, 1978). (b) Simple shear model (after Wernicke & Burchfiel, 1982). (c) Heterogeneous stretching model (after Coward & Ries, 1986). (d) Plume-related model (after White & McKenzie, 1989), from Bosence, 1998.

Examples are found in the Paraná plume and Karoo basalts of volcanic continental margins related to the Gondwana split when the South Atlantic was opened. Also, the Afar hot spot below the Red Sea and Gulf of Aden rifting in Ethiopian and Yemen are other examples of plume-related rifting.

3.2.3 Geometry/morphology of the rift system

Rift basins are normally, narrow and long, and may be asymmetric where half-graben structures dominate (Rosendahl *et al.* 1986). Initial rifting processes commonly result in asymmetric shapes (half-grabens), which tend to loose this asymmetry as the rifting evolves. Grabens are, therefore, related to late stages of rifting.

Rosendahl *et al.* (1986), studying the morphology of the Lake Tanganyika area, identified isolated half-graben as a fundamental rift unit, a building block of the rift system. According to their studies, the geometry of an isolated half-graben is characterized by a normal border fault, arcuate or crescent-shaped in plan view, a flexural border and a depocentre situated along the border fault (Figure 3.3).

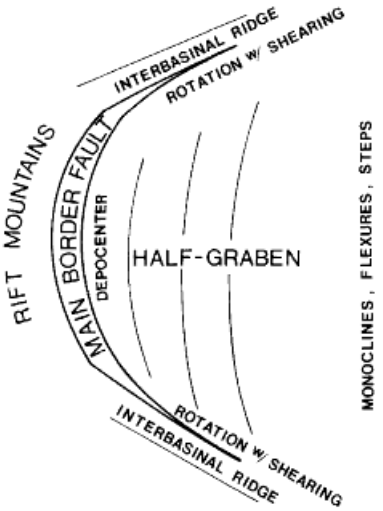

Figure 3.3 Plan view of main characteristics of the half-graben, fundamental unit for the East African Rift system (from Rosendahl *et al.* 1986).

The isolated half-graben evolve from a simple to complex border fault system according to the array of intrabasin faulting as the subsidence increase, creating synthetic and antithetic faults. Synthetic faults refer to intrabasin normal faults which are parallel to the main border faults, both in map and cross-sectional views. Antithetic faults have opposing dips to the master system in cross-section and may arc in the opposite direction in map view (Figure 3.4).

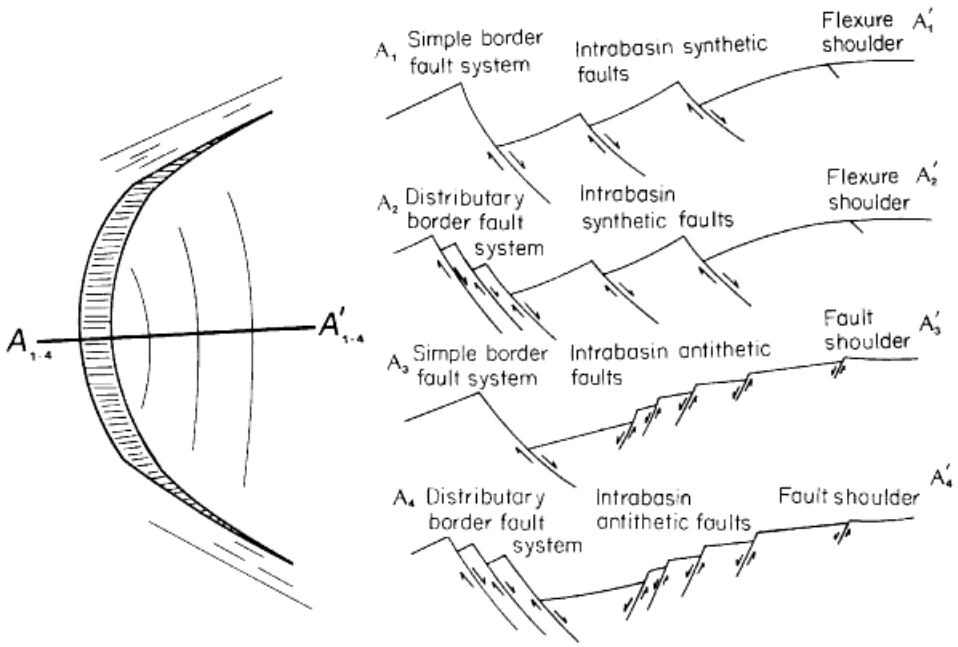

Figure 3.4 Asymmetric half-graben profiles generated by different systems of antithetic and synthetic intrabasinal faults (from Rosendahl *et al.* 1986).

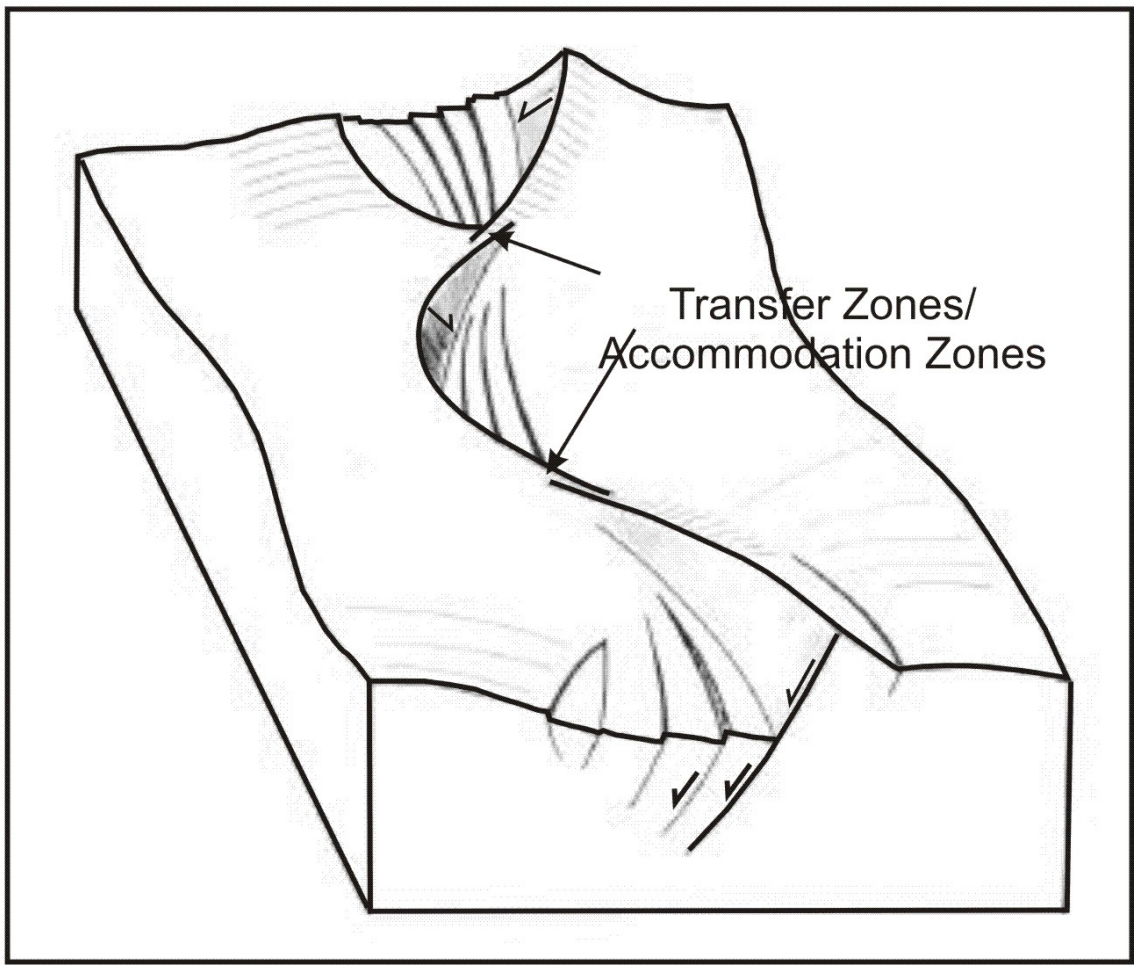

Figure 3.5 Block diagram showing a common way in which half-graben are linked together in Lake Tanganyika (from Rosendahl *et al.* 1986).

There is a large variety of ways in which these fundamental rift units can interact to link together the isolated units in time and space in order to form a rift system. The most common is an alternation of half-graben along a sinusoidal interaction of border faults and interbasinal ridges, as seen in the rift systems of the Tanganyika Lake (Figure 3.5).

In non-overlapped linkage, an interbasinal high may occur, which separates each segment of oppositely dipping border faults (Figure 3.6), or relay ramp if the separate segments dip equally. The overlapping segments can develop a complex arrangement of faults in order to accommodate the stress of the rifting (Figure 3.7). Along two interbasinal ridges in the Lake Tanganyika example, volcanic rocks may occur (Rosendahl *et al.* 1986).

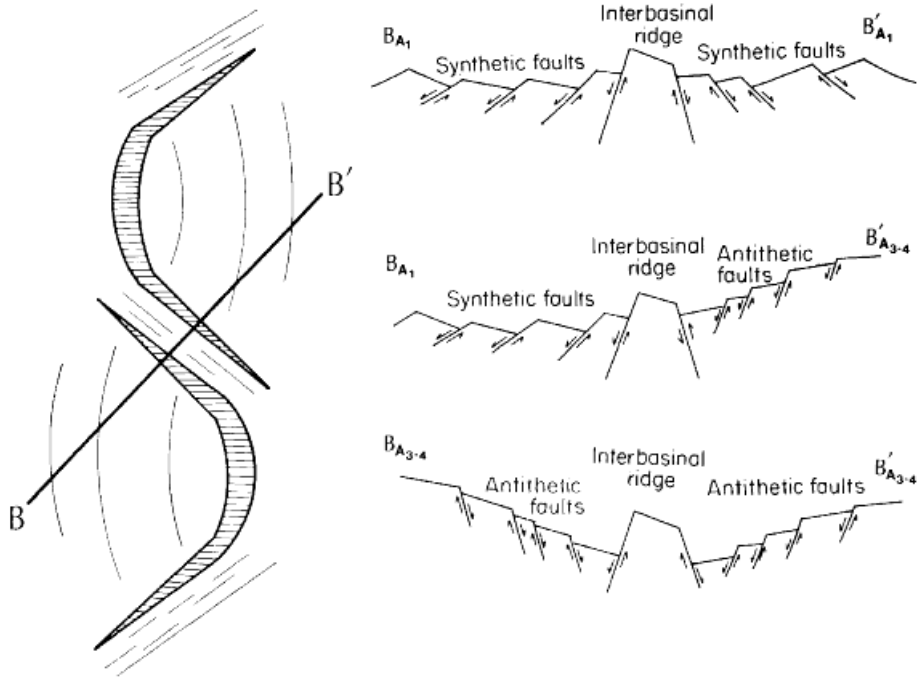

Figure 3.6 Section through back to back half-graben system (from Rosendahl *et al.* 1986).

3.2.4 Transfer Accommodation Zones

During the rifting process it is unlikely that extension has the same magnitude along the strike of rift basins (Milani, 1990). Where there is linkage between extensional fault systems, a transfer of displacement between individual faults is generated to accommodate areas with different degrees or directions of extension (Morley *et al.* 1990; Figure 3.8). Strike-slip fault systems (Gibbs, 1984, 1990), connect major normal faults with similar or opposite polarities. Walsh & Watterson (1991) named this event as hard linkage.

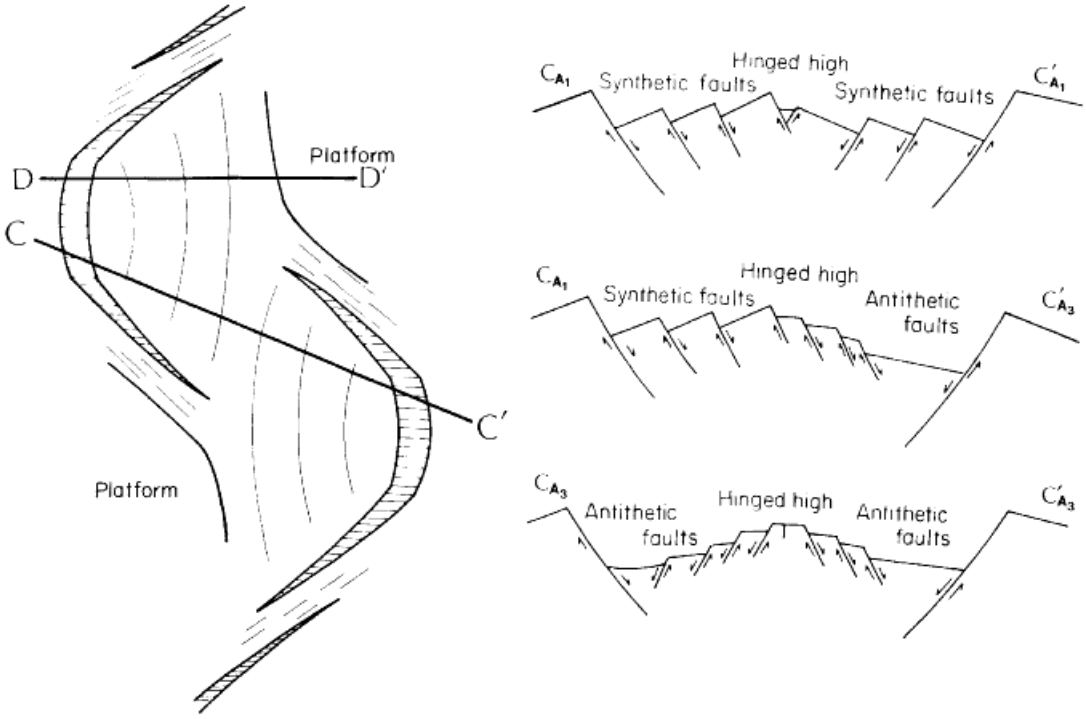

Figure 3.7 Section through the overlapping half-graben system (from Rosendahl *et al.* 1986).

On the other hand the displacement can be transferred by other mechanisms when the strike-slip transfer fault system gives place to diffuse and complex structures such as relay ramps (Larsen, 1988), accommodation zones (Rosendahl *et al*. 1986; Scott & Rosendahl, 1998) or transfer zones (Morley *et al.* 1990, Destro *et al.* 2003). These were termed by Walsh & Watterson (1991) as soft linkage. Transfer faults (Gibbs, 1984) can be defined as places where differences in strain or structural styles occur along their fault strike (e.g. Lister *et al.* 1986; Milani & Davison, 1988; Bosworth, 1995; Salah & Alsharhan, 1996; McClay & Khalil, 1998, in Destro *et al.* 2003).

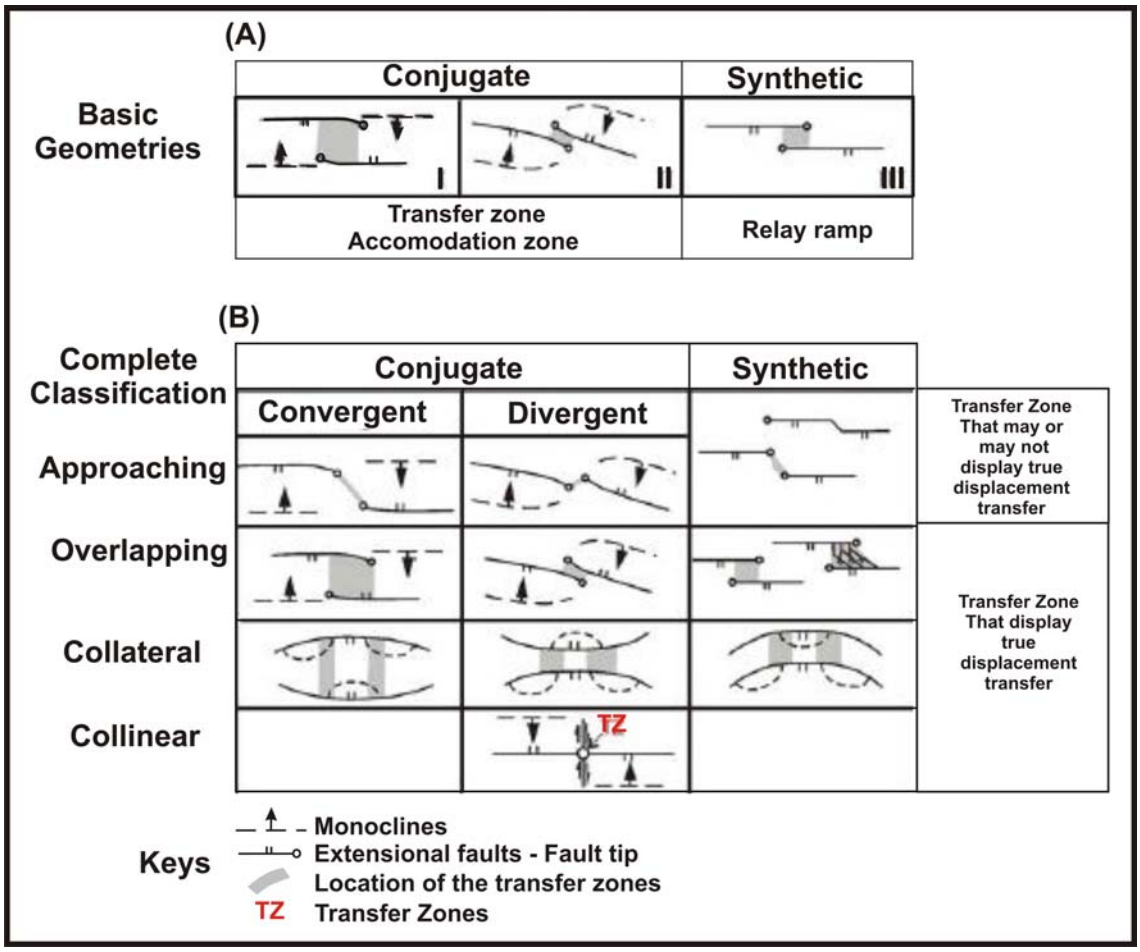

Figure 3.8 – Classification of transfer zone: (a) basic geometries and (b) complete classification (after Morley *et al.* 1990).

3.2.5 Orthogonal and oblique rifting

Pre-existent structures in the basement can play a major role during the rifting process. The most common is the reactivation of structures such as faults and lineaments during the syn-rift phase. The angle formed between the maximum extension and the rift axis, which normally is parallel to such pre-existent structures, allows a classification of the extensional stress as orthogonal, when the angle is 90º, or oblique, when the angle is less than 90º.

McClay & White (1995), using physical modelling of scaled models, showed that orthogonal rifting is characterized by long and straight border faults and intra-basin faults perpendicular to the extension direction. However, oblique rifting is characterized by shorter segmented border faults, and intra-rift faults perpendicular to the extension direction (Figure 3.9). Furthermore the rift border faults are formed in an en-echelon pattern parallel to the pre-existing lineaments in the basement. Intra basin faults are formed at right angle to the extension vector. The evolution of the rifting results in the

rotation of the intra-basin faults. As the rift evolves, the intra-basin faults rotate to become parallel with the rift border faults.

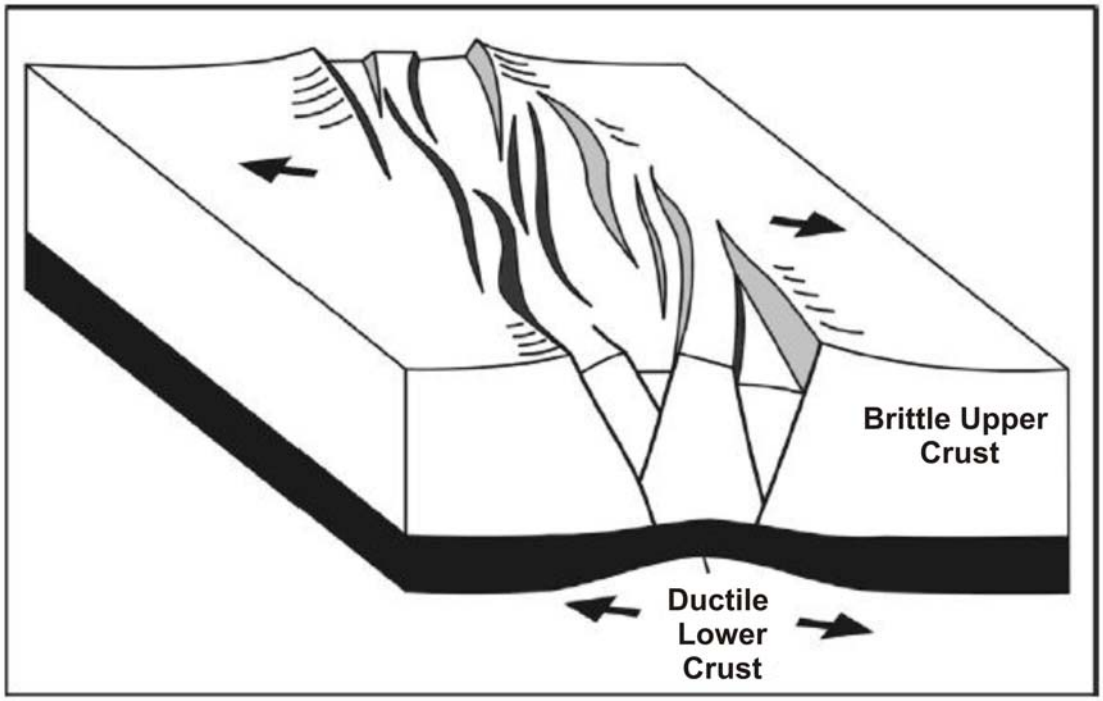

Figure 3.9 – Three-dimensional model of oblique extension rifting, after McClay & White (1995).

3.3 Conclusion

This review of extensional basin types and the structures within rift basins forms a basis for an understanding of the tectonic structures in seismic data studies in the following chapter. The application of these models will be discussed at the end of Chapter 4 when the Campos Basin structures have been studied.

CHAPTER - 4 STRUCTURAL SETTING OF PRE-SALT CARBONATES

4.1 Introduction

Tectonics is a major control on the depositional geometries and facies distribution of carbonate successions in extensional continental rift systems such as the Barremian and Aptian in the Campos Basin (Guardado *et al*. 2000). Although climatic, chemical and biological factors exert a certain influence on the production of carbonate rocks (Moore 2001; Tucker & Wright, 1990), tectonics is also considered by the present author to be quite significant. For that reason, the integrated study of tectonics and basin fill is essential. The main aim of this chapter is to propose a tectonic structural model, using 3D seismic reflection methods and subsurface well data analysis, in order to support tectono stratigraphic studies of the carbonate platform in the pre-salt succession.

This chapter begins by presenting the data set, followed by a detailed description of the methodology used. Then, a description of the seismic interpretation results is presented. Finally, a discussion of the findings and conclusions is reported.

The seismic interpretation focused essentially on the pre-salt carbonates of Barremian to Aptian age. However, the top salt and the Cabiúnas Formation (basalt - acoustic basement) were mapped as well. Seismic horizons and the main faults were therefore mapped using 3D seismic survey, well data, amplitude and others seismic attributes and Landmark software.

As a result, the analysis of sub-surface data set revealed a complex arrangement of structures and features with an overall polygonal geometric style, which is interpreted to have developed from an oblique extension rifting system. Three distinct tectonic domains (DI, DII and DIII) with three different carbonate platform geometries could be identified.

4.2. Data set

The subsurface data used for the interpretation comprises 3D seismic data covering an area 60 km wide to 125 km long (7500 km^2) with 23 wells, mostly concentrated in the shallow water sites, in the northwest the study area, covering the oil fields of Pampo, Linguado, Badejo and Trilha (Figure 4.1). Additionally, gravity data was used.

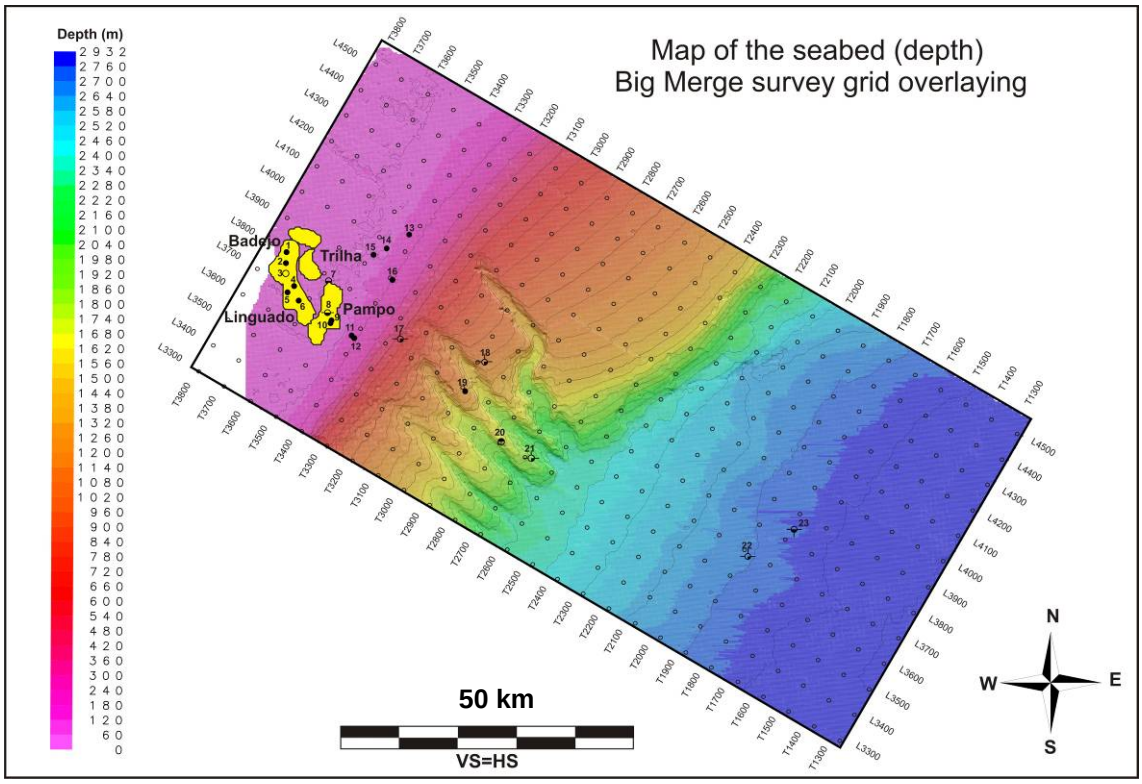

Figure 4.1 – Map of the seabed (depth) with 3D seismic grid displaying line, traces, shot points and wells overlapping.

4.2.1 Seismic Data

The seismic survey used, Big Merge, is a result of merging with four other pre-stack processed seismic surveys; Alfa, Beta, Gama and Delta (Figure 4.2), each of them with different acquisition parameters, grid characteristics and frequency content (Table 4.1). The merging was done by the Petrobras processing geophysicists previously. The grid is arranged in 1300 inlines by 2662 crosslines with the spacing between them of 50 by 50 m and an average frequency estimated of 15-18 Hz. (Table 4.1).

Seismic survey	Grid Lines x Traces	Line x Trace spacing	Average frequency	Seismic processing
Big Merge	**1300 x 2662**	**50 X 50 m**	**15-18 Hz**	
Alfa	4525 x 2981	12.5 X12.5m	25 Hz	migration with gain and filter, 32 bits
Beta	1515 x 2061	25 X 50 m	20 Hz	far offset stack migration, 32 bits
Gama	2801 x 2601	25 X 25 m	25 Hz;	pre-stack time migration with gain and filter, 32 bits
Delta	2120 x 4648	12.5 X 25 m;	18 Hz	pre-stack time migration, 32 bits

Table 4.1 – Parameters and characteristics of 3D surveys.

As the quality of subsurface seismic imaging varies in each survey within the area, the imaging quality in the merged seismic varies as well. So, in the proximal area the quality and continuity is compromised in both the original Delta and merged volumes due to the low frequency of the data (Table 4.1).

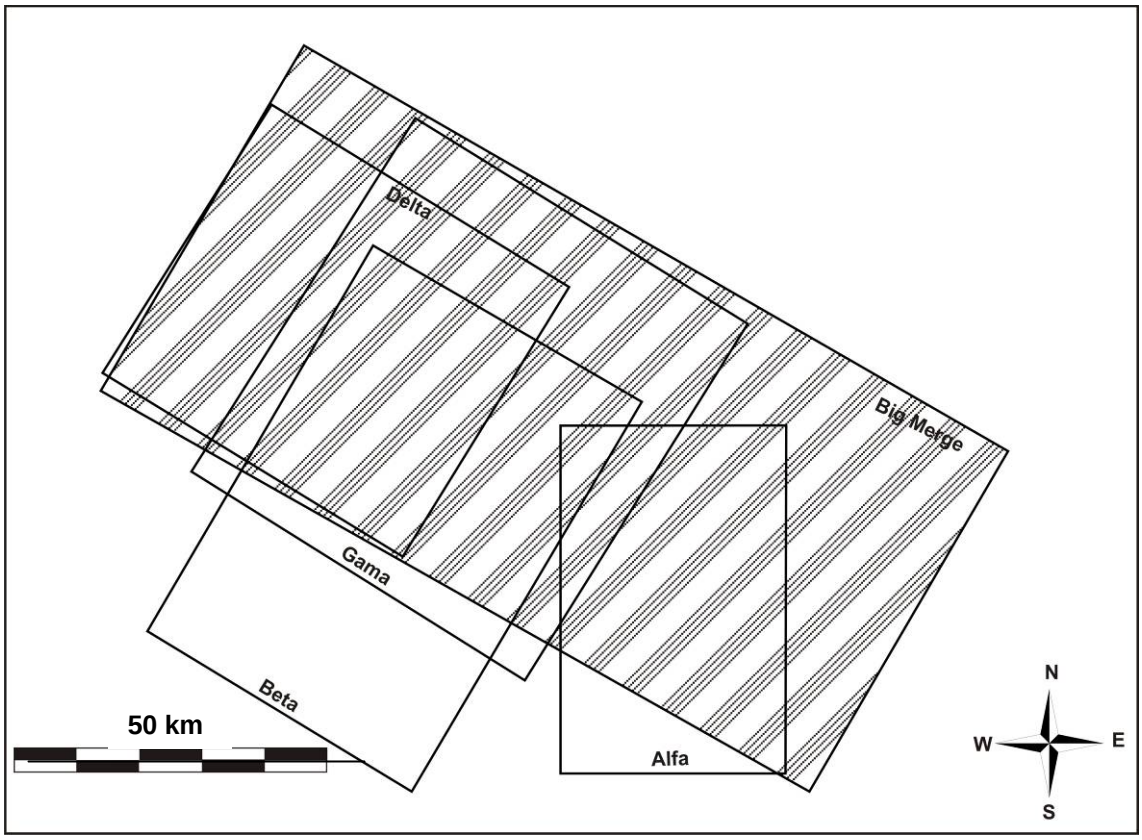

Figure 4.2 - Map with the outline of original 3D seismic volumes (white rectangles) and the hachured area shows the merged volume.

On the other hand, in the deep water areas, the resolution of the seismic is enhanced due to the better resolution of the original seismic surveys, Alfa, Beta and Gama (Table 4.1). Here the seismic reflectors are, in general, well defined. However, below salt diapirs, a strong loss of reflection signal, noise and a probable "pull up" effect (Figure 4.3) are observed.

Some irremovable processing problems, such as diffraction, smiles, multiple signals, noise as well as some gaps of data and splicing effects, mainly in the pre-salt succession, compromise the quality, accuracy of data and interpretation.

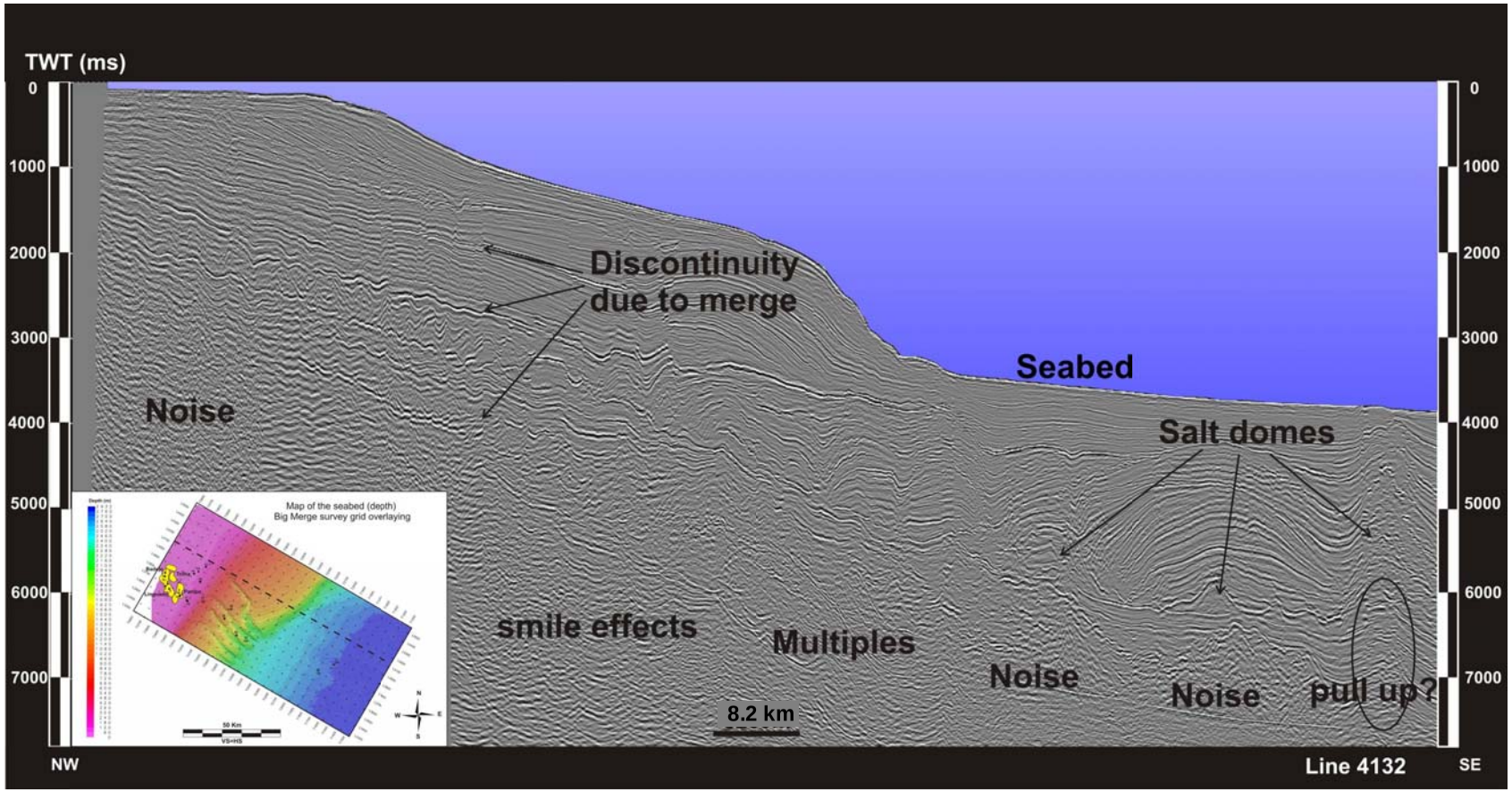

Figure 4.3 - Seismic section dip showing the seismic quality - scale: black - high amplitude; white - low amplitude.

4.2.2 Gravity data

Gravity data was available for this work. Data covering the entire study area were processed and analyzed by Petrobras. They consist of satellite Bouguer gravity anomaly maps. Published map were also used to place the data within the appropriate tectonic setting within the Campos Basin (Figure 2.3).

4.2.3 Well Data

To ensure a good interpretation of the seismic data, 23 wells and FMI logs were used for stratigraphic correlation, and to tie the seismic data to the stratigraphy. Some of them were cored in the pre-salt, Barremian-Aptian section so far.

At deep water sites, more than 900 m deep (Figure 4.1), uncored wells (wells 19 and 20) were sampled by sidewall cores and registered FMI (Full-bore Formation Micro Imager) logs, whereas in great depths offshore ultra deep water (more than 2100 m deep), there are no wells that reach the rift pre-salt Aptian section.

Wireline logs were also used, such as DT (sonic - acoustic log) and GR (gamma ray- neutron log), which are more useful for correlation between wells. But VSP (vertical seismic profile) and WST (well seismic tool) were extensively used, with check shots, in order to establish the time depth table used to tie the well to the seismic data.

4.3 Methodology

The tectonic and structural model proposed was based mainly on interpretation of seismic reflection data. This method consists of mapping subsurface reflections, faults and also to analyse and interpret the maps. For this purpose four steps were followed: 1) loading data and configurations; 2) picking manually the seismic horizons on a 3D seismic volume to generate structural and time thickness maps; 3) analyses of seismic attributes and picking faults; 4) integration and interpretation of maps and generation of tectonic and structural model. The details of the methods and sequence of work undertaken for seismic interpretation is shown in Figure 4.4.

After loading the seismic and well data the tie between well and seismic was made to establish the relationship between seismic reflectors with stratigraphy. This was achieved by control parameters such as time depth tables, picks and synthetic seismogram (Figure 4.4).

The seismic horizons were picked manually, because of the structural complexity of the area and the poor quality of some of the seismic data. At first the seismic horizons picking was made in an open grid just to be used as input to the seismic velocity model. More detailed mapping, on a grid of 20 x 20 lines, of the seismic horizon "top of the salt" was carried out in order to construct a more accurate seismic velocity model. A more precise adjustment of the time-depth table was done with supervision from Petrobras, Rio de Janeiro. This works was undertaken using the identification and picking of the main seismic reflectors and faults.

A substantial seismic attribute analysis was carried out, and the structural and tectonic model was erected by the analysis, integration and interpretation of the structural and fault maps.

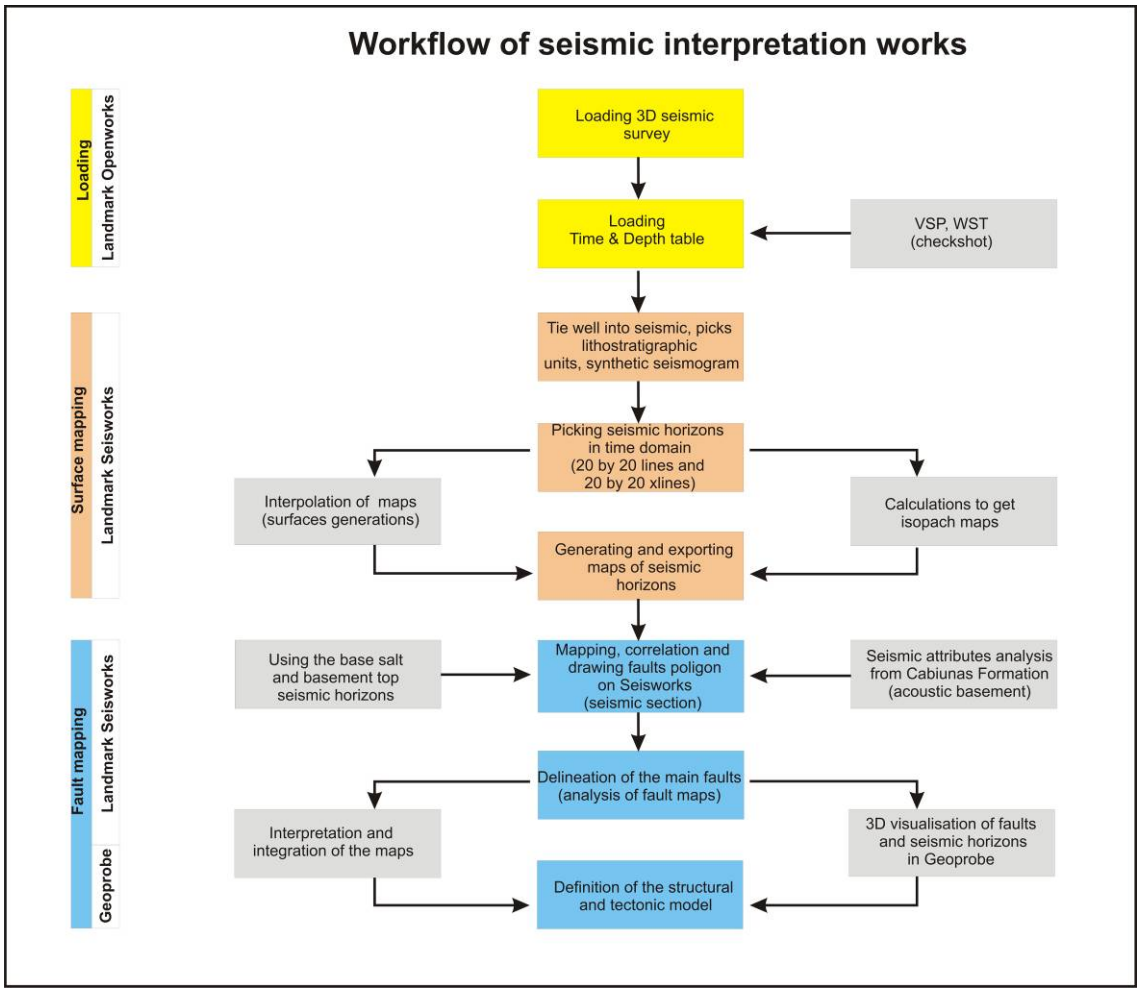

Figure 4.4 - Workflow of the method and sequence of work undertaken in the seismic interpretation.

The seismic survey was converted into depth by using TDQ (Landmark software) and from the seismic velocity analysis. Several previously mapped post-salt

seismic horizons allowed a precise adjustment using interval velocities and an accurate time-depth table was used. Although the results of conversions are good, near to the salt domes, some artifacts appear due to the pull up effects and different velocities of salt compared with the surrounding rocks (Figure 4.3).

4.3.1 Seismic horizons and fault maps

Five stratigraphic horizons were mapped in time: Top Cabiúnas Formation (basalt, acoustic basement), base and top Coquina, base and top salt (Figures 4.5 and 4.6). The criteria used to pick these structural seismic horizons were: continuity of the reflectors, seismic facies changes and endings (onlap, downlap, toplap, etc.). Some other criteria such as salt domes, which in general occur anchored over basement highs, were also used.

To map the faults, the structural maps were used, mainly the top Cabiúnas Formation map (basalt-acoustic basement). Likewise, a substantial seismic attribute analysis was done in order to delineate the main faults. Various seismic attributes were tested, such as amplitude, coherence, edge detection, dip azimuth and dip. The best results however came from dip, in which the faults were delineated more accurately.

4.4 Data Interpretation

4.4.1. Seismic Data Interpretation

This seismic interpretation aims to generate subsurface structural, isopach and fault maps, as well as cross sections through the 3D seismic survey. These maps and cross-sections were used to aid the identification and interpretation of the tectonic regimes, structural patterns, internal and external geometries of strata in the stratigraphic interval comprising late syn-rift Barremian to early post-rift Aptian succession. This study is directed to support the sedimentological, stratigraphic and tectonic interpretation in order to erect an original 3D tectonostratigraphic model in a non-marine carbonate platform environment.

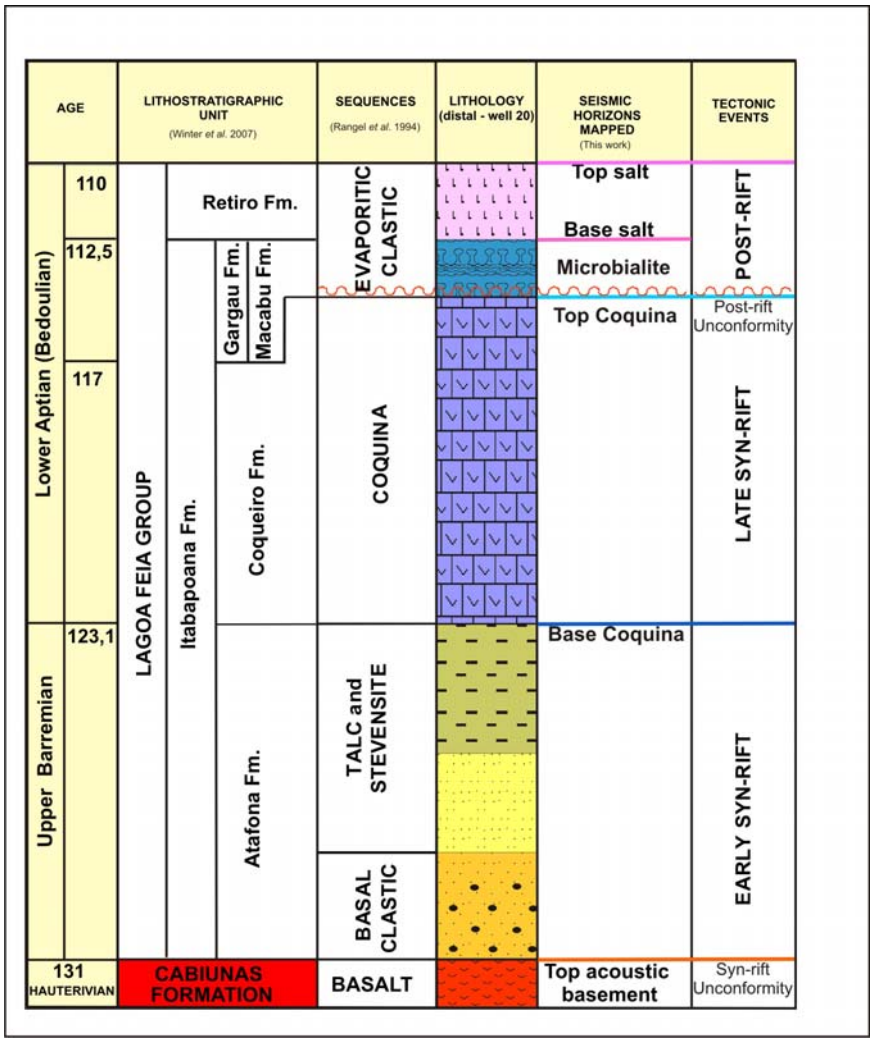

Figure 4.5 - Reference chart for the stratigraphic and tectonic settings with the top of the seismic horizons mapped.

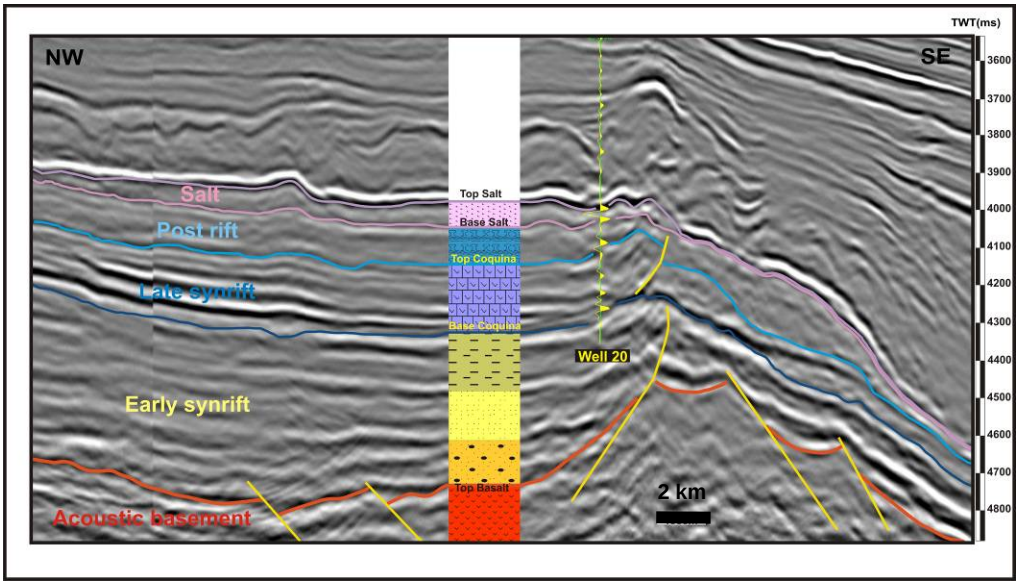

Figure 4.6 - Seismic section dip (in time), showing the seismic horizons mapped and the synthetic seismogram used to fit the well data into seismic data.

4.4.1.1 Seismic horizons

The picked and mapped horizons are within the litho-stratigraphic units Lagoa Feia Formation and Cabiúnas Formation (Rangel *et al*. 1994). They are consistent with the top of litho-stratigraphic units and denote time lines (Figures 4.5 and 4.6). Thus, the top and base salt reflectors are part of the Lagoa Feia Group, Retiro Formation (Aptian age). The top and base Coquina bound the Coqueiros Formation (Late Barremian to Early Aptian). The seismic reflector correlated to the top basalt is the Cabiúnas Formation (Early Barremian age). However, this cannot be distinguished from the Precambrian crystalline basement, due to the lack of resolution in the seismic imaging (Figures 4.7 to 4.10). For this reason, henceforward, the top of the basalts will be termed the "acoustic basement".

Top Acoustic Basement

The structural map of the acoustic basement exhibits an irregular topography and complex geometry (Figure 4.11). Most of the structures are arranged in a NE-SW direction. Secondary structures are aligned NNE-SSW. The mapped area can be subdivided into three main geometrical styles and architectural domains (Figures 4.11 and 4.12), which are: the Badejo High (Domain I), an intermediate zone in the regions near the 18 and 19 wells (Domain II) and finally a distal zone of the 22 and 23 wells (Domain III).

The first domain to the NW of the map, refers to a prominent high which is located in the vicinity of the Pampo, Linguado, Badejo and Trilha oil fields, where positive topographies are observed working up the Badejo structural high (Figures 4.11 and 4.12). This high is a horst (Figures 4.8 and 4.10) composed mainly of volcanic rocks. The Badejo high presents a steep border to the SE, like a promontory, which is narrower to the north.

The half-graben are polygonal (rhombohedral) in plan view in the Domain II, through wells 18, 19 and 20 in the intermediate zone. These half-grabens are distributed in a wide strip trending NE-SW (Figures 4.11 and 4.12). DII is bounded to the east by a curved hinge line, whose edge also defines the External High. This area also contains a large polygonal (rhombohedral) half-graben down dip to the SE. Domain III, in the SE of the map, interpreted as a site of linkage of several half-grabens, forming a large symmetric graben. This region shows relicts of a topographic high but overall has

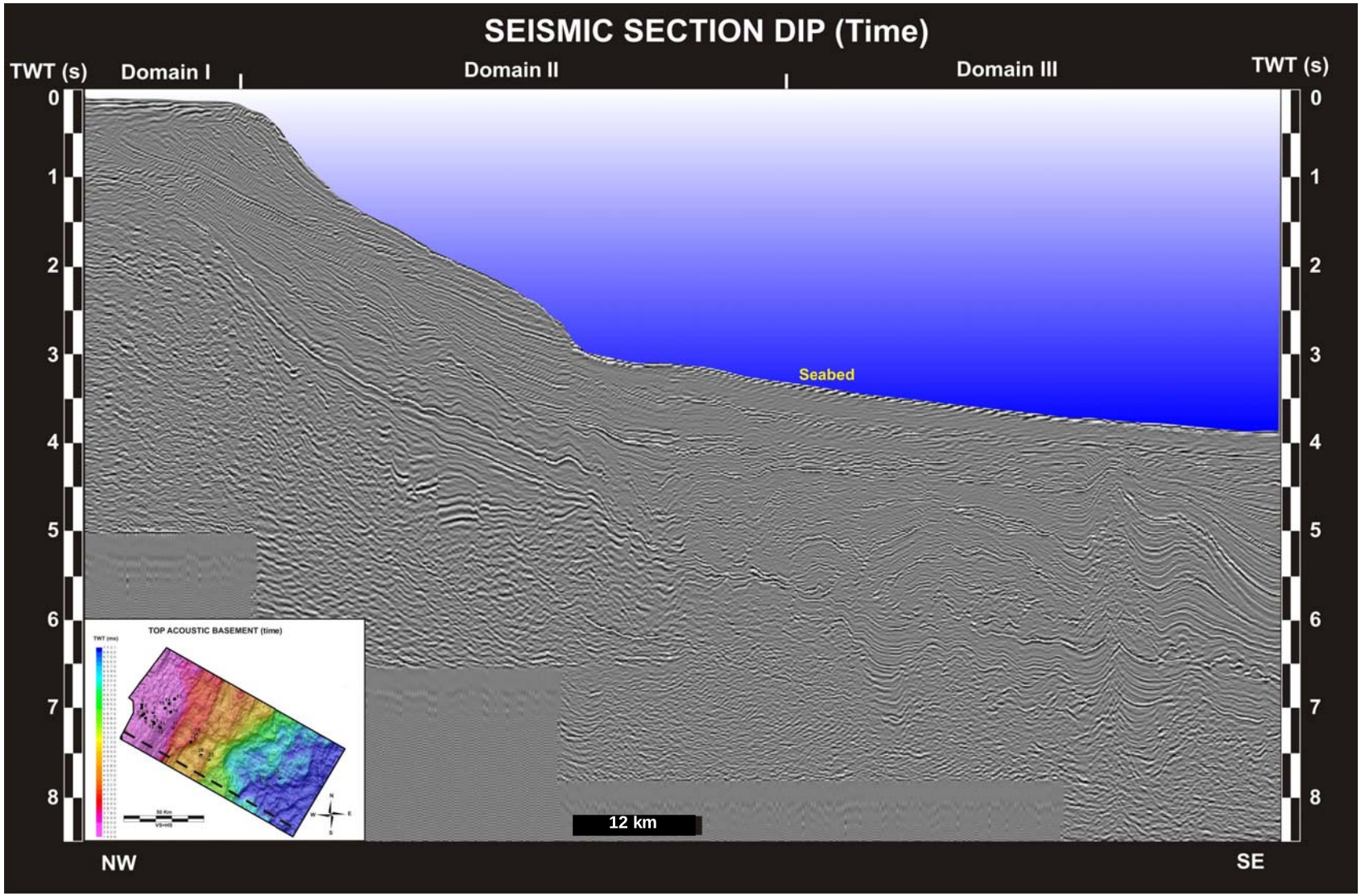

Figure 4.7- Seismic line dip section uninterpreted (in time).

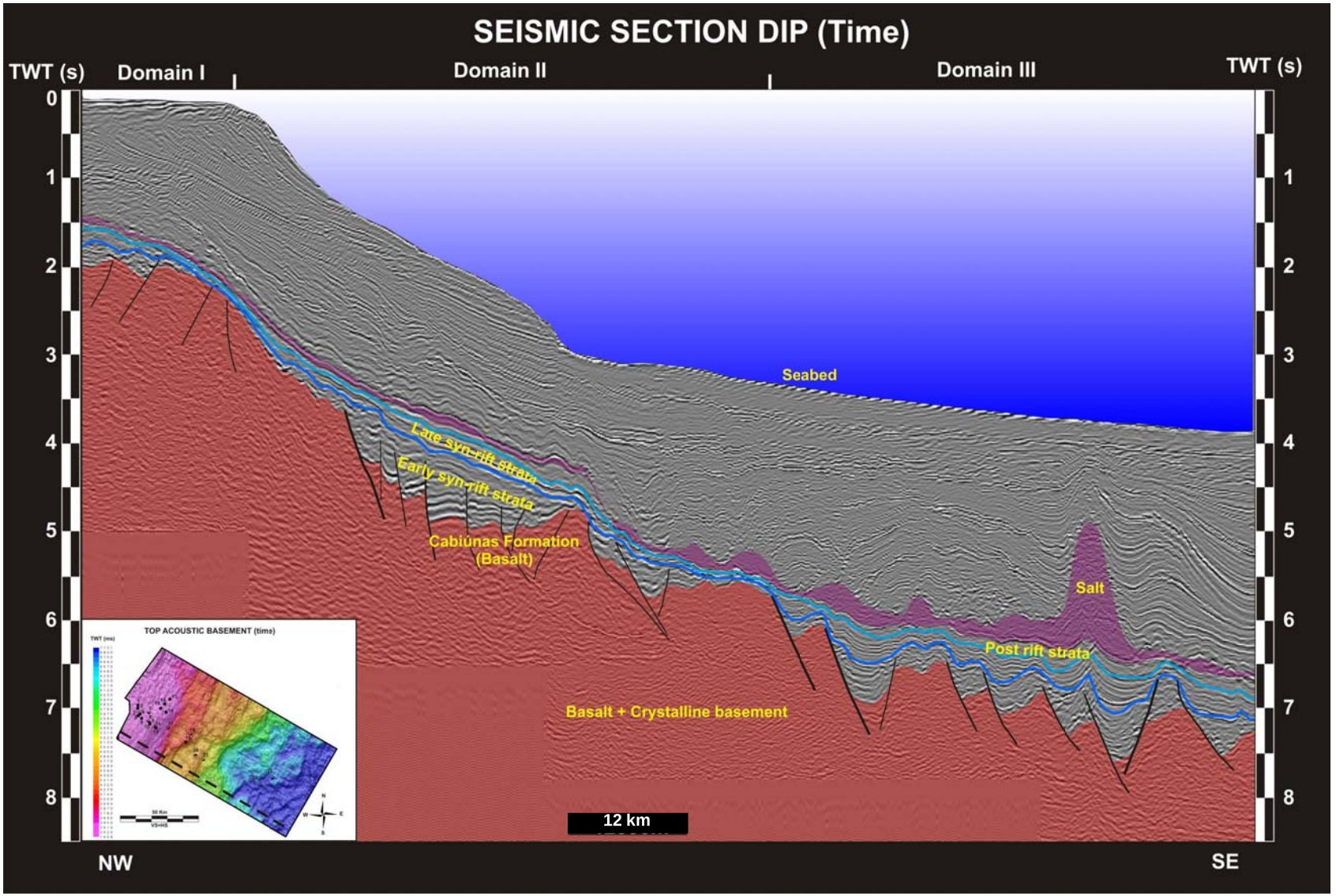

Figure 4.8 - Seismic line dip section interpreted (in time). Red= acoustic basement; Dark blue= base coquina; light blue= top coquina;; Light purple, base salt; Dark purple= Top salt.

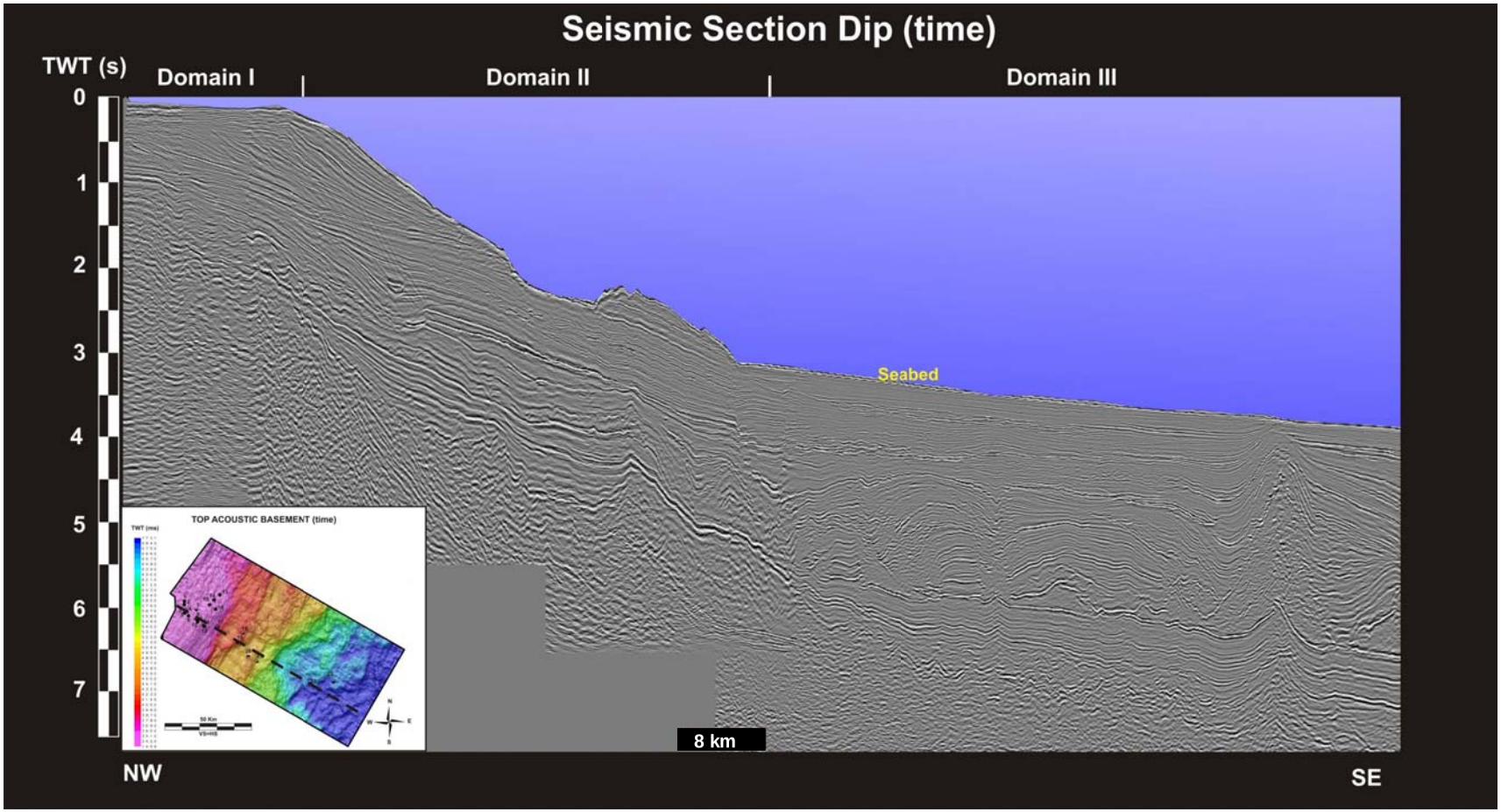

Figure 4.9- Seismic line dip section uninterpreted (in time)

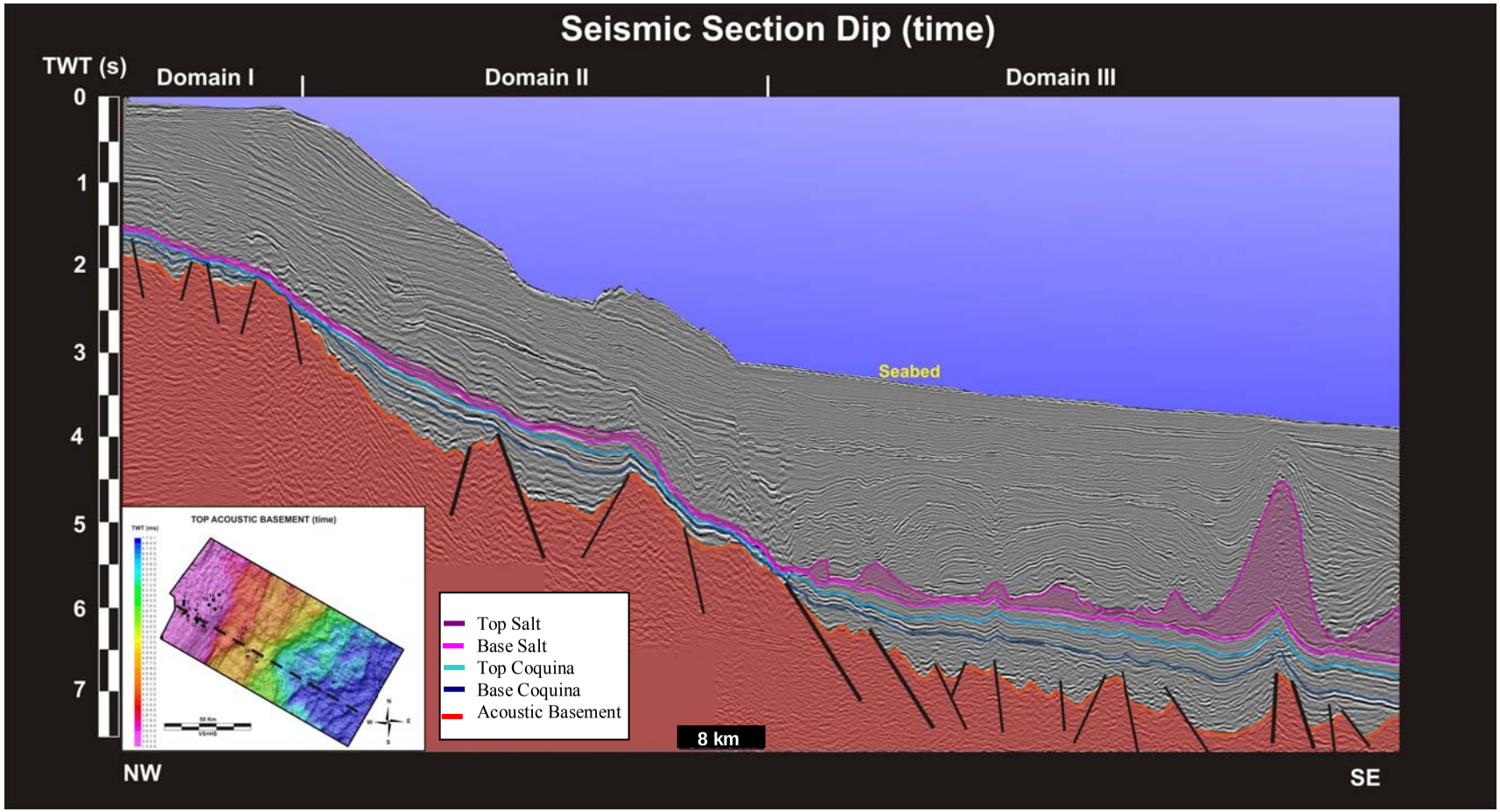

Figure 4.10- Seismic line dip section interpreted in time. Red= acoustic basement; Dark blue= base coquina; light blue= top coquina;; Light purple, base salt; Dark purple= Top salt.

developed as large topographic low, parallel to the main axis of the rift, of NE-SW directed faults.

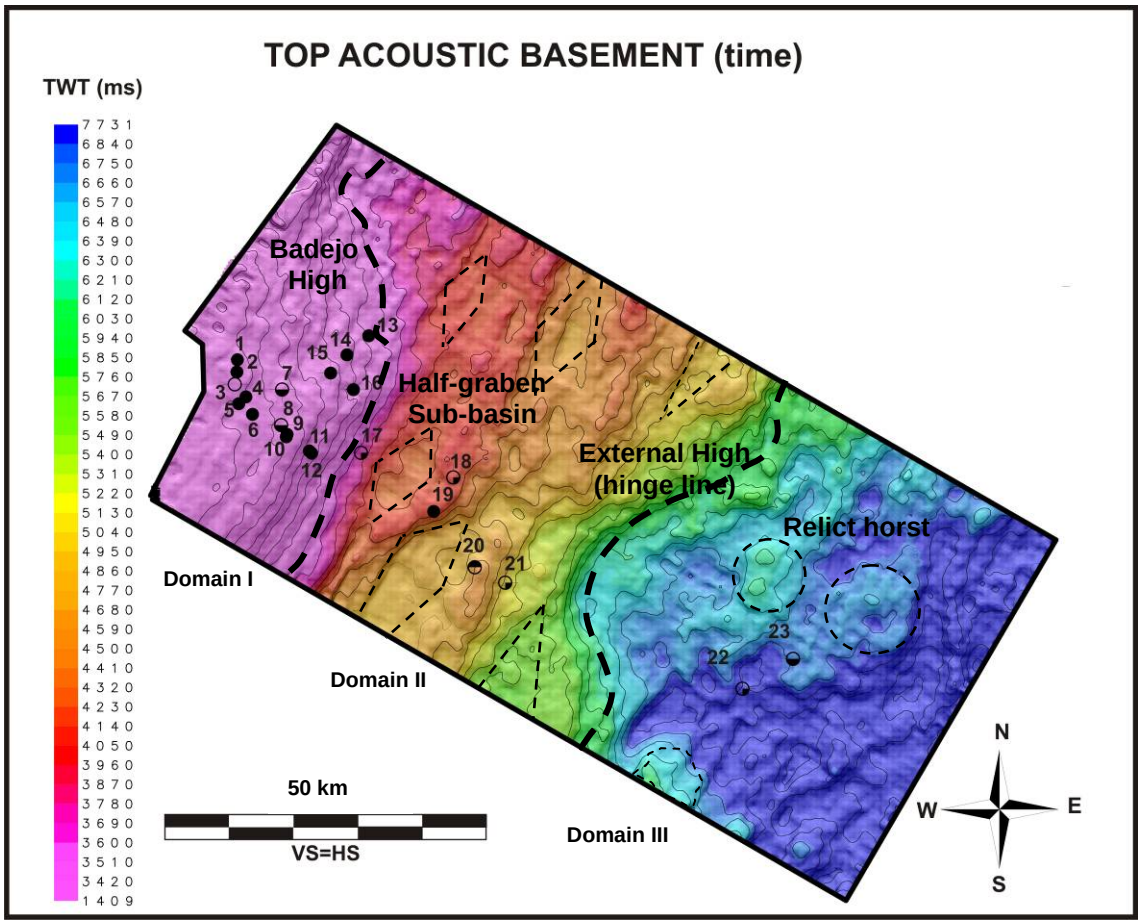

Figure 4.11 - Map of the top basalt, acoustic basement, based on 3D seismic in time (TWT- Two Way Travel time). Slim dashed lines outline the map view of the rhombohedral individual half-grabens (sub-basins – Domain II- see Figure 4.29) and the dashed circles outlines the relict horst (isolated platforms – Domain III). The coarse dashed line outline the palaeogeographical limits of the 3 domains, the hinge line.

The Base Coquina map (Figure 4.13) shows less irregular topography but still has some geometric control of the basement features. As it can be seen in the Figure 4.14, the Top Coquina map shows a smoother topography. This map represents a regional unconformity and physiographic changes can be identified. In the mid part of the map, a steep promontory and a gentle ramp are delineated, separating the proximal to distal areas. This feature is part of a hinge zone that becomes more evident with the basin evolution and tilting to the east.

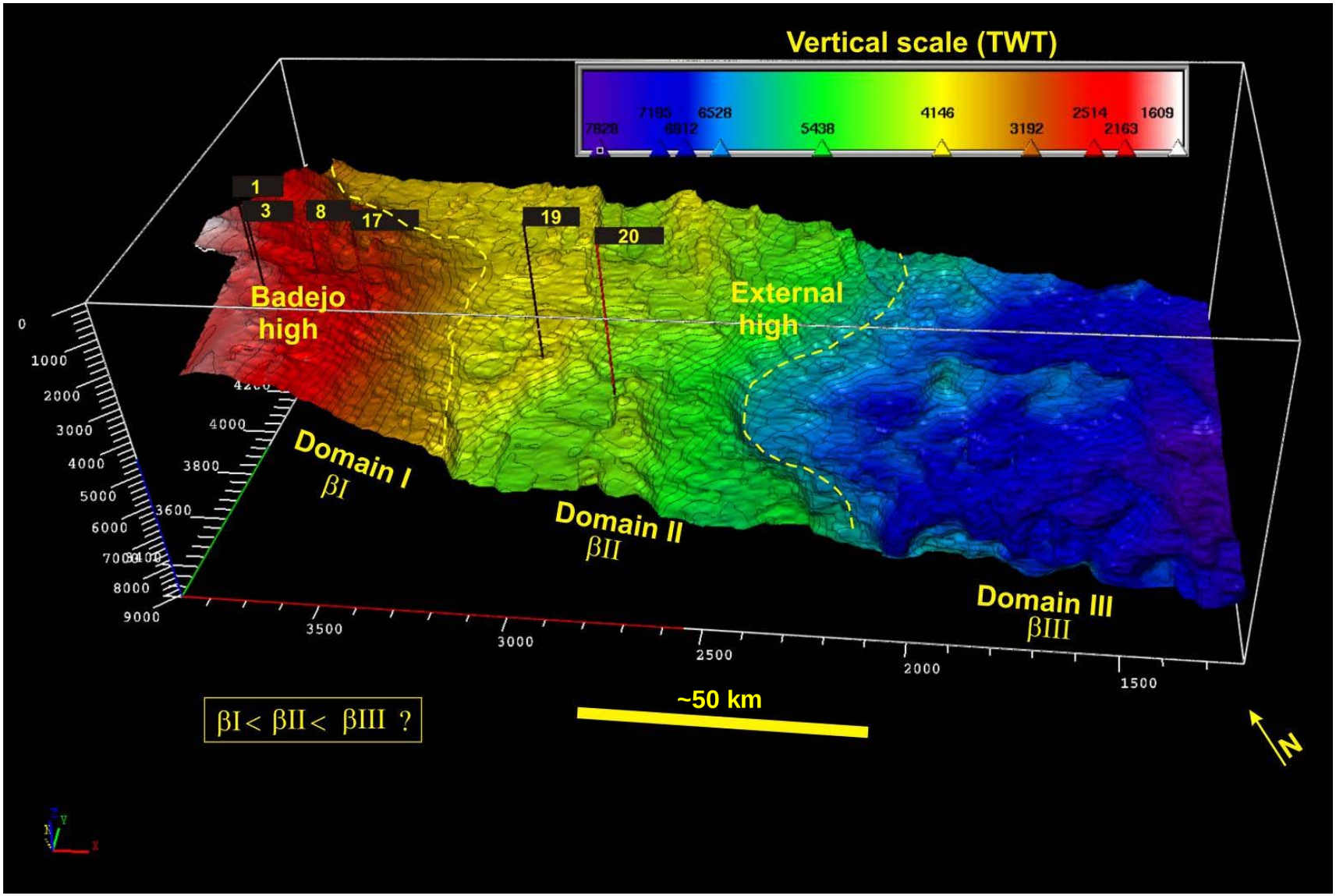

Figure 4.12 - 3D view from Geoprobe of the top basalt, acoustic basement surface, based on 3D seismic in time (TWT- Two Way Travel time).

Top and Base Coquina

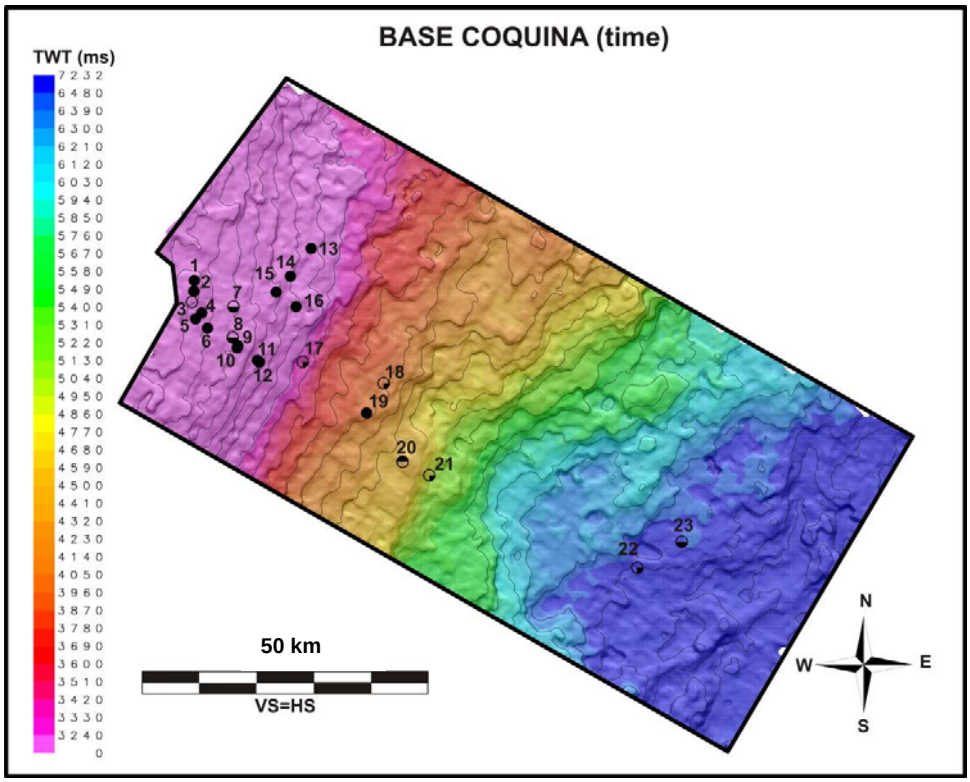

Figure 4.13 - Map of the Base coquina based on 3D seismic in time.

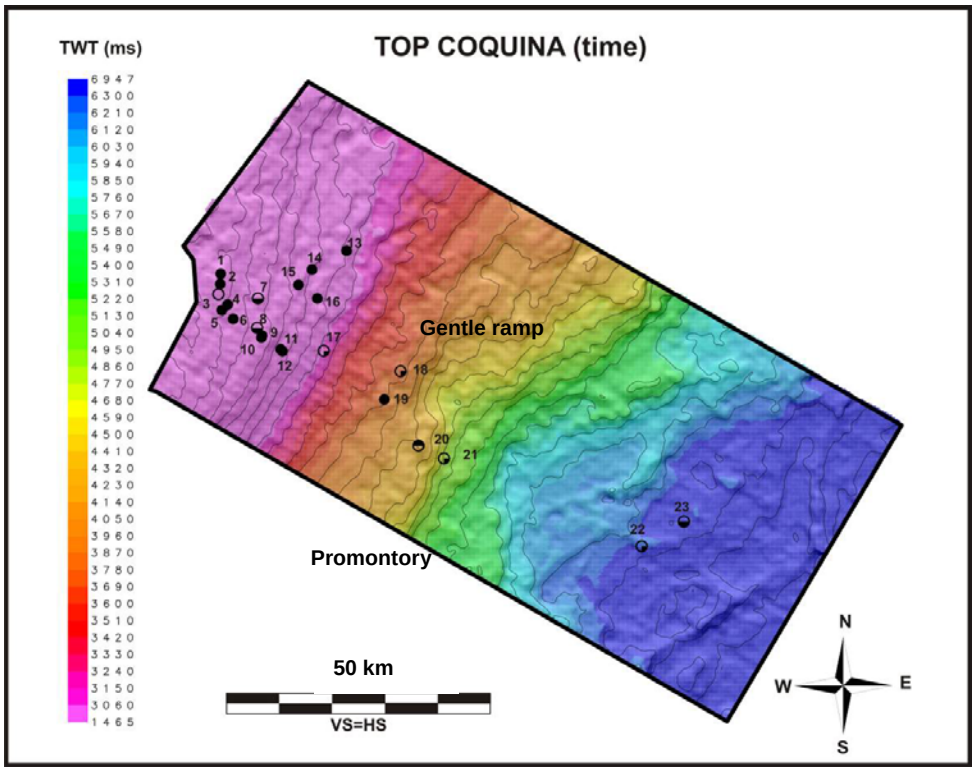

Figure 4.14 - Map of the Top coquina based on 3D seismic in time.

Base Salt

The Base Salt map (Figure 4.15) shows a gentle topography, smooth but with features which it has inherited from the basement structure. Significant features are the influence of the prominent Badejo High and the curved trace of the hinge zone of the external high which are particularly clear. A better developed promontory appears in the region of the 21 well and a smoother ramp to the north of it. In offshore regions topographic highs appear to occur. Such high topography associated with salt domes is anchored to underlying basement topographic highs (Figure 4.10).

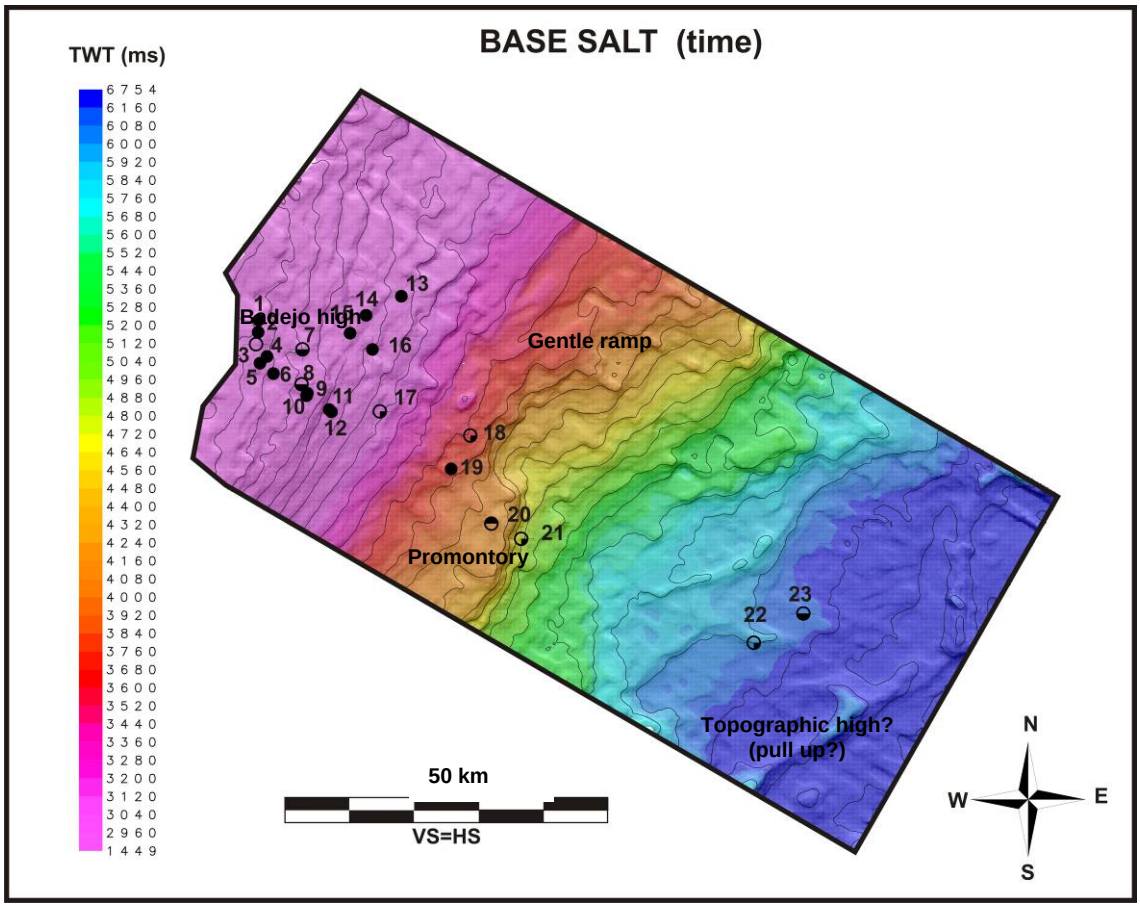

Figure 4.15 - Map of the Base salt, based on 3D seismic in time.

Top Salt

The current topography of the top salt (Figure 4.16) is smoother in proximal areas and more deformed in distal sites. The transition zone between these two areas is more ramped to the NE and steeper, like a promontory to the SW (Figure 4.16). The size and expression of the domes increases basinward where they can reach a thousand metres thick (Figures 4.8 and 4.10). This fact can be explained by the eastward gravitational sliding of the salt due to tilting of the entire pre-salt succession and also

due to sediment loading, from the west, pushing the salt downward (Figures 4.8 and 4.10).

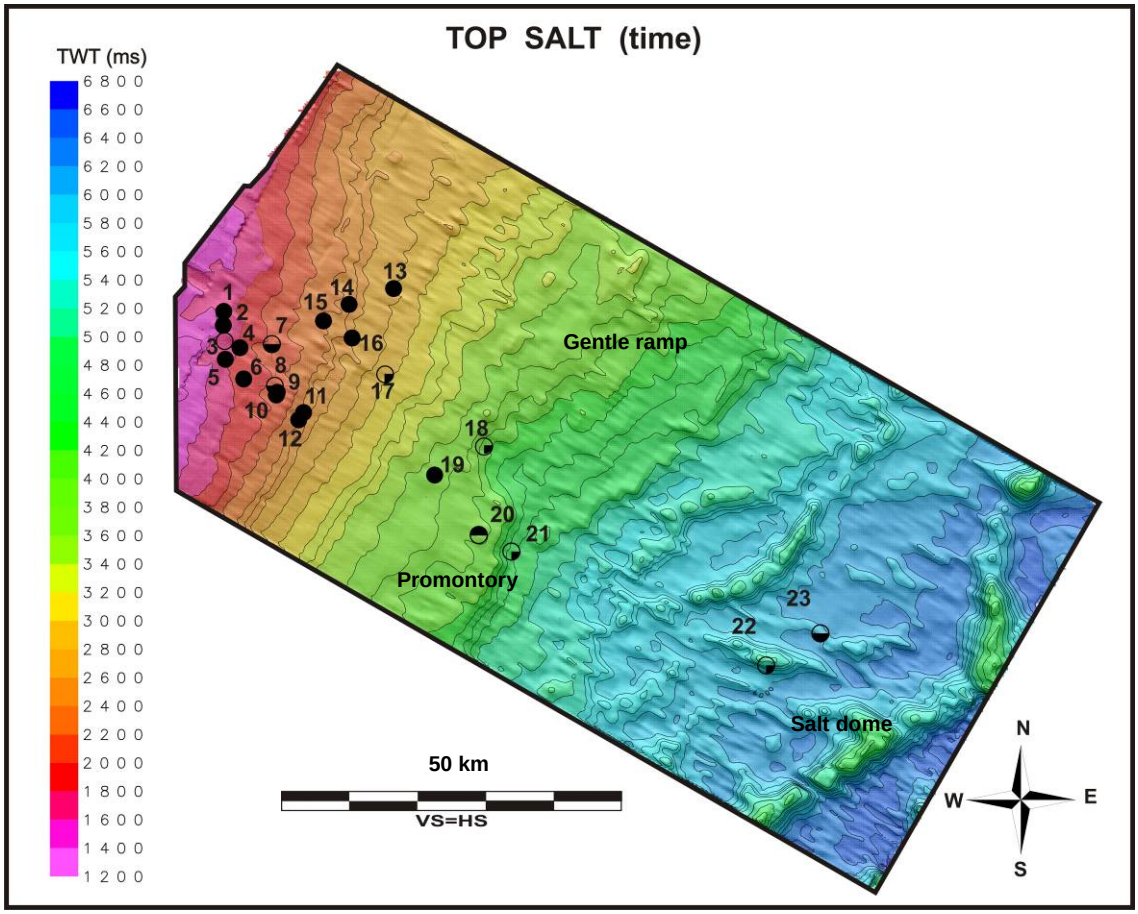

Figure 4.16 - Map of the Top salt, based on 3D seismic in time.

4.4.1.2 Seismic attributes

Seismic attribute analysis is usually used for the subsurface mapping of stratigraphical and geometrical features (Bacon *et al*. 2003). Here it was used specifically to support fault mapping as it is an effective tool for the recognition and accurate delineation of faults. Some types of attribute maps ordinarily highlight the presence of faults; even faults of small displacement can be recognized. For this reason, amplitude, coherence, edge detection, dip azimuth and dip seismic attributes were all tested. Although the edge detection and dip azimuth had good responses, the dip seismic attribute was found to be the most successful tool to highlight the faults and to support the definition of the structural elements. The amplitude maps were not accurate enough (contained potential errors) as the seismic volume was derived from the merging of four seismic surveys with different amplitudes (see Table 4.1 and Figure

4.3); compromising the lateral continuity of the dataset. Likewise, the coherence is not reliable, because of the noise that creates a non-coherent response within the map; which makes it difficult to distinguish faults.

In map view, fault traces are clearly delineated as well as the magnitude of the lateral displacement (Figures 4.17 and 4.18). The dip map was used as a control for the systematic mapping work and correlation of the faults in the seismic section. The faults mapped shows pattern of segmentation, locally linked forming straight segments in proximal areas, and curved lines in deep areas, as a result of differentiated levels of rift evolution, more evolved are the curved ones.

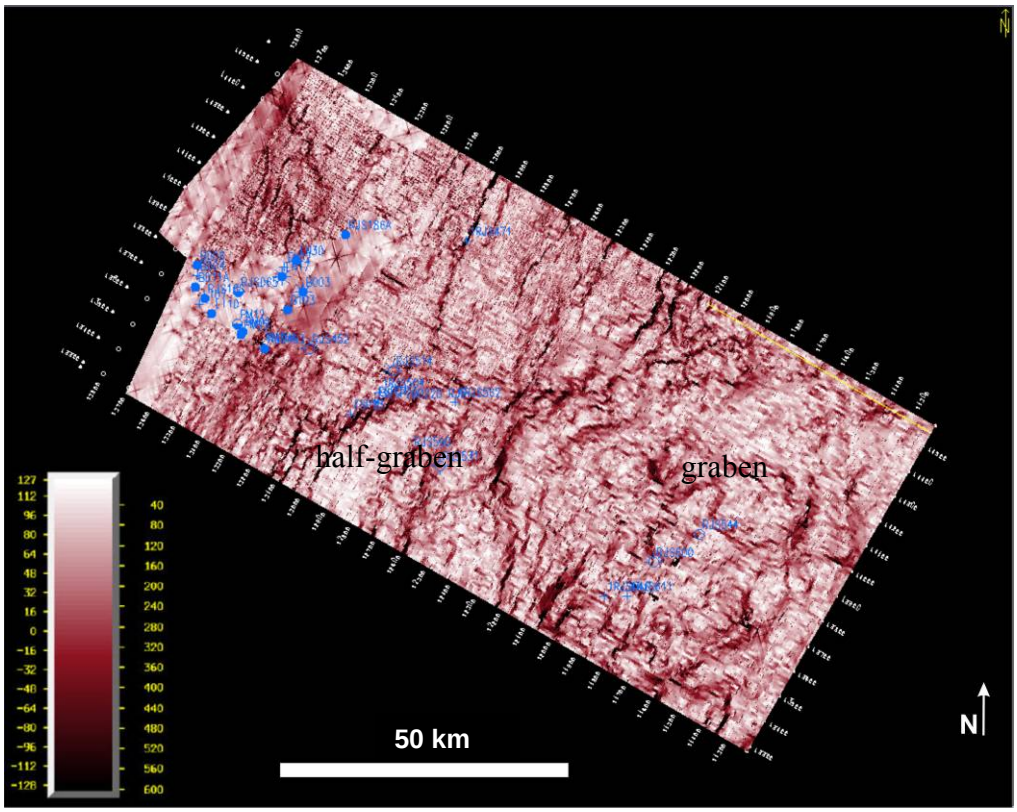

Figure 4.17 – Map of dip seismic attribute of the acoustic basement surface. This seismic attribute delineates the main faults of the study area in dark red colour.

4.4.1.3 Structural styles

Graben, half-graben and horsts are the major structural elements defined based on seismic attribute maps (Figures 4.17 and 4.18), seismic section interpretations (Figures 4.25 to 4.28) and thickness maps (Figure 4.29). They form a polygonal, rhombohedral geometry (Figures 4.11, 4.12 and 4.20). Most of the asymmetric half-graben are bounded by extensional planar, steeply dipping normal faults, which are dominantly synthetic but also with antithetic polarity (Figure 4.19). These faults are

commonly trend NE-SW, some NNE-SSW trending faults are related to prior zones of weakness in the crystalline basement, which were reactivated during the syn-rift stage (Chang *et al.* 1992). In distal basinal areas, horst and graben structures assume a much more symmetrical geometry with conjugated border faults (Figures 4.26 to 4.28).

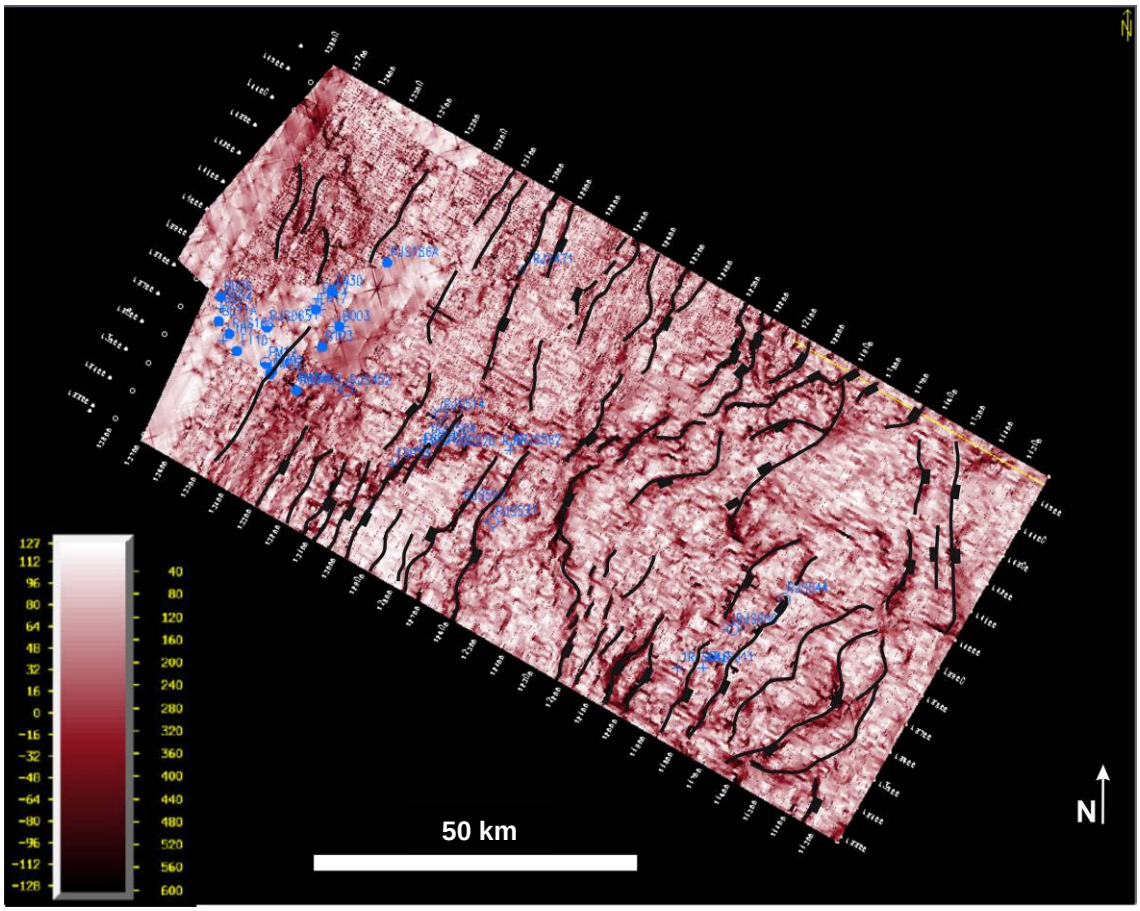

Figure 4.18 – Map of dip seismic attribute of the acoustic basement top with interpreted faults.

An ENE-WSW accommodation zone occurs separating adjacent independent half-grabens with distinct geometry and oppositely dipping faults systems (Morley *et al.* 1990). This accommodation zone shows short segmented faults (Figures 4.21 to 4.22 and 4.27 to 4.28). Additionally, the conjugate faults are shown in a section through back to back half-grabens (Rosendahl *et al.* 1986), and delimit an interbasinal ridge (close to the 18 an 19 wells), with positive topography (Figure 4.29). Toward the NE of the map the accommodation zones, in some cases, have the some fault segments with opposite dip (Figures 4.18 to 4.20).

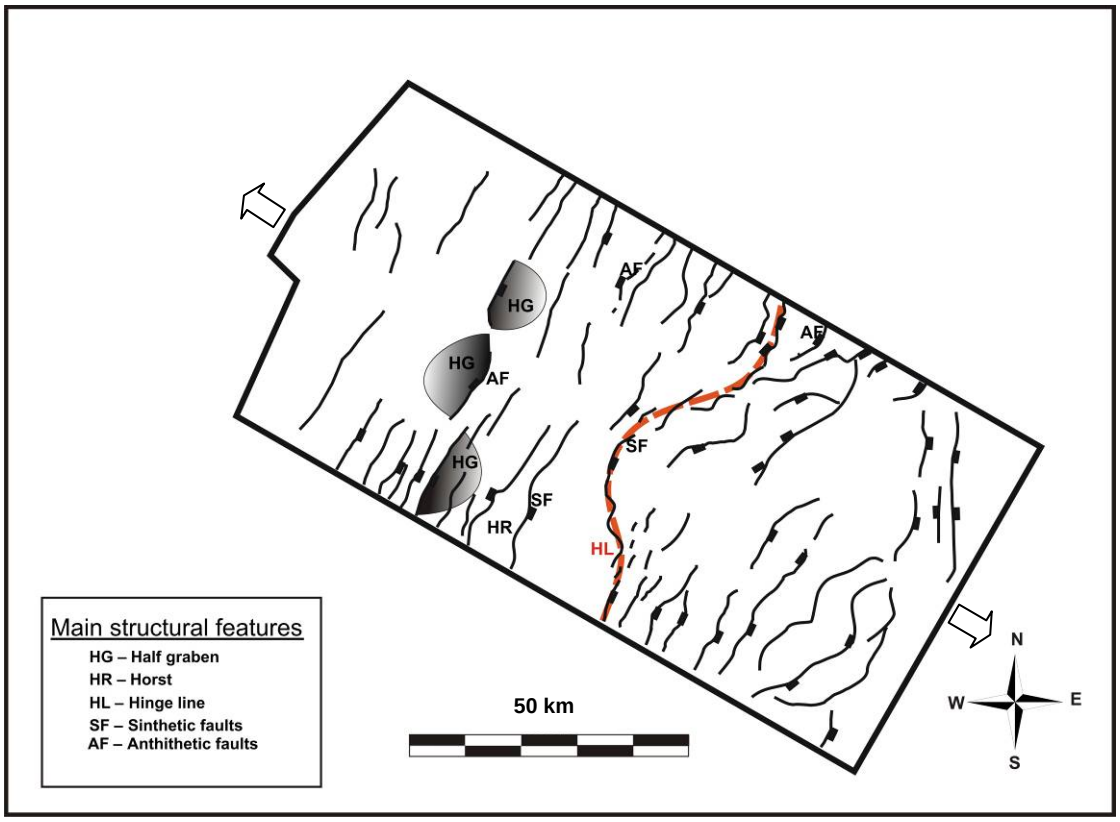

Figure 4.19 - Map of structural elements outlined from seismic dip attribute map of the top acoustic basement (Figure 4.18).

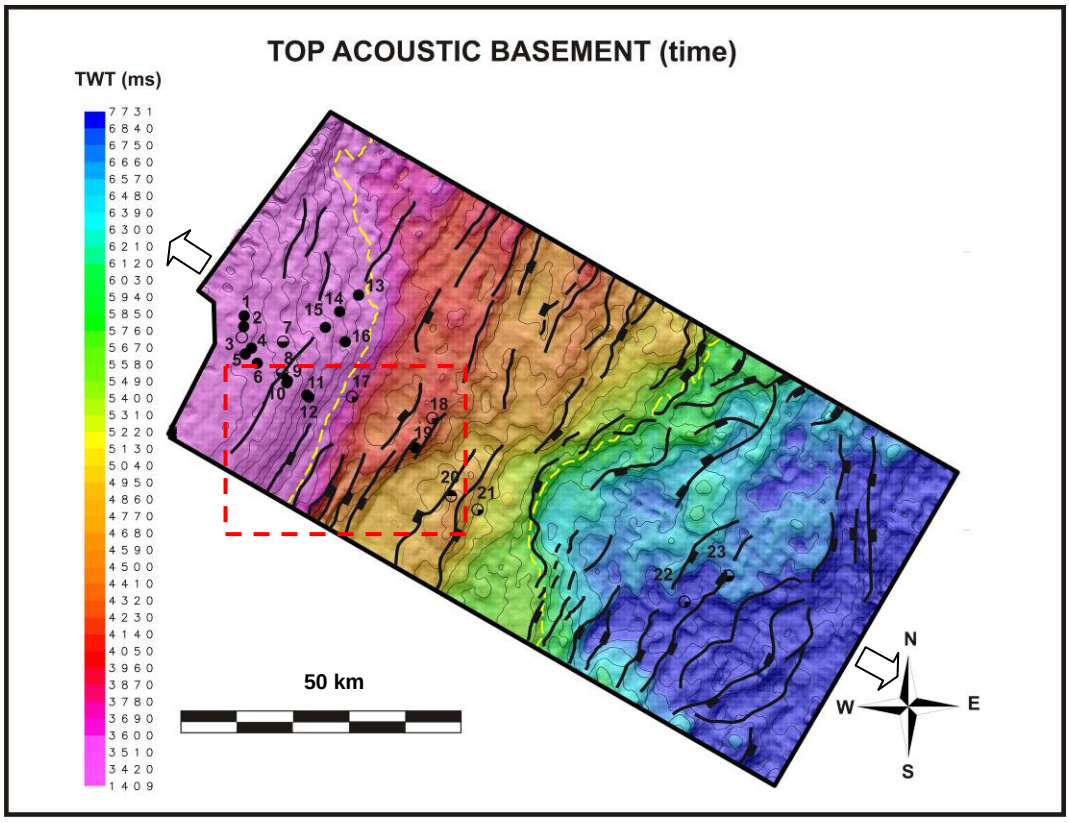

Figure 4.20 - Structural map of top acoustic basement with fault segments outlined from seismic dip attribute map (Figure 4.18). The dashed red rectangle is the coherency maps presented in the following Figures 4.21 and 4.22.

Figures 4.21 and 4.22 respectively interpreted and without interpretation, are seismic attribute coherency maps extracted from a horizon 400 ms (milliseconds) below of the seismic horizon mapped as base salt (Figure 4.10). The location of these maps is delineated in red rectangle of the Figure 4.20. Lighter colours represent coherent data, interpreted as sedimentary deposits. The reddish darker colours represent non-coherent data, interpreted as acoustic basement (basalt plus crystalline basement) or as noise.

The analysis of this map supports the interpretation of a transfer or accommodation zone NE-SW formed from a series of separated half-graben with opposite behaviour, synthetic and antithetic border faults. The accommodation zone is marked by en echelon faults NNE-SSW. (Figures 4.21 and 4.22). In a more tectonically evolved portion, NE of the map, faults with diffuse behaviour deep to both sides. These structural features are also interpreted in the pre-salt total thickness map and structural acoustic basement map (Figure 4.23). Such structures are described in Chapter 3, which were proposed by Rosendahl *et al*. 1990 (Figures 3.5 and 3.6) and classified by Morley *et al*. 1990 as basic geometries conjugate II (Figure 3.8).

Two main large scale horsts occur in the area. The proximal, nearshore horst, located in the NW of the area is related to the known Badejo High (Figures 4.25 to 4.28). Its flexural border dips smoothly to the NW and its faulted border dips steeply SE with stepped fault blocks or fault-block margins. In the distal part, the high known as External High has a sinuous outline forming a hinged margin (Figure 4.20). This feature was formed by the linkage of minor fault segments during the evolved rifting process (Figures 4.18 to 4.20).

Internally, half-graben are composed of rotated blocks arranged in a “domino style” pattern (Figures 4.25 to 4.28), a typical geometry for extensional rift systems (e.g. Mckenzie, 1978). Additionally, small-scale structures such as basement-involved normal intrabasin faults (IF) have also been mapped and described. Figures 4.19 and 4.20 show the extensional normal faults trend NE-SW, perpendicular to the main strain direction which is oriented NW-SE. The arrow indicates the main strain direction.

It is suggested that the normal faults were active for a longer interval towards the east, in the deep basin. In proximal areas, domain DI, they are short lived and the evidence for faulting terminates in the late syn-rift succession. In domain DII, the normal faults reach the top of syn-rift succession. However, in domain DIII, the normal faults are mostly long live, which cross the post-rift sag succession, in some cases reaching to the base salt (Figures 4.25 to 4.27).

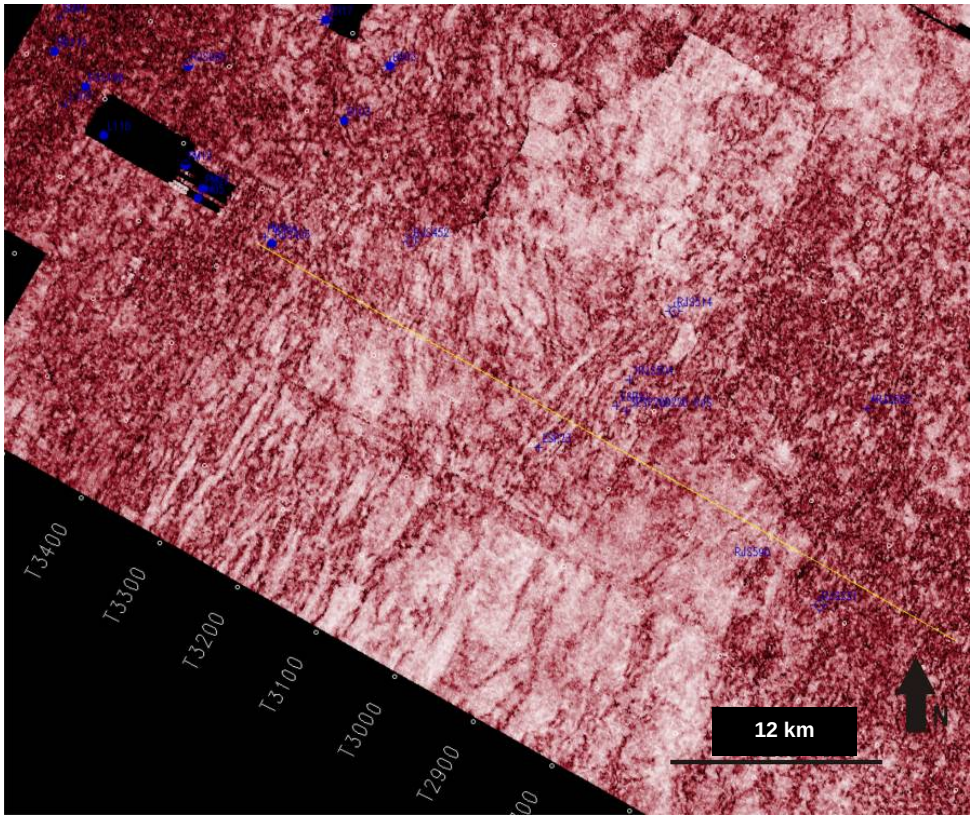

Figure 4.21 - Map of coherency extracted from a horizon 400 ms below the salt base (uninterpreted), located in dashed red rectangle of the top acoustic basement map in the Figures 4.20.

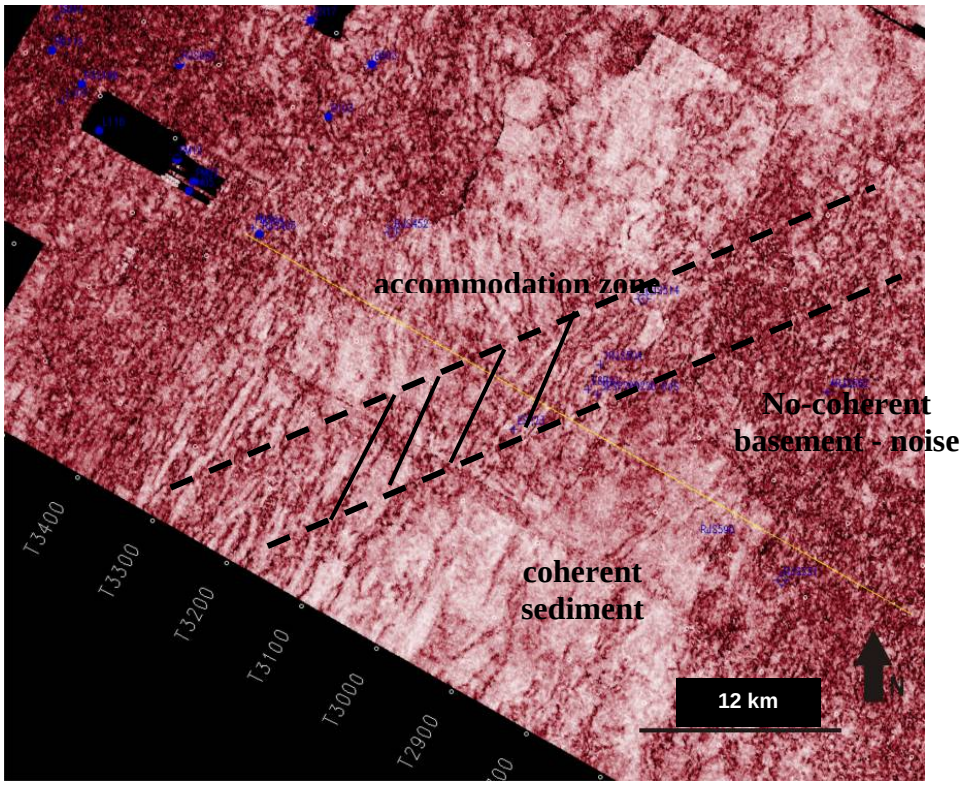

Figure 4.22 - Map of coherency extracted from a horizon 400 ms below salt base (interpreted) showing the accommodation zone with en echelon faults.

Figure 4.23 presents a summary of the structural analysis in the study area. Figure 4.23a, a map with the main structural elements and trends, shows the normal faults initially segmented. As the rifting evolved the faults tends to link each other forming longer segments. In the proximal area, northwest, the fault lines are straight. On the other hand, in a distal position, the faults are more curvilinear in plan form. This indicates a more evolved rifting process basinward (Davison, 1999, see Chapter 3). It can be seen segmented individual half-grabens, mini-basins and evolved graben basinward. The Figure 4.23b is a thickness map with the main depocentres and a projection of the proposed strain ellipsoid superimposed. The Figure 4.23c shows a proposed strain ellipsoid with main strain and deformations in an oblique extensional rifting regime.

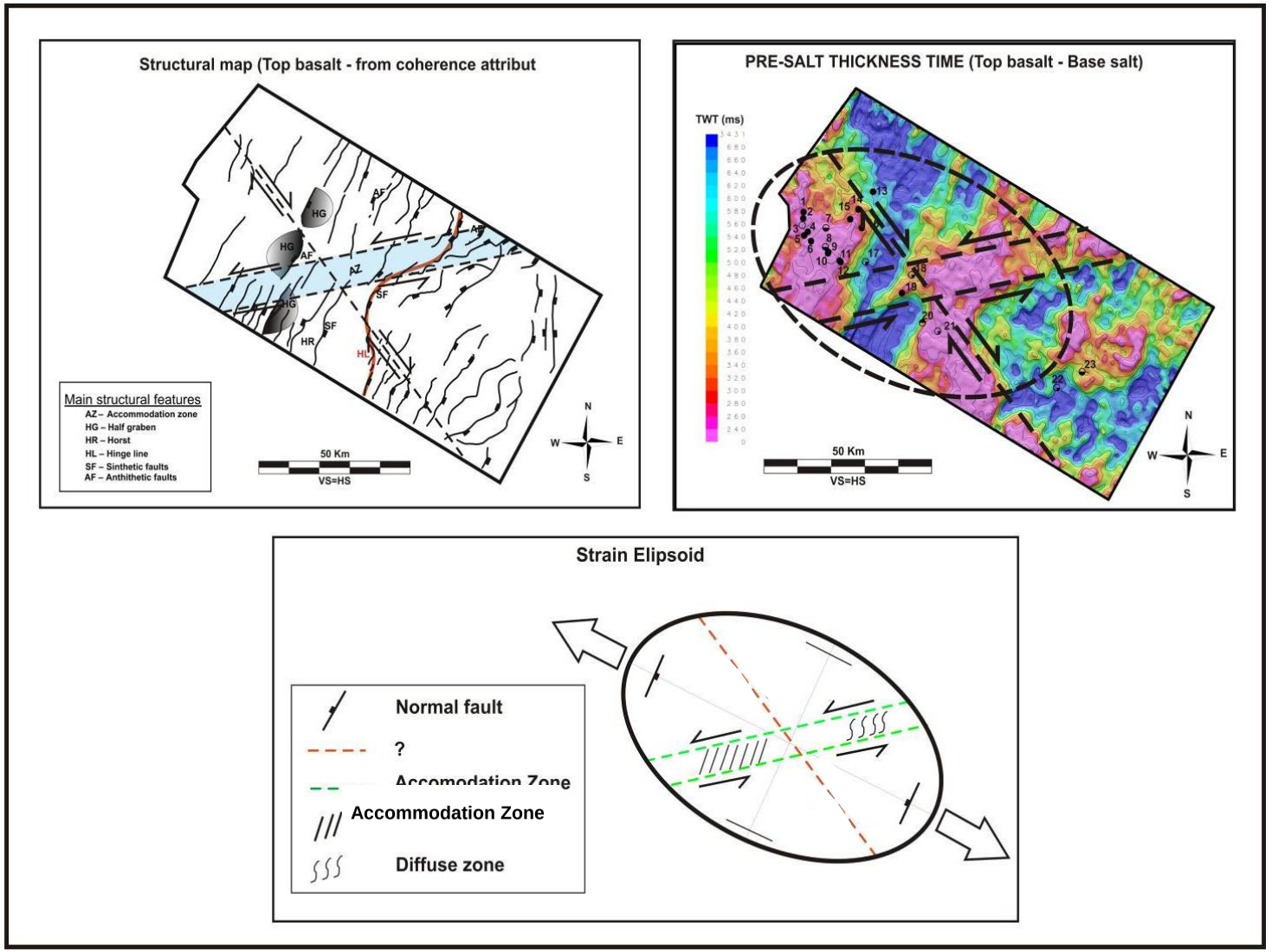

Figure 4.23 - Structural analysis of the study area: a) structural map with the main structural features. b) pre-salt thickness map (in time) shows the main depocentres (dark blue) and the main highs (pale red) and c) an attempt to summarize the rift kinematics in a strain ellipsoid.

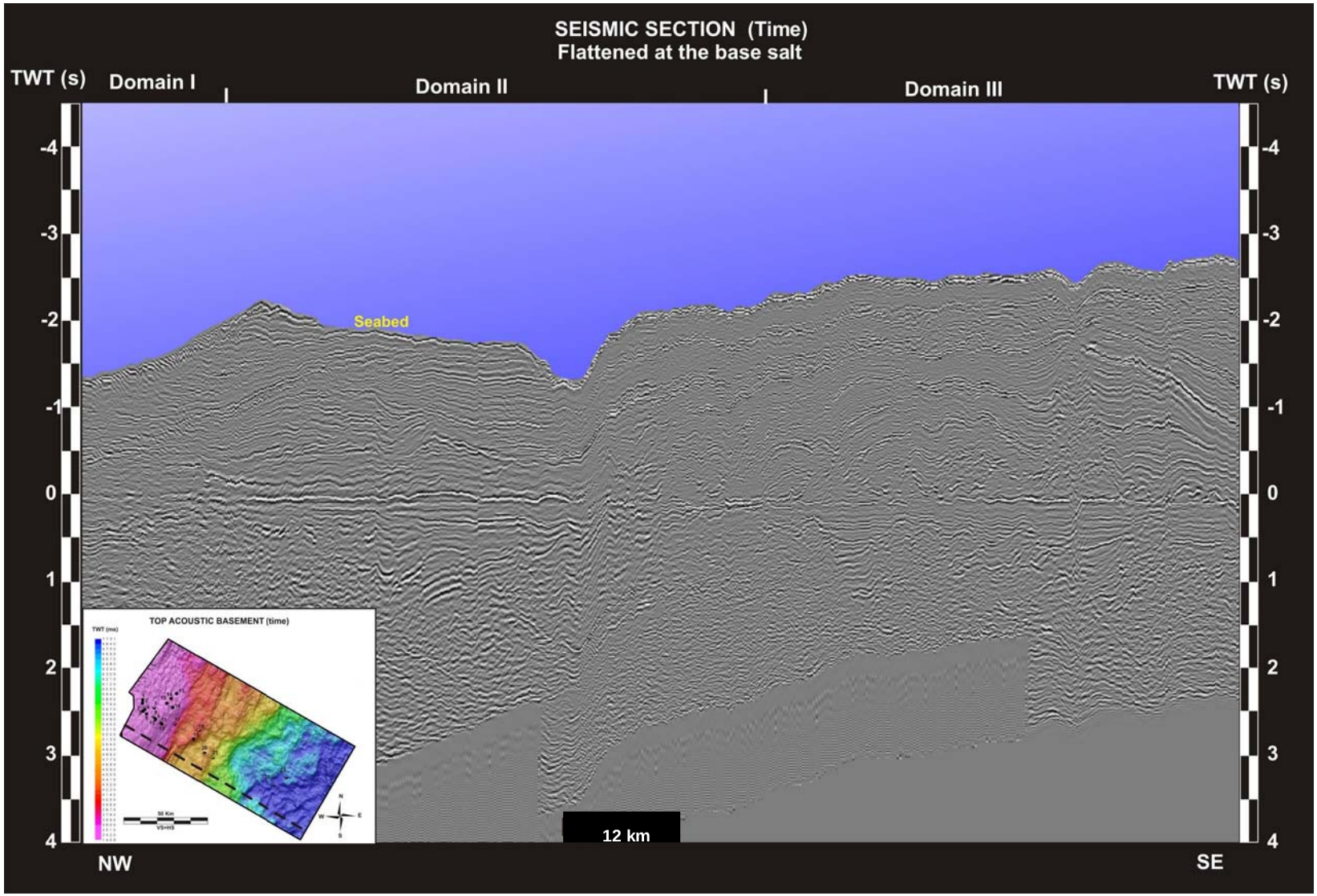

Figure 4.24 - Seismic line flattened on the base salt uninterpreted (in time)

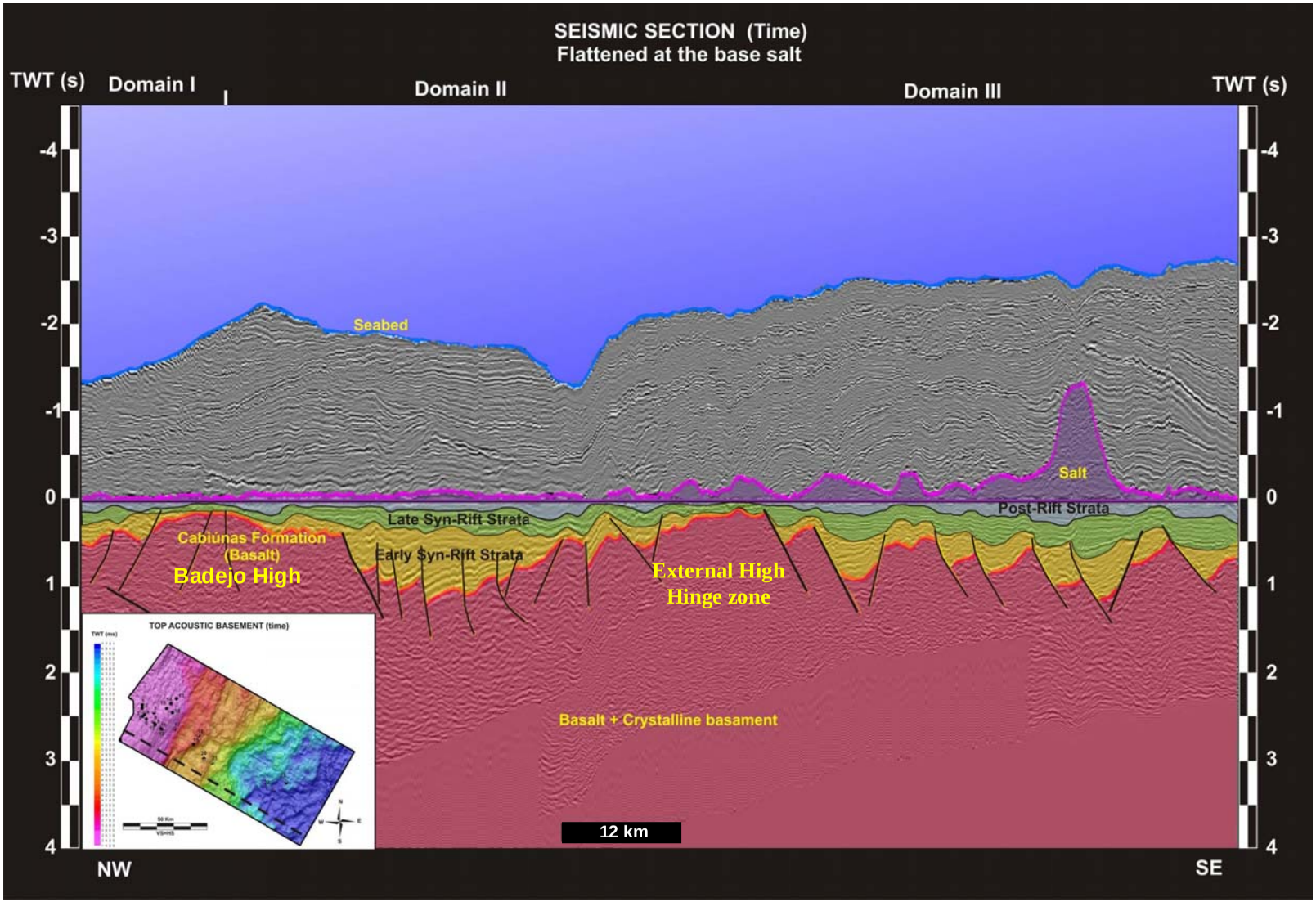

Figure 4.25 Seismic line flattened on the base salt interpreted (in time).

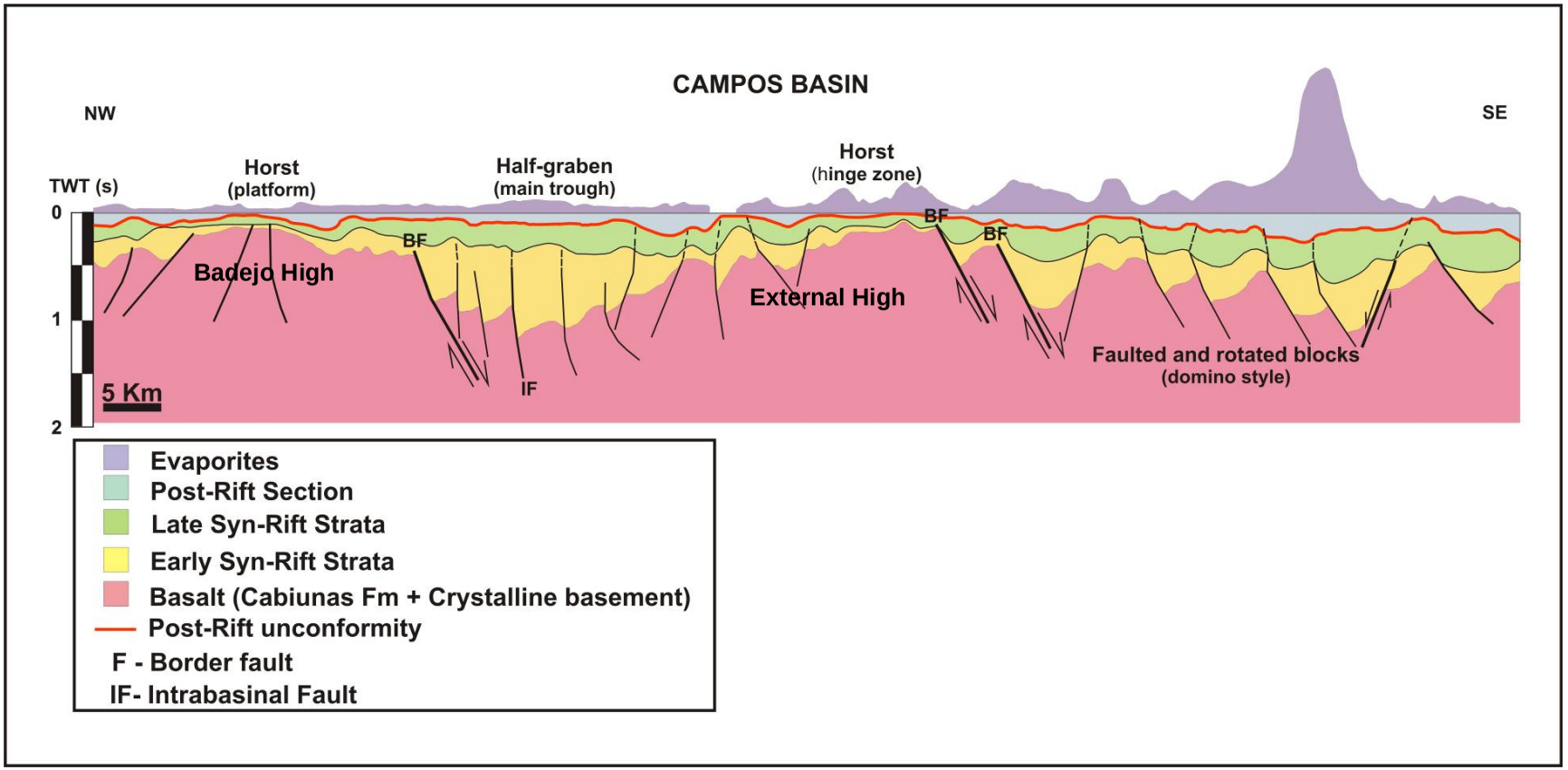

Figure 4.26 Cartoon showing the pattern of structural elements in the study area interpreted from the flattened seismic line of the Figure 4.24 and 4.25.

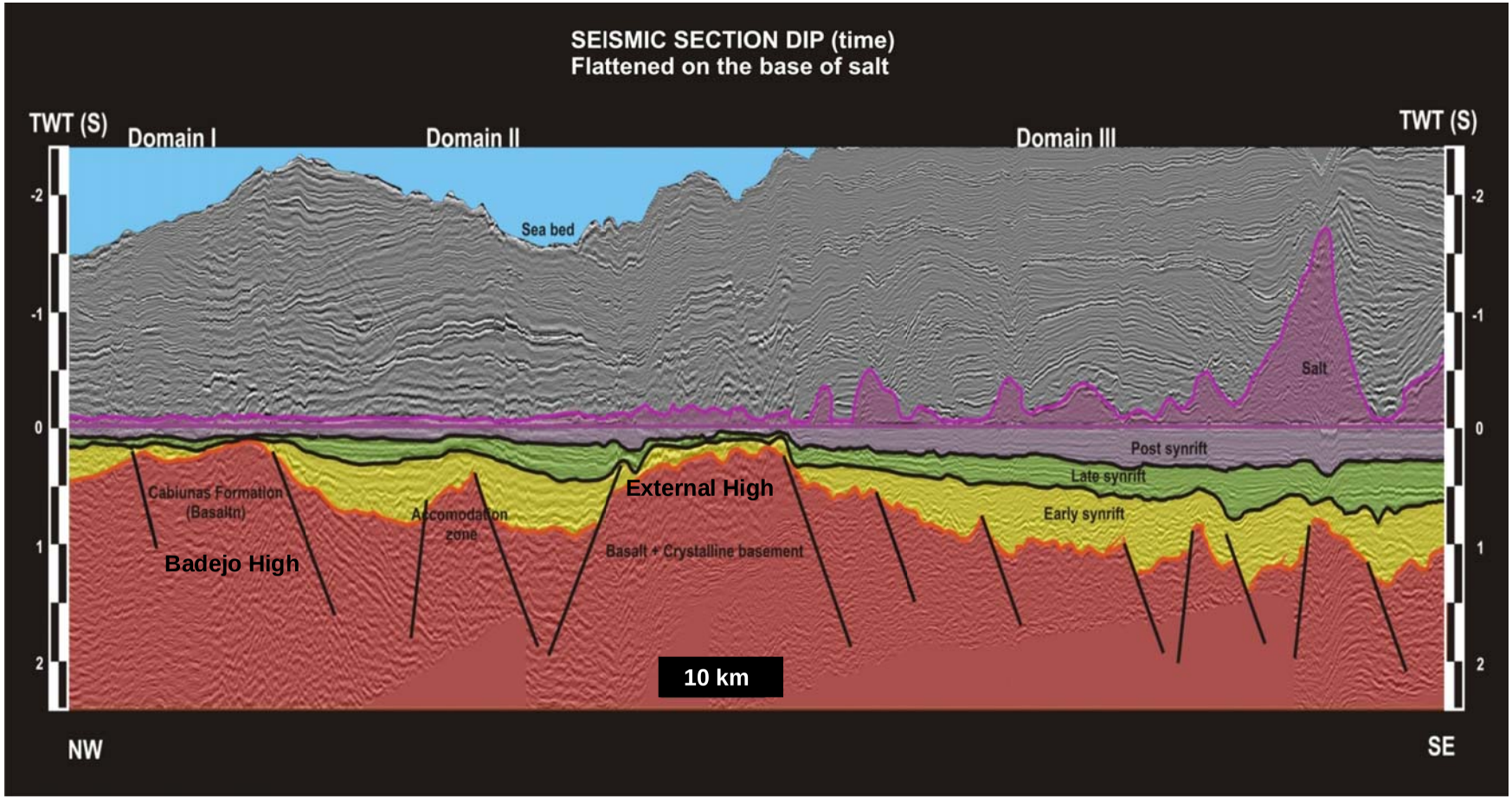

Figure 4.27 Seismic line flattened on the base salt interpreted (in time).

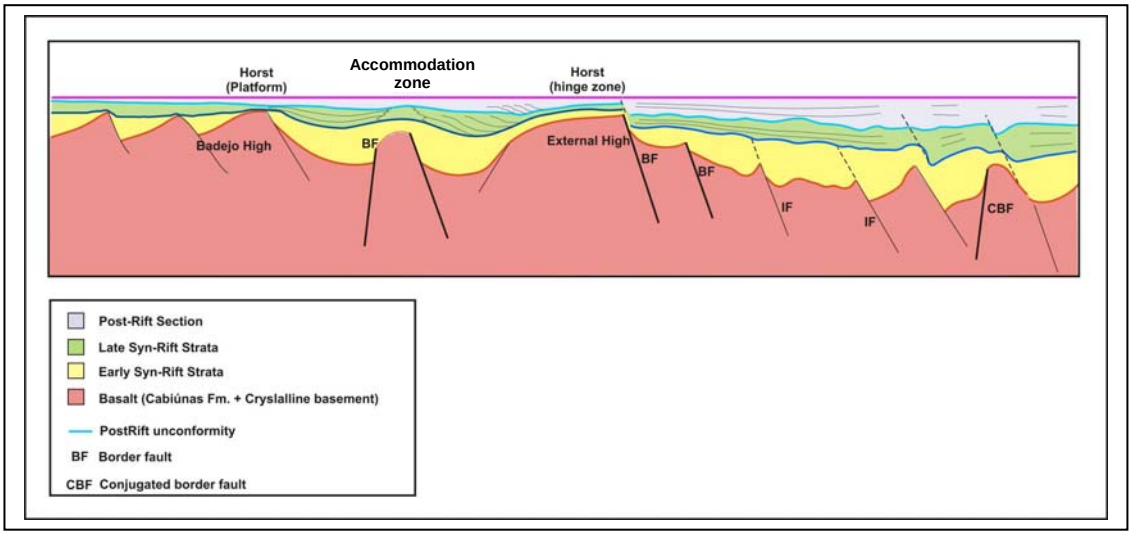

Figure 4.28 Cartoon showing the three tectonic domains and geometric patterns interpreted from the flattened seismic line of the Figure 4.27.

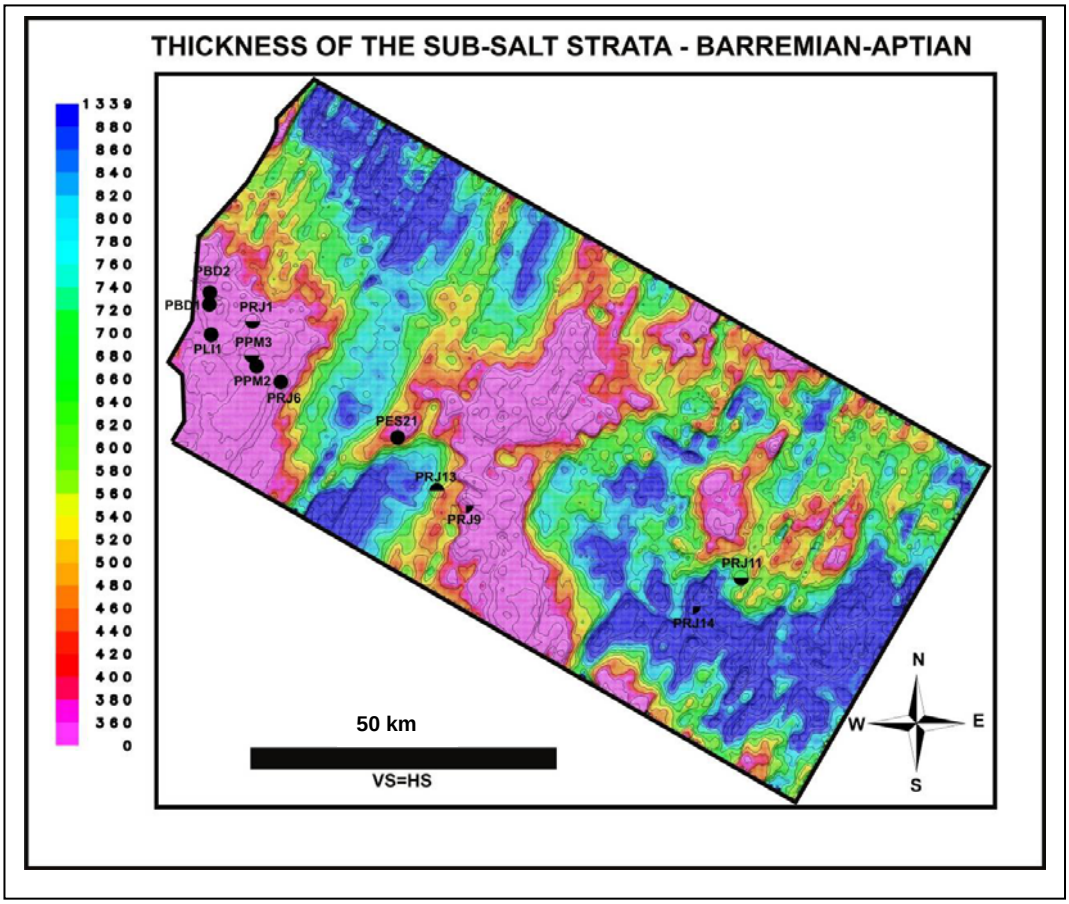

Figure 4.29 Map of thickness (in TWTT, milliseconds) of total pre-salt section, based on 3D seismic in time.

4.4.1.4 Rift evolution

Time Thickness maps

The time thickness maps of the pre-salt strata, Figures 4.30 to 4.32, displays complex geometries, resulted of the basement topography inheritance and the rift evolution (Figure 4.23). The three maps show similar geometrical configuration, with individual asymmetric depocentres, half-graben and symmetrical graben, controlled by synthetic and antithetic border faults, and zones of thin strata that match exactly with the previous positive structures such as Badejo High, External High and relicts of the horst basinward. Some half-graben lay in an elongated strip NE-SW with development of depocentres separated by very pronounced relay ramps or transfer zones. Figures 4.25 to 4.27 show differences in the structural style and geometry through the entire section, which were individualized into three tectonic domains (DI, DII and DIII), each one with different rift evolution, indubitably. The map of total time thickness of the pre-salt (Figure 4.29) shows a thicker pre-salt strata basinward, where, according this interpretation, it had greater subsidence rate and a more evolved rifting.

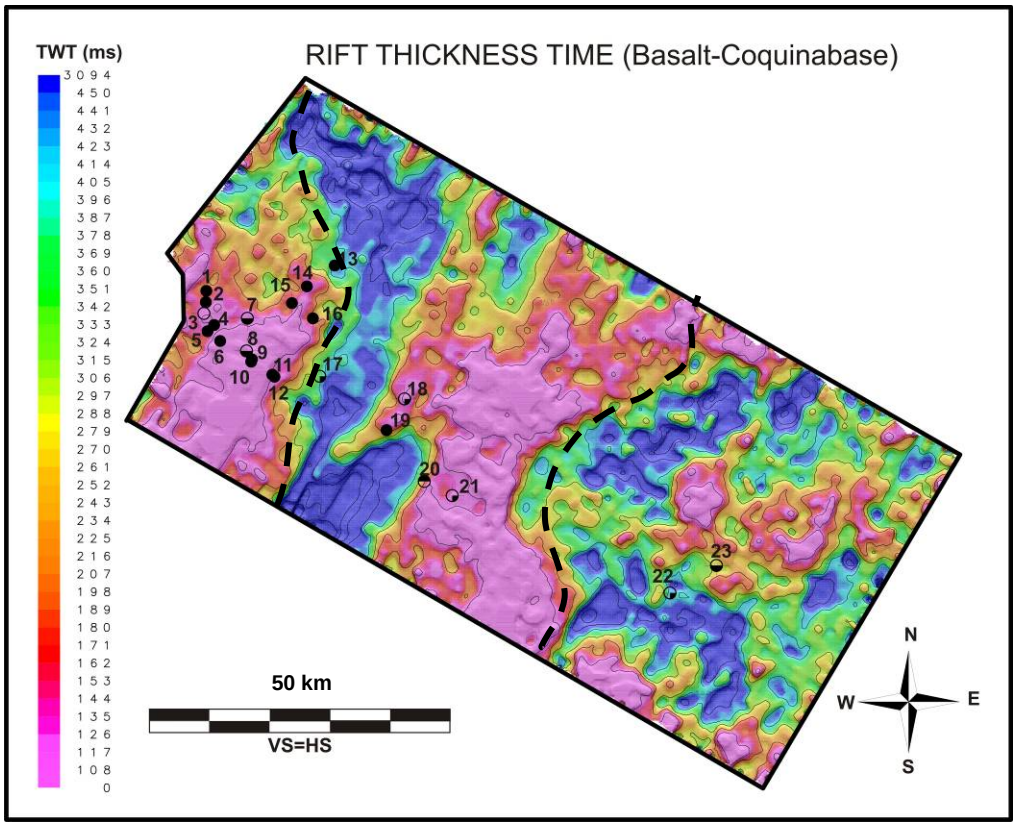

Figure 4.30 Map of thickness of early syn-rift succession, based on 3D seismic in time.

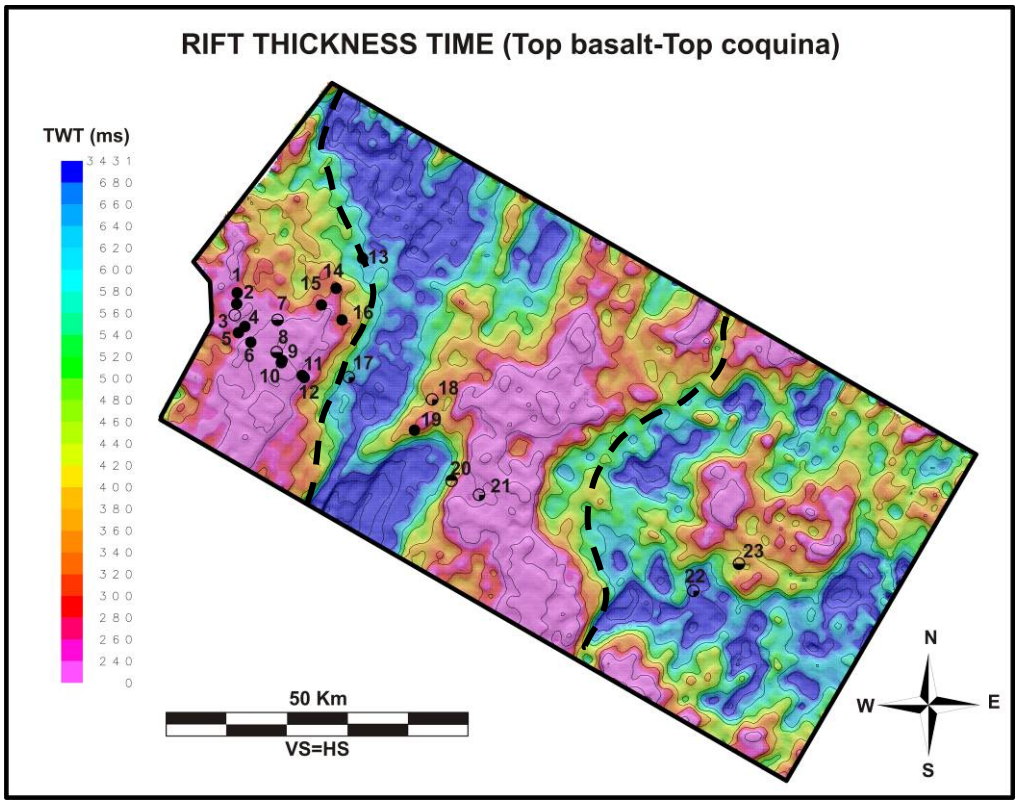

Figure 4.31 Map of thickness of early + late syn-rift succession, based on 3D seismic in time.

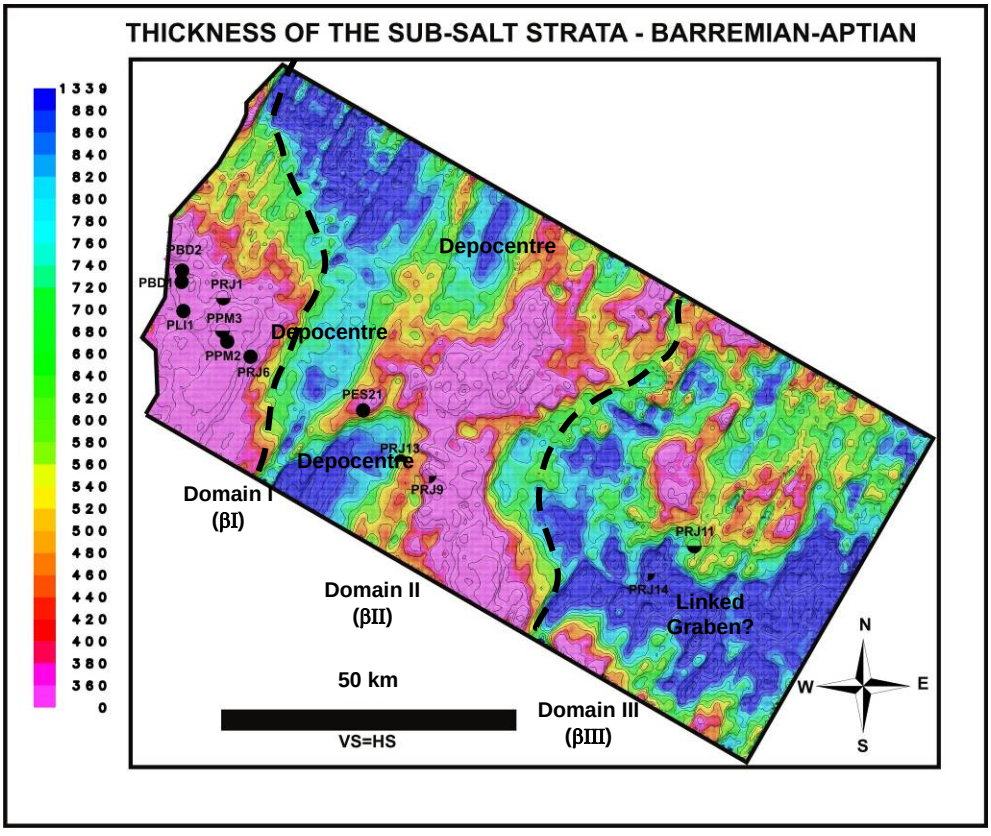

Figure 4.32 Map of thickness of total pre-salt section, based on 3D seismic in time.

4.4.1.5 Summary

The structural element arrangements interpreted in the study area define an extensional rifting system, *sensu* of Rosendahl *et al*. 1986. Also, the segmented and curved fault segments and the border of the basin (NNE-SSW) oblique to the rift faults directions (NE-SW) are strong evidence for oblique extensional rifting system (e.g. Mckenzie, 1978). The rift system is formed by individual half-grabens, grabens and horsts. Basinward, in the SE of the area, the individual half-grabens seems to have linked due to the advanced evolutionary stage of the rift, where they become more symmetric, forming a graben, with conjugated border faults (Davison, 1999).

After infilling the early syn-rift accommodation with terrigenous sediments, due to intense tectonic activity (yellow colour in the Figures 4.25 to 4.28), by the late syn-rift stage tectonic movements appear to have reduced, as strong topographic contrasts seen in the acoustic basement maps and even in seismic section (Figures 4.11 and 4.12), are replaced by a smooth and gentle topography, as seen in the base and top coquina maps (Figures 4.13 and 4.14). A post -rift uplift followed by a regional unconformity of Aptian age, normally called the "break up unconformity" (Guardado *et al*. 2000), culminates with the flattening of the basin and the thermal subsidence and sag basin commencement (Figures 4.25 to 4.28).

The architectural differences observed in the map of the acoustic basement, may be indicative of differential crustal stretching factors or due to tectonic overprinting of different evolutionary stages of the rifting. In this case, each zone certainly would have a different rate of subsidence, accommodation, and consequently distinct history and patterns of rifting infilling. The three specific tectonic domains defined in this work, based on structural styles, DI, DII and DIII, suggest a bigger stretch factor and consequently a greater subsidence rate in the DIII domain, basinward. Therefore, in deep basin is expected to have thicker strata, as we can see on the maps (Figure 4.29) and sections (Figures 4.25 and 4.26). Additionally the rifting is reactivated eastward, adding the accommodation basinward. This interpretation is supported by the fact that the rifting is still occurring in DIII sag succession (cf. Karner & Gamboa, 2007). Extensional long live faulting within the pre-salt succession occurs up to the base salt in DIII.

Significant thickness variations in late syn-rift Barremian succession, when carbonate rocks, mainly coquinas, were deposited (Figures 4.28 and 4.29), can be due to the differential rate of subsidence within the basin and also the reactivation of the early syn-rift normal faults.

The post-rift sequence is marked with smooth palaeotopography with minor changes in thickness, probably due to flattening of the basin infilling after erosion associated with the break up unconformity event. Some thicker strata could be a result of local inheriting topography,

reactivation of syn-rift normal faults or even space creation due to differential compaction (Figure 4.25 to 4.28).

4.4.2. Gravity data analysis

The outlined rectangle in Figure 4.33 delineates the area of this study, which evidenciate three tectonic domains: Badejo High (BH) and the external high (IZ), hinged zone. Also indicates the main low (LW) in the rift system, along the rift axis of NE-SW direction. The positive gravity anomaly above 30 mGal, red in the map, highlights the Badejo High (BH), Domain I in this work. The anomaly from -30 to 30 mGal, red up to light blue on the map, highlights an intermediate tectonic zone (IZ) and the external high, Domain II. Finally, the negative anomaly, below -30 mGal, highlights the main depocenters in the study area, Domain III (LW). These differential anomalies and further analysis of the structural styles from the seismic interpretation are undeniable evidences for the individualization of three tectonic domains described in Figure 4.33. The wells 1, 20 and 23 are representative for each domain, and the transfer zone NW-SE (TZ), regional transfer zone, has similar trend shown in the structural analysis of the Figure 4.27. These three different gravity anomalies domains denote three different responses to the upper crust stretching and certainly three differentiated rift evolution level (Domains I, II and III).

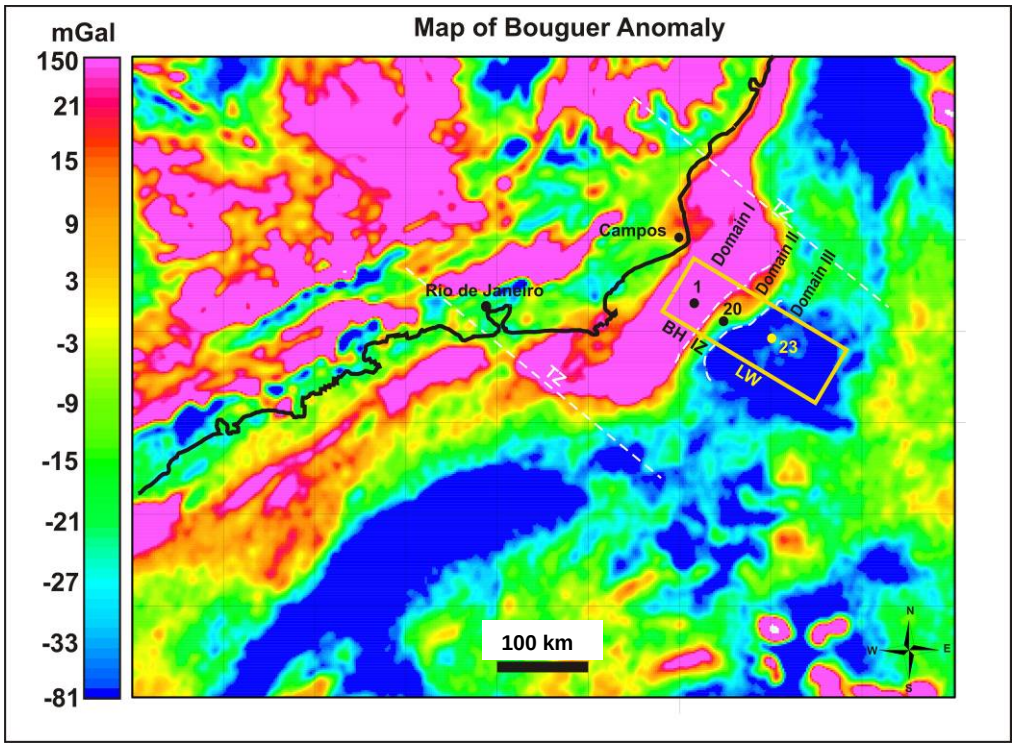

Figure 4.33 Map of satellite gravity Bouguer anomalies, Campos and Santos basins. The colour bar shows residual anomaly values in mGal.

4.5. Discussion (Structural and tectonic model)

The complexity of the tectonic evolution within a continental rift system and palaeogeography formed in response to the extensional tectonic forces, are not well understood within the context of formation of non-marine carbonate platforms in rift environments, especially in more distal zones within the rift basin. Therefore it is necessary to integrate studies of tectonics and sedimentation in the process of continental rift infilling. Most of the workers give a generic approach on this matter and focused on clastic and proximal deposits (Chang *et al.* 1992, among others). This study however aims to show the influence of tectonics on geometric arrangement and distribution of carbonate platform facies in the Aptian and Barremian in the southern part of the Campos Basin.

The results indicate that a 3D tectonic and structural model could be erected using 3D reflection seismic and well data. This tectonic and structural framework is used herein to aid understanding of the tectonostratigraphic evolution of the late syn-rift to post-rift pre-salt strata of the southern of Campos Basin (discussion in Chapters 9 and 10).

This chapter has revealed geometrical and structural features of extensional tectonics with oblique deformation in relation to the basin boundaries and also inherited structures from the crystalline basement. Such NNE-SSW structures are normally parallel to the margin of the basin, in short en-echelon fault segments. Intrabasinal structures however are, in general, perpendicular to the maximum direction of the extensional rifting (NW-SE), parallel to the main axis of the rift (NE-SW). According to McClay & White (1995), all characteristics described above are produced by oblique rifting and typical of Type 3 rift basin of Withjack & Olsen (2002). Cobbold *et al*. (2001) attributed the obliquely rifted margin and reactivation of basement structures in the Campos Basin, to the combined effects of far-field stress and a hot-spot.

As a result of oblique rifting, a rift basin with a polygonal geometric pattern, with half-grabens, horsts and evolved graben was created. The present chapter establishes the tectonic setting for the study area where the deposition took place during Barremian and Aptian time.

More complex structures such as transfer zones or areas of accommodation and fault and rotated blocks, also identified in the study area, are the product of the rotation and transfer of extensional movements during the evolutionary phases of the rift, according to Rosendahl *et al.* (1986).

From the structural map of the acoustic basement, it can be observed that the individual half-grabens in the proximal area are more asymmetrical, with straight line border faults. Basinward, the geometry of these depressions tend to be more symmetrical, forming graben as a product of several half-graben linkage, which exhibit curved line conjugated border faults.

Three tectonic domains - DI, DII and DIII - identified in the 3D seismic interpretation and analysis of the Bouguer anomaly maps, denotes three zones of particular crustal stretch factor: $\beta 1=1.24$, $\beta 2=1.4$ and $\beta 3=1.59$ ($\beta_1<\beta 2<\beta 3?$). Consequently, each domain has a specific subsidence rate and evolutionary history, resulting in a typical geometry.

Differentiated development of the rift with lateral variations in crustal characteristics may be interpreted for this fact. In the nearshore area, the crustal stretching factors have been shown to be smaller (Chang *et al.* 1992) and basinward areas the degree of crustal stretching would have higher values. This can be driven by a faster cooling of the mantle and basaltic ocean crust after the break up of the continental rift. Such a hypothesis is supported by the observations of Chang *et al.* (1992), which show that the extension on the surface and crustal thinning in the area seem to be compatible. By the analysis of deep seismic data, Manatschal (2010) and Magnavita *et al.* (2010), also interpret lateral stretching differentiation of the crust for the South Atlantic passive margin basins. They state a multiphase rifting with lateral deformation of the crust into stretched crust, thinned crust, hyper stretched crust and exhumed mantle.

Another plausible interpretation is a difference in the degree of evolution of rifted area. In this sense the rift in the DIII domain would have a more advanced evolutionary stage, and a large graben would be the result of the amalgamation of various asymmetric half-grabens during the evolution of the extensional rift cf.

Rosendahl, 1987. Davison (1999) postulated that in Hauterivian times in the Campos Basin, several individual rift basins opened simultaneously and became subsequently linked as the rifting process evolved.

Continuing the development of the rifting process, a post-rift unconformity between the Barremian and Aptian stages, marked a major change in basin configuration. A sag basin evolved in response to the thermal subsidence. Consequently the geometry and stratigraphic content changed significantly from the previous tectonic phase. The syn-rift normal faults are mostly truncated by the post-rift regional unconformity (break-up?), predominantly in domain DI. Moreover, strata tend to be more tabular with minor differences in thickness during this phase. Lateral variations in thickness are probably due to an inherited palaeogeographic configuration from the previous tectonic phase, or reactivation of some syn-rift faults, or even differential compaction, which may have generated accommodation.

However, in domains DII and DIII, the syn-rift faults cross through the sag succession up to base salt. Long lived faults allowed the rifting reactivation eastward, where the high subsidence rate adding to the continued rifting show thicker strata of pre-salt sag succession. In this sense it seems to have the rift structures superimposed on the thermal subsidence. Karner & Gamboa (2007), studying this episode in the Santos Basin, consider the syn-rift phase up to base salt, late Aptian.

Some authors (Wernicke, 1985; Allen & Allen, 1990; Coward & Ries, 1986; among others) consider an early phase of thermal subsidence due to cooling of the lithospheric mantle, with formation of a sag basin and subsequent oceanic crust in the Aptian age. This change in tectonic style, from late syn-rift to post-rift, produced significant palaeoenvironmental and palaeogeographic changes, which may be characterized in the geometry, lithotypes and fossil content. Onlaps were observed in this post-rift phase. They are interpreted together with the well data as the first marine incursions.

Published works have considered the rift succession as a whole; however, in this study the aim was not only to discriminate deposited carbonate geometries but also the different depositional controls on sites of asymmetric and symmetrical rifting.

There are number of good papers based on seismic interpretation, outcrop studies and physical modelling in the laboratory. Rosendahl (1987), Rosendahl *et al*. (1986), based on seismic data interpretation, outlined the morphology and structures styles in the extensional continental rifting of the Tanganyika Lake. Bosence (1998) described the stratigraphic response to different models of rifting. Bosworth *et al.* (1998) based on outcrop of Gulf of Suez, studied the tectonic control on sedimentation during rifting process. McClay *et al.* (2002) and McClay *et al.* (2005) produced in the laboratory the structural styles in the oblique rifting system. A similar model of oblique rifting was produced by Withjack & Jamison (1986), studying the Gulf of California and Gulf of Aden.

The major contribution of this present chapter is a new and original tectonic, structural evolutionary model in the rift system of Barremian - Aptian age in the southern part of the Campos Basin. This model, however, answers one of the research questions:

What are the syn-sedimentary tectonic controls on the depositional geometries and facies distribution of the carbonate rocks from Barremian-Aptian of the Campos Basin?

The answer is: An extensional oblique rifting system, forming three different tectonic control domains with specific subsidence rate; each one with characteristic geometry and sedimentary arrangement.

Further studies of rift kinematics and stress fields are recommended, leading to a deep understanding of rift evolution of rift. Also, further investigation of the system of fractures (both syn-depositional and post-depositional) is needed for a better understanding of the quality of fractured carbonate reservoirs.

4.6. Conclusions

Seismic interpretation was used to generate a 3D structural and tectonic model. This model is used for the understanding of the continental rifting evolution, the palaeogeography and palaeoenvironment and as a framework for the generation of a 3D facies model within the pre-salt rift environment.

As a result of the seismic data interpretation and analysis of the maps, the rifting system was defined as extensional oblique and the overall tectonic regime as syn-rift for the Barremian sequence and post-rift for the Aptian.

Major and minor structural elements were identified. Major elements are graben, half-graben, horsts and accommodation zones. Also, faulted and rotated blocks (domino style), and structural elements such as border faults and hinge zones were indentified. The geometries observed were syn-rift depocentre and accommodation zones. Transfer zones or accommodation areas divide half-grabens with faults dipping in opposite direction. The proximal individual rifts are more asymmetric, tending to the symmetry basinward, due to evolutionary stage of the rifting process.

The base of post-rift succession is strongly marked by a regional unconformity with subsequent thermal subsidence and formation of an Aptian sag basin. However, basinward the long-lived syn-rift faults are superimposed on sag succession.

Three tectonic domains were defined: DI, DII and DIII, bounded by a promontory in the eastern border of the Badejo High and a hinge zone in the eastern border of External High. Each domain has a specific stretching factor and subsidence rate and developed a distinct geometry and evolutionary history during the rifting process. These domains are:

- Domain I developed smaller half-graben with straight normal border faults.
- Domain II developed a polygonal arrangement of half-graben which border faults having synthetic and antithetic behaviour.
- Domain III, the most evolved area, basinward, a large graben is a product of several half-graben linkage.

CHAPTER 5 – CORE BASED SEDIMENTOLOGY

5.1 Introduction

The study of the sedimentological and stratigraphic framework of carbonate rocks in non-marine rift environments is challenging, due to their complexity and the scarcity of publications in this field compared to marine carbonates. The complexity results from the great spatial and temporal variation of facies, dependant upon which results from the different factors that control these sediments, such as hydrological conditions of the lake, open or closed (Talbot & Allen, 1978), the fluctuations of lake level due to climatic changes and tectonism, the rate and mode of carbonate production, and supply of sediment to the basin (Tucker & Wright, 1990). This chapter aims to address the issue through examination of cores and petrographic slides in order to erect a classification and description of sedimentary facies for integration and interpretation of data from the seven cored wells in the study area. The aim of this work is the production of facies models for the Coqueiros Fm of the early Barremian / Aptian and late Aptian Macabu Fm. These non-marine dominantly carbonate rocks comprise part of the Lagoa Feia Group that accumulated in the syn-rift of the Campos Basin pre-salt succession (see Chapter 2).

5.2 Facies classification and description

Facies is the fundamental unit for sedimentological studies. The term was firstly introduced by Gressly in 1838 to describe the lithological and palaeontological aspects of a sedimentary rock (Middleton, 1973; Tucker & Wright, 1990; Walker & James, 1992). Since then, it has been used, not only for descriptive purpose but also for genetic characteristics and environmental interpretations (Middleton, 1978; Walker, 1992).

Due to the diversity of facies within the continental lake environments of the Lagoa Feia Group carbonates, three classification schemes were used in order to satisfy the needs and goals of this work. None of these schemes have been previously used to describe these non-marine carbonates of the Early Cretaceous of the southwest Atlantic. The first scheme is based on the classification of Dunham (1962) and modified by Embry & Klovan (1971) (Figure 5.1), and further subdivided by the main components of the rocks (Figure 5.2). This classification is well suited both to the allochthonous coarse grained (mainly > 2 mm) shelly carbonates of the coquinas, the mixed clastic /

carbonate sediments and for the autochthonous, bioconstructed carbonates of the microbialites in the Macabu Fm. The clastic sediment facies are based on their Wentworth (1922) textural classes (Fig. 5.2). The facies descriptions below are followed by a discussion of their likely depositional processes, palaeoenvironments and depositional geometries. The facies, as the fundamental elements, are then grouped into facies associations in order to understand facies relations and their environmental significance (*sensu* Collinson, 1969; Walker, 1992).

The second classification scheme, is a taphonomic classification (Chapter 6, Figure 6.6) which is needed to understand the different environments of deposition of the large range of fabrics seen in the molluscan floatstones and rudstones (or coquinas) in the Coqueiros Fm. The third scheme is based on FMI data with some sidewall core thin-sections rather than on core material. This FMI-based facies classification is presented separately in Chapter 7.

5.2.1. - Carbonate Facies

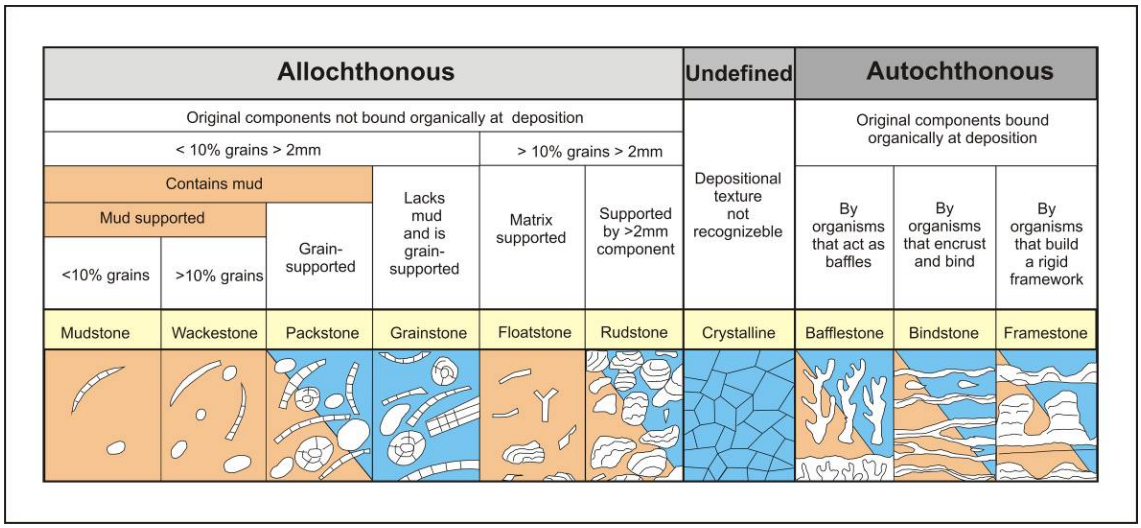

Figure 5.1 - Textural classification of limestone after Dunham (1962) and Embry & Klovan (1971).

Many lithologies have a mixture of carbonate and siliciclastic grains and these are classified by the major grain types so that any sediment with more than 50% calcareous grains is classed as a limestone and more than 50% siliciclastic grains as a terrigenous rock. Intermediate or mixed carbonate / siliciclastic classes have not been used.

Carbonate facies

Textural name Embry & Klovan (1971)		Components	Grain Size	Purity	Structure	Key
Allochthonous	Mudstone					MD
	Wackestone					WK
	Packstone	Bivalves Gastropods Ostracods Peloids				P-b,g,o,p
	Grainstone		fine (f) medium(m) coarse (c)		graded (g) laminated (l) stratified (s)	Gf - b,g,o,p
						Gm -b,g,o,p
						Gc -b,g,o,p
	Floatstone	Bivalves Gastropods Oncoids				F-b,g,o
	Rudstone			muddy (m)	graded (g) laminated (l) stratified (s)	Rm -b,g,o-
				terrigenous (t)		Rt-b,g,o-
				clean (c)		Rc-b,g,o-
Autochthonous	Bafflestone	Microbial				BaM
	Bindstone					BiM
	Framestone					FM

Terrigenous facies

Textural name Wentworth	Grain size Wentworth	Purity	Structure	Key
Shale (SH)				SH
Siltstone (ST)				ST
Sandstone (S)	fine (f) very fine (vf)	argillaceous (a)	graded (g) laminated (l) x-stratified (s)	Sf-agls
	medium (m)			Sm-agls-
	coarse (c)			Sc-agls
Conglomerate (CG)		clast / grain supported		CG
Conglomerate (CM)		matrix supported		CM

Modified facies

Textural name	Key
Chert	CH
Slump	SL
Breccia, tectonic	BT
Breccia, karst /exposure surface	BK

Figure 5.2 – Classification scheme for the facies grouping.

Thus a scheme was set up to group the diversity of the rock characteristics, texture and composition, descriptively and interpretatively, in a summary form. This scheme was divided into three main groups: carbonate facies, terrigenous and modified facies (Figure 5.2). The carbonate facies were further subdivided by their components: grain type, grain size, purity and primary depositional structures.

The textural, compositional and petrographic facies descriptions of the logged cores are summarized in Figure 5.2. The individual core logs and integration with

wireline data from the wells are discussed in the Chapter 7 and presented in the Appendices A1 to A7.

Carbonate facies - Allochthonous

Mudstone (MD)

Description

These are muddy carbonate rocks (silt and clay sized). They contain less than 10 per cent skeletons grains (Dunham, 1962). They occur in the wells 1, 2, 6 and 9 (Figure 5.3), in decimetre beds (10 to 30 cm) and rarely up to 1.5 m in thickness. The mudstones are normally interbedded with packstone, wackestone, shale and rarely with microbial laminites (Figure 5.3). This facies is light grey, brownish grey, rarely greenish. Locally the mudstone is argillaceous and with some organic matter. Locally the facies is deformed, fractured, showing calcite, pyrite and some phosphate concretions, and also chert nodules. Microscopically the mudstone is microcrystalline with some scattered bioclasts of bivalves and ostracods. The mudstone may locally be recrystallized into microspar and calcite spar.

Figure 5.3 – Core slab Mudstone with a massive aspect, fractured, brecciated, peloidal with some broken, scattered bivalve shells. Interbedded with a thin microbial laminite (above scale bar) (well 6, core 2, box 07 – Appendix A3)

Interpretation

The origin of this facies is not well understood, but it may be product of abiotic precipitation or biotically induced precipitation it (Reid *et al.* 1990) or even abrasion of shelly material. The fragmented shell material cannot be identified and palaeoenvironment assessed. Marine biotas are lacking and the context suggests a non-marine setting. This facies is either deposited in deep subaqueous environment, below storm wave base, or, depending on the facies relations, in shallow sheltered lacustrine settings but always in calm and quiet waters (Flügel, 2004). Some peloidal sediments (peloidal packstones and wackestones) assume visually the mudstone texture after mechanical compaction. Also it may be formed as product of chemical precipitation.

Wackestone (WK)

Description

These are mud-supported carbonate rocks containing more than 10% of grains (Dunham, 1962), with a mixture of carbonate mud and skeletal grains with large variations and abundance of grain types (Appendices A1, A3, A6 and A7). The wackestones occur in the wells 1, 6, 9 and 12 with centimetre to metre- thick beds with a greyish cream, brownish green, to greenish colour. Normally the grains comprise bivalves, ostracods and rarely gastropod shells (of 0.5 to 1 mm in size), scattered in a muddy matrix (Figures 5.4a to 5.4d). Peloids also occur (Figure 5.4c) with the beds that have massive aspect, but may also be laminated and bioturbated. Bed contacts are sharp, locally erosive at the base, with gradational contact upward into coarser facies, inverse grading. Most commonly they are interbedded with rudstones. This facies is locally brecciated and partially silicified with silica nodules. The beds contain vertical fractures.

Interpretation

This facies may record deposits in 1) subaqueous zone, below storm wave base (SWB), or 2) in a shallower setting such as protected and calm water lagoon (Figures 5.4a and 5.4b). In this environment terrigenous sediment may be associated, as seen in the Figures 5.4a and 5.b. Wackestone is normally associated with transgressive systems tract, so it normally occur at the base of metre shallowing cycles (see Chapter 8). When

subaerial exposure is identified due to the base level fall, the beds exhibit an erosive upper surface.

Figure 5.4a Core slab Wackestone with massive and homogeneous aspect in upper part of the sample. Below, occur root marks (rm), erosional surface and oxidation features due to subaerial exposure (se). Stevensite and fragments of volcanic rock are also seen. Well 1 core 1 box 3 (Appendix A1).

Packstone (P-b,g,o,p)

Description

Grain supported, muddy carbonate rock (Dunham, 1962; Embry & Klovan, 1971). This facies were sampled in almost all the wells logged (wells 1, 2, 6, 7, 8, 9 and 12 – Appendices A1 to A7), occurring in beds. Individual beds vary from some centimetres up to one metre in thickness. When the packstone beds are stacked they reach 2.5 m in thickness (e.g. well 1 core 7 boxes 14 to 12). The packstone is generally associated with mudstones and siltstones (well 1 core 7 box 16, well 6 core 10 boxes 8 to 2), or locally interbedded with mudstones and rudstones with erosive contacts (wells 7 core 4 box 1). The clasts in the packstone may be composed of bivalves (P-b), gastropods (P-g), ostracods (P-o) or peloids (P-p) or a combination of these

components, as shown in the classification scheme (Figure 5.2) and logs (e.g. Appendices A1 to A7).

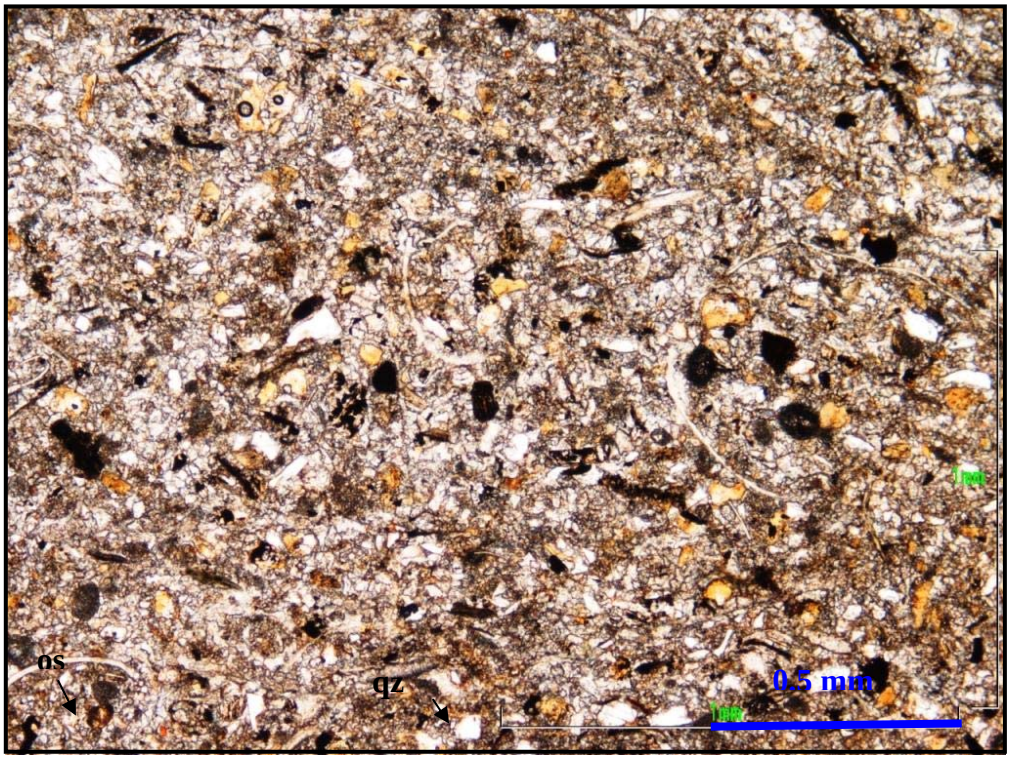

Figure 5.4b Photomicrograph of wackestone exhibiting the homogeneous texture, quartz (qz), ostracods (os).

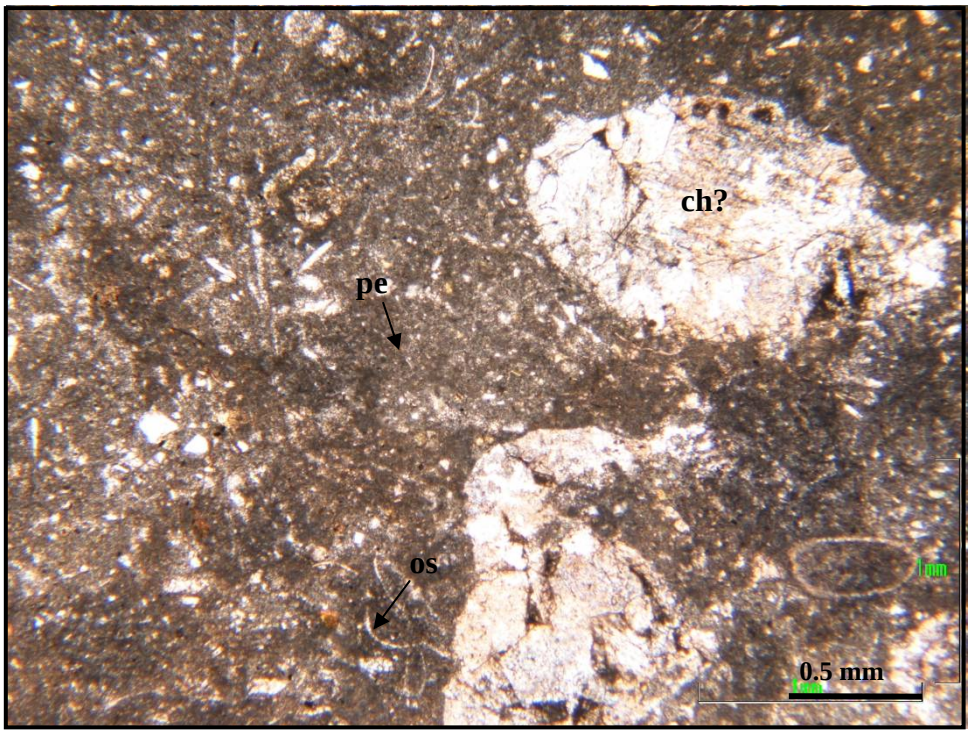

Figure 5.4c Photomicrograph of peloidal wackestone (pe), silty, sandy matrix, disarticulated shells of ostracods (os), and possible abrasively altered charophytes (ch)?

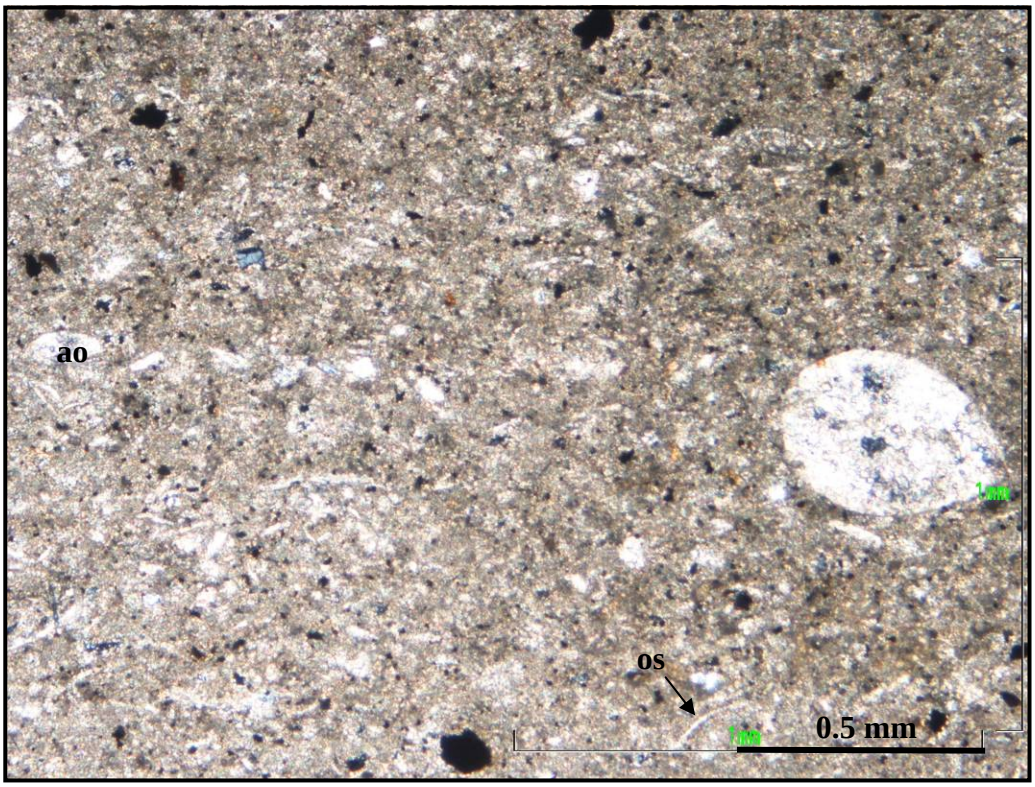

Figure 5.4d Photomicrograph of wackestone; ostracod-rich. Articulated (ao) and disarticulated (os) shells of ostracods.

The most commonly occurring lithology is a bivalve packstone with a muddy or silty matrix (P-b). It normally shows disarticulated and rarely articulated whole and broken shells within a muddy or silty matrix. Some are broken. The majority of bioclast shells are less than 2 mm in size. Some scattered shells may vary from 0.5 to 5 cm in size. In more argillaceous intervals this facies may occur moderately bioturbated. Cream, nut brown and greenish grey are the main colours. Locally (e.g. well 7 core 4 box 1) the facies contain “green minerals” (in hand specimen and thin section as well) and volcanic rocks fragments may be seen.

The packstone as a rule is poorly laminated but it may also occur with low-angle, cross-stratification, normally at the base of the bed. It commonly occurs with a sharp, erosive contact over wackestone and rudstones in shallowing-up trends (e.g. well 2 core 4 box 3, well 9 core 43 box 8). At the base of these beds the rare shells are commonly and other clasts may also occur. The amount and size of shells increase toward the top of the beds. This facies may occur with flame structures and arranged in fining-up.

Solution seams, stylolites and micro-fractures are common in this facies. Commonly the packstone matrix is neomorphosed into sparry calcite; locally it is

partially dolomitised and partially silicified. The porosity varies from no visual porosity, with microporosity in a muddy matrix up to extremely porous. Vuggy and mouldic porosities are seen where less matrix occurs and the shells are extremely broken. Three sub-varieties of packstone are also recognised as follows:

- The ostracod-rich packstone (P-o) is generally light cream colour (Figure 5.5). Its matrix is mica rich and locally occurs with stevensite.
- Peloidal packstone (P-p) also occurs, with variable contribution of disarticulated shells of bivalves of 2 mm to 1 cm size. The matrix comprises clay minerals and locally nodular features of authigenic minerals. The colour is normally greenish grey or light brown.
- Packstone (P-bgo) with bioclasts of bivalves, gastropods and ostracods. This facies has a sandy, silty, argillaceous matrix that is locally bioturbated. It also occurs interbedded with rudstones (see below). Millimetric to centimetric laminae of light cream or greyish green packstone also occurs. These laminae have very fine-grained to silt size matrix, are ostracod-rich and occur with some bivalve rudstones.

Interpretation

Packstone lithologies have various origins: mud infiltrating into previously deposited mud-free grainstones, prolific production of grains in calm to moderate water muddy settings, mixing of muddy and sandy sediments by burrowers, incomplete winnowing, partial leaching of mud or compaction and dewatering of original wackestone (Shinn & Robbin, 1983). Also the coarser particles may be carried to muddy sites by turbidite currents, washover, by waves or even storms, forming packstone textured sediment. The erosive basal contact, load and flame structures, and locally fining-up stacking pattern are evidence for the occurrence of turbidite deposits. At other sites, the erosive and bioturbated base, together with lag of coarse and disorganized sediments may be evidences for storm deposits, and the silty matrix rich associated to washover, lagoon deposits.

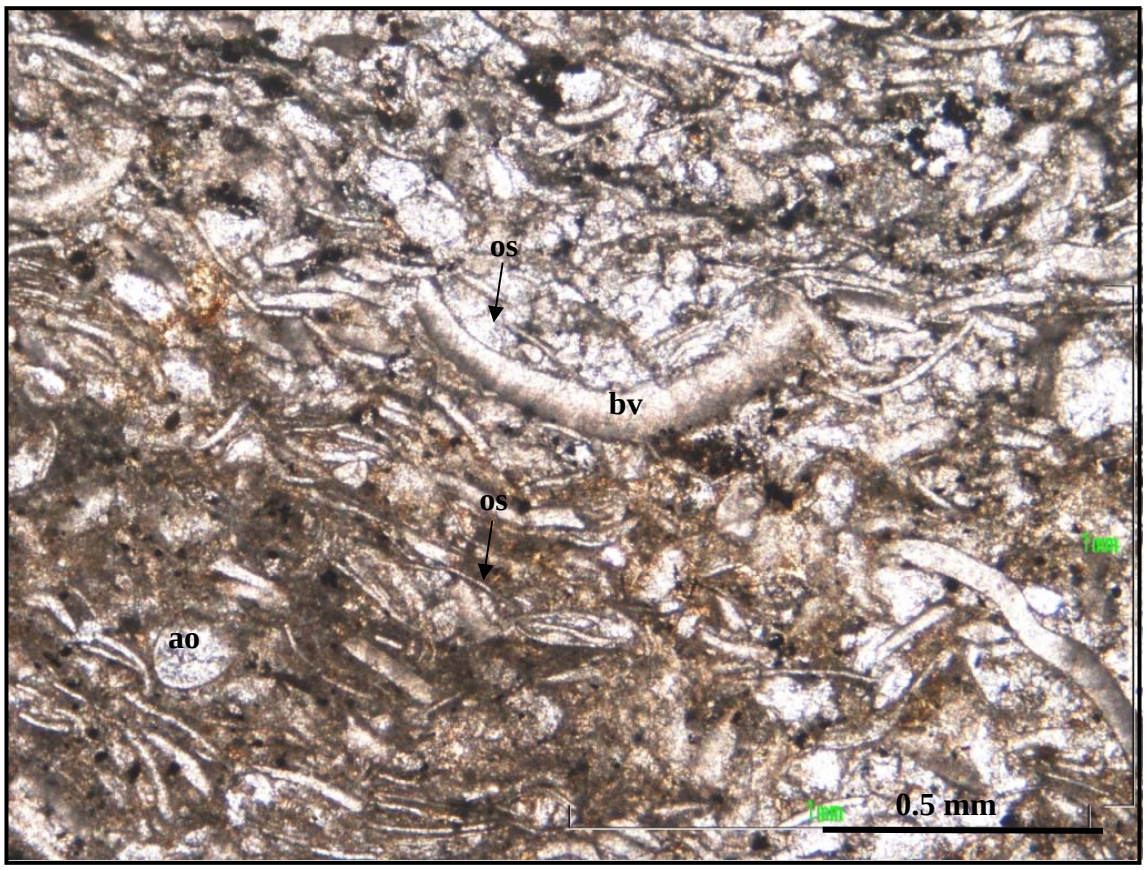

Figure 5.5 Photomicrograph - Packstone of disarticulated (os) and articulated (ao) ostracods and bivalves (bv) showing normal packing with muddy matrix also some recrystallized microspar (mc). Well 12 core 2 box 1 (Appendix A7).

Grainstones (G-b, g, o, p)

Description

Mud free, grain supported limestones. This facies occurs in thin isolated beds or thicker units of stacked up to 3 m thick (wells 1, 6, 7, 8, 9 and 12). Grainstones are normally associated with thinner (< 30 cm) beds of shale, or are interbedded with packstones and rudstones in amalgamated units greater than 1 m thick (well 6 core 3 boxes 6 to 3, well 7 core 4 boxes 6 and 5, Appendices A3 and A4).

The grainstones can be subdivided on the basis of their principle components such as bivalves (Gb), gastropods (Gg), ostracods (Go), peloids (Gp) or as mixtures (G-g,o,e,g). The grain sizes vary from fine, medium or coarse (f,m,c) and are used as indicators of the degree of hydraulic energy acting on the sediment (Folk, 1962).

Although the grainstones comprise a range of grains (bivalves, gastropods, ostracods, ooids and peloids), the commonest grains are bivalves (Figures 5.6a and 5.6b). These carbonate rocks are in general medium to coarse grained, greenish cream and with disarticulated and articulated shells. The shells may be whole or broken. The

genera *Trigonodus (A)* and *Composella* (E) can be identified. When fragmented and abraded, shells vary from 0.5 mm to 5 mm in size, but they can reach 1 cm in length. Green minerals and also some lithoclasts of volcanic rocks may occur (Figure 5.6b). According to the energy level of each depositional environment this facies may vary from moderately to well sorted, and normal to well packed. Cross stratification is quite common (well 9 core 44 box 2).

Neomorphism of shells into sparry calcite (Chapter 6) is considered the most common diagenetic process (Figures 5.6a and 5.6b). The shells appear to have been originally aragonite. Occasionally, they are dissolved and cemented by low-Mg calcite spar or replaced by silica. Interparticle pore space is invariably filled with calcite cement mosaic (Figures 5.6a and 5.6b). These facies are either porous or cemented by calcite (see Chapter 6). The most common porosity type is intergranular, primary porosity, but mouldic and vuggy porosities also occur, mainly at the top of the beds. Occasionally micro-fractures may be seen. Burial compaction is evidenced by dissolution seams and stylolites, particularly in the finer grained grainstones. Exposure surfaces on grainstones have chert, deformed beds, breccia, and reworked features.

The gastropod grainstones occur in well 6 core 3 box 4. They are normally coarse grained, porous, but also with some cement, associated with high energy facies. The ostracod grainstones are almost always fine grained, associated with lower energy facies such as shale and mudstone or wackestone. They may occur alongside broken and abraded bioclasts of bivalves.

Interpretation

Grainstones can accumulate in response to a number of processes; they may be current deposited, some product of winnowing and or mud bypass. They may also be biogenically produced and locally accumulating grains or the result of winnowing of previously deposited grainy and muddy sediment (Mazzullo & Birdwell 1989, Wright, 1990). Finally they may occur also in paludal, pedogenic carbonates environments (Flügel, 2004).

Grainstones are generally associated with high energy, mud-free environments, due to wave-induced or unidirectional currents. In a subaqueous setting this commonly occurs above Fairweather Wave Base (FWWB) where moderate to high energy conditions generate clean grain supported textures or, where mud is washed way by

wave or unidirectional currents such as foreshore settings in beaches or carbonate banks.

The grainstones in the Lagoa Feia Group, Coqueiros Formation, do not contain any marine grains. The bivalves *Camposella (E)* and *Trigonodus (A)* although endemic and extinct forms are interpreted to have lived in lagoonal environments (Hessel, 1992). The ostracods have not been identified in this project but have been interpreted by Silva-Telles (1992) to have lived in restricted fresh to brackish waters. Grainstone belts in subaqueous, lacustrine settings are reported from shoreface, subaqueous bars, delta front and washover fans (Flügel, 2004).

This facies is considered a good potential oil reservoir due to its high interparticle porosities (visual estimates of 6 to 10%) and possibility of additional secondary mouldic and vuggy porosities (10% to 12%) caused by dissolution of grains (Figures 5.6a and 5.6b).

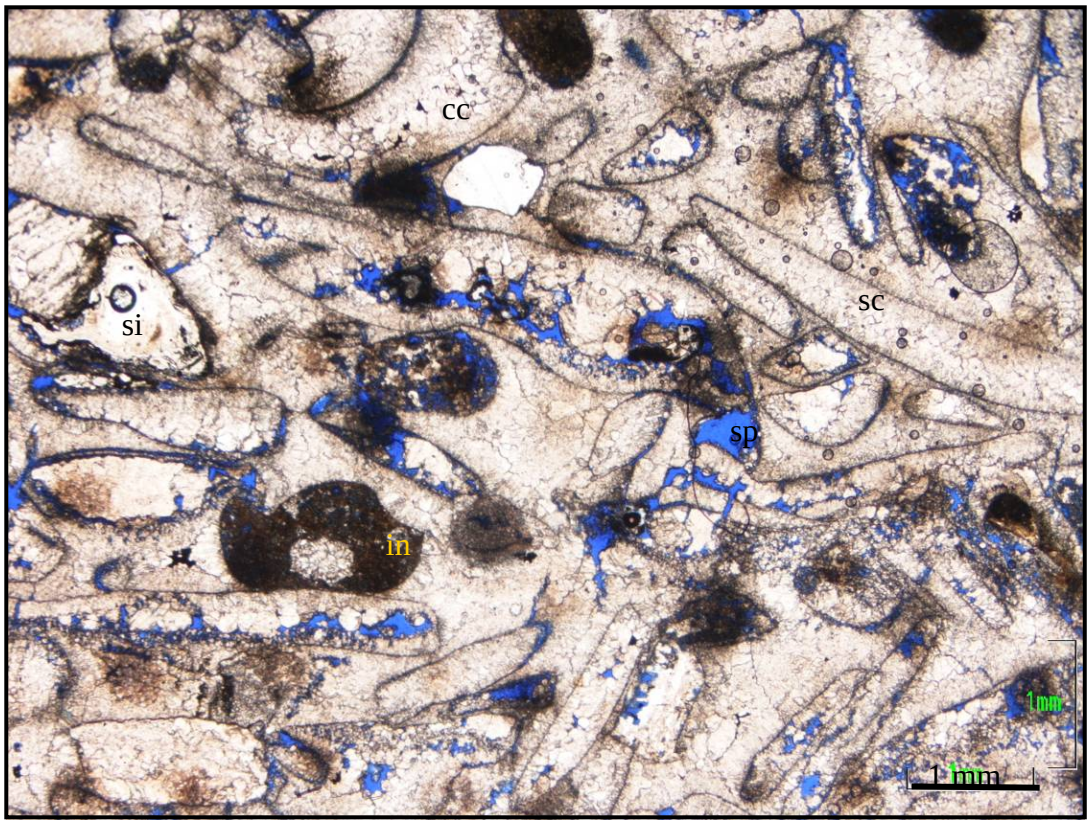

Figure 5.6a Photomicrograph - Grainstones of bivalves. Disarticulated shells of bivalve neomorphosed into spar calcite (sc). Some silicification (si) and also dissolution (sp), calcite cement (cc). Moderately to poorly sorted, normal packing subrounded grains, some intraclasts (in). Thin section with blue dyed resin.

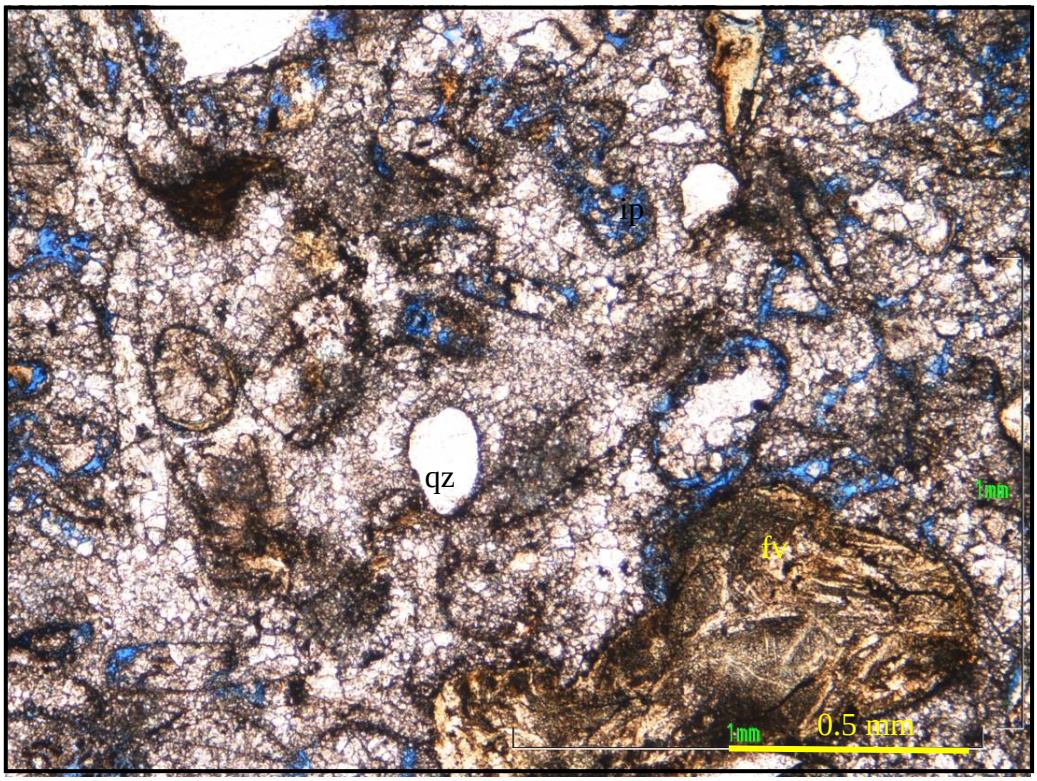

Figure 5.6b – Photomicrograph - Grainstones of rounded shells of bivalves. The grains are neomorphosed into microspar and spar calcite and the matrix recrystallized. Locally silicified. Some secondary porosities. Fragment of volcanic rock (fv). Late dissolution indicated by intercrystalline and intraparticle porosities (ip).

Floatstone (F-b, g, o)

Description

Floatstones in the Embry & Klovan (1971) scheme are matrix supported carbonate rocks with more than 10 per cent grains larger than 2 mm (Figure 5.2). These rocks are cream, with thin disarticulated shells of bivalves of up to 3 cm probably of the genera *Trigonodus (A)* and or *Camposella (E)* (Figures, 5.7a and 5.7b) and other bivalve shells up to 1 cm in size, which may be articulated or disarticulated. Locally this facies occurs with peloids of stevensite. These are floating within a silt to sand size matrix (Figure, 5.7b). Gastropods and rarely oncoids occur as grains. Floatstones occur in the wells 1 and 8, in beds that are no more than 1 m thick. Normally this facies is associated with clean and argillaceous rudstones and also siltstone. Commonly the beds show an up-section increase in shells and are overlain by clean and muddy rudstones (e.g. well 8 core 20 boxes 11 and 2). This facies generally occurs strongly recrystallised to microspar and sparry calcite and locally may exhibit stylolites.

Interpretation

The origin and processes that form floatstones are similar to the depositional environments of wackestones. However, the size of the skeletal allochems may reflect the growth stages of the shells and the matrix are in general micrite or fine grained sediments.

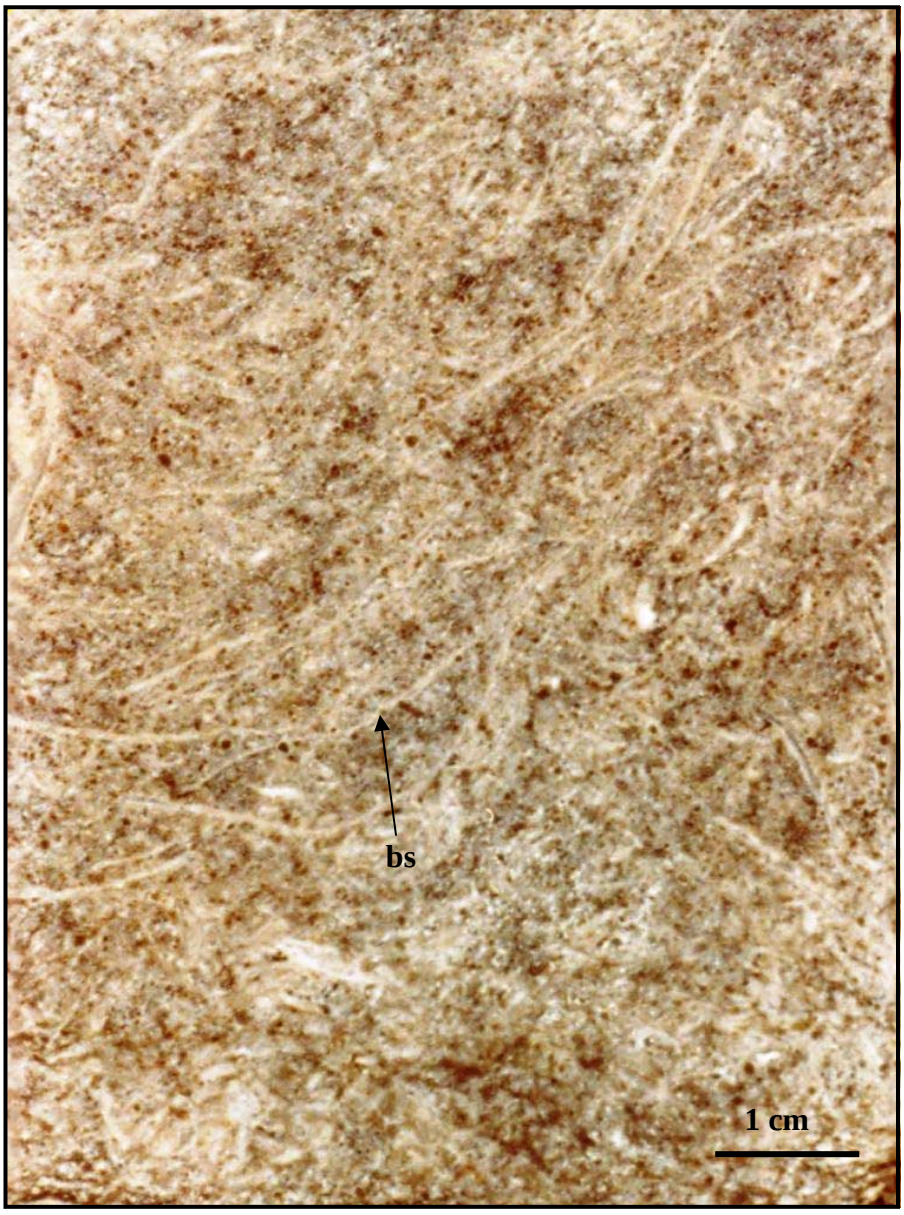

Figure 5.7a –Core slab - Floatstones of bivalves. The shells (bs) are probably disarticulated shells of the genus *Trigonodus*.

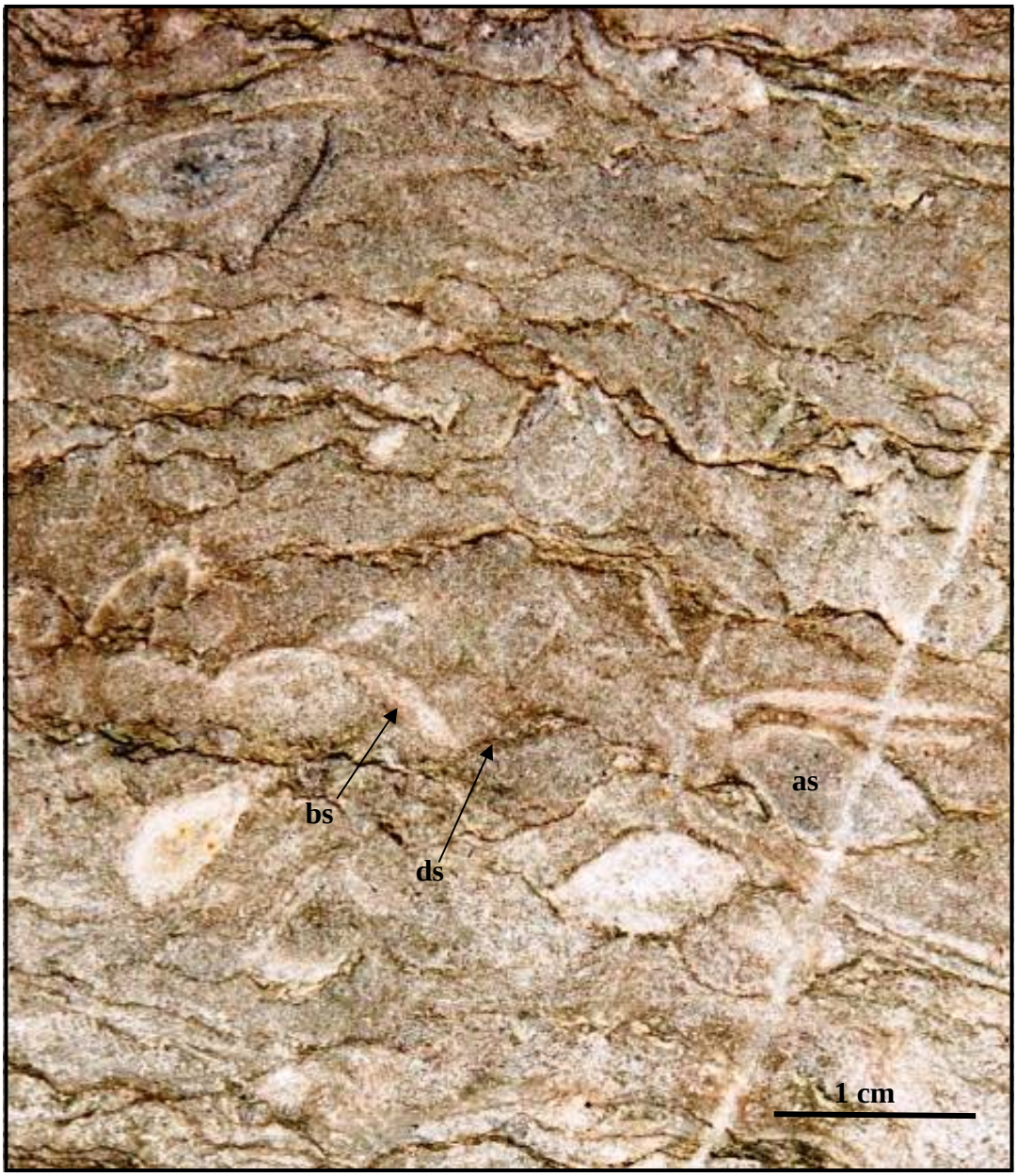

Figure 5.7b – Core slab - Floatstone of bivalves (bs), genus *Camposella* with articulated (as) and disarticulated shells (bs) set in a muddy matrix. Dissolution seams (ds) and compaction effects. Location?

Rudstone (R - m,t,c) (b,g,o) (g,l,s)

Rudstone is a grain-supported carbonate rock containing more than 10 per cent of grains more than 2 mm (Embry & Klovan, 1971).

Rudstone is commonest carbonate facies in the cores logged. In the proximal areas this facies tends to occur interfingered with terrigenous facies. Basinward, this facies is carbonate-rich. It may occur as centimetre-thick individual beds or as amalgamated packages totalling tens of metres.

For a better understanding of the sedimentary environment and hydraulic energy level that characterise this facies, some additional data was added to the Embry & Klovan (1971) textural classification (Figure 5.2). This supplementary information may complement the name of the facies. Thus, in such classification scheme (Figure 5.2), bioclastic components, bivalves (b), gastropods (g), and also oncoids (o); the matrix, muddy (m), terrigenous (t), clean (c); or even the primary sedimentary structures such as graded (g), laminated (l) or stratified beds (s), may be added to the classification for the subdivisions of this facies. For example, a rudstone facies can be described as bivalve rudstone which is clean and stratified (R-bcs). Because of the great diversity of this facies relating to its different processes and environments of deposition, only the most important and most frequent occurrences are described below. In addition the taphofacies of these molluscan floatstones and rudstones and their environments of deposition are described in more detail in Chapter 6.

Rudstone R-cb

Rudstone of bivalves that are clean, or matrix free (R-cb) are light brown, light grey, light cream and dark brown in cores. The shells are in general disarticulated and rarely articulated, commonly broken but also preserved whole (Figures 5.8a and 5.8b). Due to transport and reworking and the lithified state of these rocks, it is difficult, in most of the cases, to recognize the bivalve genera. When preserved, the most common genera identified are assigned to the non-marine, unionid bivalves; *Trigonodus (A)*, *Camposella (E)* and *Desertella* (G). The size of shells varies from 0.3 cm up to 2 cm but can reach 5 cm in size. Smaller fragments are normally rounded and articulated shells are in general smaller than 1 cm. The shells normally lie in a fine bioclastic grainstones matrix.

This facies is poorly stratified and exhibits, in general, a massive aspect, with poor sorted grains in a disorganized arrangement. But, some intervals show a degree of organisation with shells oriented parallel with bedding (e.g. Figure 5.8a), weakly laminated or cross stratified or even imbricated shells. Locally the shells may display concave-up or concave-down preferred orientations

Typically the shells are neomorphosed (Figure 5.8b) and fewer or dissolved and cemented with calcite spar. Silicification may occur partially or totally as a late

diagenetic substitution process. Rare matrix occurs due to recrystallization to sparry calcite. Stylolites are not common, unless in cemented portions, but sutured grain margins are common (e.g. Figure 5.8b). Green and clay minerals may concentrate in the stylolites. This lithology is generally strongly cemented but still preserves a primary intergranular porosity. However, locally it has interbedded tight intervals with no visual porosity. These are normally neomorphosed shells, now sparry calcite, but they also contain calcite cements, filling the pore space produced by the shell dissolution, or intergranular pore space. Some shells show dissolution, forming mouldic, vuggy and intercrystalline porosities displaying primary intergranular porosity in shell rich intervals. Silification is variable with beds being completely silicified and with a brecciated aspect. Argillaceous intervals tend to be less porous, with lower microporosity and stylolites.

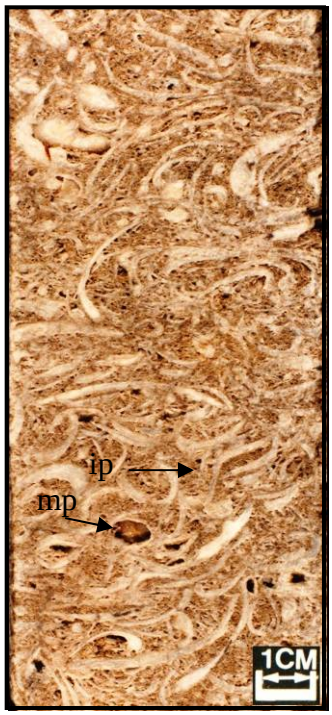

Figure 5.8a – Core slab – Clean, bivalve rudstone (Facies R-cb), disarticulated shells of bivalves, scattered in a bioclastic grainstones matrix, exhibiting intergranular (ip) and mouldic porosities (mp). Moderately to poorly sorted. Well 12 core 3 box 4 (Appendix A7).

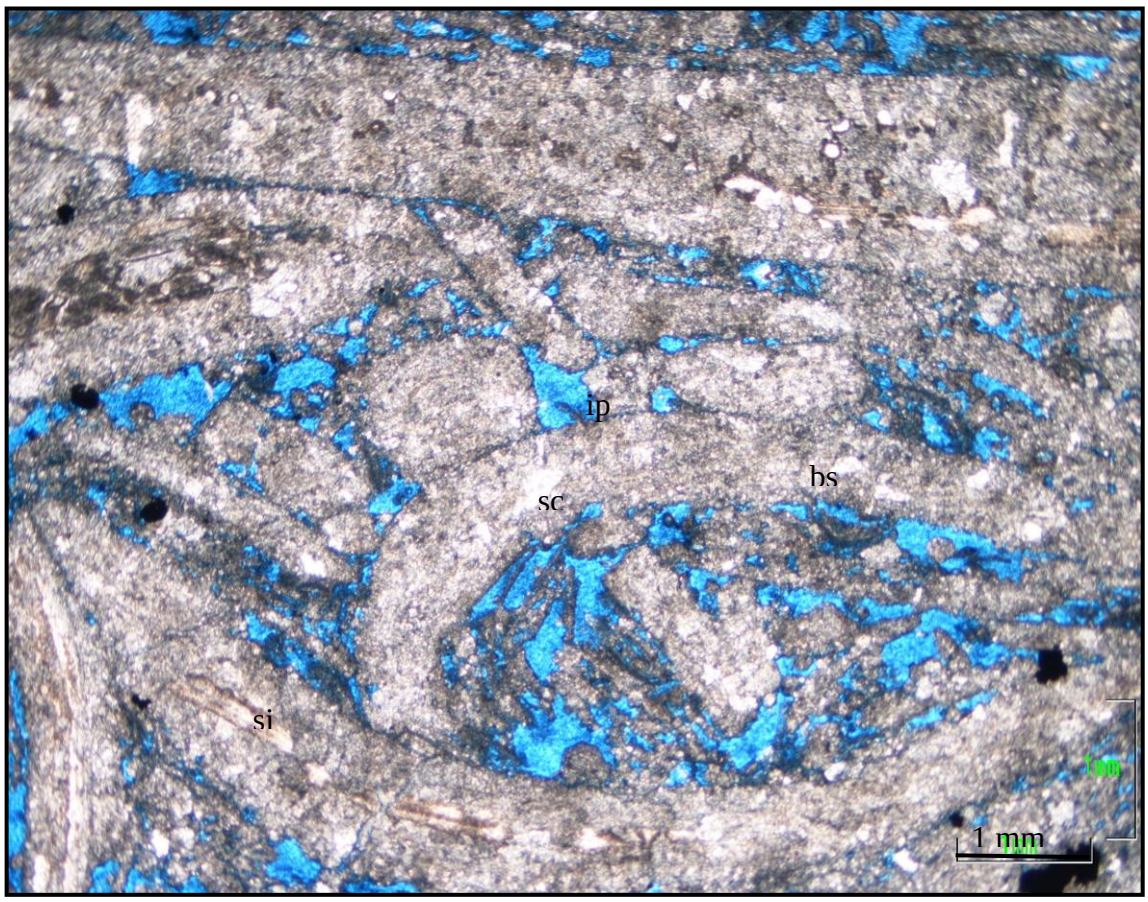

Figure 5.8b Photomicrograph showing the disarticulated shells of bivalves (bs), whole, but also broken, neomorphosed into spar calcite (sc) and locally partially silicified (si). Shows intergranular primary porosity (ip). Well 12 core 3 box 4 (Appendix A7).

Rudstone Rmb

The bivalve rudstones with muddy or peloidal matrix (Rmb) vary from light cream for the rudstones with more calcite cement content to greenish grey for the argillaceous intervals. These deposits are poorly laminated. Laminations may occur at the top of the beds. Inverse and normal grading may be seen (Appendices A1 to A7). In general, the amount and size of shells increase toward the top of the beds. Gradational contacts with muddier facies at the base and coarser grained facies at the top of the beds are the most common, but erosional surface may also occur. Locally, features of bioturbation, brecciation, nodules and fractures may occur.

Shells of bivalves are normally disarticulated. But less commonly are articulated, whole and also broken (Figures 5.9a and 5.9b). They normally vary from 1 cm to 2 cm in size, but it may reach 3 cm. The smallest are normally broken and rounded.

Disarticulated shells have been identified as *Trigonodus (A)*, *Kobayashites (D)* and *Camposella (E*) genera. The shells are preserved in disorganised fashion and scattered in a muddy, peloidal or bioclastic medium to coarse grained packstone matrix. Rarely geopetal structures may be seen.

Articulated shells of *Sphaerium (H)* and *Desertella (G)* genera, also occur but less commonly, mostly in the argillaceous or muddy intervals. Disarticulated and also articulated ostracods may also occur. In the proximal areas they are greenish and sandy and an argillaceous rich matrix is quite common. Stevensite and microbialites may also occur associated with more argillaceous beds.

The shells are generally neomorphosed into spar calcite (Figure 5.9b). Locally the calcite is partially replaced by silica. Rarely, shells are substituted by stevensite (see Chapter 6, Figures 6.29 and 6.30). The muddy matrix may be recrystallized into spar and microspar calcite. Some intervals are more argillaceous and pyrite rich, showing stylolites and no visual porosity. Locally the stylolites may concentrate stevensite and also organic matter.

Figure 5.9a – Core slab - Rudstone of bivalves with muddy matrix (Facies R-mb). Disarticulated, whole, rarely broken shells are disorganized and irregularly distributed in a peloidal and muddy matrix. Poorly sorted, moderately to well packed. Note dissolutions seams. No visual porosity. Well 1 core6 box 12.

Porosity varies from less than 5% of intercrystalline porosity to 10 % owing to dissolution resulting in intraparticle, mouldic and vuggy porosities.

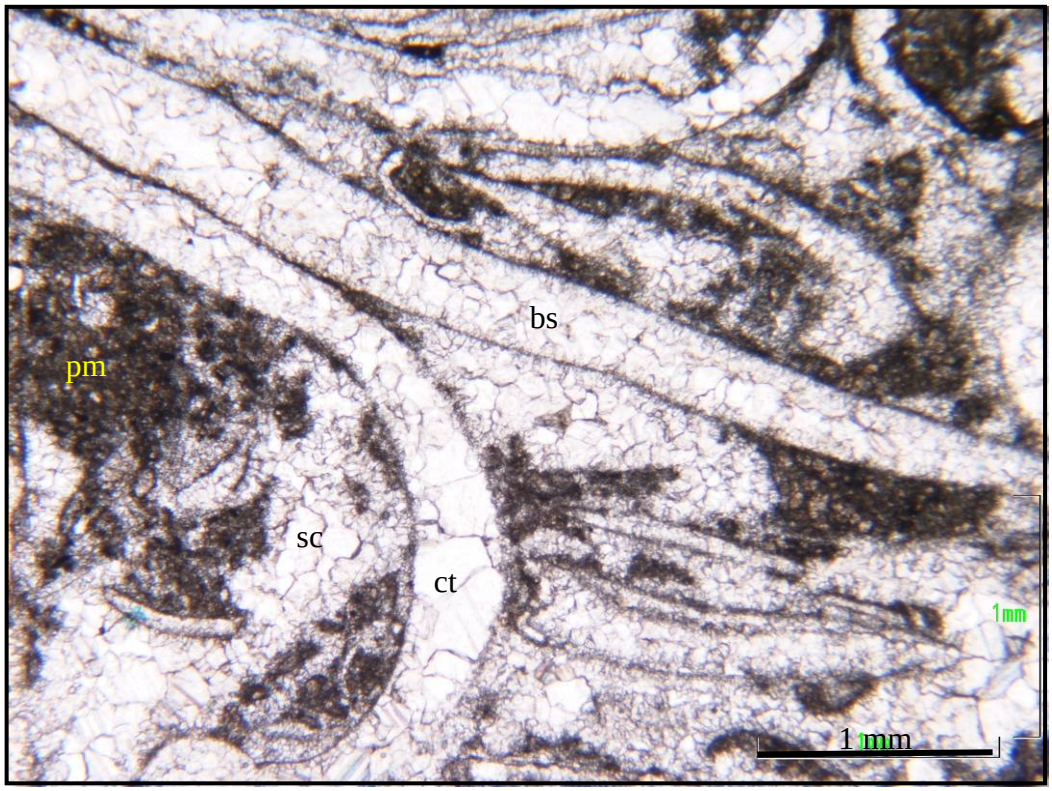

Figure 5.9b – Photomicrograph - Neomorphosed bivalves shells (bs) within a peloidal and muddy matrix (pm), partially recrystallized into spar or microspar calcite (sc). No visual porosity – Dissolution and calcite cement precipitation locally occur (ct). Well 1 core 6 box 12 (Appendix A1).

Rudstone R- gb

Rudstone of gastropods and bivalves (R-gb). This facies occurs in well 6 core 4 boxes 10 to 4 with metre thick beds stacked up to 6 m thick (Appendix A3). The facies has a homogeneous texture and is moderately to well sorted, which denotes a selective high hydraulic energy environment. The bivalve shells are disarticulated; whole and also broken, and the gastropods are 2 mm to 5 mm in size. These shells are normally neomorphosed into spar calcite, some are partially silicified, and showing mouldic and vuggy porosities (Figures 5.10a and 5.10b).

Figure 5.10a – Core slab - Rudstone of gastropod and bivalves (Facies R-gb). Core sample with bedding inclined to the right showing white coloured shells neomorphosed into sparry calcite with mouldic and vuggy porosities - Well 6 core 4 box 6 (Appendix 3).

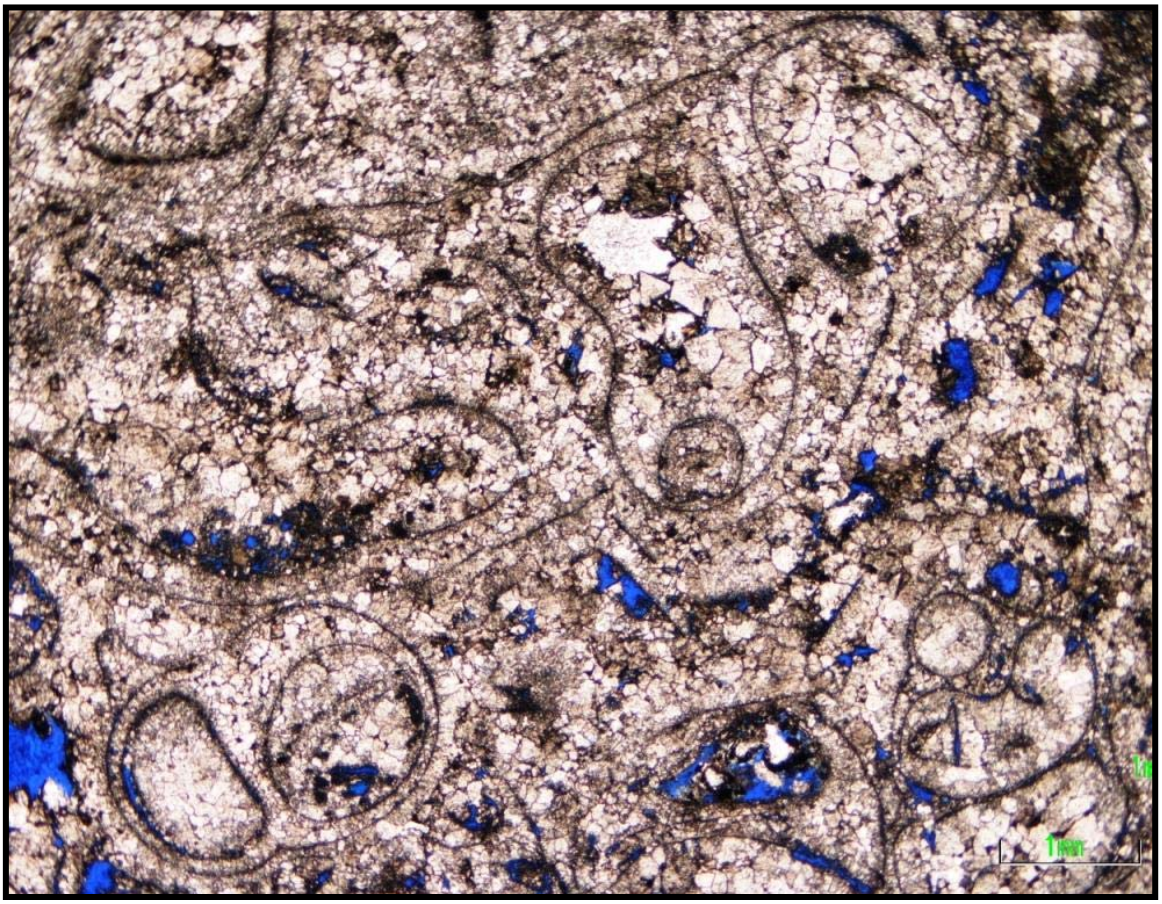

Figure 5.10b Photomicrograph of R-gb showing gastropod shells neomorphosed into spar calcite and mouldic, vuggy and intra- and interparticle porosities - Well 6 core 4 box 6 (Appendix 3).

Rudstone Rt-b

Rudstone of bivalves with terrigenous matrix (R-tb). This facies has shells, mostly *Camposella (E),* disarticulated in a terrigenous sandy matrix. They are normally 1 cm to 2 cm in size (Figures 5.11a and 5.11b). Generally, the shells are broken at the base and larger and unbroken towards the top of beds. Smaller shells are commonly reworked, abraded. Most of them display concave-down but some are concave-up orientations. Green minerals are present in the sandy matrix. Lithoclasts, volcanic rock fragments and fish bones may also occur. This facies exhibits small cycles of fining upward and plane-parallel lamination. The size of the shells decreases upward. A thin lag of coarse sediment may occur at the base of the bed overlying an erosive surface, which is interpreted as tempestite. The shells of bivalves are normally neomorphosed into spar calcite and are partially silicified (Figure 5.11b). Some grains show micrite envelope. Locally stylolites are seen as is pyrite

Figure 5.11a – Core slab - Rudstone of bivalves (bv) in a sand matrix, quartzose, feldspathic and green minerals (gm) (Facies R-tb). At the base of the photo medium to coarse grained sandstone (S-mc) with green minerals (gm) and spots of oxidized pyrite (py).

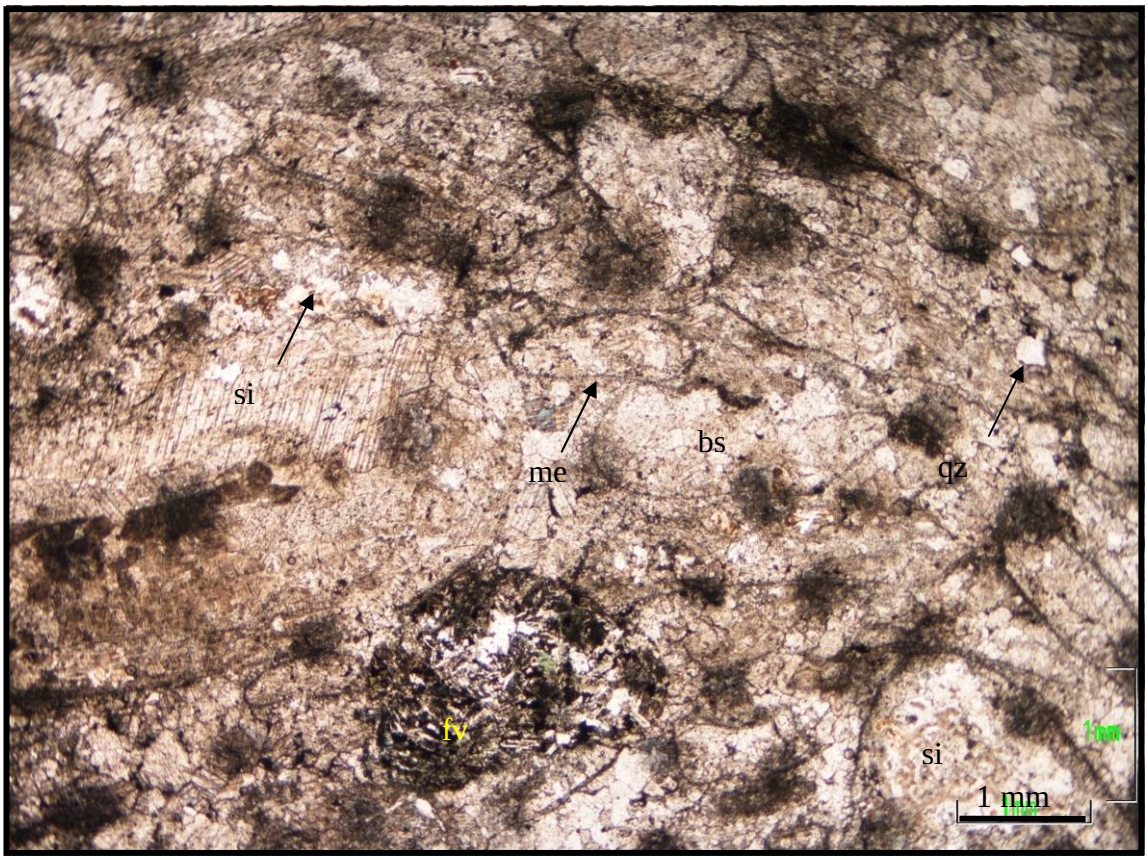

Figure 5.11b Photomicrograph of rudstone showing neomorphosed shells of bivalves (bs), locally partially silicified (si), with micrite envelope (me). Quartz (qz), feldspar, and basalt fragments (fv) are also present. The rounded black spots scattered are stains over the thin section. Well 8 core 20 box 18 (Appendix A5).

Rudstone R-o

Oncoidal rudstones (R-o) contain oncoids, in general < 0.5 cm diameter, that are well sorted, in a grainstone or packstone matrix. The oncoids exhibit an original concentric structure (Figure 5.12). They have been dissolved out to form mouldic and vuggy porosities. Interparticle and intraparticle porosities can also be seen (Figure 5.12).

Figure 5.12 Core slab - Rudstone of oncoids (Facies R-o). The oncoids are up to 0.5 cm in size, show concentric structure, and are moderately to well sorted scattered within a finer grained matrix. Well 1 core 5 box 1. They were dissolved out to form moulds.

Interpretations

Rudstone facies are widely distributed in shallow, high-energy lagoonal environments. They may occur as a result of various depositional processes such as waves and storms reworking coarse bioclastic sediments on high energy lake margins. The varying textures of the rudstones indicate accumulation at different depths but above storm wave base, in zones of agitated water. The preservation of molluscan shells within the rudstones is considered to be an important part of the interpretation of these facies and this is discussed in the following Chapter 6.

Carbonate facies - Autochthonous

Almost all the facies described in core are clastic, allochthonous, transported by currents or gravity flow. However, autochthonous or bioconstructed boundstone facies, although rare in the cored Coquina succession, dominate the microbialite rocks of the Aptian, Macabu Fm. These have been documented by sidewall core, thin sections and FMI logs, and for this reason will be treated in Chapter 7 (see section 7.3, Figures 7.6, 7.14 to 7.17).

In the Barremian coquina succession, are rare and are normally associated with very shallow water, muddy and argillaceous sediments. In this case, they generally occur at the top shallowing-upward cycles, associated with exposure features such as calcretes and breccias. This may relate to arid conditions of a closed lake environment.

5.2.2. Terrigenous Facies

Shale (SH)

Description

The shale facies occurs in the wells, 2, 6 and 9 (Appendices A2, A3 and A6). It varies in thickness from 0.3 m up to 8 m, and almost always is associated with other fine grained facies, such as mudstone and siltstone. However, locally it may occur interbedded with thin beds of coarser packstones, grainstones and rudstones. In the proximal areas (wells 2 core 6 boxes 19 to 15 and core 2 boxes 19 to 9) it is generally interbedded with sandstones and siltstones (see below). Most of the shale is reddish brown, greenish brown or dark grey but it may exhibit darker colours where rich in organic matter. It can also be silty, and mica rich. Locally it exhibits greenish colours. The shale may be poorly laminated (Figure 5.13a) and locally with gravitationally deformed structures (well 6 core 2 boxes 7 and 3). Locally it is brecciated, fractured, but rarely weathered. Nodules of calcite are relatively common (Figure 5.13b), and sandstone dykes rarely occur. Pyrite may be concentrated in some intervals.

Locally the shale is bioclastic rich, with disarticulated and articulated shells of bivalves and locally fragments of fish bones also occur, and frequently they contain ostracods. Shell fragments of up 0.2 cm in size occur in some cores and these bioclastic-rich intervals are commonly interbedded with bivalve rudstones and thin beds (< 5 cm) of packstone (wells 6 core 5 boxes 10 to 3). In wells 6 core 5 box 9 the shale occurs associated with microbial laminites.

Interpretation

Shale is normally deposited in calm water environments, below the storm wave base (Tucker & Wright, 1990). The lamination suggests little bioturbation which indicates deposition near or below the thermocline in anoxic conditions, in the deepest parts of lakes. This is also supported with the reduced biota of small articulated and disarticulated ostracod shells. The association with bivalve and gastropod rich carbonates normally occurs where shales are interbedded with gravitational or storm deposits. In proximal area (wells 2 cores 6 and 2) this facies may be associated with shallow protected lagoon or deltaic flood plain.

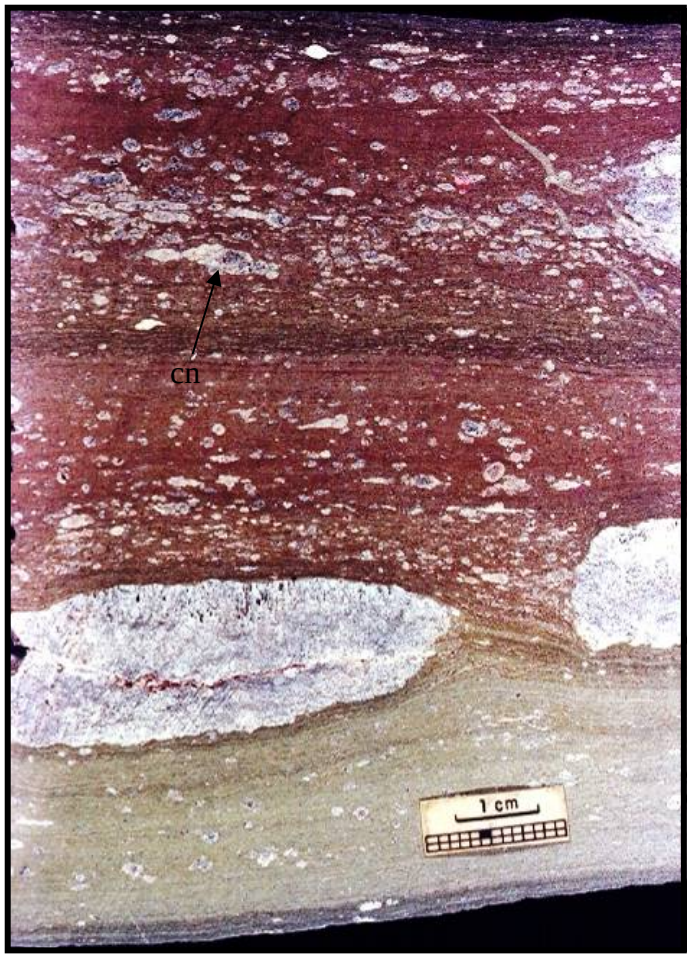

Figure 5.13a Core slab - shale reddish brown and greenish brown (SH), thinly laminated with calcite nodules (cn). Some bivalve shells completely neomorphosed / recrystallized.

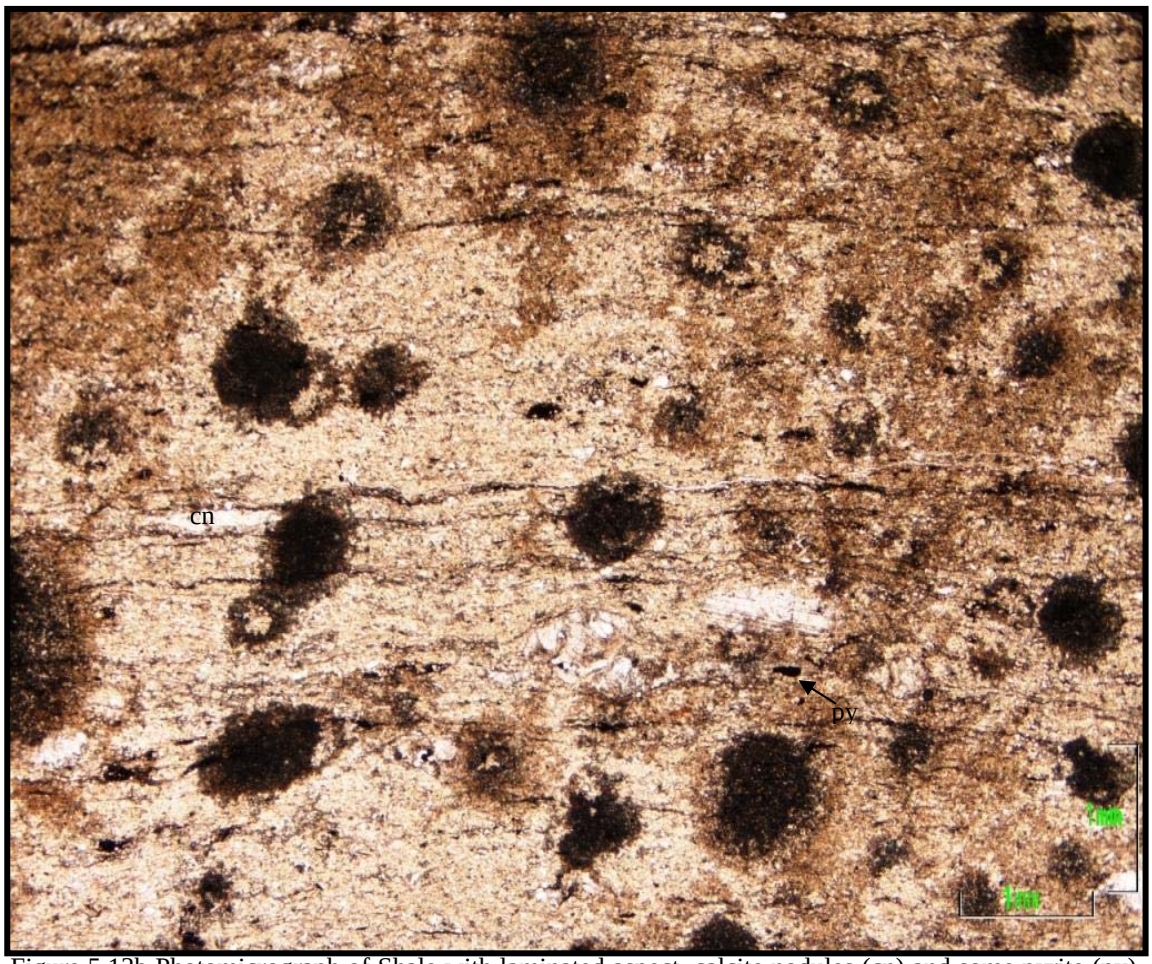

Figure 5.13b Photomicrograph of Shale with laminated aspect, calcite nodules (cn) and some pyrite (py). Rounded black stains are artefacts in old slides produced by moulds. Well 6 core 2 box 7 (Appendix A3).

Siltstone (ST)

Description

This facies occurs in wells 1, 2, 6, 7, 9 and 12, and has greatest abundance in wells close to the proximal source areas (Appendices A1 to A7). Normally the siltstone occurs in very thin centimetric beds, 0.1 m to 0.3 m thick, interbedded with thin beds of other fine-grained lithologies, such as shale and wackestone facies, but locally it may occur with very fine and fine sandstone facies (see below). The siltstone facies may also occur in 1 m to 2 m thick, amalgamated beds associated with packstone of bivalve packstones (P-b) and interbedded with thin-bedded grainstones and rudstones. When amalgamated, this facies form units totalling 7 m thick (e.g. well 9 core 33 boxes 5 to 1 and core 32 boxes 9 and 8).

The siltstones are greenish grey, greenish brown and cream and less commonly reddish brown (Figure 5.14) and dark grey. Lighter coloured lithologies are more sandy and the greener ones, more argillaceous. In general it is mica and clay rich, with quartz,

calcite and pyrite. Clasts of volcanic rocks and fragments of thin and rounded bioclasts of bivalves may occur disseminated in the siltstone. The amount and size of shells is observed to increase toward the tops of the beds, with articulated and disarticulated shells, up to 1 cm in size. Additionally fish bone fragments and some clay clasts may occur sporadically.

In more argillaceous intervals the siltstone is poorly laminated. Locally it is massive with clasts slightly deformed at the base, and associated with escape structures This facies may occurs interbedded with very fine sandstones which show low-angle cross-stratification (e.g. well 1 core 2 box 12). Microfractures are frequent.

Locally this facies exhibits calcite, pyrite nodules, and euheudral crystals of spar calcite cement. The siltstone is poorly to moderately bioturbated and locally presents a mottled aspect due to burrowing and burrows appear to have locally altered redox levels resulting in light coloured burrow fills in a reddish-brown siltstone (Figure 5.14).

Interpretation

There is a broad range of environments where siltstones may accumulate. But the facies association, in this case, in a lacustrine setting indicates calm waters, in a deep subaqueous environment, below the storm wave base. The burrowing indicates it is in oxygenated zone. Siltstones usually compose the base of the shallowing-up cycles, as part of transgression in a flooding trend. At the base it may have an erosive contact, and may relate to storm beds.

It may also occur in deltaic environments, such as the prodelta and delta front. In this context however, it may be found as density flows turbidites. Shallow protected environments may also accumulate siltstone in protected lagoons, and also in very shallow water associated with microbial facies in well 9 core 33 boxes 6, 5 and 1 (Appendix A6). Exposure and erosional features such as desiccation cracks, early diagenesis and silica nodules indicate its association with emergent surfaces.

Figure 5.14 Core slab – Siltstone (ST), reddish brown, moderately bioturbated (planolites?). Some burrows (bw) are filled with different younger sediments. Part of them is deformed by mechanical packing. Well 1 core 7 box 7 (Appendix A1).

Sandstone (c, m, f, vf) (a) (g, l, s)

The main constituents of the sandstone facies are usually quartz, feldspar, mica, and rock fragments, although the proportions of these may vary widely. Sandstones occur in wells 1, 2, 6, 9 and 12, ordinarily in individual beds (0.1 - 1.0 m in thickness), or interbedded in decimetre beds of 0.2 m to 0.3 m with shale, siltstone, and also carbonate facies, such as rudstone (well 9 core 34). When amalgamated, the sandstone units may reach up to 5 m thick (well 1 core 7 boxes 6 to 1, core 3 boxes 16 to 13 and

box 4 to 1). They vary in granulometry from very fine to coarse grained (see grain size track in the Appendices A1 to A3, A6 and A7). Most commonly they appear in cores as massive beds, normal graded beds and cross-stratified beds (well 1 core boxes 13 to 10).

To classify the broad range of different types of sandstones found they have been divided by grain size into coarse, medium, fine and very fine according to the Wentworth table (1922) (**c, m, f, vf**). The purity is measured according to the mud, or argillaceous, content (**a**), and the sedimentary structures are classed as graded, laminated or stratified **(g, l, s)** as described below:

Sandstone, coarse to medium grained, poorly laminated **(Scml**).

These greyish green sandstones comprise grains of quartz, feldspar, green minerals and bioclastic components. Scattered shells of bivalves occur up to 4 cm in size. This facies also contains lithoclasts and is pyrite rich. It exhibits tractive and normal grading structures (Figure 5.15a). This coarse sandstone occurs at the base of well 8, core 20 and box 18, in beds up to 20 cm thick interbedded with sandy bivalve rudstone (Rtb).

Sandstone, medium grained **(Sm**).

This brownish, greenish grey, or even black sandstone, is composed of quartz, feldspar, green minerals, volcanic rock fragments and garnet. It is well to moderately sorted. Usually it presents a homogenous or massive aspect, but locally it exhibits plane laminations, and also low-angle, cross-stratification and bioturbation. This facies may occur with significant mud content and with scattered pyrite. Some intervals occur with dispersed shells of bivalves. The fragments of bivalves are about 0.5 cm in size, entirely recrystallized and locally silicified. Visually estimated intergranular porosity in this facies is 5 to 15%. This facies occurs in well 2 core 2 box 1 in beds 0.1 to 1 m thick interbedded with gravitationally deformed beds, and conglomerate matrix supported (diamictite – DM). It also occurs in the well 9 core 34 box 1.

Sandstone fine to medium grained **(Sfm)**.

This facies is greenish brown or dark brown, and is composed by quartz, feldspar, volcanic rock fragments and mica grains. This facies is rare and where it occurs it is in beds of 20 cm in thickness interbedded with coarse grainstone (Gcb) (well 2 core 2 box 2). Is the beds are weakly laminated, with plane-parallel laminations

toward the top of the beds. Disarticulated shells of bivalves up to 1 cm in size occur scattered within the sandstone. However, towards the top of the beds, the shells of bivalves tend to be horizontally oriented. The basal contact of beds is erosional, with intraclasts of 1 cm to 2 cm and normal grading. This facies also occurs with a more massive aspect rich in volcanic rock fragments and with rounded bioclastic grains.

Sandstone fine **(Sf)**

These are greenish brown, greenish grey, reddish brown, sandstones composed of quartz, feldspar, mica, garnet, green minerals, opaques and volcanic rock fragments. This is the most frequent sandstone facies in the study area. Commonly the beds are 0.1 to 1 m in thickness stacked in units up to 6 m thick (well 6, core 36 boxes 02 to 01). These are massive, but locally, poorly laminated (well 2, core 2 boxes 8 to 3) and can also occur with low-angle, cross-bedding (well 6 core 12 box 1 to core 11 boxes 10 to 7). Mottled, fluidized structures, ripples or possibly hummocky (?) structures also occur. The basal contacts are normally erosive followed by lag. But less commonly, the contact is gradational. In some beds, these sandstones exhibit inverse grading (well 9 core 33 box 7). Toward the top of the beds, there are abundance of disarticulated shells of bivalves and gastropods of 2 cm to 3 cm in size, and also intraclasts.

Sandstone fine, argillaceous **(Sfa)**

Dark brown, greenish grey, silty sandstone. Composed of quartz, feldspar, mica and bioclasts. The facies occurs in beds of 0.1 cm to 1 m in thickness. The beds are poorly laminated and generally occur interbedded with bivalve rudstones (well 9, core 34 boxes 8 to 1). In these cases, the sandstones contain scattered shells of bivalves. The sandstones present irregular and erosive basal contacts. Locally at the base of the beds, rip-up clasts are observed and load cast structures (well 9 core 31 boxes 6 and 7). These beds also occur interbedded with shale and siltstone and are interpreted as turbidites. Nodules of calcite can be noted.

Interbedded very fine sandstone and siltstone **(Svf / ST)**.

Interbedded very fine sandstone and siltstone with gradational contacts. The sandstone is greenish grey, shaley, mica rich, locally with calcite cement. The siltstone is greenish grey, mica rich, and calciferous. These facies are rich in bivalve shells, and

whole shells occur in shaley sandstones. Nodules of calcite normally occur parallel to the beddings. These occur in the well 1, core 2, boxes 11 to 1.

Sandstone very fine **(Svf)**

This facies is composed mostly of quartz, feldspar, mica and volcanic rock fragments and vary between greenish grey, light cream and also brownish red. Subordinately, it contains ostracods, bivalves, peloids and rare clay minerals. Moreover it can be argillaceous and locally pyrite rich. Green minerals and stevensite rich intervals occur. Some beds are bivalve rich, with millimetre shells, smaller than 1 cm but also up to 2 cm in size. The disarticulated shells are broken and the smaller are usually rounded. Occasionally they occur larger and whole. The bioclastic grains are scattered within the sand and also horizontally oriented, with nodules of calcite enveloping the shells. No visual porosity is observed where calcite cement is present. Usually the shells of bivalves are partially neomorphosed, recrystallized, or partially replaced by silica. Some shells are dissolved and their moulds filled by calcite cement. Thin beds with nodules of calcite, calcite cement and stylolites may occur in the carbonate rich portions. Locally this facies exhibits a brecciated aspect. This facies may occur interbedded with mudstone or thin laminas of siltstone (well 1 box 3 to 1). Low angle stratification and ripples are common. At the base of the beds, the sandstone is generally more laminated. In addition, normally it shows load casts and fluidization structures. Locally this facies is moderately to poorly bioturbated. The contacts between silty and sandy facies are in general irregular, erosive, usually with lag of sandstone.

Sandstone very fine, argillaceous **(Svfa)**

This facies is normally greenish brown with irregular reddish brown stains. It is quartzose and locally mica-rich with fragments of volcaniclastic rocks and also small fragments of shale. Locally this facies is pyrite-rich and it commonly occurs interbedded with laminae of siltstone or shale, with small variations in grain size (well 1 core 2 box 16). This facies exhibits plane-parallel laminations and locally it is moderately bioturbated and fractured. Locally broken and whole shells of bivalves are present. The shells are in general totally neomorphised and occur scattered within the sandstone, and also within intervals with calcite cemented.

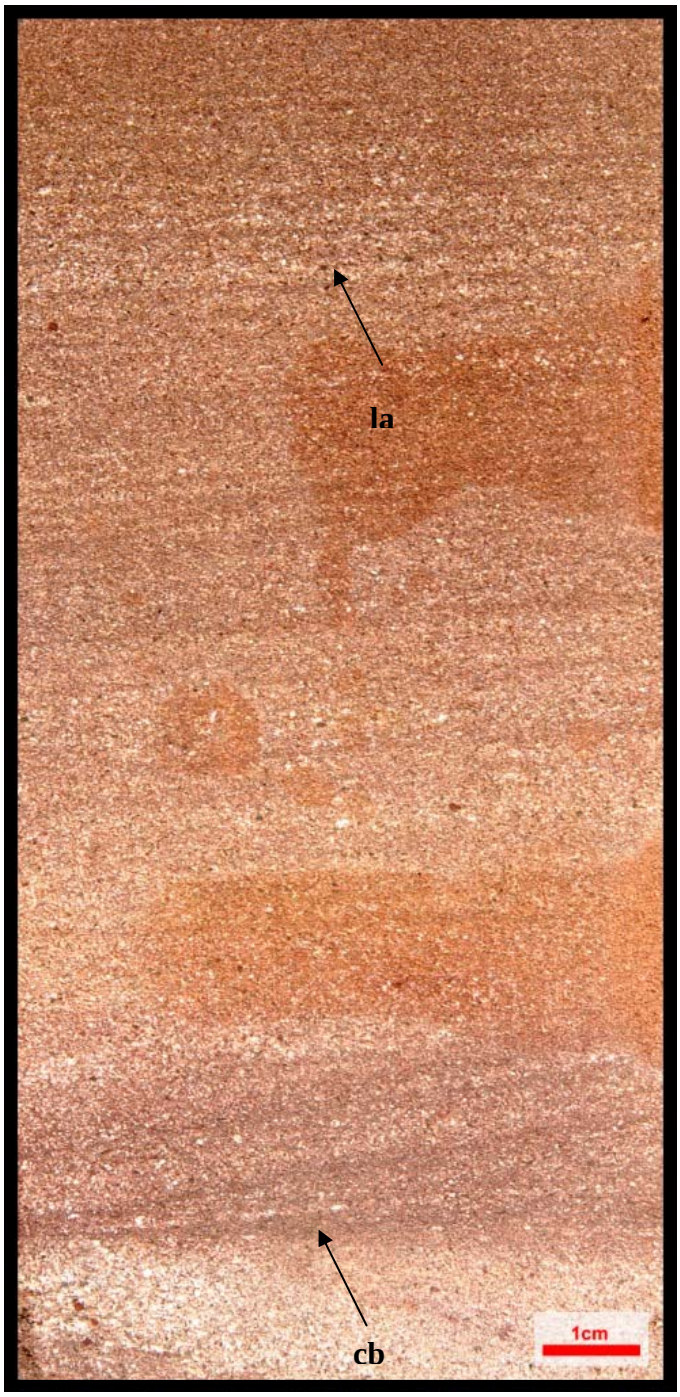

Figure 5.15a Core slab - Sandstone reddish brown, coarse to medium grained (Scml), moderately sorting, and showing cross bedding (cb) and low angle planar stratification (la).

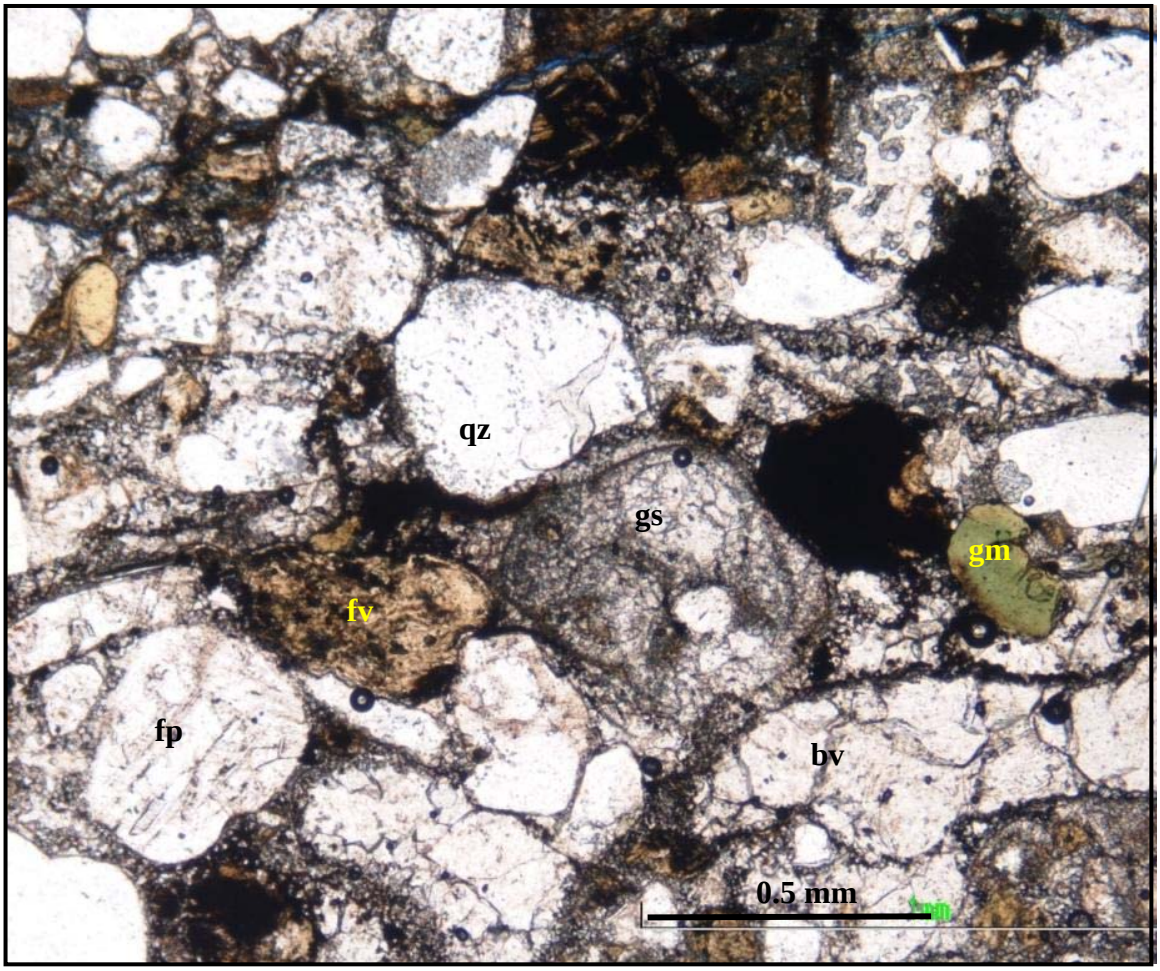

Figure 5.15b Photomicrograph showing the sandstone composed of quartz (qz), feldspar (fp), fragment of volcanic rocks (fv), green mineral (gm), bioclasts of gastropods (gs) and bivalves (bv) neomorphosed and also pyrite. The detrital grains are in general rounded to sub rounded. The rock is moderately sorted and well packed. Well 1 core 2 box 12 (Appendix A1).

Interpretation

The distribution of sandy facies in the lake environment is very broad. However, their occurrence is interpreted to be associated with subaqueous gravitational processes and also fluvial - deltaic environments. Thus, the coarser facies may have formed the distal areas of alluvial fans as or in the fluvial channels. In coastal and also shoreface areas, fine and clean sandstones with cross stratifications are more likely to occur. The fine and argillaceous sandstones are interpreted to have formed in a delta front or prodelta environment as turbidites into the lake. These more argillaceous facies also occur as crevasse deposits in the floodplain and in the slope zone as slumps and turbidites deposits (Reading, 1978).

***Conglomerate matrix supported* – (CM)**

This facies is a well lithified, conglomeratic siliciclastic rock which is unsorted, with pebbles and sand supported within a mud matrix, described as a diamictite. This facies occurs only in well 2 in metre-thick beds associated with sandstones and shales. Normally it occurs with sandy grains and shale clasts in a disorganised texture.

Interpretation

This facies may be interpreted as gravitationally derived flow deposits, e.g. debris flow (Walker, 1979), and it is commonly found on slopes in deep subaqueous zones. In well 2 it is associated with turbidities and slumps features which also support a deep lacustrine environment of formation.

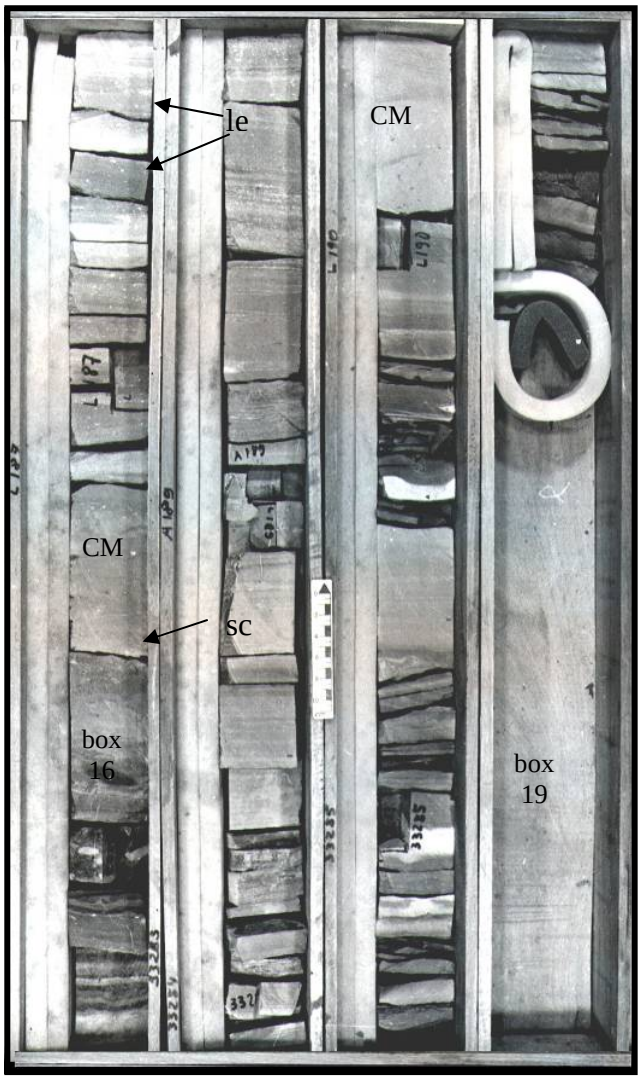

Figure 5.16 Core photo - Well 2 core 2 boxes 16 to 19. CM showing the massive, disorganized texture, and shale clast (sc), associated with deep lake facies and load structures (le). (box 0.1 m x 1 m). Appendix A2.

Conglomerate clast supported (CG)

This facies is a coarse grained rock with rounded clasts greater than 2 mm in size and occurs in wells 6 and 9. Individual beds are 0.1 to 1 m thick and stacked in units up to 3 m (well 6 core 1 and well 9 cores 26 and 27 – Appendices A3 and A6).

The conglomerates are clast supported, polymictic, composed of rounded igneous, metamorphic and volcanic rock pebbles, pelitic rock fragments and also green argillaceous clasts (Figure 5.17a). The matrix of the conglomerate is coarse grained sand, composed of sub-rounded to sub-angular grains of quartz, feldspar and volcanic rock fragments. The latter are mica rich; with some opaque and green minerals (Figure 5.17 b).

The individual beds, in well 6, core 1, present a poorly developed fining upward trend from pebbles size to coarse and very coarse grains. Laminations in the finer portions are less evident. In well 9, cores 26 and 27 (Appendix A6), beds are generally amalgamated, and the fining up beds is formed with erosional base, normally with rip up clasts of shale at the base. Locally this facies is cemented by calcite, with some levels exhibiting neomorphosed and silicified shells of scattered bivalves indicating a subaqueous lacustrine setting.

Interpretations

This facies occurs in proximal areas, close to the border faults in wells 6 and 9. It is interpreted to represent deposition in alluvial fans/fan deltas in tectonically active areas (Collinson, 1978).

Figure 5.17a– Core slab - Polymictic, clast supported conglomerate (CG) with clasts of volcanic (fv) and igneous rock (ig), pelitic fragment (pe) in a very coarse matrix (well 6 core 1 box 8, Appendix A3).

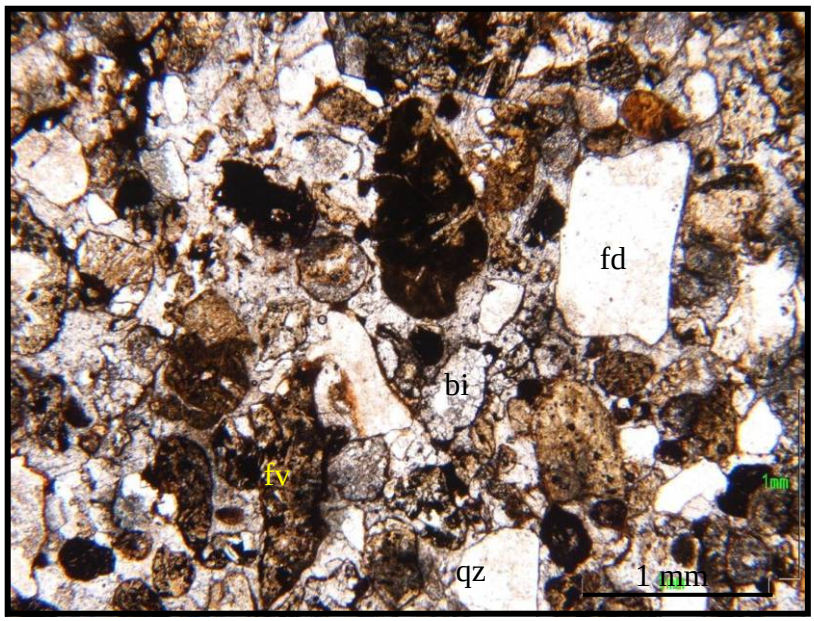

Figure 5.17b Photomicrograph showing the composition and texture of the matrix to the polymictic conglomerate: quartz (qtz), feldspar (fd), volcanic rock fragment (fv) and bioclasts (bi). Well 6 core 1 box 8 (Appendix A3).

5.2.3. Modified facies

Chert (CH)

Chert is a fine grained rock consisting of beds of cryptocrystalline silica (SiO_2), usually of biogenic, volcanogenic or diagenetic origin (Flügel, 2004). This facies occurs in the wells 1, 2, 6 and 7 (core 4 box 1), in very thin beds (< 20 cm), and also as nodules. The chert is normally brownish, deformed, brecciated, fractured and occasionally it shows silt filled veins (Figure 5.18). Fractures, shrinkage features, brecciation, concretions and pisolites are commonly associated with the chert horizons. This facies normally forms as a result of diagenetic processes involving the on replacement of host sediments. The host sediments are commonly lacustrine and palustrine carbonate rocks. However, the original fabric of the rock is usually masked by the diagenetic process of silicification.

Interpretation

The silicification is interpreted as a pedogenic overprint of exposed parts of the shores in palustrine carbonates. Such silcretes (Bustillo *et al.* 2002), are commonly associated with evaporation of silica saturated pore waters driven to the surface by capillary forces as described in modern environments by Bustillo *et al.* (2002). Various origins have been proposed for the silica source: detrital silica (Peterson & Von der Borch, 1965), siliceous skeletal material, solutions from land in semi-arid climate (Laschet, 1984), springs and seeps, hydrothermal volcanic systems (De Wet & Hubert, 1989; Smith & Mason, 1991), silica released from burial and dewatering of the surround clay rich rocks (Mahran, 1999). The temperature and pH changes in the lacustrine environment are the main factors that contribute to the chert formation. (Mahran, 1999; Bustillo *et al.* 2002).

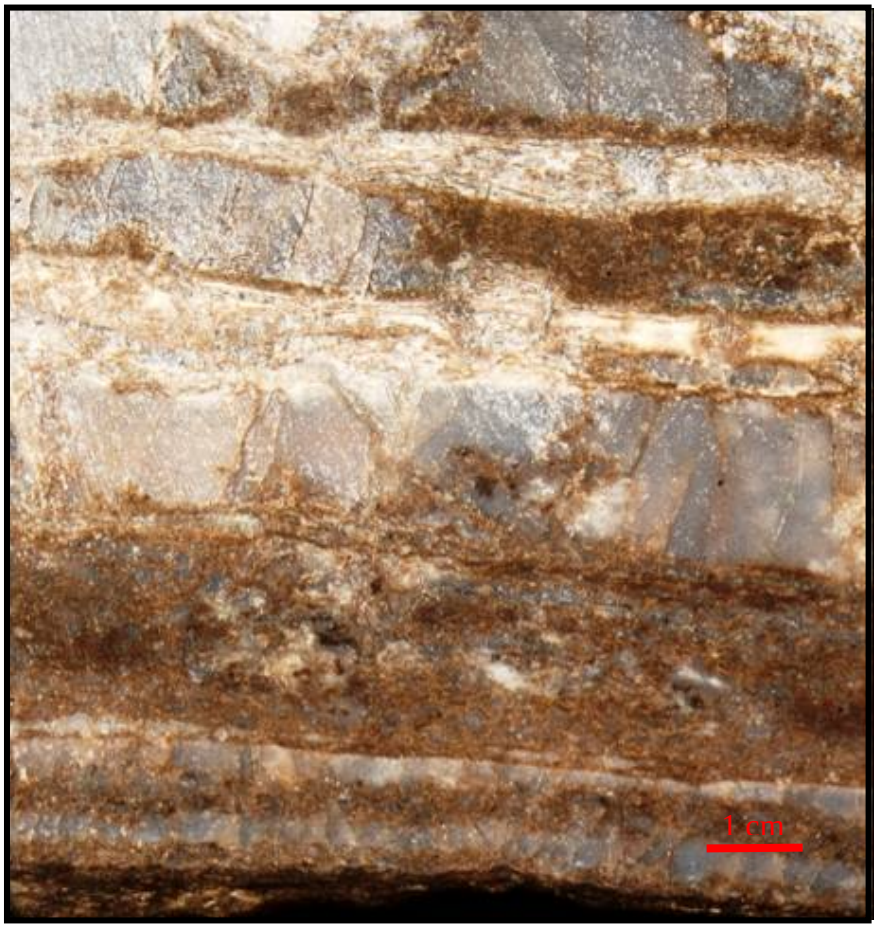

Figure 5.18 – Core slab The upper part of the photo, showing Interbedded chert and siltstone/ grainstones. The chert show fractures filled by silty material. Well 7 core 4 box 1.

Slumped deposits (SL)

A sedimentary structure consisting of overturned folds formed by downslope en mass transport of unconsolidated material, without basal detachment under the influence of gravity (Scholz, 2007, Rosendahl *et al*. 1990). This facies occurs in wells 1, 2, 6 and 9, as a contorted or deformed shales and siltstones, as a product of mass flow on a slope. The slumping deposits occur associated with shales, siltstones and also turbidite sandstones in the deep subaqueous environment, probably in fault border zones or prodelta front (cf. Tucker & Wright, 1990).

Breccia

Breccias here are coarse, siliciclastic, sedimentary rocks, made up of angular clasts. Tectonic breccias and collapse breccias occur locally; however, breccias that are formed from extensive shrinkage cracking or caliche breccia appear to be more

regional. Frequently this facies preserves the fabric of the original host rock that has been brecciated suggesting they are formed more or less in place.

The main breccia types are described here:

Tectonic breccia

BT - Breccia, greenish brown with fragments of pelitic rocks, quartz grains, feldspar, interbedded with portions of clay, shale with fractures filled with conglomeratic sandstone. This facies is normally associated with faults and fractures and milonite. These occur in the well 6 core 6.

Collapse breccia (BC)

BC- Breccia, with clay matrix, green at the top, exhibiting silicified layers, and locally silica nodules. This facies in general occurs as a product of karstification process, associated with vugs and vadose diagenetic features (Figures 5.19a and 5.19b). They are thought to result from in place dissolution, leading to collapse or pedogenic related breccias.

Breccia occurs in almost all the wells, in thin layers at the top of metre-scale shallowing-up cycles and interpreted to represent subaerial exposure surfaces.

Shrinkage breccia (BK)

Brecciated facies also occur as a result of subaerial exposure and desiccation of previously deposited sediment. Figure 5.20 shows a brecciated horizon with some younger sediments filling the interstitial space. These desiccation breccias occur due to exposure following the fluctuation of the lake level. Very fine breccia, calcrete, iron oxide; all normally occur together with calcite and silica nodules, suggesting subaerial exposure (Figures 5.20 and 5.20a).

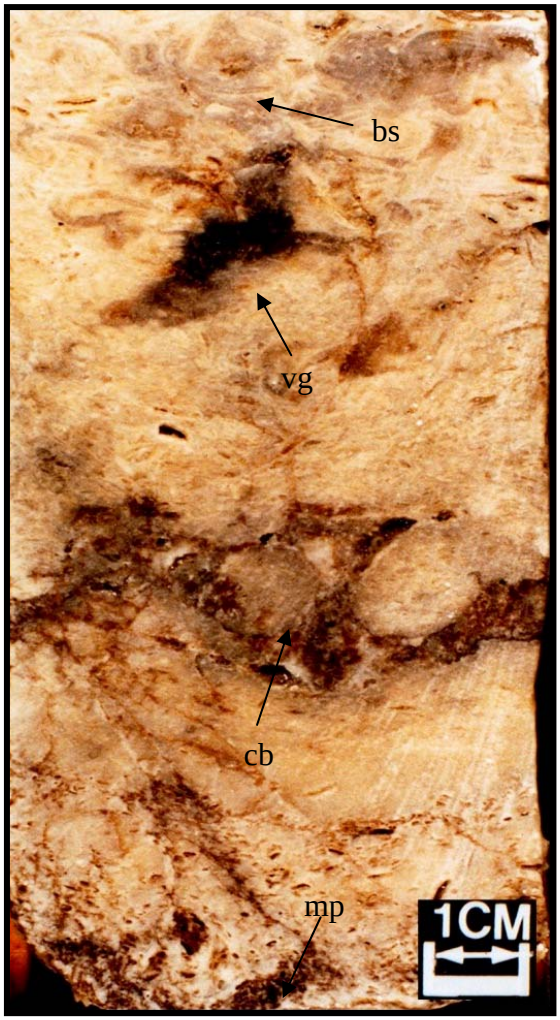

Figure 5.19a. Core slab Collapse breccia - hand sample showing bivalve rudstone (bs) cemented by calcite with vugs 3 cm (vg) some mouldic porosity (mp) and collapse breccia (cb).

Figure 5.19b Photomicrograph fragment of bivalve rudstone within a breccia showing fringe of early diagenesis, relict of neomorphic calcite (nc) and silicification (si) of the previous calcite cement. The silica cement may be chalcedony, formed during the early diagenetic process, probably due to subaerial exposure (oral communication Paul Wright). Well 12 core 1 box 1.

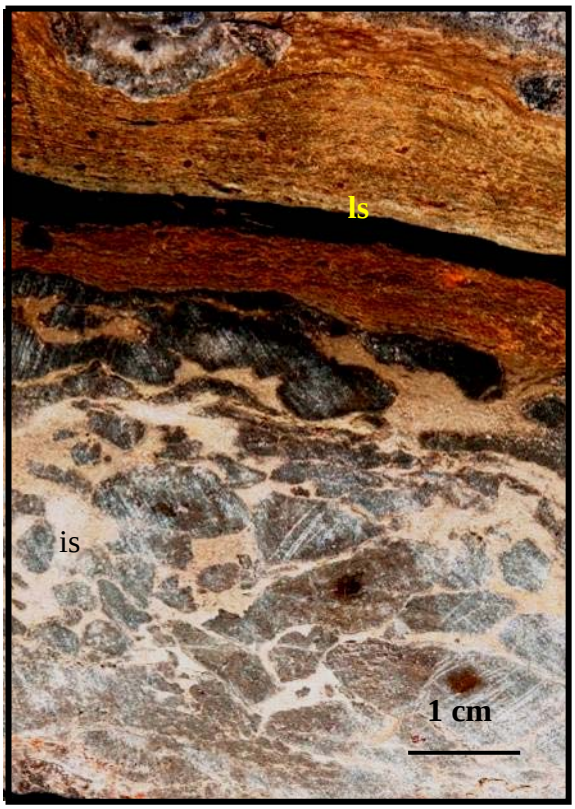

Figure 5.20a - Core slab - Mudstone brecciated with features of exposure cracks. Some younger material fills the interstitial space (is). In the upper part of the picture, overlie a laminated siltstone (ls) thin bed with crenulated aspect. Well 12 core 20 box 4 (Appendix A7).

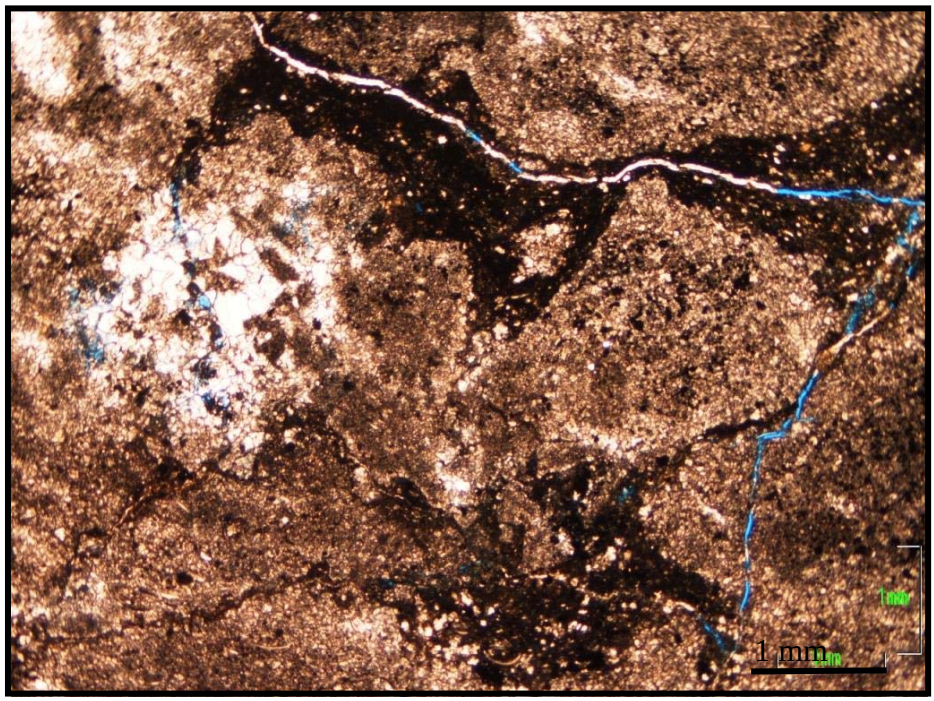

Figure 5.20b Photomicrograph showing brecciated aspect of the host rock with angular parts and interstitial space infilled by, younger black sediment. Well 12 core 20 box 4 (Appendix A7).

5.3 Depositional processes in lacustrine environments and evidence from Lagoa Feia Group facies

The sedimentary record of the earliest stages of continental rifting in extensional basins involves physical, chemical and biogenic processes (Reineck & Singh, 1980). The palaeogeography results from the extensional tectonic setting or template and the climatic and hydrological factors that control the sedimentation in such environments. Climate mainly controls the freshwater input and the rates of precipitation and evaporation, and also plays an important role in the influx of clastic sediment into the basin. There are both similarities and differences between depositional processes operating in lakes compared to those existing in the marine environment. Similarities are the aqueous environment (including waves and wind-induced currents) and differences include the absence of tidal effects and the mineralogy of carbonate deposits (Tucker & Wright, 1990).

In the lake sedimentary systems, especially in shallow areas, abrupt temporal and spatial sedimentary facies changes usually occur. The great variability of facies and complexity in the lacustrine environment is attributed to frequent lake level fluctuations, which promote the shifting of shorelines and subaerial exposure. The hydrological conditions of the lake must be taken into account to establish whether it is hydrologically open (exorheic) or closed (endorheic) as this has an important control on facies (Talbot & Allen, 1978).

The sedimentological processes within continental lake environments may be episodic or continuous. Episodic processes are, as a rule, responsible for mass transport of clastic sedimentary particles, whereas continuous processes, such as currents and waves, are usually responsible for the final deposition characteristics, features and the geometry of the sedimentary bodies (Walker & Plint, 1992). Sedimentary processes are also responsible for the mass displacement of rock, where high slope gradients exist. Among the above cited process, the most important for lacustrine sediment accumulation are storms, wind-induced waves, density flows and currents (Talbot & Allen, 1978). Less significant with low frequency is the occurrence of gravitational flows (Wright, 1990). Aeolian erosion, transport and deposition of exposed sediments can also be significant in the sedimentary record. However, aeolian derived sediments were not observed in the cores logged or the facies. The understanding of the processes that controls the formation of the studied rocks and the palaeoecological conditions

where they accumulated is fundamental for the development of Lagoa Feia Group palaeoenvironment in the following chapters.

5.3.1. Storms

This is an episodic process, often of great magnitude and effect, resulting from wind and barometric processes that form currents able to erode and transport large amounts of sediment (Figure 5.21; Aigner, 1985; Walker, 1992). The frictional coupling between wind and water produces oscillatory waves but also unidirectional wind drift onshore currents and a coastal set up, or elevation of the water level. The different water onshore and offshore water levels, results in hydrostatic gradient on the lake floor that drives a bottom return unidirectional flow (relaxation flow) offshore flow (Figures 5.24 and 5.25). Unidirectional bottom currents together with strong waves drive oscillatory motion at the bed that is responsible for the transport of sediments and skeletons (Aigner, 1985; Swift *et al.* 1986). As a result of this intricate and episodic process, the most common diagnostic sedimentary structures formed from storms are: ripples, dunes, (HCS) hummocky cross stratification and (SCS), swaly cross stratification within storm beds or tempestites (Walker, 1992). In most cases, the arrangement of the bioclastics is chaotic, with no preferential orientation.

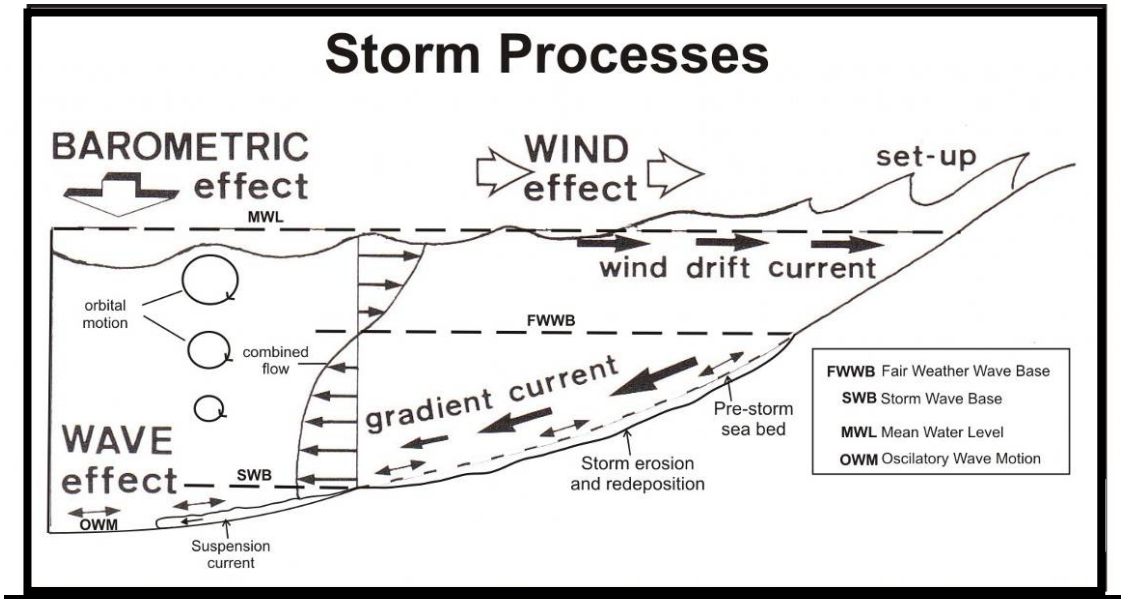

Figure 5.21 – Scheme illustrating the three main physical effects resulting from storms (mod. from Aigner, 1985).

Figure 5.22 is a proposed model for the storm-dominated hydrodynamic regime on carbonate ramps in the Upper Muschelkalk (Aigner, 1985). Surface water is pushed landward by the Coriolis and alongshore storms currents flow on the bottom to form gutter casts and distal tempestites. In shallower sites on shoals spillover deposits may be formed. Furthermore, proximal tempestites are deposited through the surge channels eroded by the compensating bottom return flows.

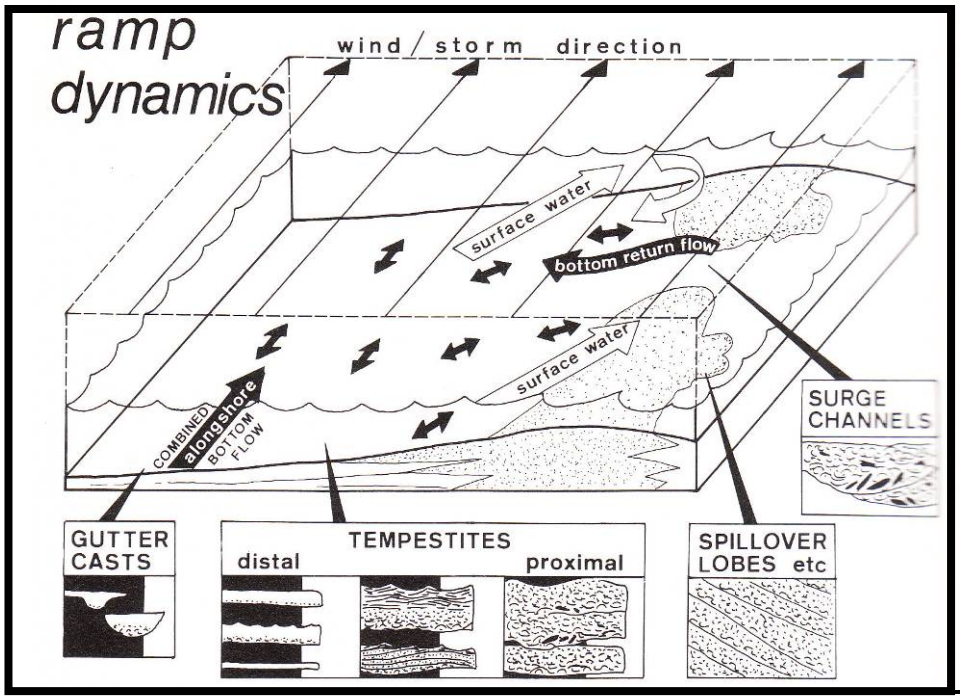

Figure 5.22 Model for the storm-dominated hydrodynamic regime and bioclastic shell accumulations on Upper Muschelkalk marine carbonate ramps. Based on in analogy with modern day shelves (Aigner, 1985).

Storm sedimentary processes, and products developed in marine environments are applied here to lacustrine settings as they both generally result in mass transport of sediment, carrying abundant shelly material. More proximal areas tend to stack several amalgamated storm beds, forming thick allochthonous shell beds with erosional bases, (Fürsich & Oschmann 1986; Goldring, 1991); whereas in distal areas, the storm beds tend to be thinner, with parautochthonous shells and interbedding of fair weather mud supported textures. Offshore they will pass into fine grained basinal muds deposited in deep, low energy environments (Fürsich & Oschmann 1986; Figure 5.23).

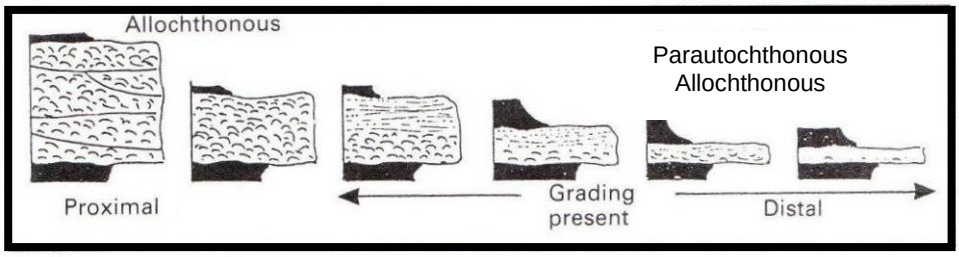

Figure 5.23 Proximal to distal sequence in a shell bed (After Fürsich & Oschmann, 1986).

Sedimentary characteristics of tempestite are not always preserved, due to the combination of different sedimentary processes acting and subsequent reworking. Figure 5.24 shows examples of commonly occurring allochthonous skeletal accumulations that are interpreted as tempestite deposits. These commonly occur with sharp or erosive basal contact. Possible storm generated structures recognized in cores from the Lagoa Feia Gp are shown and described in Figure 5.25.

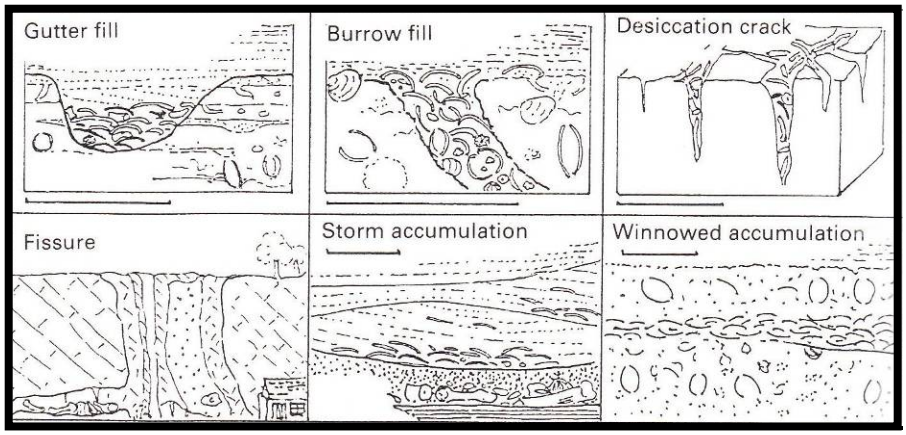

Figure 5.24 - Types of allochthonous skeletal accumulations (from Goldring 1991 after Kidwell, Fursich & Aigner, 1986). Gutter Fills, Burrow Fills, Storm accumulations and winnowed accumulations are typical of storm reworked, allochthonous skeletal accumulations Bar scale = 10 cm.

Figure 5.25a left – Bivalve rudstone (Rcb) with articulated and disarticulated (whole and broken) shells, poorly sorted. Chaotic arrangement of shells, without preferential orientation. Interpreted to have formed from a proximal storm (tempestite). Well 12 core 3 box 4 (Appendix 7).

Figure 5.25b centre Bivalve rudstone (Rmbg), disarticulated shells of bivalves and gastropods and also shale. Disperse intraclasts of shale at the base, occurring as a lag deposit of probable surge channel. Well 6 core 2 box 1 (Appendix 3)

Figure 5.25c right – Bivalve rudstone (Rmb), greenish brown 10 cm thick overlying a mudstone/wackestone (yellowish). Overlain by brown mudstone. Erosional base (possible gutter cast) and disarticulated, chaotically arranged shells suggest that this rudstone is a distal tempestite. Well 8 core 20 box 7 (Appendix 5).

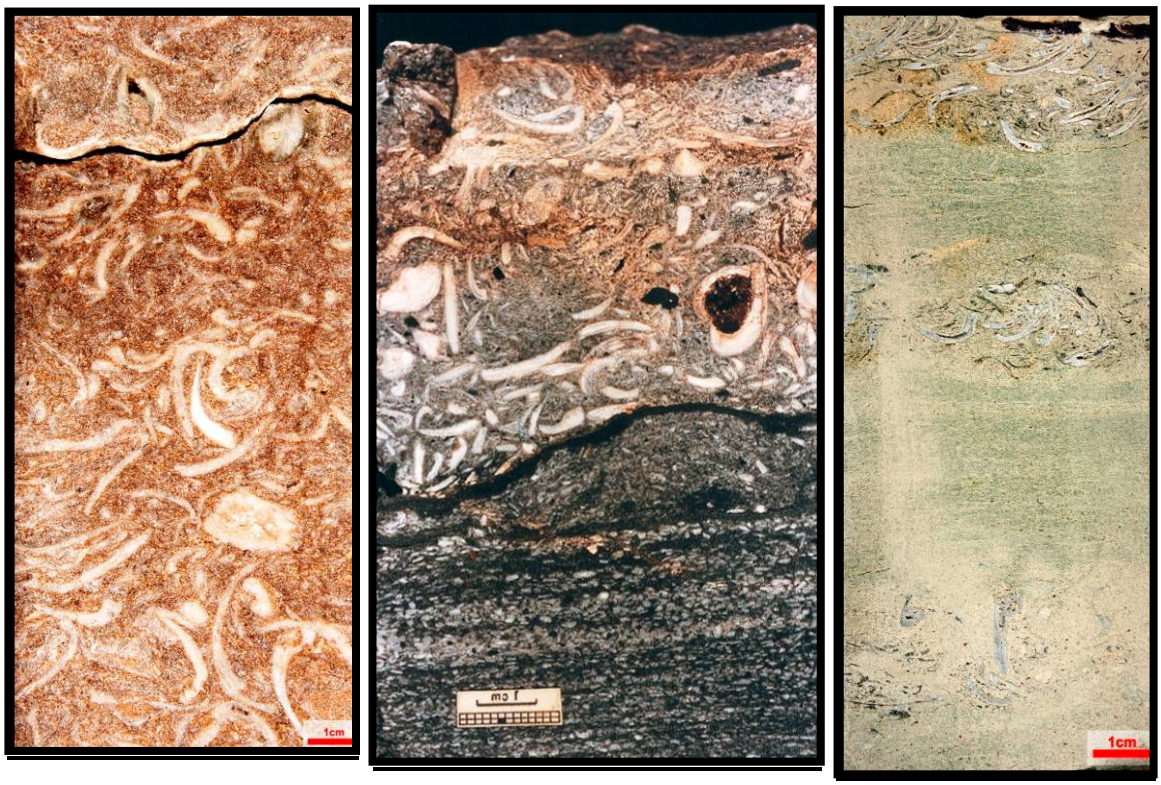

Figure 5.25d left Core slab Bivalve Rudstone (Rcb), poorly sorted disorganized and interpreted as three amalgamated beds. Disarticulated and also articulated shells of bivalves, whole, broken with little abrasion. Interpreted as proximal tempestite. Well 8 core 20 box 16 (Appendix A5).

Figure 5.25e centre – Core slab Bivalve Rudstone (Rmb), on erosional surface, showing poorly sorted, articulated disarticulated broken and rounded shells. Some intraclasts (i) and basalt (b) fragments also included. Erosional base and chaotic texture interpreted to be a proximal tempestite. Well 6 core 11 box 10 (Appendix A3).

Figure 5.25f right – Core slab Bivalve Rudstone (Rmb) 5 cm thick interbedded within green/grey siltstone. The shells of bivalves are disarticulated, mainly broken and show poor imbrication. Such occurrences are interpretated as distal tempestite. Well 1 core 6 box 1 (Appendix A1).

5.3.2. Wind-induced Waves

Wind-induced surface waves will transport and abrade sediments through the orbital motion of water particles (Figure 5.26). As a result of internal friction the energy of the wave is progressively reduced down to the epilimnium and metalimnium zones in the lake. The thermocline will baffle this turbulence and inhibit surface wave circulation in the underlying hypolimnium zone (Figure 5.26, Talbot & Allen, 1978). In this way, sediment transport on the lake floor is a consequence of the orbital velocities of water particles in the epilimnium and metalimnium zones. Fair-weather wave action is a continuous process (Talbot & Allen, 1978) and its geologic record can be found in coastal zone, high-energy, shallow-water, depositional palaeoenvironments, expressed mostly in shoreface beaches and banks (Read, 1974; Logan, 1974; Davies, 1970).

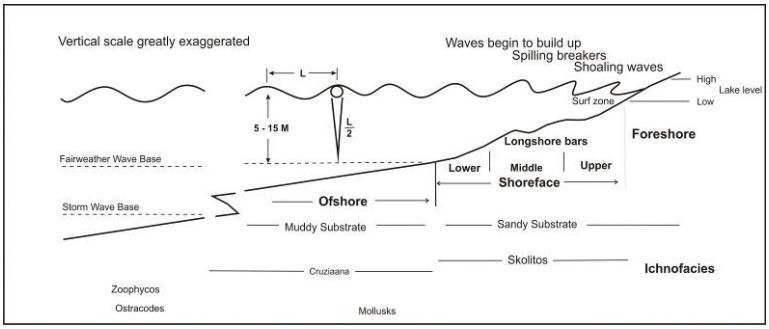

Figure 5.26 – Shoreline to shallow marine (modified from Reading & Collinson, 1978 applied to lacustrine environment) profile locating foreshore, shoreface and offshore areas. As well as fear weather wave base, and approximate ichnofacies occurrences. Note fairweather waves of wave length L, cannot agitate the bed at depth greater than approximately L/2.

In addition to sediment transport, waves may generate strong bottom currents able to erode and shape the bottom topography. Another fact to be considered is that the palaeogeography may exert a strong influence on the magnitude and products of the wave action, which are more intense and strong in windward facing coastal areas close to the shoreline (Walker & Plint, 1992). Leeward shores may form swamps (palustrine environments) with higher amounts of fine grained sediments and organic material.

The bathymetry of the lake will also have an effect on the extent of the lake floor affected by waves. In steeply sloping margins near the border fault zone, and foot-wall slopes, the wave processes will tend to form narrow and elongate zones with higher-energy grain supported textures, such as bioclastic and sandy or mixed carbonate – clastic shoreface deposits.

The latter deposits would be expected near fluvial inputs, particularly delta-mouth bars. Winnowing by wave swash and backwash may take away the fine particles of these deposits. In lake margin areas with gentler slopes, the wave action will be spread over a wider area and gradually decrease with increasing depth into sub wave-base mud supported sediments, occasional with storm reworking.

Examples of interpreted shoreface lacustrine successions are known from well 1 core 7 boxes 6 to 1 (Appendix A1). Common and diagnostic sedimentary structures observed in such depositional environments are: low-angle cross-bedding (Figure 5.27), indistinct and symmetric to asymmetric wave-ripple lamination (Reinecke & Singh, 1980). Well rounded grains of bivalves associated with quartzose sandstone are commonly present in the Lagoa Feia rudstones and these are interpreted to have formed from continuous wave-reworking in a shoreface environment (Mcglue *et al.* 2010).

5.3.3. Gravity flows

Gravitational force can move large volumes of sediment downslope (Postma, 1984). This process is episodic and is generally tectonically triggered, taking sediments from unstable areas of high relief into zones of more gentle topography. In rift basin lakes such slopes may occur close to the border faults, intrabasinal faults, or on the lake margin depositional slope. The flow may be laminar or turbulent, with plastic or fluid behaviour, and may involve low or high concentrations of particles. Both subaerial and subaqueous deposits may be generated by gravitational flow process such as deposits on alluvial fans (Figure 5.28), fan deltas and subaqueous lacustrine slopes. According to the topography gradient and the amount of interstitial water in the system, the process may evolve from sediment creep, to slides and slumps to slope aprons. Sediment textures may be matrix, or clast-supported, conglomerates (Collinson, 1978) including cohesive debris flow, paraconglomerate (*sensu* Nemec & Steel, 1984). The terminal flows may evolve into high or low density turbidity currents forming respectively muddy or sandy turbidites.

Episodic debris flows occur on gravity flow fans whereas continuous stream flow constructs fluvial fans (Postma, 1984). Blair & McPherson (1994) applied the term *gravity flow fans* to alluvial fan deposit formed by sediment gravity flows in various topographic gradients, small to high slope angle. This architectural element generally develops in arid settings on tectonically active basin margins, and adjacent to intrabasinal faults and their deposition is discontinuous as a result of sporadic and localized character of the processes (Collinson, 1978).

Gravity flows may form tens of metres of sediment (Heward, 1978a), as a product of intense tectonic activity in rift environments (e.g. Tylen & Burns, 1984; Blair, 1987b) as seen in well 9 cores 1 and 2 (Appendix A6).

Figure 5.27 – left - Core slab Sandstone fine/medium, quartz feldspar and rock fragments, exhibiting low-angle cross-stratification of abraded fragments of bivalve shells set in sandstone. Such deposits are interpreted to have formed from wave action on beach or bar. Well 1 core 7 box 3 (Appendix A1).

Figure 5.28 – right - Core slab. Clast supported conglomerate Polymictic, with fragments of sedimentary, igneous and volcanic rocks. Rock poorly sorted grains with no preferential orientation, due to episodic sedimentation. Well 6 core 1 box 8 (Appendix A3).

5.3.4. Currents

Currents in lakes are generally set up by river water inflows and persistent wind generated currents and are responsible for distribution of sediment in shallow lake areas (Talbot & Allen, 1978). As a rule the sediments are transported by traction currents in bed load and suspended load in turbulent flow regime (Collinson, 1978). These flows are usually associated with hydrographic slope, through subaerial rivers, braided or anastomosed, and subaqueous channels, which work as conduits to form lacustrine deltas. Other currents such as longshore currents are also responsible for reworking and redeposition sediments. The geostrophic effects (Coriolis force) can enhance the major water circulation (Miall, 1992). This is reported from Lake Tanganyika but it has a very low magnitude and has negligible influence on the water circulation (Naithani & Deleersnijder, 2004).

Other factor to be considered is the density difference between river and basin waters. According Bates, 1953, the river water may be more or less dense than the basin waters. The hyperpycnal flow is most frequent in fresh water lakes. In this case the river water is denser and normally colder forming density currents during floods and carring sediments into the basin beneath the basin waters. These flows bypass the shoreline and tend to deposit sediments on the lower delta front or on the prodelta (Reading & Collinson, 1978).

Coarse grained traction deposits from unidirectional currents such as cross-stratification is seen in cores from wells 1 and 6 (Figures 5.29 to 5.31).

Figure 5.29. - left - Core slab Hybrid rock, bioclastic sandstone and rudstone, with bivalve shells and intraclasts showing cross stratification. The size and shape of the shells may be due to variations on the competence of the flow, variation of the current power and source material. Well 6 core 12 box 1 (Appendix A3).

Figure 5.30. - centre - Core slab Sandstone showing cross-stratification from continuous current processes. Very fine fragments of bivalves are the white clasts. Well 1, core 2 box 12 (Appendix A1).

Figure 5.31. right - Core slab Hybrid rock, bioclastic sandstones with rounded bioclasts of bivalves, rounded intraclasts and rounded fragments of basalt. The rock shows bimodality and tractive structures of cross-stratification. Well 6 core 11 box 9 (Appendix 3).

5.4 Facies association for Lagoa Feia Group and depositional environments

Based on core logging (Appendices A1 to A7) and facies description and classification (above), the depositional facies described may be grouped into facies associations and architectural elements (Allen, 1983; Miall, 1988), as building blocks for the construction of the depositional model (Talbot & Allen, 1978). Facies associations have been defined by Collinson (1969) as "a group of facies genetically related to one another and which have some environmental significance". Four broad and distinct facies associations are recognised within the Lagoa Feia Group carbonate and siliciclastic sediments within the cored area (Figure 5.32) and are described below. More sophisticated tectono-stratigraphic models incorporating tectonic setting and seismic stratigraphic geometries are presented in Chapter 10.

5.4.1. Alluvial Fan and Plain Facies Association (AF&P-FA)

The alluvial fans occur onshore to the main lacustrine environments in the hanging wall sub-basin, close to the border fault and are represented in wells 1 and 2. They occur mainly as conglomerates, which are generally clast or grain supported. These sedimentary deposits are interpreted to be associated with braided fluvial systems that work as a conduit to transport terrigenous sediments into the basin. The occurrence of fans is restricted to the area of border faults and the fans built out basinward as sandy and muddy fluvial plains (Appendices A1 and A2). The most common facies are Conglomerate clast or grain supported (CG) and Conglomerate matrix supported (debris – CM) in the proximal area and the most common facies in the fluvial plain systems are Sc-agls, Sm-agls- Sf-agls. These facies occur in the wells 1 and 2 and represent the distal part of the alluvial fan and plain facies association.

5.4.2. Deltaic and Delta Margin Facies Association (D&DM-FA)

This system occurs on the border of the lake, where distal alluvial systems enter the aqueous environment. It comprises siliciclastic deltas at the mouths of rivers together with the delta slope, and mixed carbonate-siliciclastic shoreface deposits marginal to the delta. Such associations have been classified as high-energy, Bench type Margins (Wright, 1992), with the greatest facies diversity of the system. The siliciclastic system is represented by medium to fine grained sandstones (facies Sm-agls- Sf-agls)

interpreted to have formed in the distributary channels of the deltaic system. The finer grained facies of this association are considered to be channel-levee and delta plain deposits, and are predominantly represented by siltstones and shales (ST- SH). This association may occurs interbedded with thin and very thin sandy facies (Sf - agls, Smf – agls) that are interpreted to have formed in a deep lake environment. Similarly, this association also comprises the more distal portions of prodelta and delta front, where deformed or slide and slumped deposits (SL), and also sandy turbidite deposits are observed (Wells 1 and 2, Appendices A1 and A2). These turbidites are interpreted base on characteristic structures such as, sharp erosional bases and load and flame structures in the base of the thin sand beds.

In the lateral marginal portion of the deltas, sandy shoreface deposits may be reworked (facies Sm – Sf) and pass laterally into mixed carbonate-siliciclastic deposits such as bioclastic-rich sandstone (facies Sf - Svf) or sandy grainstone and rudstones (facies Gcb, Gm-b and Gf-b, and Rt-b). The shelly shoreface deposits also occur on the delta top (e.g. Well 1) that comprise in most cases facies: Gf - b, g, Gm-b, g, Gc-b, g - Rom-b, g, b-Rt-, g - Rc-b, g. Close to the slope reworked sedimentary deposits formed by alongshore currents may occur as recognised by the persistent preservation of tractive structures.

5.4.3. Deep Lacustrine Facies Association (DL-FA)

This is the deepest subaqueous sedimentary environment of the continental rift system. Most of it occurs below storm wave base, in the hypoliminium zone, where there is evidence of low-oxygen conditions such as preservation of organic matter and laminated muddy deposits. Quite commonly these deposits are characterised by the presence of ostracods. The DL-FA comprises interbedded siltstones, mudstones and shales (SH – ST), and distally by fine grained facies such as MR - WK and MD. The interbedding of these facies can relate to climatic changes (Platt & Wright, 1992). Close to the toe of the slope of the delta front, turbidite deposits may also occur (Well 1 and well 2, Appendices A1 and A2).

5.4.4. Lacustrine Carbonate Platform Facies Association (LCP-FA)

Shallow lake environments isolated from siliciclastic supply commonly accumulate thick successions (hundreds of metres) of bioclastic carbonates. These are referred to as high energy ramp platform border type by Platt & Wright (1992), but

because of the thickness and lateral extent, the range of facies and different settings developed in the Campos Basin they are here regarded as carbonate platforms in their own right. Bioclastic banks and bars of bivalves and, less commonly gastropod rudstones are common, and normally occur stacked; forming packages of sediments many tens of metres in thickness. These shallow-water facies pass laterally into the deep lake with lower energy facies with thinner beds of bioclastic packstones and mudstones or rudstones, which are usually ostracod-rich.

The LCP-FA, is represented by the following facies: Rm-b, g; Rt-b, g, o; Rc-b, g, o; Fb, g; Gf - b, g, o, p; Gm-b, g, o, p and Gc b, g, o, p. Such facies are interpreted to accumulate on bars, banks and shorelines in shallower moderate to high energy settings. Finer-grained facies MD, WK, Pb, g, o, p, occur in more distal and deeper settings at or below the metalimnium wave-base. Redeposition of sediments may occur in washover deposits that occur as reworked facies. Also, the peloidal facies may occur in more protected areas.

In periods of arid climate and probably closed lake conditions, the shallower areas may develop autochthonous microbial facies association that is are more common in the Aptian succession, of the Macabu Formation. These are commonly found in more distal site, e.g. well 20 and information is based mainly on FMI data that is presented in Chapter 7.

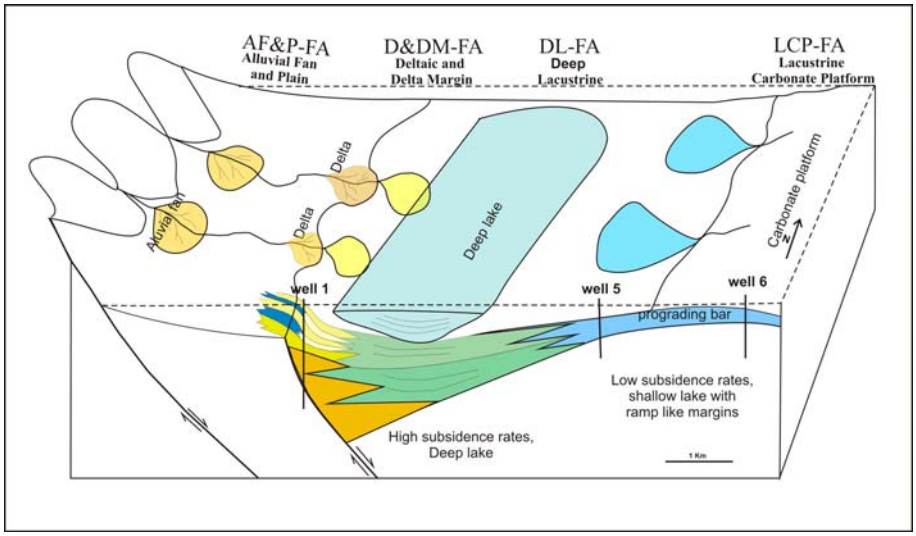

Figure 5.32. A general 3-D diagram of the Barremian Lagoa Feia Lake with some of the processes and relation with the 4 facies associations identified based on core log (mod. from Platt & Wright 1992).

5.5. Facies model for the Lagoa Feia Group, core based (coquina succession).

The lateral and vertical depositional facies variations in continental lake environments are a product of several factors acting together to form the sedimentological record. Some facies are formed and preserved *in situ* (autochthonous) or undergoes a small amount of transport (parautochthonous). However, many facies undergo reworking and transport by hydraulic processes (above) to form the final deposits (allochthonous). Unlike the marine environment, where eustacy and subsidence are key factors on the control and distribution of carbonate facies, in extensional continental tectonic setting, several factors act integrated to form the complex arrangement of sedimentary facies (Gierlowski-Kordesch, 2010). Thus, the climate changes provide an external control on sediments and the productivity of carbonates. The tectonic environment of extensional rifts moulds the overall accommodation space and the palaeogeography. Moreover the physical processes, such as waves and currents storms works on the sediments to shape the final carbonate deposits (Talbot & Allen, 1978).

Several authors (Castro & Azambuja Filho, 1980; Praça, 1996; Carvalho *et al*, 2000) have proposed facies models specifically for the Lagoa Feia carbonate rock successions of the Campos Basin. Such models are generally based on the sedimentological framework, focusing on facies association, fossiliferous content and architectural elements. Other authors have proposed an association between tectonics and sedimentation for the same lithostratigraphic unit (Abrahão & Warme, 1990; Rangel & Carminatti, 2000).

Based on some characteristic lacustrine lithofacies assemblages and absence of typical stenohaline marine organisms, Schaller (1973), Bertani (1984) and Carvalho *et al.* (1984) state that the Lagoa Feia Group was deposited in an alluvio-lacustrine complex. Abraão & Warme (1990) based on open-hole logs, cutting and core samples, proposed three depositional environments for the Lagoa Feia Group: alluvial fans, exposed lake-margin mud flats, and sublacustrine deposits. Various sub environments were recognized with further detailed core analysis.

As with the classic standard facies zones of Wilson (1975), where lateral changes in the biota and sediments are related changes in bathymetry, Fair Weather Wave Base (FWWB) and Storm Wave Base (SWB) and sea surface; the facies model proposed here, is an attempt to summarize the facies distribution along a hypothetical

transect from the northwest on the coast, through shallow subaerial and subaqueous sites to the deeper water areas in the southeast of the basin. This model, therefore, is constructed based on well data analysis of facies (above) and in particular the vertical association of facies using Walther's Law (in Walker, 1992). The tectonic structural model erected (see chapter 4), was used as background to the understanding of the carbonate depositional sites and this is used to erect the tectono-stratigraphic models in subsequent chapters (9 and 10)

As a next step, four main depositional environments are defined below which relate, in part, to the facies associations described and interpreted above: deep subaqueous, intermediate subaqueous, shallow subaqueous and emergent. Figure 5.33 shows a schematic facies model for carbonate rocks of the Coqueiros Fm of the Lagoa Feia Group based on the core logging of rocks.

5.5.1. Deep subaqueous

The deep subaqueous environment can be subdivided into two sub environments, below and above storm wave base (SWB) (Figure 5.33). Below storm wave base, in the hypoliminium zone, laminated and non-burrowed sediments are found, the result of the seasonal climate changes and lake fluctuations. In this low-energy, anoxic, basin floor environment, shales and mudstones with organic matter and early diagenetic pyrite is found. These are generally non-fossiliferous, lacking benthic organisms. However, some bottom currents allow the presence of ostracods, which are organisms resistant to environmental stress conditions (Silva Telles, 1992). Although being characterized by thin laminated facies; rare decimetre deep tempestite and turbidite beds may also occur in this environment.

In more basinward half-graben areas the trend is to find fine grained chemical or bioinduced sediments, such as mudstones, below SWB. In slightly shallower proximal positions marls occur. They are typically laminated and weakly to moderately bioturbated, indicating more oxic conditions. This equates to the Deep Lacustrine facies association (DL & FA) described above.

Within the zone between SWB and FWWB, where there is a greater productivity of bivalves, the carbonate biogenetic factory, can form *in situ* or parautochthonous deposits with articulated shells commonly buried in life position that grade in shallower areas to the deepest portion of the bioclastic packstone / grainstones textures with an

ostracod-rich muddy matrix. This area below fair-weather wave base may be influenced by storms (see above).

5.5.2. Intermediate subaqueous

The intermediate subaqueous zone is the zone of highest energy deposition, influenced by sporadic storms, infrequent but of high magnitude that are responsible for the bulk transport of skeletal grains. Continuous wave action is responsible for the swash and continues reworking and winnowing of skeletal grains. These shallow water sediments, consists of rudstone banks, shoals, beach ridges and also shoreface deposits. Disarticulated and broken shells of bivalves are quite common. Bioclastic grains may be abraded, showing rounded grains when associated with quartz grains. These sediments may form thick amalgamated packages of coquina deposits normally along the margin of the lake and includes the lacustrine carbonate platform facies association.

In the back of shoal zones, in protected areas, lacustrine oncoid rudstones (Figure 5.12) and also peloidal packstones are formed. The bivalve rudstones can occur with peloidal matrix due to remobilization of bivalve shells from the banks or shoals into the lagoon. In periods of low lake level, ooids and shallow water microbial deposits, associated with siltstone and distal terrigenous deposits may be formed.

5.5.3. Shallow subaqueous

In the shallow subaqueous environment the microbial deposits can occur interbedded with siltstones and terrigenous sediments. Normally mixed carbonate and terrigenous sediment are interbedded, due to fluctuations of the lake level. Sand flat and mud flat may occur from the influence of the alluvial, fluvial and lacustrine system in marginal areas. However, basinward, purer carbonate lithologies occur as indicated in the Delta and Delta Margin facies association (D&DM-FA).

5.5.4. Emergent

In the emergent carbonate areas features of exposure are observed such as karst, cracking and brecciation, desiccation features related to subaerial exposure due to periodic or seasonal variation in lake level. Close to the border faults the Alluvial Fan and Alluvial Plain facies association occurs (AF&P-FA).

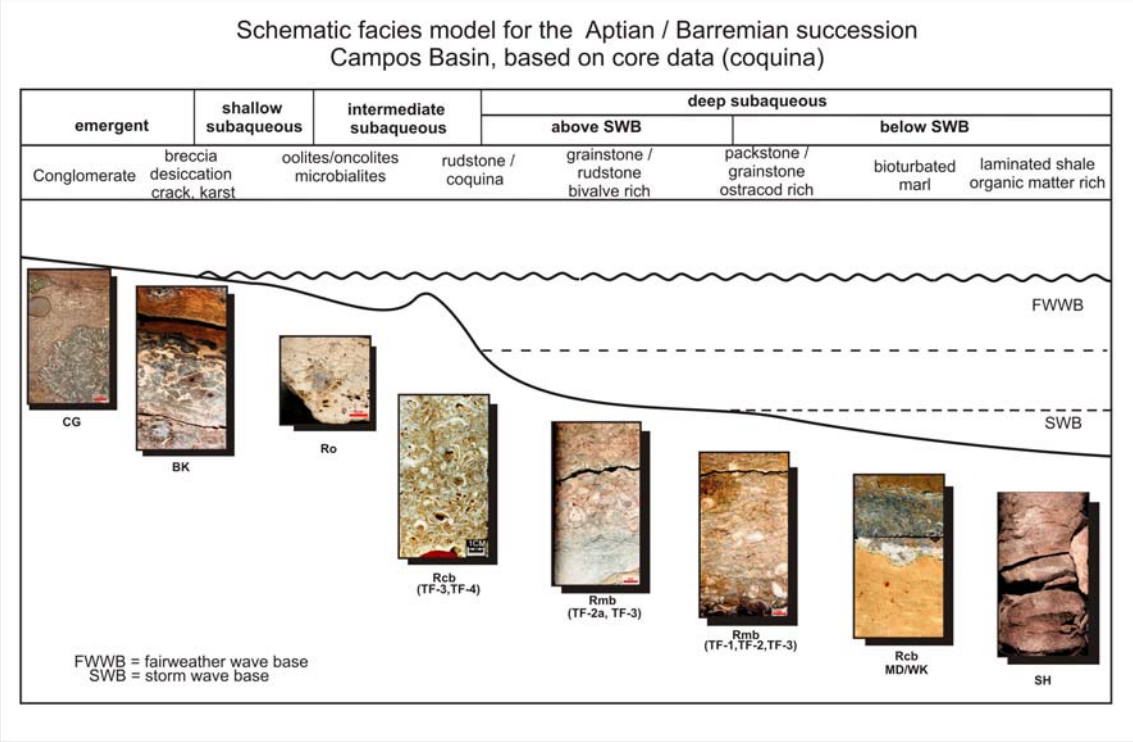

Figure 5.33 – Schematic facies model for the Barremian/Aptian succession, Lagoa Feia Group – Based on core logging - Coquinas.

Figure 5.34 shows the basic stacking pattern of an elementary metre-scale, T-R of high frequency. In this model packing, grain is not considered. This simple unity is considered in Chapter 8 in the stratigraphic analysis, stacking pattern and cyclicity.

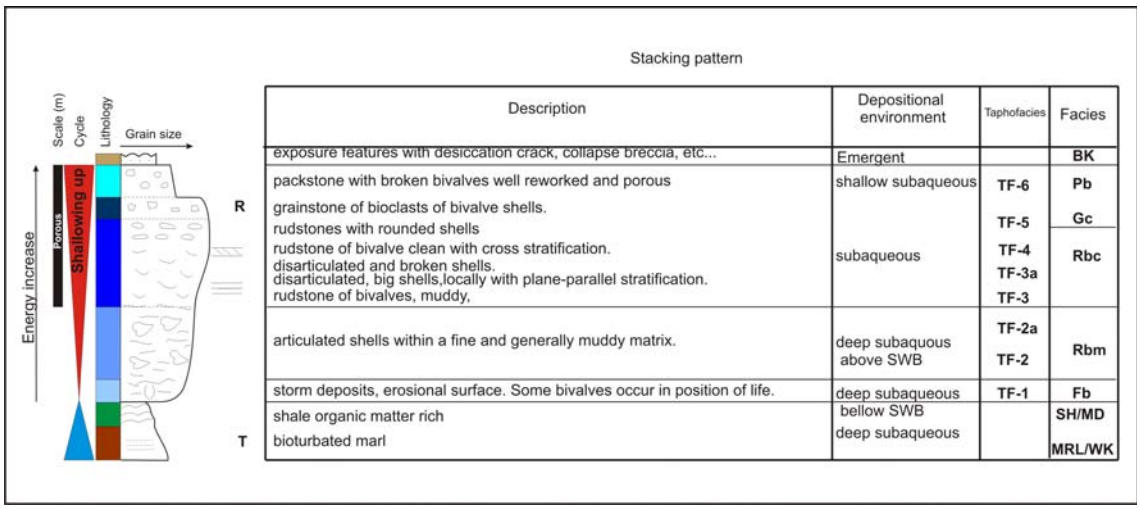

Figure 5.34 – Basic metre shallowing up cycle, lithofacies and taphofacies core based of the Lagoa Feia Group.

5.6. Palaeoecology and Palaeoenvironments

Fossiliferous sediments of the Lagoa Feia Group were deposited from the late Barremian up to the mid Aptian. This geologic record comprises abundant low-diversity

biotas which may represent opportunistic species due to lagoonal conditions, a series of lakes (Hessel, 1992). The main elements of the fauna in the study area are non-marine molluscs, bivalves, gastropods and also ostracods.

Eight species of bivalves are recognized: *Angelasina* cf. *A. plenodonta* Riedel, 1932, *Arcopagella*, longa n. sp, *Camposella rosea* n. gen et n. sp, *Desertella acarenata* n.sp, *Kobayashites brasiliensis* n. sp, *Remondia* (*Mediraon*) *magna* n. sp, *Sphaerium* cf. S. *ativum* White, 1987, *Trigonodus camposensis* n. sp. and *Angelasina* cf. ***A.*** *plenodonta* Riedel, 1932. With exception of *Sphaerium*, all are endemic to the offshore Brazilian basins. *Sphaerium* cf. S. *ativum* White, 1987, is found in Africa (Camaroon, Nigeria, Gabon and Congo) as well as elsewhere in Brazil (Bahia). Almost all the species have a seminfaunal habitat living in soft substratum, but also infaunal (*Sphaerium* and *Arcopagella*) and epifaunal (*Desertella*) on a hard substratum. Their trophic group are suspension feeders, except *Arcopagella* which is a sediment feeder (Hessel, 1992). The suspension feeders would have lived off lacustrine zoo- and phyto-plankton and algae, with the sediment feeders, subsisting from muddy sediments. They live in the subaqueous environment, below FWWB (see following chapter 6) but are thought to be carried to shallow zones by storms, where they are reworked to form the coquina deposits. After deposition, they can be reworked and retransported by other processes such as turbidites or channels and longshore currents. Coquina accumulations have also been documented in the Congo Basin in Barremian – Aptian carbonate of the Toca Formation (Harris *et al.* 2000).

Gastropods occur mostly in the mid Aptian. In the Campos Basin the most frequent are pulmonate gastropods from the family *Limneidae*, typical of fresh waters and considered by Carvalho *et al.* (1995) as living in the vicinity of river mouths. In this site it is quite common to find fossil fish of the Pycnodontidae family, genus *Pycnodus* (Gallo oral communication, 1995). This is a potential predator of the benthic molluscs and some crustaceans (Carvalho *et al.* 1995). The concentration of shells in the mid Aptian is not fully understood. Possibly this is a more freshwater interval but charophytes are rare. Alternatively it may be a preservational feature as thin shelled gastropods may fill with gas / air and float and drift to landward to form littoral shell beds. Considerable gastropod accumulations are been reported from shallow shorelines of the present day Lake Tanganyika (Mcglue *et al.* 2010).

Subordinately, fish, reptiles, algae and planktons (zoo and phyto) have been reported. Although figure 5.4c shows a component of the rock similar to a charophyte,

diagnostic charophytes were not identified in any quantity to provide evidence for a fresh water environment in any of these rocks. Musacchio (2000) also records an absence of charophyes in these offshore Brazil basins but, probably incorrectly, attributes this to Petrobras wells only sampling deep-water facies. Both deep and shallow water facies are sampled in this project. Although it has been considered non-marine or brackish because of the absence of both marine and freshwater fossils, there is evidence, presented by Hessel and Mello (1987), Silva Telles (1996), in the Aptian succession, of intermittent (periodic) marine incursions. In rock extracts analysis of organic rich shales (Hessel & Mello, 1987) describe biomarkers such as 24-*n* propilcolestans, C_{30} esterans, and biomarkers typical of marine environments associated with Chrysophytes. Hessel & Melo (1987) also record the presence of the bivalves *Angelasina* and *Remondia* characteristic of marine environments. Finally, Hessel (1992) attributed the presence of the pigment beta-carotene within preserved pink coloured bivalve shells as suggesting marine conditions. Some authors (Silva Telles, 1996) show evidence of marine forams and carbon and oxygen stable isotopic data to emphasize this view and this is discussed further in Chapter 10.

Castro & Azambuja Filho (1980) followed by Carvalho *et al.* (1984) suggest saline and alkaline conditions for the palaeolake water chemistry and Bertani and Carozzi (1985a, 1985b) oscillations in the lake water salinity. According to them, in more saline conditions, ostracods dominate and early diagenetic dolomite occurs whereas in less saline conditions, bivalves abound.

Other components such as peloids, ooids and oncoids in minor quantity also compose the sedimentary record of the carbonate rocks. The bivalves are the most abundant skeletons organisms in the period from late Barremian to Early Aptian and after long-term environmental change, in the mid Aptian, when extinction of molluscs occurred and were replaced by a bloom of microbialites.

5.7 Conclusions

This chapter includes results of the main facies that are seen in the cored intervals of the Coqueiros Formation of the Lagoa Feia Group.

The main findings are:

- The Coqueiros Fm comprises mixed carbonate and clastic lithologies and is best classified by a combination of the Dunham (1962) and Embry &

Klovan (1971) scheme for carbonates, further subdivided on the basis of composition and amount of matrix, the Wentworth scheme for siliciclastics and an informal scheme for various deformed and diagenetically altered facies.

- 13 carbonate facies are described, illustrated from split cores and thin sections and their depositional environments briefly discussed. The most abundant facies are bivalve-rich rudstones or coquinas, with 6 subfacies.
- Similarly, 7 siliciclastic facies and 4 deformed and diagenetically altered facies are considered.
- The depositional processes and environments represented by the lagoonal facies of the Lagoa Feia Gp and conclude and give examples from the cored intervals of deposits formed from storms, wind-induced waves, gravity flows and unidirectional currents.
- The facies are then discussed in more detail in terms of their associations and depositional setting within the Lagoa Feia lacustrine basins and the following facies associations are described: Alluvial Fan and Plain FA, Deltaic and Delta Margin FA, Deep Lacustrine FA and Lacustrine Carbonate Platform FA.
- A facies model is presented for these rocks based on their interpreted depositional environments and the association of the facies in vertical cored intervals. This is presented as a shore to basin cross section from emergent siliciclastic facies, through lake margin carbonate rich facies to deep water, basinal shales.
- Finally the various lines of palaeontological evidence for the nature of the lacustrine environment are presented based on this work and the literature which concludes that the lake was mainly non-marine brackish water from the abundance of brackish water bivalves and the absence of both evaporites and of charophytes. However more marine and freshwater intervals are suggested from palaeontological evidence.

CHAPTER 6 - TAPHONOMY OF THE BIVALVE RUDSTONES AND FLOATSTONES

6.1 Introduction and review

Conventional methods used for the study and interpretation of depositional palaeoenvironments, group biofacies, lithofacies into facies associations, depositional elements and then depositional environments. Additional methods such as chemical analysis (e.g. isotopes), specific palaeontological studies and others may also be needed in order to supplement palaeoenvironmental interpretation. The variety and complexity of facies that occur in the mollusc-rich limestones of the Coqueiros Formation of the Campos Basin means that a more detailed approach than the textural classification presented in Chapter 5 is needed to understand the environment of formation and accumulation of these coquinas.

For this reason, taphonomy has been used as an additional tool in the study of these carbonate rocks for the understanding of all physical and chemical, from sedimentary processes through to the diagenetic transformations. The first part of this chapter is concerned with the taphofacies of the coquinas and then the diagenetic transformations that have occurred in these rudstones are assessed through thin section and cathodo-luminescence studies.

6.2. Biostratinomy

The term taphonomy was first coined by Efremov (1940), and is defined as the science of fossil preservation (Martin, 1999). The taphonomy of the biogenic components ranges from *post-mortem* to diagenesis. Some authors, however, also consider tectonic uplift as part of taphonomic studies (Fig. 6.1). Taphonomy can be subdivided into two major parts: 1) biostratinomy, which comprises the sedimentary history of the skeletal grains, since the death of the organisms, decomposition, transport and burial; 2) fossil diagenesis, completes the process by documenting the physical and chemical changes of the fossils during and after burial (Seilacher, 1976; Flessa *et al.* 1992).

Following death, molluscs show evidence of having undergone various consecutive and overlapping taphonomic processes (Goldring, 1991). Initially transport, breakage, sorting and reworking of the shells by water, and damage by

predators and scavengers takes place (Figure 6.1). Skeletons usually pass through "taphonomic filters" before forming the final death assemblage (Kidwell & Bosence, 1991). The most severe processes of taphonomic data loss are: fracturing, abrasion, bioerosion and dissolution (Martin, 1999). Shells that survive these destructive processes form the fossil record (Kidwell & Bosence, 1986). In this sense, the balance between destruction and preservation of skeletal grains must be positive (Figure 6.1). Encrustation and early diagenetic processes can significantly increase the preservation potential of shells (Mcglue *et al.* 2010). The fossil assemblage, then, is modified prior to its final incorporation to the sediment, where compaction, chemical changes and diagenesis take place within the sediment and with burial.

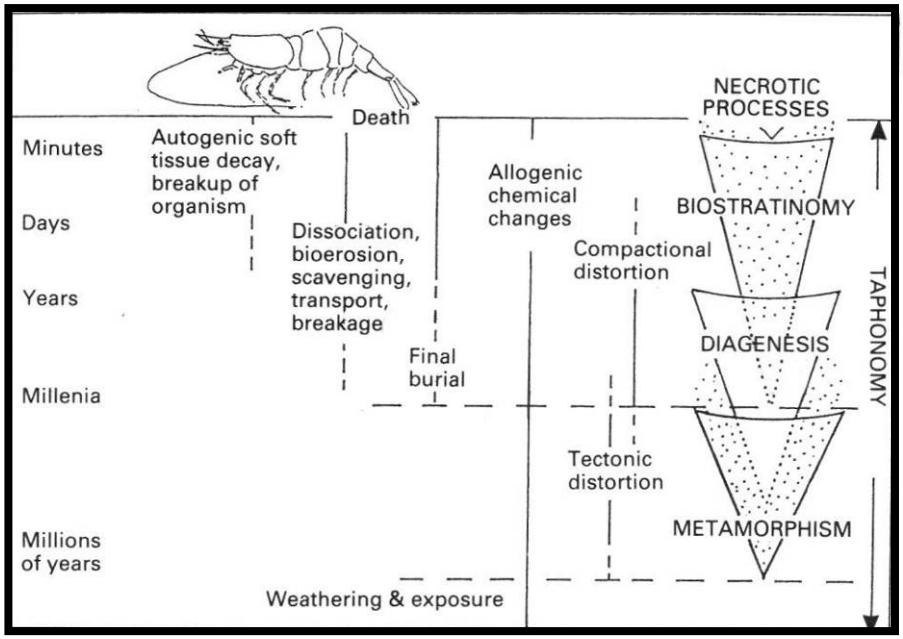

Figure 6.1 Taphonomy and its associated processes (Goldring, 1991).

6.3. Taphofacies

Taphonomic processes that take place in different depositional settings, promote differential preservation of fossils within facies (Martin, 1999). Brett & Speyer (1990), state that "taphofacies consist of a suite of sedimentary rocks characterized by a particular combination of preservational features of the contained fossils". In this work, a taphofacies is considered as a group of similar features of living conditions, organism's habitat, degree of hydraulic reworking acting on skeletal grains, degree of transport (within or out-of-habitat transport) and the position and sedimentary textures of the shells after transport.

Taphofacies therefore characterise more features of these shelly limestones than are considered in the Folk (1962) and Dunham (1962) or Embry & Klovan (1971) textural classifications. However, the basis of these textural classifications are still relevant in that the facies can be ordered into a trend from lime mud rich, lime mud with allochems and winnowed or mud-free allochems, to porous textures with sparry calcite cement fabrics. In this way the textural classifications of Chapter 5 indicate a direct association with hydraulic energy and with the maturity of the depositional process. Such processes evolve from winnowing, sorting, and rounding to textural inversion where rounded, highly abraded and very broken grains may be formed (Folk, 1962 - Figure 6.2).

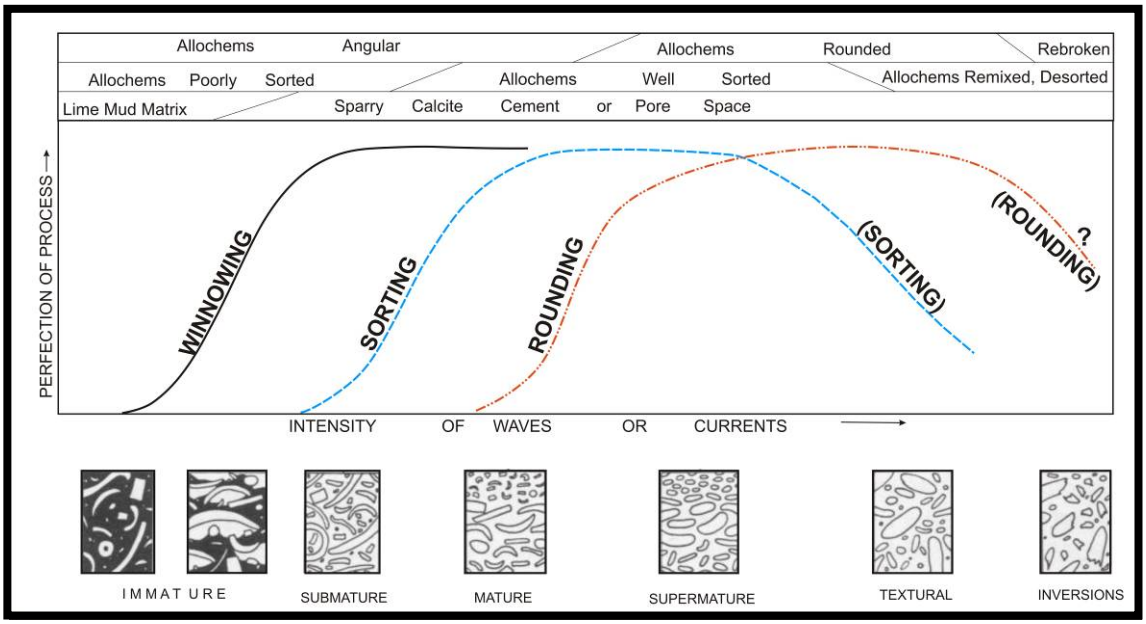

Figure 6.2 – Sketch illustrating the effect of the intensity of hydrodynamic process on texture and maturity of carbonate sediments (After Folk, 1962).

However, many facies from these non-marine carbonate rocks cannot be fitted into the classic textural classification schemes. Large, heavy shells of bivalves within deep lagoon mud and rudstone of molluscs or gastropods with peloidal matrix are such examples. Similarly the proportion of *in situ* preserved shells to transported shells cannot be characterized. For this reason, this chapter aims to give a different approach for these problems.

Since this early work, various authors have proposed contributions for a better understanding of this complex subject. Several attempts have been made to characterise and classify the physical, chemical and biogenic processes in taphonomy

(Kidwell 1993; Kidwell & Bosence; 1991, Behrensmayer *et al.* 2000; Holz & Souto-Ribeiro, 2000; Holts & Simões, 2005, amongst others). These include grouping genetic types of skeletal accumulations, position of the shells in the fossil record, hard part orientation and the implications of these interpretations to hydraulic energy, depositional processes and depositional environments. The application of this method is useful for sequence stratigraphic analysis and in the temporal resolutions of fossil concentrations studies (Holts & Simões, 2005).

Kidwell *et al.* (1986) developed a descriptive nomenclature and genetic classification of hard part concentrations consisting of end members and mixed assemblages emphasizing the genetic significance of biostratinomic factors (Figure 6.3).

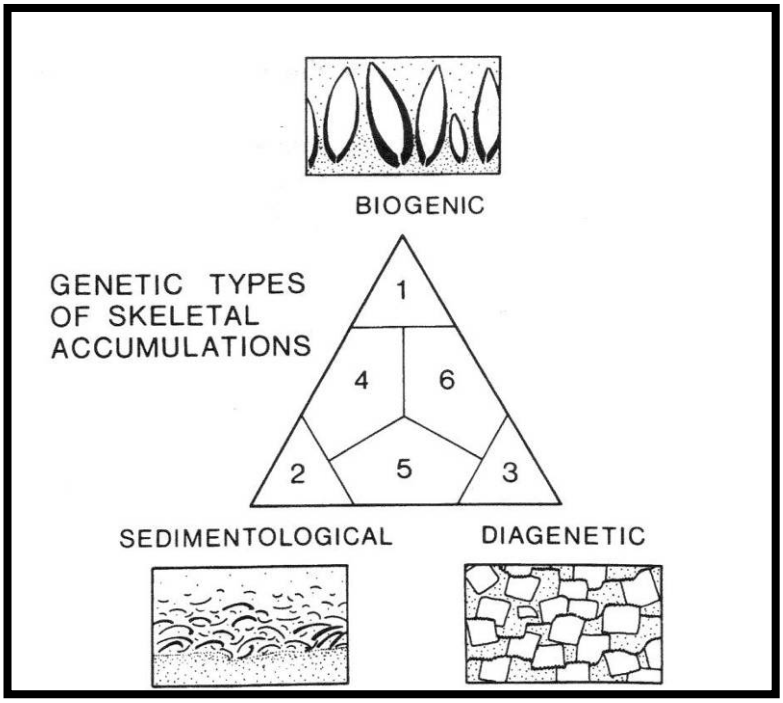

Figure 6.3 Genetic classifications of hard part concentrations consisting of end members and mixed shelly assemblages (Kidwell *et al.* 1986).

Kidwell & Bosence (1991) characterised not only the type, size, sorting but also the position of shells after post-mortem. They pointed out the significance of the position of shells for palaeoenviromental studies; such as concave-up, convex up, imbricated, disarticulated, whole, broken or rounded fabrics and textures. A specific terminology was proposed for hard part orientation and biofabrics (Figure 6.4).

Menard & Baco (1951) demonstrated that single valves buried in flume tanks, almost always tend to occur convex-up. Convex-up is common under traction flow.

These orientations are common in wave-swept shallow marine settings and turbidite deposits (Clifton & Boggs, 1970). The flume current velocities can also result in mixture of concave-up and concave-down shells (Mercand & Bancont, 1951). So concave-up and concave-down orientation of valves are not flawless indicators of environmental water energy or the top and bottom of beds (Kidwell & Bosence, 1991). However, the biofabric and the orientation of the shells are effective indicators of water energy levels and bottom currents. High energy conditions normally show imbrication, cross-bedding, stacked shells and depositional breccias (Flügel, 2004). On the other hand, low and moderately energy conditions are indicated by thin, platy skeletal grains, variable shell orientations, matrix supported textures, normally with plane-parallel orientation or a bioturbated fabric.

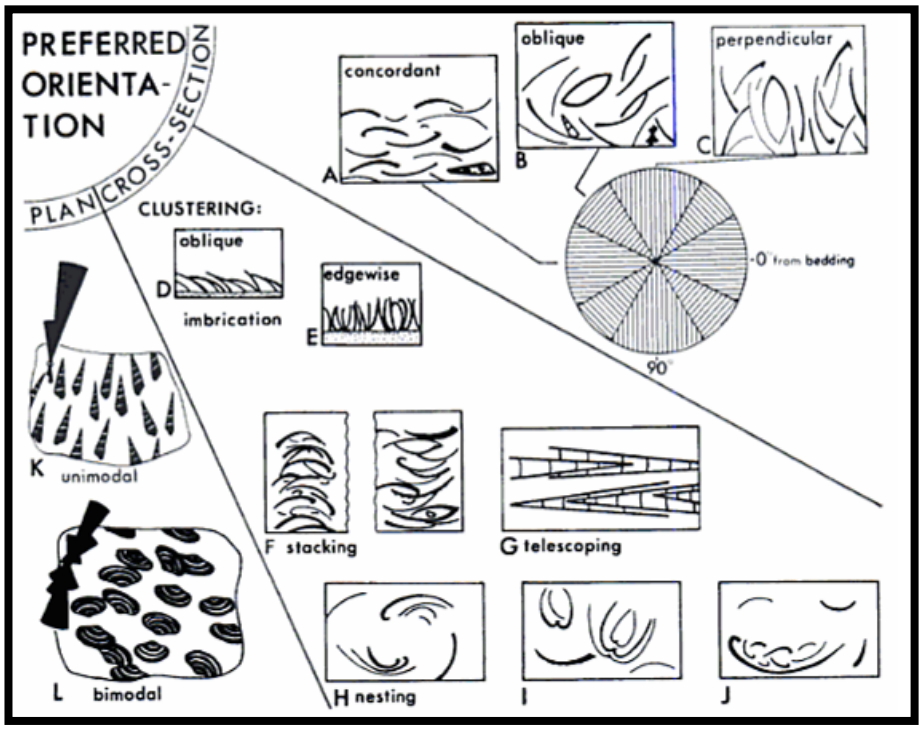

Figure 6.4 Terminology for hard part orientation and biofabric (Kidwell & Bosence, 1986).

Goldring (1991) presents a general model for the taphonomy of bivalve shells (Figure 6.5). This scheme is very useful in the description and understanding of the diagenesis processes and diagenetic evolutionary history discussed in the section 6.4.

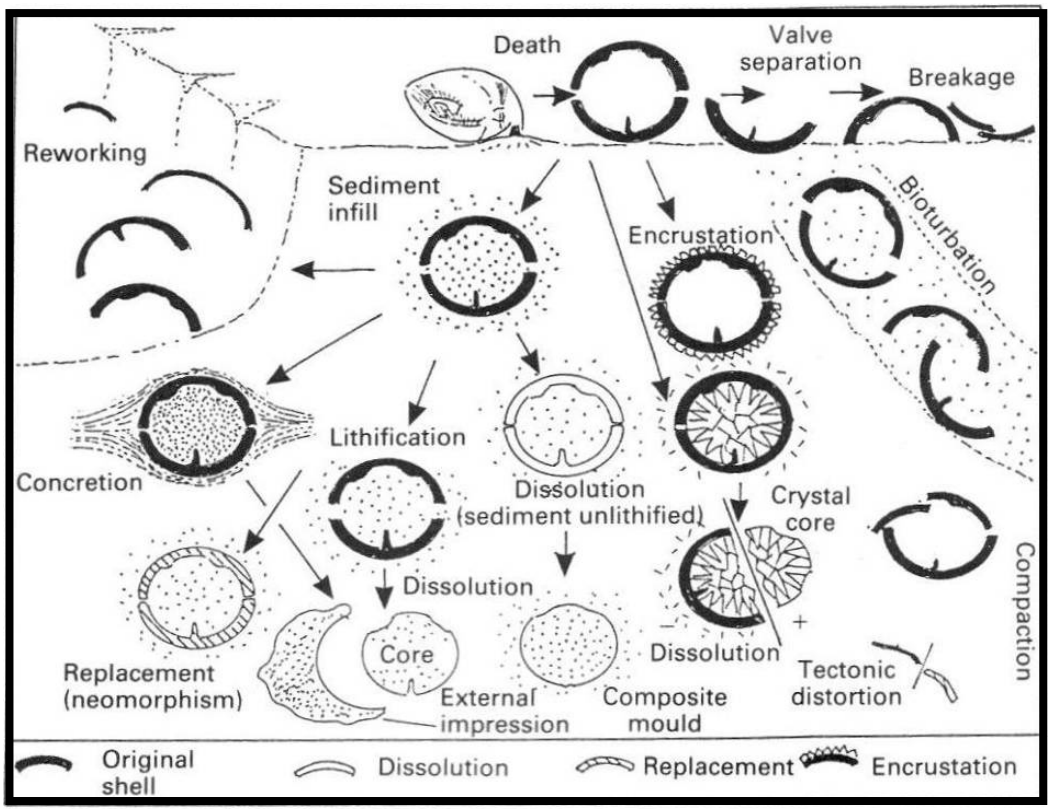

Figure 6.5 General model for the taphonomy of bivalved shells (Goldring, 1991).

Considering the conceptual background exposed above, a taphonomic classification was erected in this work focusing on the degree of hydraulic reworking and transport of bivalve skeletons and their preservation (Figure 6.6). Ten taphofacies have been identified which are grouped into autochthonous, parautochthonous and allochthonous fabrics. Taphofacies resulting from mixed terrigenous / carbonate sediments and intrabasinal carbonate rocks are also included (Figure 6.6). These are original attempts to organize the taphonomic concepts and group them into comprehensive taphofacies so that they can be applied to the subsequent stratigraphic studies, stacking patterns and cyclicity analysis, as seen in the following chapters 7 and 8 and as recorded in the core logs (Appendices A).

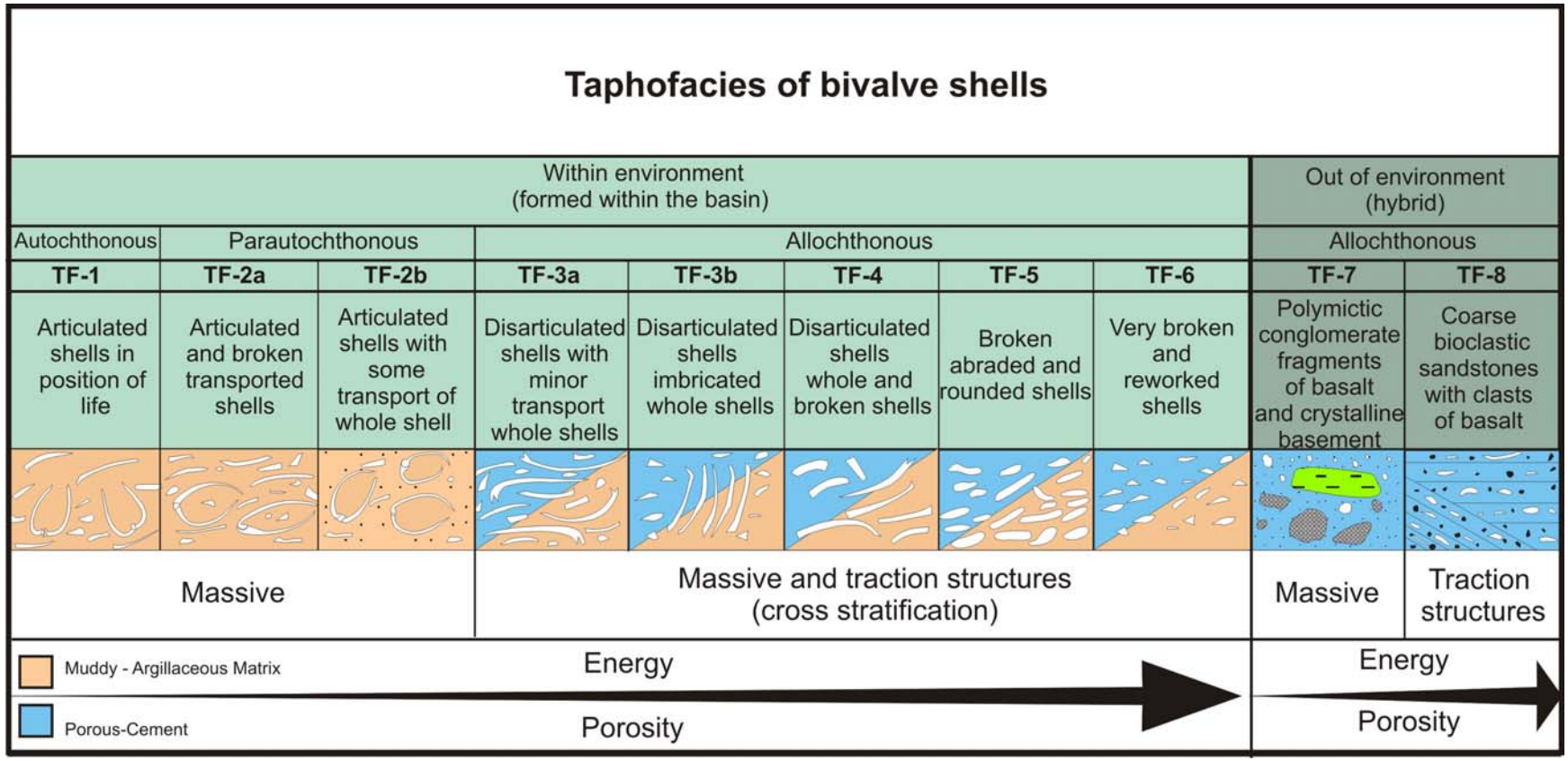

Figure 6.6 Taphofacies of bivalve shells rudstones and floatstones of the Coqueiros Formation (brown colour– matrix and blue – porosity / cement.

Within environment

Autochthonous

TF-1 Articulated shells in position of life

This taphofacies comprises rudstones and floatstones with articulated shells of bivalves in position of life without any evidence of transport. The matrix is muddy, locally peloidal but almost always rich in ostracods. This taphofacies with the in-place preservation of bivalves and the fine grained matrix and rudstone to floatstone fabric is interpreted to have formed in a low energy depositional environment and muddy sediments. It is considered to have formed below fair weather wave base but in an oxygenated lacustrine zone (Figure 6.7 a).

Parautochthonous

TF-2a Articulated and broken transported shell

This taphofacies comprises rudstones and floatstones with articulated shells of bivalves but not in their life position. There is some evidence of transport with some broken shells set within a muddy matrix. It is also interpreted to have formed in a low energy environment, occurring below wave base in an oxygenated zone (Figure 6.7 b).

TF-2b Articulated shells with some transport of whole shell

This taphofacies comprises rudstones and floatstones with articulated bivalve shells, disarticulated and broken shells and all within a muddy matrix. Commonly the internal sediment of the articulated shells is different to that of the matrix thus indicating a degree of transport from the original life habitat. This taphofacies is associated with a moderate energy environment with some transport of whole shells. This is considered to occur in a subaqueous environment at or around wave base (Figure 6.7 c).

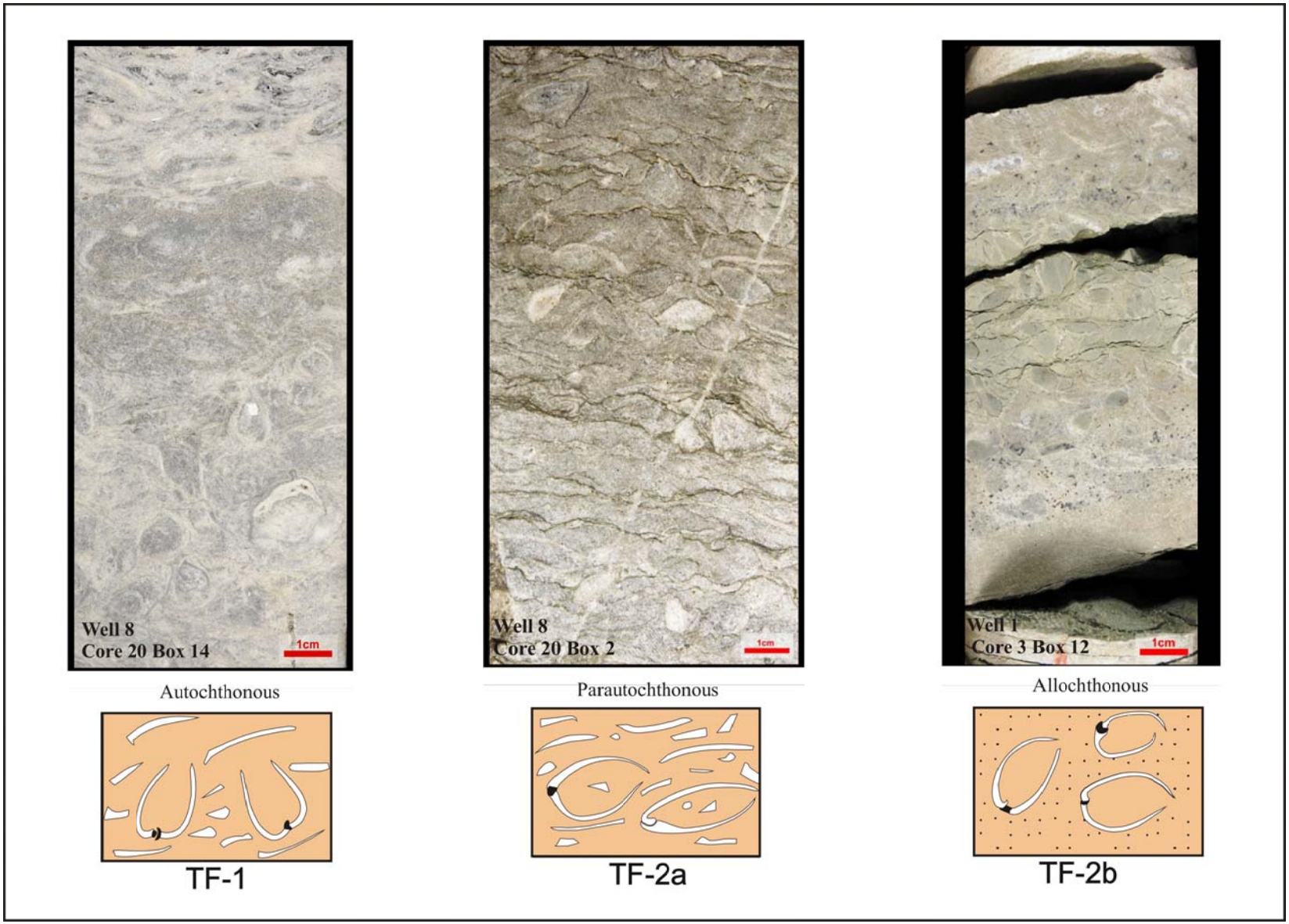

Figure 6.7 Taphofacies within environment autochthonous, parautochthonous and allochthonous a) Taphofacies 1 b) Taphofacies 2a c) Taphofacies 2b

Allochthonous

TF-3a Disarticulated shells with minor transport of whole shells

This taphofacies comprises rudstones with disarticulated and whole shells of bivalves. The shells commonly show no preferential orientation, but they may occur oriented parallel to bedding (Figure 6.8a).

Shells are also broken and abraded and with or without a muddy matrix dependant on the amount of winnowing. The mud content may also be due to amount of reworking, resedimentation or infiltration. These sediments are interpreted to have formed in the subaqueous environment but above wave base.

TF-3b Disarticulated shells imbricated whole shells

This taphofacies comprises rudstones with disarticulated but whole shells of bivalves with broken and abraded shell fragments locally set in a muddy matrix with muddy or peloidal matrix. But it may occur in grainstone or packstone matrix due to reworking process. The shells normally show some organization, stratification or imbrication as a response of high energy depositional environment, waves, currents or storms (Kidwell & Bosence, 1991). They are interpreted to occur in a subaqueous lacustrine environment above fairweather wave base (Figure 6.8b) and occasionally subjected to high energy events.

TF-4 Disarticulated shells whole and broken shells

Rudstones with disarticulated and broken shells of bivalve with some whole shells. The matrix is commonly muddy or peloidal, but it may be composed of grainstone or packstone. The shells normally show tractive structures in the form of low angle stratification and cross-bedding as a response to a high energy depositional environment, waves, currents or storms. This taphofacies is considered to form in a subaqueous environment above fairweather wave base (Figure 6.8c).

TF-5 Rounded shells

This taphofacies comprises rudstones with abraded and rounded bioclasts of bivalves, normally well sorted, and with a muddy or, more commonly, a peloidal matrix. It may show some cross-bedding as a response of traction processes. These

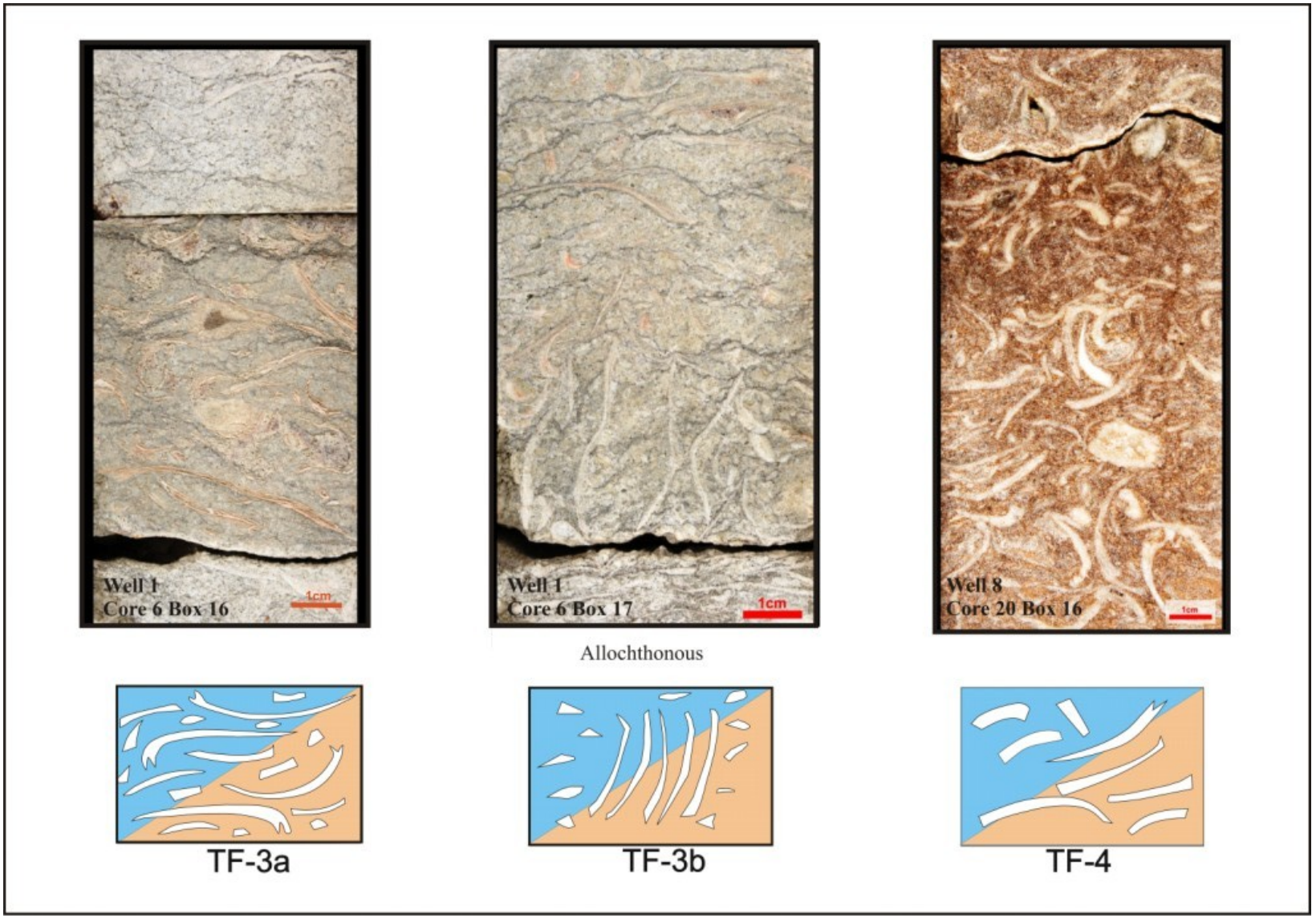

Figure 6.8- Taphofacies within environment Allochthonous a) Taphofacies 3a b) Taphofacies 3b c) Taphofacies 4

may occur in the shallow subaqueous environment above fairweather wave base and in a higher energy setting than TF-4 (Figure 6.9a).

TF-6 Very broken and reworked shells

This taphofacies comprises grainstones and packstones which are either clean or set in a filtrated muddy matrix in clast supported sediment with very broken and reworked shells of bivalves (Figure 6.9b). The finer grain size of this taphofacies to the preceding rudstones and floatstones is considered to be a form of textural inversion, where shells decrease in size with additional transport and abrasion (Figure 6.2). Although it is formed in a very high hydraulic energy environment, it may also occur with muddy matrix and this is thought to have formed through infiltration. Interpreted to occur in shallow subaqueous environment in the zone of active and continuous wave or current processes (Figure 6.11).

Out of environment

Allochthonous

TF-7 Polymictic conglomerate with fragments of crystalline basement.

This taphofacies is a polymictic conglomerate, commonly clast or grain supported, but also locally matrix supported, with fragments of basalts, crystalline basement and bioclasts of bivalves. The rock is poorly sorted, structureless, and a mix of terrigenous and carbonate lithoclasts. These are mixed in a lacustrine environment with transported and abraded shell debris. These rocks clearly formed in a high energy, shallow lacustrine setting such as Alluvial fans, but it may also have formed in deeper lake environments as gravitational deposits (Figure 6. 10a).

TF-8 Coarse bioclastic sandstone with fragments of basalt.

This taphofacies comprises bioclastic lithic sandstones or lithoclast-rich grainstones and packstones with fragments of basalt. This mixed rock normally occurs with tractive structure such as cross-bedding due to high-energy currents. It is interpreted to have formed in shallow fluvial-deltaic environments such as fluvial systems, interdistributary channels or mouth bars (Figure 6.10b).

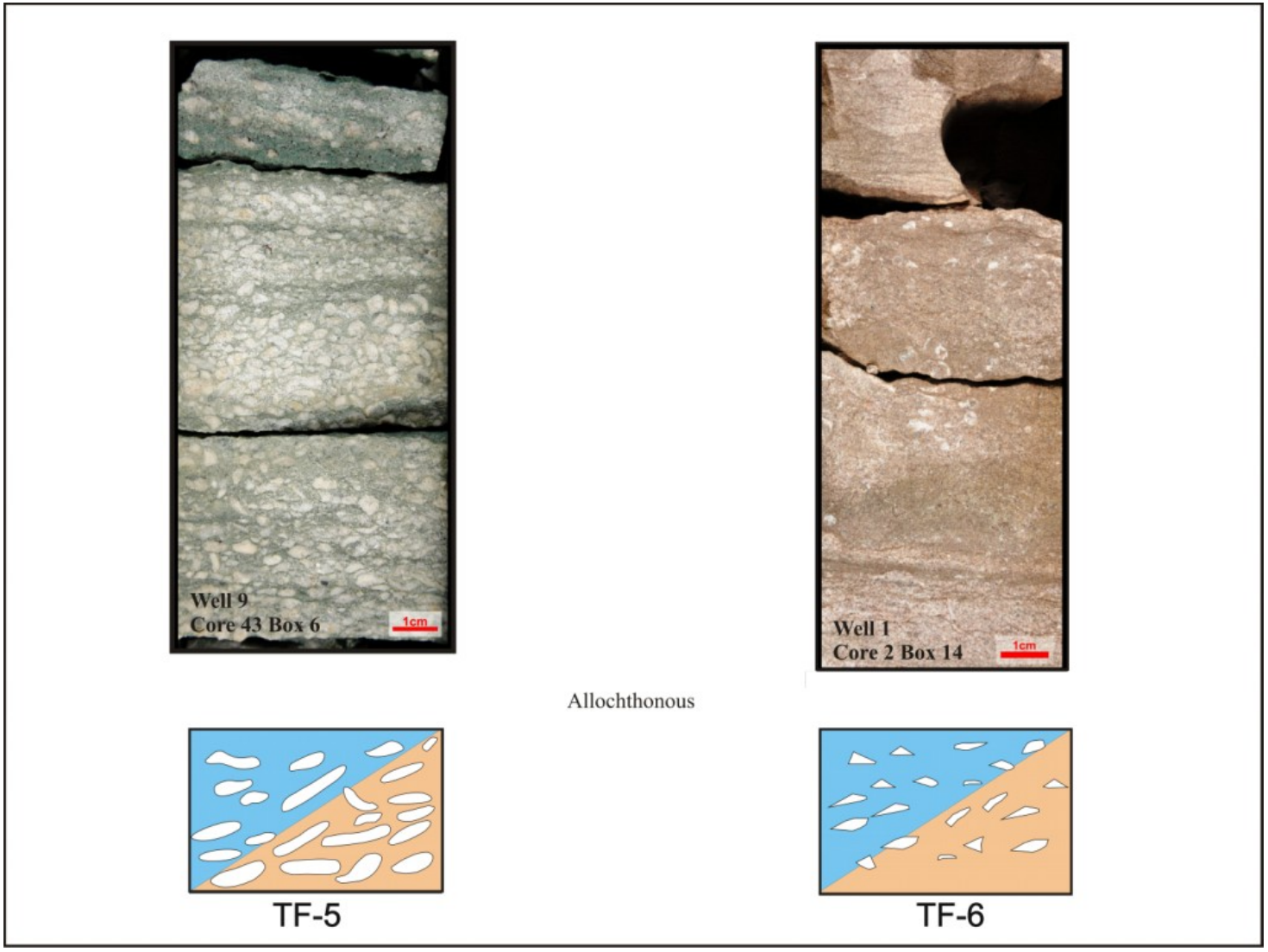

Figure 6.9 - Out of environment mix allochthonous - a) Taphofacies 5 b) Taphofacies 6

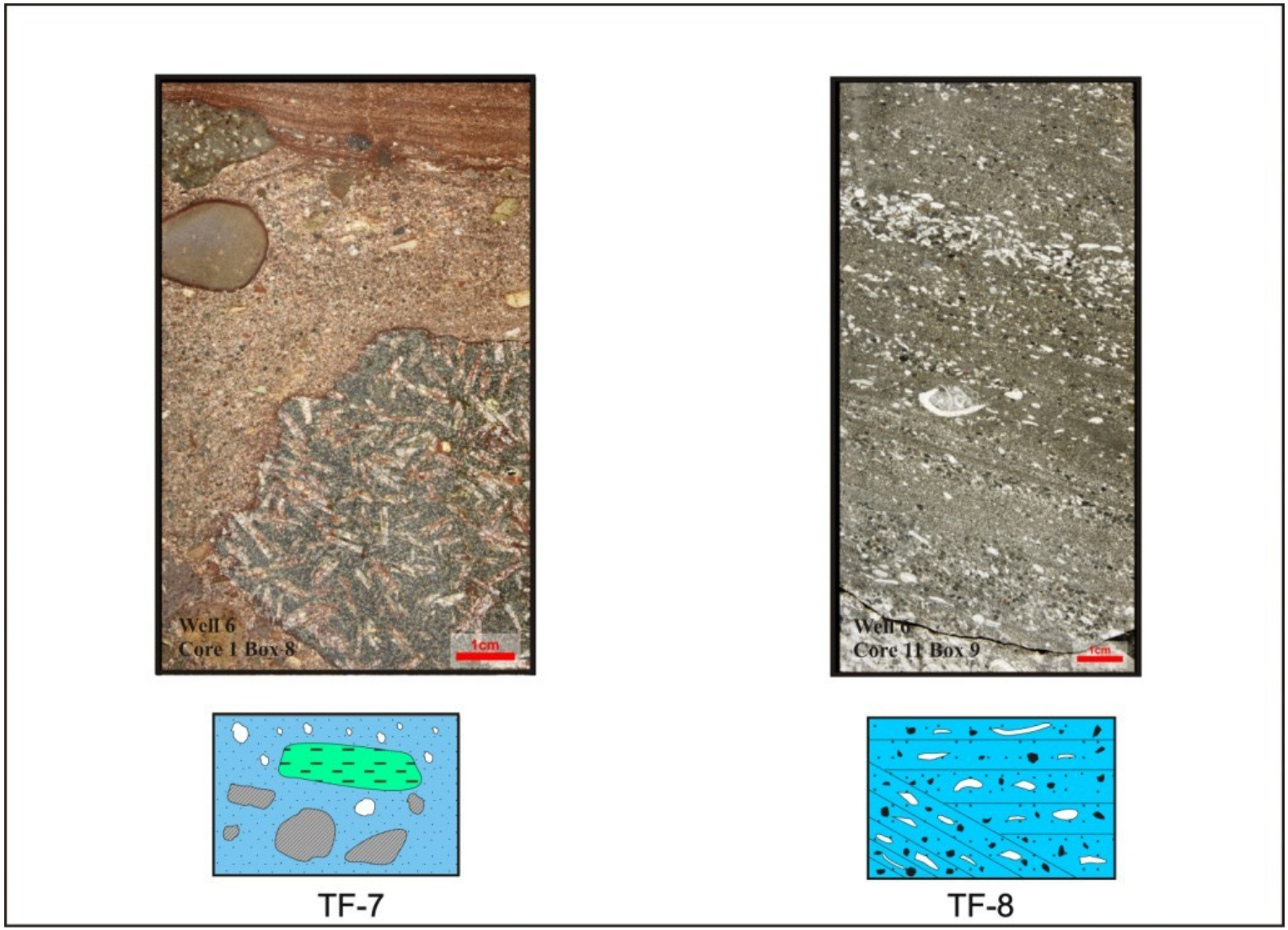

Figure 6.10 - Out of environment mixed carbonate - clastic allochthonous - a) Taphofacies 7 b) Taphofacies 8

The Fürsich & Oschmann (1993) scheme is a taphonomic model to explain the relationship between process of biogenic production, the agents of skeletal transport and the sites of bioclast deposition (Figure 6.11). Although it is devised for the marine realm it is applied here as a relevant, general model for lacustrine settings. The zone between the FWWB and SWB has the maximum biogenic productivity and concentration of sediments by the storms waves. In this research, it is observed that primary bivalve production is concentrated above SWB, below this zone the ostracod-rich facies is most likely to occur (Chapter 5). Also the concentration of shelly sediments generated by tempestites is thicker above SWB, due to amalgamation of various events. By comparison, below SWB, the thickness of tempestite tends to decrease. But the greatest thicknesses of detrital coquinas forming units many metres thick (see Chapter 7) are concentrated above FWWB zone.

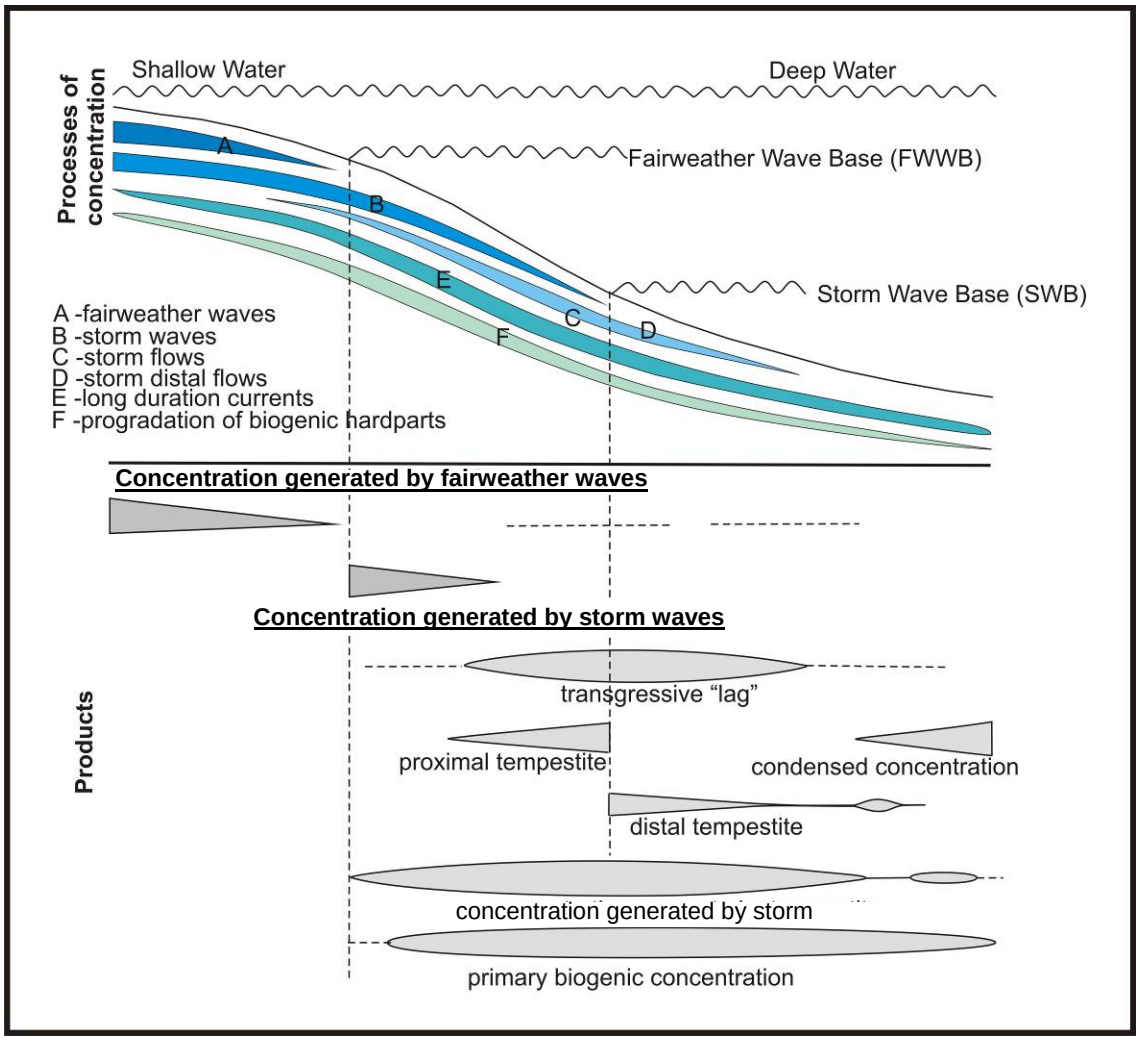

Figure 6.11 Distribution along a gradient of shallow / deep process concentrators of bioclastic sediments and their products (Fürsich & Oschmann, 1993).

6.4 Diagenesis of Lagoa Feia Group carbonates

Qualitative petrographic and diagenetic studies were made through the analysis of approximately 200 thin sections with the aim of supporting to the description of depositional facies (see above) and to support the interpretations made whilst logging cores and examining sidewall cores. In addition the thin section observations were used to establish the major diagenetic structures and textures within these cored samples to erect a general model for diagenetic evolution of the Campos Basin carbonates. Time constraints in the PhD meant that more detailed study of textures and cements using SEM, and carbon and oxygen isotopes could not be included within this study. The morphology of different cement phases and the various superimposed diagenetic events is based on petrographic microscope observations and cathodo-luminescence on the polished surface of thin sections. Therefore, most of the interpreted diagenetic history is based predominantly on petrographic observations such as diagenetic textures and structures as cement overgrowths and cross-cutting relations.

6.4.1. Original sedimentary components

The carbonate rocks analysed in thin section comprise sedimentary clasts that are mainly skeletal, microbial as well and precipitated allochthonous grains and also autochthonous components and micrite matrix. Among the skeletal allochems bivalve, ostracod and gastropod shells, in order of abundance, are the most significant bioclasts present in the Lagoa Feia Group. Secondarily, non-skeletal allochems such as peloids, and ooids occur and together with oncoids and microbial intraclasts contribute to the coarse-grained framework of these rocks. Microbialites are the most significant autochthonous components and are represented by laminites, stromatolites and thrombolites that form bioconstructions in the Macabu Formation (Aptian). Stevensite minerals and intraclasts occur locally in the wells 1, 2, 6 in the base of Coqueiros Formation (Barremian).

The original mineralogical composition of skeletal grains is an important factor in determining the diagenetic history of carbonate rocks (Moore, 2001). Such mineralogical composition of the shells can be: aragonite, low-magnesium calcite, high-magnesium calcite or calcite plus aragonite (Figure 6.12). Calcium carbonate crystals build aggregations of different layers, monophase or polyphase, according to

the shell structures and their general features (Bathurst, 1975). According Taylor and Hall (1969), many bivalve species have their shells built of aragonite. The aragonite occurs as prismatic, nacreous, complex crossed-lamellar and homogeneous structures.

		Aragonite	Low-Mg Calcite	High-Mg Calcite	Aragonite + Calcite
Mollusca:	Bivalvia	●	●		●
	Gastropoda	●	●		○
Arthropoda:	Ostracoda		●	○	

Figure 6.12 – General scheme showing the mineralogical composition of the main skeletal grains in the Lagoa Feia carbonate rocks (Scholle, 1978). Black circle means common, empty circle means rare.

All the petrographic observations indicate that the bivalves (identified and non-identified) in the Campos Basin cores had an unstable original mineralogy. The shells are either neomorphically recrystallised, or have been dissolved and replaced as described below. The same is the case for the gastropods. For this reason they are considered to have been originally aragonite in composition. Conversely, the ostracod valves still show their original fine prismatic structure and are assumed to be calcitic in composition.

The diagenetic processes and their products recognised in the Lagoa Feia carbonates are: micritization, early cementation, neomorphism, dissolution, late cementation, recrystallization, substitution (silicification and dolomitization), mechanical compaction, pressure dissolution (dissolution seams and stylolites), fractures and late dissolution. These are described and illustrated below.

6.4.2. Diagenesis

6.4.2.1. Micritization

One of the first processes interpreted to have occurred in the diagenetic environment is micritization of grains. This is very common and is seen as a micrite envelope that is formed on the surface of shells of bivalves on the lake floor or with very shallow burial. The activity of endoliths produces boring and early precipitation that eventually replaces the carbonate of the shell. Along with the micrite, organic

residues are formed due to the activities of these organisms (Bathurst, 1975). The micrite envelope normally occurs more frequently in subrounded and rounded grains in the shallow lacustrine waters.

In thin section this is seen as patches of micrite and micrite tubes embedded in shells, which may also occur in clusters (Bathurst, 1975). The organisms may also leave an insoluble organic residue after dissolution of the shell (Kendall & Skipwith, 1969a). When the carbonate rock is extremely recrystallized or neomorphised, this micrite and organic matter forms a coating or micrite envelope that defines the original external surface of the grains (Figure 6.13).

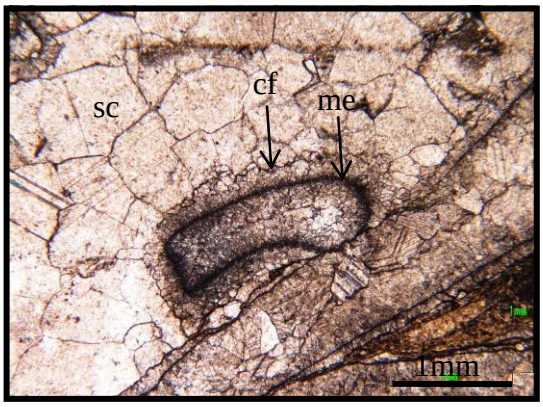

Figure 6.13 Photomicrograph of bivalve rudstone. Bivalve with subrounded margins (centre) and portion of whole shell, with micrite envelope (me) and calcite fringe (cf) cement. Coarse blocky equant sparry calcite (sc) fills subsequent interparticle pore space. No visible porosity (plane polarised light).

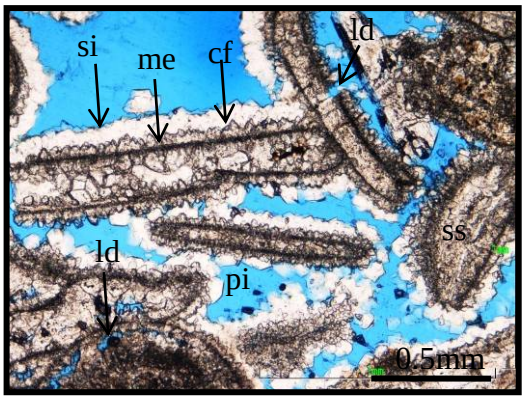

Figure 6.14 Photomicrograph of rounded and subrounded shells (ss) of bivalves, neomorphosed into spar calcite showing well packed, concavo-convex shell contacts, micrite envelope (me), fringe of calcite (cf) cement, some replacement of calcite cement by silica (si). Preserved primary intergranular porosity (pi) enlarged by late dissolution (ld). Open porous, void, filled with blue resin (plane polarised light).

In thin sections from wells 1, 2, 6, 7, 8, 9 and 12, the rudstones and grainstones show micrite coatings around rounded grains formed by abrasive process (Figures 6.13, 6.14 and 6.15). This suggests that the micritization process occurs continually with grain abrasion in shallow and agitated water, high energy depositional environment in the same way as has been reported from marine environments (Mcglue *et al.* 2010).

The micritization may also occur reducing the size of spar calcite by recrystallization and grain-diminution (Orme & Brown, 1963). This process, also called degrading neomorphism, may take place during early diagenesis and burial diagenesis phases (Dixon & Wright, 1983).

6.4.2.2. Cementation

Cementation is the chemical precipitation of crystals into primary or secondary pore space (Bathurst 1975; Harris *et al.* 1985; Tucker & Wright 1990). The pore-filling crystals of different phases of cementation have discrete and distinct morphologies related to their mineralogical composition and pore water chemistry (Bertani, 1984).

The main minerals observed to have precipitated as cements in the Lagoa Feia carbonate rocks are low-Mg calcite and silica. Low-Mg calcite is the predominant cement occurring in continental carbonates subjected to meteoric diagenetic processes (cf. Chafetz *et al.* 1985). Silica occurs sparsely (Bustillo, 2010). Evidence for aragonite and high magnesium calcite was not observed in the thin sections studied. However, this is not unexpected as these cements are recorded mainly from the marine environment (Tucker & Wright, 1990). Dolomite is similarly not common in the studied succession. It normally occurs as a replacement of calcite cement in late diagenetic stage (see below). Three phases of calcite cement are recorded as described below.

Phase 1- The first cement observed is calcite precipitated into the mouldic porous space formed from dissolved shells (Figure 6.16).

Phase 2- Following this is the isopachous rim (fringe) of calcite (dog tooth) which commonly develops on micrite envelopes around the bioclastic grains (Figures 6.13, 6.14 and 6.15). These precede the coarse interparticle sparry calcite cementation.

Phase 3- In this phase coarse sparry or prismatic calcite cement occurs infilling interparticle porous space (Figure 6.13).

Silica cement rarely occurs as original cement infilling interparticle or mouldic pore space (Bustillo, 2010). Where it occurs, it is represented by chalcedony or chert. However, silica is most likely to occur replacing the previous calcite cements (see replacement section below) (Figures 6.18 to 6.20).

The diagenetic process of cementation may produce similar petrographic features to neomorphism (see below) as they both can form equant sparry calcite. The diagnostic criteria used to indentify sparry calcite cement are the identification of euhedral crystal faces of sparry calcite, plane intercrystalline boundaries and enfacial junctions (Figure 6.16). The sparry calcite cement may occur as partially

filled cavities or as a final cement phase of void fill (Bathurst, 1975). Cathodo-luminescence is a useful tool to identify such cement. The sparry calcite has strong bright colour under luminoscope (Figure 6.17b).

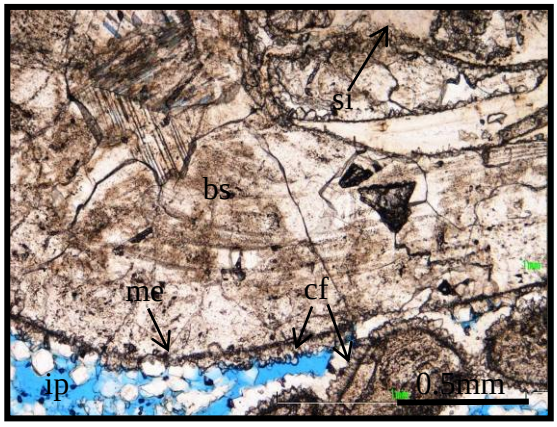

Figure 6.15 Photomicrograph of bivalve shell (bs) completely neomorphosed into spar calcite. Original fibrous structure and growth lines transect the sparry mosaic. Micrite envelope (me) and calcite fringe (phase 1) around the exterior of the grains (cf). Sutured concavo-convex contacts. Primary intergranular porosity (ip) enlarged by late dissolution. Locally amorphous silica (si).

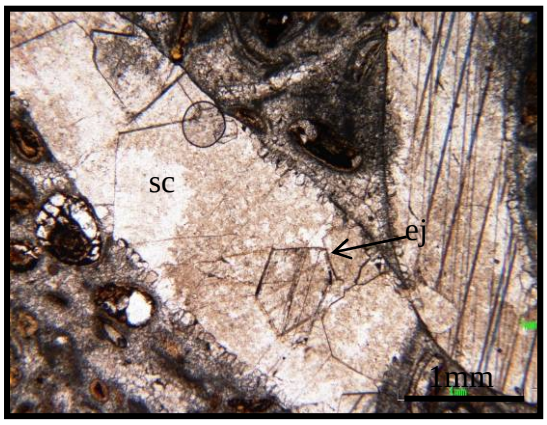

Figure 6.16 Photomicrograph of bivalve – rudstone. Shell of bivalves with micrite envelope, fringe of calcite. Interior filled with euhedral crystal of sparry calcite (sc) cement, identified petrographically by the plane intercrystalline boundaries and enfacial junctions (ej). Sutured grain-grain contact (plane polarised light).

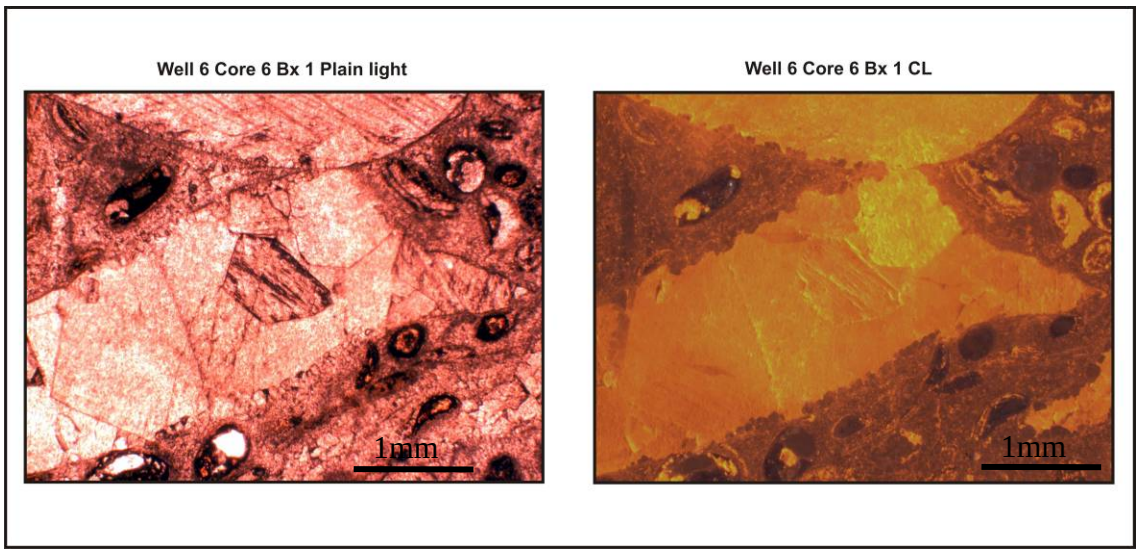

Figure 6.17 Rudstone showing bivalve shells replaced by equant sparry calcite, under plane polarised light and same view under Cathodo-luminescence (right). The sparry calcite cement fills the previously dissolved aragonite shell with equant, euhedral sparry calcite, which exhibit diagnostic enfacial junctions and compromised intercrystalline boundaries. The matrix of the rock is partially recrystallized into microspar calcite. b) CL showing bright yellow/orange colour of the spar calcite cement in the bivalves. The recrystallized matrix seems to be peloidal origin and shows dull non-luminescent colours (cf. Figure 6.16).

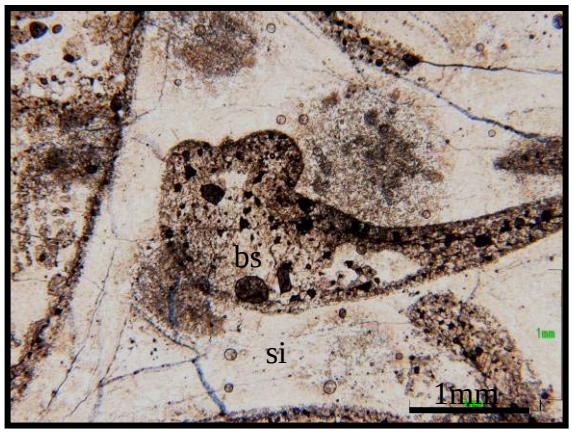

Figure 6.18 Rudstone with bivalve shells (bs) completely neomorphosed. Early calcite cements fill the intergranular pore space. Late replacement by silica (si). Some stains and bubbles on the surface of polished thin section (plane polarised light). Cement grew within the bivalve rudstone voids. Crust of equal thickness fringe form levels of cement rim.

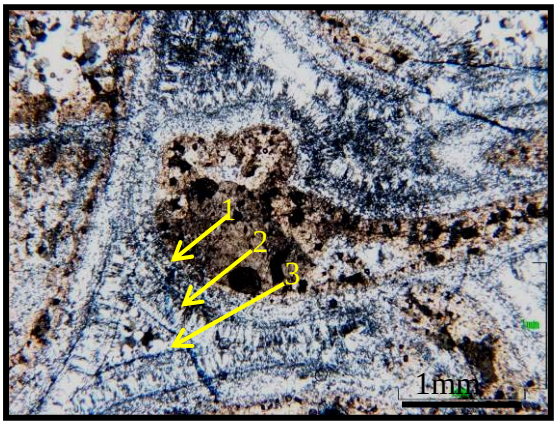

Figure 6.19 Crossed polarised light of rudstone to left (Fig 6.18). Previous void cementation occurred in 3 growth zones, substituted by silica. 1) Gravitational laminated fibrous crust coating the bivalve shell. 2) Fibrous crust covering the previous one. 3) Microcrystalline equigranular mosaic filling the remaining pore space

6.4.2.3. Neomorphism / Recrystallisation

The term ‘‘neomorphism’’ was first proposed by Folk (1965) to designate “all transformations between one mineral and itself or a polymorph”. Subsequently, Bathurst (1975) stated that in the neomorphic process, the new mineral has the same composition but assumes a new crystal shape, larger or smaller. Therefore, this term embraces the *in situ* transformation process of aragonite into calcite (inversion) (Folk, 1965). This is the most common process (cf. Tucker & Wright, 1990; Braithwaite, 2005) but in the more recent literature, neomorphism is used to express calcite to calcite diagenetic transformations and also recrystallization of micrite matrix into microspar and spar calcite (Lasemi & Sandberg, 1993). Such mineral transformation processes generally occurs in wet conditions, with a zone or front where aragonite is recrystallized into calcite and has no effect on the porosity of the rock. Although being synonymous to neomorphism, “recrystallization” is defined as any changes in crystal size, strain state, or geometry without change in mineralogy (Folk, 1965; Spry, 1969; Bathurst, 1975).

The best criteria for the recognition of neomorphism are the irregular bounding surfaces of the crystals, the preservation of relict of the original shell structure such as crystal fibres or growth lines (Bathurst, 1975) or preservation of floating patches of micrite in sparry calcite. This is the most common diagenetic

product in the studied thin sections (Figures 6.13 to 6.15 and 6.20 to 6.22). Neomorphic sparry calcite normally appears as a mosaic of anhedral crystals replacing bivalve shells.

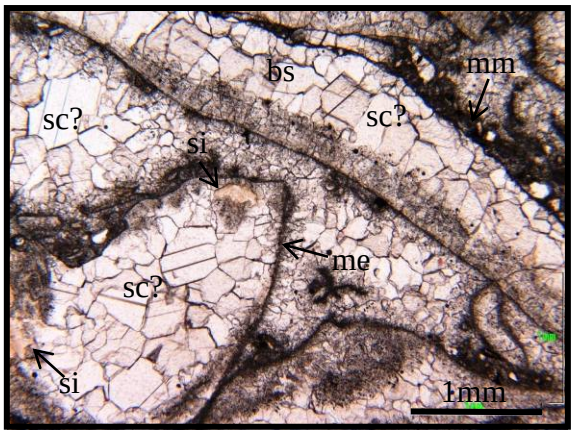

Figure 6.20 – Rudstone of bivalves. Shell (bs) recrystallized by neomorphic spar calcite. Micrite envelope coating the grains (me), some original structure of the shell partially preserved. Partial late substitution of calcite by amorphous silica (si) . Some spar calcite may occur filling the pore space (sc). Some relict of the original micrite matrix (mm) which recrystallized into microspar and sparry calcite. (Plain polarised light).

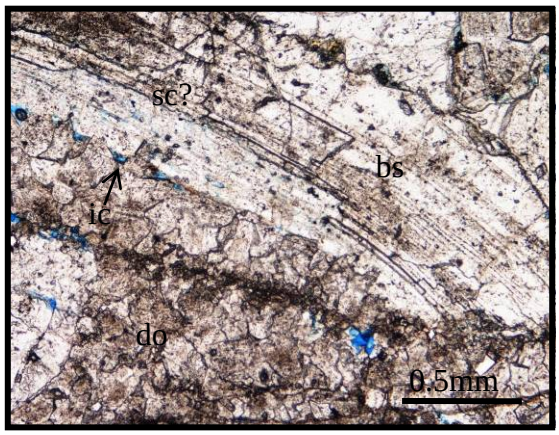

Figure 6.21 – Rudstone of bivalves. Shell of bivalve showing neomorphic spar calcite, with original fibrous structure preserved. Dolomitization (do) in the intergranular space. intercrystalline porosity (ic) (plain polarised light).

Figure 6.22 – Bivalve shell (bs) neomorphosed into spar calcite exhibiting features similar to radiaxial fibrous mosaic (plain polarised light).

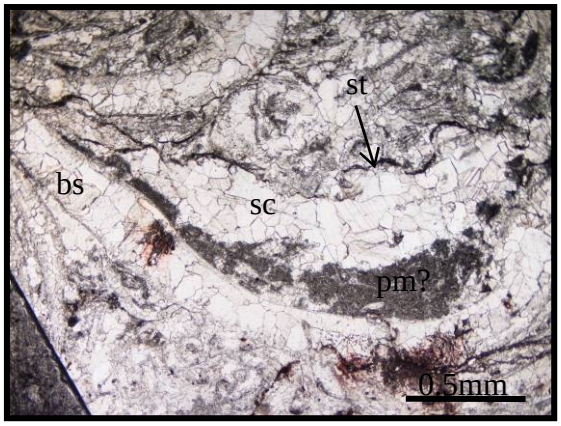

Figure 6.23 – Rudstone of bivalve (bs), completely neomorphosed into spar calcite (sc), micrite and peloidal matrix (pm) recrystallized into microspar and spar calcite (sc). Stylolite in the upper part (st).

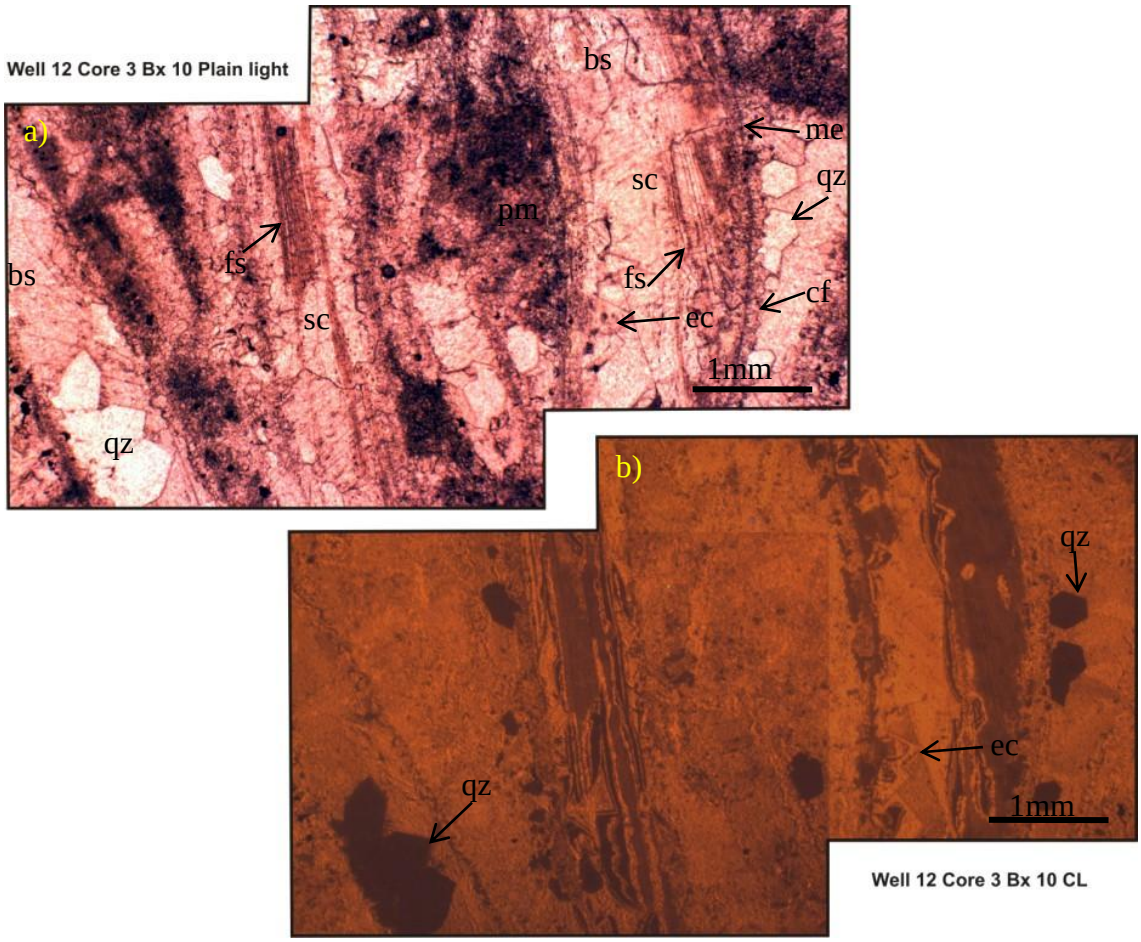

Figure 6.24 a) Bivalve rudstone. Bivalve shells (bs) showing a neomorphic sparry calcite (sc) replacing the original fibrous shell structure (fs) of the shell. Locally the neomorphic process forms euhedral crystals of calcite (ec) which are locally substituted by euhedral quartz (qz). The shells shows a micrite envelope (me) and a coating of fibrous axial fringe (rim) of calcite (cf). The peloidal or/ and micrite matrix (pm) is partially recrystallised into microspar and spar calcite. b) CL showing neomorphosed shells of bivalve. Part of the shell appears with banded colour, dull and bright. The dull colour may be interpreted as ferroan rich Mg-calcite. Locally euhedral crystals of neomorphic Mg-calcite exhibit growth lines and banded colours. Some hexagonal quartz appears non-luminescent. The banded colours represent fluctuation in diagenetic chemical conditions with different neomorphic phases.

Evidence for the neomorphism of the original micrite matrix, partially or completely, into a microspar and spar calcite is found locally (e.g. Figure 6.23). However, when the carbonate rock is completely recrystallized, few relicts of the original fabric are found to easily identify such a process (Figures 6.15, 6.21 and 6.24).

Although most studies concerning aragonite skeletons have interpreted a single generation of low-Mg calcite neomorphic spar in early diagenesis, Hendry *et al.* (1995), studying limestones from Middle Jurassic of Lincolnshire (UK), identified two phases of neomorphism. Firstly in the early diagenesis and oxic conditions, the aragonite shells are neomorphically replaced by minor volumes of non-ferroan

calcite (poor in Fe, Mg and Mn content). Subsequently, the remaining aragonite is replaced by ferroan calcite in anoxic conditions interpreted to be during burial diagenesis.

,

6.4.2.4. Replacement

Replacement is a substitution of one mineral by another or “inversion” to a different chemical composition (Bathurst, 1975). The most common replacement processes observed were dolomitization and silicification (Figures 6.18; 6.19, 6.21, 6.24 and 6.25). Dolomitization occurs partially or totally in one, well defined stratigraphic horizon (Well 20, sidewall cores 9 and 13). It occurs in grainstones and rudstones in the coquina succession, whereas silicification occurs sparsely in all stratigraphic intervals studied. In some intervals stevensite occurs as a replacement of calcite, indicating alkaline conditions (Bertani, 1984).

6.4.2.5. Dolomitization

The dolomite occurs in sidewall cores from well 20 in a well-defined stratigraphic zone in cores 9 and 13 in bivalve grainstones and rudstones. The crystal fabric is almost always xenotopic and hypidiotopic mosaic, and rarely idiotopic type (Figures 6.21, 6.24 and 6.25). Moreover, the crystals are invariably anhedral and subhedral, but they rarely exhibit euhedral textures. Dolomites may appear as sucrose mosaic (Figure 6.25) but also occurs as scattered dolomite rhombs.

Locally the original fabrics of the skeletal grains are destroyed by the dolomitization process and only the shape of the grains is preserved (Figure 6.25). But occasionally the original fabric of the rock is preserved, in fine grained texture preserving replacement of the allochems (Figure 6.26). The extensive dolomitization seems to be associated with early diagenesis (Bertani & Carozzi, 1985; Bustillo, 2010) but subsequent to dissolution of aragonitic clasts (Figure 6.25). It may be the result of pedogenetic process, as in dolocrete formation. Therefore partial dolomitization with coarser grains are possibly related to late diagenesis in the replacement process.

There are many models for dolomitization and the diagenetic process of dolomitization can occur as an early diagenetic process, (syn-sedimentary), in arid climates with evaporation and concentration of salts in shallow and restricted water environments or as late diagenetic process (Hardie, 1987; Lasemi *et al.* 1989; Tucker

& Wright, 1990) associated with clay mineral diagenesis or hydrothermal fluids. Almost all of these models were made for the marine carbonate platforms and require detailed petrographic, geochemical and isotopic analyses to establish the mode of dolomitization.

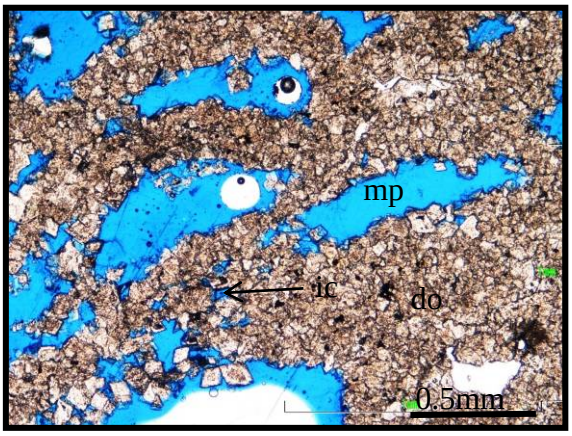

Figure 6.25 - Dolomitised limestone (do), sucrose texture exhibiting locally some euhedral and subhedral crystals of dolomite, as floating rhombs. Mouldic porosity (mp) after early dissolution and intercrystalline porosities (ic) after late diagenesis.

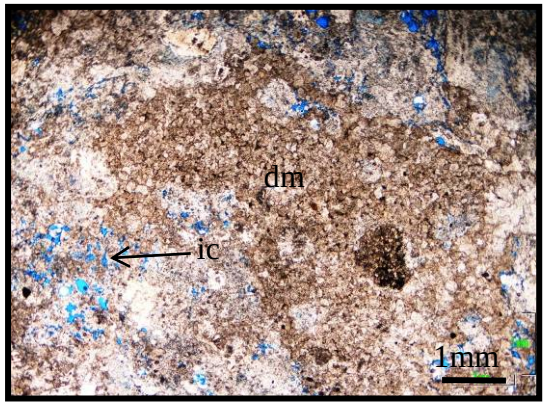

Figure 6.26 – Dolomitised microbialite (dm). Fine grained anhedral texture, xenotopic, intercrystalline porosity (ic).

6.4.2.6. Silicification

The silica is normally microcrystalline or amorphous (Figures 6.27 and 6.28). It may occur as nodular or lenticular bodies. Silicification may result from early diagenesis in emergent vadose environments (Bustillo, 2010). The emergent vadose environment, however, is prone to form chalcedony and chert, while late diagenesis is most likely to form amorphous and microcrystalline silica (Bustillo, 2010). In the late diagenesis stage, the replaced silica assumes the previous calcite crystal fabric (Figures 6.18 to 6.20, 6.24, 6.27 and 6.28).

Stevensite

Stevensite is a tri-octahedral magnesium smectite ($Mg_3\ Si_4O_{10}\ (OH_2)$), found in the Lagoa Feia Group of the Campos Basin. It is also found in the Cretaceous of the Santos Basin (Bertani, 1984) and the Green River Formation in Wyoming (Bradley & Faley, 1962). Similar magnesium smectites (e.g. Ghassoulite) occur in African lakes today (Bauman *et al.* 1975). Its high crystallinity suggests formation by chemical precipitation (Carvalho *et al.* 1984) and its presence is taken here to

indicate magnesian-rich lake waters, possibly attributable to contemporaneous volcanism. Such conditions are observed in modern African lakes (Abraão & Warne, 1990).

The stevensite occurs normally as ooids or peloids (Figures 6.31 and 6.32), but it can also occur as a diagenetic product replacing calcite cement in the shells of bivalves (Figures 6.29 and 6.30) (see also Brindley *et al.* 1977).

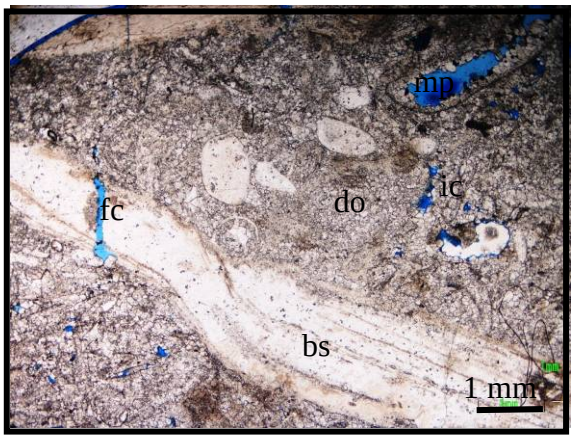

Figure 6.27 – Rudstone of bivalve (bs), with extensive dolomite (do) in the matrix, and bivalve shells replaced by silica (si), fracture (fc). Mouldic (mp) and intercrystalline (ic) porosities (plane polarised light).

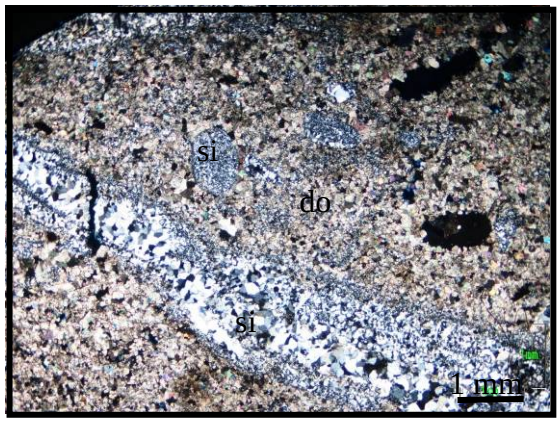

Figure 6.28 Cross polarised light view of Figure 6.27 showing bivalve shells replaced by microcrystalline and drusiform silica (si).

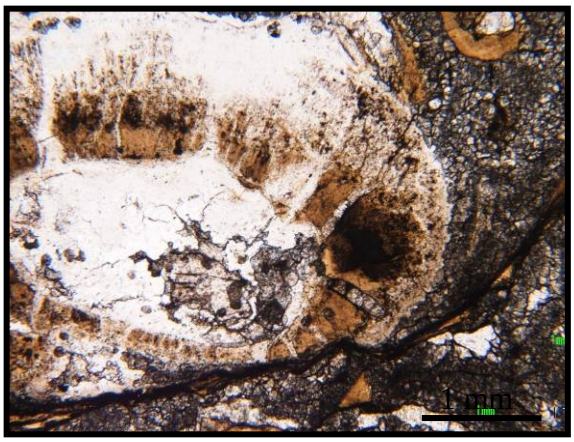

Figure 6.29 Bivalve shell replaced by microcrystalline silica and granular mosaic and also brown coloured stevensite (plain polarised light).

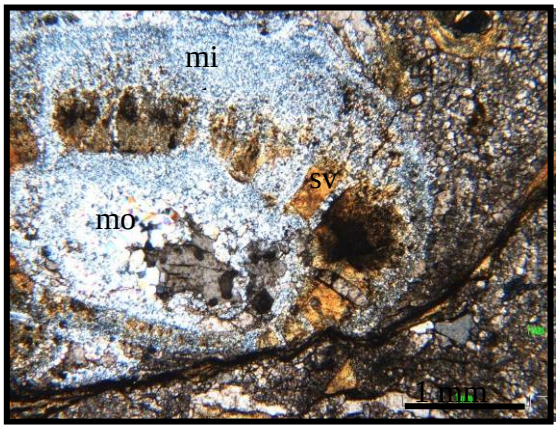

Figure 6.30 Bivalve shell replaced by microcrystalline (mi) and granular mosaic silica (mo) and also stevensite (sv) (cross polarised light).

6.4.2.6. Mechanical compaction & Pressure dissolution

Mechanical compaction accompanied with pressure dissolution occurs progressively during the burial of carbonate sediments. This process produces a reduction of pore space, dewatering, deformation and reorientation of the grains. In addition the overburden pressure and compaction results in a reduction of thickness and increasing in density of the carbonate rock. In a qualitative evaluation of the compaction effects, the degree of deformation can be measured by the type of contact between the grains, which may be: grain to grain, tangential contact, concavo-convex, sutured, and culminating in the highest degree of compaction in dissolution seams and stylolites (Bathurst, 1975).

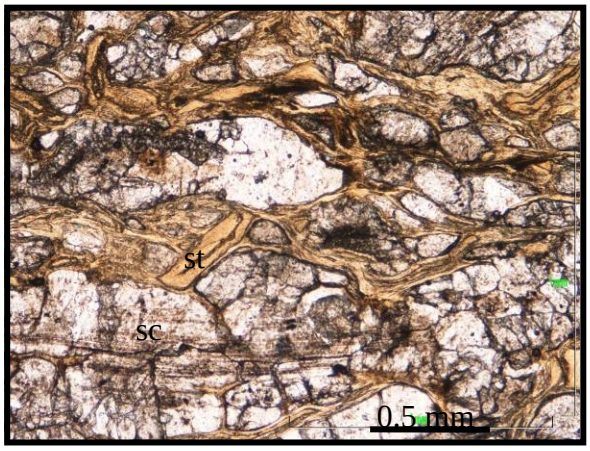

Figure 6.31 Rudstone of bivalves. Neomorphic spar calcite (sc) showing structures of original bivalve shell (bs). Ooids of stevensite (st) strongly deformed due to mechanical compaction.

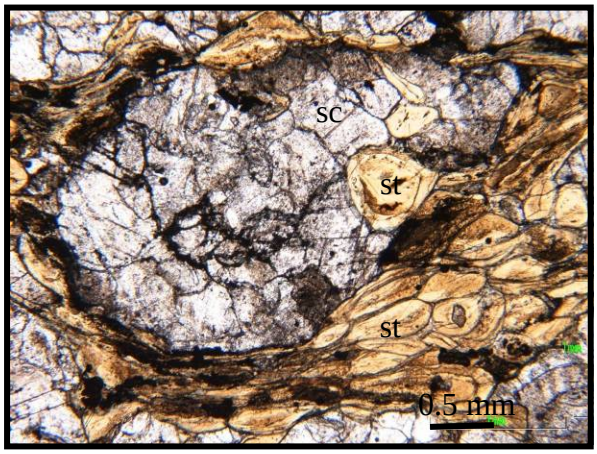

Figure 6.32 Rudstone of bivalves. Neomorphic spar calcite (sc) shell of bivalve and ooids of stevensite mechanically deformed forming pseudo matrix, occluding porosity (plan polarised light).

The rocks of the Lagoa Feia Group which have been buried to depths of 2000m to 5000m and show evidence of moderately to high mechanical compaction and pressure dissolution. Grain to grain contacts (Figures 6.15 and 6.16) are quite common, but these may also occur as concavo-convex (Figure 6.14) or sutured contacts (Figure 6.13). Non facies selective dissolution seams and stylolites with amplitudes up to 1 mm are commonly observed in thin sections. However the stylolite may also occur at a centimetre scale as seen in cores. Stylo-mottled and stylo-breccioid structures are seen locally (Flügel, 2010). The stylolite surfaces are dark and are assumed to contain concentrations of clay and organic matter (Figure 6.35). The clay minerals may be mechanically deformed forming pseudo-matrix, with reduction of the porous space and dewatering (Figures 6.31 and 6.32), changing

the chemical behaviour and consequently taking an important part in the diagenesis process.

Some skeletons grains may be protected against compaction pressure dissolution by early cementation (Figures 6.13 and 6.18). These two examples show the bivalve shell floating in surrounding early cement, possibly a loose packing fabric.

Pressure dissolutions may be associated with fractures (Logan, 1984), and also create conduits for fluids migration. At the late stage of this process the carbonate rocks may be fractured and take place a late dissolution with secondary porosity generation.

6.4.3. Diagenetic environments and diagenetic sequence history

Diagenetic environments are zones in the surface or subsurface affected by characteristic diagenetic process with specific digenetic structures and fabrics (Flügel, 2010). The major diagenetic environments in continental rift systems are: Meteoric vadose; Meteoric phreatic and shallow and deep burial environments (Moore, 1987). During the early diagenetic history the environments may change due to lake level fluctuations, tectonic activity and increasing or decreasing burial. Also, climate changes can alter the salinity of surface and shallow subsurface water circulation, affecting the diagenetic pathway.

6.4.3.1. Vadose diagenetic environment

Located between the water table and the land surface, the diagenetic vadose zone is characterised by processes related to meteoric waters, with dissolved CO_2 and strongly undersaturated in $CaCO_3$. Such attributes enable pore waters to dissolve carbonate grains and rocks in a non-selective manner, thereby increasing porosity. Subsequently supersaturated waters may precipitate cements within meniscus or as microstalactite structures (Moore, 1987).

In the upper vadose zone, close to the air-sediment interface, nearshore lacustrine facies may also be altered by wetting and drying in this zone to form soils and calcretes and silcretes may be developed (Flügel, 2010). Similarly, subaerially exposed lacustrine carbonates may occur and be altered in adjacent continental areas, where sediments are exposed, above the lake water level and the water table.

Micritization is attributed to occur in the upper part of this zone in the interface land surface air (James & Choquette, 1990).

In this project, core observations revealed exposure features, such as mud cracks, shrinkage and collapse breccia, and karst (see facies section in Chapter 5) that formed in this diagenetic zone. The vuggy and mouldic porosities described above are also considered to have formed in vadose zone (Figures 6.33 and 6.34). However, meniscus cements were not observed in thin section even though they are considered to be a diagnostic feature of vadose cementation. According to Prezbindowski & Tapp (1989), such features become progressively masked as the pore space and solubility of the carbonate minerals decrease, in the burial diagenesis.

Figure 6.33 Core slab - Rudstone of oncoids showing vadose mouldic and vuggy porosities.

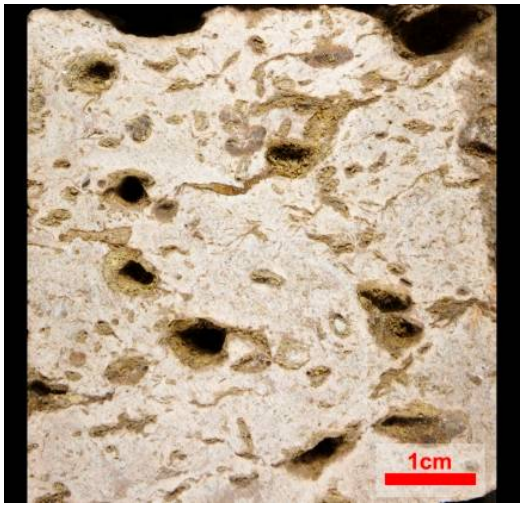

Figure 6.34 Core slab - Rudstone of bivalves showing vadose mouldic and vuggy porosities.

6.4.3. 2. Meteoric phreatic diagenetic environment

The meteoric phreatic diagenetic environment occurs where meteoric water saturates the pore space below the water table. The upper part of this diagenetic environment is the active solution zone, where extensive dissolution of aragonite and Mg - rich calcite takes place (Flügel, 2010, p. 275). This typically results in mouldic porosities and also the precipitation of calcite cement either in interparticle pores or in moulds. This zone is also marked by stabilisation of aragonite and Mg-calcite through dissolution and cementation and also neomorphism.

The first step of the diagenetic process in the meteoric phreatic zone observed in the Lagoa Feia carbonates is the precipitation of cement rims around grains that

may be isopachous or circumgranular (Tucker & Wright 1990; Flügel, 2010, p.300; Bustillo, 2010). These cement rims begin with nucleation of crystals around the grain surfaces. Subsequent cementation reduces the pore space with crystals coarsening toward the pore centres (Longman, 1980). The mosaic of sparry calcite cements occur as drusy, equant or a granular morphologies (cement phases 2 and 3) (Figure 6.13). Crusts of radial fibrous, microcrystalline with one or more growth phases may occur in this meteoric phreatic zone (Figures 6.18 and 6.19).

The aragonitic bivalve and gastropod shells are dissolved by a leaching process, producing mouldic porosity. The previous micrite envelope, formed before the extensive dissolution, delineates the original surface of the grains when mouldic and inter-particle pore space is completed cemented. Occasionally it is particularly difficult to differentiate in thin section the meteoric precipitation of calcite cement from neomorphism (Figure 6.37). Similarly, the recrystallisation of muddy matrix into microspar initial calcite cements into sparry neomorphic calcite can be difficult to recognise.

6.4.3.3. Burial diagenetic environment

The burial diagenetic environment is a zone extending from the stagnant waters of the lower phreatic zone down to the realm of low grade metamorphism. It may extend to burial depths of hundreds to thousands of metres and rocks may be affected by deep burial fluids brought in by compaction or along faults (Moore, 2001).

During burial diagenesis, physical and chemical compaction takes place (Bertani & Carozzi, 1985). With shallow burial mechanical compaction occurs and results in, a reduction of porosity and sediment thickness. In the deep burial diagenetic environment chemical compaction occurs with pressure dissolution characterized by dissolution seams and stylolites (Moore, 1987).

As the pores are usually filled with brines of different salinity, freshwater to brackish or deep burial fluids (Flügel, 2010), calcite cements, enriched in iron and manganese, precipitate in coarse drusiform and mosaic spar calcite (Hendry *et al.*1995). Mechanical compaction of peloids may also occur forming micritic pseudo matrix (Flügel, 2010). Occasionally the micrite matrix is recrystallized into microspar calcite. In rocks with early calcite cementation, in the interparticle porous space, little or no compaction is observed. Calcite cements and grains may be

dissolved by subsurface fluids rich in CO_2, derived from hydrocarbon maturation, generating a secondary porosity in the carbonate reservoir rocks (Bathurst, 1975) (Figure 6.36).

At the late stage of diagenesis, a strong replacement process of calcite by silica and dolomite occurs as described above. It may also form dolomite by the non-selective replacement of micrite matrix and bivalve shells (Bertani & Carozzi, 1985). The diagenetic environment turns more anoxic, enriched in Fe and Mg due to fluids liberated by clay mineral diagenesis in the vicinity (Hendry *et al.* 1995). At this stage, late sulphate reduction may occur, expressed by the formation of pyrite.

With continuing burial, diagenesis is characterized by grain to grain, concavo-convex and sutured grain contacts described in the previous section. Also pressure dissolution occurs with dissolution seams, stylolites and fracturing. These diagenetic features usually concentrate clay and organic matter in the surfaces of stylolite (Figures 6.35 and 6.36). Chemical dissolution may occur in these surfaces, which together with the fracturing establishing conduits for fluid flow.

Stylolites and some deep burial diagenetic features are most likely to occur in the central basin and close to the border fault of hanging wall, where subsidence and compaction were great. The maximum burial depths today in the study area are 5000 metres.

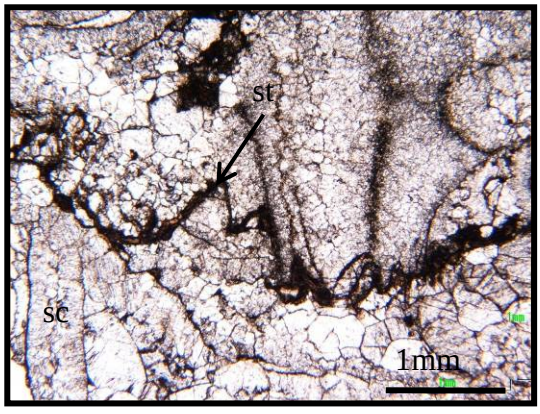

Figure 6.35 Bivalve rudstone completely neomorphosed, compacted and cemented? with spar calcite (sc) with stylolite. The stylolite (st) surface concentrates clay and organic matter (dark brown color).

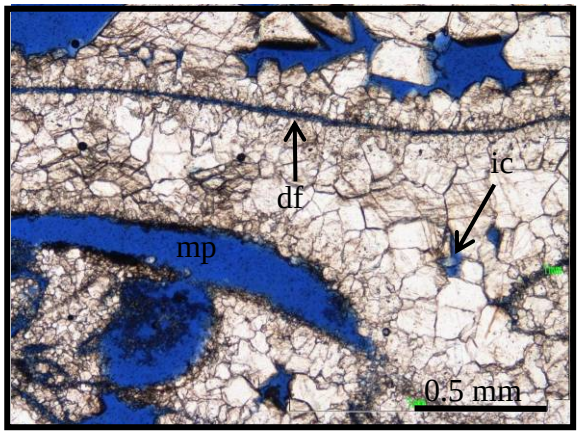

Figure 6.36 Bivalve rudstone, with neomorphosed mollusc shells. Micrite envelope and associated organic matter film dissolved away (df). Fringe of calcite cement (phase 1) surrounding the grains, mouldic, (mp) interparticle and intercrystalline porosities also visible.

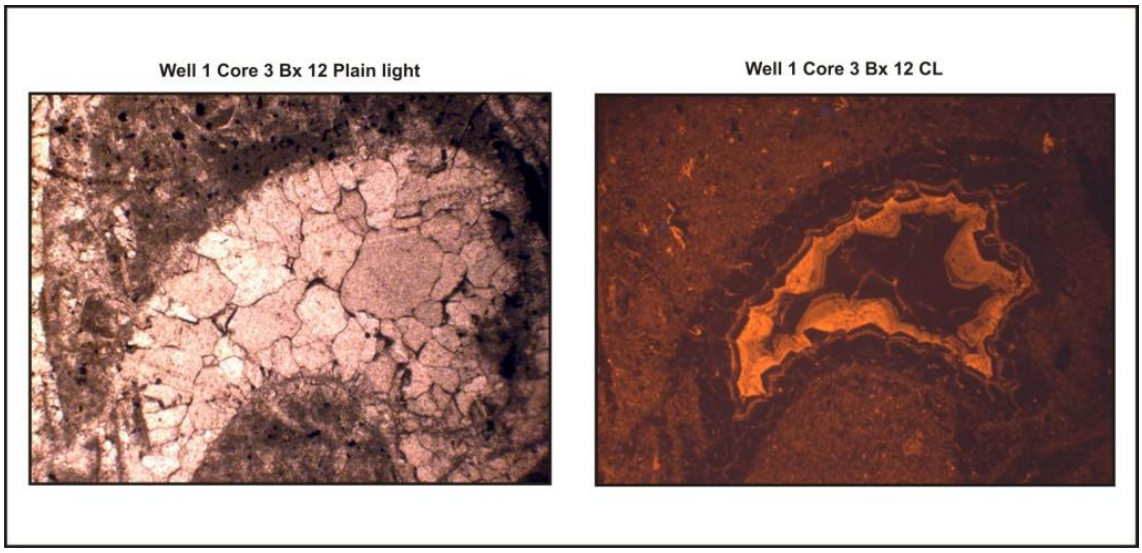

Figure 6.37 a) Mosaic of drusy fabric calcite spar. The crystal size increase toward the centre of the shell. b) CL of same area showing 3 main growth zones of crystals. The first, from the border to the centre of the shell, a non-luminescence zone. Following is a bright colour zone and finally a non-luminescent zone filling the remaining cavity. This markedly zonation reflects subtle changes in the porewater chemistry during cementation. The non-luminescent zones are more ferroan calcite. The bright one, for its turn, more low Mg-calcite rich cement.

6.4.4. Diagenetic history

The diagenetic evolutionary history of bioclastic carbonate rocks is related to the original mineralogical composition of skeletal grains and the physical and chemical changes to which these grains have passed through during the different diagenetic zones.

The diagenetic sequence, or paragenesis, based on thin section observations begins with the micritization of the external surface of skeletal grains (Figures 6.13, 6.14 and 6.15) on the lake floor.

Secondarily, a fringe of calcite cement is deposited over the micrite film on the outer surface of the grains. This fringe and the earlier micrite envelope may protect skeletal grains from the effects of mechanical compaction. This is considered to be an important factor in the preservation of porosity in the burial process (Figure 6.14). Subsequently, aragonite shells are dissolved and low-Mg sparry calcite cement precipitation takes place in the void created.

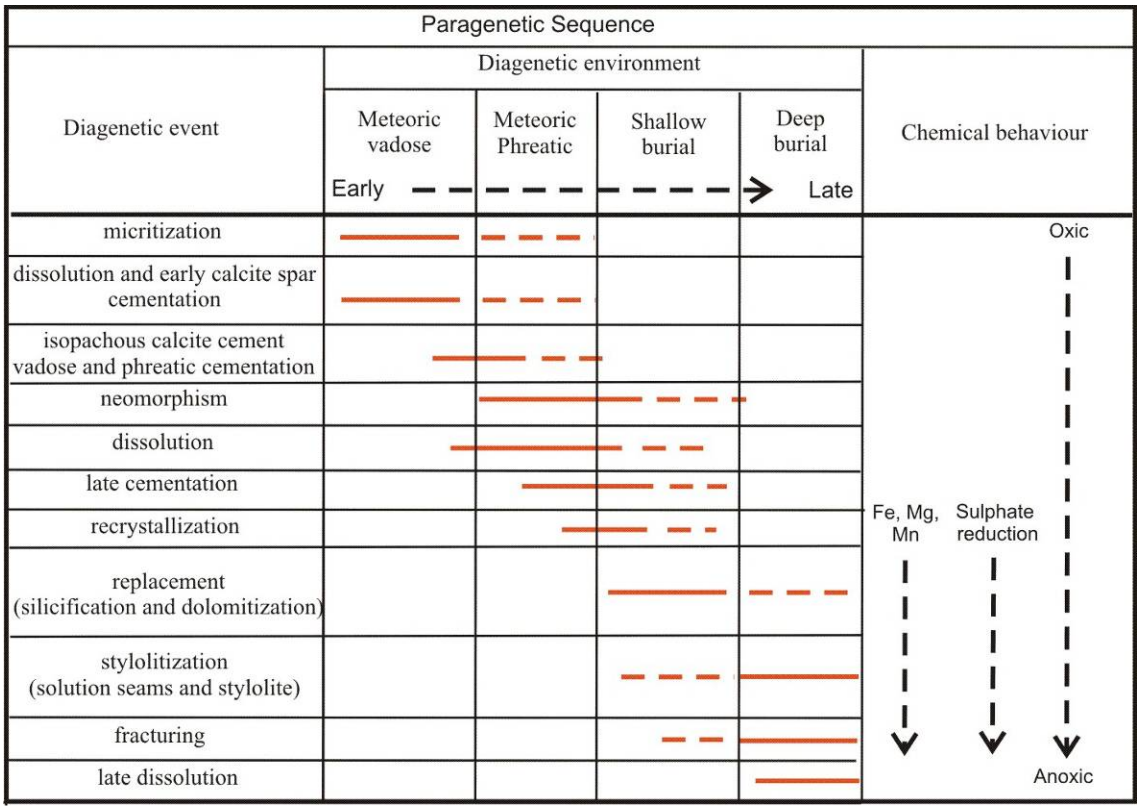

Figure 6.38 – Sequence of diagenetic events during the burial of carbonate rocks in the southern Campos Basin, in chronological order (Modified from Divet & Montjoy, 1997 and Hendry, *et al.* 1995)

Sparry calcite cements are then precipitated in available interparticle and mouldic pore space, with equant, drusiform or even fibrous cement textures, which may occur in distinct phases (Figures 6.18 and 6.19). The carbonate rock then or at same time goes through the neomorphic process which is the most common and widely occurs. Both aragonite and calcite skeletal grains may undergo this process. In some cases of neomorphic process, the original shell structures are preserved (Figures 6.15, 6.21, 6.24 and 6.31). The micrite matrix may suffer a partial or even total recrystallization into micro spar or sparry calcite, and even suffer a subsequent replacement process too (Figures 6.27 and 6.28).

With burial and increase in overburden pressure with the rocks show evidence of chemical compaction, which is in general characterised by pressure dissolution and manifested by dissolution seams and stylolite (Figure 6.35). In addition, the stress caused by overloading sediment also produces fractures (Figure 6.27).

Throughout the burial history, the paragenesis sequence indicates that the chemistry of the diagenetic environment changes from oxic to anoxic; $CaCO_3$

depleted and enriched in Fe, Mg and Mn solutions. These latter fluids generally migrate from dewatering of adjacent shales during their burial compression (cf. Hendry *et al.* 1995). As the environment becomes progressively more anoxic, sulfate reduction with precipitation of pyrite may take place. Similarly fluids rich in Mg, may be forming late stage dolomites (Figures 6.25 to 6.28). Silica is also precipitated which under transmitted light microscope, may have a pale brown color; possibly because of inclusions of organic matter (cf. Hendry *et al*. 1995) (Figure 6.20).

Burial compaction produces dissolution seams and stylolites (Figure 6.35). The surface of these diagenetic structures usually concentrated organic matter and clay minerals (Bathurst, 1975). Maturation of organic matter can release CO_2 for dissolution of carbonates within fractures and can create routes for fluid migration. Such fluids are responsible for the generation of secondary porosity in the carbonate rocks (Figure 6.36).

6. 5 Discussion and Conclusions

Taphonomic studies are powerful tools with which to elucidate the complex biostratinomic, sedimentological and diagenetic history in these lacustrine deposits. First, the nature of the *post-mortem* preservation and accumulation of the shelly fossils provides more palaeoenvironmental information than the sedimentary facies alone (Figure 6.39).

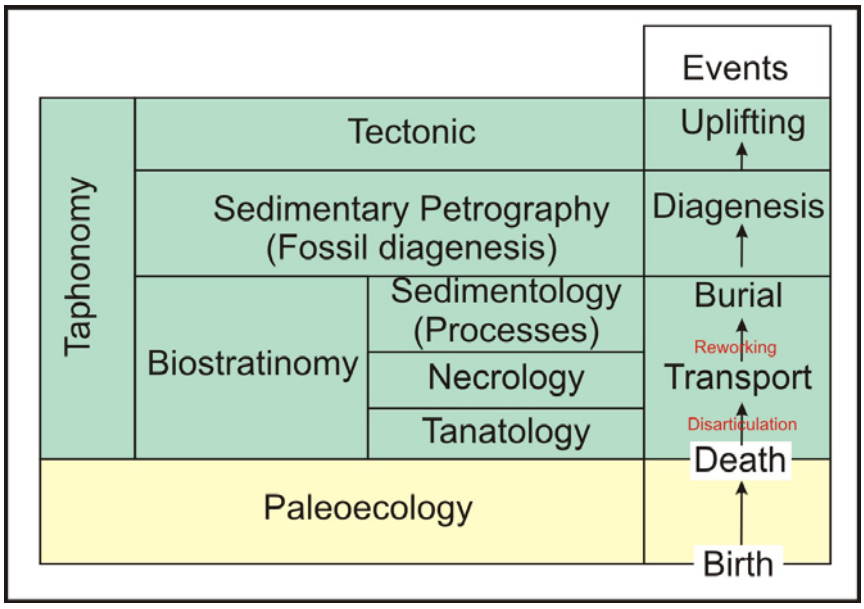

Figure 6.39 Relationship between taphonomy, its subdivisions, and the events responsible for the origin of fossiliferous assemblages (after Simões & Holz, 2002).

Biostratinomy deals with the *post-mortem* processes that affect the preservation of organisms (Figure 6.39). So, the classification of taphofacies of bivalve rudstones and floatstones shown in the Figure 6.6 is an attempt to group the textural and compositional overprints since its death and through to their final burial. This aspect is used in the next chapter where sedimentary trends are identified based on their taphofacies and related to environmental energy associated to the environments on the lake margin (Chapter 7). This method, together with sedimentological and electrical logs analysis have been extensively used in this project for the construction of cycles stacking patterns as building blocks for the stratigraphic analysis, described in Chapter 8. The taphofacies have been grouped into autochthonous, parautochthonous and allochthonous groups. The autochthonous (TF-1) and parautochthonous (TF-2 and TF-3) taphofacies represent *post-mortem* reworking in very low energy sub wave base environments. Hydraulic energy was low enough to preserve some bivalves in their position of life or with just minor reworking and transport. They are generally associated with considerable mud content; matrix supported textures and consequently has massive bedding. On the other hand, the allochthonous taphofacies (TF-3 to TF-6) experienced higher energy transport, leading to breakage of shells. These form cleaner facies with traction structures and preserve greater primary porosity. The allochthonous mixed carbonate-clastic taphofacies are normally associated with alluvial environments (TF-7) or specifically fluvial channels (TF-8). These may have reworked previously deposited shells as second generation bioclasts.

Finally, after the burial of sediments, the diagenetic history has to be understood as a series of *in situ* mineral transformations. The dynamics of the diagenetic process begins with the original shell mineral composition. On the subsequent diagenetic history is dependant on whether the shells are calcite or aragonite (Figure 6.12). Goldring (1991), has established a general model for the taphonomy of bivalved shells (Figure 6.5) in which he shows the diversity of possible processes that the shell may undertake to form the final depositional record and many of these are recognized in these lacustrine bioclastic carbonates.

Based on the petrographic and cathodo-luminescence analyses, and cross-cutting and overgrowth observations, a diagenetic sequence of events or paragenesis has been constructed (Figure 6.38). The carbonate rocks analysed in this project have most of their shelly components formed of unstable aragonite. Some were dissolved and filled by early low-Mg calcite cement, but others were neomorphosed into stable

spar calcite. The final porosity seems to be influenced by original mineralogy and taphofacies type. Despite the generation of some secondary porosity in the late diagenetic stage, the best porosities observed in thin section are related to carbonate reservoir facies which have an original primary porosity, followed by early dissolution, forming mouldic porosity. Minor, meteoric fringe cements then preserve the rock from the effects of mechanical and chemical compaction that lead to the occlusion of porosity. This facies selective porosity is typically found in porous shallow lacustrine carbonate banks. Their occurrence and stacking patterns are discussed in the subsequent two chapters.

CHAPTER 7 - CORE AND WELL DATA ANALYSIS

7.1 Introduction.

This chapter presents the description and interpretation of the logged core and FMI log focusing mostly on the temporal and spatial facies variations. The analysed carbonate successions range from the upper Barremian to mid Aptian. They comprise the mid to upper parts of the Lagoa Feia Group, between the lower clastic sediments of the Basal Clastic Sequence and Stevensite Sequences and the overlying Aptian evaporites (Dias *et al*. 1988). Almost all of the cores logged are within the tectonic Domain I (Chapter 4) characterized by half-graben 1 and half-graben 2 (Figures 7.1 and 7.2). The cores are 7 cm diameter, commonly 9 or 18 metres long, generally arranged in boxes of 1 m long, commonly with good recovery. The cores are placed in their correct context (Figure 7.1). Although they were cut more than 20 years ago, most of the cores are in good condition, but some are discontinuous, due to extensive sampling for petrophysical, petrographic and palaeontological studies. Some of these cores, particularly where shaley, are very broken and others have gaps of small pieces. In these cases, the original black and white core photos, and also thin sections obtained from plugs were used as support for the core descriptions. The location, size and also the percentage of recovery of each core are described next to each core in each well in the Figure 7.1. The core logs and descriptions were done in 1:20 scale, but the integration of all informations is plotted in ANASETE (Petrobras in house software) and edited in the CorelDraw in a 1:40 scale, which are presented in the Appendices A1 to A7.

The uncored well 20 was sampled with sidewall cores and 600 m of wireline resistive image log FMI. This encompasses the entire stratigraphic interval, from Barremian (Coquinas) up to Aptian (Microbialites) within tectonic Domain II (Figure 7.1). This is an unconventional tool for facies analysis and the facies are defined as FMI facies (cf. Thompson, 1999) and used to generate a facies model for the Aptian microbialites carbonate succession.

The first half of this Chapter, describes the cored intervals and interprets the lateral and vertical facies variations, based on logged core. Most of the core was recovered from the Barremian coquina succession (Figure 7.1) and the facies and facies model for this succession were presented in Chapter 5. The second half of this Chapter

focuses on the FMI interpretations and the facies model for the Aptian microbialites succession.

Approximately 400 m of core from seven wells were logged (wells 1, 2, 6, 7, 8, 9 and 12). The cores sampled encompass the Barremian biochronozones A to D (Chapter 2, Figure 2.7) of the late syn-rift tectonic stage. However, wells 6 and 9 also contain cores of the Aptian post-rift succession, biochronozone E (Figure 7.2). Such biochronozones, previously cited in the Chapter 2 and detailed in chapter 8 section 8.4 (Figure 2.7), are based on non-marine ostracod fauna and are correlated, in this thesis, with Gamma Ray log curve variations. The integration of data, descriptions, analysis and interpretation of all the wells are presented as integrated logs in ANASETE software, plotted on expanded scale and available in Appendices A1 to A7, and the FMI interpretations in Appendices B1 and B2.

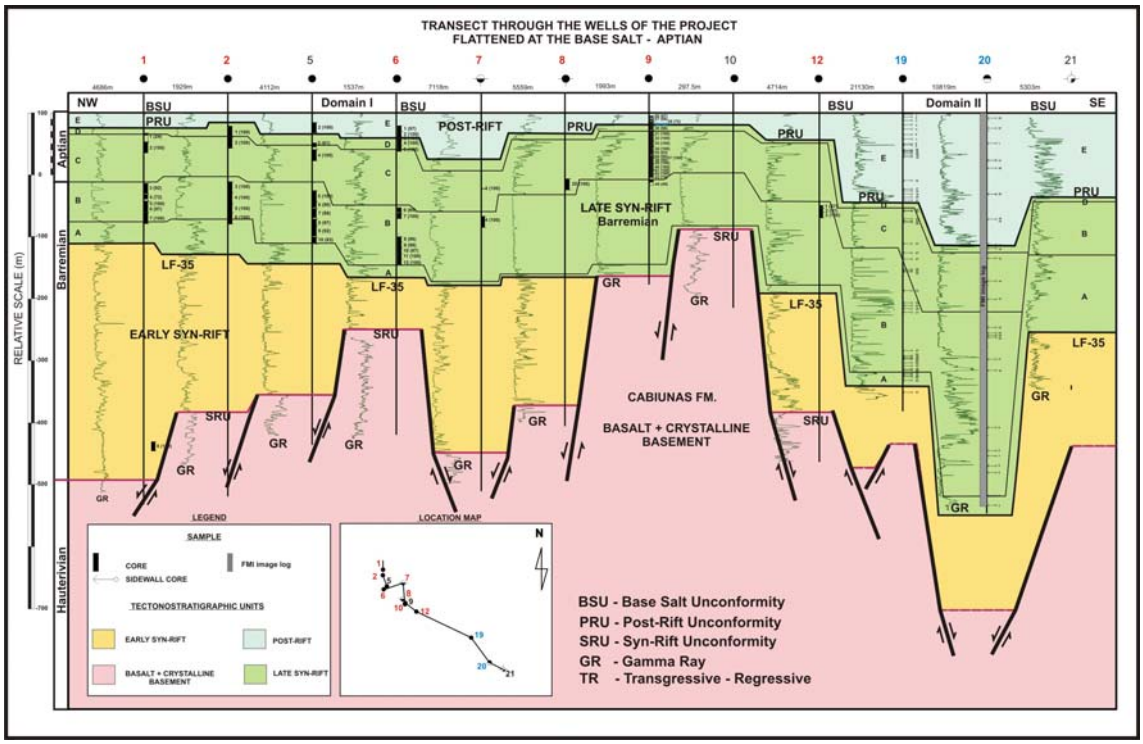

Figure 7.1 – Transect through the wells of the project, flattened at the base Aptian salt.

As a result of the core logging and interpretations, the FMI image log interpretation and also the side wall core descriptions (thin sections), an uninterrupted sedimentological and stratigraphical analysis and the construction of a simplified facies model has been undertaken. Such facies models allowed the recognition and definition of cycles and the analysis of their stacking pattern, temporal and spatial distribution of the facies and arrangement of the facies in the stratigraphical geometries, and this work is presented in the succeeding Chapter 8.

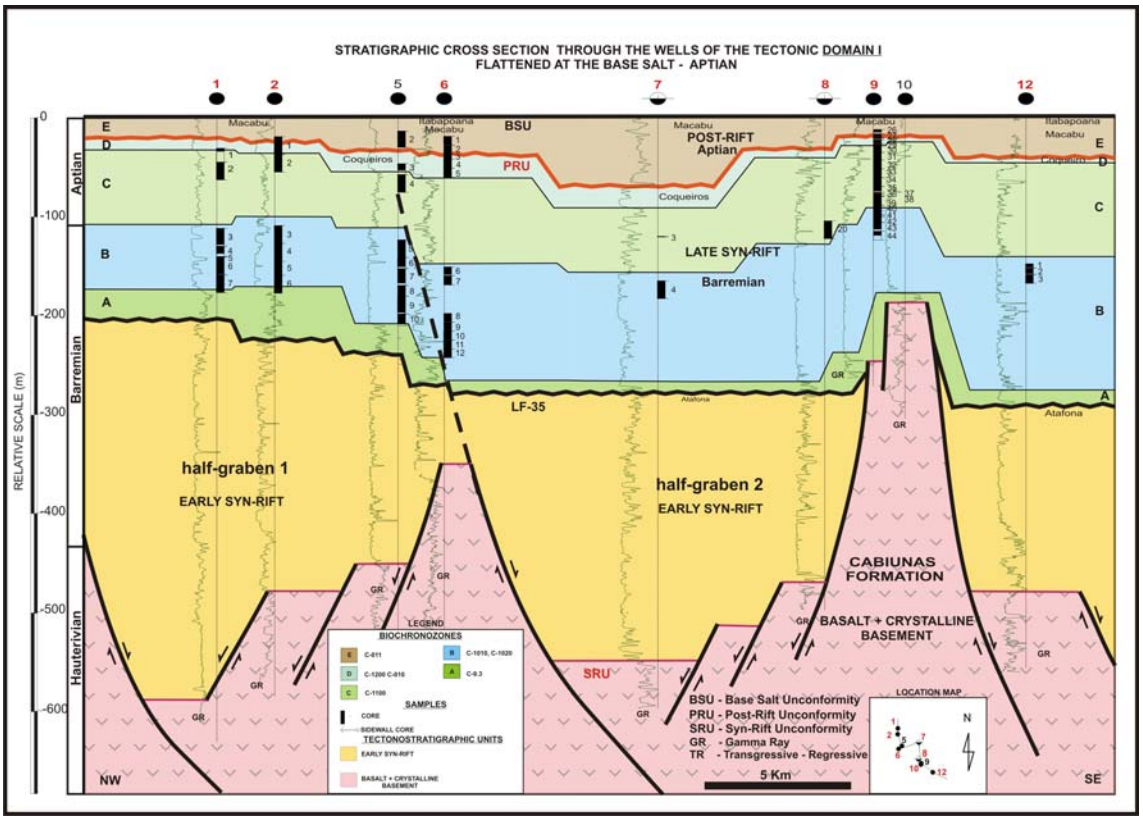

Figure 7.2 – Stratigraphic cross section through the wells logged in tectonic Domains I, half-grabens 1 and 2.

7.2 Description of logged cores, and Facies Associations, stacking and trends

Well 1

Well 1 is the most proximal in the west - east transect positioned at the hanging wall close to the border fault of the half-graben 1 (Figures 7.1 and 7.2). The well has seven cores totalling 85 m, taken from an interval of 146 m of bore hole with gaps (Appendix A1). The lithologies indicate a mixed depositional system with successions of carbonate and terrigenous facies alternating through the cored interval

Description:

Initially (box 18), core 7 has bioturbated siltstone (ST), ostracod rich and with plane-parallel laminations at its base (Appendix A.1). The siltstone passes upwards into packstone (Pb) and bioclastic grainstones and then to bivalve rudstones (box 17) with disarticulated and, in some cases, broken shells (boxes 11 to 8). The upper portion of the siltstone succession (boxes 16 to 14) underlies a 2 m thick packstone ostracod rich (Po) (boxes 14 to 12). A 20 cm thick laminated sandy bed (box 13) occurs interbedded with these packstones. The packstone succession is topped abruptly by a 5 m thick bivalve

rudstone layer. The top of this rudstone (Rmb) succession is marked by a 50 cm thick siltstone bed which underlies a 30 cm bed of rudstone with normal grading (box 7). Then, the succession continue in boxes 6 to 1 by 7m thick layer of fine grained sandstones with low-angle cross-bedding (Sfas) with basal erosive contact. This unit is capped at the top of core 7 by rudstones (Rmb) with plane-parallel stratification (box 1).

In the core 6, following mixed successions of interbedded carbonate rocks, rudstones of bivalves and packstones (boxes 18 to 15, 12 to 11 and 7 to 4) with sandy deposits (boxes 15 to 12, 10 to 7 and 3 to 1) occur. The rudstones occur in amalgamated beds reaching up to 2.5 m (boxes 7 to 5) or interbedded with sandstones (boxes 12 and 11). They generally exhibit abrupt basal contact with sandy (boxes 17, 14 and 7) or silty facies (box 12). Locally occurring with a sandy matrix (Rtb), normal grading and passing gradationally into packstones (boxes 17 to 15 and 7 to 4). The packstone is bivalve-rich (Pb) at the lower part of the core 6 (boxes 15 and 16) and ostracod rich (Po) upward (boxes 1, 2 and 4), occurring in 1 m thick beds, generally. Some imbricate shells are observed at the base of the box 1. The sandstones are fine, bioclastic (bivalve-rich) occasionally massive (boxes 14 and 15), but generally with plane-parallel stratification (boxes 10 to 7).

At the top of the core 6 are noted hybrid facies, composed of reworked sandstones and deposits of bioclastic carbonate rocks, with bivalve shells, ostracod-rich, and rare ooids (boxes 3 and 1). The core 5 sampled 0.5 m of packstone ostracod-rich (Po). At the base of the core, a 5 cm thick bed of floatstone of oncoid with mouldic and vuggy porosity occurs. A gap of 2.9 m occurs between cores 5 and 4. The core 4, however, is characterized by a thick layer of amalgamated beds of rudstone of bivalve (Rcb) totalling approximately 8.5 m. Beds of rudstones are bivalve rich. Most of them are replaced by silica. The basal contacts of the beds are normally abrupt, but also erosive (boxes 6 and 3). Core 3 is characterized by intercalation of carbonate rocks and sandstones. The carbonate rocks vary from 1 m (box 17) to 7 m in thickness (boxes 12 to 6) and the sandstones varies about 3.5 m (boxes 16 to 13 and 4 to 1). Carbonate facies (Rmb and Rcb) are composed of bivalve shells, and have abrupt and erosive contact with underlying beds of sandstones. Exposure features can be seen at the top of some beds (box 5). Sandstones occur in layers of 3.5 m (boxes 16 to 13) amalgamated with plane parallel stratification, locally bioturbated (boxes 4 to 1) and with abrupt contacts. However, at the top of box 4 the contact with the siltstone is gradational.

Core 2 shows a sequence of sandstones and siltstones intercalations, locally with metric carbonate beds (box 14). The first third of core 2 is dominated by siltstone (boxes 19 to 15) with plane parallel laminations interbedded with sandstone (fine grained-(Sf)) with bioclasts of bivalves and basal irregular contact (box 19). At the top of this lower siltstone succession (boxes 14 and 15), occur a 1 m thick packstone (Pb), with plane parallel laminations, that are bivalve rich (Pb).

In the middle of core 2 (boxes 13 to 10), sandstone occurs with plane-parallel laminations (Sfl), low angle cross bedding, tabular cross bedding (Sfs) and normal grading. Locally these facies occur with bioturbation (boxes 13 and 11). The upper portion of the core comprises 4 m (boxes 10 to 6) of laminated siltstones interbedded with thin beds of fine sandstone (< 20 cm). The following upward succession (boxes 6 to 1) is characterized by dense interbedded siltstone sandstone. The sandstone is fine (Sf), laminated, argillaceous, locally bioturbated and locally with slump structures. The beds commonly have gradational contacts but abrupt contacts are also quite common. In box 2 a 20 cm of packstone of bivalve ostracod rich is observed.

Core 1 shows an alternating succession of siltstones and fine sandstone (Sf) at the base (Boxes 4 to 3) and fine sandstones with peloids, ostracods and root marks at the top. The upper part of the core (boxes 2 to 1) is marked by a transitional succession of carbonate rocks upward, from wackestone peloidal (WK) through packstone (Pb) and a 1.5 m thick bed of rudstone of bivalve (Rmb).

Interpretation:

The facies associations observed in the vertical stacking is interpreted to represent the occurrence of marginal depositional environment, predominantly fluvial-deltaic (Reading & Collinson, 1978). The non-marine environment is indicated by the presence of throughout the well of bioclasts interpreted to be non-marine bivalves and the absence of any marine fossils. The bivalve shells are not well preserved due to the presence of abundant terrigenous sediments which is thought to have aided the breaking and abrading of the shells. For this reason the original bivalve species cannot be identified but are thought to be the remains of taxi preserved in more distal wells (Chapter 6). The extensive erosion of the clasts and the gravitational processes acting on these sediments, thus, hinder the taphofacies analysis as outlined in Chapter 6.

These deposits range from rhythmic siltstones, rich in organic matter and ostracod in deeper sites, to slumped deposits and turbidites, both products of

gravitational flows downslope, to shallower marginal carbonate (bivalve-rich) banks, in the lake margin (Talbot & Allen, 1978). A shallow origin for the carbonate rocks is indicated by the occurrence of low-angle cross-stratification. Platt & Wright (1991) have described the relationship of depositional facies and facies association with the continental rift palaeogeography. Such a relationship is also interpreted in this research. The successions of rocks described here, may also be compared with the fluvial-lacustrine facies dominated basin fill depositional sequence of Carrol & Bohacs (1999).

The facies association observed at the base of core 7 (boxes 18 to 15) is interpreted as pro-delta deposited in deep subaqueous lake environment (Tiercelin *et al*. 1992). This ostracod rich siltstone succession then passes gradually into bioclastic carbonates deposited in prograding banks of grainstones and rudstones in a shallower subaqueous environment (boxes 14 to 7). This is indicated by the coarsening-upward succession in this core. Upward, these banks are interrupted by laminated sandy deposits with low-angle cross bedding, which are interpreted as a high-energy shallow subaqueous environment facies. These sandstones are most frequent in shoreface facies, shoreline, and high energy environment or may occur as a reworking product of axial currents (Talbot & Allen, 1978). Overlying these is a succession of carbonate bank rudstone and packstone of bivalve (box 1, core 6 boxes 18 to 15) with thin beds (10 cm) of siltstone (box 16) and sandstone with plane-parallel and occasionally tabular cross bedding (box 17). This facies association is interpreted to have formed in fluvial-deltaic succession with bioclastic shelly banks, deposited in high energy environments (cf. Tiercelin *et a*l. 1992). Continuing upward in core 6, mixed successions of interbedded with sandy deposits are interpreted as delta front turbidites (boxes 15 to 7). Evidence for this comes from the fining up, depositional load structures and locally load and flame structures at the base of the beds. At the top and shallower positions this succession passes upward into carbonate bar succession (boxes 18 to 15 and 6 to 4). Some imbricate shells (box 1) associated with hybrid rocks are ostracod rich (boxes 4 to 1 and core 5) suggesting proximal shallow lagoon deposits, which are overlain by delta-top carbonates. These deposits form amalgamated prograding bars in periods of high lake level, regressive system tract with similar geometry proposed in Bosence (2005) and also Leeder & Strudwick (1987) for delta top carbonate platform in a marine environment. Such carbonates extend upward in cores 4 and 3 (boxes 12 to 5) with bioclastic bars, possibly as elongate long-shore banks.

At the base of the core 2 (boxes 19 to 15), the facies association of fine sandstones (Sf) with flame structures (box 16), burrows and fining-up trends, associated with siltstone with plane parallel laminations is interpreted as subaqueous environment with deep lacustrine prodelta turbidites (cf. Platt & Wright, 1991). This succession is overlain by a facies association of distributary sandy channels near the river mouth. In the middle of the core 2 is observed facies with normal grading, intraclasts, slump structures, which is considered to be of delta front origin followed by a typical deltaic plain distributary channels upward.

The facies association and the presence of root traces described in the base of core 1 (boxes 4 and 3) characterize a deltaic plain with interdistributary channels (cf. Tiercelin *et al*. 1992). These deposits may also occur as proximal siltstone of mud flat facies association, with thin beds of fluvial deltaic crevasse. These terrigenous successions are overlain by a 2 m thick layer of bivalve rudstones.

A 3 cm long fragment of vertebrate bone (Figure 7.3) was found in the core 2 box 15. This is the first reported occurrence of such a fossil in the Campos Basin. The bone has a triangular cross-sectional shape, lamellar porous aspect and is surrounded by hybrid sandstone, possible a turbidite. Professor Anusuya Chinsamy Turan (pers comm. 2010. University of Cape Town) diagnosed that this is a largely cancellous bone with the outer edges showing a parallel fibred structure. She identified, in the photomicrograph, darker lines that look like hypermineralised rest lines (Figure 7.3). Dr. Alexander Kellner (written communication, 2011), a researcher from Brazilian National Museum, suggested that this bone is near an articulation, possibly, with various growth lines (Figure 7.3) suggesting an animal of low metabolism, maybe a reptile; but not a pterosaur, or a theropod dinosaur. He reported it is likely to be a crocodilomorphous reptile or a dinosaur. Because of the small size of the bone and the fact to be found in redeposited sediments (turbidities), no further palaeoenvironmental considerations can be made except that it is consistent with a fresh water or brackish environment as interpreted by the other preserved biota.

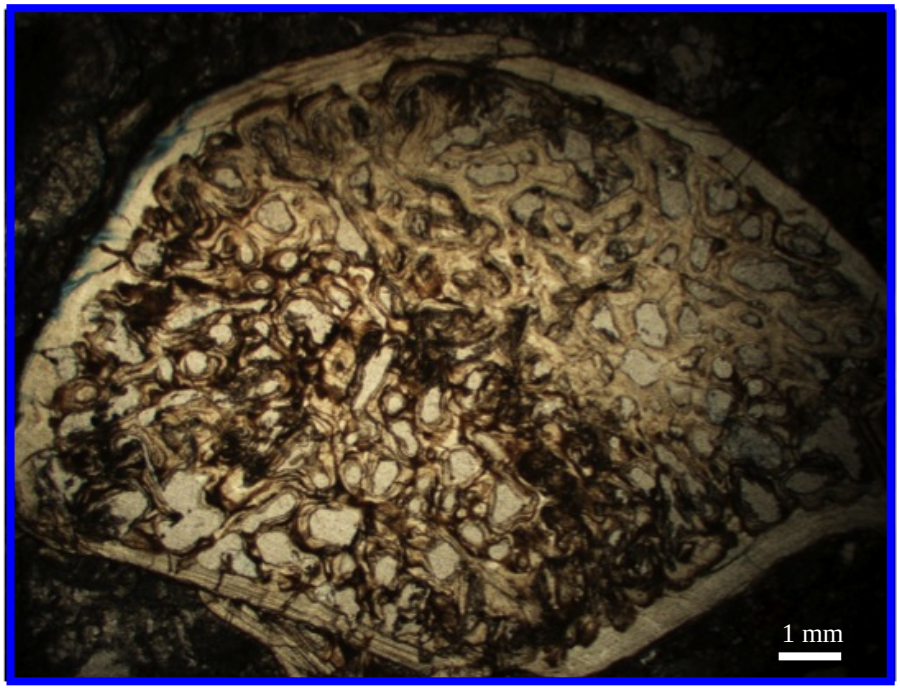

Figure 7.3 – Photomicrograph of vertebrate bone exhibiting triangular shape, internal structures largely cancellous bone with parallel fibred structure in the outer edges.

Well 2

Description

Well 2 is located approximately 2 km eastward from well 1 (Figure 7.1), in the mid-part of the hanging wall of half-graben 1 (Figure 7.2). Here, 6 cores were retrieved totalling 108 m (Appendix A.2). As with well 1, well 2 shows a mixed carbonate-siliciclastic succession as a consequence to the proximity of the siliciclastic source area. The stacking of the sedimentary succession shows a recurrent intercalation of carbonate rocks (cores 6, box 14 to core 4, box 14) and siltstones core 4, boxes 13 to 2, core 3, boxes 12 to 3). Shale (SH) occurs locally (core 6 boxes 19 to 14, core 2, boxes 19 to 9). The occurrence of fine sandstones (Sf and Sfl) decreases laterally in relation to well 1 (core 2, boxes 8 to 3, core 1 boxes 6 to 1). The facies in well 2 generally occur with pyrite concretions and poorly developed plane-parallel laminations. In addition, they are associated with a diamictite (DM or CM- muddy supported conglomerate) with flame structures at its base (core 6 box 17), and followed by packstone of bivalve (Pbo), ostracod rich (core 6, box 13).

The sedimentary succession summarised above underlies thick deposits of bivalve rudstones (Rcb and Rmb). Such deposits, are stacked in coarsening-up metre sets that begin with packstone (Pb) at the base (core 6, boxes 13 and 7, core 5 boxes 15 and 8) culminating with bivalve rudstones (Rmb) at the top (core 6 boxes 1 and 3, core

5, boxes 14 to 10). When amalgamated, the rudstones total some 25 m thick. Locally they show normal grading (core 5 box 5 to core 4 box 14). The basal contacts of the sets are in general erosive, when identified (core 6 box 7, core 5 box 8). These coarsening-upward successions may be overlain by a thin conglomerate bed, which exhibits an erosive basal contact (core 4, boxes 14 to 13). These conglomerates underlie a succession of laminated siltstones (core 4 boxes 14 to 3) which occur interbedded upwards in core 4 with thin beds of bivalves, ostracods packstones (Pob) and muddy packstone (Pmb). The packstones are ostracod rich, display plane-parallel stratification, rarely tabular cross-stratification and load structures at their base. Normal grading (core 4 box 2, core 4 box 4), weak bioturbation and escape structure (core 4 box 4) are also present.

Toward the top of core 4 and base of core 3, the succession described above is overlain by 7 m of muddy bivalve rudstones (Rmb) intercalated with thin beds of medium grained bivalve grainstones (Gmb) and bivalve and peloid packstones (Pbp and Pb) with disarticulated bivalve shells, intraclasts, exhibiting normal grading and wave ripples (core 3 box 18). These facies are, in general, moderately bioturbated (core 4 box 1, core 3, boxes 18 to 13). In the lower to mid portion of the core 3 an association of gravitationally deformed structures, scours and ripple marks and flames structures within the siltstones (ST) and carbonate layers (Pbp and MD). This succession underlies packstone and mudstone moderately bioturbated (core 3, boxes 3 to 1), with slide structures, calcite concretions, pyrite and phosphate nodules. The base of the core 2 shows shale (SH) interbedded with sandstone (Sfl) with plane-parallel and redepositional structures, such as slumps (core 2 boxes 19 to 16). Locally a diamictite (DM-diamictite or CM-conglomerate matrix supported) occurs with flame structures, calcite, pyrite and phosphate concretions. These successions are overlain by laminate shale (SH), which shows locally gravitational deformed structures, such as slumps (core 2 boxes 11 and 12) and calcite concretions (core 2 box 14 and 10). This succession coarsens progressively upwards, with transitional contacts, into interbedded laminated and moderately bioturbated 1 m thick bed siltstone (ST) and laminated and strongly bioturbated 2 m thick bed of fine sandstone (Sf) (core 2 boxes 9 to 3). These occur with bioclasts of bivalves, calcite concretions, wavy ripples and incipient cross-bedding.

At the top of this succession of siltstones and sandstones, is a 1 m thick bed of coarse grained bivalve grainstone (Gcb), associated with a 10 cm thick bed of rudstone (Rmb) and medium grained sandstone (Sm) (core 2, boxes 3 and 2). Bivalve and

gastropod-rich rudstones (Rmb) continue upward and are amalgamated into a 14 m thick succession (core 2 boxes 1 and 2, core 1 boxes 19 to 7). The Rmb shows in all sampled interval, tabular cross bedding, poorly-defined plane-parallel stratification and imbrications of the shells. Locally is noted the occurrence of dish structures (core 2 box 1) and clay clasts (core 1 boxes, 17 and 15).

The top of the core 1 is represented by fine grained sandstones (Sf) with shells of bivalves, and locally, scattered ostracods (core 1 boxes 7 to 1). These sandstones overlie the previous rudstones with an erosive basal contact. The sandstones occur with pyrite, calcite concretions and plane-parallel laminations; and locally present weak bioturbation (core 1 boxes 5, 3 and 1).

Interpretation

Well 2 is located 2 km eastward from well 1. The successions of the rock cored are quite the same, and the succession is still considered overall as a marginal lacustrine environment. At the base of the core 6 the rock is interpreted as sublacustrine facies association, with shales and siltstones exhibiting tractive and load structures and also weak bioturbation. Such facies associations are common in deep subaqueous environments and are interpreted as prodelta deposits (Pratt & Wright, 1991). As in well 1 the bivalve shells are not well preserved due to the presence of abundant terrigenous sediments and evidence for reworking, breaking and abrading of the shells. For this reason it is difficult to recognise the original bivalve species. The extensive reworking of these sediments enables them to be assigned to particular taphofacies as outlined in Chapter 6.

A series of meso-scale coarsening and shallowing-up successions (7 to 10 m thick, from core 6 box 14 to core 4 box 14), form bioclastic carbonates totalling approximately 32 m thick. These shallowing- up trends, normally begin with bivalve and ostracod rich packstone (Pob) and wackestone (WK) at the base and culminate with clean bivalve rudstones (Rcb) at the top (cores 6, 5 and 4). Locally these sets have a basal erosive contact (core 6 box 7 and core 5 box 8) but the first shallowing upward trend is gradationally up from fine grained siliciclastics (core 6 boxes 15-13). These trends are interpreted to occur in subaqueous conditions from amalgamated bioclastic prograding bars or banks (Figures 5.33 and 5.34). Such packstone and rudstone bivalve

bars are reported in Platt & Wright (1991, p. 61) as accumulating from steep-gradient 'bench' margins in low energy.

A shift of facies association and consequently depositional environment is marked by an erosive surface overlain by a 20 cm thick bed conglomerate (core 4, box 14) at the base of a 12 m thick unit of siltstone and interbedded bivalve and ostracod packstones (core 04 boxes 14 to 2). This facies associations interpreted to have accumulated in a deep subaqueous lacustrine depositional environment probably in a prodelta setting (cf. Talbot & Allen, 1978). The laminated packstones with local load structures are considered to be calciturbidites derived from a shallower lake margin environment and emplaced by density flow in the deep lacustrine setting.

This siltstone rich succession (core 4, box 14 to 2) represents a deepening or flooding of the depositional system as a result of active tectonism and /or climate change to a more humid setting. The basal conglomerate, overlying the erosion surface, is considered to have been generated from erosion associated with the transgression or flooding surface. The interbedded siltstones and packstones are followed by a thick amalgamated bed of packstone, grainstone and rudstone (Rmb), arranged in a coarsening and shallowing-up trend (core 4 box 2 to 1, core 3 boxes 18 to 13). The carbonate successions, suggests subaqueous lacustrine conditions, which are moderate to high. For rudstones energy, represent prolonged periods, of clastic-free, reworking and winnowing which suggests tectonic quiescence conditions and/or arid climate periods (Soreghan & Cohen, 1996). These shallowing upward successions are recurrent in time but develop at a lesser magnitude up section (core 3 boxes 12 to 1).

The strong presence of shale with gravitationally deformed structures, matrix supported conglomerate in the lower portion of the core 2 (boxes 19 to 10), and the progressive upward appearance of fine grained bioturbated sandstones and siltstones (boxes 9 to 3), indicates an increased clastic supply, increased accommodation space and a shallowing-up succession. Such a succession is interpreted to form following base level rise with the progradation of a clastic depositional system from prodelta (slope to deep lacustrine conditions), to delta front to sandy delta plain. These terrigenous successions are common in subaqueous to shallow subaqueous environments but this succession culminates with a 1 m thick, coarse bivalve grainstones interpreted as shoreface facies (core 2, boxes 2 and 2), and a 14 m thick amalgamated beds of muddy bivalve rudstone (Rmb), which is interpreted as a bar or beach deposits formed in a

subaqueous environment (core 2 boxes 2 to 1, core 1, boxes 19 to 7). The facies association reported above is typical of shallow water and high energy environments, such as beach, bars and shoreface deposits; evidenced also by the presence of cross-stratification, imbricate shells of bivalves and gastropods and also by the presence of clay clasts.

The overlying succession shows an erosional base (core 1 box 7), and is composed by fine grained weakly bioturbated sandstones interbedded with thin beds of shale (core 1 boxes 7 to 1). This facies association is interpreted as distal alluvial-fluvial settings as part of the Aptian progradational depositional system (Chapter 6). The strong shift of facies association and the erosional surface at its base is consistent with the presence of the Post -Rift Unconformity (PRU) which occurs at this level and is which is discussed in Chapter 9.

Well 6

Description

This well is located between the wells 5 and 7 (Figure 7.1) on the structural basement high of half-graben 1 (Figure 7.2). It was sampled in 12 cores totaling approximately 103 m. The entire cored interval is represented by interbedded sandstones, carbonate rocks and thin argillaceous beds (Appendix A3).

Core 12 comprises dark shale with a massive aspect (SH) at its base (boxes 10 to 3). Locally this facies occurs interbedded with thin beds of muddy rudstones (Rmb). These rudstones are composed of disarticulated shells of bivalves and ostracods (boxes 3 and 5), which normally exhibit erosive basal contact (boxes 10 and 3). of the lower rudstone (box 1) has a basal erosive surface, then a massive aspect at the base composed of shells up to 3 cm, most of them rounded. These skeletal grains occur in association with rounded bimodal volcanic grains. This passes up to a rudstone with 5 cm diameter shale clasts scattered toward the top. At the base of the core 11 a mix of fine-grained sandstone (Sfs) with fragments of disarticulated and whole bivalve shells, within bimodal sandy deposits is observed (boxes 10 to 8). The sandstones occur with low-angle cross stratification, bioclasts of bivalve shells of up to 3 cm in size, that are commonly rounded, and also scattered mud clasts (box 10). At some levels the beds of hybrid sandstones reach 2 m thick (boxes 9 and 8). In the upper portion of the core, where shale (SH) occurs interbedded with thin rudstones bivalves (Rmb), slump

deformations are present (boxes 3 and 1). The shale is black, organic matter rich and has, in general, massive aspect (boxes 7 to 1).

The core 10 is composed of siltstone (ST) interbedded with mudstone (MD) and also massive black shale (SH). Such intercalation normally occurs with beds of up to 1 m thick, where the rudstones of bivalves and rare gastropods exhibit inverse grading (box 9). In the upper part of this core slumped features are observed (box 1).

Shale (SH) with soft sediment deformation and bioturbation occur at the base of the box 9. The shale is black, organic matter rich and underlies muddy rudstones (boxes 10 to 8). These rudstones occur with disarticulated bivalve shells and with smaller and finer fragments toward the top of the beds. Similar beds also form amalgamated strata totaling approximately 7m occurring in boxes 7 to 1. Cross-stratification is poorly defined. Usually mouldic and intergranular porosities may be observed in this succession.

At the base of core 8, black shale (SH) underlies a layer of 1 m thick of muddy rudstones (Rmd) composed of disarticulated and also articulated shells of bivalves, with rare gastropods in a fine grainstone matrix, partly within taphofacies (see chapter 6) TF2a, TF2 and TF3a (box 9). Above this succession, occurs thick units of fine sandstones (Sf) and 2 m thick bioclastic rudstone beds (box 1 and 2), at the top of the core. The sandstones occur with plane-parallel laminations that are weakly defined.

Core 7 is composed by shale of massive aspect with a basal tectonic breccia (BT) with deformation, features, at its base (box 10). Sandstone (box 6) and rudstone (box 3) with slump features and further tectonic breccias are also seen. In the upper portion, up to10 cm thick beds of shale, slumped, bioturbated and with calcite nodules are found.

Core 6 has poorly laminated mudstone (MD) with associated black shale (SH). At its base, this core presents a silty portion with tectonic breccia and associated deformation features. Toward the top, occurs a bed of ostracod rich limestone which is 20 cm thick, exhibiting an abrupt and erosive basal contact. Some thin beds of siltstones (ST) or fine sandstones (Sf), show ripples, tectonic breccia and deformation, such as slumps (boxes 5 and 4).

From the base to the top of the core 5 shale with plane-parallel laminations is observed (boxes 5 to 4). These have with concretions of calcite, and are interbedded with rudstones of bivalves (Rmb). This facies has a peloidal matrix, occasionally replaced by stevensite. Some grains of quartz are commonly occurring along with disarticulated, broken and whole shells of bivalves. The shells range from 0.5 cm up to 3

cm in size. They lie in both concave-up and concave-down positions. The smallest shells occur at the base of the interval. Gastropods are quite common in this interbedded packstone and rudstone succession (boxes 8 to 5). In the upper part of this succession muddy rudstones (Rmb) occur composed by disarticulated bivalves, gastropods, with some intraclasts. This succession occurs above an erosional base in amalgamated beds (boxes 3 to 1). At the top rudstones of just bivalves and gastropods are more common. In thin section this facies is completely neomorphised, with a recrystallized matrix, some coatings of fringe cement. The skeletal grains have a preserved micrite envelope. The Rmb facies shows some substitution of silica and pressure dissolution features in the form of stylolites (boxes 3 to 1).

Core 4 is composed almost entirely of rudstone of bivalves and gastropods (Rcb/g) with muddy rudstones (Rmb) in the upper part of the core (box 3 to 1), when amalgamated; this facies reaches units 7 m thick. Locally the rudstones are interbedded with thin beds (20 cm) of wackestone (WK) and packstone (PK), with rounded to very rounded bioclastic grains, and rarely fragments of fish (box 5). The rudstone shows a recrystallized matrix, some visual porosity and stylolites. The shells exhibit micrite envelope and neomorphic calcite spar in thin section (Chapter 6.4, Figures 6.13 and 6.14). In addition to the abraded and small broken bioclastic grains, siliciclastic and argillaceous intraclasts are present.

Cores 3 and 2 are composed of coarsening up successions with coarse grained grainstones (Gbc) in the base and bivalve rudstones (Rmb) at the top. An erosional surface is noted at the base of the 2 m thick beds (boxes 6 and 4). A 40 cm bed of chert; deformed, brecciated and fractured, occurs in the base of core 4 (box 6). Shale with calcite concretions (boxes 8 to 3) and siltstone (box 2) occurs interbedded with thin beds of packstones (Pb) and bivalve rudstones (Rmb) with rare gastropods, in the top of the succession. At the top of the core 2 occur a 1 m thick bed of muddy rudstone of bivalve (Rmb) is found which has an erosional basal contact, clay clasts and gastropods. The rudstone is poorly sorted with small rounded fragments and peloids. At the top of the core 1 terrigenous conglomeratic sandstone and polymitic conglomerate (CG) occur arranged in a metric fining up stacking pattern, with markedly erosional basal surface. These units show plane-parallel and low angle cross stratification (box 10 and 5), and locally, slump features (box 9).

Interpretation

Well 6 is located in the basement high, footwall of the half-graben 1 (Figure 7.2), however the facies association and depositional context shows sedimentary successions that normally occur close to a normal fault (Tiercelin *et al*. 1992). This unpredictable occurrence is probably related to long lived fault in the hanging-wall of the half-graben 2 (Figure 7.2), as suggested by the presence of tectonic breccia (core 7 boxes 10 and 3, core 3 box 6) and deformation in the facies logged (core 12 box 7, core 11 boxes 3 and 1, core 10, box 1, core 7, boxes 10, 6 and 3, core 2, box 7 and 3, core 1 box 9).

From the base of the cored intervals toward to the top; core 12 presents black shale interpreted as a deep subaqueous environment (Platt & Wright, 1991) and a deep lacustrine facies association (DL & FA) (Chapter 5). This facies association occurs with some intercalated thin beds of rudstone (boxes 10 and 5) that are interpreted as bioclastic carbonates transported in by gravity flows, i.e. calciturbidites (cf. Platt & Wright, 1991). This succession is followed by what is interpreted as a shallowing upward lake margin succession shallow subaqueous deposits of marginal bioclastic bars with argillaceous beds at their base, which are common to occur in sublacustrine environments (cf. Talbot & Allen, 1978). A 12 m thick unit of siltstone and shale (cores 10 boxes 10 to 1 and also core 9 box 9 to 8) with centimetric mudstone interbeds is interpreted as deep subaqueous conditions (Tiercelin *et al*. 1992). This former succession is topped erosively by 10 m of muddy bivalve rudstone (core 9, box 7 to 1). These rudstones are overlain by fine grained sandstones (Sf) which are again topped erosively by rudstones (core 8). A thick succession of shale (SH) interbedded with sandstones and rudstones, is considered to be deposited in marginal lacustrine environment (Soreghan & Cohen, 1996).

Following a 29 m break in core 7, a 40 cm tectonic breccia is a strong evidence of active tectonism recorded in the vicinity of the well. This is suggested in well 6 by the presence of fine grained sandstones into a shale and siltstones deposits, with slumped structures and tectonic breccias (core 6, box 5).

The facies association in cores 7, 6 and 5, is considered to be deep subaqueous environment with thin beds of rudstones and packstones interpreted to be turbidites or tempestite. These deep water deposits are overlain by bioclastic bar deposits (core 5, boxes 3 to 1) again sharply overlying deeper water deposits. This suggests that another

plausible interpretation for these sequences is that the whole succession is interpreted as being deposited originally in a protected lake margin environment (McGlue *et al*. 2010).

Upward, from core 5 are amalgamated beds of muddy and clean bivalve rudstones (core 5 boxes 3 to 1, core 4 boxes 10 to 1) showing clearly aggradational deposits of shallow mollusc-rich bars followed by a shallowing and coarsening up stacked rudstones (core 3). These facies association is common to occur in high energy environment, bar or beach (Carvalho *et al*. 2000). At the top of the core 4 it is identified a 50 cm thick of brecciated chert.

The upper part of the core 2 shows shale and siltstone with thin beds of rudstone interbedded topped by metre bed of rudstone. These rudstones, gastropod reach, may represent beaches or bars deposits (Carvalho *et al*. 2000).

The polymict conglomeratic succession in the top of the cores (core 1 boxes 10 to 1), with its 10 metre thick of stacked beds, erosive surface and bed loads, is characteristic of an alluvial fan succession and is interpreted to be the product of uplift of the source area and associated climate change to more humid conditions. This succession is considered to be part of the Aptian post-rift progradational clastic succession (Dias *et al*. 1988).

Well 7

Description

This well is located in a structural basement low in the distal hanging wall basin (half-graben 2), approximately 2.8 km eastward from well 6 on the structural high (Figure 7.2). 19 m of core was studied; one metre from core 3 and 18 metres from core 4. core 4 is characterized by a thin bed of laminated shale (SH) and siltstone (ST) at its base, passing gradually upward in a coarsening-upward trend from bivalve packstone (Pb), to muddy rudstone (Rmb), culminating with clean rudstone (Rcb) at the top (boxes 14 to12, Appendix A4). This coarsening upward trend is repeated above in boxes 12 to 5 and 5 to 1. These meso-scale sets are capped by exposure features, such as tepee, caliche or mud cracks (core 4, boxes 12, 6 and 2). Calcite, pyrite and silica concretions are seen in all cored intervals. Some of the bivalve species can be recognized in these bioclastic carbonates. In general, *Desertella* (G) and *Esphaerium* (H) are found in fine grained, low energy facies, whereas the genera *Camposella* (E) and *Trigonodus* (A), which have bigger and thicker shells, are found in the high energy facies. The shells are normally disarticulated and only rarely found articulated. The taphofacies are most

commonly assigned to classes 2 and 3a. core 3 comprises shale (SH) with a centimetric bed of fine peloidal grainstones (Gfp). The shale is laminated, and at one horizon has thin silicified layers and exposure features (box 1).

Interpretation

The depositional environments interpreted for all succession in the core 4, vary from deep subaqueous, below the storm wave base (SWB), to shallower zones above FWWB, where the shells of bivalves form banks and shoals in marginal lacustrine areas (Chapter 5, Figure 5.33). The 3-4 mesoscale coarsening up sets are interpreted as shallowing upward trends formed as progradational fill of the basin margin. The facies trends are mirrored in the identified of taphofacies variations which also reflect shallowing trends and increase in hydraulic energy. These sets are markedly capped by erosive surfaces which may represent arid periods with lake dried (Platt & Wright, 1992). At the top of the core 4, a silica-rich facies occurs associated with subaerial exposure features, such as strong brecciation and caliche. The shale in core 3 is interpreted as either a deep lacustrine environment with sporadic episodic carbonate turbidite event to emplace the grainstone, or as a shallow, protected lagoon behind a coquina bank, with the thin grainstone as washover deposits (Aigner, 1985).

Well 8

Description

Well 8 is located approximately 5.5 km eastward of the well 7 and 2 km west of the well 9. The single core 20 sampled 18 m of rock (Appendix A5) from near the flexural border of the half-graben 2 (Figure 7.2). At its base, the core comprises tabular cross-stratified bivalve rudstones (Rcb) associated with coarse grained sandstones with normal grading, clay intraclasts, plane-parallel laminations and low angle cross stratifications (Scl) (cores 18 and 17). The basal contacts of the 0.5 to 1 m thick rudstone beds are in general erosive.

Amalgamated coquinas (Rcb) with disarticulated and also broken shells of bivalves occur at the intermediate part of the core (cores 16 to core 10). In this interval, allochthonous taphofacies TF3, TF4 and rarely TF6 are identified. Also, the bivalve genera *Camposella* (E), *Desertella* (G) and *Trigonodus* (A) can be identified. Locally at the base of some of the beds articulated shells, in position of life, are observed that indicate low depositional hydraulic energy probably at the SWB level (Figure 5.33).

At the top of the core 20 finer packstone (Pb) occur interbedded with clean rudstone (Rcb) facies. At some levels these facies occur with mud cracks laminated fabrics and nodules of silica, pyrite and calcite (boxes 6 to 4). It is possible to see faint bioturbation in the fine grained facies (box 7). In the upper part of the core plane-parallel lamination and low angle cross stratifications are noted in the carbonate facies (box 1). In the upper portion of the core the rocks are stacked in coarsening-up style, normally with an erosive base (boxes 9 to 7, 7 to 4 and 4 to 1).

Interpretation

Core 20 is interpreted as being deposited in subaqueous and deep subaqueous lacustrine environment above SWB (Figure 5.33) and with sporadic exposure. The depositional elements at the base (boxes 18 and 17) are normally observed in shallow, high energy carbonate and siliciclastic facies lake margin environments (e.g. Platt & Wright, 1992). The middle portion of the cored succession (boxes 17 to 9) is characterized by subaqueous carbonate platform with progradational, lake margin, bioclastic bars with tractive depositional structures (box 10), indicating the shallow conditions. Locally these successions are topped by erosive surfaces (e.g. box 10).

A deeper subaqueous succession with intercalation of bivalve packstones and clean bivalves rudstones overlies the bars successions. These two shallowing and coarsening-up 2 to 3 m successions form from sets of progradational bars and bar fringe in marginal lake conditions (boxes 9 to 1).

The presence of siltstone in the upper section, however, shows a possible climate change and increment of terrigenous input in the depositional system (Tucker, 1990). Rounded to subrounded bioclastic grains associated with quartz at the base of the interval may be considered as a redeposition or reworking of these sediments, in a sandy beach or delta mouth bar (McGlue *et al*. 2010).

Well 9

Description

This well is located between Wells 8 and 10 on a basement high in the footwall of half-graben 2 (Figure 7.2). It comprises approximately 105 m of rock, from a 108.3 m interval with gaps, totaling 18 cores (cores 26 to 44). From the bottom to the top, the successions are composed of a mix of carbonate rocks and terrigenous sediments (Appendix A6). The basal portion is predominantly carbonate rocks (cores 44 to 36),

whereas the upper successions are terrigenous (cores 35 to 26) interbedded with 3 to 7 m thick units of carbonates (cores 36 to 26), which are represented by clean (Rcb) and muddy rudstones (Rmb), with disarticulated and broken bivalves. The taphofacies identified in this interval are TF3 and TF4 and, more rarely TF6. At some horizons taphofacies TF2 with articulated shells and also disarticulated bivalve shells is also present. Recognized genera are predominantly *Esphaerium* (H), *Desertella* (G) and subordinately *Camposella* (E).

The carbonate succession range from packstones (Pb) to rudstones (Rcb and Rmb) with low-angle cross stratifications and poorly developed plane-parallel laminations (core 44 to 37). In thick rudstone intervals, e.g. core 39, amalgamated beds with cross-tabular cross-stratifications may be seen (core 39 box 1). From core 44 to 42 these bioclastic carbonates are arranged in 2 to 6 m thick coarsening-up trends with erosive bases (core 44 box 3, core 43, boxes 8, 6 and 3, core 42, box 5). Rarely the rudstone facies occurs with what is interpreted as hummocky sedimentary structures (core 42 box 6). The packstones to rudstones may also occur with silica and calcite concretions (core 44, boxes 2 and 1 and core 43, boxes 8 and 3). Bioturbation is quite common in the lower energy facies (core 42, box 2, core 35, box 5 and core 33, box 9). Pressure dissolution features (stylolites and dissolution seams) are also present (core 41, core 46, boxes 10 to 6). On the top of core 40 and 39 rudstones (Rcb and Rmb) are interbedded with siltstone (ST) and muddy wackestone (WK), with plane-parallel laminations. In this interval, carbonate rocks are ostracod-rich and microbialites with exposure features also occur. Core 36 comprises thin bedded argillaceous sandstone, laminated at the base, with silica nodules and locally is brecciated. Cores 35 to 34 to show an upward gradual change from bioclastic carbonates to interbedded sands and then siltstones. At its base a sequence of interbedded packstone with bivalves shells (Pb) and some intraclasts, with bioturbation and silica nodules is present. The recognized genera of bivalves are *Trigonodus* (A) and *Camposella* (E). The genus *Esphaerium* (H) is also identified with disarticulated and fragmented shells of the taphofacies TF3, TF4, and TF6. Locally the tabular cross-stratification tabular occurs.

From the upper half of boxes 33 to 30 is a succession of silt and sandstone interbedded with packstone and mudstone, and then siltstone at the top. The lower portion shows plane-parallel laminations, weak bioturbation with calcite and locally disarticulated shells of bivalves. The cores exhibit slip / slide surfaces. In the sandstones flame structures occur at some levels and intraclasts are associated with thin microbial

laminite horizons. Thin muddy rudstones, with ostracods occur interbedded in the siltstones. Pressure dissolution features occur in the form of stylolites and dissolution seams.

The succession that extends from core 30 to the base of core 27 is composed of shale and packstone at the base and the rudstones bivalves at the top. The shale shows plane-parallel laminations and calcite concretions.

The upper portion the carbonate facies varies from bivalve packstone to rudstones with the species *Camposella* (E), *Desertella* (G) and *Esphaerium* (H), and taphofacies TF3, TF2 and TF6. Taphofacies TF4 and TF5 rarely occur. At the top of this succession, ostracods and bioclastic rich rudstone are arranged in two coarsening-up trends (cores 29 to 28).

This succession is capped by an erosion surfaces overlain by polymitic conglomerates in the upper half core 27 and in core 26.

Interpretation

The overall successions seen in well 9 represent coarsening-up, progradational depositional systems, which vary from subaqueous to deep subaqueous to shallow subaqueous and emergent environments (Figure 5.33). The subaqueous facies are represented by banks or bars of bioclastic carbonate lacustrine margins at the base of overall succession (cores 44 to 40 box 3, and cores 39 box 9 to core 37, core 35 to core 34 box 8). The lower part of these progradational banks, are characterized by shallowing up stacking pattern (cores 44 to 40) whereas the upper part of the progradational shallowing up system by amalgamated aggradational sets of rudstones (cores 41 to 40, box 4, and core 39 box 9 to core 37). These successions are interbedded upward with shallow subaqueous facies, interpreted as marginal protected shallow lagoon environment accumulating siltstone with common emergent surfaces (core 40, box 3 to core 39, box 10). This is followed by further aggradational stacking of shallow, high energy bioclastic bars. The lacustrine carbonate margin, is then influenced at two levels by clastic supply (core 36 to core 34 box 8) with shallow sandy bioclastic shoreface facies gradationally overlies the previous carbonates (cores 37 to 36 and core 34 box 8 to box 1). These mixed deposits are characterized by interbedded rudstones and packstones with shoreface fine sandstones (core 34, box 8 to box 1) that continue with emergent surfaces into core 33 boxes 9 to 6. The carbonate dominated system, is however, interrupted by an erosion surface and a deepening up succession into deep

subaqueous pro-delta basinal depositional system. These facies are characterized by siltstones with plane-parallel stratifications at the base (core 33 to core 32, box 8) and siltstone interbedded with fine sandstones with flame structures, clay clasts and slumps features. These are interpreted as turbidites formed off the front of a delta (core 32 box 8 to core 31 box 4). This facies association normally occurs in muddy plain or river mouth and generally is topped by delta top carbonate, which is characterized by grainstones and rudstones interbedded with siltstone (core 31 box 4 to core 30 box 9). Accumulation continued with deep subaqueous basinal lacustrine shales (core 30, boxes 9 to 1). This facies coarsens upwards into subaqueous lacustrine carbonate bar facies (cores 29 to 27, box 3). Normally these facies occurs in the lake and marginal lake and common in subaqueous fringe bar environment.

The overall succession culminates with stacked polymict conglomerates, interpreted as alluvial fan deposits. These correlate with the post-rift prograding clastic succession and represent the emergent to shallow subaqueous part of this progradational clastic system (core 27, box 2 to core 26 box 1).

Well 12

Description

This is the most offshore cored well in the studied basin margin section. It is located 5 km eastward of the well 9, in the Domain 2 sub-basin in the hanging wall (Figure 7.2). Three cores were sampled totaling approximately 15 m: 0.4 m in core 1, 5.7 m in core 2 and 8.9 m in core 3. The cored successions consist essentially of bivalves and ostracod-rich rudstones (Rcb) and packstones (Pob, Pb) (Appendix A7). Locally these successions are rhythmic alternations of wackestones (core 3 boxes 10, 11 and 2) with coarser bioclastic carbonates and rarely thin beds of siltstones (ST) are noted (core 3 boxes 9, 2 and 1). The rudstones occur in two 5-6 m thick amalgamated successions with articulated shells of bivalves in core 3, boxes 4 and 2), and predominantly disarticulated shells in core 2 (boxes 7 to 3). Taphofacies TF2 and TF3 are the most common, but locally taphofacies TF4 and TF5 occur with imbricate shells and cross stratification (core 3, box 6 and core 2, boxes 6 and 5) in higher energy and shallower environments. The dominant genera of bivalves observed at the base of the beds are: *Camposella* (E), *Desertella* (G) and rare *Esphaerium* (H). *Camposella* (E). *Trigonodus* (A) is more common in the upper part associated with high energy facies. The finer grained facies are in general ostracod-rich, with plane-parallel laminations,

locally with exposure features, such as mud cracks, and bounded by erosional surface (core 3, box 9, core 2, box 1).

The amalgamated banks of coquina (Rcb) are generally cleaner than those from more proximal wells but can also occur with the packstones (Pb) and wackestone (WK). Occasionally gastropod-rich rudstones occur with normal grading (core 3, boxes 10 and 11) planar stratification and imbricate shells. These facies have stylolites and dissolution seams but locally occur uncemented with high porosity (core 3, box 8). They have calcite, pyrite and phosphate concretions (core 2, boxes 1 and 2) and locally exhibit exposure features.

Interpretation

The overall cored succession in the well 12, shows a recurrence between fine grained facies, ostracod-rich (Pob, Pb, WK), and coarse grained facies, bivalve-rich rudstones (Rcb). These occur in two coarsening up and shallowing-up successions (core 3, boxes 11 to 3 and core 3, boxes 2 and 1 to core 2, box 3) both capped by erosive surfaces (core 3, box 2 and core 2, box 3). These facies associations are likely to occur in the border of an isolated lake with little influence of terrigenous material (Pratt & Wright, 1991). They are interpreted to form from progradation of such a margin preserving facies from Storm Wave Base (SWB) up to exposure and erosion. However, it may also occur in deep subaqueous to subaqueous environments. (Figure 5.33), occasionally with exposure features due to the lake level fluctuations (Talbot & Allen, 1978). These successions occur in amalgamated beds and have previously been described as constructing banks or bars in proximal areas and fringe bar in more distal sites (Carvalho *et al*. 1995). Fine grained turbidites or distal tempestite may also be present interbedded with low energy facies in deep subaqueous conditions (Talbot & Allen, Op. cit.; Wright, 1991). The upper part of core 1 is a facies that is interpreted to be modified by subaerial exposure, such as collapse breccia, karst and silicification. Such features are result of the lake desiccation (cf. Talbot & Allen, 1978), but the underlying facies unfortunately was not cored.

7. 3 Description and interpretation FMI facies in well 20

7.3.1. FMI log interpretation

Fullbore Formation Micro Imager log (FMI), is proving an important tool for the identification and interpretation of rocks in uncored wells during subsurface analysis (Thompson, 1999). Good quality data provides continuous information about sedimentary textures and structures, sedimentary heterogeneities, cyclicity, stacking pattern, and significant features such as porosity types and fracture density (Al-Rhougha *et al*. 2005). In addition, in this thesis, micro-faults, vugs, fractures, stylolites, thinly laminated and graded bedding textures; also distorted and slumping features can all be identified on FMI resistive images.

Thus, the textural heterogeneity of carbonate rocks can be characterized by high resolution borehole image logs; particularly, as in this study, when integrated with the analysis of thin sections from sidewall cores, and combined with traditional gamma ray and sonic wireline log analysis (Appendices B1 and B2). Research using these techniques in well 20 where there are no conventional cores is aimed at generating a substantial framework for sedimentological and stratigraphic studies. Almost 600 m of FMI log, combined with gamma and sonic logs and 19 thin sections from sidewall cores were studied and interpreted; 200 m in the Aptian and 400 m within the Barremian succession. As a result, 10 FMI facies were recognized and interpreted, structures and depositional features were recognized and with textural observations used to erect facies succession, and identify possible sedimentary cycles.

7.3.2 Methodology

Figure 7.4 shows the flowchart of work undertaken, the software used and also further data analysed in the FMI interpretation. The work is divided into three distinct phases: 1) acquisition and pre-processing, 2) analysis and interpretation and 3) final graphical presentation. The acquisition was made onsite by Schlumberger, followed by data processing previously performed by geophysicists and geologists in Petrobras headquarters, using appropriate software.

Gamma Ray, sonic electric logs and thin sections from sidewall core samples were used as additional data in order to interpret and classify FMI facies. Thin section

analyses together with electrical borehole image log interpretation were later loaded into the integration software (Fig. 7.4).

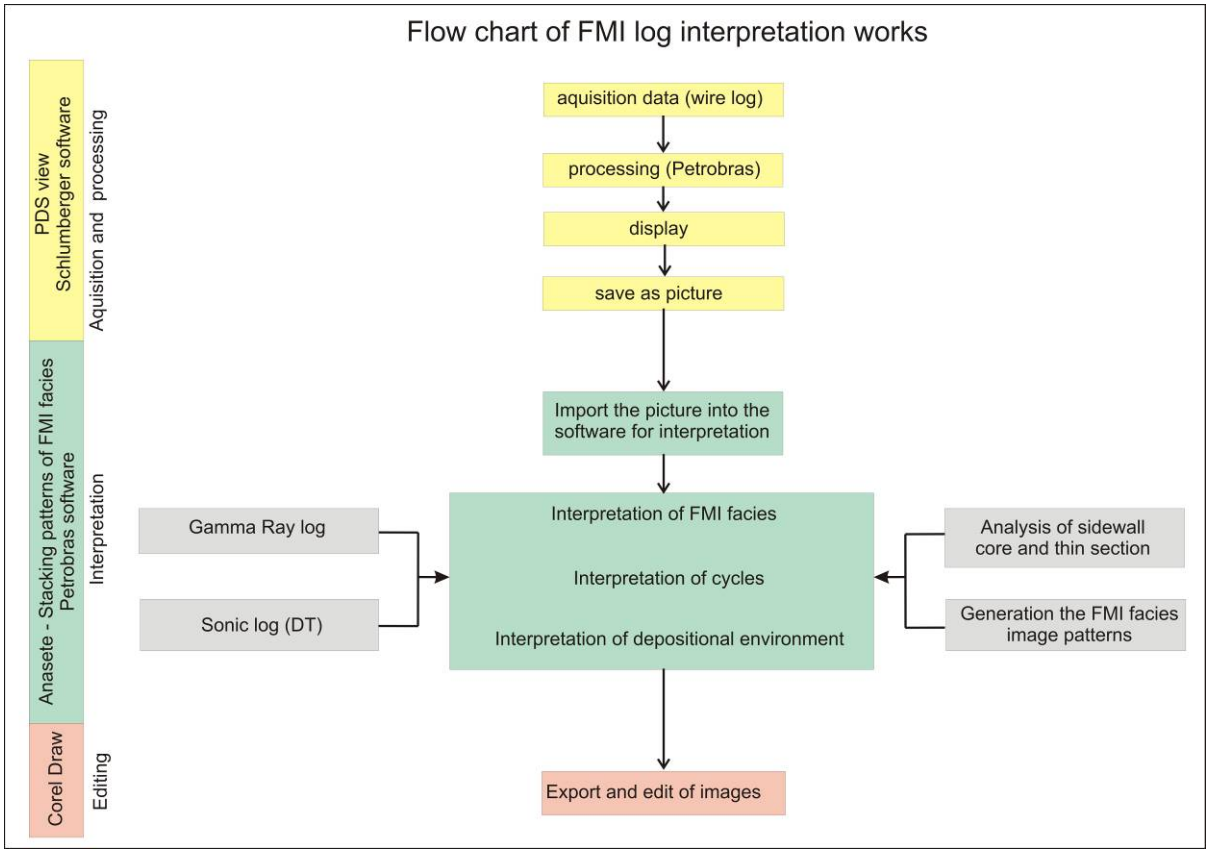

Figure 7.4 – Flowchart of FMI log interpretation work undertaken and software used for data from well 20

The FMI Image is coded into colours ranging from pale-yellow to dark brown and presented in dynamic and static displays. These variations in colour denote differences in resistivity of the wall rocks and pores. Lighter colours, for example, equate to denser and cemented rocks, or organic matter or hydrocarbon occurrence in the pores of the rock (Akbar *et al*. 1995). On the other hand, dark brown colours denote conductive clays and shale-like rocks (e.g. tight shale beds). Dark colour may also reflect water content in void, vuggy and porous rocks (Zhang *et al*. 2005).

The criteria used to interpret the FMI facies were basically the FMI patterns of colour variation, grain size image textures, sedimentary and the diagenetic structures identified. In addition, the conductivity reflects the composition, porosity, and the type of fluid contained in the rock. Analysis of the FMI image log from well 20 allowed the identification of ten FMI facies.

A high resolution display scale (1:10), was used for the FMI interpretation. The Gamma ray log was then used to indicate clay content (Appendices B1 and B2). This

was then used together with the FMI facies to establish larger scale trends of shallowing-up (increase in grain size, sedimentary structures and decrease in gamma values, locally capped by brecciated horizons) or deepening upward trends (decrease in grain size, sedimentary structures and increase in gamma values). These repeated trends are then interpreted as possible cycles of shallowing or deepening related to variations in the lake level. Density electric log is used mainly to correlate composition and porosity or diagenesis in the rock.

The repeated vertical association of the FMI facies in the interpreted shallowing and deepening trends has been used to propose a facies association scheme and depositional environment (Figure 7.18).

Although the data used is of good quality, some limitations are noted, such as: lack of sidewall core sample for the interpretation of some FMI facies, the scarcity of publications on FMI interpretation and facies recognition; diagenesis of carbonate rocks and also artefacts such as noise in the FMI image (Figure 7.17, and Appendices B1 and B2, red track) resulting from the borehole and tool problems.

7.3.3. FMI Facies

Ten FMI facies (FMI-1 to FMI-10) were interpreted after the establishment of distinct associations of structures and textures seen on the images (Figures 7.5 and 7.6). These FMI facies probably include a wider range of lithologies than those that can be detected in core and thin sections. For this reason they are given a separate classification scheme. The interpreted lithologies range from shale (FMI-2) and mudstones (FMI-5) associated with low energy depositional environments, to high energy grainstones (FMI-6) and rudstones (FMI-07) and abraded shells of bivalves. Autochthonous laminites (FMI-8) and stromatolites (FMI-9) were also identified with distinctive external shape and internal structures. Deformed, contorted, gravity deposited facies such as slumps and debris flows and diagenetically modified facies such as breccias (FMI-1) could also be recognized (Figure 7.6). The characteristics of the facies and some physical criteria to interpret the FMI facies are given in Figure 7.5 and examples of each facies are given in Figure 7.6.

Facies	Facies name	Features	Colour	Structures	Resistivity	Comments
FMI-1	Breccia	Broken, deformed, discontinuous	Light brown	Angular clasts? diffuse, contorted	High	
FMI-2	Shale	Thinly laminated	Dark brown	Laminated	Low	High resistivity when rich in organic matter or calcite nodules
FMI-3	Marl	Coarsely laminated	Light brown	Bioturbated	Medium-high	
FMI-4	Conglomerate/ debris /slump	Homogeneous, chaotic, contorted	Medium to dark	Coarsely grained structureless	Medium-high	
FMI-5	Mudstone	Massive aspect	Light brown	Homogeneous blocky	High	
FMI-6	Grainstone	Grainy	Light to medium brow	Homogeneous stratification	Intermediate	
FMI-7	Rudstones	Grainy, shelly,	Dark brown light brown	Homogeneous, strat	High intermediate	The resistivity and colour depends on the diagenetic processes and the type of fluid in the pores.
FMI-8	Laminite	Laminated, distinguish from FM2 and 3	Light to medium	Crenulated	High medium	Resistivity varies due to the heterogeneity and texture of the rock.
FMI-9	Stromatolite	Columnar	Light to medium	Laminated	High medium	
FMI-10	Thrombolite	Irregular shapes chaotic	Light	Structureless, diffuse	High	

Figure 7.5 – Main characteristics of the 10 FMI facies recognised and interpreted in the FMI log for well 20.

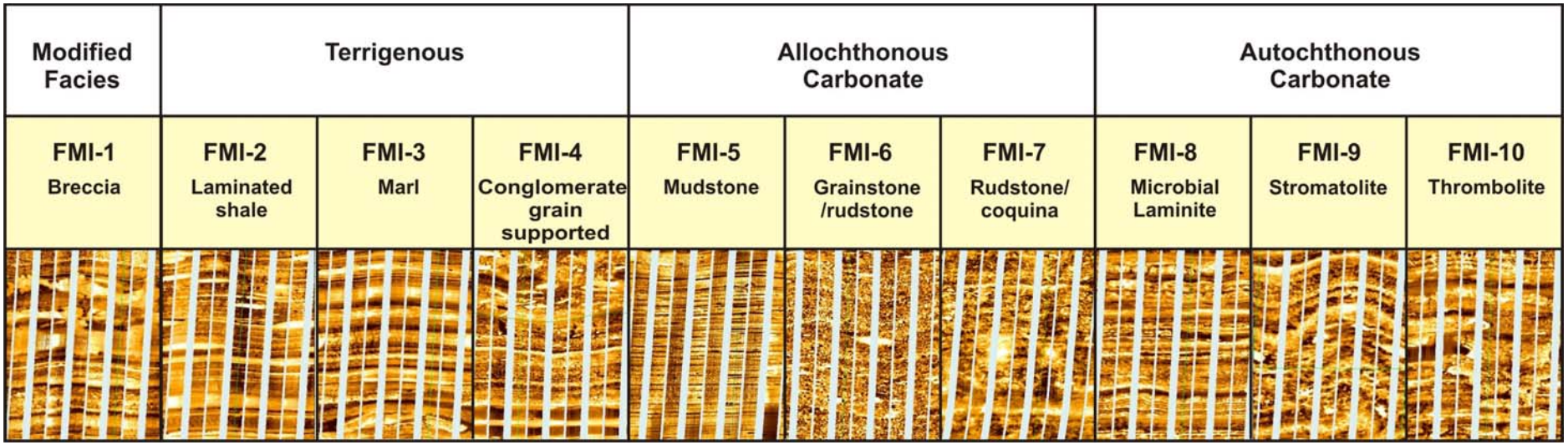

Figure 7.6 – Ten facies based on FMI log interpretation. The scale of each image is 10 cm wide cm 12 cm high and shows the complete dynamic image of the wall to the well. Detailed discussion of each facies is given in the text 7.3.3.

Modified facies

FMI -1- Breccia

This FMI facies shows discontinuity of thin beds and laminations of high resistivity (Figure 7.7), probably due to meteoric vadose diagenesis. Most of the occurrence represents exposure features with desiccation cracks, tepee structures, calcrete and silcrete, but also collapse breccia, or even tectonic breccia. The voids, holes and fractures between cracks are normally filled with younger material of different resistivity. This facies occurs in thin units, occasionally at the top of high frequency metre cycles (Purple track in the strip log, Appendix B2). Breccias such as this can have multiple origins and the following are all possible: 1) Caliche breccia, formed by in situ brecciation in arid and semiarid climates, controlled by soil-forming processes, and linked to extensive weathering, erosion, dissolution and shrinkage; 2) Collapse breccia, formed by collapse of beds due to the removal of soluble material within some beds (e.g. evaporites). 3) Tectonic breccia associated with faults.

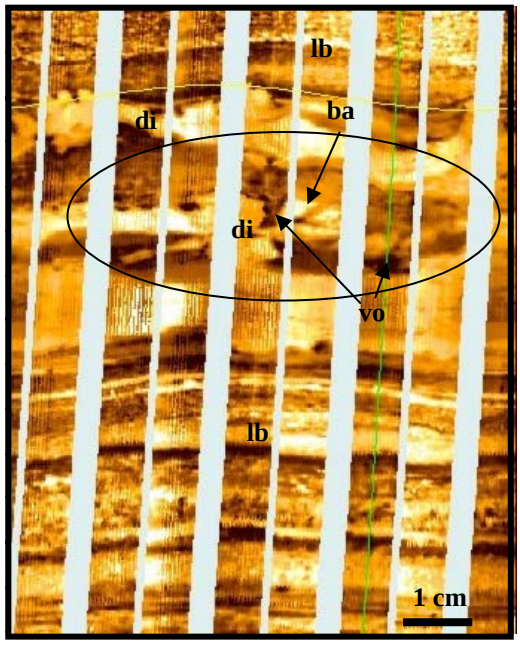

Figure 7.7 – (FMI 1) - Breccia - In the middle of the picture there are discontinuous (di) and broken aspect (ba) of the 10 cm bed with the holes and void between cracks filled with different sediment (vo). The breccia lost its original bedding continuity. However, this facies is bounded by bedded horizons above and below (lb).
(purple track in the strip log, Appendix B2).
Vs = Hs (This Figure is indicated in Appendix B2, track Sidewall core).

Terrigenous and bioclastic

FMI -2 – Shale

Normally the shale is very conductive with darker colours (Figure 7.17), but in some cases, this facies may occur interbedded with more resistive layers of calcite nodules or organic rich lithologies (Figure 7.8). When the shale is rich in organic matter or with higher carbonate content, the colour tends to be lighter due to the high resistivity. This FMI facies is thinly laminated and in some cases associated with

crenulated laminae suggesting microbial activity. The shales commonly show calcite nodules, rare bioturbation, and some conductive dark spots, interpreted as pyrite (Figure 7.8). These features are also commonly seen in the cores of the Shale facies (Chapter 5). An associated high Gamma ray response is an additional criterion for the interpretation of this facies. This FMI facies is generally associated with interpreted transgressive units (Tucker and Wright, 1990) and at the base of the metre cycles, representing flooding of the lake. Examples are seen in core in well 7 (core 4 box 18). In figure 7.17 (Appendix B1) and Appendix B2, it is represented by green color in the track lithology. This facies, as with its equivalent seen in cores (Chapter 5), is interpreted to have formed below the storm wave base (SBW), in deep subaqueous or profundal environments (cf. Tucker & Wright, 1990).

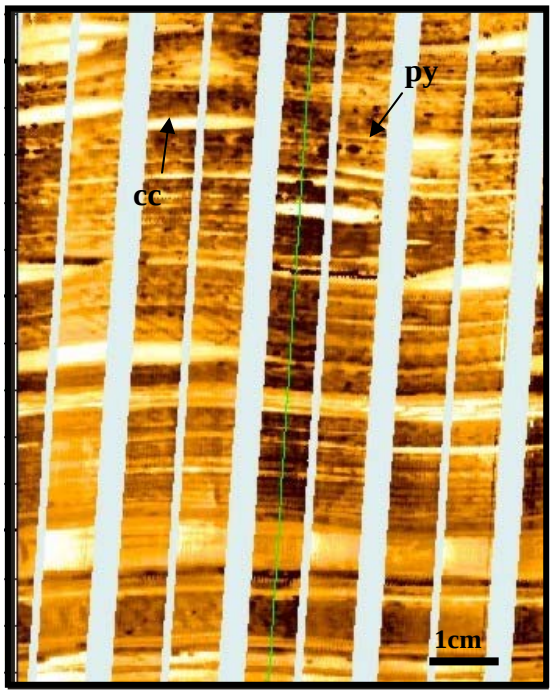

Figure 7.8 – (FMI 2) Shale - Thinly laminated shale (dark brown) with pyrite (py) and calcite concretion (cc) interbedded with marl and / or mudstone (light brown 1 cm beds).
Vs = Hs (This Figure is indicated in Appendix B2, track Sidewall core).

FMI -3 – Marl

This facies has intermediate resistivity, with lighter colours varying through to pale browns. When rich in organic matter or fossil content the colour tends to be lighter. The interpreted marl occurs in medium bedded (10-20 cm) units (Figure 7.9). The Marl occurs in units up to 10 m thick, in well 20 and good examples are seen in Figure 7.17 (sample 19). It differs from the shale FMI image in having thicker and lighter beds (more resistive) and some bioturbation (cf. Figure 7.9). Tucker & Wright, 1990 state that in lakes with prolonged periods of bottom oxygenation the profundal sediments may be bioturbated. This facies is interpreted to have accumulated below wave base in a

stratified lake because of its laminated aspect. This facies is normally associated with the interpreted transgressive units, occurring generally at the base of the metre cycles as seen in the base of the Figure 17 (track lithology, purple colour). It is bounded at the base by erosional surface and transitional contact to shale at the top. Is interpreted to have been deposit in a deep lake environment; below of the storm wave base.

Figure 7.9 – (FMI 3) Marl – Coarsely laminated marl with bioturbation. (b). At the base of the picture, may be seen the interpreted tee-pee (tp), a exposure feature.
Vs = Hs (This Figure is indicated in Appendix B2, track Sidewall core).

FMI -4- Conglomerate

The light small particles denote a grainy matrix with surrounding coarse clasts interpreted as limestone fragments (Figure 7.10). The clasts reach sizes up to 2 cm. Dark, small-sized conductive spots, rounded and sub-rounded, are interpreted as porosity. The resistive, light colour, bigger and planar-shaped fragments are interpreted as limestone fragments and the conductive, darker as shale clasts. The rock illustrated in Figure 7.10 appears to be a grain-supported conglomerate, poorly to moderately sorted, containing, probably, different types of rock fragments, as its components vary in size, shape and colours. Clasts are arranged parallel to bedding or in more chaotic orientations and also as contorted structures. In well 20, this facies occurs in the entire logged interval, mostly where the GR log presents higher values. It may reach thicknesses of up to 70 cm (Figure 7.17 and Appendix B2, track Terrigenous, FMI-3, MR). This FMI facies is interpreted to have formed as a high energy event in the lake basin as it erodes underlying strata and redeposited coarse pebble sized clasts.

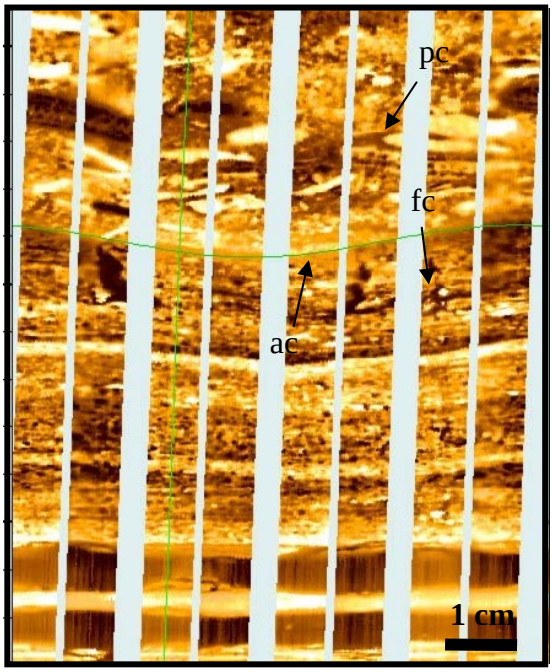

Figure 7.10 - (FMI 4) The upper part of the picture shows planar clasts (pc) of limestone in muddy to grainy matrix. Abrupt contact (ac) with underlying bed of grainstones which is laminated with fracture (fc) and vuggy porosities (vp).
Vs = Hs (This Figure is indicated in Appendix B2, track Sidewall core).

Allochthonous carbonate

FMI -5 – Mudstone

A high resistivity, bright colour, dense and finely laminated lithology (Figure 7.11). Commonly this FMI facies occurs with a blocky texture, but it also occur interbedded with shale of a darker brown colour (Figure 7.17 and Appendix B2, track Limestone, FMI-5, MD). It occurs in units, varying from 10 cm to 30 cm thickness. This FMI facies as with the Mudstone facies seen in cores (Chapters 5 and 6) is interpreted to have been deposited in deep subaqueous sites below the storm wave base (SWB), and in quiet waters.

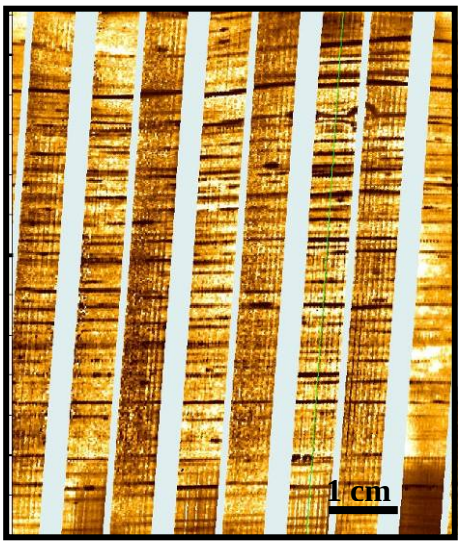

Figure 7.11 (FMI 5) Mudstone thinly laminated showing interbedded with more resistive calcareous beds.Vs = Hs (This Figure is indicated in Appendix B2, track Sidewall core).

FMI -6 – Grainstone/rudstone

This FMI facies has a coarse grain supported fabric. It shows intermediate resistivity and a medium colour due to the resistivity of different components (Figures 7.12a, 7.12b and 7.12c). Small dark colour spots are interpreted to be cavities filled by water. Otherwise, light coloured particles are interpreted as fragments of shells and the irregular shaped areas as a calcite or even silica cement. Visually the textures appear moderately to well sorted (Figure 7.12.c), and relatively homogeneous (Figure 7.12.a). In some cases with cross-bedding and plane-parallel stratification, indicating high hydraulic energy transported process (Figure 7.12.b). This facies occurs in units less than 1 m thick. But, where amalgamated, beds form deposits of tens of metres in thickness (e.g. Appendix B2, track Limestone, FMI 6, GR / RD). The basal contact is normally gradational and the top erosive. Locally this facies exhibits large irregular pores interpreted as karst features and the product of meteoric vadose diagenesis. The stratification types and interpreted coarse textures indicate a high energy environment of deposition. Clean washed traction deposits such as these commonly occur in the lake margin environments as discussed in Chapter 5 sections 5.2 to 5.4.

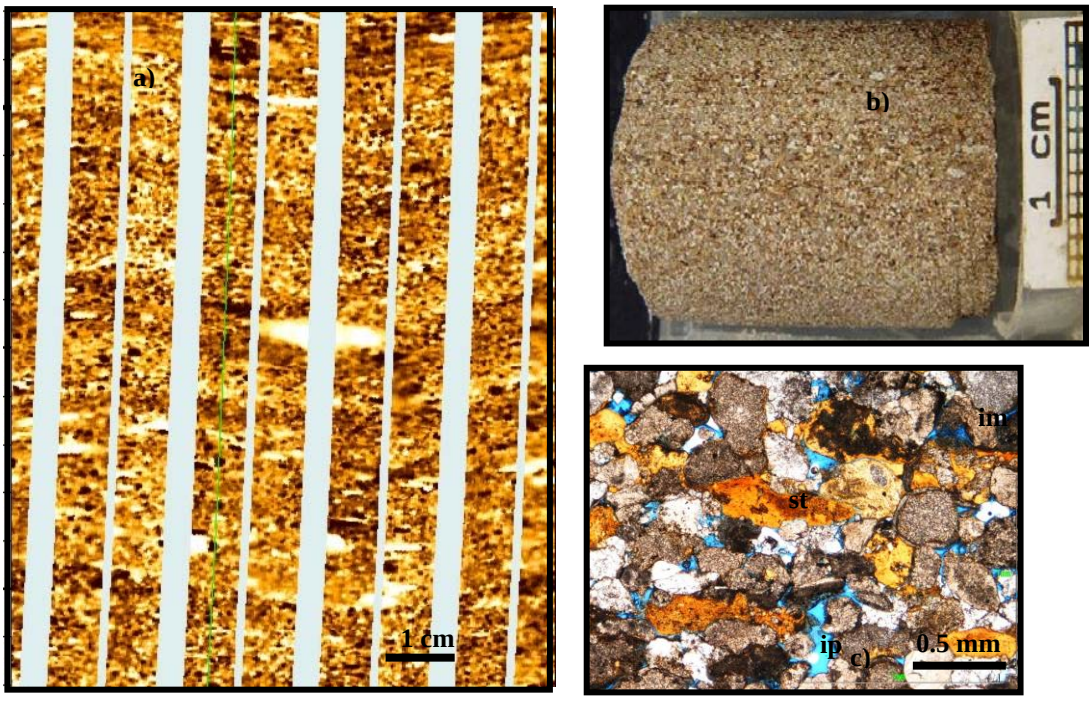

Figure 7.12 – (FMI 6) - a) Spots showing grainy textural aspect, well sorted. Vary in size and composition. The black small holes are interpreted as porosity, mouldic, intergranular, and vuggy. The resistive light colours are interpreted as calcite cement and limestone fragments. b) – sidewall core showing poor plane-parallel stratification. c) photomicrograph of the grainstones showing intraclasts of microbialites (im) and stevensite (st) mechanically deformed, reducing the primary intergranular porosity (ip). Vs = Hs (This location of this figure is indicated in Appendix B2, track Sidewall core).

FMI -7- Rudstones/ coquina

Facies of coarse grainy aspect, light conductive, with visible shells, and pores represented by dark brown colours (Figures 7.13a and 7.13b). Normally, the imaged shells appear disarticulated, broken or entire. Articulated shells are rare. The coquina occurs as massive units up to 10 m thick. When individual beds are amalgamated, it may reach tens of metres thick (e.g. Figure 7.17 and Appendix B2, track Limestone, FMI-7, RD / CQ). It may also occur with cross-bedding, indicated in the track structure (Appendix B1).

These texture and structures indicate this FMI facies is the product of high hydraulic energy, shallow lacustrine sites, such as shoreface deposits or shallow storm deposits (Carvalho *et al*. 2000). These would occur in the shallow to intermediate subaqueous, littoral zone, above fairweather wave base; forming subaqueous bank deposits (Davies, 1970). Often exhibits inverse grading, coarsening and shallowing up. The size and quantity of shells increase upward within the bedded units.

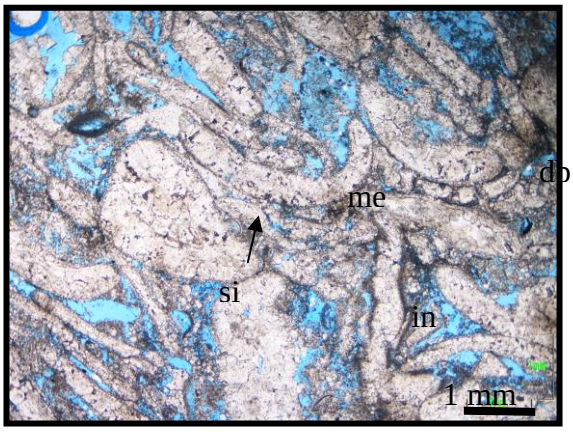

Figure 7.13 – (FMI 7) a) Rock of grainy texture with black spots of porosity and irregular light colour of cementation, fractured. b) - Photomicrograph showing rudstone of disarticulated bivalves (db), whole and broken shells, some with micrite envelope (me). The shells are neomorphosed into spar calcite, intergranular (in) primary porosity. Some shells are broken due to mechanical compaction. Some shells are partially replaced by silica (si). Vs = Hs (This figure is indicated in Appendix B2, track Sidewall core).

<u>Autochthonous carbonate</u>

FMI -8 – Microbial Laminite

This FMI facies is a finely laminated carbonate lithology (Figures 7.14a and 7.14b). Dark and light colours indicate both high and low resistivity. The laminae may occur in bundles and the laminae are characteristically crenulated which distinguishes

this facies from the laminated shale and marl (above). Two types of laminite may be recognized: The first are thin laminae, normally associated with facies such as shale and marl, the second, containing trapped coarser sediments. By the premises of the microbial rocks composition components, levels of different colours are interpreted to be carbonate with microbial and / or organic matter and also porosity or mud content. Two types of laminite may represent different settings: the first with the thin laminae, and associated with shale and marl are interpreted to have formed in deep subaqueous settings and the second with trapped coarser sediments, may relate to shallow subaqueous environments. Both formed in a calm water, low hydraulic energy environment. This facies are very common in lithologies of Aptian age (Figure 7.17, Microbialite succession and Appendix B2, track Microbial, FMI-8, LM).

Figure 7.14 – (FMI 8) a) At the base of the picture, a laminite shows a crenulated fabric. At the top of the unit a small low amplitude stromatolite is developed. The alternation of colours is interpreted to be due to the alternation of organic- rich shale and calcite rich intervals. Some dark brown colour may be porous space filled with water. b) – Sidewall core showing crenulated laminae with alternating dark and lighter laminae Vs = Hs (This Figure is indicated in Appendix B2, track Sidewall core).

FMI -9 - Stromatolite

This facies has laminated benthic mound-like microbial deposits (cf. Riding, 1999), with includes trapped limestone fragments, showing alternating colours reflecting resistivity variations due the diverse carbonate materials (Figure 7.15a). Dark brown colours suggest cavities filled with water whereas light colours represent continuous, carbonate laminae. Light coloured patches suggest trapped calcareous

fragments in the stromatolite mounds. The stromatolites imaged show the structures of up 1.5 m thickness. Small size cavities normally occur. In thin section are seen stained of different colours of different material and preserved fenestral porosity (Figure 15b). This facies is interpreted to occur in a sublittoral zone (Riding, 1999) in a restricted but high energy environment with strong microbial activity, normally associated with grainstones, clastic sediments (see Appendix B2, track Microbial, FMI-9, ST).

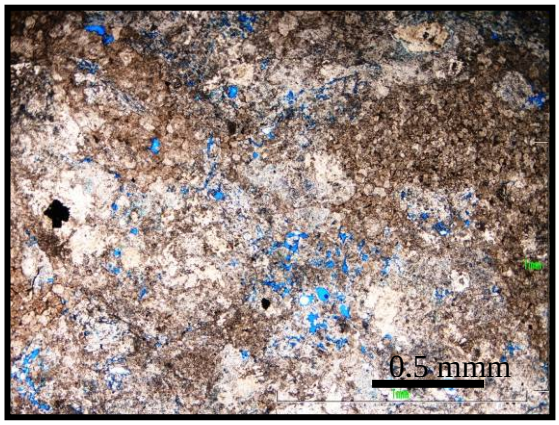

Figure 7.15 (FMI 9) a) Stromatolite showing convex-up layered structure with limestone fragments (lf) trapped. Some dark irregular voids but regularly distributed long of laminae, are interpreted as fenestral porosity. b) Photomicrograph of the stromatolite now dolomitized, with porosity, and few relicts of the original laminated fabric. Vs = Hs (This Figure is indicated in Appendix B2, track Sidewall core).

FMI -10- Thrombolite

This facies shows an irregular distribution of colours (Figure 7.16a). The resistivity varies due to the heterogeneity and texture of the rock. It has a lumpy or clotted aspect and occurs in association with stromatolite. Fragment of limestone are trapped, within thrombolite voids and fenestral porosity are common. In thin section a mottled or clotted fabric is seen with no preferential arrangement of particles (Figure 7.16b). Calcite and silica cement is quite common and mid-sized cavities show a dark colour. This facies is not common in the well 20, but is found in the Aptian Microbialite successions. It generally occurs in beds of less than 30 cm in size (Appendix B2, track Microbial, FMI-10, TB). This facies is interpreted to occur in subaqueous zone associated with medium to low energy environment (Riding, 1999; Feldmann & McKenzie, 1998).

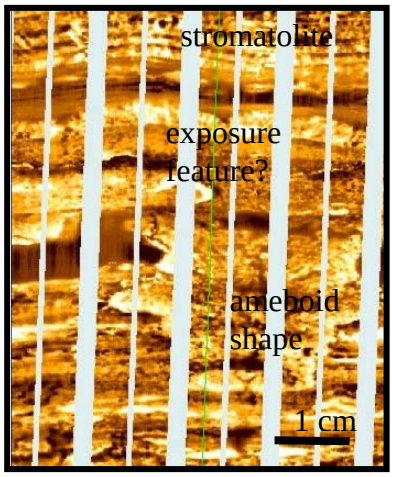

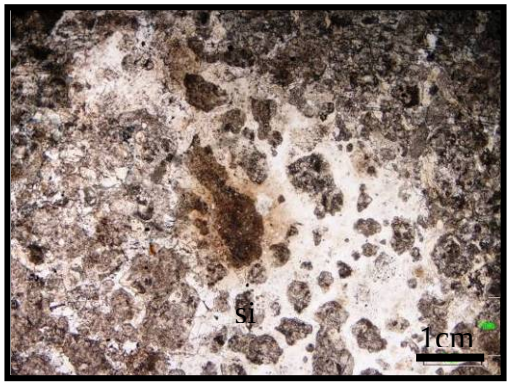

Figure 7.16– (FMI 10) a) Thrombolite with irregular clotted aspect with an amoeboid shape, with adjacent irregular and indistinct laminations, b) Photomicrograph showing clotted fabric, mottled aspect, silicified (si). Vs = Hs (This Figure is indicated in Appendix B2, track Sidewall core).

7.4 FMI based Facies Model for the Aptian Macabu Formation - Microbialites

The Appendices B1 (Figure 7.17) and B2 are Figures summarizing FMI image log interpretation from the well 20, which comprise Lagoa Feia group, coquina and microbialite successions. Some figures described in the text in the Chapter 7 are indicated: the main unconformities and also the main source rock of the pre-salt successions. Also the position of the sidewall core samples are indicate in these Figures.

The FMI facies in this formation are dominated by microbialites, facies that are only poorly developed in the more proximal, cored wells. A simplified facies model is therefore presented (Figure 7.18) which has been constructed from observations and interpretations of the FMI facies, recording the vertical association of FMI facies, and backed up with analysis of sidewall core samples and thin sections from well 20. In addition, Gamma Ray and Sonic log analysis, observations of the modern and ancient occurrences of microbialites have been used in the construction of the facies model and some major concepts are reviewed below.

Microbialites are defined as “organosedimentary deposits that accrete as a result of a benthic microbial community, which traps and binds sediment and / or forms the locus of mineral precipitation due to the cyanobacteria activities” (Kennard & James, 1986; Burne & Moore, 1987), or more simply as “benthic microbial deposits” (Riding, 1991). These structures can be found in a wide range of environments such as alkaline, freshwater lakes, hypersaline and marine settings (Dupraz *et al*. 2011; Riding, 1999), recorded in modern and ancient outcrops. The growth of microbialite structures is

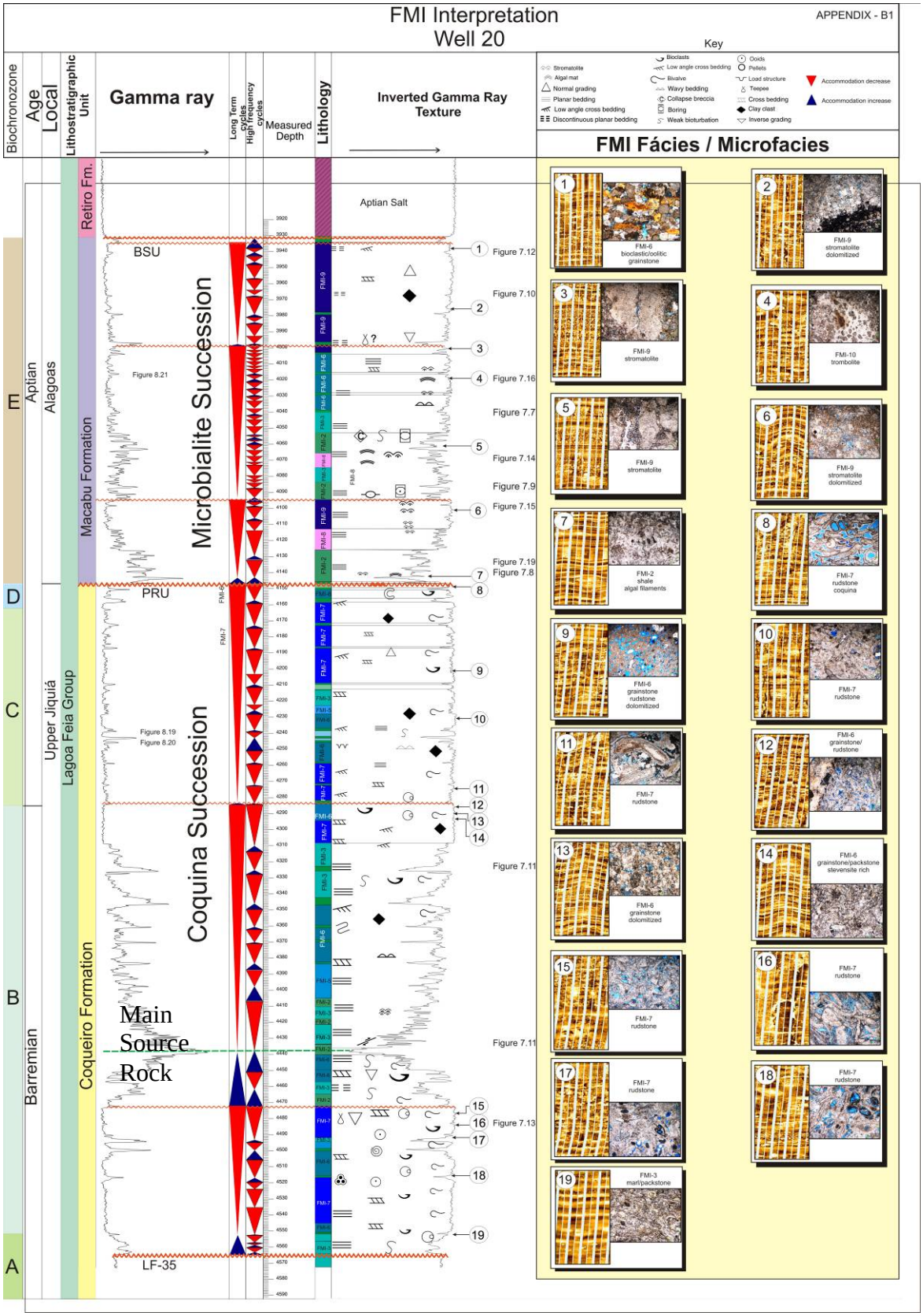

Figure 7.17 - Composite log of the pre-salt carbonate successions in the well 20, based on FMI log interpretations (Appendix B1).

normally associated with poor nutrients in the environment, absence of grazers such as gastropods, due to stressed conditions inhospitable to eukaryote organisms. They can be classified as laminites (laminated), stromatolites (laminated), thrombolites (clotted), and leiolites (structureless) (Dupraz *et al*. 2011).

According to various authors, (Playford, 1990; Feldmann & McKenzie, 1997 among others), the variation in type of microbialite is related to water depth, or degree of hydraulic energy. The first facies models for microbialites (or stromatolites as they were then labelled) were based on observations from Shark Bay, which established the lateral facies distribution within different depositional environments (Logan, 1961). Logan's model has microbial laminites in intertidal, shallower portions whereas subtidal, deeper water environments have stromatolite mounds. Where the water depths are greater, the greater the size of the stromatolite heads. In addition to microbialite morphology the degree of energy the environment may be incorporated into the model, for example, the highest energy environments have intermound bioclastic or oolitic grainstones with tractive sedimentary structures (Figure 7.12). An outstanding question in the study of microbialite palaeoenvironments are the different conditions that lead to development of either stromatolites or thrombolites. Feldmann & McKenzie (1997), show in Santa Pola, Messinian, SE Spain a thrombolite - stromatolite association that places the heads of stromatolites in positions of moderate to high energy in back reef environments whereas thrombolites occur in deeper positions of the front reef. Similar statements they have made for microbialite occurrences in the modern environment of Lee Stocking Island, Bahamas (Feldmann & McKenzie, 1998). They proposed that the stromatolite-thrombolite associations in Bahamas did not grow contemporaneously, but the environmental changing caused by sea-level fluctuations, controls the development of each type of microbialite. On the other hand Mancini *et al*. (2004), studying Upper Jurassic thrombolite reservoirs from the northeast Gulf of Mexico, argue that thrombolites are formed in low-energy and eurytopic palaeoenvironments.

Based on the literature cited above and the interpreted shallowing-upward facies relations in the FMI log, a schematic facies model has been erected in order to show the distribution of microbialite FMI facies for the Aptian of the Campos Basin (cf. Muniz *et al*. 2004; Muniz & Bosence, 2008). Four environments are interpreted: deep subaqueous (below storm wave base), intermediate subaqueous (below fair-weather wave base), shallow subaqueous (above fair weather wave base, very shallow conditions) and

emergent (or, subaerial). Each environment has a characteristic facies and facies association.

Although some previous studies from the Campos Basin consider facies as tidal related (Dias *et al*. 1988), in this study no evidence has been found of marine conditions (see section 2.6, Chapter 2) so that environmental zones based on tides, such as those used in Shark Bay (e.g. intertidal) have not been used. Moreover, the arguments are presented for a non-marine (brackish to freshwater) lacustrine environment for the accumulation of non-marine ostracods and endemic non-marine molluscs rich carbonate facies (Chapter 2).

The Figure 7.18 show the schematic facies model based on FMI log for the microbialites of the Aptian succession, Campos Basin. This simplified scheme shows the environment, the lateral facies association and the characteristic FMI facies. This facies model is used for the understanding of the arrangement and the stacking pattern of the cycles (Figure 7.20) developed in Chapter 8.

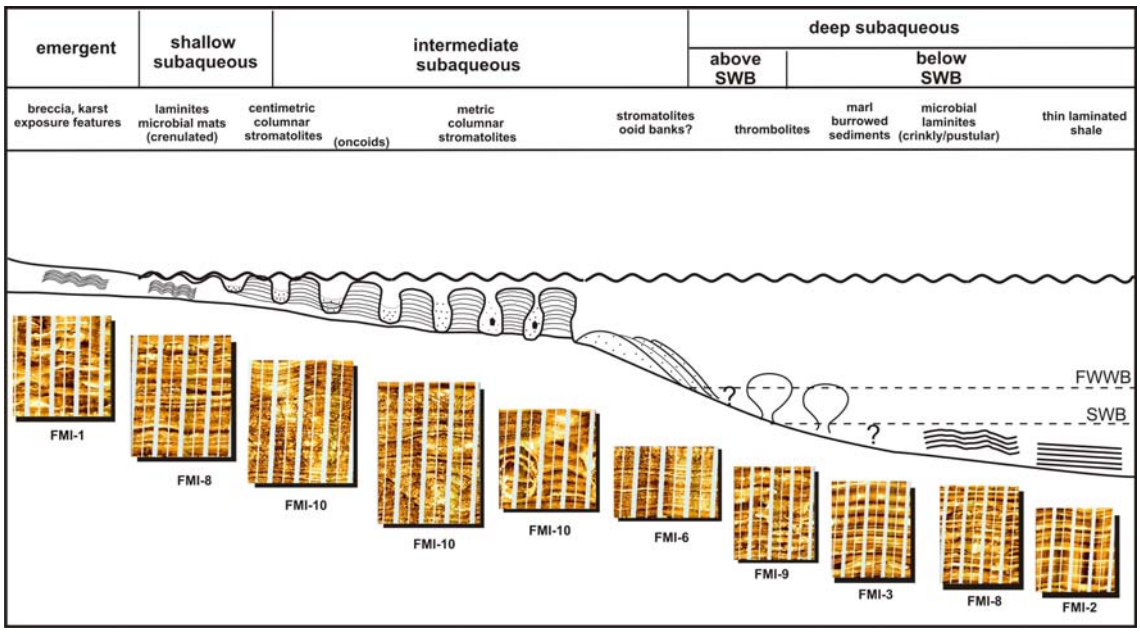

Figure 7.18 – Schematic facies model based on FMI log for the microbialites of the Aptian succession, Campos Basin.

Deep subaqueous

In the deep subaqueous environment, finely laminated shales (FMI 2) are interpreted to occur in restricted, basinal sites. These shales are generally poor in fossils, organic matter and pyrite rich, and show high values on the Gamma Ray log (Figure 7.18 and Appendices B1 and B2). Associated with these facies are the microbial

laminites (FMI-8), pustular and crinkly, which in some cases have microbial filaments, indicating a biotic origin for these sediments (Figure 7.19).

A shallower setting is interpreted for laminated marls (FMI-3) as these indicate some degree of oxygenation from the occurrence of bioturbation (Figure 7.9). They are thought to occur close to SWB and are observed vertically adjacent to thrombolite occurrences in well 20. Although in the literature examples of thrombolites are given from higher energy environments (Feldmann & McKenzie, 1997 and 1998), Mancini *et al*. (2004) consider the thrombolite construction in low energy deep water conditions. It is considered here that the thrombolites occurred in deep lake environments because of their occurrence, in thin beds (< 30 cm) in association with low energy facies (FMI-2, FMI-3 and rarely with FMI-9 - Appendix B2). However, the possibility of associated hydrothermal fluids or lake floor springs cannot be discounted because long-live faults occur in the vicinity of well 20 (Figure 7.1 and 7.16). These thrombolites occur in well 20 both dolomitised and silicified (Figure 7.16).

Above SWB and below the FWWB occur in the position of platform margin, prograding grainstone banks, which may occur with the intraclasts of reworked stromatolites, and also ooids (Figure 7.12). These deposits occur in areas of highest energy are normally clean with tractive structures such as cross bedding (see FMI-6 in the Figure 7.15) and planar bedding. The mounds of stromatolites from the deep subaqueous environment are typically 1-2 m forming columnar structures and intermounded areas are filled by clastics and or ooids (Appendices B1 and B2).

Intermediate subaqueous

Considering the observations from modern occurrences and the ancient outcrops, the intermediate subaqueous zone, is interpreted to be located around fairweather wave base water (FWWB) in shallow and also protected zones (Figure 7.18). This zone, however, occur next one Shallow subaqueous and centimetre scale stromatolite mounds can be seen (FMI-9, Figure 7.15). Intraclasts, ooids and oncoids are interpreted to have been deposited as intermound sediments (see Appendix B2). These deposits exhibit tractive structures such as plane-parallel stratification. Toward the shallower sites close to the shoreline, the stromatolite heads decrease progressively in size to less than one metre. Thus, the size of the bioconstructions, in such conditions, may become a good lake depth indicator (cf. Logan, 1970).

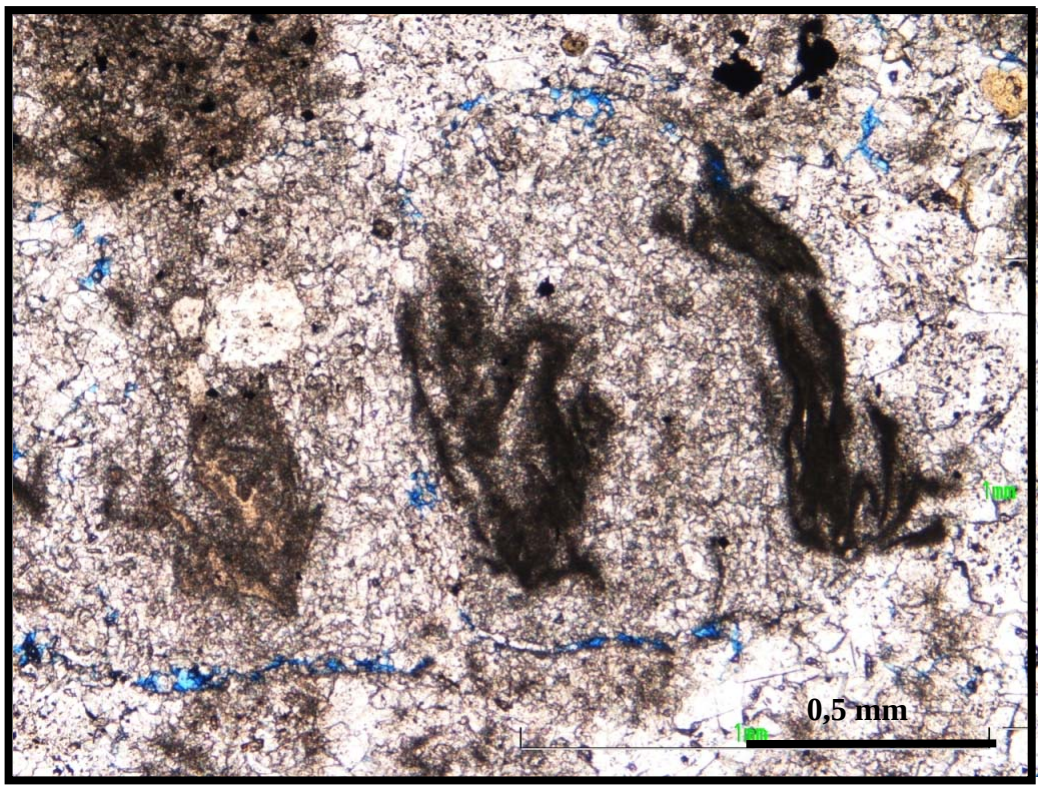

Figure 7.19– Filaments with micrite walls indicating algae or filamentous cyanobacteria suggesting the biotic origin of the microbialites studied. laminite partially recrystallized, dolomitized and silicified (This Figure is indicated in Appendices B1 and B2, track Sidewall core).

Shallow subaqueous

This zone is interpreted to be located above FWWB in shallow, low energy environment (Figure 7.18). It can be compared to the upper intertidal zone of Logan (1970). In these shallower conditions with limited accommodation space, the bioconstructions tend to be smaller and thinner bedded than the previous described zone. In the shallow subaqueous environment, planar microbialites, such as microbial laminites (FMI-8) are present. These facies tend to occur associated with terrigenous sediments, in more proximal areas, and small sized stromatolites (see Appendix B2). Locally they can show desiccation cracks and exposure breccia due to the sporadic subaerial exposure resulted from the lake level fluctuation. The characteristic microbial laminites are generally crenulated (Figure 7.14). This facies, however, is texturally different from the deep subaqueous laminites. In shallow setting, the crenulated laminites are rougher, commonly trapping coarse terrigenous sediments and often times with bioturbation organisms, such as worms and even gastropods (grazers).

Emergent

Located above the level of high lake level, in proximal areas of low relief this zone is flooded only occasionally. The diagnostic characteristics of the emergent environment are subaerial exposure features generated by early vadose diagenesis such as, karst, collapse breccias, shrinkage cracks (well illustrated in the Chapter 8 section 8.3.2) and tepees (FMI-1, Figure 7.15). These represent FMI facies FMI-1. The geometry and some characteristic features of this environment can be compared with supratidal environment of the marine conventional facies model (Logan, 1970). The presence of terrigenous sediments is commonly associated with these facies in more proximal areas. However, the analysed well 20 is located offshore with little influence of terrestrially derived sediments. The modified facies (FMI-1) that characterize the emergent environment, therefore, is most likely to occur associated with shale (FMI-2) and marl (FMI-3) of the subsequent transgression (lake level rise – see Appendix B2), or even microbial laminite (FMI-8).

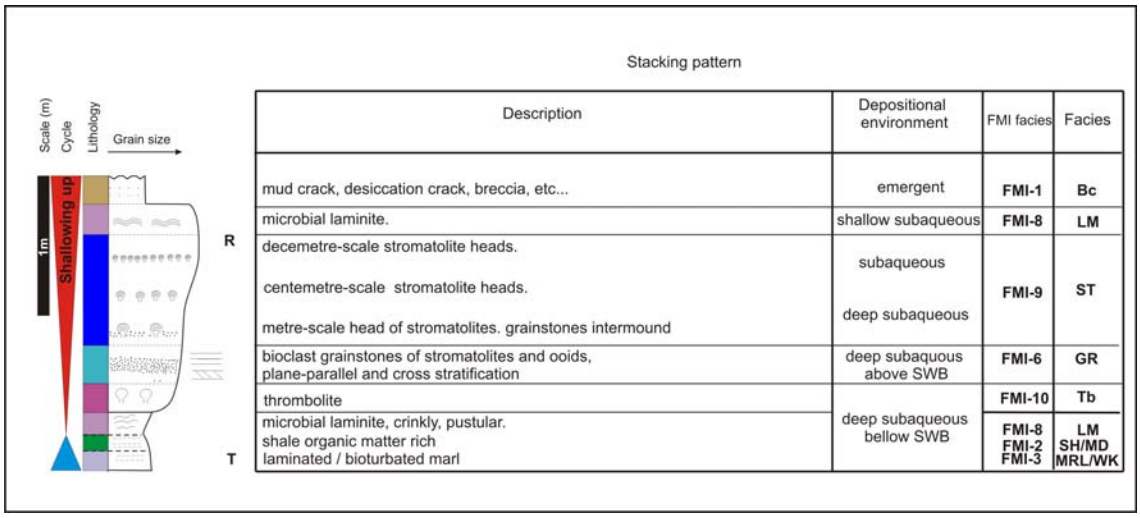

Figure 7. 20 – Schematic stacking pattern of a fundamental cycle in the microbialites, based on presumed progradation of the FMI facies as depicted in the facies model in Fig 7.18.

7.5 Discussion and conclusions

In order to carry out the regional sedimentological and stratigraphic study of the Barremian, Aptian carbonate successions cores and FMI image log, with additional help from sidewall core data have been studied. The cores sampled the more proximal area, covering Domain I, penetrated by wells 1, 2, 6, 7, 8 and 9 (see Figure 7.1 and Chapter 4, for Domains). The facies classification and facies model and stratigraphic analyses are core based. In the more offshore Domian II core was taken in well 12 and the FMI log

and sidewall core samples and also Gamma Ray logs were used to complement the study in well 20. However, in Domain III, where no wells have been drilled, the sedimentological and stratigraphic model is completely based on 3D seismic interpretations undertaken and these results are discussed in Chapter 10.

The core logging presented in section 7.2, through wells 1, 2, 6, 7, 8, 9 and 12, revealed a succession of facies association that compose alluvial fan (AF & P FA), deltaic and lacustrine environments (DL & FA) in more proximal areas and lacustrine environments with carbonate platforms in shallower locations, away from the influence of terrigenous supply (Appendices A1 to A7 and Figures 7.32 and 5.33). The Barremian and early Aptian section of the southern portion of the Campos Basin, comprises a mix of sandstone, conglomerates, and carbonate rocks. This system is increasingly purer in carbonate with distance from the rift border. Near the edge of border fault (Figure 7.2) in the hangingwall situations there is influence of gravitational processes expressed in slumps and resedimentation of previously deposited sediments, forming turbidite deposits (wells 1, 2 and 6). Fluvial-deltaic systems are seen to operate in the process of filling the sedimentary basin with coarsening upward clastic successions. In the footwall of the half-graben, where shallower conditions prevail, and away from clastic supply, carbonates tend to dominate. At this location, bioclastic carbonates are stacked to form thick deposits of amalgamated shallow bar or bank deposits (wells 5, 7, 8, 9 and 10). The lake level fluctuations promotes partial or total exposure of the carbonates allowing the formation of diagenetically modified facies, and the preservation of pedogenetic features (Freytet & Verrecchia, 2002). These facies are not common in the facies succession in the hanging wall zone. Exposure may occur due to low lake levels in dry periods or to tectonic uplift in footwall sites. The post-rift section (sag phase) of Aptian age is sampled in wells 6 and 9 (section 7.2 and Figures 7.1 and 7.2). Conglomerates and sandstones interpreted to have been deposited from alluvial fans and an alluvial system that prograde into the basin. Basinward this system tends to become more carbonate rich with microbialite carbonate rocks. This tendency is noted in the Gamma Ray log curve pattern, which becomes cleaner, and box like offshore (Figure 7.1).

A similar partition of clastic and carbonate facies was described by Burchette (1988) regarding the fill pattern of the various half-graben that comprise the marine rift of the Gulf of Suez basin. Here the deposition of the Mid-Miocene marine carbonate and clastic succession was controlled by extensional fault-block topography. In his model, shallow marine carbonates and clastics were deposited in marginal positions,

while the central troughs were filled by slope aprons and turbidite and pelagic mudstone. This was developed by Bosence (2005) in a review of marine carbonate platforms formed on rotated fault blocks where the footwall highs are characterised by carbonates and the hanging wall lows by clastics.

Soreghan & Cohen (1996), correlated sediments and sedimentary bodies in relation to particular tectonic-geomorphic settings within Lake Tanganyika. Their arguments involve climate, tectonism and volcanism and how these influence the sedimentary framework. Seven half-graben are identified, arranged with 4 morphological elements, including border fault margins, littoral platforms, mid lake structural highs and axial-deep margins. Each tectonic-geomorphic setting is related to particular facies geometry, which comprises sediments of allochthonous and autochthonous origin. As an example, the border fault margins have piedmont deposits, colluvial rockfalls, fan deltas and downslope bars. The littoral platform is characterized by deltas and particular littoral carbonate deposits, such as ooid shoals, coquinas and stromatolites. Homogeneous or laminated mud sedimentation, generally organic matter rich and formed under anoxic conditions, are normally relate to deep basins (DL & FA). In this environment, distal turbidite sedimentation occurs as episodic events interbedded with heterolithic facies. Therefore the occurrence of clastic and carbonate facies in the Southern Campos Basin is similar to that described from other extensional non-marine and marine environments. In distal sites, Domain II, represented by the wells 12, 19, 20 and 21, the sedimentological record differs considerably from that described above in the Domain I. Apart from well 12, no further wells have been cored, but well 20 is extensively imaged with FMI log. Additional data such as sidewall core, Gamma Ray log, along with maps and seismic sections (see in Chapter 4) were used for the study of this area. As a result of such studies a series of half-graben with synthetic and antithetic normal faults were recognized. In this tectonic setting, transfer zones have been described (Chapter 4) and where thick packages of autochthonous carbonate rocks are stacked (Figure 7.1). These sediments form aggradational (recognized in the Gamma Ray curve box pattern in the well 19). and progradational (recognized in the Gamma Ray curve bell pattern in the well 20), bodies constructing deposits of up to 400 m thicknesses in the syn-rift Barremian coquina succession and 200 m thick in the post-rift, microbialite succession (well 20 – Figure 7.18). In the Barremian coquina succession, a thick mud rich section of high Gamma Ray values (around 4400 m depth, Appendices B1 and B2) divides two major coquina successions, informally called lower

and upper coquinas sequence. These muddy, organic rich rocks are considered the main source rock of the Campos Basin reservoirs (wells 12, 19 and 20). However, this unit is poorly developed in wells cored in the more proximal area.

In conclusion, it should be noted that the traditional core logging has been effective in determining the temporal and spatial facies distribution, the facies associations and depositional environments. However the sampling of the stratigraphy by cores is still limited and few correlations can be made between adjacent wells. This aspect is considered in more detail in the next chapter. The author is not aware of any literature that integrates FMI image log and other wireline logs for the construction of FMI based facies and a facies model. It is likely that this approach will become more common in the future as more results from FMI are in the public domain. The results can be easily compared with ancient and modern tectono-stratigraphic models for sedimentation in extensional rift settings. However, little is known in the literature about the 3-D model established for Domain II; half-grabens with synthetic and antithetic faults, forming a polygonal arrangement with a transfer zone. Few references referring to the transfer zones (e.g. Cross & Bosence, 2005). Most of these references emphasise the bypass for terrigenous sedimentation in marine environment and also the important connection between half-graben drainage networks. Carbonate environments are known to accumulate thick progradational geobodies possibly due to the low relief of the relay ramp (e.g. Abu Shaar carbonate platform – Gulf of Suez, Egypt). Tectonostratigraphic models are considered in more detail in chapter 10 after the stratigraphic analyses of chapters 8 and 9.

CHAPTER 8 - SEQUENCE STRATIGRAPHIC ANALYSIS

8.1. Introduction

This chapter focuses initially on the principles of Sequence Stratigraphy and discusses how this method may be applied to carbonate depositional systems in rift basins. The second half of the chapter deals with cyclicity and stacking pattern of the Barremian Aptian carbonate succession. In this section 4 hierarchical levels of cyclicity are identified through core logging, Gamma Ray and sonic logs, and also FMI image log interpretation. The controls on cycle formation are discussed and lateral correlation of the 3rd order sequences is shown to be an effective way of correlating strata through the south Campos Basin. However, it is not possible to correlate the 4th and 5th order cycles regionally, through the wells, due to the significant vertical and horizontal facies variation and the fact that each half-graben behaves as an individual sub-basin in the rift system. Finally, a brief discussion compares and summarises the findings of the chapter.

8.2. Sequence stratigraphy and cycles

8.2.1 - Sequence Stratigraphy

Sequence stratigraphy is an interdisciplinary tool that has revolutionised the methods of facies and stratigraphic analyses (Miall, 1995). It was originally applied to siliciclastic depositional systems (Vail *et al.* 1977; Van Wagoner *et al.* 1989) and subsequently to carbonate systems (Sarg, 1988). The method focuses on facies cyclicity, facies associations and their correlation across a basin; and also the stacking patterns of the stratal successions and major surfaces that subdivide stratigraphy (Catuneanu *et al.* 2006).

The fundamentals of sequence stratigraphy start with the publication of AAPG Memoir 26 (Payton, 1977) followed by other publications by the Exxon group (Vail *et al*. 1984, Wilgus *et al*. 1988). However, Sloss *et al*. (1949) were the first to coin the term ‘sequence’ to define a stratigraphic unit bounded by subaerial unconformities. He subdivided six major sequences in the North America Phanerozoic interior craton (Sloss, 1963) and pointed out the significance of tectonism in the creation of sequences and bounding surfaces. Mitchum *et al*. (1977) expanded the term sequence to a ‘relatively conformable succession of genetically related strata’. They considered these

sequences to be of a higher order (lower frequency) than those proposed initially by Sloss *et al.* (1949).

Since then, sequence stratigraphy has developed to include the stacking patterns of strata and a more refined treatment of systems tract, i.e., 'transgressive', 'normal regressive' and 'forced regressive' (Hunt & Tucker, 1992; Posamentier & Morris, 2000), moreover several types of sequence such as 'depositional', 'genetic' and "transgressive-regressive" have been established (Figure 8.1) based on their facies trends and bounding surfaces (Figure 8.2). In exploration geology, the attraction of this model is due to its predictive abilities in that facies and unconformities can be predicted away from data points or wells. The following discussion addresses the development and application of sequence stratigraphy to the carbonate depositional systems in rift basins.

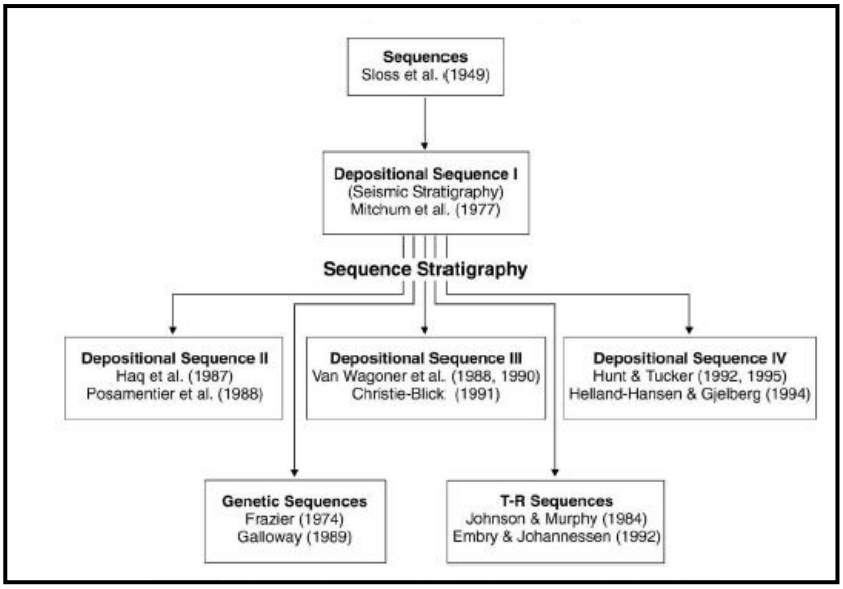

Figure 8.1– Sequence stratigraphic models (from Catuneanu, 2006; modified after Donovan, 2001). The Depositional Sequences are bounded by subaerial unconformities and their correlative conformities. The Genetic Sequences model uses maximum flooding surfaces as sequence boundaries. T-R Sequences uses composite sequence boundaries: subaerial unconformity and the maximum regressive surface as the sequence limit.

8.2.2 - Sequence stratigraphy in carbonate depositional system

The development of sequence stratigraphic principles for carbonate depositional systems in passive margin settings was initiated by Sarg (1988) and subsequently by other authors (Handford & Loucks, 1993; Hunt & Tucker, 1993; Cathro *et al.* 2003; Schlager, 2005). The key bounding surfaces are similar for both clastic and carbonate systems being formed and modified by depositional and erosional process controlled by eustasy, tectonic subsidence, sedimentation rate and climate.

Although the application of the sequence stratigraphy to carbonate depositional systems started in the late 1980s it was not until the 1990s that the fundamental differences between the clastic and carbonate stratigraphic models was presented (Coniglio & Dix, 1992; James & Kendall, 1992; Jones & Desrochers, 1992; Pratt *et al.* 1992; Schlager, 1992; Erlich *et al.* 1993; Hunt & Tucker, 1993; Long, 1993; Loucks & Sarg, 1993; Tucker *et al.* 1993).

The fundamental concepts of carbonate sequence stratigraphy are the same for both siliciclastic and carbonate systems. However, some significant differences exist. Such differences relate mainly to the sediment supply and the fact that most carbonates are produced close to where they are deposited. Whilst in the siliciclastic systems the sediments comes from extra basinal sources and the accommodation space dictate the geometry of the systems tract, in carbonate systems, the sediment supply (carbonate factory) is intrabasinal and the productivity depends on the climate, water depth, and illumination, nutrients, salinity, palaeogeomorphology and rate of base-level changes (Walker & James, 1992). Three main types of carbonate factories are recognised in the literature (e.g. Schlager 2005): Warm water carbonate factories, cold water carbonate factories and pelagic carbonate factories. Additionally, for this thesis, it should be recognized that there are non-marine and fresh-water carbonate factories that, to date have not been defined.

To date most of the work on sequence stratigraphic principles has concerned marine carbonate systems where there has often been an assumption of a eustatic control on accommodation space (e.g. Sarg, 1988). In tectonically active environments, such as the Campos Basin, and in non-marine successions, such as the Lagoa Feia Group the application of these principles needs to be undertaken with care as the drivers on accommodation space and the nature of the carbonate factory will be expected to be different from the previous models. This is explored in the section below before undertaking a sequence stratigraphic analysis of the Early Cretaceous of the Campos Basin.

8.2.3 – Application of sequence stratigraphy to rift basins

Different basin types have specific tectono-stratigraphic controls on their evolution as they have different subsidence and sediment supply rates, and palaeogeography. Sequence stratigraphy has been applied to continental divergent margin basins (Posamentier *et al*. 1988; Posamentier & Vail 1988 and Galloway 1989),

to foreland basins (Van Wagoner & Bertram, 1995, Plint & Nummedal, 2000), and also to rift basins (Dolson *et al.* 1996; Ranzy *et al.* 1996, Prosser, 1993).

Vail *et al.* (1977) initially proposed that accommodation space was controlled by linear tectonic subsidence and eustatic change for passive margin stratigraphy. They argued that while the magnitude of depositional sequences was due to tectonic subsidence, facies and internal strata geometries are controlled by eustatic fluctuations (Vail *et al*. 1977, 1984; Vail, 1987, Haq *et al.* 1988; Posamentier *et al.* 1988). However, Hubbard (1988) demonstrated that the second and third order cycles of rifted margins of the North Atlantic, South Atlantic and Arctic Oceans were controlled by local events or factors instead of being global and synchronous as claimed by Vail *et al.* (1977). A similar conclusion was reached by Bosence (1998), when reviewing the stratigraphy of the Red Sea-Gulf, Aden rift basin.

In active rift basins the stratigraphic patterns and facies distributions would be expected to be tectonically controlled and Payton (1977), proposed methods for analysis of such basins considering the accommodation space as a result of the interaction between tectonic subsidence, change in base level, climate and changes in sedimentary supply. These factors are generally responsible for the limit of sequence and systems tract formation. Changsong *et al.* (2001) agree with this statement. But, on the other hand, they state that, in marine basins, mainly continental margins, the stratigraphic patterns and facies distribution are controlled predominantly by eustatic variations.

According to Scholz *et al.* (2007) in lacustrine rift basins, the structural and geomorphological elements of half-graben have different rates of subsidence and uplift. This results in subsidence in one portion of the basin and uplift in another. This could result in the simultaneous generation of aggradational or retrogressive transgressive systems tract on the hanging wall with high rates of subsidence, at the same time regressive, progradational systems tract on the footwall margin, with low rate of subsidence (Gawthorpe *et al.* 1994; Bosence, 1998). Prosser (1993), Gawthorpe *et al.* (1994) and Cross (1996) used the term tectonic systems tract to label such depositional systems with a tectonic origin. Prosser (1993), studying the structural control on siliciclastic rift basin stratigraphy, affirms that systems tract are related to structural evolution of a rift basin rather than to eustatic sea level changes. In accordance with this statement, some authors describe sequence boundaries as relating to tectonic eustasy (e.g. Bally, 1982; Thorne & Watts, 1984).

Other important factor of depositional systems in the study of non-marine carbonate systems in the continental rift environment is the nature of the climate and drainage system and their control on changes in lake level. Chiossi (1997), studying these relations in the Sergipe-Alagoas Basin, in the northeast of the Brazil, classified four main types of drainage systems: associated with the border faults, associated with axial drainage, associated with flexural ramps and associated with accommodation zones (Larré, 2009). The drainage associated with accommodation zones is important as they may link individual half-graben.

8.2.4 - Transgressive-regressive sequence model (T-R)

Although being initially proposed for shallow water marine settings, the T-R sequence model of Embry and Johannessen (1992) and Embry (1993, 2002), is considered the most suitable sequence model to be applied in this thesis for the study of continental rift basin carbonates. The identification of various systems tract in rift settings is generally difficult, due to a broad variety of facies and stacking patterns. Moreover, the rift basin is composed of several segments of half-graben and has many factors acting to control the sedimentary fill framework that may not be expressed regionally. However transgressive and regressive trends have been identified in most of the cores (Chapter 7) and can be interpreted from the continuous downhole logs from the wells studied in this thesis. Furthermore, it has been possible to identify key surfaces, such as subaerial erosion (exposure surfaces) in marginal areas and maximum regressive surface from deep water facies in basinward locations.

Johnson & Murphy (1984); Johnson *et al.* 1985 and also Embry & Johannessen (1992) defined a transgressive–regressive sequence (T-R) as '*a sedimentary unit deposited during the time between the beginning of one transgressive event and the beginning of the next*'. The transgressive-regressive sequence corresponds to the accumulation of strata during the shift of the coastline within a regressive - transgressive cycle. The T-R sequence model uses composite sequence boundaries: subaerial unconformities at the basin margin, *sense* of the depositional sequence stratigraphy school (e.g., Haq *et al.* Posamentier *et al.* 1988; Van Wagoner *et al.* 1988, 1990; Christie – Blick, 1991), and maximum regressive surfaces (MRS) basinward (Embry & Johannessen, 1992). These key surfaces define the sequence boundaries (SB). Also the maximum flooding surface (MFS) defines the end of the transgression (Figures 8.2 and 8.3).

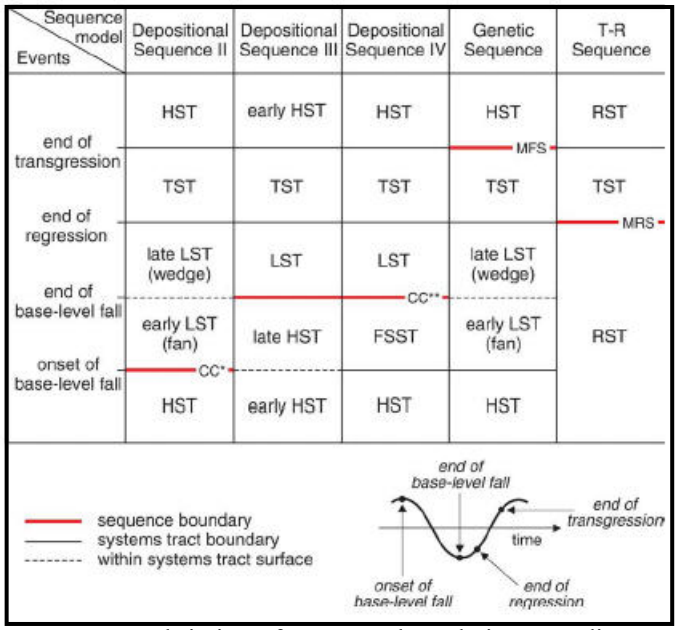

Figure 8.2 - Organisation of systems tract and timing of sequence boundaries according to the different sequence stratigraphic models (from Catuneanu, 2006). Abbreviations: LST - lowstand systems tract - highstand systems tract; FSST - falling-stage systems tract; RST - regressive systems tract; TST - transgressive systems tract; HST; T-R - transgressive–regressive; CC*- correlative conformity *sensu* Posamentier & Allen (1999); CC** - correlative conformity *sensu* Hunt & Tucker (1992); MFS - maximum flooding surface; MRS - maximum regressive surface.

As a sequence boundary, the recognition of a subaerial unconformity is a key step in the definition of depositional sequences. Problems arise because correlative conformities (Vail *et al.* 1977) and also maximum flooding surface, used as a sequence boundary in the genetic stratigraphic sequence model (Galloway, 1989), are not objectively recognized in most cases. The difficulty of recognising these surfaces arises with well data (Catuneanu, 2006). In this way the transgressive - regressive sequence is considered as an alternative model as it uses the maximum regressive surface (MRS, Figure 8.2) as a submerged correlative key surface. The MRS can be determined from facies and wireline responses.

In each half-graben the subsidence rate varies in relation to deformation and rotation of the fault block (Figure 8.3; Cross & Bosence, 2006). While the footwall area undergoes uplift, a regressive succession (R), locally with subaerial exposure, is expected, whereas in the hangingwall depocentre, close to the border fault, subsidence occurs and transgressive successions (T) develop that are synchronous with the regressive successions in the footwall. Similarly, the Maximum Flooding Surface (MFS) in the hangingwall may be synchronous with regression in the footwall (Figure 8.3). Mancini & Puckett (2002) consider that these key surfaces may represent time lines.

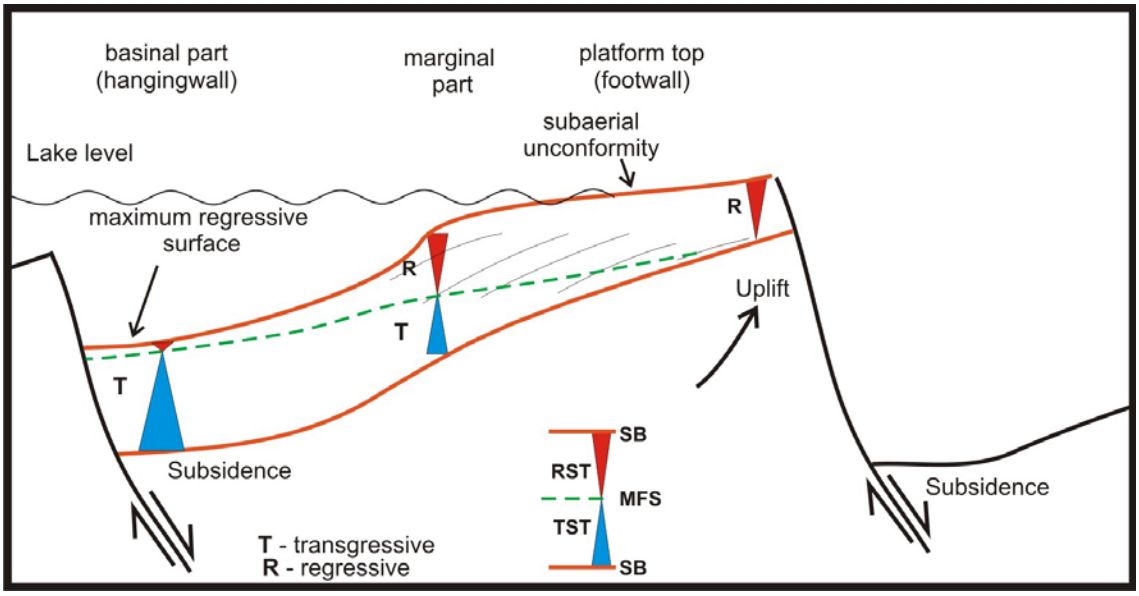

Figure 8.3 Transgressive-regressive sequence model (T-R) as applied in this thesis for continental rift basin carbonates. More explanation can be found in the text.

As well as changes in accommodation space being driven by tectonics, changes in lake level may be driven by climate or rearrangement of fluvial systems. Widespread desiccation surfaces may therefore also be important in the identification of maximum regressive surfaces and boundaries to depositional sequences and systems tract. With extremely low base level, from desiccated lakes the deep lake bottom facies in hangingwall sub-basins may show exposure features (Figure 8.4). These facies, however, need to be distinguished from the syneresis features that also occur in subaqueous conditions.

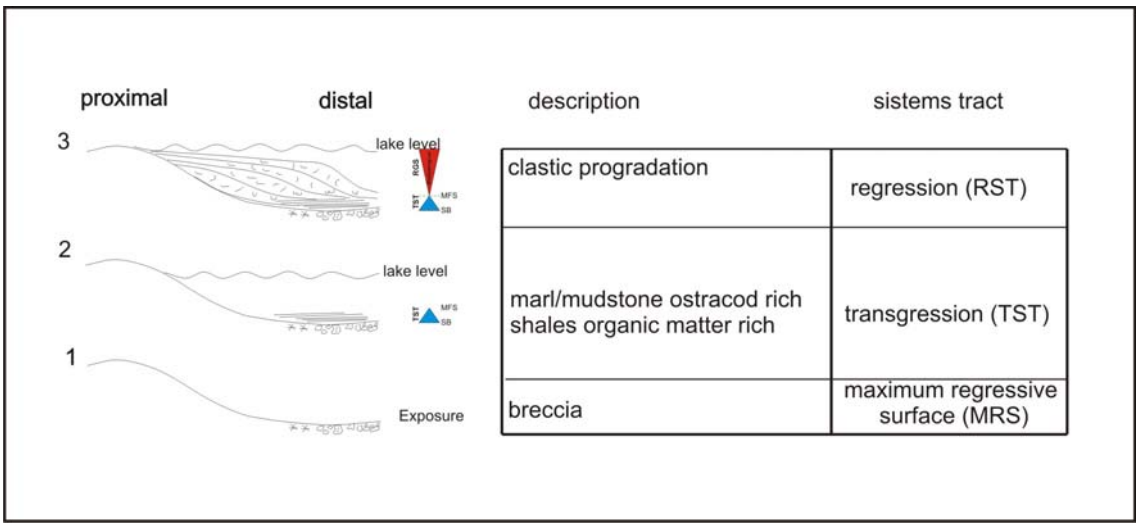

description	sistems tract
clastic progradation	regression (RST)
marl/mudstone ostracod rich shales organic matter rich	transgression (TST)
breccia	maximum regressive surface (MRS)

Figure 8.4 – Illustration of predicted T-R sequence during desiccation (1) and flooding (2 and 3) of a lake with carbonate progradation based on facies trends recognized in cores presented in Chapter 7.

8.3 Cyclicity and stacking patterns in the Barremian-Aptian successions

The Barremian-Aptian-age carbonates of the Coqueiros and Macabu Formations respectively, were deposited within a lacustrine environment in a late syn-rift and post-rift tectonic context in a semi-arid climate (Chapters 2, 5 and 7). In the Barremian succession the biogenic sediments comprise predominantly molluscs (bivalves and gastropods) and arthropods (ostracods), whereas the Aptian carbonates are dominated by more autochthonous bioconstructions, aided by microbial induced precipitation.

Based on core logging analyses (facies and taphofacies), FMI log interpretations and wireline log analysis (GR and Sonic), coarsening and fining-upward trends and repeated facies shifts have been identified on the logs (see Chapter 7 and Appendices A1 to A7 and B1 to B2). These trends of textures and facies are separated by erosive and / or exposure surfaces that are recorded in the logs and these repeated trends are interpreted as sedimentary cycles. The cycles have been identified at various scales, from high frequency, metre-scale (commonly shallowing-up) to low frequency cyclicity on a scale of hundreds of metres from the wireline logs. Based on the magnitude of the cycles (thickness), a hierarchy for the 4 levels observed was established. The biostratigraphy has no resolution for the high frequency cycles. However the long term cycles can be correlated with Vail *et al*. 1992 time table. In this chapter the metre-scale cycles are described and interpreted from both core and FMI logs and then the longer term trends are identified in the Gamma Ray logs. Cyclicity can be observed in almost all the wells. They are normally irregular in size and areal distribution and may be incomplete.

Some cycles from the well 1, core 2 (Figures 8.5a and 8.5b) and well 2 are clastic dominated and deepen-up. But others from wells 7 (core 4) and 12 (core 3), for instance, are carbonate dominated and mostly shallow-up (Figures 8.6 to 8.9).

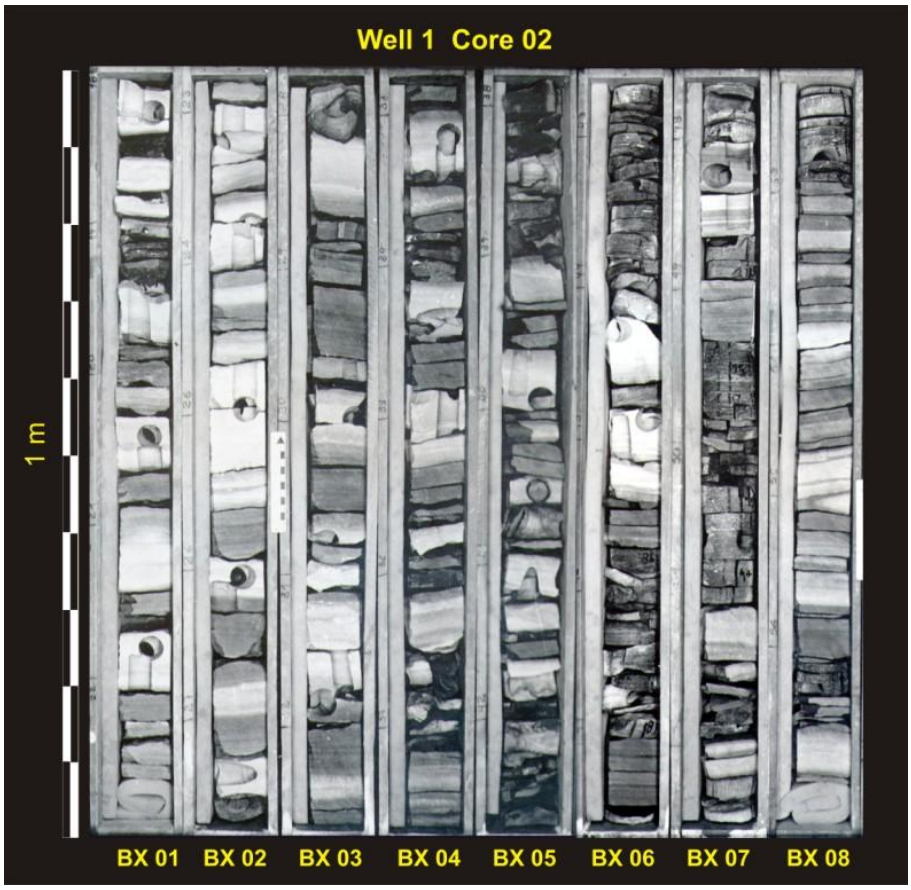

Figure 8.5a – Core photos from the upper 8 boxes of well 1, core 2 showing facies variation within the hierarchical level 3 (5th order) cycles. The facies and taphofacies (TF) criteria were use to stack the succession.

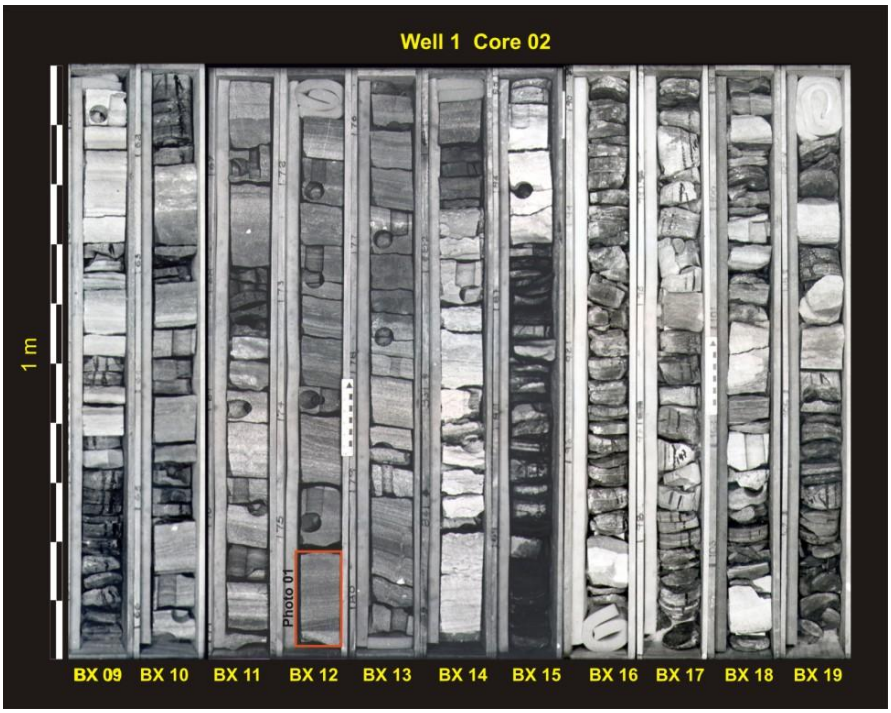

Figure 8.5b – Core photos from the lower 11 Boxes of well 1, core 2 showing facies variation within the hierarchical level 3 (5th order) cycles. The facies and taphofacies (TF) criteria were use to stack the succession.

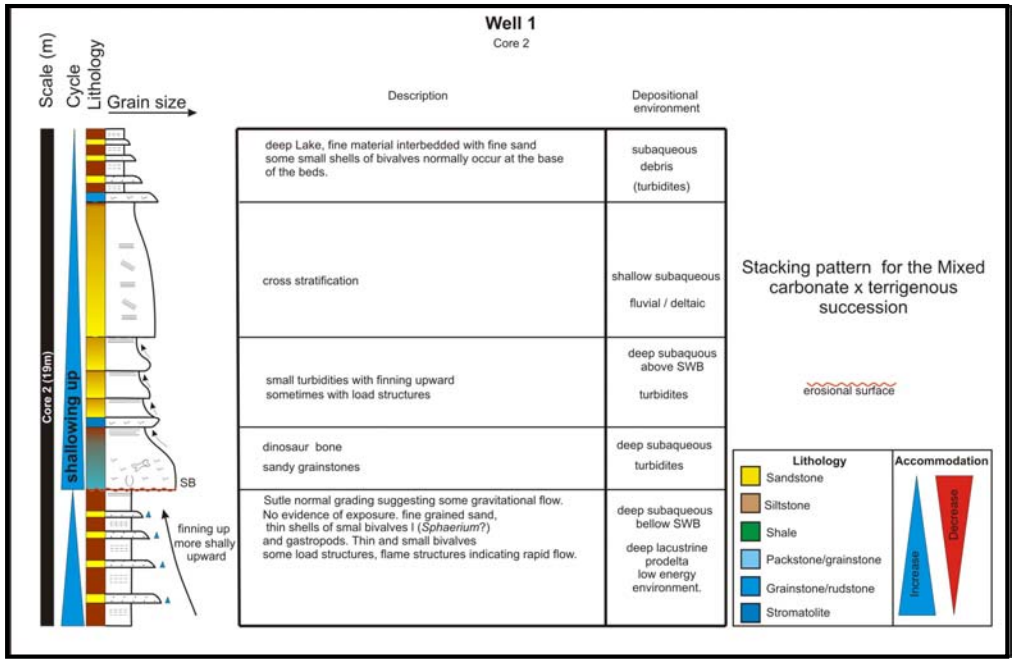

Figure 8.6 - Metre-scale cycles from a siliciclastic rich proximal part of the succession. The well is sited in a hangingwall sub-basin. The cycles show 2 fining, thinning and deepening upward trends over 19 metres in Well 1 - core 2.

8.3.1 Cycles identified in cores

In well 1 individual cycles are seen in Core 2 (Figures 8.5a, 8.5b and 8.6). These metre-scale cycles are less than 2 m thick, composed predominantly of fine sandstones. Figures 8.5a, 8.5b and 8.6 shows a series of fluvial deltaic sedimentary deposits also including delta front turbidites (Well 1 - core 2), which vary from shallow subaqueous to deep subaqueous environments. These cycles are typical of those occurring in basins close to the border fault, in the hangingwall portion of each individual half-graben. Other examples are seen in Well 2 (core 2). These cycles are dominated by transgressive systems tract so that the cycles are fining, thinning and deepening upwards. The complete description of cores 1 and 2 can be seen in the Appendices A1 and A2 and the facies trends are described and interpreted in Chapter 7.

In Wells 7, 8 and 12, cycles varying in thickness from some centimetres to some metres, comprise an initial, thinly-laminated, deep subaqueous (below SWB) shale and marl facies (well 7 core 4 box 18), and packstone in carbonate-rich successions (Figures 8.7 to 8.12). These facies grade upward into intermediate subaqueous basin margin grainstones and rudstones (Well 7, core 4 boxes 18 to 12). This is interpreted as a shallowing upward to more high energy facies and these are commonly capped by erosive surfaces or brecciated horizons (e.g. Well 8 core 20 box 04, 3006.20 m). Commonly these key surfaces have exposure features in the form of desiccation breccia

(Figure 8.13d). Occasionally (e.g. well 7 core 4 box 18, well 8 core 20 box 3, and well 12 core 3 box 11) the base of the cycle comprises a shale with slump structures, turbidites or a thin storm deposit (Figure 8.13g), and these are interpreted to have formed as a transgressive lag deposits or possibly they represent some lowstand deposits.

In carbonate-rich offshore successions the base of high frequency cycles is composed of packstones with bioclasts of bivalves and ostracods (Figures 8.7 to 8.9), followed by floatstones and rudstones and culminating with exposure feature facies. The facies textures and taphofacies vary upward from low energy environment, represented by Rmb and taphofacies TF-1 to TF-2 (Figures 8.7 to 8.9 and 8.10 to 8.13b, 8.13c, 8.13f and 8.13g) to high energy environment, Rcb, TF-3 to TF-6 (Figures 8.7 to 8.8 and 8.10 to 8.13a and 8.13e).

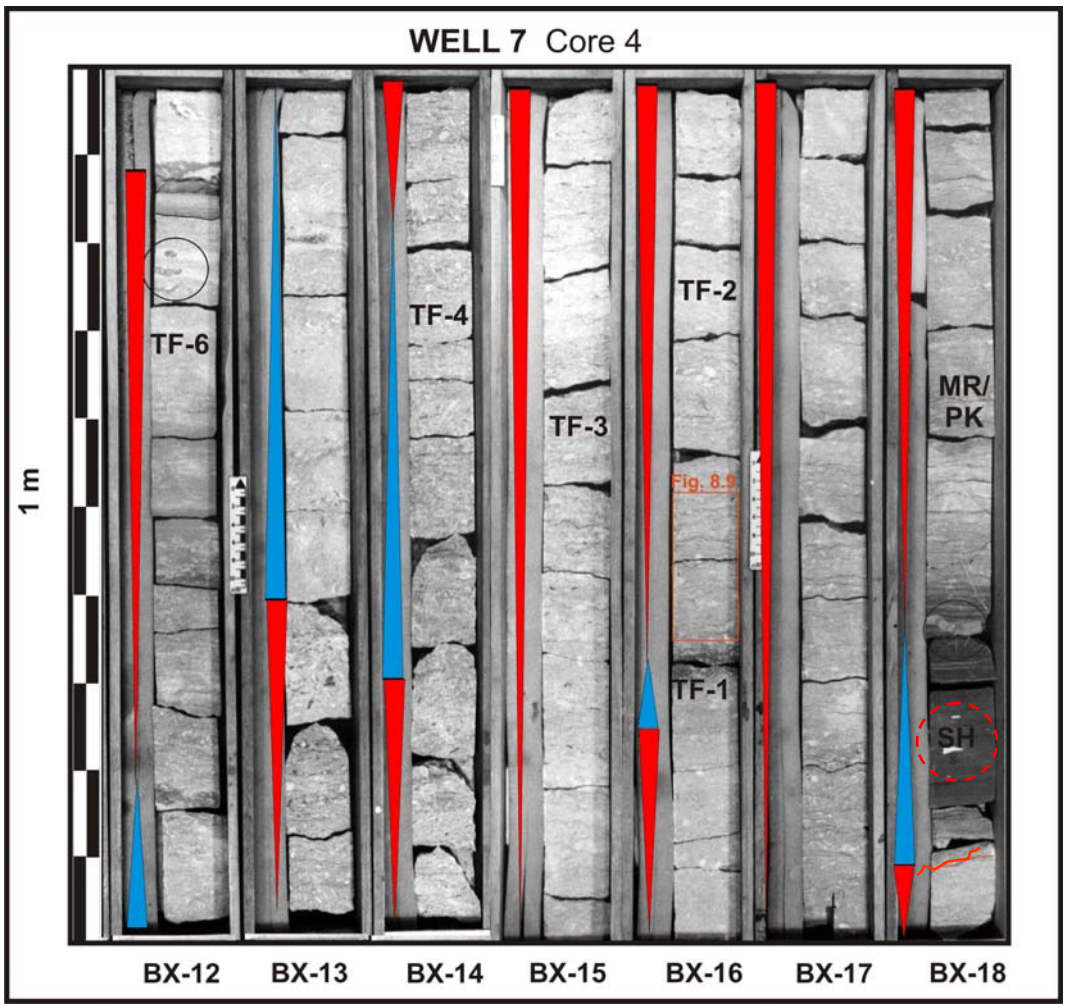

Figure 8.7 – Core photos from the upper 7 Boxes of well 7, core 4 showing facies variation within the hierarchical level 2 (4^{th} order) cycles. The facies and taphofacies (TF) criteria were use to stack the succession. The outlined red rectangle is magnified in Figure 8.9.

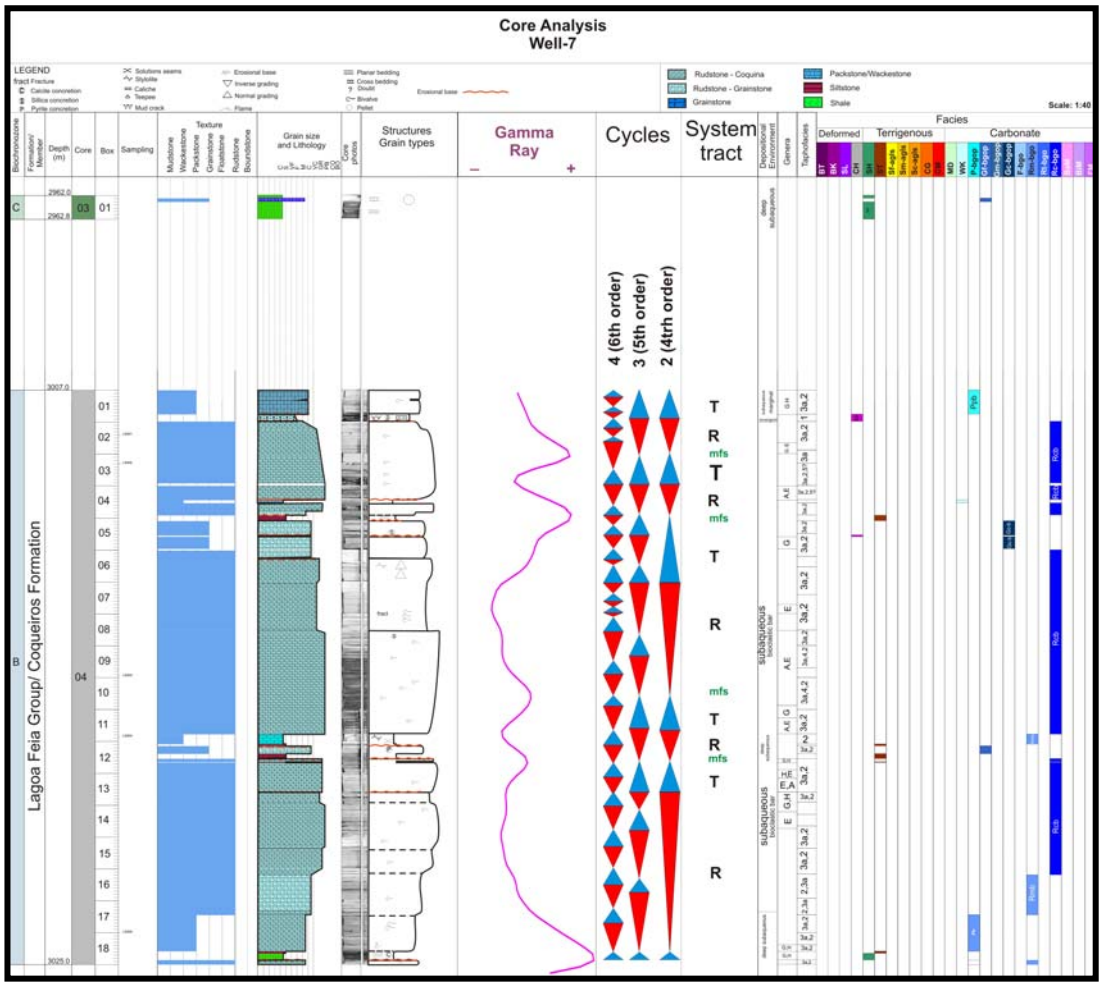

Figure 8.8 - Core log analysis of the well 7, cores 3 and 4. Detail of cyclicity in 3 different hierarchical levels. Regressive and transgressive systems tract of hierarchical level 2 fits well with the trends identified on the Gamma Ray curve. More explanation can be found in the text.

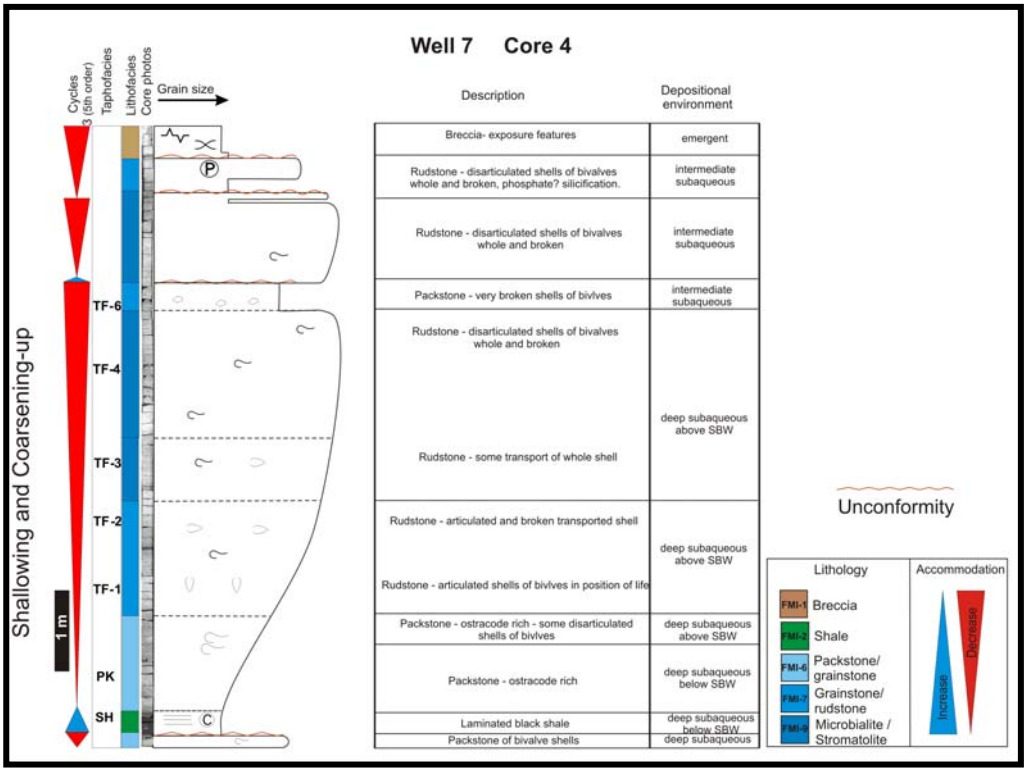

Figure 8.9 – Analysis of the lower interval from the previous figure 8.7, well 7 core 4, and boxes 12 to 18. Facies and taphofacies description and cyclicity in hierarchical level 2 in transgressive regressive cycles in a predominantly carbonate succession.

In shallow sites of the rift system (Figure 8.3) the cycles normally occur with predominantly regressive systems tract (RST), capped by an erosion surface and overlain by a thin subsequent deepening upward transgressive systems tract deposits of marls and shales and also packstones (TST) (Figures 8.7, 8.8 and 8.10). These transgressive deposits are, in most of the cases, organic matter rich, exhibiting elevated values in the gamma ray curve. The shallow-water sediments are in general arranged in an aggradational style in platform top locations and shallowing-up, progradationally stacked in hangingwall basin margin locations (Figure 8.3). Such geometries are interpreted as a possibly response to high carbonate productivity in relation to available accommodation space.

Transgressive cycles are shown above (Figure 8.6) and their occurrence predominates at the deepest part of the half-graben (Figure 8.21 wells 1 and 2). Accommodation space is considered to have been created by the active border fault to the northwest. In this proximal area, however, the composition of the rocks is dominated by terrigenous sediments (Figures 8.21 and 8.22, wells 1 and 2).

Figure 8.10 – Detail of red rectangle area in Well 7 core 4 box 16 (Figure 8.6). The photo shows Rudstones of articulated shells of bivalves (Rmb) in position of life (TF-1) at the base, parautochthonous Rmb, shells with small transportation but still articulated (TF-2) in the middle. Finally, Rmb with disarticulated shells (TF-3) at the top of the figure.

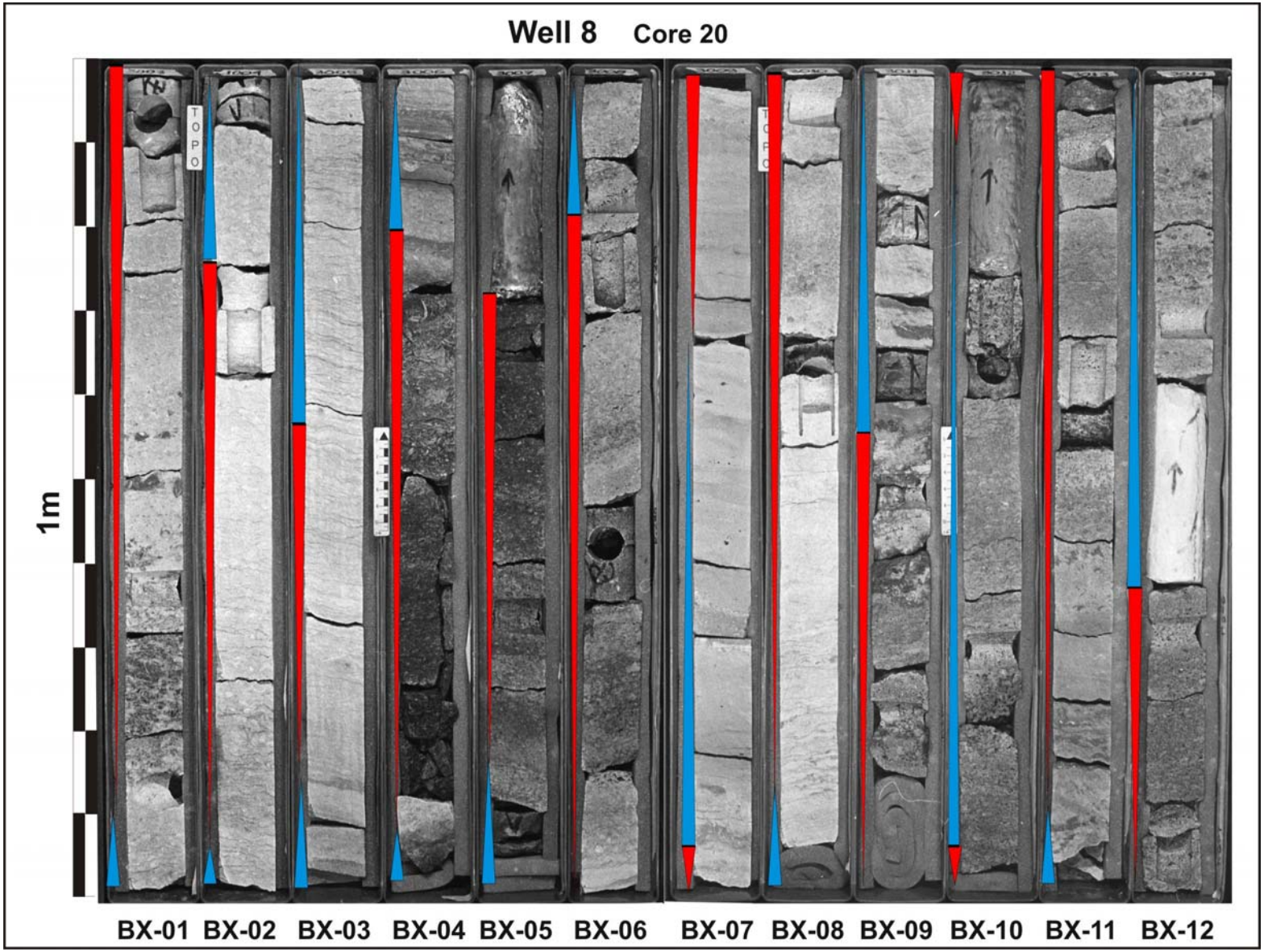

Figure 811a – Core photos from the upper 12 boxes of well 8, core 20 showing facies variation within the hierarchical level 2 (4^{th} order) cycles. The facies and taphofacies (TF) criteria were use to stack the succession.

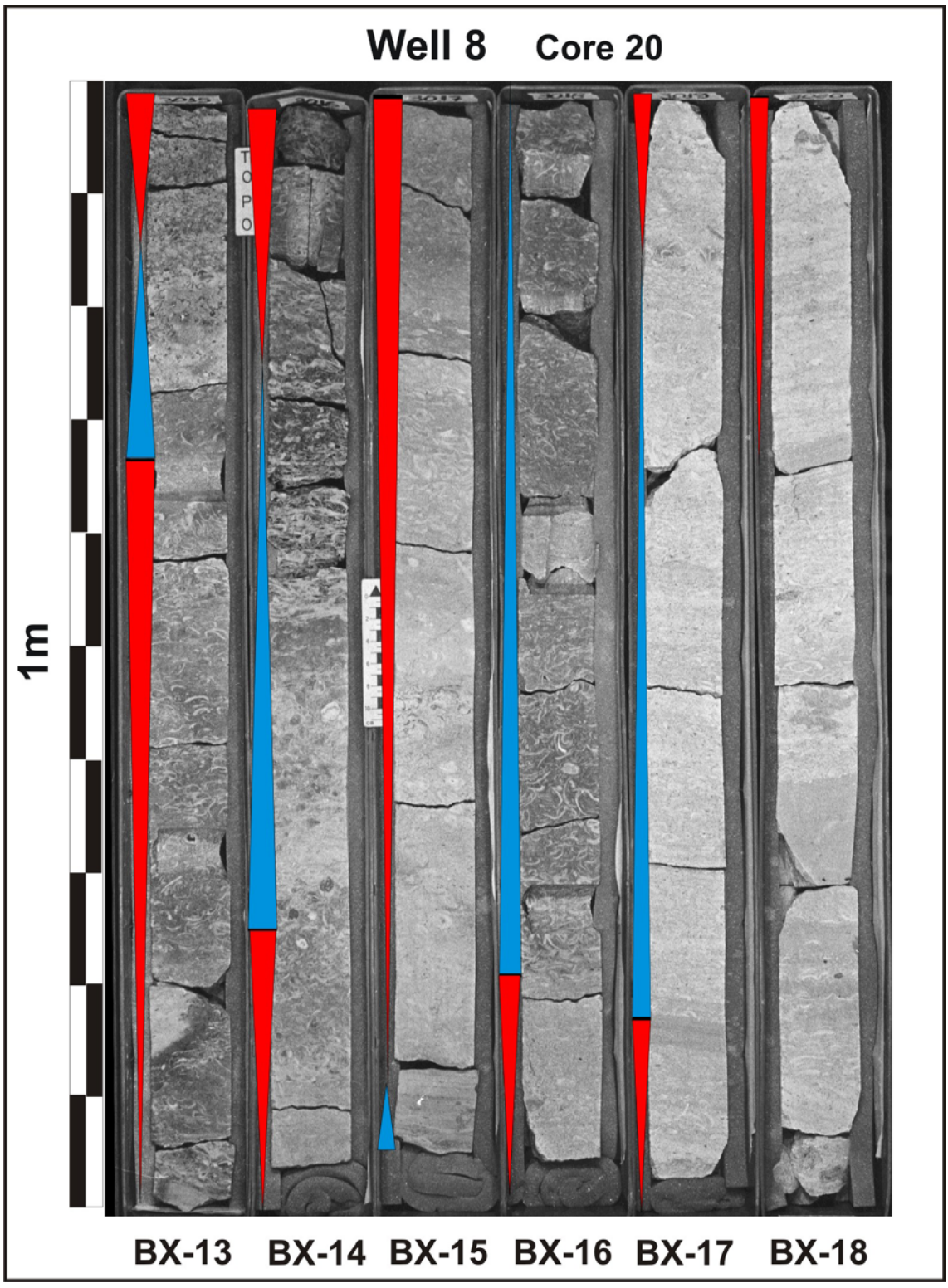

Figure 811b – Core photos from the upper 6 boxes of well 8, core 20 showing facies variation within the hierarchical level 2 (4th order) cycles. The facies and taphofacies (TF) criteria were use to stack the succession.

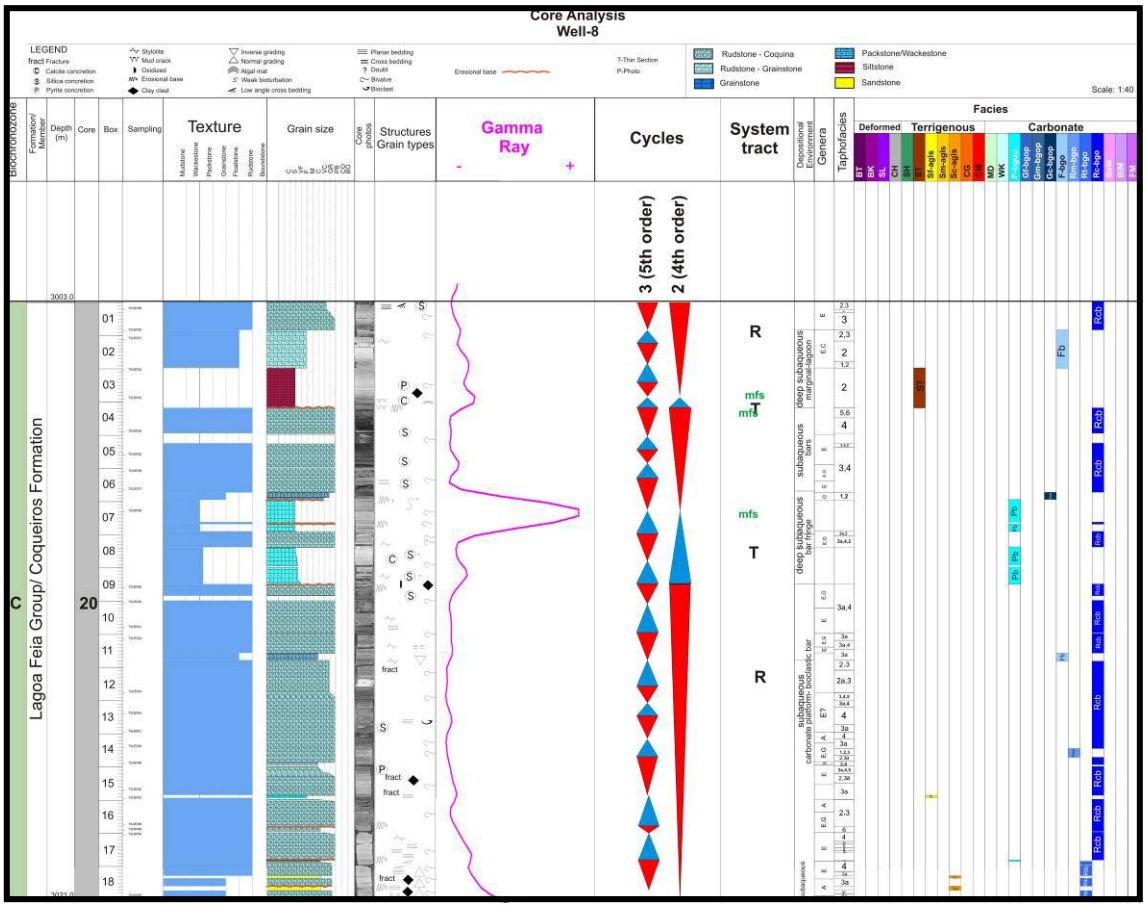

Figure 8.12 – Sequence analysis of the core log of the well 8, integration of all analyzed data.

Summarizing, the cycles are separated by different key surfaces such as subaerial exposure and the correlative maximum regressive surface (MRS) or lacustrine flooding surfaces (MFS). Not all the cycles are bounded by flooding surfaces alone, and thus they do not conform to the definition of parasequences *sensu* Van Wagoner *et al.* (1988). However, some cycle types are parasequence and others are high-frequency sequences *sensu* Lehrmann & Goldhammer (1999). The range of cycle types and bounding surfaces found here is encompassed by the broader definition of parasequences proposed by Spencer & Tucker (2007).

Figure 8.13a Rudstone of bivalves (Rcb). Disarticulated shells of bivalve, whole and broken. Taphofacies TF-3 and TF-4. Well 8 core 20 box 01.

Figure 8.13b Rudstone of bivalves (Rmb). Taphofacies TF-1 at the base and TF-2 in the upper part.
Well 8 core 20 box 02

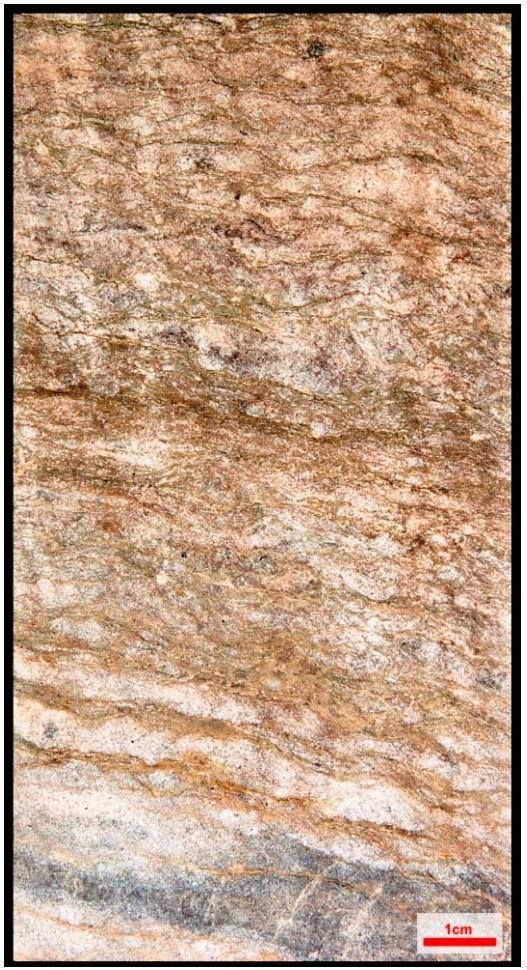

Figure 8.13c Packstone (Pb) with bioclasts of bivalves and ostracods Well 8 core 20 box 03

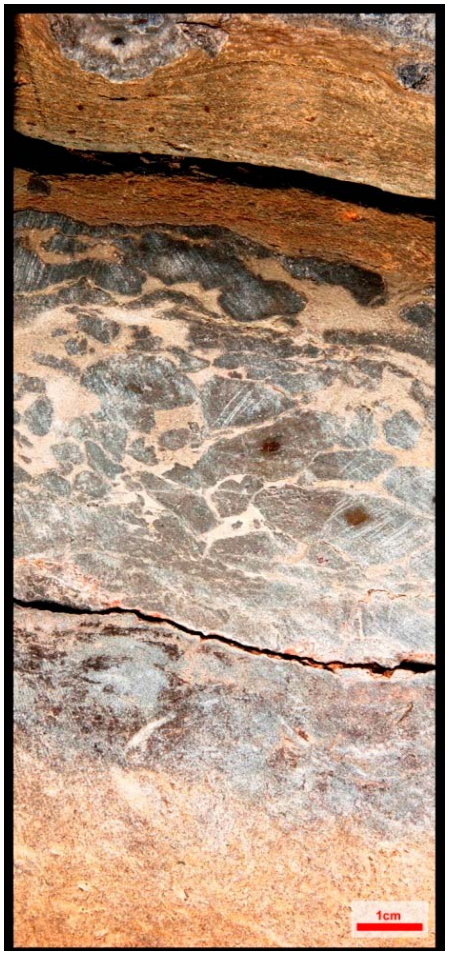

d) Packstone of fragment of bivalves very broken (TF-6) in the base followed upward by an exposure surface breccia, Well 8 core 20. box 04

e) Rudstone of bivalve with subtle cross stratification (TF-4). Well 8 core 20 box 04

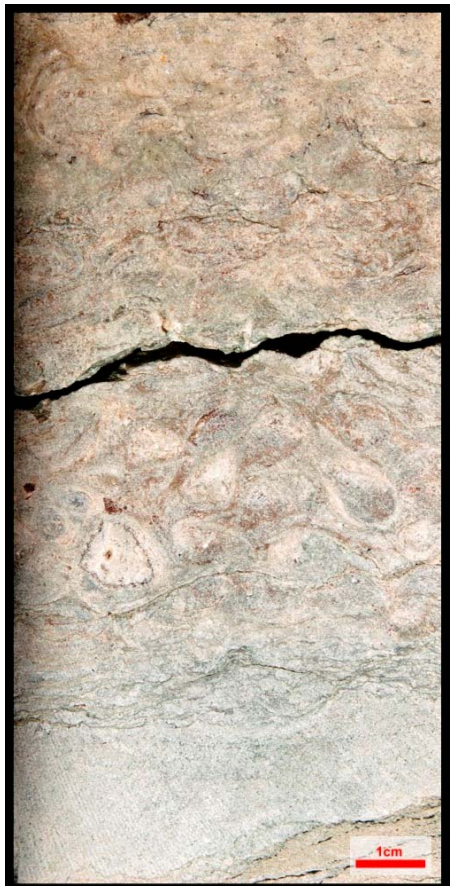

f) Rudstone of bivalves shells in position of life (TF-1), in the base of the picture, and TF-2 and TF-3 at the top. Well 8 core 20 box 6.

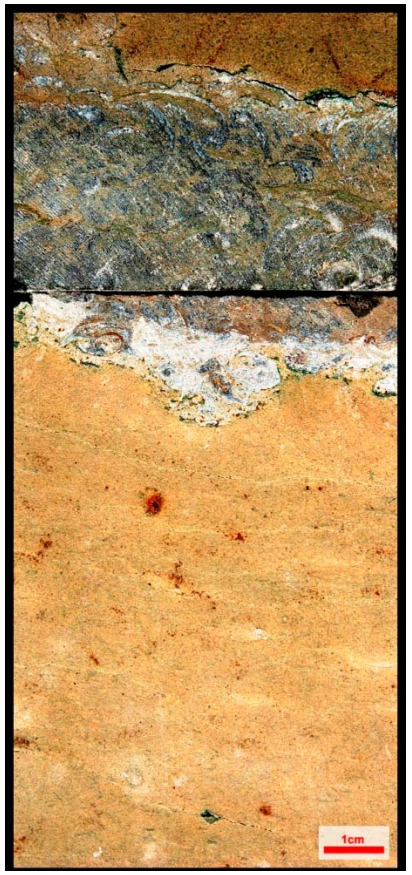

g) Packstone/ wackestone cut by a 5 cm layer of rudstone with erosive base (distal tempestite). Well 8 core 20 box 07

8.3.2 Cycles imaged in FMI logs

The FMI log from Well 20 has been used to identify facies, but can also be used to identify facies trends and erosional surfaces so that cycles may also be interpreted. Although the quality of the data on the lithologies is inferior to that from the cored intervals it has the advantage of being a continuous record through all the Barremian and Aptian carbonates. Cycles are identified in both the coquina and the microbialite successions that show either transgressive and regressive systems tract, or just a regressive systems tract.

Transgressive-regressive cycles

The presence of laminated horizons at the base of these cycles (Figure 8.14) indicates sedimentation in deep subaqueous environment. These pass upwards into coarser lithologies interpreted as grainstones and rudstones that suggest intermediate to shallow subaqueous settings and these may be capped by brecciated surfaces, suggesting exposure (Figures 8.13d and 8.14). The features and textural characteristics of exposure observed in the FMI image logs is very similar to that observed in core logs (e.g. Figures 8.7 to 8.9 and 8.13d).

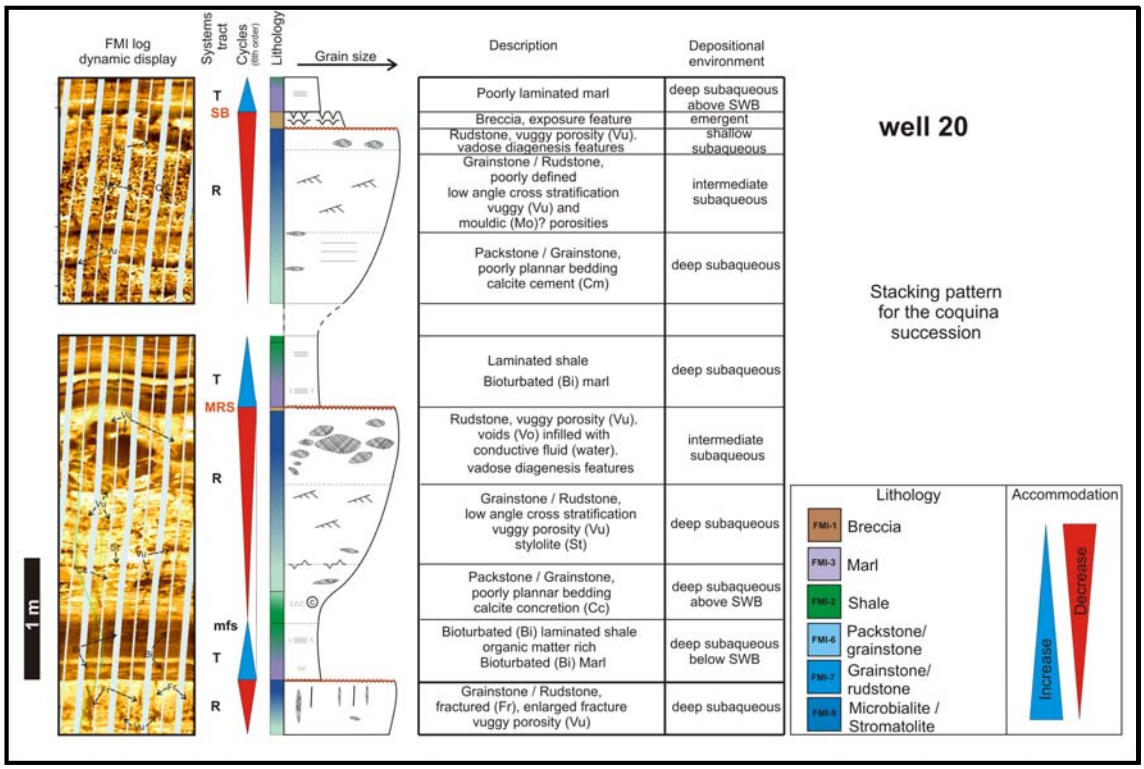

Figure 8.14 – Transgressive - regressive metre-scale cycles in the coquina succession. The cycles exhibit deepening and shallowing trends and are separated by sharp, erosional surfaces (SB) or maximum regressive surface (MRS) marking the transition from coarse grained lithologies to fine laminated lithologies. These successions of carbonate rocks are interpreted to form in deep to shallow subaqueous and emergent lacustrine environments.

These metre-scale cycles generally show an initial fining-upward trend followed by thicker coarsening-upward trend. These are interpreted as transgressive-regressive high frequency cycles and they commonly occur in the marginal (footwall) parts of the half-graben (Figures 8.3, 8.9 and 8.14).

Regressive cycles

Regressive cycles normally have low energy facies at their base grading upward into coarser, high energy facies. The facies normally vary from marl or packstone up to grainstones and rudstones of bivalve shells, usually with traction structures (Figures 8.15 to 8.16), arranged in coarsening- and thickening-up stacking patterns. Exposure features such as desiccation cracks and breccias, or even vugs suggestive of vadose diagenetic zone, suggest emergence and shallow-water depositional conditions (Figures 8.15 to 8.17 and 8.13d). In the Aptian microbialite successions, the regressive cycles normally vary from grainstone with plane-parallel and cross stratification, to heads of stromatolites with up to 1.5 m to underlying emergent features, such as imbricate textures and breccia (Figures 8.16 and 8.17).

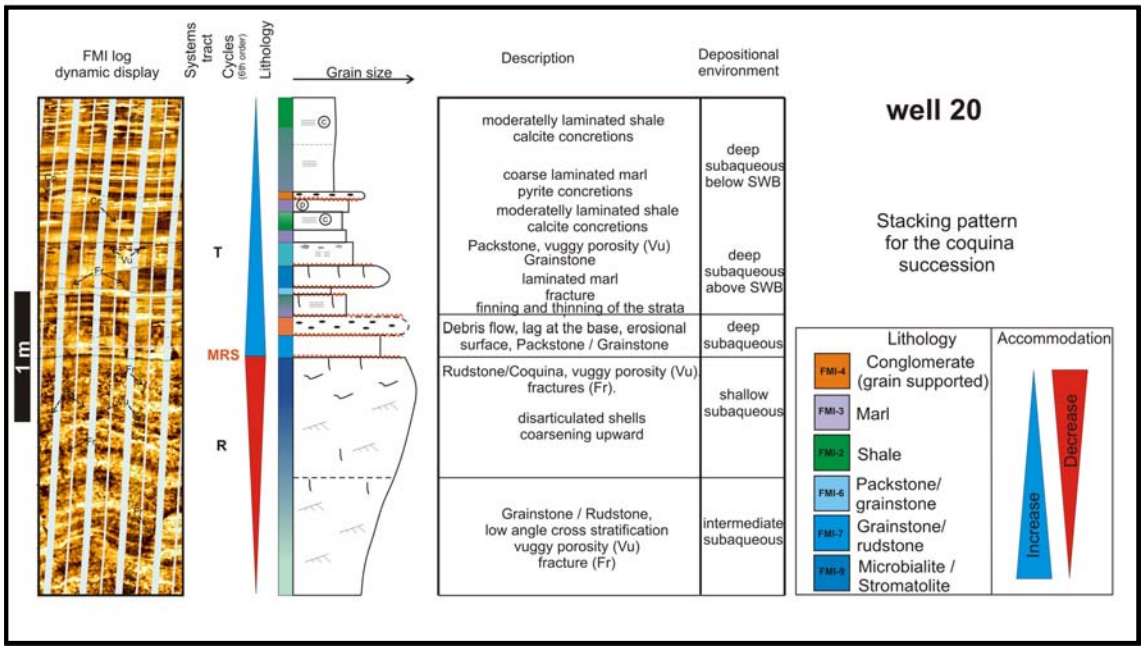

Figure 8.15 – Elementary regressive followed by a transgressive high frequency metre cycle in the coquina succession. The cycles exhibit a shallowing and then a deepening up stacking pattern. The lag or debris on the erosional surface of the shallowing-up trend, may represent a deposit resulted from tectonic movement of the fault-block associated with the deepening. These successions are interpreted to occur in shallow to deep subaqueous basinal parts of the basin above SWB.

Recurrent successions are noted in the analysis of the stacking patterns. However, the cyclicity studies conclude that the cycles are generally irregular and in most of the case incomplete. It is common that in shallower locations regressive stacking patterns arranged in shallowing upward cycles are found, whereas at the basin margin of the carbonate platform deepening up and shallowing up transgressive-regressive cycles, with a MFS dividing the succession (Figures 8.3 and 8.12 to 8.15) are more commonly found. As was pointed out earlier, close to the border faults successions of transgressive cycles are arranged in fining-up stacking patterns (Figure 8.5).

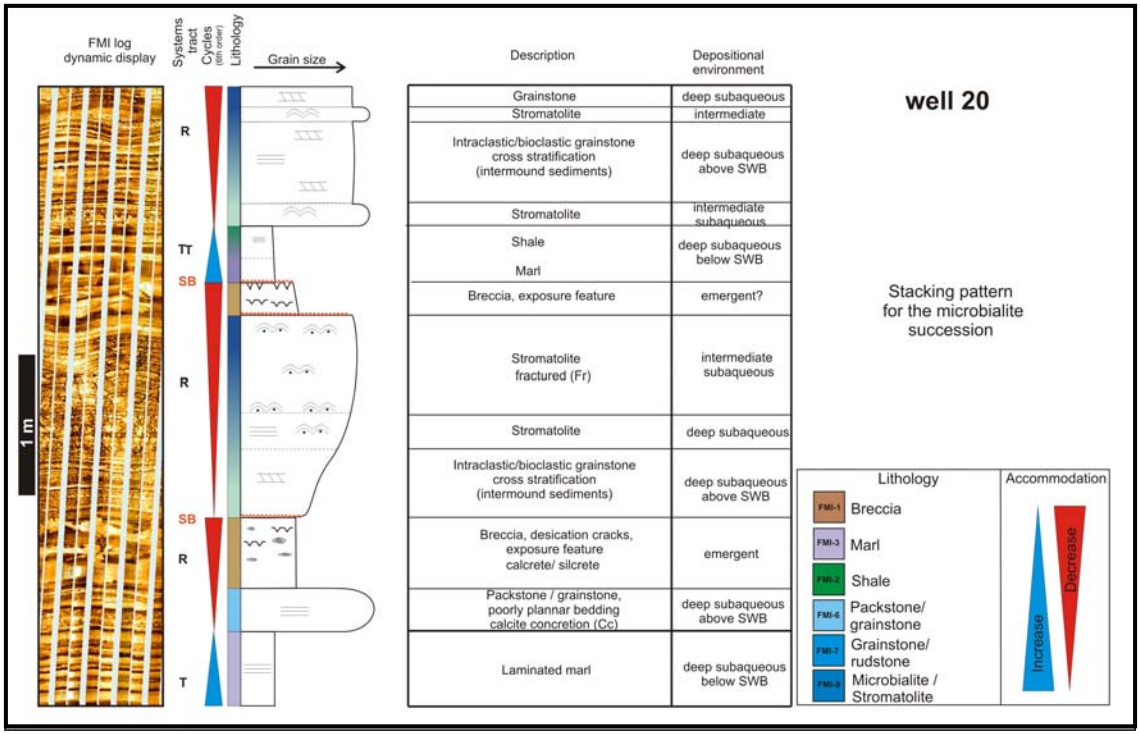

Figure 8.16 – Regressive, high-frequency, metre-scale cycles in the microbialite succession (Well 20), deposited in shallowing lacustrine environments with emergent surfaces suggested by vertical cracking and brecciation. The cycles exhibit in the base of the picture T-R cycle, a central R cycle and an overlying T-R cycle.

The cyclicity observed in core in the Barremian coquina sequence appears to be similar to those in the FMI image logs. Both examples shallowing-up cycles and provide evidence that the biological productivity was commonly outpacing accommodation space. The cycles have similar dimensions and temporal and spatial variations. Moreover it is common to observe erosional or exposure feature as bounding surfaces in both cases. The FMI examples although providing lower quality data than the cores from their continuous record provide evidence of the stacking patterns and the hierarchy of cycles and how this links to the gamma ray curve (Fig 7.17).

The differences between the core based cycles and the FMI log (well 20, Figure 7.17) are due mainly in the location of the wells but also in the dimensions of the transgressive cycles. The cycles in the core examples, are more proximal, and the influence of terrigenous source area can be seen, whereas in the FMI log analysis, in a more offshore position, has purer carbonates facies within the cycles. For this reason, the transgressive cycles in proximal areas are thicker and better defined.

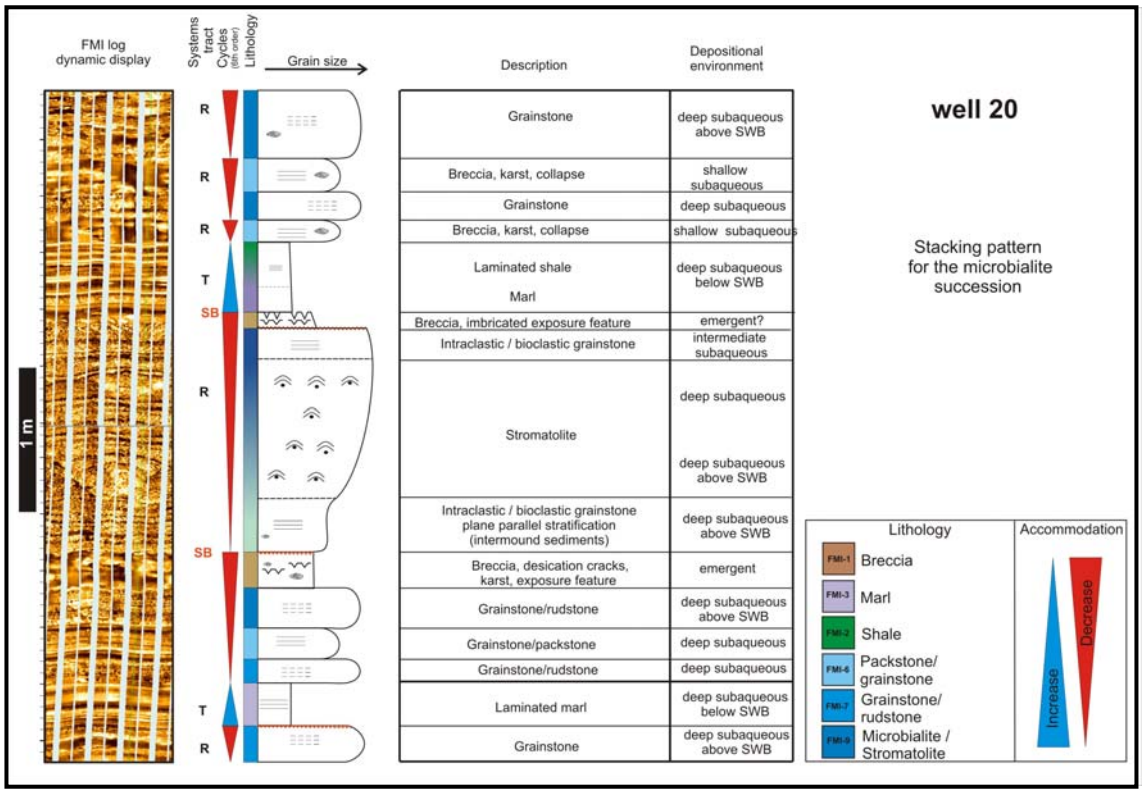

Figure 8.17 - Elementary regressive, high-frequency, metre-scale cyclicity in the microbialite succession, deposited in shallow marginal part, above SWB. The cycles exhibit a shallowing trend and are bounded by erosion surfaces.

8.3.1. Discussion on nature and origin of cycles

In this study of cyclicity in the Barremian and Aptian rocks the high-frequency (or elementary) cycles within these stages have different characteristics. In the Barremian succession, the elementary cycles are metre-sized and usually bounded by erosive surfaces or subaerial exposure. Shale and marl commonly overlie these surfaces, and represent the subsequent transgression. Commonly this transgression culminates with shale, as recorded in high values on the Gamma Ray electric log. The textural fining trend is then followed by a textural coarsening and shallowing-upward trend to reach shallow, high energy lake conditions, represented by molluscan grainstones and rudstones. These carbonate facies show an increase of hydraulic energy toward the top,

passing from more massive facies cross-bedded units at the top of the cycle. Related to this shallowing is an increase in porosity, dissolution features, shrinkage breccias and occasionally karst features. Occasionally, low energy subaqueous facies show features of emergence in the form of shrinkage cracks and brecciation indicating that deeper lake floor settings may also be exposed (Figure 8.4). Figure 7.3 shows a schematic model of lateral facies distribution and the Figure 7.25 vertical stacking pattern of these cycles in different sites of the basin.

In the Aptian succession the carbonates are more autochthonous, and interpreted to have formed by extensive microbial activity, trapping and binding sediments, forming microbial laminites, stromatolites and also thrombolites. Associated with these facies are also observed bioclastic facies and ooids (Figure 7.12). The shallowing-up cycles begin with the lake exposure facies stacked with carbonaceous shales and marls followed by microbialites towards the top of the cycle (Figures 8.14 and 8.15). These facies are interpreted to have formed in a very shallow subaqueous environment, with widespread microbial activity. However, such elementary high-frequency cycles are quite irregular and frequently incomplete. So the correlation of these high frequency cycles between the wells is difficult and has not been attempted. On the other hand, the lower frequency cycles (e.g. 3rd order) can be correlated regionally. This lower order cyclicity is clearly seen in the Gamma Ray log curve variations. Cyclicity is identified by trends of lower and higher Gamma Ray values (Figures 8.25 and 8.26). The cored intervals indicate that the lower values represent carbonate rocks, whereas the high Gamma Ray indicates terrigenous sediments.

8.3.1.2 Cycle hierarchy and controls on cycle formation

One of the main characteristics of marine carbonate platforms are the arrangement of the beds and strata in cyclical repetition of carbonate facies (Wilson, 1975; Kendal & Schlager; 1981, Algeo & Wilkinson, 1988). Very few studies of this nature have been published for lacustrine carbonates (e.g. Platt & Wright; 1990; Terra *et al.* 2012 and Sarg *et al.* 2012). Even fewer are published from rift basin stratigraphy, where tectonism is responsible for the rift geometry and structural elements, and varying basin subsidence rates. A model for cycle development in such settings is proposed above (Figure 8.3). Climate, in its turn, can also be an allocyclic control on cycle formation at a larger scale with fluctuation of humid and arid periods, affecting lake level, production of carbonate sediments and also terrigenous supply (Figure 8.18).

The cyclicity record shown in the wells from the South Campos Basin varies hierarchically from metre-scale, high frequency cycles (described above) to lower order, larger scale cycles (Figures- 8.19 to 8.25).

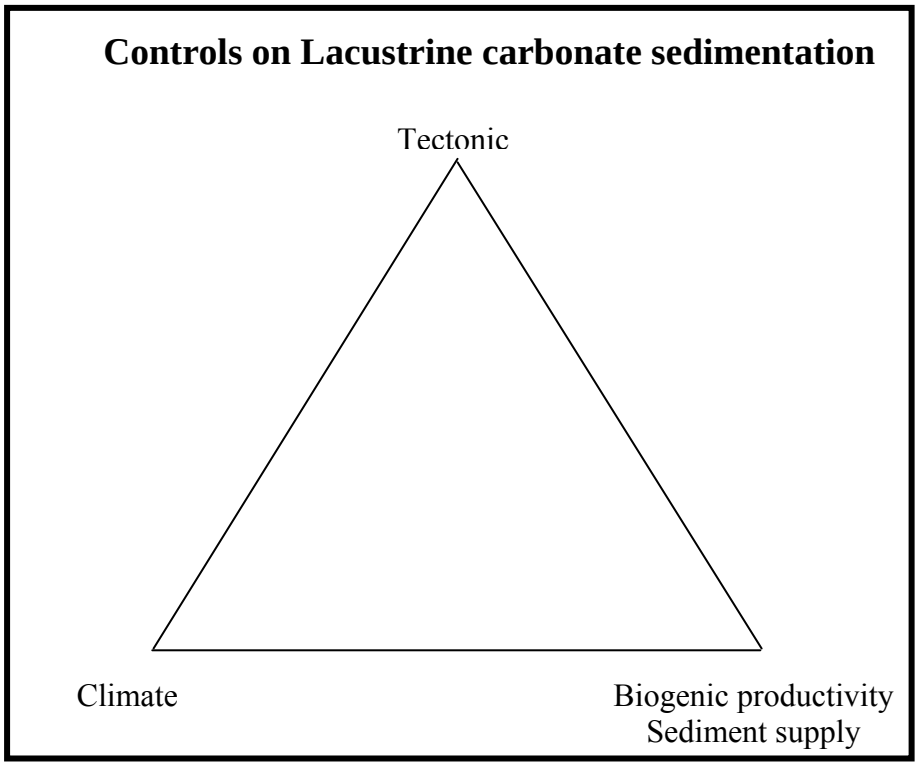

Figure 8.18 - The main controls suggested for the lacustrine carbonate sedimentary record.

Metre-scale cycles form the most basic, or elementary cyclic unit in the carbonate successions and are reported to most commonly occur as shallowing-up stacking of facies, (Pratt *et al.* 1992; Lehrmann & Goldhammer, 1999). These shallowing-up, metre-scale cycles, however, can form from a variety of processes either intrinsic to the sedimentary process of shallow water sedimentation, known as autocyclic process or from an allocyclic control from sea-level fluctuations or local tectonic movements (Pratt *et al*. 1992). In lacustrine environments these controls would also be expected to occur with the added complication of different drivers on lake level, as discussed above (sections 8.2 and 8.3). In the Campos Basin carbonates such elementary shallowing-upward, metre-scale cycles are present, in most of the cored wells and the FMI images (Figures 8.20, 8.21 and 8.23).

The cycles are set into four hierarchical levels. Namely, 1, 2, 3 and 4, corresponding in time to the 3rd, 4th, 5th and 6th order of Vail *et al.* (1992) respectively.

The Level 1 cycle is considered to be equivalent to 3rd order cycles of Vail *et al*. 1992). This cycle relates to rift basin evolution and the generation of accommodation space for the syn to post-rift of the Pre-salt and the infill of a series of half-graben fills. It is hundreds of metres thick and endures for about 4 Ma. The tectonic activity and creation of accommodation space in rift basins occurs in pulses (Paz & Rossetti, 2005), with more tectonically active periods and periods of tectonic quiescence (Figures 8.19 and 8.20). The periods of tectonic quiescence usually form carbonate deposits and in the tectonically active phases, the trend is erosion, transport and sedimentation of terrigenous deposits through reactivation of the source area. In more distal areas in extensional margins, progressive reactivation of previous faults results in long-lived faults and more accommodation space. In such areas in the Southern Campos Basin, away from clastic supply, high productivity of carbonates can fill or overfill the accommodation space resulting in aggradational or progradational geometries seen in the offshore sites as illustrated and described in seismic sections in the Chapter 9 and interpreted from shallowing upward successions in wells (Figures 8.23, 8.25 to 8.27).

Level 2 cycles (4th order in Vail terms) is about hundred metres thick. These cycles are interpreted from the GR log signature, and commonly are an alternation of terrigenous and carbonate facies (wells 1, 2, 7, 8, 9 and 10, Figures 8.20, 8.25 and 8.26). It is suggested that in more humid periods, there is greater input of terrigenous sediments, which are evidenced in cores, cutting samples and high values of GR. Humid periods therefore form the transgressive portions of cycles. In arid periods the conditions are more conducive to the accumulation of carbonate rocks and these are commonly stacked in shallowing upward and regressive phases. In the offshore well (well 20) such climate changes are represented by considerably variation in the preserved biota (Hessel & Mello, 1987) and this aspect is discussed further in Chapter 10. Level 2 climatic changes are regional and widespread in the study area, and can be correlated from well 1 to well 12, (Figures 8.19, 8.20, 8.25 and 8.26).

Level 3 cycles (5th order) are 10 to 30 m thick, and are considered to be driven by changes in lake level that are thought to be responses to a higher frequency climate variations than those in level 2 cycles. These changes are more local, seasonal, and may also be associated with tectonic subsidence to generate the required accommodation space. The cyclicity is observed in facies variations, which form symmetrical cycles strongly expressed in the rise and fall of the GR values, as shown by the arrowed trends in Figures 8.19 to 8.22. These trends (green spike in the Figures 8.21 to 8.22) occur with

a superimposed higher frequency cycle (level 4, 6th order), which appear to be ubiquitous in the cores and FMI log (light blue in the Figures 8.21 to 8.22).

Level 4 cycles (6th order) are commonly 1 to 2 metre thick and attributed to be related to high bioproductivity and bioconstructions, and also to small transportation and building out of shallow lake margin facies of bioclasts and intraclasts. These cycles are controlled by intrinsic sedimentary processes of the lake margin and are progradational in style (Figures 8.14 to 8.17 and 8.21). The cycles are therefore considered to be autocyclic. They are described in detail (section 8.2 and 8.3 above) and also show similarities to shallowing-up cycles (Strasser, 1991), or parasequences (e.g. Spencer & Tucker, 2007; Nichols, 2009), and also high frequency sequences (e.g. Lehrmann & Goldhammer, 1999). Separating these different influences using subsurface data and in a tectonically active rift basin lacustrine setting is beyond the scope of this project.

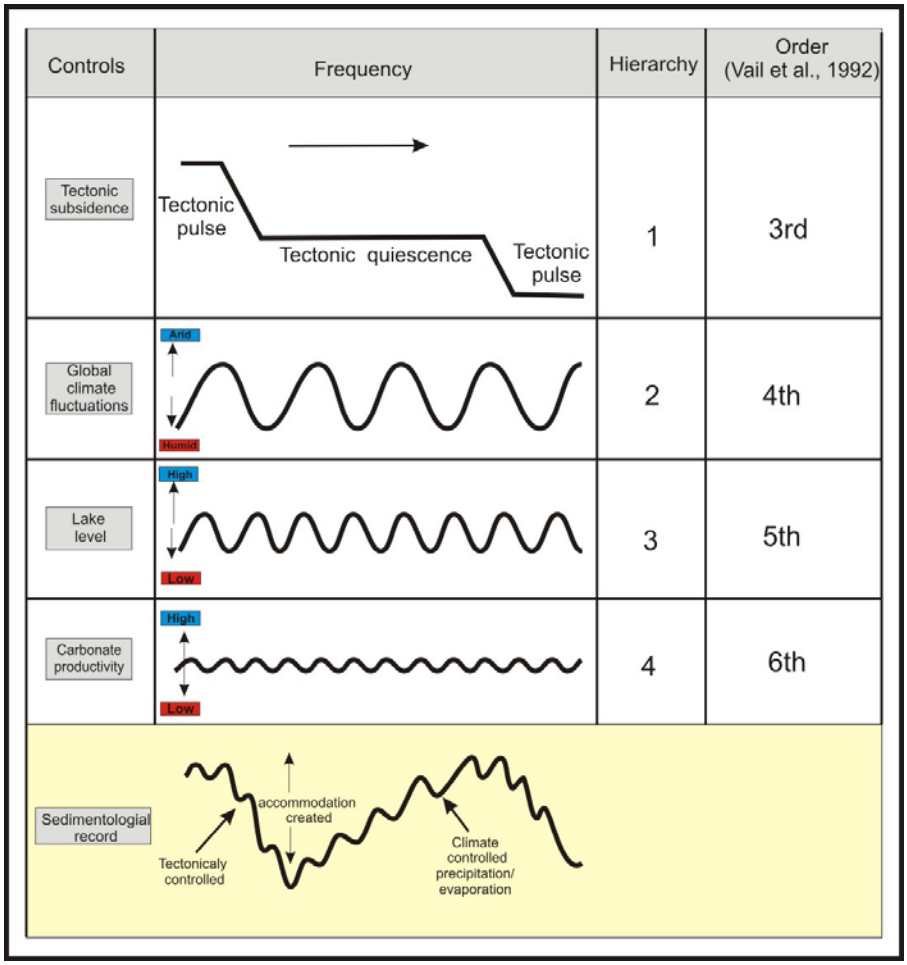

Figure 8.19– Hierarchy of cyclicity in Campos Basin Pre-salt and composite curve resulting from different frequencies of cyclicity recorded in the wells. The fourth column shows there possible equivalence to the Exxon orders of cyclicity.

The sedimentological record is a result of a composite curve of changing accommodation space made up from the convolution of curves of different frequencies of cycles (Figure 8.19). It is not easy to isolate these superimposed controls when they are not mutually exclusive (Hardie *et al.* 1991, Read *et al*. 1991; Van Wagoner *et al.* 1990; Church & Coe, 2003; Perlmutter & Azambuja Filho, 2005).

Figures 8.14 and 8.15 show elementary shallowing-upward cycles of about 2 metres thick at the base of well 20. This stratigraphic unit is mainly formed by grainstones (FMI-6), interpreted to have been deposited in a lower subaqueous environment, and breccias (FMI-1) representing emergent conditions at the cycle top (Chapter 7). These Level 4 cycles are interpreted (above) to be autocyclic, controlled by the local sedimentary dynamics (Macurda, 1997). However, an allocyclic event of Level 3 of approximately 10 m thick is superimposed on the Level 4 cycles (Figure 8.20) as explained in the previous section. The Level 3 cycle, is interpreted to be related to the variation in lake level (*sensu* Fitchen, 1997). But, the high frequency cycles, of hierarchy level 4, are continuous and persistent, exhibiting thickening shallowing-up stacking patterns in the lower part of the Coqueiros Fm. And also in the Macabu Fm. (Figures 8.21 and 8.22).

Hierarchy		Magnitude (m)	Cyclicity type	Controls		Systems Tract	
						Transgressive	Regressive
1	(long term)	>100	Allocyclic	tectonic	active quiescence	deltaic and lacustrine depositional systems (active)	carbonate platform (quiescence)
2	Intermediate frequency	100		climate	arid humid	terrigenous (humid)	carbonate (arid)
3		10-30		lake level fluctuation (tectonic & climate)	allochthonous sediment supply	deepening, flooding, mud organic matter	shallowing, exposure grainstones, rudstones
4	high frequency	1-2	Autocyclic	*in situ* bioproductivity intrinsic sedimentary process (shallowing up cycles progadation)	autochthonous parautochthonous	shale, marls, mudstones pustular laminites	grainstones, rudstones, stromatolites breccia

Figure 8.20 – Summary of the stratigraphic and cyclicity controls and lithological characteristics of transgressive and regressive phases. More explanation may be found in the text.

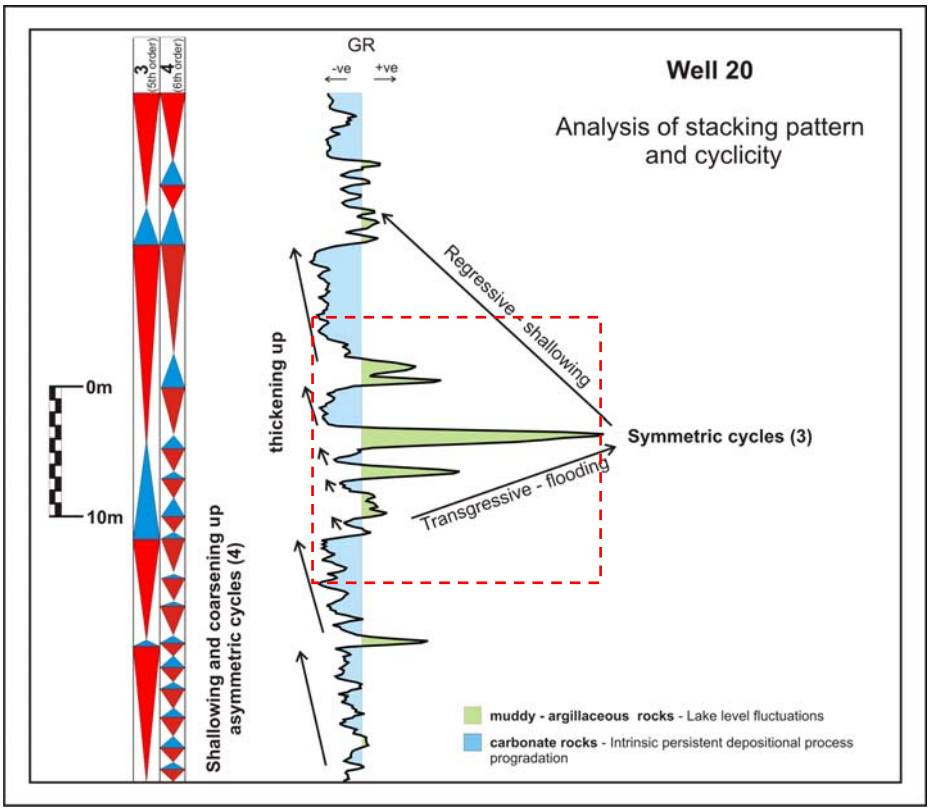

Figure 8.21 – Analysis of stacking pattern and cyclicity of the 4th and 3rd hierarchy level cycles in the Coquinas of well 20. Blue colour in the low Gamma Ray log values indicates carbonate rocks deposit in shallowing and thickening up trend, interpreted as high frequency autocyclic asymmetric cycles. The green colour indicates more argillaceous sediment and the symmetry is interpreted as lake level variation. The dashed red Box is a magnification of this interval (Figure 8.20).

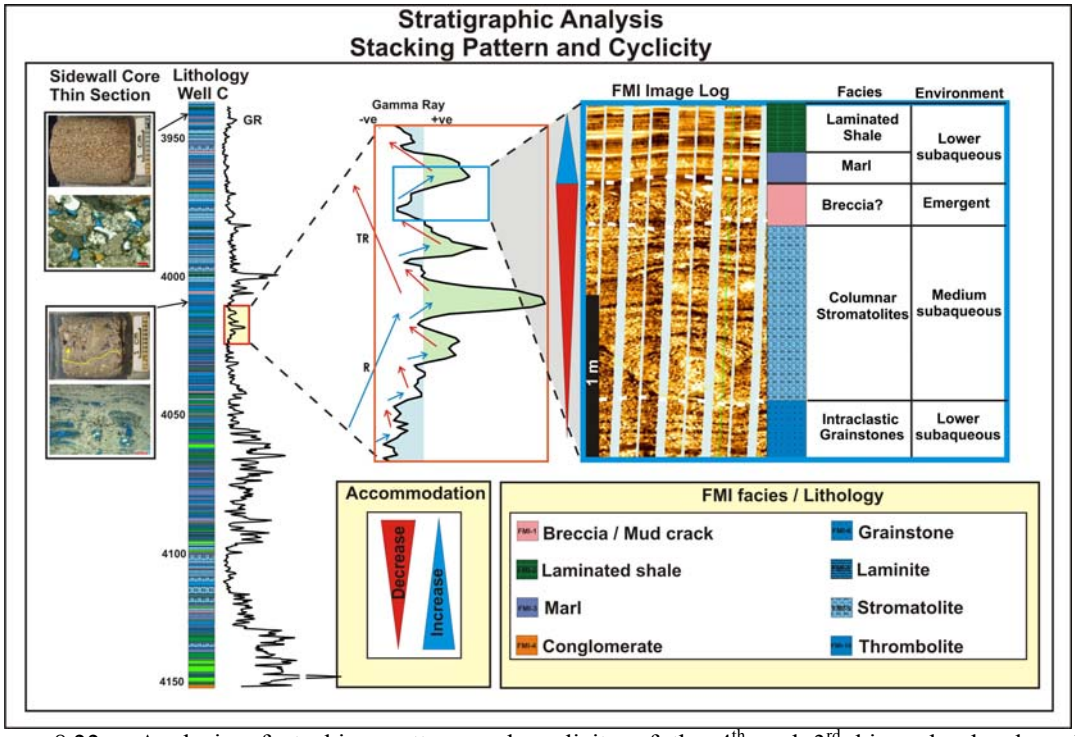

Figure 8.22 - Analysis of stacking pattern and cyclicity of the 4th and 3rd hierarchy level cycles (Microbialites). The same interpretation as the previous Figure 8.14, but in the Aptian microbialite succession.

A Fischer plot was made of the high frequency cycle thickness variations (Level 4) in well 20 (Figure 8.23). This method is normally used as a graphical analysis of parasequence thickness data in order to determine trends in accommodation space (*sensu* Fischer, 1964; Read & Goldhammer, 1988 and Sadler *et al*. 1993). The analysed interval is 200 m thick, ranging from 4650 m to 4850 m depth. A trend of decreasing followed by increasing accommodation space is identified in the Aptian succession, spanning up to 4.5 Ma. (112.5 to 117 Ma.). This long term (Level 1) curve may be interpreted as 3rd order (Exxon type) regressive-transgressive succession or the upper part of one cycle and the base of another (Figure 8.23).

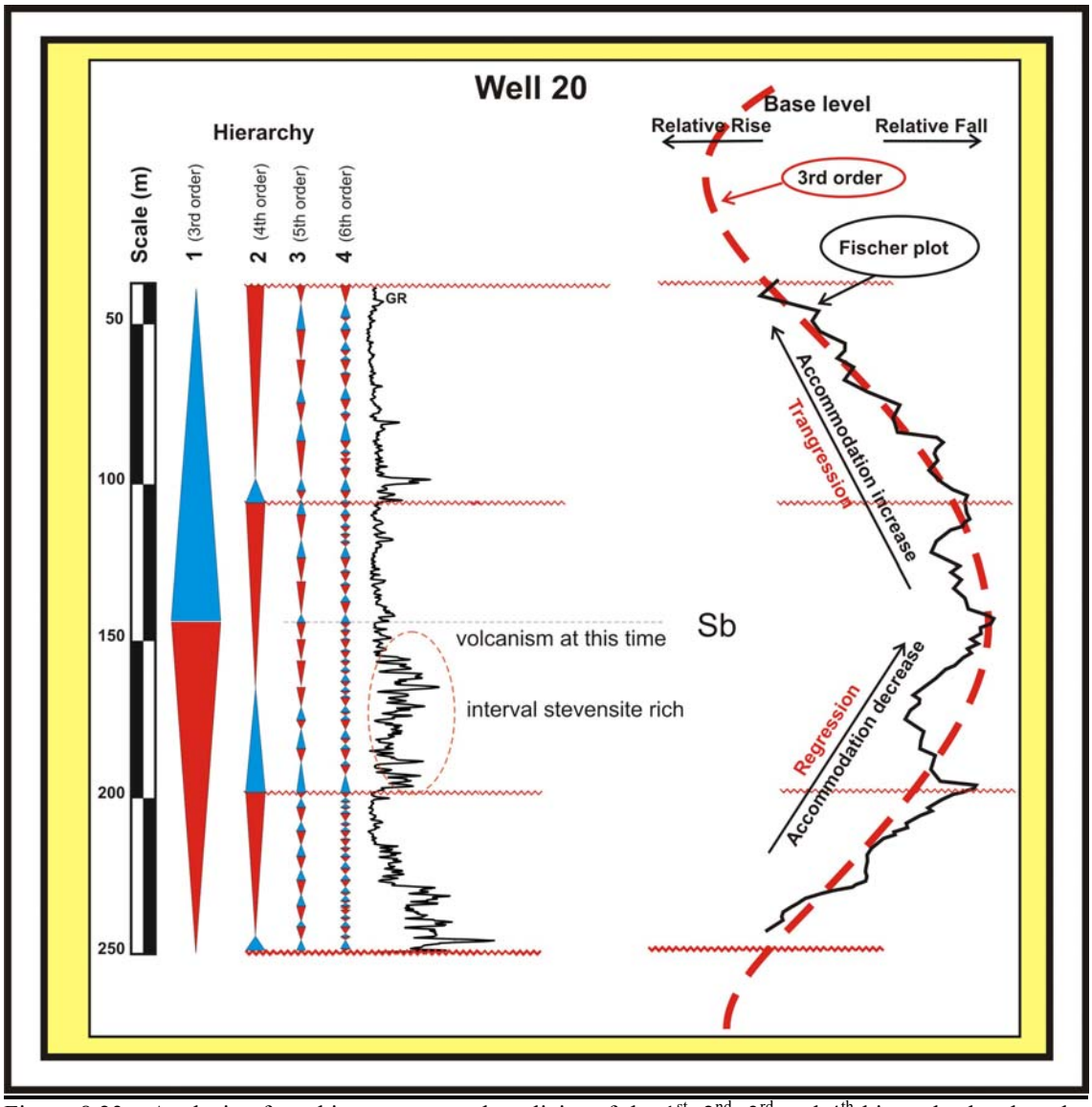

Figure 8.23 - Analysis of stacking pattern and cyclicity of the 1st, 2nd, 3rd and 4th hierarchy level cycles Aptian microbialites. The Fischer plot was based on the thickness variations of the cycles in level 4 (using the method of Fischer, 1964 and Sadler *et al*. 1993). The dashed red line shows the trend enveloped in 3rd order (*sensu* Vail *et al.* 1992).

One plausible explanation for this inverted sequence (RT-3) is that the sedimentary succession in the interval from 4700 m to 4800 m is stevensite rich. This mineral, a tri-octahedral magnesium smectite, indicates magnesium-rich lake waters, possibly attributable to contemporaneous volcanism (see Chapter 6). The third order Aptian cycle (Figure 8.23) may therefore be strongly governed by earlier tectonic-related uplift, which might have promoted a reduction in the accommodation space in the middle part of the Aptian carbonate succession (4700 to 4800 m, Figure 8.23).

Related to this Rodrigues (2005) has documented changes in carbon and oxygen stable isotope values in the Aptian in the Campos Basin. This demonstrates enrichment in the $\delta^{18}O$ content followed by a decrease in the $\delta^{18}O$ values (Figure 8.24). These curves indicate increased evaporation and higher salinity in the trends to heavier $\delta^{18}O$ followed by, increased water inflow indicated by the trend to lighter $\delta^{18}O$. The stable isotope trends of $\delta^{18}O$ and $\delta^{13}C$, therefore follow the trends of the Fischer plot and support the hypothesis of regression followed by transgression. Sarg *et al.* (2012) presented similar stable isotope values indicating more closed and more open lacustrine palaeoenvironments for the Cenozoic Green River Formation.

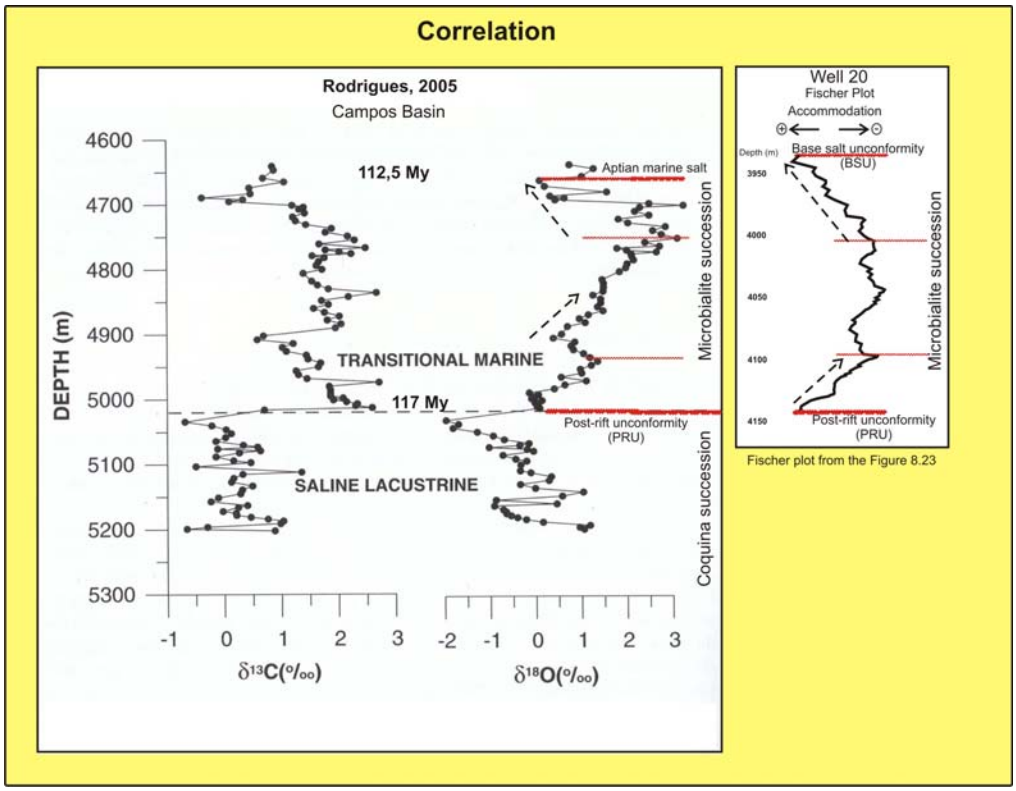

Figure 8.24 – Stable isotope analysis of the Campos Basin Aptian succession (Rodrigues, 2005), compared with Fischer plot analysis undertaken with high frequency cyclicity for the Aptian succession in the well 20.

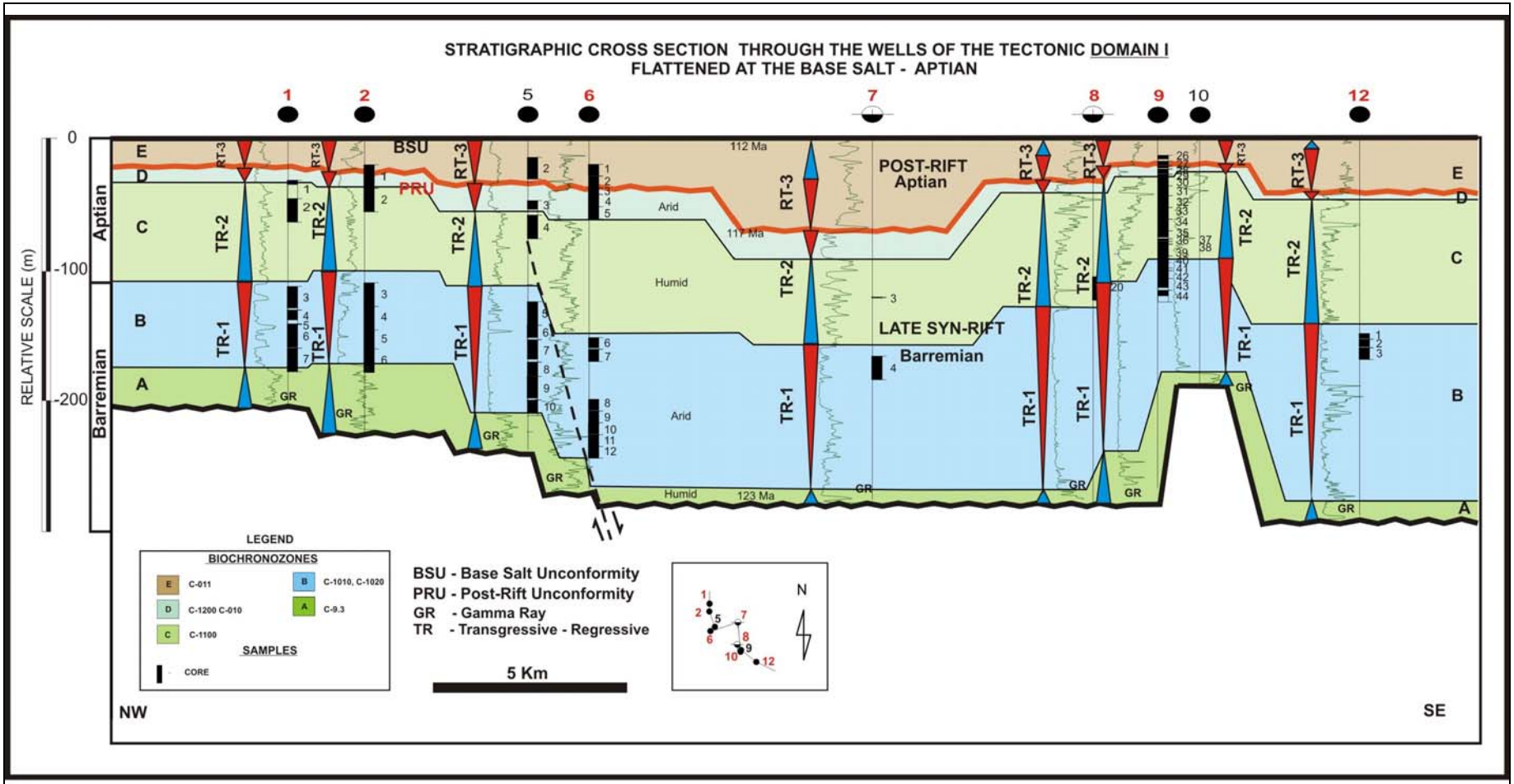

Figure 8.25 - Transect through the wells of the project area, flattened at the base Aptian salt. The gamma logs as well as the cored intervals have been used to identify clastic rich (higher gamma), transgressive, humid phases as opposed to carbonate rich (lower gamma) and regressive phases. These together make up the Level 2 cycles of the southern Campos Basin

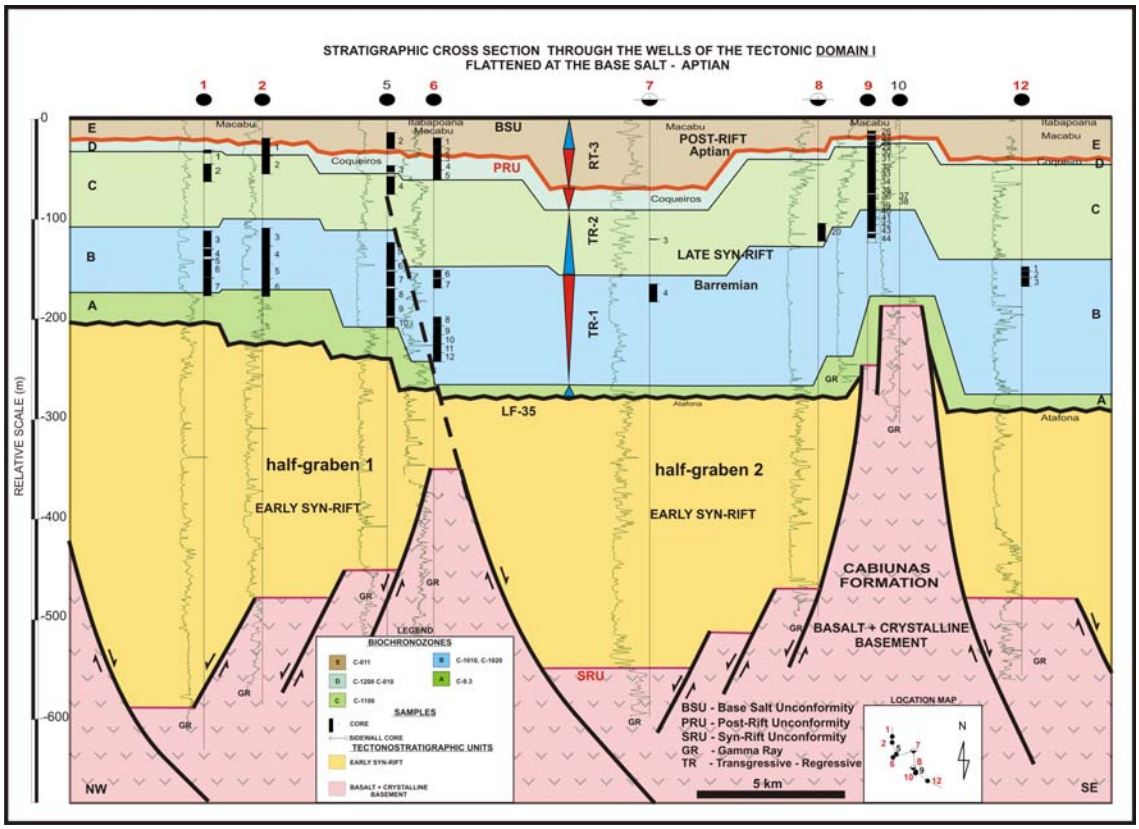

Figure 8.26 - Stratigraphic cross section through the wells of tectonic domain I, flattened at the base Aptian salt.

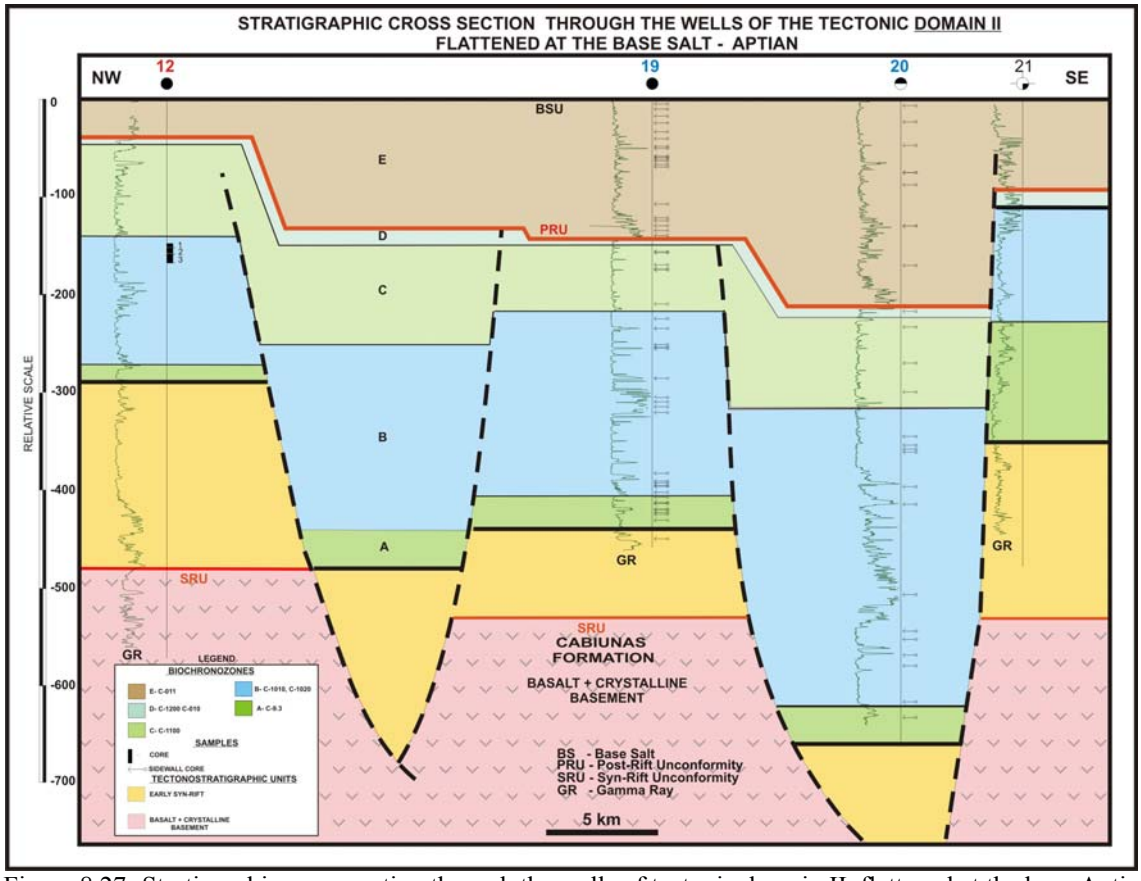

Figure 8.27- Stratigraphic cross section through the wells of tectonic domain II, flattened at the base Aptian salt.

8.4. Facies and cycle variation between wells

The sediments of the Lagoa Feia Group of the Campos Basin unconformably overlie the acoustic basement, which comprise basalts of the Cabiúnas Formation, of Neocomian age. These non-marine syn to post-rift successions culminate in a marine evaporitic deposit, which covers all the rift succession in the basin (Castro & Azambuja Filho, 1980).

During the progressive rifting process, various half-graben formed that were filled initially by alluvial clastic sediments in the tectonically active phase of the early syn-rift. (Figures 8.25 to 8.27). Then, fluvio-deltaic-lacustrine sedimentation took place in a continuous basin fill process. In this case, mixed carbonate and sandstone successions were deposited in shallower conditions in more proximal areas whereas basinward, carbonate tends to dominate in areas less influenced by terrigenous supply.

Successive transgressive - regressive phases represented by facies alternation of sandstones and carbonates, respectively, occur in proximal sites. Through the analysis of cycles of various scales three major transgressive-regressive sequences are defined: TR-1, TR-2 and RT-3 (Figures 8.25 to 8.27). The TR sequences, as defined by Johannessen (1992), are limited by unconformities in the shallow areas and surface of maximum regression (SMR) in the submerged portions. The maximum flooding surface separates the transgressive systems tract from the regressive systems tract (Figure 8.3).

Each Transgressive Systems Tract (TST) is characterised by the increase of terrigenous sediments as indicated by cores and wireline logs from the wells. Deeper lacustrine waters, lower energy environments, accumulating finer grained lithologies such as shale and marl, show an increase in ostracod content, and are interpreted to have formed below SWB. Such facies association may be expressed in the high value of GR due to the considerable content of feldspars and organic matter in the sediments. This systems tract, as it is regionally expressed throughout the basin, may be associated with humid climate phases, and tectonically active periods (Fitchen, 1997; Church & Coe, 2003). Overlying this is the Regressive Systems Tract (RST) which is characterised by the high productivity of filter feeding and grazing carbonate components; bivalves and gastropods molluscs. The abundance of such components in matrix free textures and accumulation of the shells by in high energy waters are expressed in low values of GR. These events are interpreted to occur in more arid and tectonically quiescent periods (Cross *et al*. 2008).

In order to have a better spatial and temporal correlation five subzones were defined in the entire studied interval: biochronozones A, B, C, D and E (see Chapter 2; Figure 2.7). These stratigraphic zones are based on non-marine ostracod biozones (Silva Telles, 1992) that are tied to the gamma ray electric log signatures (GR). The boundaries between biochronozones are markedly expressed by shifts in the gamma ray logs leading to the recognition of the biochronozones.

The TR-1 sequence is limited at its base by the stratigraphic mark LF-35, a seismically traceable regional unconformity (Chapter 2.5 – Figure 2.7) and at the top by the chronozone C 1020 and the biochronozone B. This sequence comprises biochronozones A and B and varies laterally in thickness and geometry according to the palaeogeography (Figures 8.25 and 8.26).

The biochronozone A is characterized by the chronozone C-093 (Figures 2.7 and 8.25). It is thicker in the proximal sites and thinner in distal areas. It was not sampled by core, but the descriptions of cutting samples previously made by Petrobras, and lateral samples collected from wells 19 and 20, show that this biochronozone is characterized mainly by shale, stevensite and siltstone ostracod-rich in more proximal sites. The Gamma Ray log shows high values and a crenulated pattern (Figures 8.25 to 8.27). In the intermediate locations a considerable presence of marl is noted. Mudstone, however, occurs in the most distal portions of the basin. This zone is thick in the proximal sites and represents the initial transgressive phase of the studied interval. The subsequent biochronozone B of the regressive phase of TR-1 is characterised by chronozones C-1010 and C-1020 (Figures 2.7 and 8.25). In the proximal areas, this chronozone tends to occur amalgamated in pack of sediment with an average of hundred metres. In the proximal area, it is represented by mix of terrigenous and carbonate rocks which laterally pass into an amalgamated carbonate platform forming a thick unit on the foot wall of half graben 1 and 2 (Figure 8.26). This facies association is characterized by high GR values intercalated by low GR, with a clean Box-like pattern, representing the regressive phase of the TR-1 sequence (Figures 8.25 and 8.26). However deeper in the basin, in half-graben, it tends to have more shaley sediments, similar to the T interval. It is extensively cored in wells 1, 2, 5, 7, 9 and 12 (see Appendices A1 to A7) and with sidewall core samples in the wells 19 and 20 (Figure 8.27).

In more distal areas, basinward, Domain II, these carbonate rocks thicken considerably, due to the greater accommodation space and possible high biogenic

productivity of molluscs shells. At these sites progradation of banks and bars commonly occur.

The TR-2 sequence is identified at its base by the chronozone 1020 and at the top by the syn-rift regional unconformity (Figure 8.25). This sequence comprises C and D biochronozones and is almost isopachous (Figure 8.25). However, close to the border fault of the half-graben the thickness increases considerably and above structural highs it thins due to non deposition or erosion. In the well 21, for example, the biochronozone C is not present (Figure 8.27).

Biochronozone C, is characterized by chronozone C-1100, cored in the wells 1, and 2 and sidewall core samples in the well 20. In more proximal areas there is alternation of mixed terrigenous and carbonate rocks, clearly showing in the variations of high and low GR log curves. In the wells 8, 9 and 10 there is a progressive increase of terrigenous sediments expressed in the GR log curve trend, with a bell-like pattern (Figure 8.26). This is interpreted as representing the progradation of fluvial system. This stratigraphic horizon, which is a hundred metres thick on average, represents the transgressive phase of the TR-2 sequence. These are interpreted as turbidites from a delta system in proximal areas (Chapter 7). Basinward within this zone, the diversity of the bivalves decreases due to environmental change, probably this phenomenon occurs as a result of an increase in salinity, as also suggested by dolomitization and an enrichment in the pink colour of the bivalve species, which is also taken as indicating environmental changes (Hessel, 1987). The carbonate rocks offshore are more pure, formed predominantly by coquina of high-energy depositional environment showing progradational geometries. They present crenulated-like GR pattern with high values of Gamma Ray log (GR).

The biochronozone D is characterized by chronozone NRT-010 and was sampled in the wells 1, 2, 5, 6 and 9. It is represented predominantly by rudstones that are gastropod rich. These stratigraphic layers are not very thick (< 20 m) but thicken in the most proximal and thin in the most distal areas. This represents the regressive phase of the TR-2 sequence and shows a cleaner GR, Box-like pattern, which indicate pure carbonate (Figure 8.25). It is bounded at the top by chronozone 1100 and the post-rift unconformity (PRU). The gastropods may have lived in a variety of environments both fresh water and more saline but the species have not been used as palaeoenvironmental indicators. Clearly it was less favorable to be bivalve species. It is believed that during the period of deposition of this, the last unit of the syn-rift phase, the rift was practically

filled, with very shallow water conditions, with possibly some influx of marine water. The subsequent post-rift unconformity shows subaerial exposure, as shown by karst features; porosity enlargement and shallow vadose and phreatic diagenesis in the cores. Evidence shows that some significant environmental changes do occur in zone D, probably due to the environmental stress that results in the exclusion of the molluscs; probably due to a possible first influx of marine water to the basin or a global climate change.

The RT-3 is interpreted as an inverted sequence, Regressive – transgressive, of Biochronozone E, limited by the syn-rift unconformity and base salt unconformity. The zone E, is sampled in wells 2, 5, 6 and 9 and is characterised by sandstones and polymict conglomerates interpreted as forming in an alluvial system in the proximal areas. However, in the distal portions it is characterized by microbial carbonates associated with reworked grainstones. Thickness varies according to the accommodation space. In proximal areas the thickness varies from 20 to 50 m, in distal areas the thickness reaches 200 m (well 20). This considerable increase in thickness may be due to thermal subsidence and a basinward tilt, possibly magnified by long-lived faults reactivated in the post-rift phase.

8.5 Conclusions

In reviewing the literature about sequence stratigraphy, it is clear that initial models are based on siliciclastic environments (Vail *et al.* 1977; Van Wagoner *et al.* 1989). This original sequence stratigraphy method has been adapted to the study of carbonate platforms with modifications made to include carbonate production in shallow carbonate factories (Sarg, 1988; Bosence & Wilson, 2003). However, the assumed continuous subsidence and global eustasy working together to control accommodation and the arrangement of systems tract in a predictable and correlatable fashion can not be applied to carbonates accumulating continental rift basins. In this context, other factors such as climate, tectonic, sedimentary supply, work together to form the sedimentological record and the interpretation of trends and cycles is far more complex. The transgressive - regressive sequence stratigraphic model, proposed by Johannessen (1992) initially for interpreting the marine successions is found to be applicable to the rift tectonic settings. This method uses the maximum regressive surface (MRS, Figure 8.2) as a submerged correlative key surface. Thus, the MRS, can be objectively

determined and it is an alternative model to overcome the problems of sequence definition.

As an early example of application of a similar method, Castro & Azambuja Filho (1980) defined four transgressive regressive cycles in the Lagoa Feia Group, for alluvial fans underlying lacustrine shales, sandstones coastal shoreface and shallow platform carbonates. Rangel & Carminatti (2000), based their subdivisions on unconformities, and stratigraphic markers, which are identified in well logs and seismic, defined seven depositional sequences, deposited during the rift stage and three depositional sequences deposited in the post-rift context, sensu Mitchum *et al.* (1977) for the same basin.

In this study a clear cyclic character of the sedimentological record is recorded for the entire interval studied of the Coqueiros and Macabu Formations. The cyclicity is observed in a hierarchy of four different levels and the sequences are defined using the T-R models of Johannessen (1992). Although higher frequency cycles are irregularly arranged, in both space and time, they are the building blocks to the construction of the stacking patterns and transgressive regressive sequences of a lower order. These lower order T-R sequences (3^{rd}) are found to be correlatable throughout the study area and can be used to study the fill of the rift basin. The different orders of cyclicity are shown to have different controls on their development including autocyclicity, climate, and tectonics.

The findings of this chapter addresses and answers the second scientific question postulated for this research: Can the strata be subdivided using sequence stratigraphic principles to organise and understand the sedimentological framework and are these the same or different from standard sequence stratigraphic models?

From the analysis of stacking patterns and key surfaces in seven wells, a hierarchy of 4 different orders of transgressive-regressive sequences has been identified. These are used to further the understanding of the different stages of the rift basin and some of the controls on sediment accumulation.

CHAPTER 9 – SEISMOSTRATIGRAPHY

9.1. Introduction

Seismic stratigraphy was a revolutionary technique when introduced to sedimentary geology by Vail *et al*. in 1977. Since early in the last century, stratigraphy has been investigating the interaction between base level changes, unconformities and sedimentation rates (e.g., Grabau, 1913; Barrell, 1917; Sloss *et al*. 1949; Wheeler & Murray, 1957; Wheeler, 1958, 1959, 1964; Sloss, 1962, 1963; Curray, 1964; Frazier, 1974). However, Vail *et al*. (1977) proposed a seismic stratigraphic method for the identification of depositional sequences that has lead to facies prediction in the subsurface. This seismic stratigraphic method consists of the recognition of key surfaces that bound the strata together with stratigraphic geometries based on seismic data. Such surfaces may be considered as time-stratigraphic horizons rather than lithological boundaries and have been used define sequences, systems tract and also geometric stratal patterns (Macurda, 1997).

The Vail *et al*. (1977) seismic stratigraphic method has been used for the mapping of key surfaces and the recognition of the main sequences (3^{rd} order) within the south Campos Basin dataset. Five time-stratigraphic seismic reflectors have been recognised and mapped through the 3D seismic volume in a dense mesh. The criteria used for the mapping of these seismic horizons is the identification of seismic reflector terminations, such as erosional truncation, onlap, downlap, toplap, and continuity of the reflectors as well as the stratal geometries (Figure 9.1). The quality of the data within the seismic volume is variable and in the proximal area of study (Domain I) the resolution is not good enough to define accurately all five key surfaces. The reflectors are poorly defined.

However, elsewhere the surfaces have been mapped in Landmark software (Figures 4.3 and 9.1). For this reason, another seismic survey (Alfa July 2010) with better resolution for the base and top and top Coquina surfaces has been used for this area. The reflectors showing in the Domain I region is a result of merge.

The variable quality of the seismic, which, in places, is noisy and with low seismic vertical resolution, is compensated in this study by density sampling of subsurface data, with cores and wireline logs. The main surfaces mapped and their stratigraphic significances are described in the following sections.

9.2. Key surfaces mapped and sequences

Thus, the main surfaces mapped are:

1) Top acoustic basement (Syn-rift unconformity -SRU),
2) Base coquina (LF-35 stratigraphic mark),
3) Top coquina (Post-rift unconformity - PRU),
4) Top of microbialites (base salt unconformity - BSU
5) Top Salt

Such surfaces correspond to the three main TR sequences (*sensu* Embry and Johannessen, 1992) described in Chapter 8. The LF-35 and PRU form the lower and upper surfaces of the stratigraphic sequences TR-1 and TR-2. The PRU and BSU form the bounding surfaces of the RT-3 sequence (Figure 9.1).

The Syn-rift Unconformity corresponds to the base of the Lagoa Feia Group and overlies the basalt of the Cabiúnas Formation (Schaller, 1973). This is a regional unconformity dated at 128 Ma. (Winter *et al.* 2007). This surface forms the base of the entire rift sedimentary succession (Cordani *et al.* 1972). The basal clastic terrigenous sediments, of the early syn-rift succession, lie unconformably on it (Figures 9.1 and 9.2) and it is therefore named here as the Syn-rift Unconformity (SRU) (cf. Bosence, 1998).

The LF-35 chronostratigraphic marker (Figures 9.1 and 9.2) forms the lower limit of the TR-1 sequence (Chapter 8.24 and 8.25) and the coquina sequence (K38) of Winter *et al.* (2007). The coquina sequence corresponds to the intermediate portion of the Lagoa Feia Group, comprising the Itabapoana and Coqueiros Formations, deposited during an interval ranging from the late Barremian to the early Aptian, between 117 Ma and 123.1 Ma (Chapter 2.3, Figure 2.5). This is a significant surface representing the passage from basal clastic alluvial-fluvial strata of the early syn-rift succession to carbonate platforms of the late syn-rift succession. The upper surface of this stratigraphic unit (TR-1) is the LF-60 chronostratigraphic marker (Figure 2.5), which divides the coquina sequence (K38) into two parts. This surface is an unconformity at the base of the main transgression of the TR-2 sequence. It is bounded at its top by the post-rift unconformity (PRU).

The PRU is a marked regional erosive event, easily identified on seismic sections (Figures 7.1, 7.2 and 9.1). The RT-3 sequence is bounded by PRU at its base at 117 Ma and the base salt surface (BSU) at 112.5 Ma at the top, and corresponds to the upper part of the Lagoa Feia Group (Figure 2.5). This sequence comprises the post-rift

or sag phase (*sensu* Dias *et al.* 1987) of the rift succession and is characterised by clastics and evaporites. This sequence represents an expansion of the basin and transition from continental to marine related evaporites. The sequence comprises conglomeratic alluvial fans of the Itabapoana Formation in the proximal zone, marl and shale of the Gargaú Formation in the intermediate sites and microbial carbonates of the Macabu Formation in the most distal areas (Winter *et al.* 2007).

9.3. Seismic stratigraphic geometries of the syn-rift carbonate successions

Little has been published concerning the sequence stratigraphy of carbonate rocks in the non-marine environment. In such carbonate successions, the stacking patterns, sedimentary facies, and arrangement and geometry of the sedimentary depends not only on eustasy and constant subsidence such as the standard sequence stratigraphic model (Vail *et al.* 1977), but several other factors act individually or together to control the depositional architecture. This is discussed in detail in Chapter 8 (section 8.2.3). However, in general, the seismics commonly show aggradational geometry with parallel, sub-parallel and also divergent reflectors. However, at the platform edges regular progradational patterns are seen (*sensu* Macurda, 1997) are observed (Figures 9.1, 9.3 and 9.3a).

Within the syn-rift succession aggradational parallel and sub-parallel seismic reflectors are normally related to the available space for sediment to accumulate, and on a large scale to regional increase in the accommodation potential (cf. Macurda, 1997). On the other hand, divergent or fanning reflectors are related to the regional differential accommodation, such as in half-graben where the asymmetric geometry controls the pattern of arrangement of the stratal geometries (Figures 9.1 and 9.3). The differential accommodation results in faster rates of deposition in the more rapidly subsiding parts of a depression. However, in shallow areas, the facies models suggest that carbonate production is higher but accommodation space is more limited. In general the reflectors of the mapped area present plane-parallel and divergent configurations in the syn-rift successions (Figure 9.1). In the late syn-rift, where carbonate platforms are formed, there are differences in the stratal geometries and platform morphologies from onshore to offshore positions (see below). These differences appear to relate to different styles of continental rifting.

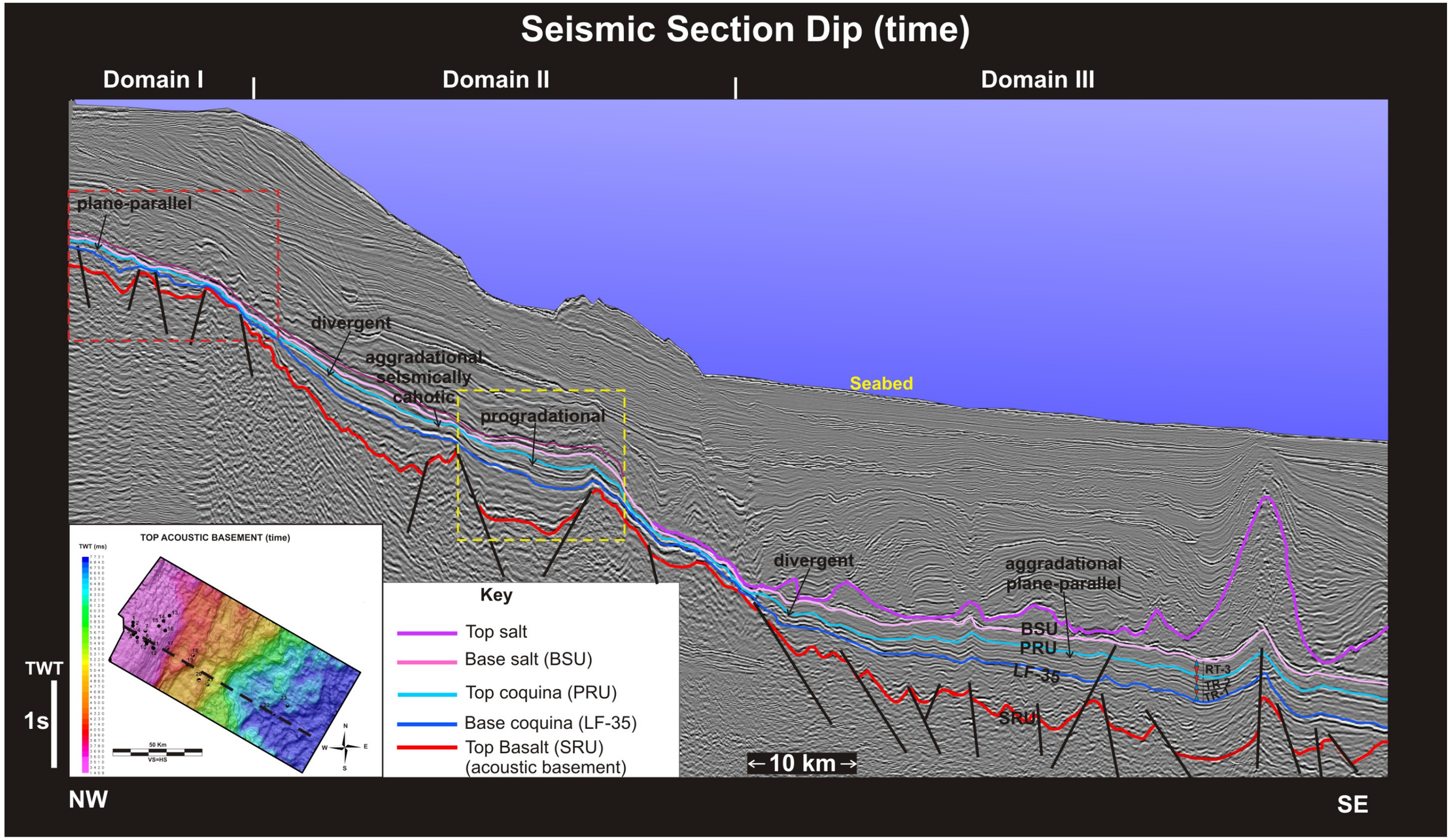

Figure 9.1 – Dip oriented seismic section from NW to SE (for location see inset) showing the main horizons mapped, and the unconformities that bound the 2 T-R and an R-T sequences identified and the geometric patterns of the basin fill.

The post-rift carbonate succession relates to the eastward tilting of all the sequences related to long live basinward fault and thermal subsidence that together provide the accommodation space for the post-rift carbonate succession.

Domain I

In the proximal zone (Domain I) the seismic data are noisy and has low vertical resolution, hindering the identification of the seismic reflectors. However, the horizons mapped with help of a better seismic quality Alfa survey, which was merged to the presented one, it has been possible to identify and map physical time-stratigraphic surfaces. Domain I is characterized by half-graben systems, and within these thickened successions the seismic reflectors are not easily identified. But, the depositional trends, based on the cores logged in wells 1, 2, 6 and 9 are shallowing up and interpreted to be progradational (see Chapter 7, section 7.2). Plane-parallel and also divergent geometries are recognised within the syn-rift strata (Figure 9.2). Post-rift successions show prograding geometries with chaotic seismic facies interpreted as alluvial fan deposits. (Figures 9.1 and 9.2).

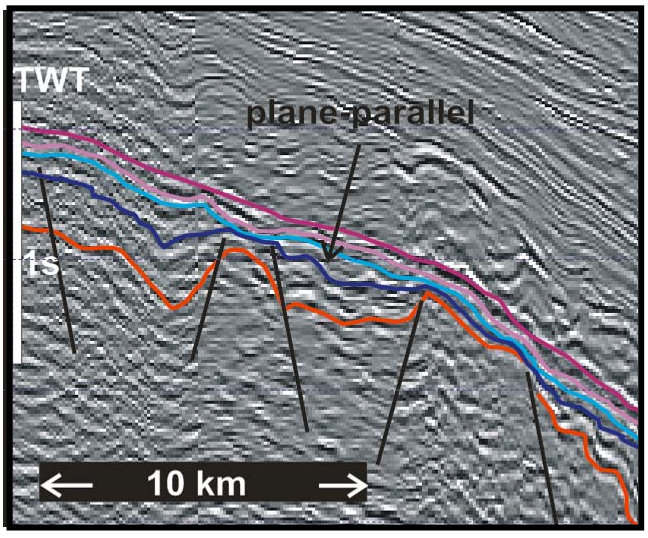

Figure 9.2 – Detail outlined in red, Domain I area of Figure 9.1, showing internal geometry and characteristics of the key surfaces explained in the text for Domain I.

Domain II

In this Domain II agradational, plane-parallel and divergent and also progradational reflectors (Figures 9.1 and 9.3) are seen. Eastward, on the topographic high (Figures 9.3 and 9.4) is a zone exhibiting plane-parallel, aggradational and divergent reflectors. Also present are agradational and chaotic areas which may

correspond to bars, banks or shoals. Well 19 suggest that these may be high-energy bioclastic rudstone units. Its either plane parallel or sub-parallel or divergent reflectors are resulted of the half-graben asymmetry added to the differential compaction from the intrabasinal highs, accommodation and transfer zones (Figures 9.1 and 9.3).

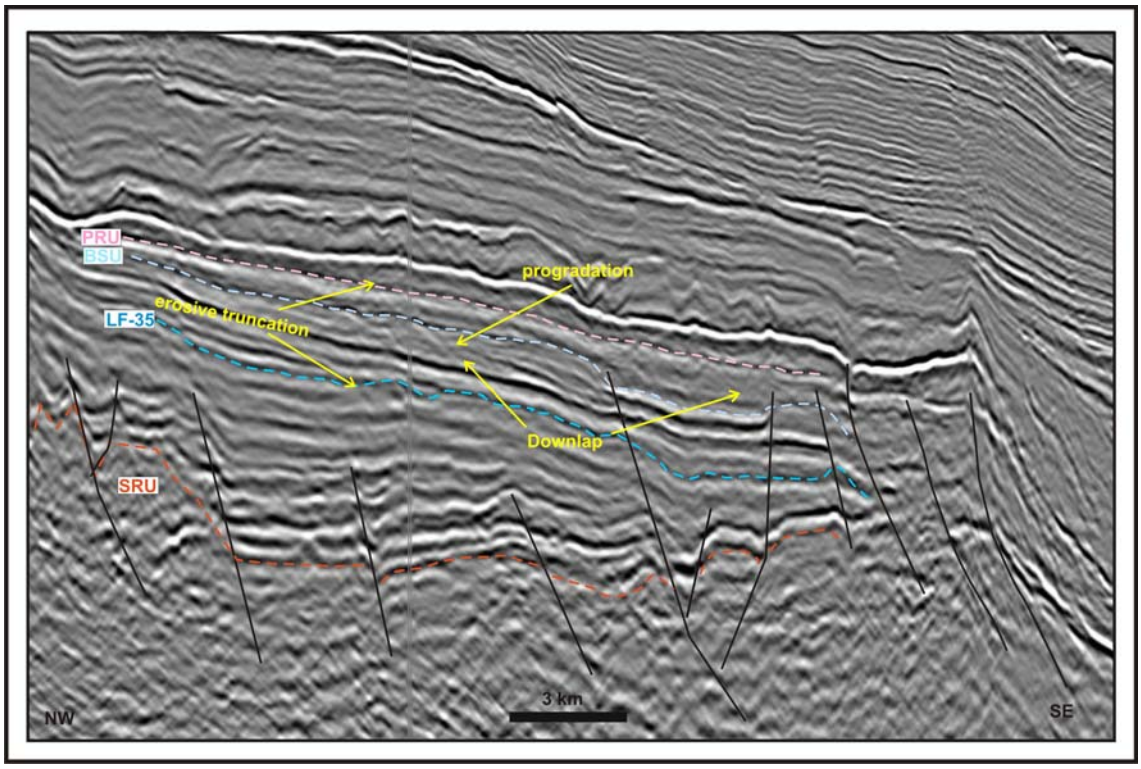

Figure 9.3 – Detail outlined in yellow, Domain II area of the Figure 9.1, showing internal geometry and characteristics of the key surfaces explained in the text for Domain II. Note the thickening of the succession into the half-graben and identification of surfaces with some erosive truncations.

Basinward prograding reflectors are also seen in areas with variably developed downlap, toplap and locally erosional truncation (Figures 9.1, 9.3 and 9.6) These prograde imply that the high carbonate productivity is in excess of accommodation space in these very shallow water environments resulting in geometries similar to those seen in shallow marine tropical environments (Figure 9.3). Long-lived antithetic faults also occur in this area, which were active during the late syn-rift and also post-rift phases. These faults allowed the progressive creation of accommodation space for the deposition of thick carbonate deposits in shallow water environment.

Domain III

In the most distal domain the basinward thickening of the stratigraphy indicates a relatively high rate of subsidence. The reflectors indicate is observed agradational and

sub-parallel reflectors (Figures 9.1 and 9.5). These features both indicate a relatively high carbonate productivity which is also supported by the lack of clastics in this area. However, comparatively lower than the subsidence rate. In some buried highs, there is progradation at the margin of the interpreted isolated platform (Figures 9.4 and 9.6). This is followed by an onlapping fill perhaps due to an increase in the rate of subsidence in this distal area. The whole sequence is truncated by a regional unconformity at the base of the Aptian salt, which can be interpreted as a major climate change associated with regional tectonic uplift and regional palaeogeographic rearrangement.

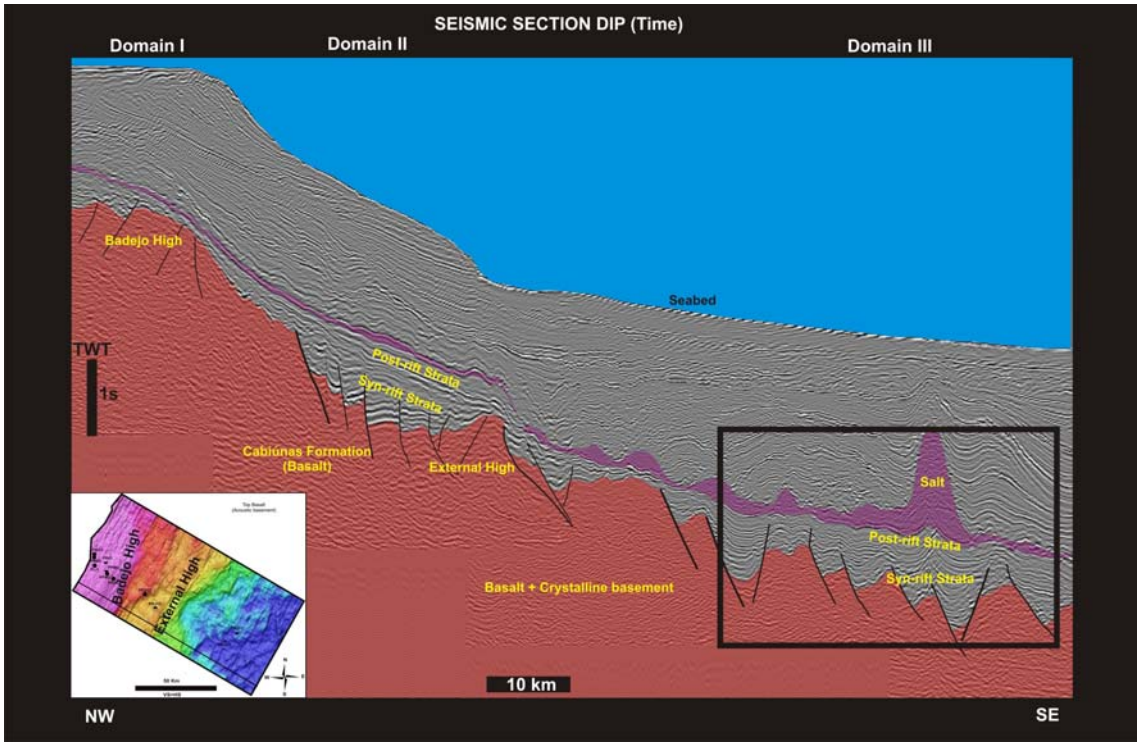

Figure 9.4 – Regional seismic section interpreted in time showing different types of tectonic domains and the main seismo-stratigraphic units. Black box indicates area of Figure 9.5

Figure 9.4 presents a regional seismic dip section showing the main geometric characteristics of the three main domains. The main geometric and seismo-stratigraphic characteristics of the Domain III are indicated. Figure 9.5 shows the internal reflectors within an isolated platform with high-energy, prograding carbonates being onlapped by the Aptian deep basin low energy facies. The prograding carbonate deposits show chaotic seismic-facies whereas the aggradational basin fill sediments shows plane-parallel seismic facies.

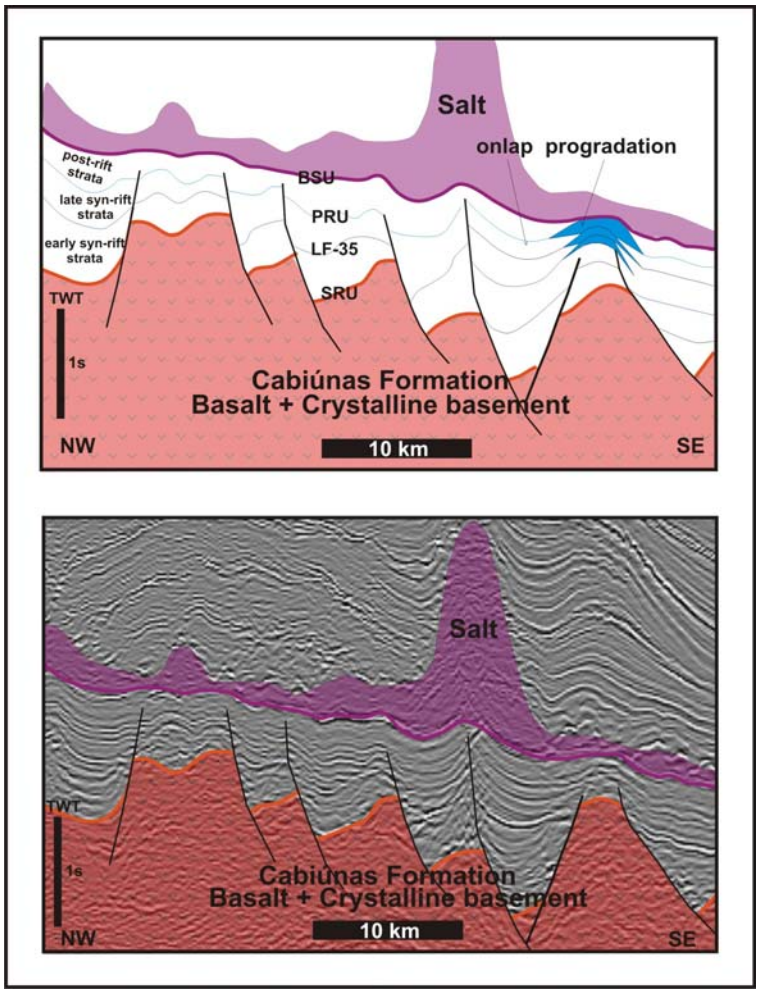

Figure 9.5 – Detail of the isolated platform with Aptian deep basin facies onlapping on high energy prograding (Domain III).

9.4 Discussion and Conclusions

The seismic stratigraphy has been an efficient tool to subdivide and map the key surfaces within the Lagoa Feia Gp and illustrate some relations between accommodation space and sedimentation rates. Also it has enabled the recognition and mapping of key surfaces which limit the depositional sequences, as well as the systems tract. In this way an evolutionary history of the basin fill dynamic may be described, and the main result is possibility of facies prediction.

Figure 9.6 summarizes the entire seismic stratigraphic framework identified in the study area. In Domain I, despite the poor seismic quality, fanning and plane-parallel reflectors are observed. This plane-parallel geometry is interpreted as a balance between accommodation space and sedimentary fill. The carbonate platforms in this domain are located on footwall highs and show progradation into the hangingwall sub-basins.

In Domain II, a configuration of a sub-basin separated by an accommodation zone, creates different geometric arrangements. Over the accommodation zone aggradational reflectors with chaotic seismic facies are observed. This is interpreted as a high energy depositional environment, where the carbonates catch up and aggrade. Up dip from this site, the reflectors are aggradational divergent which may mean differential deposition and compaction of low energy facies. But downdip of the accommodation zone progradational geometry is seen. This progradation relates to high sedimentation rate supplanting the created accommodation space. Some terminations like downlap and erosional truncations are evident.

In distal zones, Domain III, the plane-parallel reflectors indicate potential depositional space and accumulation of low energy, deep subaqueous environment. But, on the relict highs, isolated platform type, the dynamic of the depositional process seems to be different with agradational facies at the top of these highs and progradation in the border of the platform. Carbonate platforms in these locations are founded on interbasinal highs in the accommodation zone.

The limits of main 3rd order sequences, LF-35, PRU and PSU, are also shown in the Figure 9.6. Such seismic horizons bound the Clastic Sequence, the Coquinas and Microbialites sequences that corresponds respectively to tectono-stratigraphic units, early syn-rift, late syn-rift and post-rift.

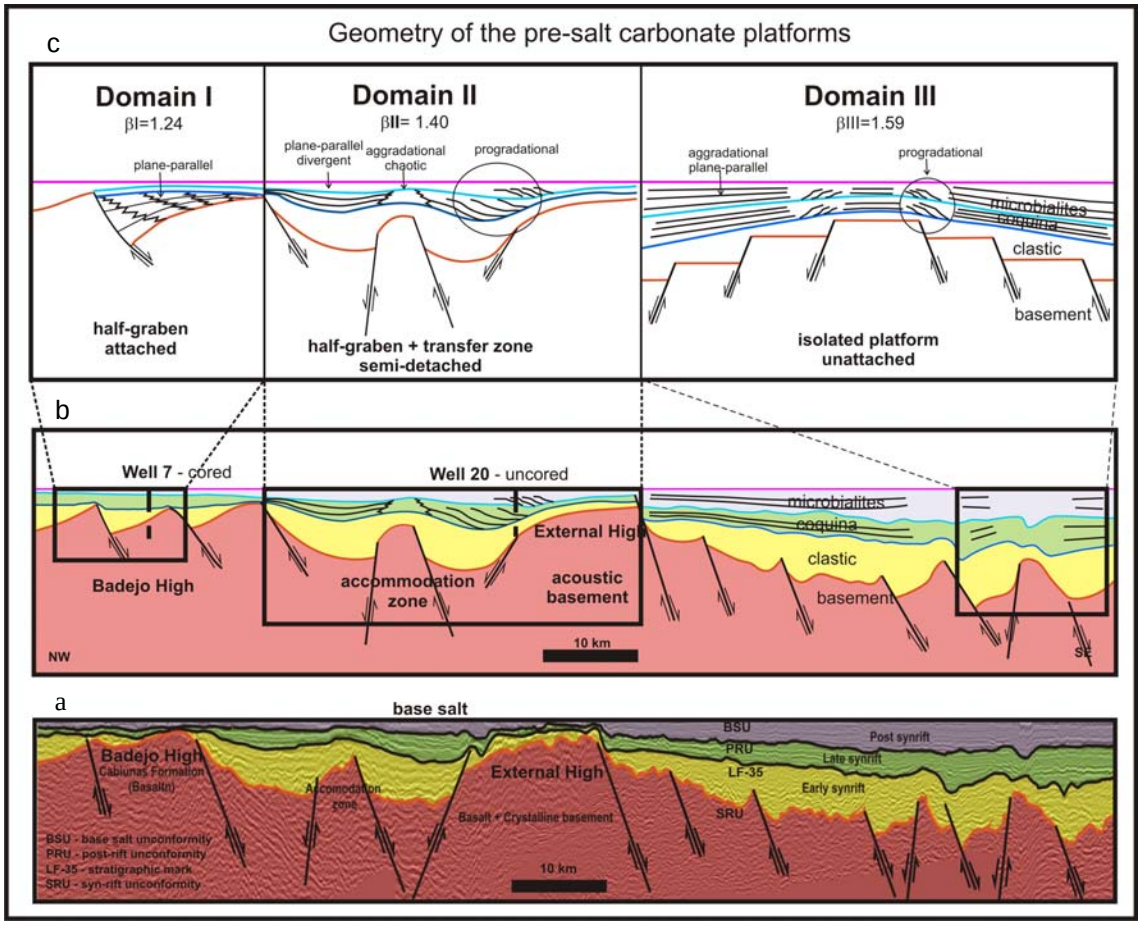

Figure 9.6 – a) Seismic section and flattened on base salt showing the main structural features, the stratigraphic sequences and the key surfaces mapped. b) A cartoons showing the 3 identified domains and the geometric pattern of basin fill in each case. c) Sketches to indicate structural template and interpreted stratigraphic geometries and carbonate platform morphologies interpreted from 3D seismic.

Whilst not cored the stratigraphic geometries here strongly suggest an isolated carbonate platform develops over buried horst blocks. These occur in both the coquina and the microbialite successions and pass basinward into presumed deeper water facies.

CHAPTER 10 - TECTONO – STRATIGRAPHIC MODELS AND DISCUSSION OF MAJOR RESULTS

10.1. Introduction

The study of carbonate platforms in continental rift basins is a complex task due to their diverse evolutionary histories, geometric characteristics and sedimentary fill types and types of carbonate platforms (Chapters 4, 7 and 9). This chapter presents and discusses new tectono-stratigraphic models of the carbonate / siliciclastic sediments of Barremian to Aptian age, for the southern Campos Basin, Brazil. These tectono-stratigraphic models are based on an integration of all well data analysis (Chapters 7 and 8), core analysis (Chapters 5 and 6) and the 3D seismic interpretation (Chapters 4 and 9). It also aims to compare the evolutionary history of the Campos Basin with other similar sedimentary basins around the world, and investigate the hydrological nature of the sub-basins and their possible connectivity.

Based on the initial study of the seismic data (Chapter 4) the southern Campos Basin was divided into three different tectonic domains: I, II and III, with three different structural characteristics, stretching factors (β), subsidence rates and accumulation rates. Domain I was studied using 3D seismic interpretation and well data analysis (core and electrical logs). Domain II by seismic interpretation and FMI log analysis whereas Domain III is only known from seismic. To support and give more credibility to the proposed models, ancient syn-rift successions from the Miocene of the Gulf of Suez, Egypt and also the microbialites of the Jurassic / Cretaceous from the Wessex Basin, Dorset, UK are used as analogues (Appendix C).

10.2. Subsidence history for Domains I and II

The late syn-rift of Domain I (Figures 7.1 and 7.2) is sited in the proximal zone of the basin and is sampled by wells 1 to 9. These penetrate strata up to approximately 200 m thick that accumulated in half-graben with only minimal thickness changes. This syn-rift unit thickens basinward from the well 12, to about 400 m in the area of well 20 position (Domain II). Likewise, the post-rift stratigraphy thickens basinward from 20 to 50 m in the proximal area of Domain I to 100 m thickness in well 7 and 200 m in well 20 in the more offshore Domain II. This is interpreted to be due to differential thermal subsidence and tilting to the east. The main extensional faults stop at the top of the syn-rift sequence, indicating reduction of tectonic activity. However the greater thicknesses

of this succession in well 20 (Domain II) indicates continued stretching and crustal thinning associated with subsidence and accommodation formed by long live faults increased in a basinward direction (Figures 10.1a and 10.1b).

The type of sediment fill, the sedimentary arrangement and geometry of the strata are different in each domain and are detailed and discussed in the chapters 7 and 9.

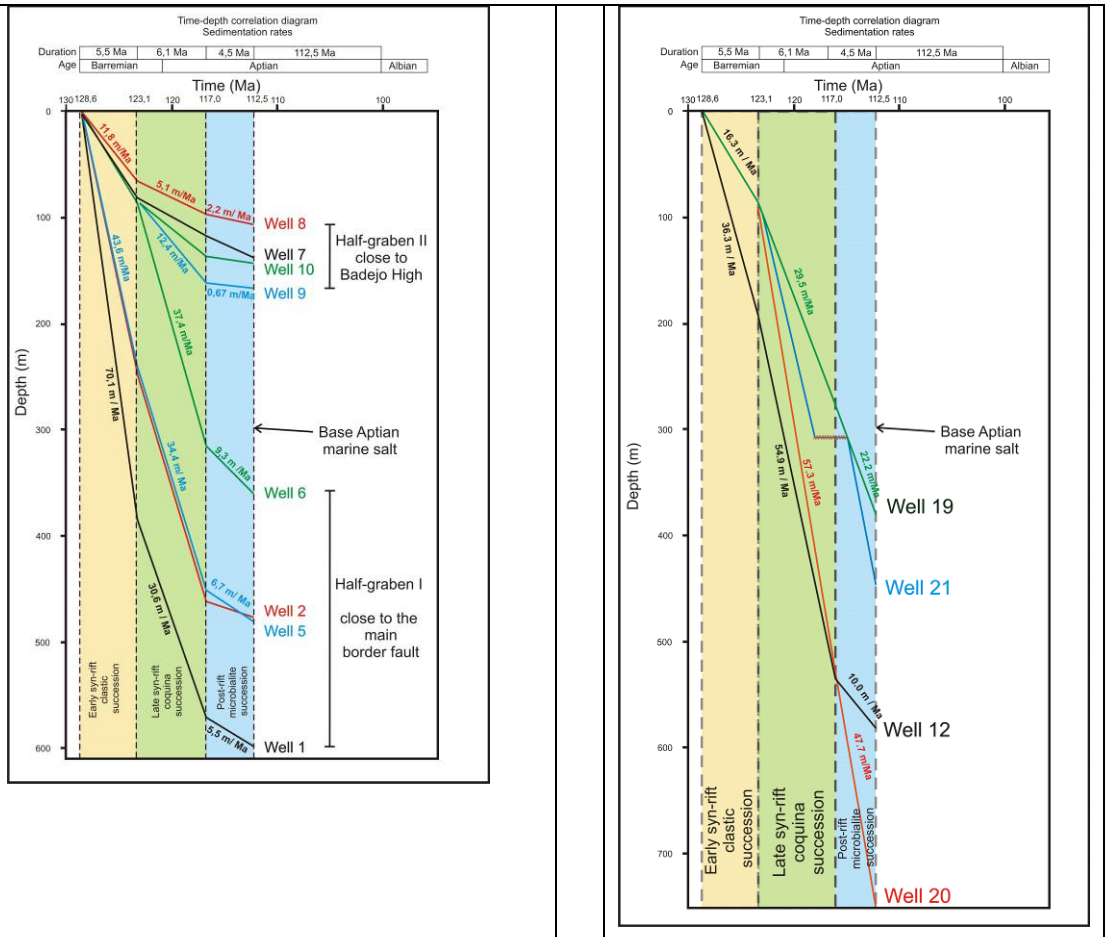

Figure 10.1 Time-depth correlation diagrams showing the subsidence history and accumulation rates in a-left) Domain I and b-right) Domain II (for discussion see text).

The time-depth correlation diagram shown in Figure 10.1a-left, represents the history of the accumulation rates in Domain I. A high subsidence rate is seen in early syn-rift tectonic phase in each of the wells (yellow). However, as the stratigraphy evolves the subsidence rate tends to decrease (late syn-rift green). So, the post-rift phase shows low subsidence rates probably related to thermal subsidence (blue). It is also seen that in the vicinity of the hangingwall areas (wells 1, 2, 5 and 6) the subsidence rate also tends to be greater, while in the vicinity of the foot wall (wells 6, 7, 8 and 10), the

subsidence rate tends to be smaller. This differential subsidence influences the sedimentary history of each particular sub-basin in Domain I.

Almost all the wells traced in Figure 10.1 b-right, that represents Domain II, display a relatively high rate of subsidence, and accumulation rate. Even in the post-rift tectonic phase, the subsidence rates are still high. As explained in chapter 4 the post-rift or sag phase is affected by progressive, basinward reactivation of the rift faults.

10.3. Tectono-stratigraphic model for proximal half-graben – Tectonic Domain I

The sedimentary facies in tectonic Domain I indicates it is close to the siliciclastic supply and is interpreted to be attached to the land. The tectonic setting is a system of several half-graben, asymmetrical, commonly with faults synthetic to the rift border fault. The lateral displacement of the normal faults suggests a crustal stretching β value, of 1.24. These half-graben are filled mainly with sediment from alluvial and deltaic-lacustrine depositional systems (Figure 10.2). In the Barremian this system is predominantly alluvial with progradation of conglomerates and sandstones into the hangingwall basin. The facies suggest proximal alluvial fan systems that evolve basinward to braided fluvial systems and Gilbert type deltas in lacustrine environments (cf. Wright, 1992). Within this dominantly clastic system this bench-type carbonate platforms built up (cf. Wright, 1992). These comprise bioclastic carbonate sediments accumulating in mixed carbonate-siliciclastic beaches, beach ridges, and also mollusc rich subaqueous bioclastic bars and shore face deposits (Chapter 6). These are predominantly sited in the relatively clastic free footwall areas to the fault blocks (Figure 10.2).

In the footwall and hangingwall dip slope a ramp profile (cf. Wright, 1992) carbonate platform is developed with shallow subaqueous banks or bars modified by storms and reworked by waves (see Chapter 6). Large and thick amalgamated packages of bioclastic carbonates accumulated in both shallow high-energy and deeper low energy sites. These shallow, lake margin carbonates were also redeposited into deeper hangingwall positions as calci-turbidites. These carbonate platforms form narrow and elongate geometries along the structural highs and the platform ramp edges (Figure 10.2) and forming bioclastic carbonate accumulations interpreted to be some km in length, wide and up to 150 m thick.

Domain I has two graben systems (1 and 2 in Figure 7.2). The first is more proximal and more influenced by terrigenous sediments. The second one, more distal, is carbonate rich, but with accumulations of terrigenous deposits in the hangingwall, where bioclastic turbidities are found. These are the product of reworking and gravitationally redeposited sediments from adjacent footwall carbonate platforms. Similar depositional systems accumulating in half-graben are widely reported in the literature, but from marine environments e.g., Burchette (1988) and Cross & Bosence (2008) from the Gulf of Suez, and Dorobek (2008) from Southeast Asia. Examples from lacustrine environments are less well known e.g. Cohen & Thouin, (1987) and Soreghan & Cohen (1996) in Lake Tanganyika, Tanzania and Lambiase & Morley (1999) from Lake Turkana, Kenya, As well as being less well known the modern examples of the lacustrine platforms do not appear to be as extensive as those from the Campos Basin.

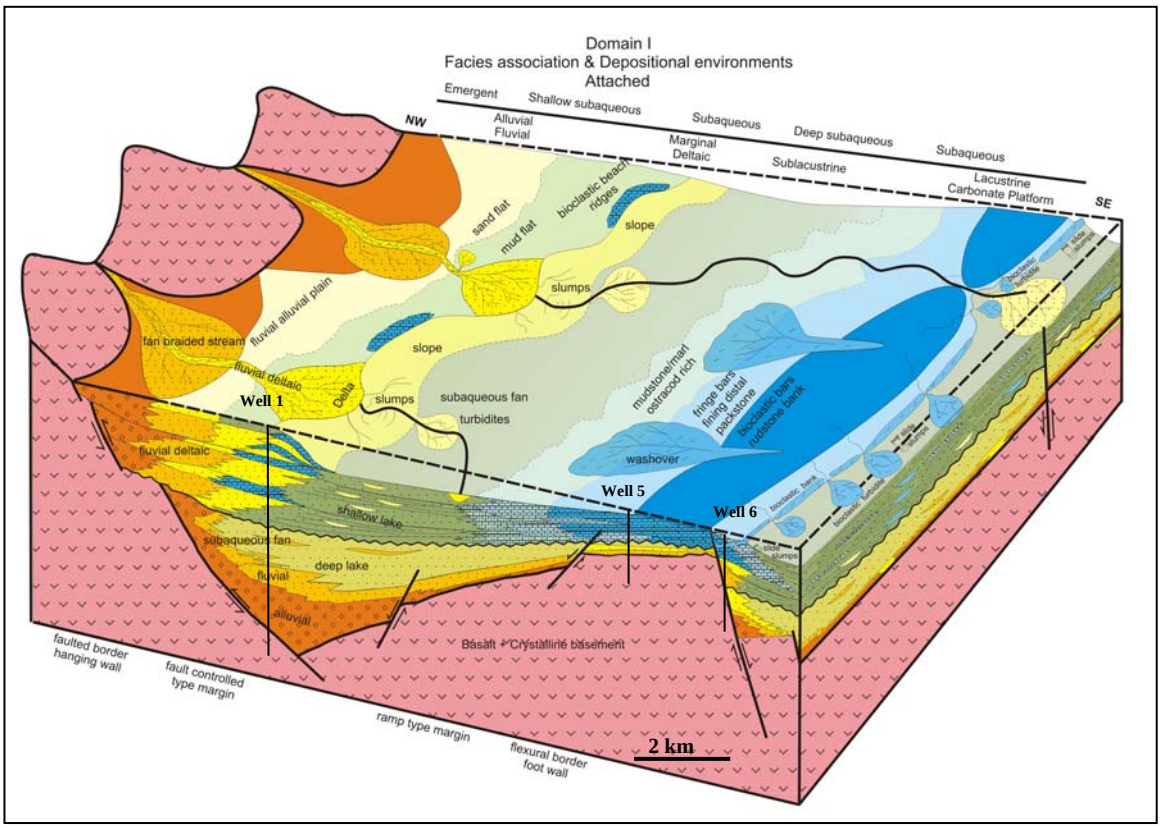

Figure 10.2 - Block diagram showing the structural setting, facies associations and depositional environments for mixed siliciclastic – carbonate sediments of Domain I. Based on wells and seismic data from half-graben I.

10.4 Tectono-stratigraphic model for accommodation zone setting, Tectonic Domain II

The second domain, in the intermediate portion of the basin, is in a more offshore location with differential crustal stretching and estimated overall β values of 1.40. Synthetic and antithetic rotated half-graben occur, separated by accommodation or transfer zones (Figure 10.3). This domain has a complex geometric arrangement of acoustic basement, in a polygonal, or rhombic, style (section 4.4.1.1, Figures 4.11 and 4.12) which has influenced the stratigraphic history.

On the basement high, which is a horst, an accommodation zone, is formed with thick packages of high energy, bioclastic carbonate banks and bars that are deposited in an aggradational arrangement (Figure 10.3). These are seismically chaotic (Figures 9.1 and 9.6). These shallow lacustrine sediments prograding laterally toward the basin. The progradations can be observed at different levels, from large scale, e.g. seismic, but also may be interpreted from the coarsening-upward profiles on a metre scale, on electrical logs and FMI image logs. (Figure 7.17). In the interior of the banks on the horst block the seismic sections show aggradational parallel seismic geometries (Figure 9.6). This seismic facies is interpreted to reflect low energy mud-rich carbonate sediments such as marls, mudstones or even shales.

Domain II is limited to the west by the prominent Badejo High and to the east by the External High, which is a hinge zone (Figure 10.9). The depositional system appears to be isolated from clastic supply and accumulates autochthonous and parautochthonous bioclastic carbonates. These are transported and locally reworked mainly by storm and wave processes as evidenced by the commonly occurring, high energy, shallow lacustrine rudstone facies. Hundreds metres of Barremian bioclastic carbonates accumulated in sub-basins with large amounts of accommodation space (Figure 10.1 b). In this context, bioclastic sediments commonly accumulated in the progradational sets in the area of well 20. The productivity of these molluscan carbonate communities appears to have exceeded the accommodation space maintaining keep-up and progradational, shallow facies, locally exhibiting subaerial exposure.

No similar configuration of tectonic template and thick lacustrine carbonate deposits have been found in the literature. This appears to be a new occurrence, and a new type of lacustrine carbonate platform for the continental rift environment. Miocene carbonate platforms in the Gulf of Suez rift, however, show the aggradational and progradational accumulation of carbonates in the transfer zone in the Wadi Kharaza area

of Abu Shaar (Appendix C; Cross & Bosence, 2008). In the southern tip to Abu Shaar the accommodation zone accumulates up to 200 m of shallow marine and slope facies carbonates that prograde to the south into the accommodation zone. Many descriptions of accommodation zone in the literature are cited as zones of terrigenous sediment accumulation, where they act as bypass zones, developing a drainage system or a transport pathway between sub-basins in rift systems.

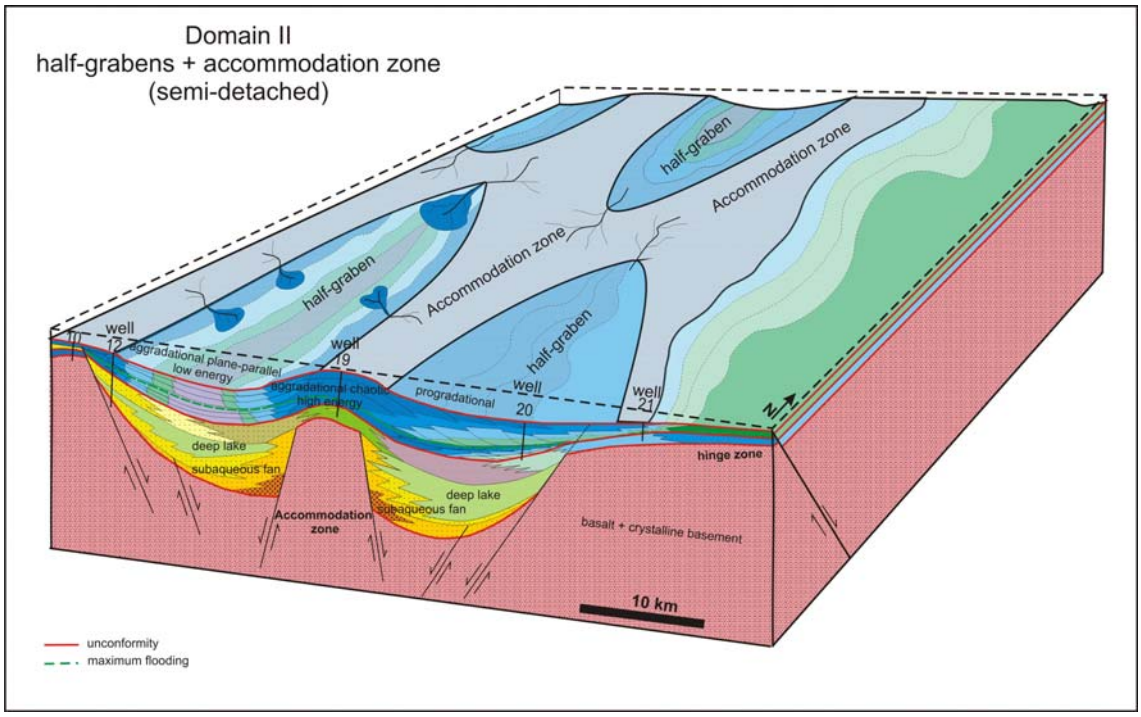

Figure 10.3 – Block diagram showing the Domain II tectono-stratigraphic model. Carbonate platform forming on an accommodation zone (horst block) with an aggradational build-up and basinward progradation. Model based on 3D seismic interpretation (Figure 9.6a), sidewall core analysis and FMI interpretation in the well 20 (Figure 7.17), with support of rift total thickness map (Figure 4.26).

10.5 Tectono-stratigraphic model for **unattached carbonate platform** *in offshore – Tectonic Domain III*

This tectonic domain is located in the distal portion of the basin and is formed from the linkage of several half-graben which results in a large symmetrical graben area with an estimated stretch factor (β) of around 1.59. This value is matched by a considerable thickening of the Early Cretaceous strata in response to a high rate of subsidence. Relict horsts formed morphological highs and that acted as the basement for isolated platforms (Figure 10.4). These carbonate platforms developed aggradational and progradational seismic geometries of presumed high energy, progradational bioclastic molluscan and also possibly microbialite facies on the margins of the highs.

Seismic lines show progradation of platform carbonates with lenticular / sigmoidal geometries into deeper basinal areas and these are onlapped by deep basinal sediments with aggradational parallel reflectors (Figure 9.5). On the platform top aggradational and also chaotic seismic facies are seen (Figure 9.6).

No similar carbonate platforms of this scale have been found in the literature on lacustrine environments. However, counterparts are very well known from the marine environment, such as the isolated platforms of the Tengiz oil field (Harris, 2008) and Bahamas (Eberli *et al.* 2002). Surprisingly, the geometries of the two systems are rather similar despite the major differences in facies and environments.

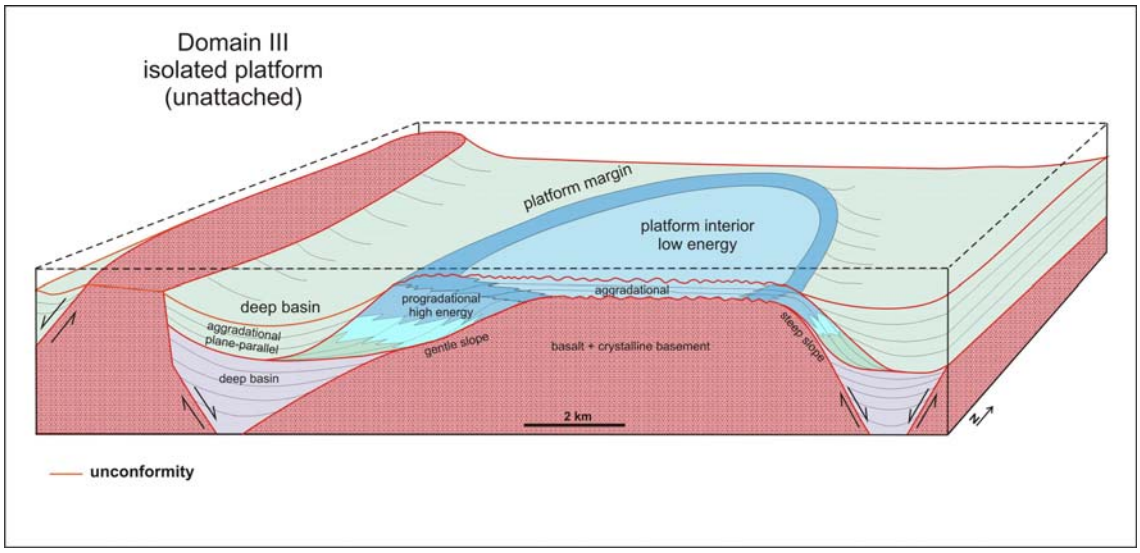

Figure 10.4 – Block diagram showing a Domain III isolated carbonate platform. In this tectonic context, a carbonate platform is formed over the relict horst, showing progradation of the platform margins that are subsequently onlapped by deeper water sediments basinward. This model is based purely on seismic interpretations.

10.6 Discussion of major findings of research

10.6.1 Tectono-stratigraphic setting

The continental rifting occurred during the Neocomian and Aptian in the South Atlantic. This event separated South America from the African continent in an extensional oblique rifting regime (Chapter 4). This process resulted in a complex framework of basins and sub-basins with varying degrees of crustal stretching and consequent subsidence (Davison, 1999). Various authors have proposed different levels of rift evolution related to the stretching of continental crust. Karner & Gamboa (2007), for example, postulate depth-dependent crustal extension causing rift and post-rift (pre-salt sag) basin formation that created space for the deposition of thick evaporite strata in

the Aptian of the South Atlantic salt basins. In this sense, the rate of lower crustal extension (Karner *et al.* 2003) determines the basin accommodation and subsidence. Moreover, extensional, long-live faulting occurs progressively from west to the east, (i.e. basinward) in the Brazilian margin, with some faults reaching the base of the evaporites (Figure 9.6). Manatchal *et al.* (2010) and Magnavita *et al.* (2010) assume differentiation of the continental crust underlying the South Atlantic passive margin basins. Based on deep seismic profiles they have interpreted layers within the crust that are: deformed, stretched, super-stretched and with exhumed mantle toward to the areas of thinner crust. Ranero & Perez-Gussinyé (2010) compared crustal thinning with measured fault extension, using depth-migrated seismic images. They modeled the kinematics of the sequential faulting to explain the asymmetry of the conjugate margins and extension discrepancy. The short-live faulting gives place to long-live faulting system toward the rift axis.

In the Campos Basin, work presented in Chapter 4 shows that different stretching factors and subsidence rates are found in the pre-salt settings on a basinal scale. These were termed in Chapter 4: Domain I, Domain II and Domain III. A simple calculation of β values was obtained from the lateral displacement of the extensional faults. Although imprecise, due to the fact that this technique does not take into account sub-seismic faults, these values support the hypothesis of the progressive basinward development of the rift. In addition the more offshore areas are more likely to have long-lived fault systems in the late syn-rift and post-rift stages due to the thinning of the crust and eastward tilting. Added to the thermal subsidence, these faults provided large amounts of accommodation space in an area far from the clastic supply for the accumulation of thick packages of carbonate strata as carbonate platforms.

The passive margin basins of the South Atlantic appear to be a unique setting in the Earth's in geological history and in its recent deposits. They appear to have no analogue due to their large dimensions and apparently unique sedimentological and palaeoecological characteristics. Analogue studies do, however help with an understanding of geometries. The Gulf of Suez (Appendix C), despite being a marine rift, of smaller size and not developing and oceanic crust, has significant similarities, which have proved useful for understanding the development of rifting and carbonate platform geometries and evolution in the Campos Basin. Cross & Bosence, (2008) have studied the fault block carbonate platform of Abu Shaar mapping out tectono-sedimentological relationships, facies associations and 3D morphology. Other authors

have studied the structural settings of the Miocene carbonates of the Gulf of Suez (Colletta *et al.* 1988; Bosworth, 1995; Garfunkel & Bartoe, 1977, Patton *et al.* 1994; Stickler *et al.* 1977; Steckler *et al.* 1988). These and other studies have demonstrated the well-preserved geometries (Purser *et al*. 1993, Cross *et al.* 1996, Young *et al*. 2003) (Appendix C) that have been used as analogues for the construction of the tectono-stratigraphic models above. In these studies it was noted that the rotated fault blocks are bounded by northwest-southeast trending extensional faults and fault-blocks. Overlying these basement fault-blocks are firstly a mixed carbonate – clastic succession and then a fault – block carbonate platform (James *et al*. 1988; Burchette, 1988; Evans 1988; Richardson & Arthur, 1988, Bosworth *et al.* 1998, Purser *et al.* 1998; Cross, 1998).

Bosence (2005) and Cross & Bosence (2008) have established new tectono-sedimentary models for the Gulf of Suez marine rift basin carbonate systems. Syn-tectonic and post-tectonic carbonate platforms can be discriminated and also carbonate successions occupying transfer zones. During the main rift phase, with active faulting and strong subsidence, clastic deposition dominates along the basin margins. In these settings, high rates of clastic supply contrast with lower rates of carbonate production in continental and marginal marine environments. However, in the late syn-rift phase (Serravalian), fault-driven subsidence slowed down, and with less fault-block rotation, footwall highs, isolated from clastic supply, provided good shallow-marine conditions for the development of fault-block carbonate platforms like Abu Shaar (Appendix C).

Similarly, the rifting process in the Campos Basin developed an oblique, extensional fault system, forming rotated blocks in a domino style (Figure C.2 Appendix C). Like the Gulf of Suez, the early tectonically active period of rifting is largely dominated by siliciclastic supply, mainly in the proximal areas, Domain I (Figure 10.2). In this period, uplift in the uplifted source area resulted in a development of drainage systems that, associated with a humid climate setting, carried terrigenous sediments into the rift basin. The deposition of large packages of carbonate sediments is commonly associated with tectonic quiescent and dry climates (Carroll & Bohacs 1999). In both of these two rift systems carbonate platforms are limited to the topographical highs, with shallow-water conditions, with little terrigenous influence.

However, the Gulf of Suez, which is a short live or aborted rift does not show any equivalents of the platforms developed in Domains II or III. Rifting developed to a more mature phase in the Campos Basin with intermediate sites (Domain II) that developed a complex polygonal or trapezoidal plan geometry forming a series of half-

graben with synthetic and antithetic faults (Fig. 10.3). This configuration of sub-basins with intervening transfer or accommodation zone, results in carbonate rocks deposited in an aggradational arrangement on interbasinal highs, and progradation into adjacent sub-basins (Figure 10.3). Equivalent areas are not known in the Gulf of Suez.

Far from the basin margins, in offshore sites, the rift has evolved into linked half-graben, producing a large graben, with relict of topographic highs in what appears to be an open-water high-energy lacustrine environment (Figure 10.4). High energy molluscan rudstones are thought to have formed on the margins of this prominent structure, arranged in aggradational and progradational geometries (Figure 10.4). The slopes of this unattached platform prograded into surrounding basins where they were subsequently onlapped by deep lake sediments. Thus the carbonate platforms in the southern Campos Basin developed progressively towards offshore clastic free areas with high bioproductivity. These areas were associated with development of large amounts of accommodation from extensional faulting, thermal subsidence and sediment-water loading. The combination of these two factors is considered to be the main reason why such large and previously unknown types of lacustrine carbonate platform could develop. The size of the lake is unknown from current data but seismic lines through the study area suggest it was at least 100 km in width and an unknown length within the study area (Figure 4.27).

Both of these occurrences in Domains II and III appear to be unique and the author has not been able to find similar structures in the published literature on lacustrine environments. These carbonate platforms form reservoirs that are of great economic interest and are considered as a new exploratory frontier in the petroleum industry.

10.6.2 Climate and Hydrological settings

The Early Cretaceous was marked by a mild "Ice House" world (Figure 10.5). During the winter seasons, snow and ice were quite common and the temperate forests covered the low latitude regions. However, in the Gondwana supercontinent, high latitude in the south hemisphere, the arid, dry and warm climate predominated during Barremian and Aptian ages (http://www.scotese.com/ecretcli.htm). This characteristics climate created ideal conditions for the carbonate rocks formation.

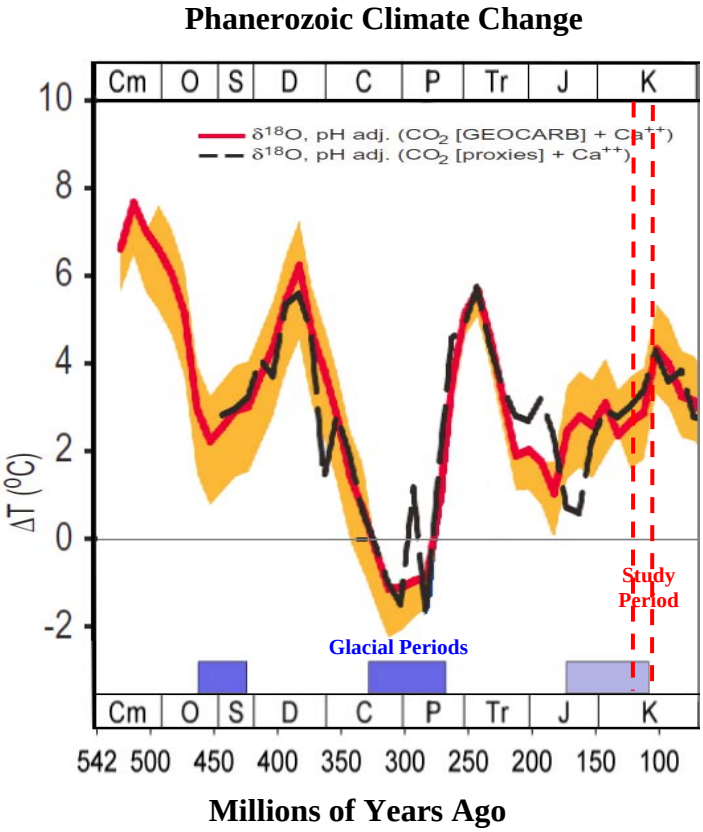

Figure 10.5 – Phanerozoic climate change (from Ron Blakey, NAU Geology, http://en.wikipedia.org/wiki/File:Blakey_90moll.jpg , http://en.wikipedia.org/wiki/Palaeoclimatology).

The long-term climate changes can be shaped by plate tectonics. This hypothesis arises from the relatively warm that occurred associated with the breakup of supercontinents during the Cretaceous (Figure 10.5).

Another factor to be considered in the evolution of pre-salt rift systems in the Campos Basin is the palaeohydrological conditions of the lake or lakes; whether these are hydrologically open or closed systems. These conditions exert a considerable control on the water circulation pattern and the resultant sedimentary fill of lakes (Talbot & Allen, 1987). Silva Telles (1992) addressed the palaeohydrological conditions of the Lagoa Feia palaeolake through the analyses of stable isotope values of $\delta^{13}C$ and $\delta^{18}O$ in Barremian sediments of the Campos Basin. Well 5 is located 2 km westward from well 6 (Figure 8.25) and the results from whole rock analysis of core samples is given in Figure 10.6. An interpretation is made by Silva Telles (1992) based on the Talbot (1990) model, where a positive correlation index between $\delta^{13}C$ and $\delta^{18}O$ indicates a hydrological closed lake phase. This is seen in the upper third of the core from well 5 (Fig. 10.5) According to Talbot's model under these conditions the influx

of fresh water will carry large amounts of nutrients into the lacustrine basin, resulting in an increase in biodiversity of primary photosynthetic organisms, increasing values of $\delta^{13}C$. However Valero-Guace *et al.* (1995), studying the covariance of isotopes in fresh water lake intakes, suggested that this relates to the stratification of producing primary biota. They associated the positive shift of $\delta^{13}C$ to the change of type of primary producing organisms, and not the increase in input of nutrients into the lake.

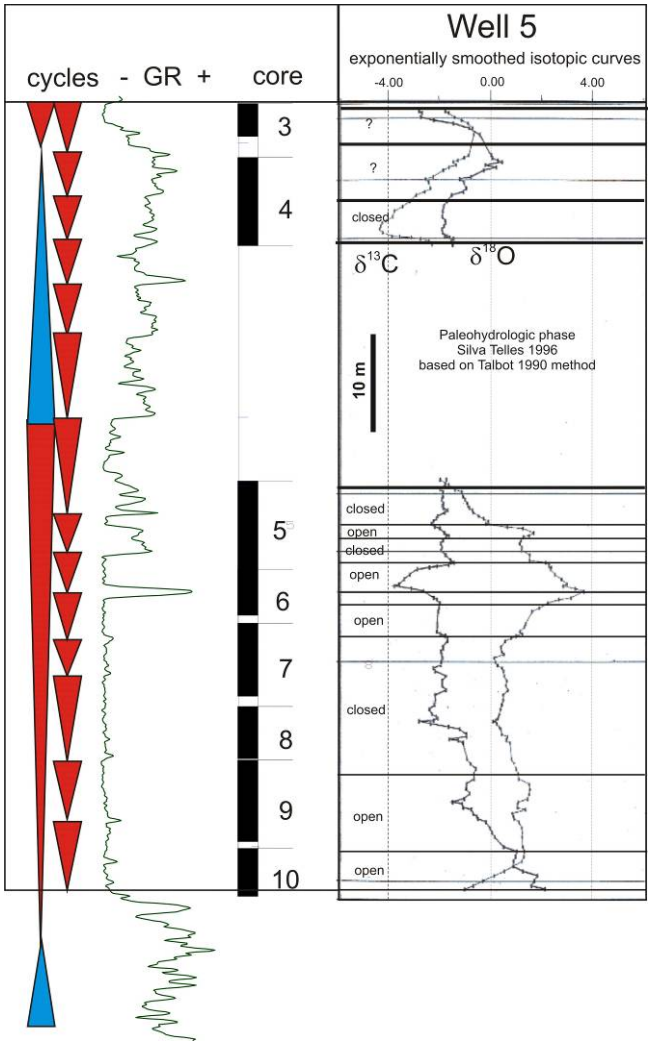

Figure 10.6 – Exponentially smoothed isotopic curves of $\delta^{13}C$ and $\delta^{18}O$ for well 5 in study area – Barremian late syn-rift coquina succession (Silva Telles, 1996) plotted against cycles interpreted in this study from gamma ray log.

Based on descriptive analyses of cores and thin sections and also of Gamma Ray logs, a marked cyclicity in drilled wells in Domain I is seen in the southern Campos Basin pre-salt interval (Figure 8.25). This cyclicity may be related to the third order cycles linked to climatic variations (Chapter 8 section 3) with more humid periods indicated by increased gamma values. In the model proposed by Silva-Telles, (1992) one shift to more open lake conditions is suggested whereas this research suggests a

number of alternations of more humid and more arid periods (Figure 8.25). Humid phases are correlated with the input of freshwater into the lake and more open lake conditions with influx of terrigenous sediments and associated with low carbonate productivity.

The analysis of cores and wireline data in Chapter 8 indicate correlatable 3rd order cycles through Domains I and II with clean carbonate rich, regressive arid phases and more terrigenous (higher gamma) transgressive humid phases. The humid phases would be characterised by more turbid water with increased nutrients and these waters would be less conducive to the development of extensive filter feeding communities of bivalve molluscs, may inhibit the primary productivity of photosynthetic organisms by making the lacustrine water more turbid near the river mouth and delta (fluvial deltaic system). Besides, the predator organisms such as fish, live close to the mouth of these rivers (Carvalho, 2005). However, in the more arid periods, the cleaner waters seem to have favoured higher carbonate productivity from the filter feeding bivalve communities.

These limiting factors appear to be differentiated along a basinward direction as there is an increase of carbonates in offshore areas. There are also more aggradational and progradational carbonate geometries in wells 12 and 20 which also show thicker successions. This suggests that carbonate production is not a limiting factor and that production rates in these cleaner offshore waters could always, either keep-up, or outpace subsidence rates. Whilst the production profile of these mollusc dominated skeletal carbonates is not known the evidence from sediment textures and facies (Chapter 5) suggests that production was highest in shallow waters and is most similar to the shallow marine photozoan system (cf. Schlager, 2005).

Carroll & Bohacs (1999) proposed a balance between tectonic and climatic controls to the occurrence, distribution and characteristics of lake sediments. They classify lake stratigraphy according the balance of these rates in overfilled, balanced fill or underfilled lake basins. Overfilled lake basins refer to where the influx rate of water and sediment fills and exceeds accommodation space. In these circumstances fluvial-lacustrine facies dominate the basin fill. Balanced fill lake basins, are where the accommodation approximately equals water and sediment fill. Profundal facies dominate the basin fill. Underfilled lake basins are where there is more accommodation than sediment supply. They attribute the overfilled lake basin to the hydrological conditions of open lakes and relatively stable depositional environments. While a

balanced fill and underfilled lake basin have rapidly fluctuating lake levels resulting in rapidly changing in depositional palaeoenvironments, even at the parasequence scale.

The sedimentological and palaeontological information in the Lagoa Feia Group indicate some major up-section changes in lake hydrology and chemistry (Figure 10.7). Biochronozone A is ostracod-rich and associate with stevensite (Chapter 6, section 6.4.2) represent alkaline water environments (Figure 10.7). The lower part of Coqueiros Formation carbonates and clastics (Biochronozone B) contain variable amounts of the mineral stevensite that is known from alkali lakes (Chapters 5 and 6). Apart from this mineral no other evaporite minerals are seen and, together with the preserved bivalve genera and rare occurrence of charophytes (Chapter 5), indicate brackish, alkali lake conditions (Figure 10.7) for the accumulation of the coquinas. At the top of the late syn-rift in biochronozone D the bivalves are replaced by gastropod-rich horizons. These have been attributed to an increase in the salinity of the environment by Silva Telles (1996) and Hessel & Mello (1987) as discussed in Chapter 5. Finally the post-rift strata have no abundant metazoan communities but are replaced by microbialites (Figure 10.7). The clastic facies suggest fresh water fluvial – lacustrine settings but some unknown environmental parameter is excluding metazoans. There are no clear indications in the sediments of what this may be.

10.6.3 Phases of evolution in Campos Basin

In Chapter 4 it was shown that initially the rift system was a series of individual sub-basins in the early syn-rift during the Hauterivian (see total isopach map of the rift, Figures 4.25 and 4.26). Strong activity of faults formed accommodation space for thick successions of terrigenous sediments (Figures 7.1 and 7.2). After this period, in the late syn-rift (Figure 8.25) the rift changes to a more connected basin with a number of depocentres and sub-environments varying from conditions of open to closed lakes. This is shown by the correlation of Level 2 cycles throughout the late syn-rift and post-rift (Figure 8.25). Humid periods, for example, are manifested by an increase of terrigenous sediment which is expressed by the widely distributed high Gamma Ray curve values (Figure 8.25 biochronozones A and C). More arid periods are characterised by cleaner carbonates and less terrigenous supply. But in the latest stage of the late syn-rift (Figure 8.25, biochronozone D) the widespread occurrence of gastropods and decreasing occurrence of bivalves suggests an environmental change occurred that was a precurser to the post-rift unconformity and facies changes into biochronozone E.

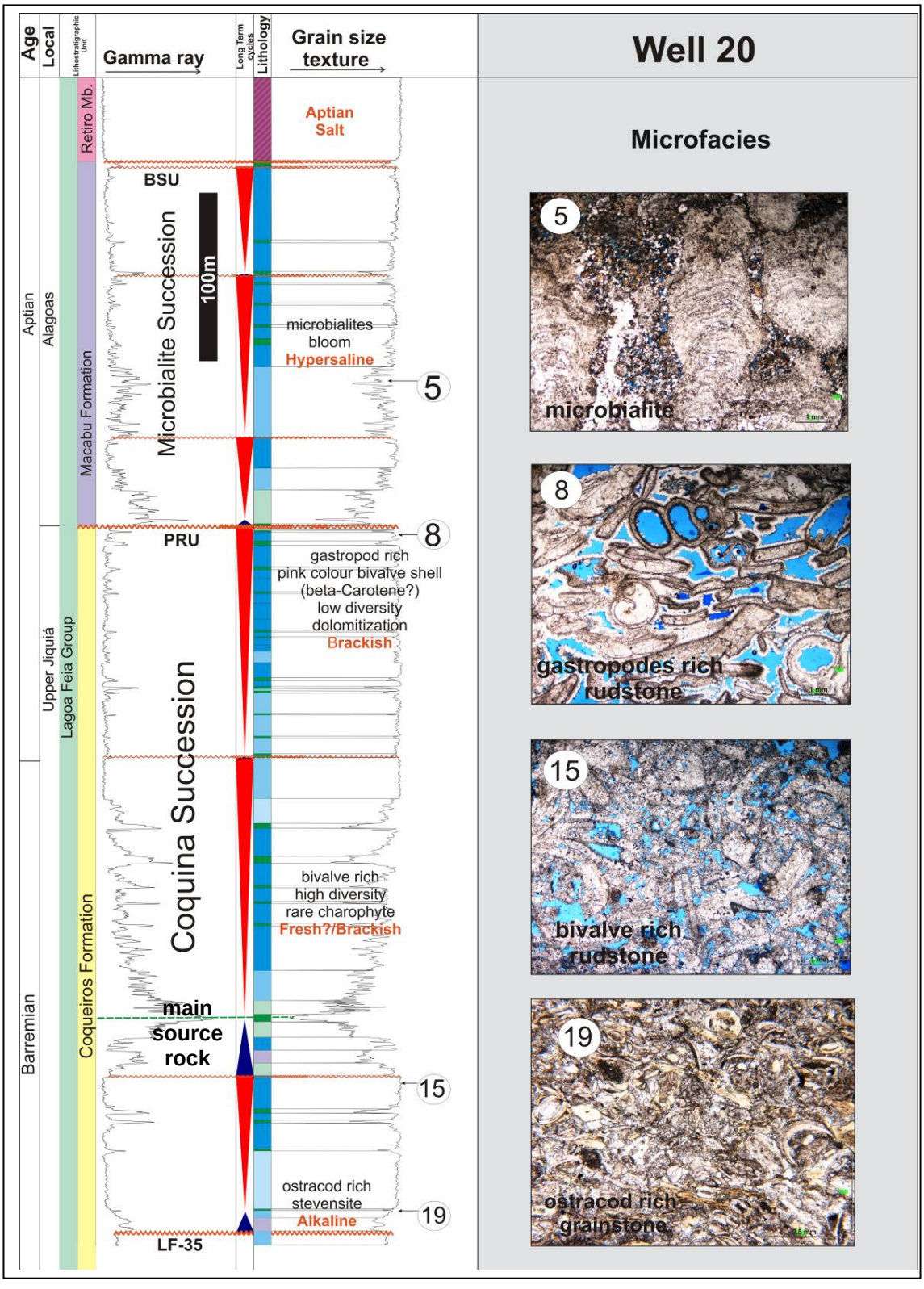

Figure 10.7 – Summary of evolution of the pre-salt palaeoenvironments (well 20). Late syn-rift coquina succession, alkaline to brackish water. Post-rift, microbialite sag phase, brackish to hypersaline. All the successions are capped by the Aptian marine-sourced salt.

To conclude, the rift probably evolved from a series of mini basins to a single big lake, intercalating periods of closed lake to open lake according to the balance of climate, sediment supply and tectonically generated accommodation space. Following the active continental rifting is a phase of post-rift, thermal subsidence and active long-live fault systems in more basinward areas which evolved to the open marine, drift phase and formation of the passive margin basins and the South Atlantic.

The sedimentology the Lagoa Feia Group would be expected to show some reflection of these different tectonic phases of rift evolution. It has already been mentioned above that the early syn-rift is dominated by continental clastics. The late syn-rift equates to the coquina succession of Barremian age and the post-rift is dominated by clastics and microbialite successions in the Macabu Fm of Aptian age. The sedimentological and fossil record is of an entirely non-marine, endemic biota. These successions were deposited in a continental palaeolake of large dimensions that made it unique in the geological record.

However, some similarities may exist with modern and ancient examples (e.g. Shark Bay and Green River Formation). It is tempting to correlate the association of coquinas and microbialites in the Campos Basin with that of Shark Bay. However, the occurrence of coquina in the Barremian of the Campos Basin, differs significantly from that in modern shelly deposits of Shark Bay, one of the best known examples for thick accumulations of bivalves, but from a restricted marine environment (Jahnert, 2012). Most of the coquina in Shark Bay occurs in beach or bank deposits, formed by waves and tidal currents (Davies, 1970a) but in a restricted marine setting rather than a brackish lake. The marine bivalve shells live in the deepest subtidal part of the lagoon. After death, they float and are transported by wind or tide currents to the coast, were they are reworked by waves to form banks and beaches. The adjacent microbialites of Shark Bay are able to proliferate in intertidal and subtidal conditions, in shallower water environment, due to the absence of grazers (Jahnert, 2012). So, in this specific occurrence the bivalves and microbialites are contemporaneous communities, living within the bay in conditions of increased marine salinity, and accumulating in adjacent palaeogeographic sites (Davies, 1970a). By contrast, in the Campos Basin, there is no evidence of marine conditions and fresh to brackish waters are interpreted and there are few geological records of the microbialite carbonates being preserved adjacent to or interbedded with the Barremian coquina succession. There is a clear temporal differentiation between the syn-rift coquinas and the post-rift microbialites. These are

separated by an important regional hiatus, the post-rift unconformity. Clearly a major environmental change occurs that leads to the extinction of the bivalve communities and an increase in microbial activity in the strata above the post rift unconformity (Figures 7.14 to 7.16).

The thin sections of the stromatolites indicate preserved algal or cyanobacterial filaments and therefore suggests that they are biotically induced structures (*sensu* Della Porta, 2012). However these are not diagnostic for different environments. The associated sediments in more proximal areas are coarse alluvial fans and reworked stromatolite intraclasts in fluvial sands and conglomerates suggests a proximal fluvial environment for the microbialites passing to shallow lacustrine environment in Domain II (well 20) (Chapter 5). However, outstanding questions remain as to why no charophytes are seen in the microbialites?

10.7 Conclusions

The major conclusions of this chapter and of the thesis are:

- The stratigraphic fill of the southern Campos Basin rift basin is strongly affected by increasing subsidence rates from rift border Domain I, through intermediate Domain II to be basinal Domain II.
- Each domain has different tectonic framework that has acted as a major control on the nature of the basin fill so that tectono-stratigraphic models can be erected for each domain.
- Domain I is characterised by half-graben basin fills. Hangingwall sub-basins are characterised by siliciclastic supplied from the rift margin whilst footwall areas develop carbonate platforms dissected by basinward dipping faults.
- Domain II is more carbonate rich and a fault accommodation zone with an interbasinal high form the template for aggrading and prograding carbonate platforms. Basinal facies accumulate in deeper areas.
- Domain III is only known from seismic data where relic, buried horsts provide highs for the accumulation of unattached carbonate platforms that prograde into basin areas.
- Comparisons with the Cenozoic Gulf of Suez rift indicate a number of similarities in basin evolution despite the marine nature of this younger marine rift. Similarities include the clastic dominated early syn-rift and carbonate

dominated late rift phases and the control of sediment accumulation in rotated fault blocks and fault transfer zones. However the Campos Basin develops into a larger lacustrine system with more pure carbonate facies and unattached offshore platforms.

- A review of the evidence for the hydrological conditions within the Lagoa Feia palaeolake combines evidence from this thesis and from the literature and concludes that it alternates from three low-order (Level 2) T-R cycles of humid (T) to arid (R) phases that are expressed as clastic- rich and carbonate rich respectively.
- Major up section changes in the evolution of the lacustrine environments are shown for the syn-rift Coqueiros Fm to be an early alkali lake phase replaced by brackish waters when the main coquinas accumulate to a possible marine influenced interval at the top of the syn-rift. The post-rift Macabu Formation is characterised by fluvial to hypersaline environments prior to the marine sourced evaporites of the Aptian related to the initial stages of marine flooding in the south Atlantic.

CHAPTER 11 – CONCLUSIONS

11.1 Introduction

The present study proposes to answer questions that still exist for tectonic and stratigraphic context in the continental rift settings, and contribute with new finds to the sparse literature on this subject. The research focused on the tectono-stratigraphic analysis for the extensional rifting settings. This is a multidisciplinary and integrated study including 3D seismic data interpretation, sedimentological studies and taphofacies of molluscs analysis, aiming the tectono-stratigraphic model. Moreover, the electric and FMI image logs analysis allowed a detailed stratigraphic and cyclicity analysis. Thus this integrated and multidisciplinary study was a landmark in this project because it supports the holistic understanding of the dynamics of such complex environment, as the pre-salt Lagoa Feia Group are; where several factors such as climate, tectonics, sediment delivery among others highest frequency local factors, working together or separately to form the geologic record. In such a way, all the scientific questions and hypotheses of this research were answered and are summarised in the following topics.

11.2 – Regional geology and background for the research

- Three main evolutionary stages were created as a result of the break up of the Gondwana: continental rifting, gulf or proto-oceanic stage and finally marine stage. The focus of this project, however, is on carbonate platforms formed in the continental lacustrine environment, in the Campos Basin, Brazil. The interval of study comprises the carbonate rocks of the Coqueiros and Macabu Formations, bounded by the stratigraphic marker LF-35 and the base salt unconformity (BSU).
- Few publications are known on non-marine carbonate platforms, especially these formed in rift basins. The background for this research however, are published lithostratigraphic and biochronostratigraphic frameworks, the tectonic settings and structural patterns in the Campos Basin. The depositional sequences previously defined by its sequence boundary in the Barremian to Aptian intervals are used as well.

11.3 – Structural and tectonic review

- Considering the tectonic and structural complexity of the study area, a review of standard models for the extensional basin types and the structures within rift basins, forms a basis for an understanding of the overall context and the structures seen in seismic sections. Such tectonic and structural concepts were largely applied in the models constructions.

11.4 – Structural and tectonic models for the Barremian Aptian of the southern of the Campos Basin.

- As a result of the seismic data interpretation and analysis of the maps, the rifting system was defined as extensional oblique of NE-SW direction and the overall tectonic regime as late syn-rift for the Barremian sequence and post-rift for the Aptian. In this tectonic context, Major and minor structural elements were identified: synthetic and antithetic normal faults, border faults, half-graben, host, hinge zones, faulted and rotated block (domino style). These structural elements compose geometries like syn-rift depocentres, accommodation zones and also erosional areas.
- The geometry and structural patterns identified allowed the individualization of three different types of carbonate platforms controlled by tectonic setting, named: Domain I, Domain II, and Domain III. Each domain has specific stretching factor and subsidence rate and developed an individual geometry and evolutionary history during the rifting process.
- Domain I - Classical rift – developed smaller half-graben with straight normal border faults with great contribution of siliciclastic sediments.
- Domain II - Polygonal framework – developed a polygonal arrangement of half-graben which border faults having synthetic and antithetic behaviour forming an accommodation with the carbonate platform being aggradational over the topographic highs and progrades into the depocentres.
- Domain III - the most evolved area, basinward, show a large graben, product of linked half-graben. Isolated platform is formed as relict of the horsts.

- The proximal individual rifts are more asymmetric, tending to the symmetry basinward, due to evolutionary stage of the rifting process. The base of post-rift succession is strongly marked by a regional unconformity with subsequent thermal subsidence and formation of an Aptian sag basin. However, basinward the long-live syn-rift faults is superimposed on sag succession.
- The seismic interpretation was effective to generate a 3D structural and tectonic model. This model is used for the understanding of the continental rifting evolution, the palaeogeography and palaeoenvironment and as a framework for the generation of a 3D facies model within the pre-salt rift environment.

11.5 – Core based sedimentology.

This chapter includes results of the main facies that are seen in the cored intervals of the Coqueiros Formation of the Lagoa Feia Group. The main findings are:

- The Coqueiros Fm comprises mixed carbonate and clastic lithologies and is best classified by a combination of the Dunham (1962) and Embry and Klovan (1971) scheme for carbonates, further subdivided on the basis of composition and amount of matrix, the Wentworth scheme for siliciclastic and an informal scheme for various deformed and diagenetically altered facies.
- 13 main carbonate facies are described, illustrated from split cores and thin sections and their depositional environments briefly discussed. The most abundant facies are bivalve-rich rudstones or coquinas, with 6 subfacies.
- Similarly, 7 siliciclastic facies and 4 deformed and diagenetically altered facies are considered.
- The facies are then discussed in more detail in terms of their associations and depositional setting within the Lagoa Feia lacustrine basins and the following facies associations are described: Alluvial Fan and Plain FA, Deltaic and Delta Margin FA, Deep Lacustrine FA and Lacustrine Carbonate Platform FA.

- A facies model is presented for these rocks based on their interpreted depositional environments and the association of the facies in vertical cored intervals. This is presented as a shore to basin cross section from emergent siliciclastic facies, through Lake Margin carbonate rich facies to deep water, basinal shales.
- Finally the various lines of palaeontological evidence for the nature of the lacustrine environment are presented based on this work and the literature which concludes that the lake was mainly non-marine brackish water from the abundance of brackish water bivalves and the absence of both evaporites and of charophytes. However more marine and freshwater intervals are suggested from palaeontological evidence.

11.6 – Taphonomy of the bivalve rudstones and floatstones.

- Taphonomic studies are definitively powerful tools to elucidate the complex biostratinomic, sedimentological and diagenetic history in lacustrine deposits. First, the nature of the post-mortem preservation and accumulation of the shelly fossils provides significant palaeoenvonmental information normally not observed in sedimentary facies alone.
- Biostratinomy deals with the post-mortem processes that affect the preservation of organisms. The classification of taphofacies of bivalve rudstones and floatstones group the textural and compositional overprints since its death through to their final burial. Sedimentary trends of environmental energy associated to environments on the lake margin are identified.
- This method with sedimentological and electrical logs analysis has been extensively used for the construction of cycles stacking patterns as building blocks for the stratigraphic analysis.
- The taphofacies have been grouped into autochthonous, parautochthonous and allochtonous groups. The autochthonous (TF-1) and parautochthonous (TF-2 and TF-3) taphofacies represent very low energy sub wave base environments. Allochthonous taphofacies (TF-3 to TF-6) were submitted a higher energy, transport and breakage of shells.

These form cleaner facies with traction structures and preserve greater primary porosity. The allochthonous mixed carbonate-clastic taphofacies are normally associated with alluvial environments (TF-7) or specifically fluvial channels (TF-8).

- After the burial of sediments, the diagenetic history has to be understood as a series of in situ mineral transformations. Based on the petrographic and cathodo-luminescence analyses, a diagenetic sequence of events or paragenesis has been constructed. In the Lagoa Feia carbonates are: micritization, early cementation, neomorphism, dissolution, late cementation, recrystallization, substitution (silicification and dolomitization), mechanical compaction, pressure solution (dissolution seams and stylolites), fractures and late dissolution.

11.7 – Core and well data analysis

- In order to carry out the regional sedimentological and stratigraphic study of the Barremian, Aptian carbonate successions cores and FMI image log, with additional help from sidewall core data have been studied. The cores covering Domain I, penetrated by wells 1, 2, 6, 7, 8 and 9.
- The facies classification and facies model and stratigraphic analyses are core based. In the more offshore Domian 2 core was taken in well 12 and the FMI log and sidewall core samples and also Gamma Ray logs were used to complement the study in well 20.
- In Domain III, where no wells have been drilled, the sedimentological and stratigraphic model is completely based on 3D seismic interpretations undertaken.
- The Barremian and early Aptian section of the southern portion of the Campos Basin, comprises a mix of sandstone, conglomerates, and carbonate rocks. This system is increasingly purer in carbonate as it moves away from the rift border. The core logging through wells 1, 2, 6, 7, 8, 9 and 12, revealed a succession of facies association of alluvial fan, deltaic and lacustrine environments with carbonate platforms in shallower locations, away from the influence of terrigenous supply.

- The carbonate facies can be compared with Lake Tanganyika and the tectonic and structural settings with Abu Shaar carbonate platform, marine rift of the Gulf of Suez basin. Therefore the occurrence of clastic and carbonate facies in the Southern Campos Basin is similar to that described from other extensional non-marine and marine environments.
- In distal sites, Domain II, the sedimentological record differs considerably from the Domain I. A series of half-graben with synthetic and antithetic normal faults, transfer zones have been described where thick packages of autochthonous carbonate rocks are stacked. These sediments form aggradational and progradational bodies constructing deposits totalling 400 m thicknesses in the syn-rift Barremian coquina succession and 200 m thick in the post-rift, Aptian microbialite succession.
- In the Barremian coquina succession, a thick mud rich section of high Gamma Ray values divides two major coquina successions, informally called lower and upper coquinas sequence. These muddy organic rich rocks are considered the main source rock of the Campos Basin.
- The traditional core logging has been effective in determining the temporal and spatial facies distribution, the facies associations and depositional environments. To overcome the difficulties in doing the same in uncored well, the construction of FMI based facies and a facies model was undertaken. Although unusual, it is likely that this approach will become more common in the future as more results from FMI are in the published domain.

11.8 – Sequence stratigraphic analysis

- The original sequence stratigraphy method has been adapted to the study of carbonate platforms with modifications made to include carbonate production in shallow carbonate factories because the assumed continuous subsidence and global eustasy can not be applied to carbonates accumulating in continental rift basins.

- The interpretation of trends and cycles in a rift basin context is far more complex where climate, tectonic, sedimentary supplies are factors that work together to form the sedimentological record.
- The transgressive - regressive sequence stratigraphic model is found to be applicable to the rift tectonic settings. Because this method uses the maximum regressive surface as a submerged correlative key surface. Which can be objectively determined and it is an alternative model to overcome the problems of sequence definition.
- The findings of this chapter addresses and answers the second scientific question postulated for this research: Can the strata be subdivided using sequence stratigraphic principles to organise and understand the sedimentological framework and are these the same or different from standard sequence stratigraphic models
- From the analysis of stacking patterns and key surfaces in seven wells, a hierarchy of 4 different orders of transgressive-regressive sequences has been identified.

11.9 – Seismic Stratigraphy analysis

- An evolutionary history of the basin fill dynamic may be described, and the main result is possibility of facies prediction with the seismic stratigraphy has been an efficient tool to subdivide and map the key surfaces within the Lagoa Feia Gp and illustrate some relations between accommodation space and sedimentation rates. Also it has enabled the recognition and mapping of key surfaces which limit the depositional sequences, as well as the system tracts.
- Domain I, fanning and plane-parallel reflectors are observed. This plane-parallel geometry is interpreted as a balance between accommodation space and sedimentary fill. The carbonate platforms in this domain are located on footwall highs and show progradation into the hangingwall sub-basins.
- In Domain II, a configuration of a sub-basin separated by an accommodation zone creates different geometric arrangements. Over the accommodation zone aggradational reflectors with chaotic seismic facies

are observed. This is interpreted as a high energy depositional environment, where the carbonates catch up and aggrades. Up dip from this site, the reflectors are aggradational divergent which may mean differential deposition and compaction of low energy facies. But downdip of the accommodation zone progradational geometry is seen. This progradation relates to high sedimentation rate supplanting the created accommodation space. Some terminations like downlap and erosional truncations are evident.

- In distal zones, Domain III, the plane-parallel reflectors indicate potential depositional space and accumulation of low energy, deep subaqueous environment. But, on the relict highs, isolated platform type, the dynamic of the depositional process seems to be different with aggradational facies at the top of these highs and progradation in the border of the platform. Carbonate platforms in these locations are founded on interbasinal highs in the accommodation zone.
- The limits of main 3rd order sequences, LF-35, PRU and PSU; such seismic horizons bound the Clastic Sequence, the Coquinas and Microbialites sequences that corresponds respectively to tectono-stratigraphic units, early syn-rift, late syn-rift and post-rift.

11.10– Tectono stratigraphic models

The major conclusions of this chapter and of the thesis are:

- The stratigraphic fill of the southern Campos Basin rift basin is strongly affected by increasing subsidence rates from rift border Domain I, through intermediate Domain II to be basinal Domain II.
- Each domain has different tectonic framework that has acted as a major control on the nature of the basin fill so that tectono-stratigraphic models can be erected for each domain.
- Domain I is characterised by half-graben basin fills. Hangingwall sub-basins are characterised by siliciclastic supplied from the rift margin whilst footwall areas develop carbonate platforms dissected by basinward dipping faults.

- Domain II is more carbonate rich and a fault accommodation zone with an interbasinal high form the template for aggrading and prograding carbonate platforms. Basinal facies accumulate in deeper areas.
- Domain III is only known from seismic data where relic, buried horsts provide highs for the accumulation of unattached carbonate platforms that prograde into basin areas.
- Comparisons with the Cenozoic Gulf of Suez rift indicate a number of similarities in basin evolution despite the marine nature of this younger marine rift. Similarities include the clastic dominated early syn-rift and carbonate dominated late rift phases and the control of sediment accumulation in rotated fault blocks and fault transfer zones. However the Campos Basin develops into a larger lacustrine system with more pure carbonate facies and unattached offshore platforms.
- A review of the evidence for the hydrological conditions within the Lagoa Feia palaeolake combines evidence from this thesis and from the literature and concludes that it alternates from three low-order (Level 2) T-R cycles of humid (T) to arid (R) phases that are expressed as clastic-rich and carbonate rich respectively.
- Major up section changes in the evolution of the lacustrine environments are shown for the syn-rift Coqueiros Fm to be an early alkali lake phase replaced by brackish waters when the main coquinas accumulate to a possible marine influenced interval at the top of the syn-rift. The post-rift Macabu Formation is characterised by fluvial to hypersaline environments prior to the marine sourced evaporites of the Aptian related to the initial stages of marine flooding in the south Atlantic.

REFERENCES

Abrahão, D. & Warme, J. E. 1990, Lacustrine and associated deposits in a rifted continental margin – Lower Cretaceous Lagoa Feia Fm., Campos Basin, Offshore Brazil. *In*: Katz, B.J. (ed). *Lacustrine basin exploration, case studies and modern analogs*. *American Association of Petroleum Geologists*, Memoir 50, p. 287-305.

Aigner, T. & Wernicke, B. 1985, Storm deposicional systems: dynamic stratigraphy in modern and ancient shallow-marine sequences. *In*: Friedman, G.M., Neugebauer, H.J.; Seilacher, A. (eds.). *Lecture notes in Earth Sciences*, Berlin, Springer, p.174.

Akbar, M., Petricola, M., Wafta, M., Badri, M., Charara, Boyd, Austin, Cassel, B., Nurmi, R., Delhomme, J. P., Grace, M., Kenyon, B., Roestenburg, J. 1995, Classic interpretation problems: Evaluating Carbonates. *World oil review*, p. 38-57.

Algeo, T. J., & Wilkinson, B. H. 1988, Periodicity of mesoscale Phanerozoic sedimentary cycles and the role of Milankovitch orbital modulation. *Journal of Geology*, vol. 96, p. 313-322.

Allen, N. H. 1983, Recent temperate carbonate deposits on the continental shelf north and west of Scotland: distribution, sedimentation and reserves Ph.D. Thesis University of Strathclyde, p. 292.

Allen, P. A. & Allen, J. R. 1990, *Basin Analysis – Principles and Applications*, Oxford, Blackwell Science, 451 p.

Al-Rhougha H. B., Shebl, H., Chakravorty, S. 2005, Heterogeneity quantification, fine-scale layering derived from image logs and cores (Reservoir Characterization) *World Oil online*, vol. 226 nº 10. Available from: http://www.worldoil.com/October-2005-Heterogeneity-quantification-fine-scale-layering-derived-

ANP, 2012 - Boletim da Produção de Petróleo e Gás Natural Superintendência de Desenvolvimento e Produção – SDP. Agência Nacional do Petróleo, Gás Natural e Biocombustíveis S.A., Março 2012.

Asmus, H. E. 1975, Controle estrutural da deposição mesozóica nas bacias da Margem Continental Brasileira. *Revista Brasileira de Geociências* vol.5, p. 160-175.

Asmus, H. E. & Guazelli, W. 1981, Descrição Sumária das Estruturas da Margem Continental Brasileira e das Áreas Oceânicas e Continentais Adjacentes - Hipótese Sobre o Tectonismo Causador e Implicação para os Prognósticos de Recursos Minerais - Projeto Remac – Cenpes / Petrobras, vol. 9, p. 187-269.

Asmus, H. E. 1982, Geotectonic significance of Mesozoic-Cenozoic magmatic rocks in the Brazilian continental margin and adjoining emerged area. *In*: Congresso. Latino Americano de Geologia, 5, Buenos Aires: Serviço Geológico Nacional, vol. 3, p.761-779.

Bacon,.M., Simm, R. and Redshaw, T. 2003, *3-D seismic interpretation*, Cambridge University Press, 212 p.

Bally, A. W. 1982, Musings over sedimentary basin evolution (and discussion). Philosofical Transactions of the Royal Society, London, A 305, p. 325-338.

Barrell, J. 1917, Rhythms and the measurements of geological time. *Geological Society of America Bulletin*, vol. 28, p. 745–904.

Barros, M. C. 1980, Geologia e Recursos Petrolíferos da Bacia de Campos. Anais do XXXI Congresso Brasileiro de Geologia, vol. 1, p. 254-265.

Bathurst, R. G. C. 1975, *Carbonate sediments and their diagenesis*. 2nd ed. Amsterdam, Elsevier. 658 p. (Developments in Sedimentology, 12).

Baumgarten, C. S. 1983, Evolução estrutural da Formação Lagoa Feia em Pampo Badejo-Linguado: Petrobras/Depex/Dirsul, Relatório interno 10 p.

Baumann, A., Forstner, U. and Rohde, R. 1975, Lake Shala, water chemistry, mineralogy, and geochemistry of sediments in an Ethiopian rift lake: *Geologische Rundschau*, vol. 64, p. 593- 609.

Behrensmayer, A. K., Kidwell, S. M., and Gastaldo, R. A., 2000, Taphonomy and Paleobiology. *In*: Erwing, D. H. & S. L. Wing, eds.*Deep Time – Paleobiology's perspective*, *Supplement to Paleobiology.* vol. 26 (4), p. 103-147.

Bertani, R. T. 1984, Microfacies, depositional models and diagenesis of Lagoa Feia Formation (Lower Cretaceous), Campos Basin, Offshore Brazil: Ph.D. thesis, University of Illinois at Urbana-Champaign, 199 p.

Bertani, R. T. & Carozzi, A. V. 1985, Lagoa Feia Formation (Lower Cretaceous), Campos Basin, offshore Brazil: Rift valley stage carbonate reservoirs. *In*: *Journal of Petroleum Geology*, 8, p. 37-58.

Bertani, R. T. & Carozzi, A. V. 1985a, Lagoa Feia Formation (Lower Cretaceous), Campos Basin, Offshore Brazil—Rift valley stage lacustrine carbonate reservoirs, *In*: *Journal of Petroleum Geology*, vol. 8, nº. 1, p. 37-58.

Bertani, R. T. & Carozzi, A. V. 1985b, Lagoa Feia Formation (Lower Cretaceous), Campos Basin, Offshore Brazil—Rift valley stage lacustrine carbonate reservoirs, *In*: *Journal of Petroleum Geology*, vol. 8, nº. 2, p. 199-220.

Blair T. C. 1987b, Tectonic and hydrologic controls on cyclic alluvial fan, fluvial and lacustrine rift basin. Sedimentation, Jurassic lowermost Cretaceous todos os Santos Formations, Chapas, México, *Journal of Sedimentary Petrology*, 57, p 845-862.

Blair, T. C &. McPherson, J. G. 1994, Historical adjustments by Walker River to lake-level fall over a tectonically tilted half-graben floor, Walker Lake Basin, Nevada *Sedimentary Geology* vol. 92; Issue 1; p. 7-16 Elsevier.

Blair, T. C. & McPherson J. G. 1994, Alluvial fans and their natural distinction from rivers based on morphology, hydraulic processes, sedimentary processes and facies assemblages. *Journal of Sedimentary Petrology*, 64 (3): p. 450-489.

Bosence, D. W. J. 1987, Porrtland and Purbeck Formations of the Isle of Portland. *In*: Riding, R. (ed.*) International Symposium on Fossil Algae*, Excursions Guide.

Bosence, D. W. J. 1998, Stratigraphic and sedimentological models of rift basins. *In*: Purser, B. H. & Bosence, D. W. J., eds. *Sedimentary and Tectonic Evolution of Rift Basins-The Red Sea-Gulf of Aden*: London, Chapman & Hall, p. 9-25.

Bosence, D. W. J. & Wilson, C. L. 2003, Carbonate depositional systems. *In*: Coe, A. L. ed. 2005, *The sedimentary record of sea-level change*. Cambridge University Press, Cambridge. p. 209 - 233.

Bosence, D. W. J. 2005, A genetic classification of carbonate platforms based on their basinal and tectonic setting in the Cenozoic: *Sedimentary Geology*, vol. 175, p. 49-72.

Bosworth, W. 1995, A high strain rift model for the southern Gulf of Suez, Egypt, *In*: Lambiase, J. J., ed., *Hydrocarbon Habitat in Rift Basins*: Geological Society of London, Special Publication 80, p. 75–102.

Bosworth, W., Crevello, P., Winn, R. D., JR., and Steinmetz, J. 1998, Structure, sedimentation, and basin dynamics during rifting of the Gulf of Suez and north-western Red Sea, *In*: Purser, B. H., and Bosence, D. W. J., eds., *Sedimentation and Tectonics of Rift Basins*: Red Sea–Gulf of Aden: London, Chapman & Hall, p. 77-96.

Bradley, H. & Fahey J. J. 1962, Occurrence stevensite C.J.R., 2005 the Green River Formation of Wyoming: Braithwaite,. Carbonate Sediments and Rocks. A Manual for Earth Scientists and Engineers. Whittles Publishing, Dunbeath, Scotland, 164 p.

Braithwaite, C. J. R. 2005, *Carbonate Sediments and Rocks*. A Manual for Earth Scientists and Engineers. Whittles Publishing, Dunbeath, Scotland, p. 164.

Brett, C. E. & Speyer, S. E. 1990, Taphofacies. *In*: Briggs, B. E. K. & Crowther, P. R. eds., *Palaeobiology*: *a Synthesis*, p. 258-263. Oxford: Blackwell.

Brindley, G. W., Bish, D. L., Wan, H. M. 1977, Nature of kerolite and its relation to talc and stevensite. *Mineralogical Mag* 41, p. 443–452.

Buck, W. R., Steckler, M. S. and Cochr, J. R. 1988, Thermal consequences of lithospheric extension: Pure and simple. *Tectonics*, 7, p. 213-234.

Burchette, T. P. 1988, Tectonic control on carbonate platform facies distribution and sequence development: Miocene, Gulf of Suez. *Sedimentary Geology*, vol. 59, p. 179-204.

Burchfiel, B. C. 1980, Tectonic of non-collisional regimes - the modern Andes and the Mesozoic cordilleran orogen of the western United States. *In*: Burchfiel, B. C: (ed.) *Continental tectonics*. Washington D. C., National Academy of Sciences, p. 65 -72.

Burne, R. V. & Moore, L. S. 1987, Microbialites: organosedimentary deposits of benthic microbial communities. *Palaios* 2, p. 241-254.

Bustillo, M. A., Arribas, M. E, Bustillo, M. 2002, Dolomitization and silicification in low-energy lacustrine carbonates, Paleogene, Madrid Basin, Spain. *Sedimentary Geology*, vol. 151, Issues 1–2, p. 107-126.

Bustillo, M. A. 2010, Silicification of Continental Carbonates. *In*: Alonso-Zarza A. M. & Tanner, L .H. eds., *Carbonates in Continental Settings*: Geoquemistry, Diagenesis and Applications. Developments in Sedimentology vol. 62, p. 153-174.

Bosworth, W. 1995, A high-strain rift model for the southern Gulf of Suez (Egypt). *In*: Lambiase, J. J., ed., *Hydrocarbon Habitats in Rift Basins*. Geological Society of London Special Publication, 80, p. 75 -102.

Carroll, A. R. & Bohacs, K. M. 1999, Stratigraphic classification of ancient lakes: Balancing tectonic and climatic controls Geology; February; vol. 27; nº. 2; p. 99-102.

Carvalho, M. D., Monteiro, M., Pimentel, A. M., Rehim, H. A. A. A. and Dultra A. J. 1984, Microfácies, diagenese e petrofísica das coquinas da Formação Lagoa Feia em Badejo, Linguado e Pampo – Bacia de Campos – Projeto 03.01.02, Evolução diagenética dos reservatórios carbonáticos da formação Lagoa Feia, Bacia de Campos, Rio de Janeiro, Petrobras. Unpublished internal report, 130p.

Carvalho, M. D.; Praça, U. M. Dias, J. L. Silva-Telles Jr., A. C. Horschutz, P.; Hessel, M. H.; Hanashiro, M.; Scuta, M. S.; Barbosa, A. S. C.; Freitas, L. C. S.; Sayd, A. D. 1995, Coquinas da formação Lagoa Feia da bacia de Campos estudo sedimentológico na caracterização da qualidade de reservatório: Petrobras Internal Report, Rio de Janeiro, 188 p.

Carvalho, M. D., U. M. Praça, Silva-Telles A. C., Jahnert, R. J., and Dias J. L. 2000, Bioclastic carbonate lacustrine facies models in the Campos Basin (Lower Cretaceous), Brazil. *In*: E. H. Gierlowski-Kordesch & K. R. Kelts, eds., *Lake basins though space and time*: *American Association of Petroleum Geologists*. Studies. *In*: *Geology* 46, p. 245-246.

Castro, J C. & Azambuja Filho, N. C. 1980, *Fácies, análise estratigráfica e reservatórios da Formação LagoaFeia. Cretáceo Inferior da Bacia de Campos.* Rio de Janeiro, Petrobras, 116 p. (Internal Report , unpublished).

Cathro, D. L., Austin, J. A., and Moss, G. D. 2003, Progradation along a deeply submerged Oligocene-Miocene heterozoan carbonate shelf: how sensitive are clinoforms to sea level variations? *American Association of Petroleum Geologists Bulletin*. vol. 87, nº. 10, p. 1547-1574.

Catuneanu, O. Khalifa, M.A. and Wanas, H.A. 2006, Sequence stratigraphy of the Lower Cenomanian Bahariya Formation, Bahariya Oasis, Western Desert, Egypt. *Sedimentary Geology*. vol. 190, Issues 1–4, p. 121–137.

Catuneanu, O. 2006, *Principles of Sequence Stratigraphy*. Elsevier, Amsterdam. 375 p.

Chafetz, H.S.,Wilkinson, B.H., Love, K.M.1985, Morphology and composition of non-marine carbonate cements in near-surface settings. *In*: Schneidermann, N., Harris, P.M. (Eds), *Carbonate Cements*. Society of Economic Paleontologists and Mineralogists, Special Publication 36.

Chang, H. K., Kowsmann, R. O., Figueiredo, A. M. F. and Bender, A. 1992, Tectonics and stratigraphy of the East Brazil Rift system: an overview. *Tectonophysics*, vol. 213, p. 97-138.

Changsong, L., Eriksson, K., Sitain, L., Yongxian, W., Jangye, R., and Jingyan, L. 2001, Sequence architecture, depositional systems, and computer simulation of lacustrine basin fills in Erlian Basin, northeast China. *American Association of Petroleum Geologists Bulletin*, vol. 85, p. 2017–2043.

Chiossi, D. N. S. 1997, Estratigrafia de seqüências e condicionamento tectono-climático num rifte continental (Bacia de Sergipe-Alagoas). Universidade Federal do Rio Grande do Sul, Curso de Pós-Graduação em Geociências. Dissertação (Mestrado), 205 p.

Christie-Blick, N., Mountain G. S., and Miller, K. G. 1990, Seismic stratigraphic record of sea-level change. *In Sea-level change*, R. Revelle, ed., p. 116–140. National Research Council, Studies in *Geophysics*. National Academy Press, Washington.

Church, K. D. & Coe, A. L. 2003, Process controlling relative sea-level change and sedimentary supply. *In*: Coe, A.L. ed. 2005. *The sedimentary record of sea-level change*. Cambridge University Press, Cambridge. p. 99 - 117.

Clifton, & Boggs, Sam, Jr. 1970, Concave-up pelecypod (Psephidia) shells in shallow marine sand, Elk River Beds, southwestern Oregon. *Journal of Sedimentary Petrology*, vol. 70, p. 888-897.

Cobbold, P. R., Meisling K. E. and Mount V. S. 2001 - Reactivation of an obliquely rifted margin, Campos and Santos basins, southeastern Brazil, *American Association of Petroleum Geologist Bulletin*, vol. 85, Issue 11, p. 1925 - 1944

Cohen, A. S. & Thouin C., 1987, Nearshore carbonate deposits in Lake Tanganyika. Geology 15:p. 414–418

Colletta, B., Le Quellec, P., Letouzy, J., and I., Moretti, 1988, Longitudinal evolution of the Suez rift structure (Egypt): Tectonophysics, vol. 153, p. 221–233.

Collinson, J. D. 1969, The sedimentology of the Grindslow Shales and the Kinderscout Grit: a deltaic complex in the Namurian of northern England. *Journal of Sedimentary Petrology*, vol. 39, p. 194–221.

Collinson, J.D. 1978, Vertical sequence and sand body shape in alluvial sequences. *In*: Miall, A. D. (ed). *Fluvial sedimentology.* Canadian Society of Petroleum Geologists. Memoir, 5, p. 577-586.

Collinson, J.D. 1996, Alluvial Sediments. *In*: H.G. Reading (ed) *Sedimentary Environments and facies*, 3rd edn. Elsevier, New york, p.37-82.

Coniglio, M. & Dix, G. R. 1992, Carbonate slopes. *In Facies Models: Response to Sea Level Change* (R. G. Walker & N. P. James, Eds.), p. 349–373. Geological Association of Canada.

Cordani, U.G., A.M. Coimbra, J.A. Boettura, and E.C.M. Rodrigues, 1972, Idades Potassio-Argonio da regiao leste brasileira: Anais do XXVI Congresso Brasileiro de Geologia, p. 71-75.

Coward, M.P. & Ries A.C. (edt.) 1986, *Collision Tectonics*. Geological Society of London Special Publication. 19, Blackwell Scientific Publications, Oxford, 415 p.

Cross, N.E. 1996, Sedimentology and sequence stratigraphy of a Miocene fault-block carbonate platform, Gulf of Suez, Egypt: unpublished Ph.D. thesis, University of London, 268 p.

Cross, N.E., Bosence, D.W.J., and Purser, B.H. 1998, The tectono-sedimen- tary evolution of a rift margin carbonate platform: Abu Shaar, Gulf of Suez, Egypt, in Purser, B.H., and Bosence, D.W.J., eds., Sedimentation and Tectonics of Rift Basins: Red Sea–Gulf of Aden: London, Chapman & Hall, p. 271–295.

Cross, N. E., & Bosence D. W. J. 2006, Controls on Carbonate Platform and Reef Development Society for Sedimentary Geology (SEPM) Special Publication No. 89, p. 83–105.

Cross, N.E. & Bosence, D. W. J. 2008, Tectono-Sedimentary models for rift-basin carbonate systems. Controls on Carbonate Platform and Reef Development SEPM Special Publication nº. 89, Society for Sedimentary Geology, p. 83-105.

Davies, G. R. 1970a, Algal Laminated sediments, Gladstone embayment, Shark Bay, Western Australia. *In*: *Carbonate sedimentation and environments, Shark Bay, Western Australia*: *American Association of Petroleum Geologists* Memoir 13, p. 169-203.

Davies, G. R., 1970b, Carbonate bank sedimentation, eastern Shark Bay, Western Australia, *In*: *Carbonate sedimentation and environments, Shark Bay, Western Australia*: *American Association of Petroleum Geologists* Memoir 13, p. 85-168.

Davison, I., 1999, Tectonics and hydrocarbon distribution along the Brazilian South Atlantic margin, *In:* Cameron, N. R., Bate, R. H. and Clure, V.S. eds., *The oil and gas habitats of the South Atlantic*: The Geological Society [London] Special publication 153, p. 133-151.

De Wet, C. C. & Hubert, J. F. 1989, The Scots Bay Formation, Nova Scotia, a Jurassic carbonate lake with silica-rich hydrothermal springs. *Sedimentology* 36, p. 857–875.

Della Porta, G., Barilaro, F., Capezzuoli, E., 2012, Non Marine Carbonates: Microbially Mediated vs. Abiotic Fabrics and Porosity. *American Association of Petroleum Geologists*, Hedberg Conference Microbial Carbonate Reservoir Characterization, Houston, Texas (abstract).

Demercian, L. S. 1996, A halocinese na evolução do Sul da Bacia de Santos do Aptiano ao Cretáceo Superior. M.Sc thesis, Universidade Federal do Rio Grande do Sul, Porto Alegre, Brazil, p 201.

Destro, N., Szatmari, P., Alkmim, F. F. and Magnavita, L. P. 2003, Release faults, associated structures,fans and their control on petroleum trends in the Reconcavo Rift, northeast Brazil. *American Association of Petroleum Geologists Bulletin*, 87 (7), p. 1123-1144.

Dias, J. L.; Vieira, J. C.; Catto, A. J.; Oliveira, J. Q.; Guazeli, W.; Trindade, L. A. F.; Kowsmann, R. O.; Kiang, C. H.; Mello, U. T.; Mizusaki, A. M. P. & Moura, J.

A. 1987, Estudo regional da Formação Lagoa Feia. Petrobras/Depex, Relatório Interno, Rio de Janeiro.

Dias, J. L., Oliveira, J. Q., Vieira, J. C. 1988, Sedimentological and stratigraphic analysis of the Lagoa Feia Formation, rift phase of Campos Basin, offshore Brazil. *Revista Brasileira de Geociências*, vol. 18 (3), p. 252-260.

Drivet, E., & Mountjoy, E. 1997, Dolomitization of the Leduc Formation (Upper Devonian) Southern Rimbey-Meadow book reef trend, Alberta: *Journal Sedimentary Research*, vol., 67, p. 411-423.

Dixon, J. & Wright, V. P., 1983, Burial diagenesis and crystal diminution: the origin of crystal diminution in some limestones form south wales. *Sedimentology*, vol. 30, p. 537-546.

Dixon, J., & Wright, V.P 1983, Limestone diagenesis during deep burial and its relationship to deformation mechanisms of calcite. *Sedimentary Geology* vol. 35; Issue 2; p 153-155 Elsevier.

Dolson, J., El-Gendi, O. H. Sharmy, Fathalla M., and Gaafar I. 1996, Gulf of Suez rift basin sequence models-Part A: Miocene sequence stratigraphy and exploration significance in the greater October field area, northern Gulf of Suez. In: Youssef, M. ed., Proceedings of the 13th Petroleum Conference: Cairo, Egypt, Egyptian General Petroleum Corporation, p. 227-241.

Donovan, A. D. 2001, Free market theory and sequence stratigraphy. Hedberg Research Conference on "Sequence Stratigraphic and Allostratigraphic Principles and Concepts", Dallas, August 26-29. *American Association of Petroleum Geology*, Program and Abstracts, p. 22.

Dorobek, S. L. 2008, Tectonic and depositional controls on syn-rift carbonate platform sedimentation. In: Lukasik, J. & Simo, J. A., eds., Controls on Carbonate Platform and Reef Development, SEPM, Special Publication 89, p. 57-81.

Dunham, R. J. 1962, Classification of carbonate rocks according to depositional texture. *In*: Ham, W. E. ed., *Classification of carbonates rocks*, *American Association of Petroleum Geologists* Memoir 1: 107-121, Tulsa, Oklahoma.

Dupraz, C., Visscher, P. T., and Reid, P. 2011, Modern Microbialite. Encyclopedia of Geobiology, Springer, accepted for publication.

Eberli, G. P., Anselmetti, F. S., Kroon, D., Sato, T., Wright, J. D. 2002, The chronostratigraphic significance of seismic reflections along the Bahamas Transect, *Marine Geology*, vol. 185, issues 1-2, p. 1-17.

Ebinger, C. J., Petit C. and Burov E. 2002, Causes and consequences of lithospheric extension: the ups and downs of continental rifts. In: Robin, W. Renault and Ashley, M. eds., *Sedimentation in continental rift*, Tulsa, SEPM Special publication. 73, p. 11-23.

Efremov, J. A. 1940, Taphonomy: New branch of paleontology, *Pan-American Geologists* 74: p. 81-93.

Embry, A. F. & Klovan, J. E. 1971, A Late Devonian reef tract on northeastern Banks Island, N.W.T.: *Bulletin of Canadian Petroleum Geology*, vol. 19, p. 730 -x 781.

Embry, A. F. & Johannessen, E. P. 1992, T–R sequence stratigraphy, facies analysis and reservoir distribution in the uppermost Triassic-Lower Jurassic succession, western Sverdrup Basin, Arctic Canada. *In:* Vorren, T. O., Bergsager, E., Dahl-Stamnes, O. A., Holter, E., Johansen, B., Lie, E. and Lund, T. B. eds., *Arctic Geology and Petroleum Potential* p. 121-146. *Norwegian Petroleum Society* (NPF), Special Publication 2.

Embry, A. F. & Johannessen, E. P. 1992, T–R sequence stratigraphy, facies analysis and reservoir distribution in the uppermost Triassic–Lower Jurassic succession,

Western Sverdrup Basin, Arctic Canada. *In*: Vorren, T. O., Bergsager, E., Dahl-Stamnes, O. A.

Embry, A. F. 1993, Transgressive-regressive (T–R) sequence analysis of the Jurassic succession of the Sverdrup Basin, Canadian Arctic Archipelago. *Canadian Journal of Earth Sciences*, vol. 30, p. 301-320.

Embry, A. F. 1995, Sequence boundaries and sequence hierarchies: problems and proposals. *In*: Steel, R. J., Felt, V. L., Johannessen, E. P., Mathieu, C. eds., *Sequence stratigraphy on the Northwest European Margin*. *Norwegian Petroleum Society*, Special Publication, vol. 5. p. 1-11.

Embry, A. F, 2002, Transgressive-regressive (T-R) sequence stratigraphy. *In*: Bob F. Perkins Research Conference Annual Gulf Coast Section, 22, Texas: GCS SEPM Foundation, p. 151-172.

Erlich, R. N., Longo, A. P., Jr., and Hyare, S. 1993, Response of carbonate platform margins to drowning: evidence of environmental collapse. *In:* Loucks, R. G. & Sarg, J. F. eds., *Carbonate Sequence Stratigraphy – Recent Developments and Applications American Association of Petroleum Geologists,* Memoir 57. p. 241–266.

Evans, A. L. 1988, Neogene tectonic and stratigraphic events in the Gulf of Suez: Insights into syn-rift unroofing and uplift history: *American Association Petroleum of Geologists*, *Bulletin*, vol. 74, p. 1386-1400.

Feldmann, M. & McKenzie, J. A. 1997, Messinian stromatolite-thrombolite associations, Santa Pola, SE Spain: An analogue for the Palaeozoic: Sedimentology, vol. 44, p. 893–914.

Feldmann, M. & McKenzie, J. 1998, Stromatolite-Thrombolite Associations in a Modern Environment, Lee Stocking Island, Bahamas *Palaios*, 1998, vol. 13, p. 201-212.

Fischer, A. G. 1964, The Lofer cyclothems of the Alpine Triassic: *Kansas Geological Survey Bulletin*, vol. 169, p. 107–149.

Fitchen, W. M. 1997, Carbonate Sequence Stratigraphy and its Application to Hydrocarbon Exploration and Reservoir Development. *In*: Palaz, I. & Manfurt, K., J. eds, *Carbonate Seismology*, *Geophysical Developments Series*, nº. 6. *Society of Exploration Geophysicists*, p. 121-178.

Flessa, K. W., Kowalewski, M., and Walker, S., E. 1992, Post collection taphonomy: shell destruction and the Chevrolet, *Palaios* 7: p. 553-554.

Flügel, E. 2004, Microfacies of carbonate rocks: analysis, interpretation and application. Berlin: Springer, 976 p.

Flügel, E. 2010 - Microfacies of carbonate rocks 2nd ed. Springer-Verlag Berlin, Germany. p. 275-300,

Folk, R. L. 1962, Spectral subdivision of limestones types. *In* Ham, W.E. ed. *Classification of carbonate rocks*: p. 62-85. Tulsa: *American Association of Petroleum Geologists*. Memoir 1.

Folk, R. L. 1965, Some aspect of recrystallization in ancient limestones. *In*: Pray, L. C. & Murray, R.C. eds., Dolomitization and limestone diagenesis: a Symposium – Soc. Econ. Paleontologists Mineralogists, Special Publications, vol. 13: p. 14-48.

Freytet, P. & Verrecchia, E. P. 2002, Lacustrine and palustrine carbonate petrography: an overview: *Journal of Paleolimnology*, vol. 27, p. 221–237.

Fürsich, F. T. & Oschmann, W. 1993, Shell beds as tool in basin analysis: The Jurassic of Kachchh, western Índia. *Journal of the Geology Society*. London, vol. 150. p. 169-185.

Fürsich, F. T. & Oschmann, W. 1986, Storm shell beds of Nanogyra virgule in the Upper Jurassic of France. *Neues Jahrbuch fur Mineralogie, Geologie und Palaontologie. Abhandlungen*, vol. 172, p. 141-161,

Galloway, W. E. 1989, Genetic stratigraphic sequences in basin analysis, I. Architecture and genesis of flooding-surface bounded depositional units. *American Association of Petroleum Geologists Bulletin* 73, p. 125-142.

Garfunkel, Z. & Bartov, Y. 1977, The tectonics of the Suez rift: *Geological Survey of Israel, Bulletin*, vol. 71, p. 1-44.

Gawthorpe, R. L., Fraser, A. J., and Collier, R. E. L. 1994, Sequence stratigraphy in active extensional basins: Implications for the interpretation of ancient basin fills: *Marine and Petroleum Geology*, vol. 11, p. 642-658.

Gibbs, A. D. 1984, Structural evolution of extensional basin margins, *Journal of the Geological Society,* London, 141, p. 609-620.

Gibbs, A. D. 1990, Linked fault families in basin formation. *Journal of Structural Geology* 12, p. 795-803.

Goldring, R. 1991, *Fossils in the field. Information potential and analysis*. Longman *Scientific & Technical*. P. 218. Harlow: Longman; New York: John Wiley.

Grabau, A. W. 1913, *Principles of Stratigraphy*. A. G. Seiler, New York, p. 1185.

Grosdidier, E. 1967, Quelques ostracodes nouveaux de la série antésalifère ("Wealdienne") des bassins côtiers Du Gabon et du Congo. *Revue de Micropaléontologie*, vol. 10 (2), p. 107-118.

Grotzinger, J. P. & Knoll, A. H. 1999, Stromatolites in Precambrian carbonates: evolutionary mileposts or environmental dipsticks. *Annual Review of Earth and Planetary Science*, 27: p. 313-358.

Guardado, L. R., Spadini, A. R., Brandão, J. S. L, and Mello, M. R. 2000, Petroleum System of the Campos Basin, *In*: M. R. Mello and B. J. Katz, eds., *Petroleum Systems of South Atlantic margins*: *American Association of Petroleum Geologists Memoir* 73, p. 317-324

Handford, C. R. & Loucks, R. G. 1993, Carbonate depositional sequences and systems tracts-responses of carbonate platforms to relative sea level changes, *In:* Loucks, R. G., and Sarg, J. F., eds., Carbonate sequence stratigraphy: recent developments and applications: *American Association of Petroleum Geologists*. Memoir 57, p. 3-41.

Haq, B. U., Hardenbol, J., and Vail, P. R. 1988, Mesozoic and Cenozoic chronostratigraphy and cycles of sea-level change. *In: Sea Level Changes–An Integrated Approach* (Wilgus, C. K., Hastings, B. S., Kendall, C. G. St. C., Posamentier, H. W., Ross C. A. and Van Wagoner, J. C. eds., p. 71-108. SEPM Special Publication 42.

Harris P. M., Kendall, C. G., Lerche, J. 1985, Carbonate cementation:a brief review. – *In*: Schneidermann, M., Harris, P. M. eds., Carbonate cements. – *Society of Economic Paleontology and Mineralogy*, Special Publication, vol. 36, p. 79-95.

Harris, N. B. 2000, Toca Carbonate, Congo Basin: response to an evolving rift lake, *In* Mello, M. R. & Katz, B. J. eds., *Petroleum systems of South Atlantic margins*: *American Association of Petroleum Geologists* Memoir 73, p.341-360.

Harris, P. M. 2008, Geologic Framework for the Tengiz and Korolev Fields, Kazakhstan – Carboniferous Isolated Carbonate Platforms. *American Association of Petroleum Geologists* International Distinguished Lecture.

Hardie, L. A. 1987; Harris P. M., Kendall, C. G., Lerche, J. 1985, Carbonate cementation: a brief review. *In*: Schneidermann, M., Harris, P. M. eds.,

Carbonate cements. – *Society of Economic Paleontology and Mineralogy*, Special Publication, vol. 36, p. 79-95.

Hardie, L. A., Wilson, E. N., and Goldhammer, R. K. 1991, Cyclestratigraphy and Dolomitization of the Middle Triassic Latemar Buildup, the Dolomites, Nothern Italy, 56p. Guidebook Excursion F. Tourist office, Ortisei, Italy, September.

Harris, P. M., Kendall, C. G., Lerche, J. 1985, Carbonate cementation:a brief review. – *In*: Schneidermann, M., Harris, P. M. eds., *Carbonate cements*. – *Society of Economic Paleontology and Mineralogy*, Special Publication, vol. 36, p. 79-95.

Hendry, J. P., Ditchfield, P. W., Marshall, J. D. 1995, Two-stage neomorphism of Jurassic aragonitic bivalves: implications for early diagenesis *Journal of Sedimentary Research*. vol. 65, nº 1, p. 214 - 224.

Hessel, M. H. R. 1993, Paleogeografia dos bivalvios da Formação Lagoa Feia, Eocretáceo de Campos Simpósio de Geologia do sudeste, Rio de Janeiro, Boletim de resumos e breves comunicações. p. 22-23.

Hessel M. H. & Mello M. R. 1987, Caracterização das primeiras incursões marinhas na bacia de campos caracterizadas por biomarcadores e bivalvios. *Anais do VI Congresso Brasileiro de Geoquímica*, p. 484-487.

Heward, A. P. 1978, Alluvial fan and lucustrine sediments from lhe SlCphanian A and B (La Magdalen: Cinera-Malaliana and Sabcro) coal fields. nonhero Spain. Sedimentology. 25: p. 451-488.

Holz, M. & Simões, M. G. 2005, Taphonomy. Overview of main concepts and Applications to sequence stratigraphic Analysis. *In*: Koutsoukos E. A. M. ed., *Applied Stratigraphy*, Springer p. 249-279.

Holz, M. & Souto-Ribeiro, A. W. 2000, Taphonomy of the South-Brazilian Triassic vertebrates, *Revista Brasileira de Geociências*: p. 487-490.

Hunt, D., & Tucker, M. E. 1993, Sequence stratigraphy of carbonate shelves with an example from the mid-Cretaceous (Urgonian) of southeast France. *In:* Posamentier, H. W., Summerhayes, C. P., Haq, B. U., and Allen, G. P. eds., *Sequence Stratigraphy and Facies Associations* p. 307–341. *International Association of Sedimentologists*, Special Publication 18.

Hunt, D. & Tucker, M. E. 1992, Stranded parasequences and the forced regressive wedge systems tract: deposition during base level fall. *Sedimentary Geology*, vol. 81, p. 1-9.

Ingersoll, R. V. 1988, *Tectonics of Sedimentary Basins, Geological Society of America Bulletin*, vol. 100, p. 1704-1719.

James, N. P., Coniglio, M., Aissaoui, D. M., and Purser, B. H. 1988, Facies and geological history of an exposed Miocene rift margin carbonate platform: Gulf of Suez, Egypt: *American Association of Petroleum Geologists, Bulletin*, vol. 72, p. 555-572.

James, N. P. & Choquette, P. W. 1990, Limestone the meteoric diagenetic environment. *In*: McIlreath, I. A., Morrow, D. W. eds., *Diagenesis. Geoscience Canada*, Reprint Series 4, p. 35-73.

James, N. P. & Kendall, A. C. 1992, Introduction to carbonate and evaporite facies models. *In:* Walker R. G. & James, N. P. eds., *Facies Models: Response to Sea Level Change,* p. 265-275. *Geological Association of Canada, GeoText 1*.

Johannessen, J. 1992, Net Shore-Drift of San Juan and parts of Jefferson, Island and Snohomish Counties, Washington. Shorelands and Coastal Zone Management Program, Washington Department of Ecology, Olympia, Washington.

Johnson, J. G. & Murphy, M. A. 1984, Time-rock model for Siluro–Devonian continental shelf, western United States, *Geological Society of America Bulletin* 95 , p. 1349-1359.

Johnson, J. G., Klapper, G. and Sandberg, C. A. 1985, Devonian eustatic fluctuations. In: *Euramerica: Geological Society of America Bulletin*, 99, p. 567-587.

Jones, B & Desrochers, A. 1992, Shallow platform carbonates. *In:* Walker, R. G. & James, N. P. eds., *Facies Models: Response to Sea Level Change* p. 277-301 *Geological Association of Canada*, GeoText 1.

Karner, G. D., Driscoll, N. W., and Barker, D. H. N. 2003, Syn-rift region subsidence across the West African continental margin; The role of lower plate ductile extension. *In*: Arthur, T. J., Macgregor, D. S. and Cameron, N. eds., *Petroleum Geology of Africa: New Themes and Developing Technologies*: Geological Society of London Special Publication 207, p. 105-129.

Karner, G. D. & Gambôa, L. A. P. 2007. Timing and origin of the South Atlantic pre-salt sag basins and their capping evaporites. *In*: Schreiber, B. C., Lugli, S., & Babel, M. eds., Evaporites through space and time. *Geological Society, London, Special Publications*, vol. 285, p. 15-35.

Kendall, C. G., St C. & Skipwith, P. A. D. E. 1969a, Holocene shallow-water Carbonate and evaporate sediments of khor al Bazam, Abu Dhabi, southwest Persian Gulf. *American Association of Petroleum Geologists*, *Bulletin* vol. 53:p. 841-869.

Kendall, C. G. St C. & Schlager, W. 1981, Carbonates and relative changes in sea level: *Marine Geology*, vol. 44, p. 181-212.

Kennard, J. M. & N. P. James, 1986, Thrombolites and Stromatolites: *Two Distinct Types of Microbial Structures*. *Palaios*, 1, p. 492-503.

Kidwell, S. M., Fürsich, F. T., and Aigner, T. 1986, Conceptual framework for the analysis of fossil concentrations, *Palaios* 1: p. 228-238.

Kidwell, S. M. & Bosence, D. W. J. 1991, Taphonomy and time-averaging of marine shelly faunas. *In*: Allison P.A. & Briggs, D. E. G. eds., *Thaphonomy*: *Releasing the data locked in fossil record*,New York, Prenum Press, p. 115-209.

Kidwell, S.M. 1993, Patterns of time-averaging in the shallow marine fossil record, *In*: Short courses. *In*: Kidwell S. M. & Behrensmayer, A. K. eds., *Paleontology Taphonomic approaches to time resolution in fossil assemblages, Paleontological Society* nº 6, p. 275-300.

Klemme, H. D. 1980, Petroleum basins: classification and characteristics. *Journal of Petroleum Geology*, 3, p. 187-207.

Gierlowski-Kordesch, E. H. 2010, Lacustrine Carbonates. *In*: Alonso-Zarza A. M. & Tanner L. H. eds., *Developments in sedimentology Carbonates in continental settings: Facies environments, and processes*. vol. 61, p-1-101. Elsevier.

Krömmelbein, K. 1965, Zur Taxonomie und Biochronologie stratigraphiche wichtige Ostracoden-Arten aus der Oberjurassic. Unterkretazischen Bahia-Serie (Wealden-Fazies) NE-Brasiliens. Senck-embergiana Lethaea, vol. 43 (6), p. 437-528.

Krömmelbein, K. & Weber, R. 1971, Ostracoden des "Nordost-Brasilianischen Wealden". Beihefte zum Geologischen jahrbuch Heft, vol. 115, p. 145-162.

Kusnir, N. J. & Egan, S. S. 1990, Simple-shear and simple-shear models of extensional sedimentary basin formation: application to the Jeanne d'Arch Basin, Grand Blanks of Newfoundland. *In*: Tankard A. J. & Balkwill, H. R. eds., *Extensional Tectonics of the North Atlantic Margins*, America *Association of Petroleum Geologists* Memoir 46, p 305-322.

Lambiase, J. J. & Morley, C. K. 1999, Hydrocarbons in rift basins: The role of

stratigraphy: Philosophic Transactions of Royal Society of London A, vol. 357, p. 877-900.

Larré, L. J. C. 2009, Seismic stratigraphic analysis of syn-rift deposits of the Coqueiro Seco Formation (lower to middle Aptian), Sergipe-Alagoas Basin. Boletim de Geociencias da Petrobras, Rio de Janeiro, vol. 16, nº. 1, p. 87-101.

Larsen, P. H. 1988, Relay structures in a Lower Permian basement -involved extension system, East Greenland. J. *Structural Geolology*, vol.10: p. 3-8.

Lasemi, Z., Boardman, M. R., Sandberg, P. A. 1989, *Journal of Sedimentary Research*. vol. 59; nº. 2; p. 249-257.

Lasemi, Z. & Sandberg, P. 1993, Microfabric and compositional clues to dominant mud mineralogy of micrite precursors. *In*: Rezak, R., Lavoie, D. L. eds., *Carbonate Microfabrics*. *Frontiersin Sedimentary Geology*, Springer-Verlag, Berlin, p.173-185.

Leeder, M. R. & Strudwick, A. E. 1987, Delta- marine interactions: a discussion of sedimentary models for yoredale-type cyclicity in the Dinantian of Nothern England. *In*: Miller, J., Adamns A. E., and Wright, V. P. ed., *European Dinantian Environments*, p. 115-130.

Lehrmann, D. J. & Goldhammer, R. K. 1999, Secular variation in parasequence and facies stacking patterns of platform carbonates: a guide to application of stacking pattern analysis in strata of diverse ages and settings. *In*: Harris, P. M., Saller, A. H., and Simo, J. A., eds., *Advances in Carbonate Sequence Stratigraphy*, SEPM, Special Publication 63, p. 187-225.

Lister, G. S., Etheridge, M. A. and Symonds, P. A. 1986, Detachment faulting and the evolution of passive continental margins. *Geology*, 14: p. 246-250.

Logan, B. W. 1961, Cryptozoon and associate stromatolites from the Recent, Shark Bay, Western Australia. *Journal of Geology*, vol. 69: p. 517-533.

Logan, B. W., Rezak. R., Ginsburg. R. N. 1964, Classification and environmental significance of algal stromatolites. *Journal of Geology*, vol. 72, p. 68-83.

Logan, B. W., Read, J. F., Davies, G. R. 1970, Carbonate sedimentation and environments, Shark bay, Western Australia, *American Association of Petroleum Geologists*, Memoir 13, p. 38-84.

Logan, B.W., Hoffman, P., Gebelein, C. D. 1974, Algal mats, cryptalgal fabrics and structures, Hamelin Pool, Western Australia. *American Association of Petroleum Geologists* Memoir, 22: p. 140-194.

Logan, B. W. 1984, Pressure responses (deformations) in carbonate sediments and rocks – analysis and application, Canning Basin. – *In*: Purcell, P. G. ed., *The Canning Basin*, W. A. – Proceedings of the Geological Society of Western Australia/ *Petroleum Exploration Society of Australia*, p. 235-251, Perth.

Long, D. G. F. 1993, Limits on late Ordovician eustatic sea-level change from carbonate shelf sequences: and example from Anticosti Island, Quebec. *In: Sequence Stratigraphy and Facies Associations* Posamentier, H. W., Summerhayes, C. P., Haq, B. U. and Allen, G. P. eds., p. 487-499. *International Association of Sedimentologists*, Special Publication 18.

Longman, M. W. 1980, Carbonate diagenetic textures from nearshore diagenetic environments. Bulletin of the *American Association of Petroleum Geologists* 64, p. 461-487.

Loucks, R. G. & Sarg, J. F. eds., 1990, Carbonate *Sequence Stratigraphy – Recent Developments and Applications*. *American Association of Petroleum Geologists* Memoir, 57, p.545.

Macurda Jr., D. B. 1997, Carbonate seismic facies analysis, *In*: Palaz, I. and Manfurt, K. J. eds., *Carbonate Seismology. Society of Exploration Geophysicists* Geophysical development series, vol. 6, p. 95-120.

Magnavita, L. P., Zalán, P. V., Severino, M. C. G., Rigoti, C. A., Amorin, W. N., Viana, R. A., Gomes, L. C., Guerra, M., Araujo, M. N. C., Lograd, J. C. G., Gontijo, R. C., Urasaki, E. N. A., Mohriak, W. U., Oliveira, J. A. B., Szatmari, P., Santana, G. C. 2010, Estrutura profunda da crosta de uma margem hiperestirada: evidências de exumação do manto na transição crosta continental - crosta oceânica no sudeste brasileiro. *In*: 45º Congresso Brasileiro de Geologia, Belém. *Anais de 45º Congresso de Geologia*, Belém: SBG/Núcleo Norte.

Mahran, T. M. 1999, Late Oligocene lacustrine deposition of the Sodmin Formation, Abu Hammad Basin, Red Sea, Egypt; sedimentology and factors controlling palustrine carbonates. *Journal of African Earth Sciences* 29, p. 567-592.

Manatschal, G. 2010, Extreme crustal thinning and mantle exhumation in deep water rifted margins: the lessons from the Iberia-Newfoundland and Alpine Tethys margins and applications to the pre-salt sag basins of the S-Atlantic. 45º Congresso Brasileiro de Geologi., *In*: *45º Congresso Brasileiro de Geologia*, Belém. Oral presentation: SBG/Núcleo Norte.

Mancini, E.A. & Puckett, M. 2002, Transgressive–regressive cycles in Lower Cretaceous strata, Mississippi Interior Salt Basin area of the northeastern Gulf of Mexico, USA. *Cretaceous Reservoir*, 23, p. 409-438.

Mancini, E. A., Llina´s J. C., Parcell W. C., Aurell M., Ba´ denas, B., Leinfelder R. R., and Benson D. J. 2004, Upper Jurassic thrombolite reservoir play, northeastern Gulf of Mexico. *American Association of Petroleum Geologists*. *Bulletin*, vol. 88, n^{o}. 11 (November), p. 1573-1602.

Martin, R. E. 1999, *Thaphonomy, a Process Approach*. Cambridge Paleobiology Series 4. 508 p.

Mazzullo, S. J., Birdwell, B. A. 1989, Syngentic formation of grainstones and pisolites from fenestral carbonates in peritidal settings. *Journal of Sedimentary Petrology* 59, p. 605-611.

McClay, K. R. & White, M. J. 1995, Analogue modelling of orthogonal and oblique rifting. *Marine and Petroleum Geology*, vol. 12, p. 137-151.

McClay, K. & Khalil, S., 1998. Extensional hard linkages, eastern Gulf of Suez, Egypt. *Geology*, 26, p. 563-566. In: Destro, N., Szatmari, P., Alkmim, F. F. and Magnavita, L. P., 2003, *Release faults, associated structures, and their control on petroleum trends in the Reconcavo Rift, northeast Brazil*. E., 1958. Time stratigraphy. *American Association of Petroleum Geologists Bulletin*, 87 (7), p. 1123-1144.

McClay, K.R., Dooley, T., Whitehouse, P., Mills, M. 2002, 4-D evolution of rift systems: insights from scaled physical models. *American Association of Petroleum Geologists*, 86, p. 935-959.

McClay, K. R., Dooley, T., Whitehouse, P. S. and Anadon-Ruiz, S. 2005, Analogue models of extensional fault systems. *In*: Dore´, A. G. & Vining, B. A. eds., *Petroleum Geology: North-West Europe and Global Perspectives*—Proceedings of the 6th Petroleum Geology Conference, p. 1543–1556. Petroleum Geology Conferences Ltd. Published by the Geological Society, London.

Mcglue, M. M., Soreghan, M. J., Michael, E., Todd, J. A., Cohen, A. Mischler J., O'Connell, C. S., Castanheda,O. S., Hartwell, R. J., Leazzar, K. E. and Nkotagu, H. H. 2010, Environmental controls on shell-rich facies in tropical lacustrine

rifts: A view from Lake Tanganyika's litoral. *Palaios*, vol. 25, p. 426-438. Research Article, SEPM (Society for Sedimentary Geology).

McHargue, T. R. 1990, Stratigraphic development of proto-South Atlantic rifting in Cabinda, Angola petroliferous lake basin. *In*: Katz, B. J. ed., *Lacustrine basin exploration case studies and modern analogs*: *American Association of Petroleum Geologists* Memoir 50, p. 307-326.

Mckenzie, D. P. 1978, Some remarks on the development of sedimentary basins. *Earth Planetary Sciences Letters*, 40, p. 25-32.

Meisling, K. Wheeler, H. E.; Cobbold, P. R.; Mount, V. S. 2001, Segmentation of an obliquely rifted margin, Campos and Santos basins, southeastern Brazil, 1959. Unconformity bounded units in stratigraphy. *American Association of Petroleum Geologists Bulletin*, vol. 85, nº. 11, p. 1903-1924.

Miall, A. D., 1988, Architectural element and bounding surfaces in fluvial deposits: anatomy of the Kayenta formation (Lower Jurassic), southwest Colorado. *Sedimentary Geology* 55: p. 233-262.

Miall, A. D. 1992, Exxon global cycle chart: an event for every occasion. *Geology*, vol. 20, p. 787-790.

Miall, A. D. 1995, Whither stratigraphy. *Sedimentary Geology* 100, p. 5-20.

Middleton, G. V. 1973, Johannes Walther's Law of the Correlation of Facies. *Geological Society of America Bulletin*, vol. 84, p. 979-988.

Milani, E. J. & Davison, I. 1988, Basement control, and transfer tectonics in the Reconcavo–Tucano–Jatoba´ rift, Northeast Brazil. *Tectonophysics* 154, p. 41-70.

Milani, E. J. 1990, Estilos estruturais em bacias sedimentares – revisão conceitual. *In*: G. P., Raja Gabaglia, & E. J., Milani (coordenadores.) *Origem e Evolução de Bacias Sedimentares* Petrobras, p. 75-96.

Mitchum, Jr., R. M., Vail, P. R., Thompson III, S. 1977, Seismic stratigraphy and global changes of sea-level, part 2: the depositional sequence as a basic unit for stratigraphic analysis. *In*: Payton, C. E. ed., *Seismic Stratigraphy* — Applications to Hydrocarbon Exploration. *American Association of Petroleum Geologists* Memoir, vol. 26. p. 53-62.

Mitchum, Jr. & R. M. 1977, Seismic stratigraphy and global changes of sea-level, part 2: glossary of terms used in seismic stratigraphy. *In*: Payton, C. E. ed., *Seismic Stratigraphy — Applications to Hydrocarbon Exploration*. Memoir, vol. 26. *American Association of Petroleum Geologists*, p. 205-212.

Mitchum, R. M. JR & Van Wagoner, J. C. 1991, High-frequency sequences and their stacking patterns: sequence-stratigraphic evidence of high-frequency eustatic cycles. *In*: Biddle K. T. & Schlager W. eds., *The Record of Sea Level Fluctuations*, *Sedimentary Geology* 70, p. 131-60.

Mohriak, W. U. & Dewey, J. F. 1987, Deep seismic reflectors in the Campos Basin, offshore Brazil, *In*: Drummond, M., Smith, C. (Prefacers), *Deep seismic reflection profiling of the continental lithosphere*. *Geophysical Journal of the Royal Astronomical Society*, vol. 89 1: p. 133-140. *Royal Astronomical Society*. Blackwell, London, United Kingdom.

Mohriak, W. U., Mello, M. R., Karner, G. D., Dewey, J. F. and Maxwell, J. R. 1990, Petroleum geology of the Campos Basin, offshore Brazil, ed., *In*: *Classic petroleum provinces*, *American Association of Petroleum Geologists*. Geological Special Publication, nº. 50, p. 119-141.

Mohriak, W. U., Macedo J. M., Castellani R. T., Rangel H. D., Barros A. Z. N., Latge M. A. L., Mizusaki A. M. Szatmari P., P., Demercian L. S., Rizzo J. G., and Aires, J. A. 1995, Salt tectonics and structural styles in the deep-water province

of the Cabo Frio region, Rio de Janeiro, Brazil. *In*: Jackson, M. P. A., Roberts, D. G., and Snelson, S., eds., *Salt Tectonics: A Global Perspective*, *American Association of Petroleum Geologists* Memoir 65, p. 273-304.

Mohriak, W., Nemcok M. and Enciso G. 2008, South Atlantic divergent margin evolution: rift-border uplift and salt tectonics in the basins of SE Brazil: *Geological Society, London*, Special Publications; vol. 294; p. 365-398.

Moore, J.G. 1987, Subsidence in the Hawaiian Ridge. *In*: Decker, W., Wright, T. L., Stauffer, P. H. eds., *Volcanism in Hawaii*. U.S. Geological Survey Prof. Paper 1350, vol. 1: p. 85-100.

Moore, J. G., Campbell, J. F. 1987, Age of tilted reefs Hawaii. J. Geophysics Reservoirs 92, p. 264..

Moore, C. 2001, *Carbonate reservoirs*, p., 460 Amsterdam (Elsevier).

Morgan, W. J. 1972. Plate motion and deep mantle convection. *Geological Society of America.* Memoir, 137: p. 7-22.

Morley, C. K., Nelson, R. A., Patton, T. L. and Munn, S. G. 1990, Transfer Zones in the East African Rift System and their relevance to hydrocarbon exploration in rifts. *American Association of Petroleum Geologists Bulletin*, 74 (8): p. 1234-1253.

Moura, J. A. 1987, Biocronoestratigrafia da sequencia não-marinha do Cretáceo Inferior da Bacia de Campos, Brasil: ostracodes. *In*: *Congresso Brasileiro de Paleontologia*, 10. Rio de Janeiro, SBP, 1987. Anais, p 717-731.

Muniz, M.C., Grassi, A. A.; Hoerlle, M. R. 2003, Considerations about the Stratigraphic and Tectonic Evolution of the Macaé Formation in the Southern of the Campos Basin - Aracajú (SE), (poster section) - IV Petrobras Internal Exploratory Interpretation Symposium – Umpublished.

Muniz, M. C. Grassi, A. A.; Hoerlle, M. R. 2003, Considerations about the Stratigraphic and Tectonic Evolution of the Macaé Formation in the Southern of the Campos Basin - Aracajú (SE), (poster section) - IV Petrobras Internal Exploratory Interpretation Symposium – Umpublished.

Muniz, M. C.; Hoerlle M. R.; Magalhães. J. L. C.; Andrade, H.; Matsuda, N. S.; Carvalho, M. D. 2004, Aptian Stromatolites, A New Exploratory Play? - II Petrobras Internal Symposium of Sedimentology and Stratigraphy – Maragogi (AL) Unpublished.

Muniz, M. C. & Bosence, D. 2008, Sedimentary Evolution in the Aptian of the Campos Basin, Brazil. 14th British Sedimentological Research Group Annual General Meeting - Liverpool, UK, oral presentation (Abstract). Available from: http://www.bsrg.org.uk/meetings_agms_reviews/BSRG 2008_Programme_Abstracts_Volume.pdf

Muniz, M. C., Oliveira F. R. B., Souza Cruz C. E., and Matsuda N. S. 2008, Stratigraphic Analysis and Facies Distribution Model in the Aptian of Campos Basin, Brazil. *American Association of Petroleum Geologists*. International Conference and Exhibition, Cape Town, South Africa – oral presentation Available from: http://www.searchanddiscovery.com/abstracts/html/2008/.../471446.htm?

Naithani, J. & E. Deleersnijder 2004, Are there internal Kelvin waves in Lake Tanganyika, *Geophysics*.

Nemec, W. & Steel, R. J. 1984, Alluvial and coastal conglomerates: their significant features and some comments on gravelly mass-flow deposits. *In*: Koster, E. H. & Steel, R. J. ed., *Sedimentology of Gravels and Conglomerates*. *Canadian Society of Petroleum Geology*, Memoir 10: p. 1-31.

Neuman, E. R. & Ramberg I. B. 1978, Paleorifts concluding remarks. *In* :Neuman, E. R. & Ramberg, I. B. eds. *Tectonics and Geophysics of Continental Rifts*. Dordrecht, D. Reidel, p. 409-424.

Nichols, G. 2009, Sedimentology and Stratigraphy. 2nd ed., Wiley-Blackwell. 419 p.

North American, Commission on Stratigraphic Nomenclature (1983).

Nurnberg, D. & Muller, R. D. 1991, The tectonic evolution of the South Atlantic from Late Jurassic to present: *Tectonophysics*, vol. 191, p. 27-53.

O'Beirne, E. 2011, Pore systems in Mesozoic microbialites: An analogue study from the Purbeck Formation, Dorset, southern England. MSc. project report, Royal Holloway University of London.

Orme, G. R., & Brown, W. W. M. 1963, Diagenetic fabric in the Avonian limestones of Derbyshire and North Wales. Proc. *Yorkshire Geological Society*, 34: p. 51-66.

Patton, T. L., Moustafa, A. R., Nelson, R. A., and Ardine, S. A. 1994, Tectonic evolution and structural setting of the Suez Rift. *In*: Landon, S. M., ed., *Interior Rift Basins*: *American Association of Petroleum Geologists*, Memoir 59, p. 7-55.

Payton, C. E. ed., 1977, *Seismic Stratigraphy – Applications to Hydrocarbon Exploration*. *American Association of Petroleum Geologists Memoir* 26, p. 516.

Paz, J. D. S. & Rossetti, D. F. 2005, Linking lacustrine cycles with syn-sedimentary tectonic episodes: an example from the Codó Formation (late Aptian), northeastern Brazil. *Geology Magazine* 142 (3), p. 269-285. Cambridge University Press. Printed in the United Kingdom.

Peterson, N. M. A. & Von der Borch, C. C. 1965, Chert: Modern inorganic deposition in a carbonate- precipitating locality: *Science* 149, p.1501-1503.

Perlmutter, M. A. & Azambuja Filho, N. C. 2005, Cyclostatigraphy. *In*: Koutsoukos, E. A. M. ed., *Applied Stratigaraphy*. Springer, vol. 23, p. 301-338.

Perry, C. T. 1994, Freshwater tufa stromatolites in the basal Purbeck Formation (Upper Jurassic), Isle-of-Portland, *Dorset Geology Journal*, vol. 29, p. 119-135.

Platt N. H. & Wright V. P. 1991, Lacustrine carbonates: facies models, facies distributions and hydrocarbon aspects. *In*: Anadón, P., Cabrera L., and Kelts, K. eds., *Lacustrine Facies Analalysis*. *Special Publication International Association of Sedimentologists*, 13, p. 57-74.

Platt, N. H. & Wright, V. P., 1992, Palustrine carbonates and the Florida Ever glades: towards an exposure index for the fresh-water environment. *Journal of Sedimentary Petrology* 62, p. 1058-1071.

Platt, N. H. & Wright, V. P. 2009, Lacustrine Carbonates: Facies Models, Facies Distributions and Hydrocarbon Aspects. *In*: Anadón, P., Cabrera, L. and Kelts, K. eds., *Lacustrine Facies Analysis*, Blackwell Publishing Ltd., Oxford.

Playford, P. E. 1990, Geology of the Shark Bay area, Western Australia. *In*: Berry, P. F., Bradshaw, S. D., and Wilson, B. R. eds.,: *Research In Shark Bay*. p. 13-31, West Australian Museum.

Plaziat, J.-C., Baltzer, F., Choukri, A., Conchon, O., Freylet, P., Orszag-Sperber, F., Raguideau, A., and Reyss, J.-L. 1998, Quaternary marine and continental sedimentation in the northern Red Sea and Gulf of Suez (Egyptian coast): influences of rift tectonics, climatic changes and sea-level flucuations *In*: Purser, B. H. & Bosence, D. W. J. eds., *Sedimentation and Tectonics of Rift Basins: Red Sea - Gulf of Aden*: Cambridge, Chapman and Hall, p. 537-573.

Plint, A. G., Nummedal, D. 2000, The falling stage systems tract: recognition and importance in sequence stratigraphic analysis. *In*: Hunt, D., Gawthorpe, R. L. eds., *Sedimentary Response to Forced Regression*. Special Publication, vol. 172. Geological Society of London, p. 1-17.

Posamentier, H. W., Jervey, M. T., Vail, P. R. 1988, Eustatic controls on clastic deposition I - conceptual framework. *In*: Wilgus, C. K., Hastings, B. S., Kendall, C. G. St. C.

Posamentier, H. W., Vail, P. R. 1988, Eustatic controls on clastic deposition II — sequence and systems tract models. *In*: Wilgus, C. K., Hastings, B. S., Kendall, C. G. St. C.

Posamentier, H. W., Morris, W. R. 2000, Aspects of the stratal architecture of forced regressive deposits. *In*: Hunt, D., Gawthorpe, R. L. eds., *Sedimentary Responses to Forced Regressions. Geological Society of London*, Special Publication, vol. 172. p. 19-46.

Posamentier, H. W., Ross, C. A., Van Wagoner, J. C. eds., 2008, Sea Level Changes — An Integrated Approach. *Society of Economic Paleontologists and Mineralogists* (SEPM), Special Publication, vol. 42. p. 125-154.

Postma, G. 1984, Mass-flow conglomerates in a submarine canyon: Abrioja Fan-Delta, Pliocene, Southeastern Spain. *In*: Koster, E. H. & Steel, R. J. ed., p. 237-258. *Sedimentology of Gravels and Conglomerates. Canadian Society of Petroleum Geologists*, Memoir 10, Calgary.

Praça, U. M. 1996, Calcários de águas rasas e calcários palustres da Seqüência das Coquinas, Formação Lagoa Feia, Bacia de Campos. Dissertação de Mestrado, UFRJ.

Pratt, B. R., James, N. P. and Cowan, C. A. 1992, Peritidal carbonates. *In*: Walker, R. G. & James, N. P. eds., *Facies Models: Response to Sea Level Change*, *Geological Association of Canada, GeoText* 1.p. 303-322.

Prezbindowski, D. R. & Tapp, J. B. 1989, Asymmetric dissolution textures as evidence of subaerial exposure. *Journal of Sedimentary Petrology* 59 (5), p. 835-838.

Prosser, S. 1993, Rift-related linked depositional systems and their seismic expression Geological Society, London, Special Publications, vol. 71. p. 35-66.

Purser, B. H., Barrier, P., Montenat, C., Orszag-Sperber, F., Ott D'Estevou, P., Plaziat, J.-C., and Philobbos, E. 1998, Carbonate and siliciclastic sedimentation in an active tectonic setting: Miocene of the north- western Red Sea rift Egypt. *In*: Purser, B. H. & Bosence, D. W. J. eds., *Sedimentation and Tectonics of Rift Basins: Red Sea–Gulf of Aden*: London, Chapman & Hall, p. 239-270.

Purser, et al 1993, Sedimentation and Tectonics. *In*: Larré, L. J. C., 2009. *Seismic stratigraphic analysis of syn-rift deposits of the Coqueiro Seco Formation* (lower to middle Aptian), Sergipe-Alagoas Basin. *Boletim de Geociencias da Petrobras*, Rio de Janeiro, vol. 16, nº. 1, p. 87-101.

Ramzy, M., B. Steer, F. Abu-Shadi, M. Schlorholtz, J. Mika, J. Dolson and M. Zinger 1996, Gulf of Suez basin sequence models - Part B. Miocene sequence stratigraphy and exploration significance in the central and the southern Gulf of Suez. *In*: *Egyptian general petroleum corporation. Thirteen Exploration Conference*, Cairo, Egypt, vol. 2, p. 242-256.

Ranero, C. R. & Perez-Gussinyé, M. 2010, Sequential faulting explains the asymmetry and extension discrepancy of conjugate margins, Month 2010,Nature|3, Macmillan Publishers Limited.

Rangel, H. D., Martins, F. A. L., Esteves, F. R. and Feijó, F. J. 1994, Carta Estratigráfica da Bacia de Campos. *Boletim de Geociências da Petrobras*, vol. 8. (1), p. 203-217.

Rangel, H. D. Martins, C. C. 1998, Main exploratory compartments, Bacia de Campos. Buenos Aires: Schlumberger, Petrobras E&P.

Rangel, H. D. & Carminatti, M. 2000, Rift Lake Stratigraphy of the Lagoa Feia Formation, Campos Basin, Brasil. *In*: E. H., Gierloski-Kodesch and K. R. Kelts, eds., *Lake basins through space and time*: *American Association of Petroleum Geologists* Studies in Geology 46, p. 225-240.

Read, J. F. 1974b, Carbonate bank and wave-built platform sedimentation, Edel Province, Shark Bay, Western Australia: *American Association of Petroleum Geologists*, Memoir 22, p. 1-60.

Read, J. F. & Goldhammer, R. K. 1988, Use of Fischers plot to define third-order sea level curves in peritidal cyclic carbonates, Ordovician, Appalacians: *Geology* 16, p. 895-899.

Read, J. F., Osleger, D., and Elrick, M. 1991, Two-dimensional modeling of carbonate ramp sequences and component cycles. *In*: Franseen, E. K., Watney, L.W., Kendall, C. G. St. C., and Ross, W. eds., *Sedimentary modeling: Computer simulations and methods for improved parameter definition*: *Kansas Geological Survey Bulletin*, 233. p. 473-488.

Reading H. G. & Collinson J. D. 1978, Clastic coast. *In*: Reading H. G. ed., *Sedimentary Environments and Facies, Alluvial sediments*, Oxford, Blackwell Scientific Publications, p 4-14.

Reading H. G. & Collinson J. D. 1978 (1996 3rd ed), Clastic coast. *In*: Reading H. G. ed., *Sedimentary environments, processes, facies and stratigraphy*, Oxford, Blackwell Scientific Publications, p 154-228.

Reading, H. G. 1982, Sedimentary basins and global tectonics. *Proceedings of the Geologists' Association*, 93, p. 321-350.

Reid, R. P., Macintyre, I. G., James, N. P. 1990, Internal precipitation of microcrystalline carbonate: a fundamental problem for sedimentologists. *Sedimentary Geology*. vol. 68, p. 163-170.

Reid, R. P., Macintyre, I. G., and Post, J. E. 1992, Micritized skeletal grains in northern Belize lagoon: a major source of Mg-calcite mud. *Journal of Sedimentary Petrology*, 62, p. 145-156.

Reid, R. P., Macintyre, I. G., Browne, K. M., Steneck, R. S. & Miller, T. 1995, Modern marine stromatolites in the Exuma Cays, Bahamas: Uncommonly Common. Facies, 33: p. 1-18.

Reid, R. P., Visscher, P. T., Decho, A. W., Stolz, J. K., Bebout, B. M., Dupraz, C., Mactintyre, I. G., Paerl, H. W., Pinckney, J. L., Prufert-Bebout, L., Steppe, T. F., and Des Marais, D. J. 2000, The role of microbes in accretion, lamination and early lithification of modern marine stromatolites. Nature, 406: p. 989-992.

Reid, R. P. & Macintyre, I. G. 2000, Microboring versus recrystallization: further insight into the micritization process. *Journal of Sedimentary Research*, 70: p. 24-28.

Reid, R. P., Dupraz, C., Visscher, P. T., Decho, A. W., and Sumner, D. Y. 2003a, Microbial processes forming modern marine stromatolites: microbe-mineral interactions with a three-billion-year rock record. *In*: Krumbein, W. E., Paterson, D. M.

Reid, R. P., James, N. P., Macintire, I. G., Dupraz, C. P., and Burne, R. V. 2003b, Shark Bay Stromatolites: Microfabrics and reinterpretations of origins. Facies, 49: p. 243-270.

Reidel, L. 1932, Die Oberkreid vom Mungofluss in Kamerum und ihre Fauna. Beitrage für Geologische Erforschung. *Deutsche Schutzgebirge*, vol. 16, p. 1-154.

Reineck, H. E & Singh, I. B. 1980, Depositional, sedimentary environments, with reference to terrigenous clastics Springer - Verlag, Berlin and New York, Springer study edition.". p. 505-542.

Richardson, M. & Arthur, M. A. 1988, The Gulf of Suez–northern Red Sea Neogene rift: a quantitative basin analysis: *Marine and Petroleum Geology*, vol. 5, p. 247-270.

Riding, R. 1991, Classification of microbial carbonates. *In*: Riding R. ed., *Calcareous Algae and Stromatolites*. Berlin: Springer-Verlag, p. 21-51.

Riding, R. 1999, The term stromatolite: Towards an essential definition. Lethaia, 32: 321-330.

Riding, R., 2000, Microbial carbonates: the geological record of calcified bacterial-algal mats and biofilms. *Sedimentology*, 47: p. 179-214

Rodrigues, R. 2005, Chemostratigraphy. *In*: Koutsoukos, E. A. M. ed., *Applied Stratigaraphy*. Springer, vol. 23, p. 165-178.

Rosendahl, B.R., Reynolds D. J., Lorber P. M., Burgess C. F., McGill J., Scott D. L., Lambiase J. J. and Derksen S. J. 1986, Structural expressions of rifting: lessons from Lake Tanganyika, Africa. *In*: Frostick L. E., R W Renault, I. Reid and J. J. Tiercelin. eds., *Sedimentation in the African Rifts. Geological Society Special Publication*. London, 25: p. 29-43.

Rosendahl, B. R. 1987, Architecture of continental rifts with special reference to East Africa. *Annual Review Earth Planet. Science Letters*, 15: p. 445-503.

Rosendahl, B. R., Scholz, C. A. and Scott, D. L. 1990, Development of coarse-grained facies in lacustrine rift basins: examples from East Africa, *Geology*, 18: p. 140-144.

Sadler, P. M., Osleger, D. A., Montañez, P. 1993, On the labeling, length, and objective basis of Fischer plots. *Journal of Sedimentary Research* 63, p. 360-368.

Salah, M. G. & Alsharhan, A. S. 1996, Structural influence on hydrocarbon entrapment in the Northwestern North Sea, Egypt. *American Association of Petroleum Geologists Bulletin* 80, p. 101-118.

Salvesen, J. 1978, Variations in the geology of rift basins: a tectonic model: Conference Proceedings, Los Alamos Laboratory, Los Alamos, New Mexico, vol. 7487, p. 82-86.

Sarg, J. F. 1988, Carbonate sequence stratigraphy. *In*: Wilgus, C.K., Hastings, B.S., Kendall, C.G.St.C., Posamentier, H.W., Ross, C.A., VanWagoner, J.C. eds., Sea Level Changes-An Integrated Approach. Special Publication, vol. 42. Society of Economic Paleontologists and Mineralogists (SEPM), p. 155-181.

Sarg J. F., Huang, S., Tanavsuu-Milkeviciene, K., Feng, J. 2012, Lacustrine Carbonates – Facies Evolution, Diagenesis: Eocene Green River Formation, Piceance Creek Basin, Colorado *American Association of Petroleum Geologists*, Hedberg Conference Microbial Carbonate Reservoir Characterization, Houston, Texas (abstract).

Schaller, H. 1973, Estratigrafia da Bacia de Campos, *Anais do XXVII Congresso Brasileiro de Geologia*, vol. 3, p 247-258.

Schlager, W. 1992, Sedimentology and sequence stratigraphy of reefs and carbonate platforms. Continuing Education Course Note Series nº 34. *American Association of Petroleum Geologists*. 71 p.

Schlager, W. 2005, Carbonate Sedimentology and Sequence Stratigraphy. Concepts in Sedimentology and Paleontology nº 8. *Society of Economic Paleontologists and Mineralogists* (SEPM). 200 p.

Scholle, P. A. 1978, A Color illustrated guide to carbonate rock constituents, textures, cements and porosities. *American Association of Petroleum Geologists*, Memoir nº.27, p. 1-241.

Scholz, C. A., Johnson, T. C., Cohen, A. S., Kinge, J. W., Peck, J. A., Overpeck, J. T., Talbot, M. R., Brown, E. T., Kalindekafe, L., Amoako, P. Y. O., Lyons, R P., Shanahan, T. M., Castan˜eda, I. S., Heil, C.W., Forman, S.L., McHargue, L.R., Beuning, K.R., Gomez, J., Pierson, J. 2007, East African mega droughts between 135 and 75 thousand years ago and bearing on early-modern human origins. Proceedings of the National Academy of Sciences 104, p.16416–16421.

Scott, D. C. & Rosendahl B. R, 1998. North Viking Graben: An East African Perspective. *American Association of Petroleum Geologists Bulletin*, 73: p. 155-165.

Seilacher, A. 1976, Preservational history of compressed Jurassic ammonites from southern Germany. Neues jahrbuch für Geologie und Paläontologie Abhandlungen 152: p. 307-56.

Sengor, A. M. C. & Burke, K. 1978, Relative timing of rifting and volcanism on Earth and its tectonic implications. *Geophysics Reserch Letters* 5: 4 1, p. 9-21

Shinn, E. A. & Robbin, D. M. 1983, Mechanical and chemical compaction in fine grained shallow-water limestones. *Journal of Sedimentary Petrology*. 53, p. 595-618.

Silva-Telles, A. C. 1996, Estratigrafia de seqüências de alta resolução do Membro Coqueiros da Formação Lagoa Feia (Barremiano / Aptiano da Bacia de Campos - Brasil). Dissertação de Mestrado. Universidade Federal do Rio Grande do Sul. Curso de Pós-graduação em Geociências Área de Concentração em Estratigrafia.

Silva-Telles, A. C. JR. 1992, Novo Zoneamento das coquinas da formação lagoa feia (Neojiquiá da Bacia de Campos) com base em ostracodes – aspectos evolutivos. *In*: *Congresso Brasileiro de Geologia*, 37., São Paulo, SP, 1992. Boletim de resumos expandidos, - São Paulo: SBG, vol. 2, p. 489.

Simões, M. G., & Holz, M. 2002, Tafonomia: processos e ambientes de fossilização. *In*: Carvalho, I. S. ed. *Paleontologia* , Rio de Janeiro, Interciência. p. 19-45.

Sloss, L. L., Krumbein, W. C., and Dapples, E. C. 1949, Integrated facies analysis. *In:* Longwell, C. R. ed., *Sedimentary facies in geologic history Geological Society of America*, Memoir 39. p. 91-124.

Sloss, L. L. 1962, Stratigraphic models in exploration. *American Association of Petroleum Geologists Bulletin*, vol. 46, p. 1050-1057.

Sloss, L. L. 1963, Sequences in the cratonic interior of North America. *Geological Society of America Bulletin*, vol. 74, p. 93-114.

Smith, A. M. & Mason, T. R. 1991, Pleistocene, multiple-growth, lacustrine oncoids from the Poacher's Point Formation, Etosha Pan, northern Namibia. Sedimentology 38, 591–599. Silicification of Continental Carbonates.

Soreghan, M. J. & Cohen, A. S. 1996, Textural and compositional variability across littoral segments of the Lake Tanganyika: The effect of asymmetric basin structure on sedimentation in large rift Lakes. *American Association of Petroleum Geologists Bulletin*, vol. 80. nº 3, p. 382-409.

Soreghan, G. S., Elmore, R. D., Katz, B., Cogoini, M., Banerjee, S. 1997, Pedogenically enhanced magnetic susceptibility variations preserved in Paleozoic loessite. *Geology*, vol. 25, p. 1003-1006.

Soreghan, M. J., Scholz, C. A., and Wells, J.T. 1999, Coarse-grained deep-water sedimentation along a border fault margin of Lake Malawi, Africa: Seismic stratigraphic analysis: *Journal of Sedimentary Research*, vol. 69, p. 832–846.

Spencer, G. H. & Tucker, M. E. 2007, Perspectives - A proposed integrated multi-signature model for peritidal cycles in carbonates. *Journal of Sedimentary Research*. 77, nº. 9, p. 797.

Spry, A. 1969; *Metamorphic Textures. Pergamon*, Oxford, 350 p.

Stecker, M. S., Berthelot, F., Lyberis, N., and Le Pichon, X. 1988, Subsidence in the Gulf of Suez: implications for rifting and plate kinematics: *Tectonophysics*, vol. 153, p. 249-270.

Stolz, J. F. 2000, Structure of microbial mats and biofilms. *In*: Riding, R. E., Awramik, S. M. eds., *Microbial Sediments*. New York: Springer-Verlag, p. 1-9.

Storey, B. C., Alabaster T. and Pankhurst R. J. 1992, Magmatism and cause of continental break-up, *Geological Society of London Special Publication* p. 68.

Strasser, A. 1991, Lagoonal-peritidal sequences in carbonate environments: autocyclic and allocyclic processes. *In*: Einsele, G., Ricken, W, and Seilacher, A. eds., Cycles and Events in Stratigraphy: Berlin (Springer- Verlag), p. 709-721.

Swift, D. J. P.; Figueiredo, A. G.; Freeland, J. L. and Oertel, G. F. 1983, Hummoki cross-stratification and megarripples: a geological double-standard *Journal do Sedimentary Petrology*, vol. 53, p. 1295-1317.

Swift, D. J. P., Thorne J. A. & Oertel G. F. 1986, Fluid process and sea floor responses on a storm dominated shelf; middle Atlantic shelf on North America. Part II. Response of the shelf floor. *In*: Knight R. J. & Mclean J. R. eds., *Shelf sands and sandstones Canadian Society of Petroleum Geologist,* Memoir 11, p. 191-211, Calgary.

Talbot, M. R. & Allen, P. A. 1978, *Lakes – Sedimentary Environments, process, facies and stratigraphy*, Reading H. G. ed., Blackwell.

Talbot, M. R. 1990, A review of the palaeohydrological interpretation of carbon and oxygen isotopic rations in primary lacustrine carbonates. *Chemical Geology* (Isotope Geoscience Section), vol. 80, p. 261-279.

Taylor, J. D. & Hall, A. 1969, Environmental and Biological controls on bivalve shell mineralogy. *Biological Reviews*, 44: 499-530.

Terra, G. J. S., Rodrigues, Freire, E. B. E. B., Lykawka, R., Raja Gabaglia, G. P., R. M., Hernández, J. I. 2012, Salta Basin, Argentina: A Good Analog for Hernández, Phanerozoic Lacustrine Microbialite-Bearing Reservoirs *American Association of Petroleum Geologists*, Hedberg Conference Microbial Carbonate Reservoir Characterization, Houston, Texas (abstract).

Thompson, L. 1999, Atlas of Borehole Imagery, *American Association of Petroleum Geologists* Discovery Series, nº. 4.

Thorne, J. A. & Watts A. B. 1984, Seismic reflectors and unconformities at passive continental margins, Nature, 311, nº. 5984, p. 365-368.

Tiercelin, J-J; Soreghan, M.; Cohen, A.S.; Lessar, K-E.; and Bouroullec, J-L. Sedimentation in large rift lakes: Example from the middle Pleistocene- modern deposits of the Tanganyika Trough, east African rift system. Bulletin Centres Research Exploration-Production. Elf Aquitaine, 16, 1, p. 83-111.

Tucker, M. E., Calvet, F., and Hunt, D. 1993, Sequence stratigraphy of carbonate ramps: systems tracts, models and application to the Muschelkalk carbonate platforms of eastern Spain. *In:* Posamentier, H. W., Summerhayes, C. P., Haq, B. U. and Allen, G. P. eds., *Sequence Stratigraphy and Facies Associations*

International Association of Sedimentologists, Special Publication 18, p. 397-415.

Tucker, M. E. 2007, A proposed integrated multi-signature model for peritidal cycles in carbonates. *Journal of Sedimentary Research* 77, p. 797-808.

Vail, P. R., Mitchum, R. M. Jr., and Thompson, S. III 1977, Seismic stratigraphy and global changes of sea level, part four: global cycles of relative changes of sea level. *American Association of Petroleum Geologists Memoir* 26, p. 83-98.

Vail, P. R., Mitchum, R. M., Jr., Thompson III, S. 1977, Seismic stratigraphy and global changes of sea level, part 3: relative changes of sea level from coastal onlap. *In*: Payton, C. E., ed., *Seismic Stratigraphy - Applications to Hydrocarbon Exploration*. *American Association of Petroleum Geologists*, Memoir, vol. 26, p. 63-81.

Vail, P. R., Hardenbol, J., and Todd, R. G. 1984, Jurassic unconformities, chronostratigraphy and sea-level changes from seismic stratigraphy and biostratigraphy. *In:* Schlee, J. S. ed., *Interregional Unconformities and Hydrocarbon Accumulation* p. 129-144

Vail, P. R. 1987, Seismic stratigraphy interpretation procedure. *In:* Bally, A. W., ed., *Atlas of Seismic Stratigraphy, American Association of Petroleum Geologists* Studies in Geology 27, p. 1-10.

Valero Garce´s, B.L., Kelts, K., Ito, E. 1995, Oxygen and carbon isotope trend sand sedimentological evolution of a meromictic and saline lacustrine system: the Holocene Medicine Lake basin, North American Great Plains, U.S.A.. *Palaeogeography, Palaeoclimatology, Palaeoecology* 117, p. 253-278.

Van der Pluijm, B. A. & Marshak S. 1997, Earth Structure: *An introduction to structural geology and tectonics*. p. 495. WCB/McGraw-Hill.

Van Wagoner, J. C., Posamentier, H. W., Mitchum, R. M., Vail, P. R., Sarg, J. F., Loutit, T. S., Hardenbol, J. 1988, An overview of sequence stratigraphy and key definitions. *In*: Wilgus, C. K., Hastings, B. S., Kendall, C. G. St. C., Posamentier, H. W., Ross, C. A., Van Wagoner, J. C. eds., *Sea Level Changes – An Integrated Approach*. *Society of Economic Paleontologists and Mineralogists* Special Publication, vol. 42. (SEPM), p. 39–45

Van Wagoner, J. C., Mitchum Jr., R. M., Campion, K. M., Rahmanian, V. D. 1990, Siliciclastic sequence stratigraphy in well logs, core, and outcrops: concepts for high-resolution correlation of time and facies. *American Association of Petroleum Geologists* Methods in Exploration Series, vol. 7, p. 55.

Van Wagoner, J. C. & Bertram, G. T. eds., 1995, Sequence Stratigraphy of Foreland Basin Deposits, *American Association of Petroleum Geologists* Memoir 64, p. 487.

Walker R. G. ed., 1979, *Facies models Geosciences Reprint Series*, 211 p.

Walker, R. G. 1992, Facies, facies models and modern stratigraphic concepts. *In*: Walker R. G. & James N. P. eds., *Facies Models: Response to Sea Level Change* p. 1-14. *Geological Association of Canada*, GeoText 1.

Walker, M. R. & Plint, A. G. 1992, Facies, Wave- and storm dominated shallow marine systems. *In*: Walker, R. G, James, N. P. eds., *Facies Models – Response to sea level change*. *Geological Society of Canadá*, p. 219-238.

Walsh, J. J. & Watterson, J. 1991, Geometric and kinematic coherence and scale effects in normal fault systems. *In*: Roberts, A. M., Yielding, G., Freeman, B. eds., *The geometry of Normal Faults*. *Geological Society Special Publication* 56, p. 193-206.

Wentworth, C. K. 1922, "A scale of grade and class terms for clastic sediments", *Journal of Geology*, vol. 30, p. 377-392.

Wernicke, B. & Burchfiel, B. C. 1982, Modes of extensional tectonics: *Journal of Structural Geology*, 4, p. 105-115.

Wernicke, B. 1985, Uniform sense normal simple shear of continental lithosphere. *Canadian Journal of Earth Science*, 22, p. 108-125.

Wheeler, H. E. & Murray, H. H. 1957, Base level control patterns in cyclothemic sedimentation. *American Association of Petroleum Geologists Bulletin*, vol. 85, nº. 11, p. 1903-1924.

Wheeler, H. E. 1958, Time stratigraphy. *American Association of Petroleum Geologists Bulletin*, vol. 42, p. 1047-1063.

Wheeler, H. E. 1959, Unconformity bounded units in stratigraphy. *American Association of Petroleum Geologists Bulletin*, vol. 43, p. 1975-1977.

Wheeler, H. E. 1964, Baselevel, lithosphere surface, and timestratigraphy. *Geological Society of America Bulletin*, vol. 75, p. 599–610.

White, R. S. & McKenzie, D. P. 1989, Magmatism at rift zones: the generation of volcanic continental margins and flood basalts. *Journal of Geophysical Research*, 94, p.7.685–7.729.

Wilgus, C. K., Hastings, B. S., Kendall, C. G. St. C., Posamentier, H. W., Ross, C. A., and Van Wagoner, J. C. eds., 1988, *Sea Level Changes–An Integrated Approach*. (*Society of Economic Paleontologists and Minera*logists), SEPM Tulsa, Oklahoma, Special Publication 42, p. 407.

Wilgus, C. K., Hastings, B. S., Kendall, C. G. 2008, Salt tectonics in the basins of SE Brazil South Atlantic divergent margin evolution: rift-border uplift and Geological Society, London, Special Publications 2008; vol. 294; p. 365-398.

Wilson, J. L. 1975, *Carbonate facies in geologic history*: Springer-Verlag. New York, 471 p

Winter, W. R., Jahnert, R. J., França, A. B. 2007, Carta Estratigrafica da Bacia de Campos, *Boletim de Geociências da Petrobras*, Rio de Janeiro, vol. 15, nº. 2, p. 511-529.

Withjack, M. O. & Jamison, J. R. 1986, Deformation produced by oblique rifting. *Tectonophysics*, vol. 126, p. 99-124.

Withjack, M. O. & Olsen, P. E. 2002, Rift basin structure and its influence on sedimentary systems. *In*: Robin W. R. & Ashley, M. eds., *Sedimentation in continental rift*, Tulsa Oklahoma USA, SEPM Special publication nº 73 p. 57-81.

Withjack, M. O., Schlische, R. W., Eisenstadt, G. 2002, An Experimental Study of the Secondary Deformation Produced by Oblique-Slip Normal Faulting *American Association of Petroleum Geologists. Bulletin* vol. 86; Issue 5; p. 885-906.

Wright, V. P. 1990, Singenetic formation of grainstones and pisolites from fenestral carbonates in peritidal settings – discussion. *Journal of Sedimentary Petrology*, 60: p. 309-310.

Wright, V. P. 1992, Speculations on the controls on cyclic peritidal carbonates: icehouse versus greenhouse eustatic controls: *Sedimentary Geology*, vol. 76, p. 1-5.

Young, M. J., Gawthorpe, R. L., and Sharp, I. R. 2003, Normal fault growth and early syn-rift sedimentology and sequence stratigraphy: The Fault, Suez Rift, Egypt: *Basin Research*, vol. 15, p. 479-502.

Zhang, R., Zhang, R., X. Zheng, Chen, L. 2005, Major Chinese field evaluated using combined seismic and well logging methods (Reservoir Characterization) *World*

oil online, vol. 228 nº. 10 Â. Available from: http://www.worldoil.com/October-2007-Major-Chinese-field-evaluated-using-combined-seismic.

Appendix C- Outcrop Analogue Studies; Gulf of Suez (Egypt) and Dorset (UK).

C.1 Introduction.

A good 3D subsurface geological model may be made with seismic data, well data, such as electric logs and cores. However its validity can be improved by comparison with outcrop analogues. Seismic data provide the geometric observations on the stacking and correlation of sedimentary deposits. Well data provides sedimentological and stratigraphical information through the analysis of depositional facies, petrography and diagenesis and also biostratigraphy. Outcrop analogues, however, are useful in that field observations can provide information on lateral facies distribution, geometries and also to validate the tectono-stratigraphic relations.

In order to compare and validate the model erected, short field trips to the Gulf of Suez, Egypt and also to the Isle of Portland, Dorset, UK were undertaken. The field trip to the Gulf of Suez focused on the geometries and carbonate- clastic interactions of a fault-block carbonate platform and the visit to Dorset studied the textures fabrics of stromatolites and thrombolites, the distribution of these facies and their likely reservoir characteristics.

C.2. Abu Shaar carbonate platform, Gulf of Sue, Egypt

The Abu Shaar carbonate platform, Miocene of the Gulf of Suez, Egypt is one of the best exposed examples of a carbonate platform that developed in rift system (Figure C.1). Despite being a marine rift of a smaller dimension than the South Atlantic passive margin there is a marked similarity in the evolutionary history of the stratigraphy in relation to the tectonic phases. However, the facies differ in that they are mostly formed in a marine environment with the exception of the upper most, non-marine units. Figure C.2 points out the similarities and differences between the carbonate platforms in the Gulf of Suez and Campos Basin. From this it is evident that the rift of the Gulf of Suez has a developed pre-rift succession on top of the basement that is not observed in the Campos Basin. Conversely the post-rift sequence with high rate of thermal subsidence and formation of oceanic crust are present in the South Atlantic but not in the Gulf of Suez (Figure C.2).

Analysis of the Barremian-Aptian age interval of the Campos Basin reveals a particular tectono-stratigraphic evolution for the pre-salt succession. This evolution is characterised by an oblique rift system with extensional faults and synthetically rotated domino style fault blocks (Chapter 4, Figure 4.26). It is not possible to differentiate seismically between the Precambrian basement from the initial basal syn-rift basalt. So the term “acoustic basement” is used for the material below the syn-rift unconformity.

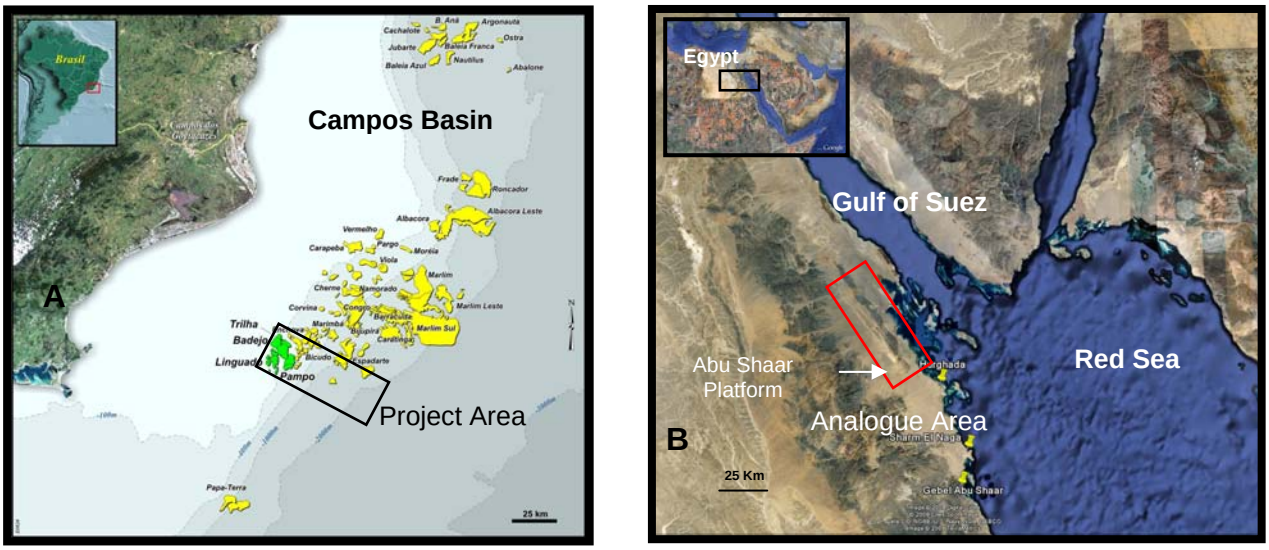

Figure C.1 - Maps of location. A - Study area in the Campos Basin, Brazil; B - Area of the analogue study in the Gulf of Suez, Egypt. Note the difference of scale of the two areas.

The half-graben formed during the initial rifting in both cases are filled with alluvial fan conglomerates and fluvial sandstones in the early syn-rift stage. This sedimentary succession is followed upward by a bioclastic carbonate platform, predominantly bivalve rudstones (coquinas) in Campos Basin but photozoan marine carbonates in the Gulf of Suez, in the late syn-rift stage, which is less tectonically active. The post-rift sag phase in both cases is marked by abundance of non-marine microbialites (stromatolites and laminites) and rarely oolites. Both of the successions underlie a thick layer of salt; both halite and anhydrite.

		Gulf of Suez				Campos Basin			
Tectonic Regime	Phase	Time-Age	Tectonic Structures	Sediments and Stratigraphy	Unit	Phase	Time-Age	Tectonic Structures	Sediments and Stratigraphy
RIFT	Late Syn-rift	Late Miocene	tectonic quiescent	evaporites gypsum + anhydrite	C2	Post	Aptian	thermal subisidence	evaporites halite + anhydrite
				dol. microbial laminites restricted	C1		Aptian	thermal subisidence	stromatolites+ microbial laminites
	Mid Syn-rift	Mid. Miocene	fault blocks transfer faults corredors	more restricted fine terrigenous + stromatolites + marginal corals	B3	Late Syn	Aptian	less accommodation	rudstones of bioclasts (coquinas gastropods) + microbial mats
		Early Mid. Miocene	more eustatic influenced	shelf edge reefs + rudstones of marine bioclasts	B2	Mid. Late Syn	Aptian Barremian	fault and rotated blocks	rudstones of non marine bioclasts (coquinas)
		Mid. Miocene	block faulting/tilting	fan deltas + reefs	B1	Mid. Syn	Barremian	fault / rotated blocks	clastics + coquinas +Ostracods
	Early syn-rift	Early Miocene	tilting block graben subsidence	marine marls + gypsum bed	A2	Early Mid. Syn	Barremian	fault blocks	talc stevensite siltstone
		Early Miocene	normal faults - tilting	alluvial fans (reddish) +playa+basalt	A1	Early syn	Barremian	fault blocks	alluvial fans (reddish) +Basalts
	Pre-rift	Oligocene + Eocene		pre-rift strata	N	Pre-rift			(Acoustic Basement)

Fresh water continental environment Open marine environment Restrict environment

Figure C.2– Similarities and differences between the pre-salt Barremian / Aptian successions in the Campos Basin and the Miocene Carbonate Platform in the Gulf of Suez.

In contrast to the Campos Basin, in the Gulf of Suez, the Precambrian basement (P) is well exposed in outcrops (Figure C.6), and all the rift succession can be seen with exception of the evaporates that are only known from the subsurface (Figures C.3 and C.5). The pre-rift cover in the Gulf of Suez is characterised by the Nubian sandstones, Upper Cretaceous-Paleocene - Eocene strata (N), (Figures C.2 and C.5). The syn-rift stage is expressed by domino style, rotated fault-blocks, formed by extensional tectonics (Figure C.5). As a consequence, the Gulf of Suez basin is filled by syn-rift units: terrigenous sediments, sandstones and basal conglomerates (Figures C.3 and C.4) interpreted by Plaziat et al. (1998) as continental alluvial fans-playa deposits, interbedded with basalt flows of the Abu Ghusun Formation (A1), marine marls with gypsum beds of the Rosa Member of the Ranga Formation (A2); and coarse terrigenous fan-deltas with capping reefs (B1).

Continuing the sedimentation process, the late syn-rift stage in the Gulf of Suez is characterized by carbonate sediments, rudstones of marine bivalves (Figure 10.4) and coral reefs close to the shelf-edge (Figures C.4, C.8 and C.9). The footwall shelf-edge coral reefs are commonly associated with mixed clastic/carbonates marine sediments (B2) (Plaziat et al. 1998). At the upper part of these successions, finer terrigenous deposits with widespread stromatolites and marginal coral biostromaes (B3); microbial laminites and stromatolites associated with oolites and marine ostracods (Figures 10.5 and 10.6), encrusting the platform and peripheral slope (C1). These microbial carbonates are commonly formed in period of restricted basin (Figures C.4, C.10 and C.11).

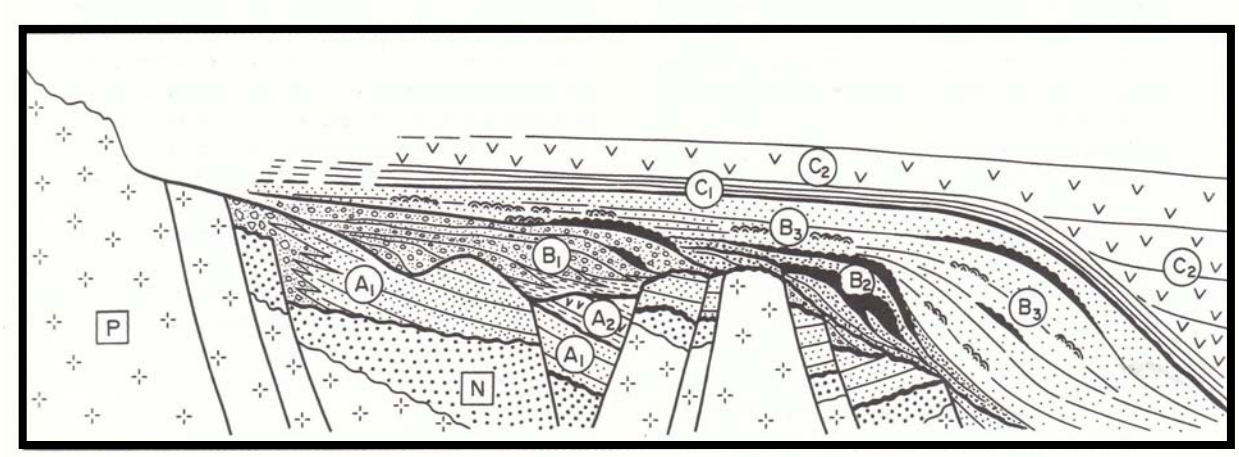

Figure C.3 – Generalized chronological and spatial relationships between the diverse settings of the North-western Red Sea coast and the informal lithostratigraphic units proposed in Plaziat *et al.* (1998).

This non-marine succession formed in more tectonically quiescence settings with the rift almost filled of sediments and very little new accommodation generated. The microbial laminites and stromatolites formed in this context are dolomitized, brecciated and are capped by onlapping late Miocene gypsum, with fine terrigenous intercalations (Plaziat *et al*. 1998). Figures C.6 to C.11 show outcrops of the Abu Shaar carbonate platform, aggradational parallel stacking patterns, and lateral continuity of the Miocene carbonate sequence, exposed in Wadi Kharasa, on the southern tip of Abu Shaar, Egypt.

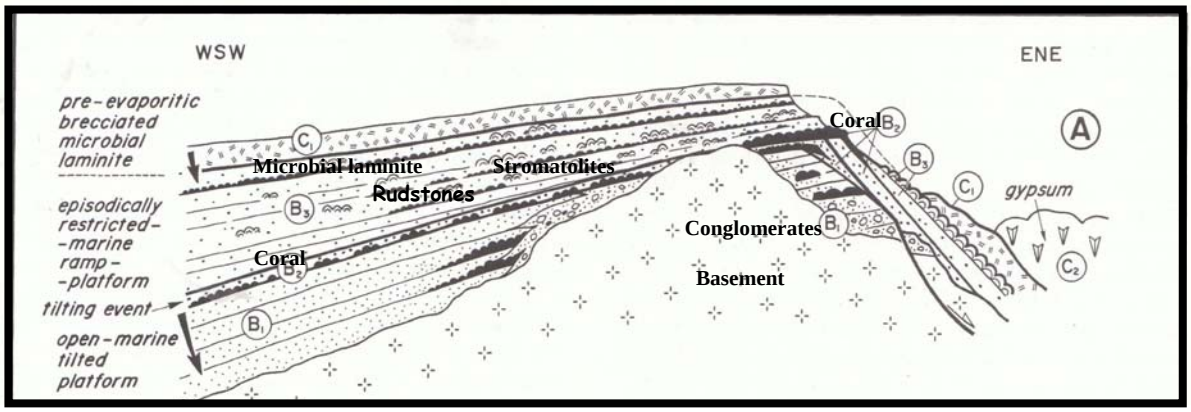

Figure C.4 – Major lithostratigraphic units of the Abu Shaar platform proposed in Plaziat *et al*. 1998.

The Figure C.2 shows the tectonic and stratigraphic framework similarities of the Campos Basin and Gulf of Suez. Apart from main differences in evolution and dimensions, both basins show extensional tectonics with a similar structural pattern of fault and rotated blocks, forming horst and graben that control the deposition, facies distribution and geometry of syn and post-rift strata.

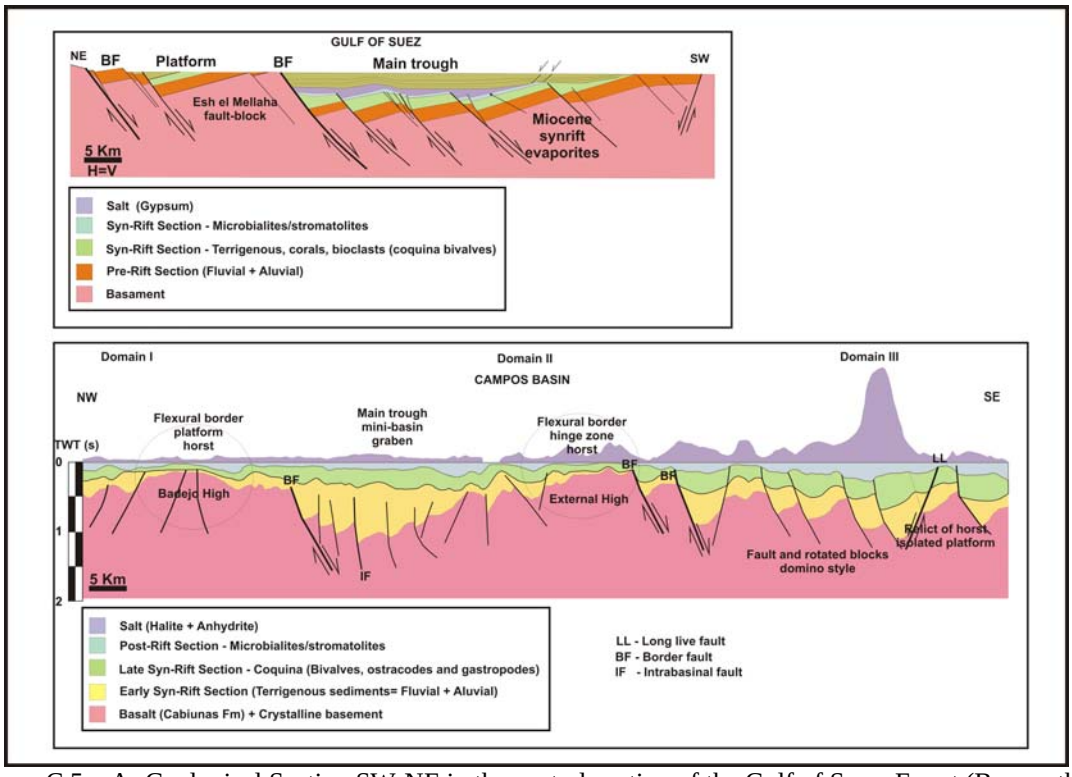

Figure C.5 – A- Geological Section SW-NE in the central portion of the Gulf of Suez, Egypt (Bosworth *et al*. 1998) Withjack *et al*. 2002, after Colletta *et al*. 1988. B - Geological Section NW-SE in the south central portion of the Campos Basin, Brazil (after. Muniz *et al*. 2003).

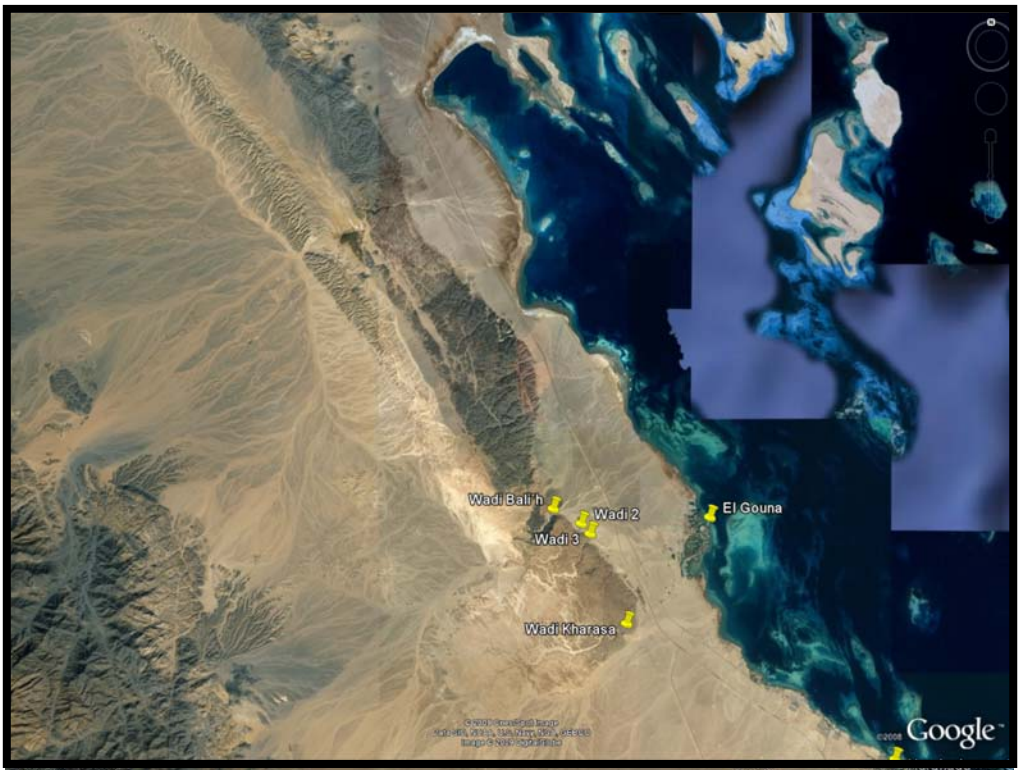

Figure C.6 – Satellite image of the Abu Shaar platform, Gulf of Suez, Egypt. Showing the exhumed Esh el Mellaha fault-block dissected by various incised wadi sections.

Figure C.7 – Panoramic view showing the stacking pattern, aggradational parallel beds with lateral continuity of the Miocene carbonate sequence, desiccated by the Wadi Kharasa, Egypt.

Figure C.8 – Abu Shaar platform edge, footwall margin, showing progradational lenticular geometry of bioclastic and reefal carbonates.

Figure C.9 – Mollusc rudstones exhibiting mouldic and vuggy porosities. They occur at the intermediate stratigraphic zone in the Miocene carbonate platform.

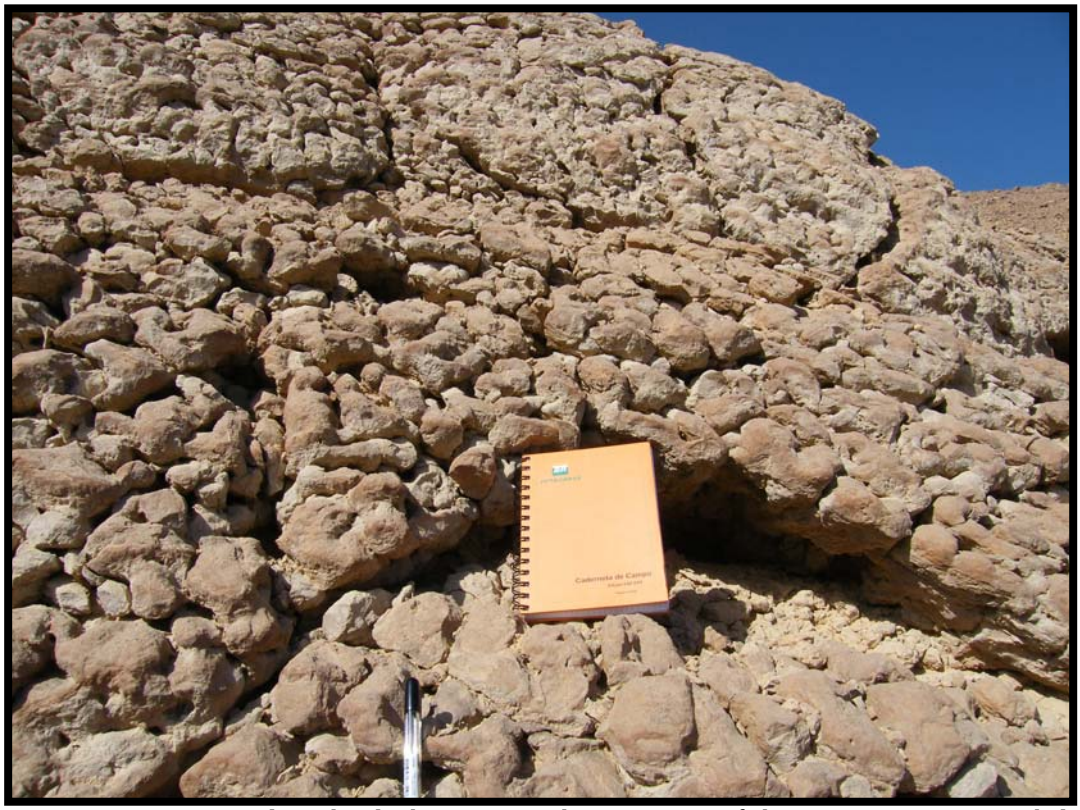

Figure C.10 - Stromatolites, heads that occur at the upper part of the Miocene succession, below the onlapping strata of salt (gypsum).

Figure C.11 – Loose block showing stromatolite heads. Detail of laminar internal structures and porosity. This type is trapping and bedding style forming semi-continuous sheets or laterally linked hemispheroids of Logan *et al*. (1964).

C.3 Thrombolites and stromatolites of the Purbeck Formation, Upper Jurassic, Isle of Portland, Dorset, UK.

The microbialites of the Lower Purbeck Formation (Upper Jurassic / Lower Cretaceous) are extensively exposed on the Isle of Portland, Dorset, UK (Figures C.12 to C.14). They show characteristic features of freshwater tufas (Bosence, 1987; Perry, 1994), with mainly thrombolitic textures. Three outcrops in disused quarries were visited over 2 days in order to examine microbialite facies and associated sediments. Samples were collected from each the facies and compared with those described and interpreted by Bosence (1987).

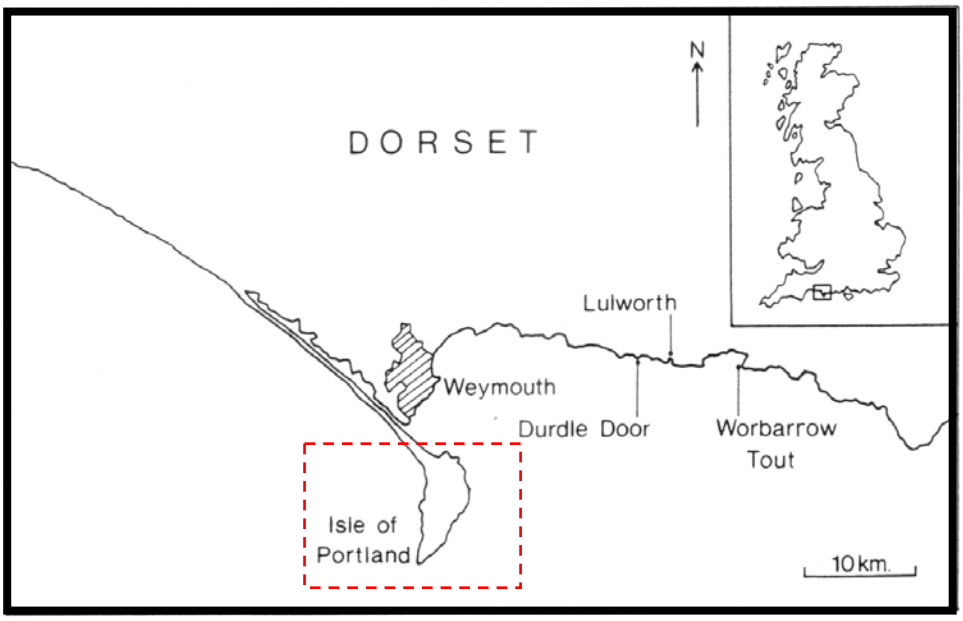

Figure C.12 - Location map of the microbialite studies, Isle of Portland, Dorset, southern England (Perry, 1994).

Three Two main potential reservoir facies is identified were studied in the outcrops visited: The coquinas and within the Portland oolites carbonates of Jurassic age, and also the thrombolites of the Purbeck Formation, Lower Cretaceous both of Late Jurassic age (Figure C.14). The coquinas, bivalve shell rich limestones, and also the oncoids and oolitic carbonates, are interpreted to form in a shallow marine environment. These marine carbonate deposits are overlain by a fossil soil which marks the passage from marine succession to non-marine microbialite carbonates of the Purbeck Formation (Top Cap) (Fig C.14)

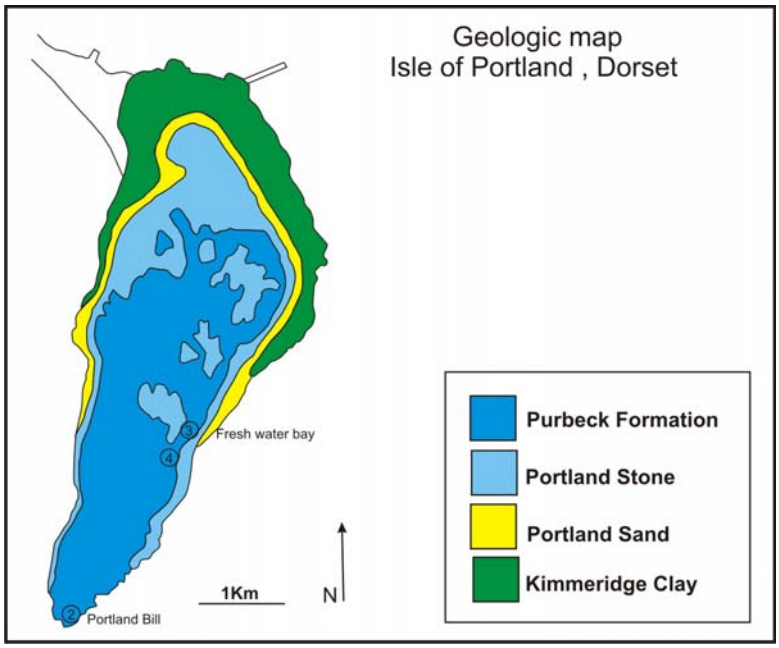

Figure C.13 - Geologic map of Portland, Dorset, UK. The numbers 2, 3 and 4 are outcrops of microbialites from Purbeck Formation visited in disused quarries.

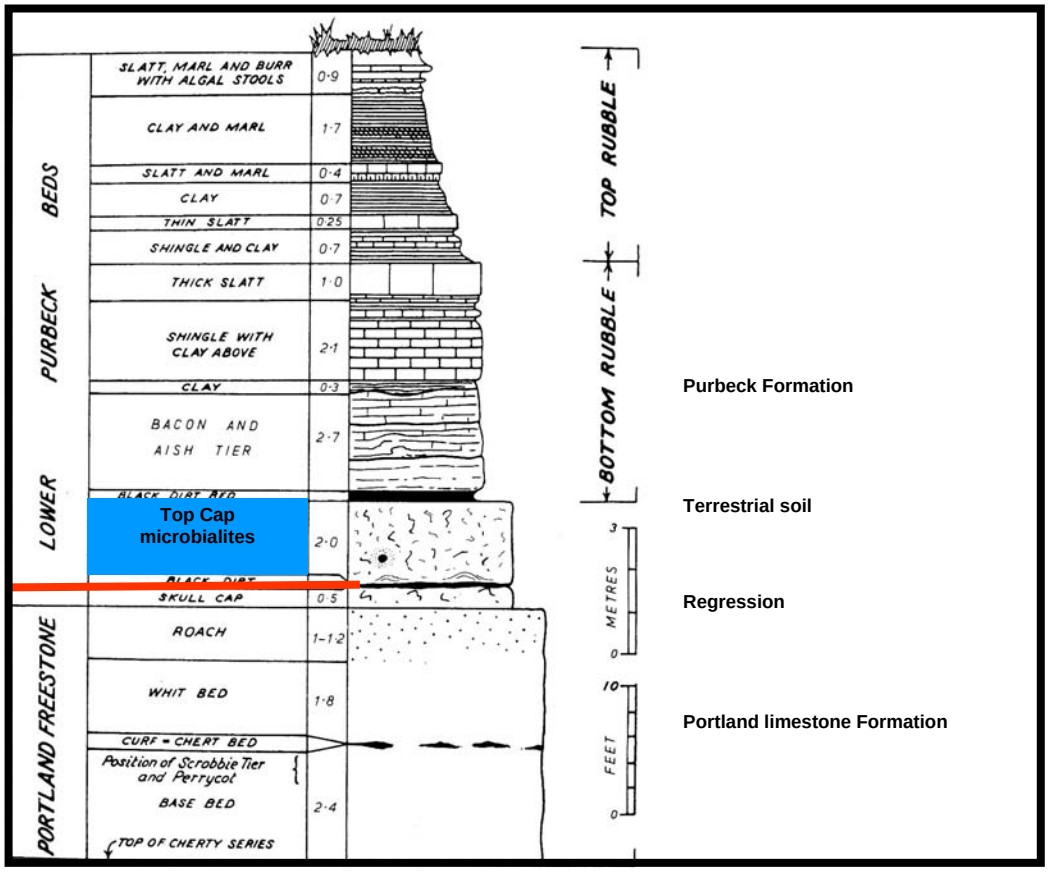

Figure C.14 – Isle of Portland stratigraphy, from House (1989). The blue rectangle marks the stratigraphic interval studied.

The carbonates of the Lower Purbeck Formation comprise microbialites, (thrombolites and stromatolites) occurring as unusual growth pattern. Four subfacies have been recognized in the Purbeck stromatolites (Bosence, 1987): basal laminated microbialite, burrowed collar, intramound thrombolite, and intermound grainstones (Figure C.15). The microbialites accumulated around the trunks of standing and fallen trees, forming doughnut-shaped “burrows”, similar occur in a modern Coorong Lagoon, South Australia. The thrombolites then grew up forming irregular, metre-scale mounds, with irregular framework porosity and also burrows (Figure C.15; Bosence, 1987). Commonly the pore space in the thrombolites, is filled with peloids (Figure C 16) and shows geopetal structures (Figure C.17). Stromatolites show framework porosity with expected good connectivity among the pores (Figure C.18). Intermound areas accumulate grainstones / rudstones with intergranular porosity (Figure C.19). These deposits comprise 75% of the area of 3 m by 10 m studied quarry sections (O’Beirne, 2011). The carbonate rocks generally exhibit good visual porosity and also good connectivity despite of the high heterogeneity of the rock (Figures C17 and C.19).

The microbialite-rich Aptian succession of the Campos Basin, studied in the well 20 and described in Chapter 7 (section 7.3) shows in sidewall core samples and FMI image logs, areas of microbialites, as stromatolites (Figure C.18), laminite facies, and also rare thrombolites (Figure C.21) with similar characteristics to those seen in the Purbeck Formation, Dorset (Figure C.20). However whilst the Purbeck Formation was deposited marginal to a shallow marine area during regression, the Macabu Formation, in the Campos Basin, was deposited in a fluvio-lacustrine conditions prior to the first marine incursions and salts of the South Atlantic (Hessel & Mello, 1987).

The bioclastic grainstones section of the Macabu Formation in the Campos Basin, are interpreted to be an intermound facies and displays intraclasts of grainstones with ooids occasionally with nuclei of stromatolite intraclasts (Figures C.22 and C.23). In the Campos Basin, the high porosity of the Purbecks is not preserved due to the high degree of compaction (Figure C.23) and mechanical deformation of the stevensite grains to form a pseudo-matrix. Comparing the thrombolite textural features from the two areas shows remarkable similarities (cf. Figures C.21 and C.22) even though the processes that formed these two rock types are still poorly understood.

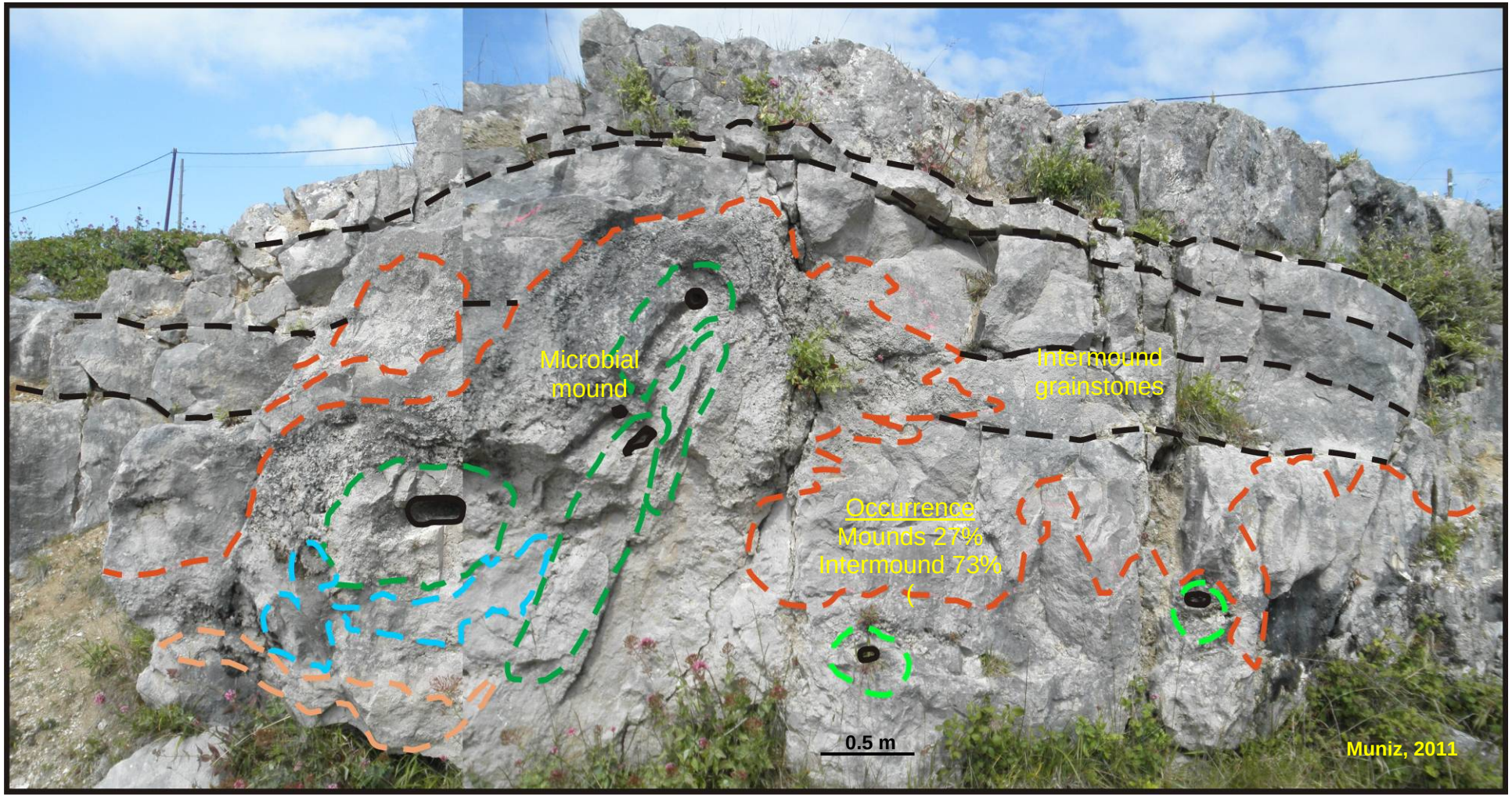

Figure C.15 – Four subfacies is identified in the outcrop in a disused quarry at Freshwater Bay, Portland Island. The internal geometry and facies distribution of the thrombolites and stromatolites of the Lower Purbeck Formation in the three metre thick are seen. The outcrop is composed of 27% of mound structures and 73% of intermound sediments (Bosence, 1987; O'Beirne, 2011).

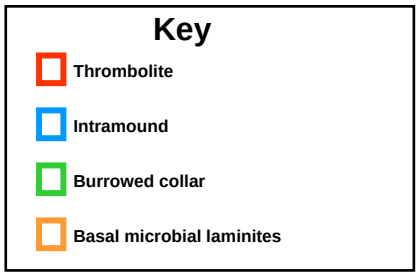

Figure C.16 - Basal laminated portion of mound exhibiting trapping and binding sediment structure. Porous spaces filled with peloids.

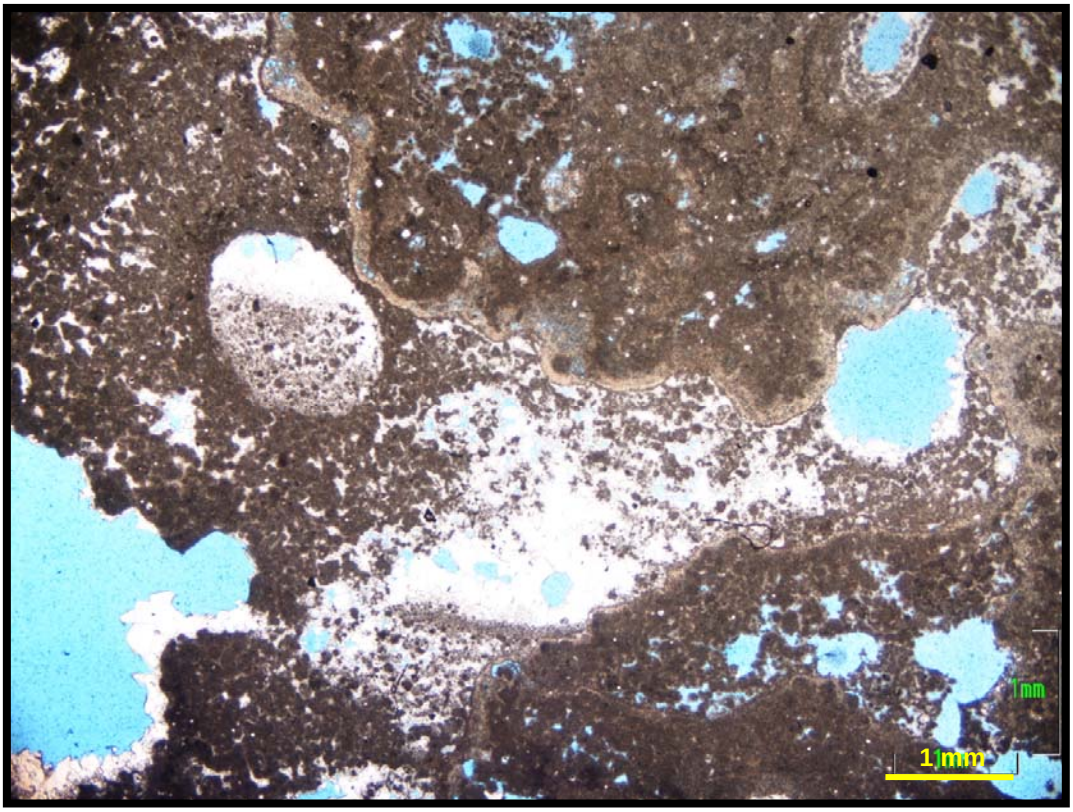

Figure C.17 Burrowed collar –irregular structure showing agglutinated peloidal sediment. Some rounded holes are burrows partially filled with peloids to form geopetal structures. Irregular borders, agglutinated peloids and thin (brown) cement fringe of calcite.

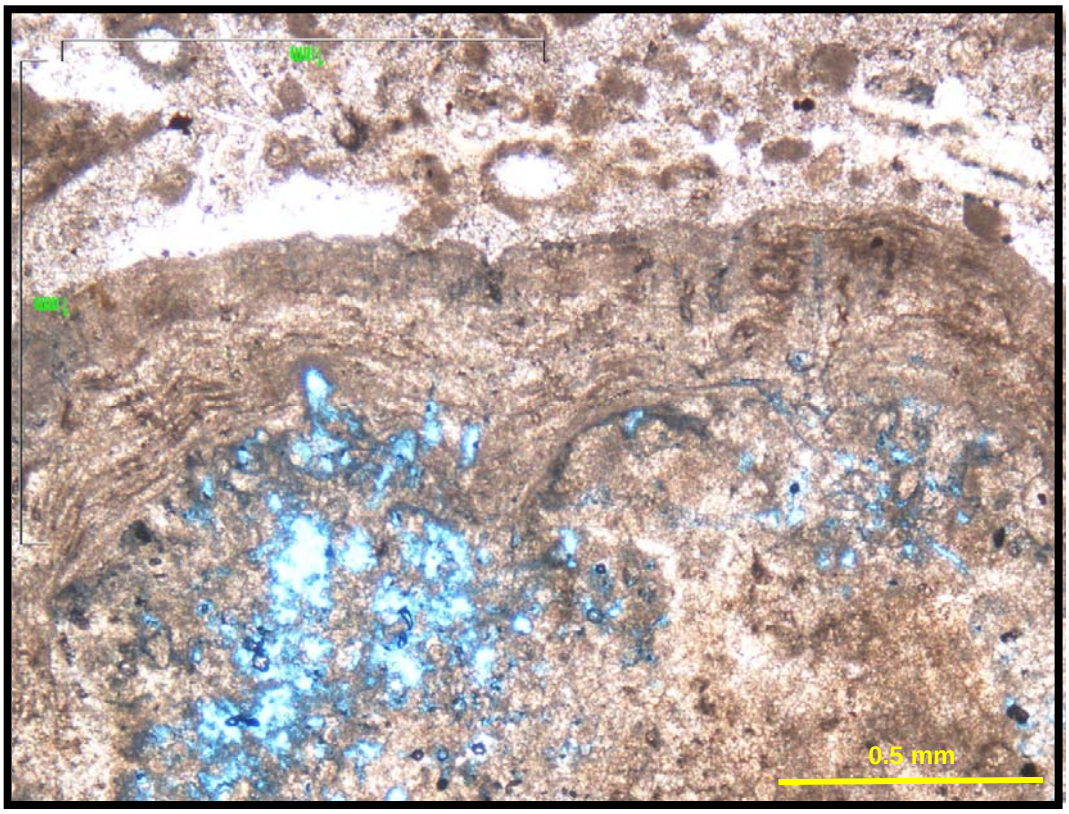

Figure C.18 Intra mound stromatolites showing some laminated structures, algal filaments. Some holes filled by calcite microspar or spar calcite. Intercrystalline and mouldic porosities. The upper part is burrowed and cemented.

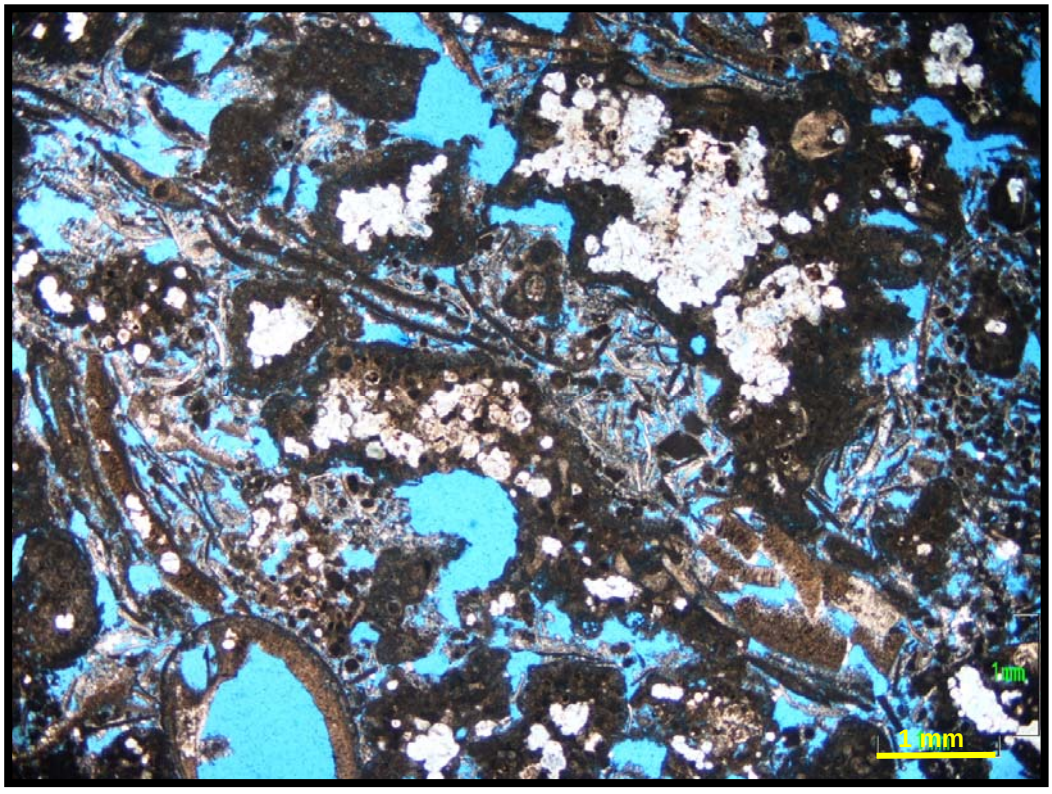

Figure C.19 intermound bioclastic grainstone with broken shells of bivalves and peloids some silica replacement. Very porous, with intergranular and mouldic pores.

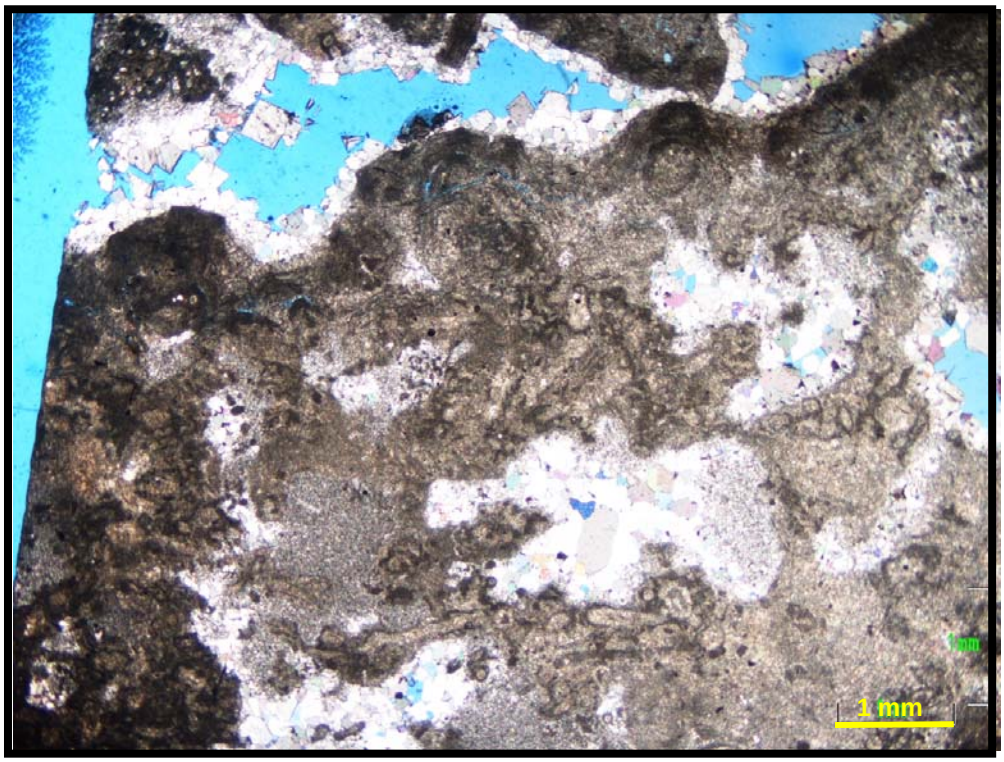

Figure C.20 Thrombolite irregular structures, trapping peloids, filament holes filled with calcite cement. Calcite spar in fracture and framework pore space.

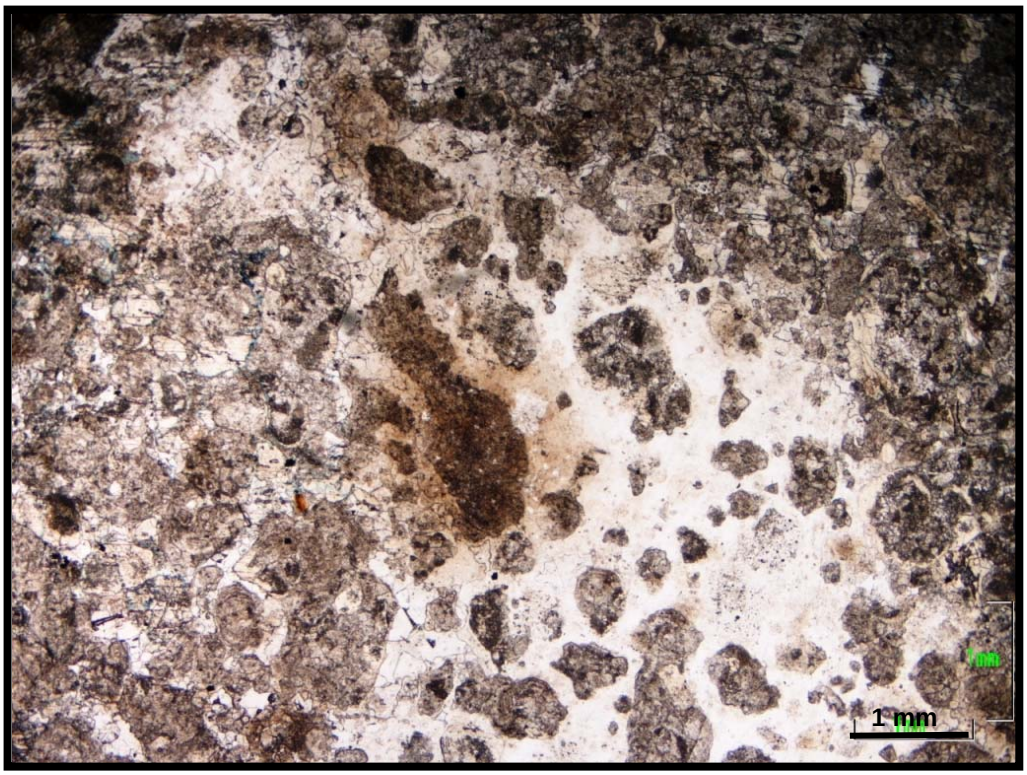

Figure C.21, Thrombolite - Photomicrograph showing clotted fabric, mottled aspect, partially silicified with lumpy aspect, irregular and poor laminations, well 20, Campos Basin.

Figures C.22, intermound – grainstone of intraclasts and ooids. Weakly laminated, in sidewall core sample from well 20 and matching thin section.

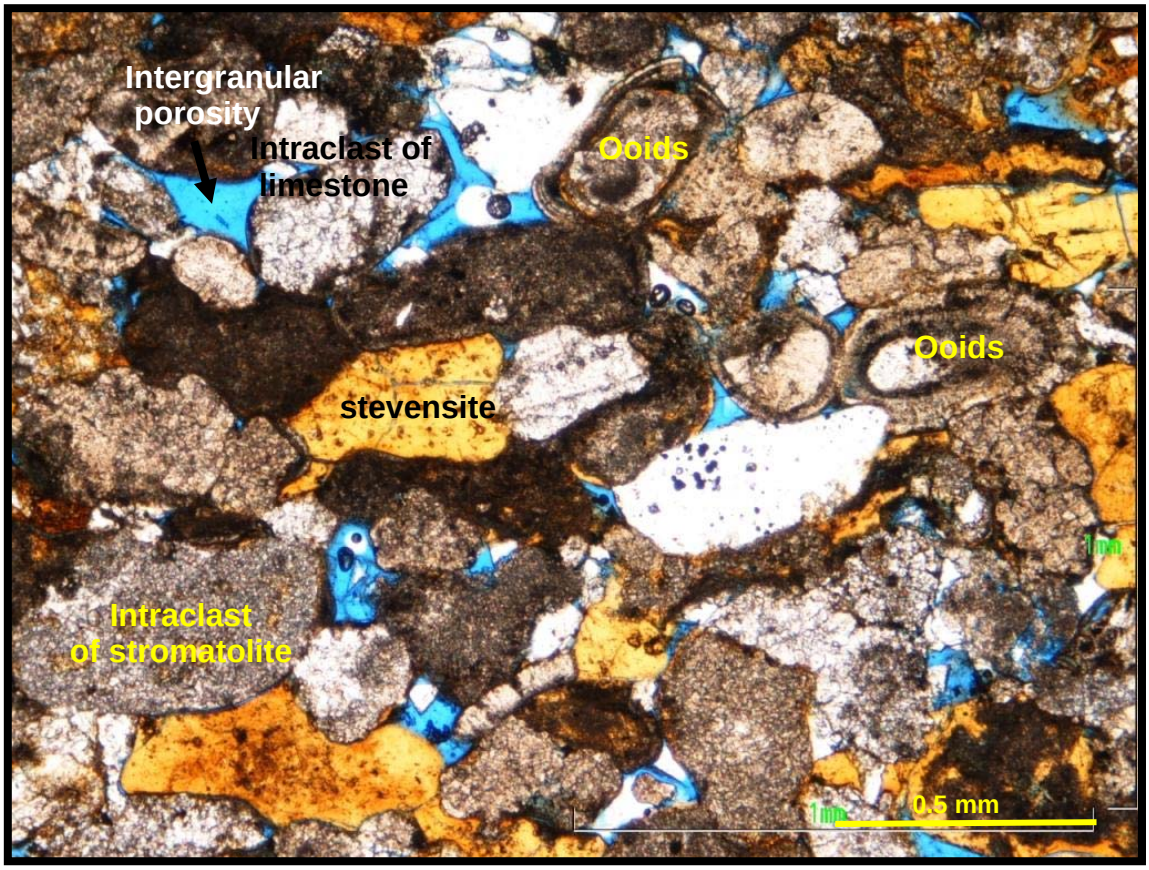

Figure C.23, Intermound thin section grainstone of intraclasts of stromatolite, deformed grains of stevensite and ooids and intergranular pore space (blue) well 20.

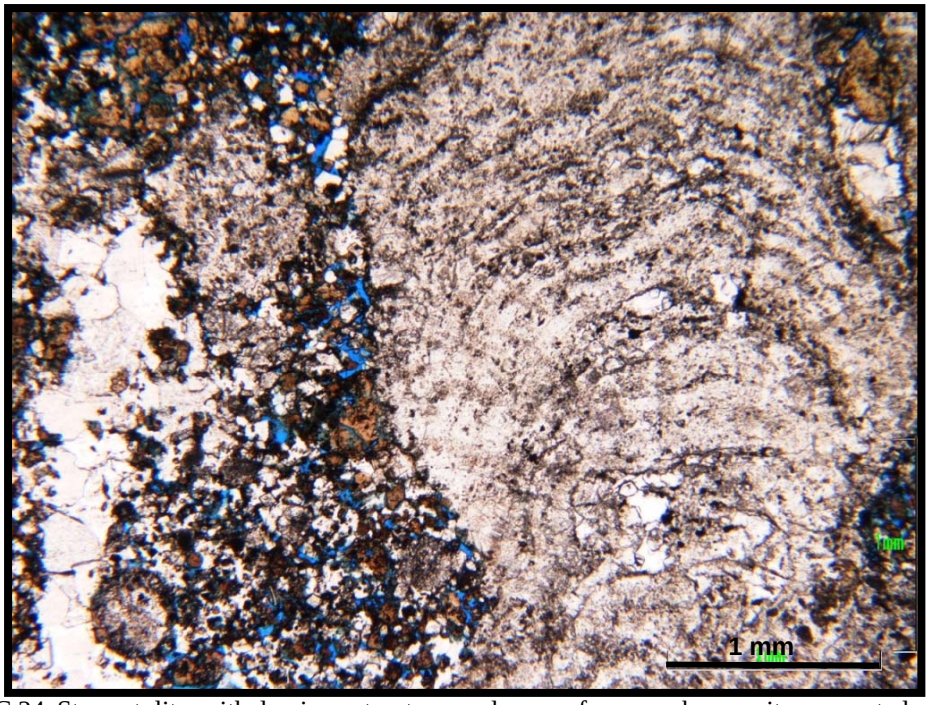

Figure C.24 Stromatolite with laminar structure and some framework porosity cemented with calcite cement. In the intermound pore space filled with Fe-Mg minerals, dolomite, and peloids.

Figure C. 25 Outcrop view of clotted textured microbialite (Thrombolite) with framework porosity

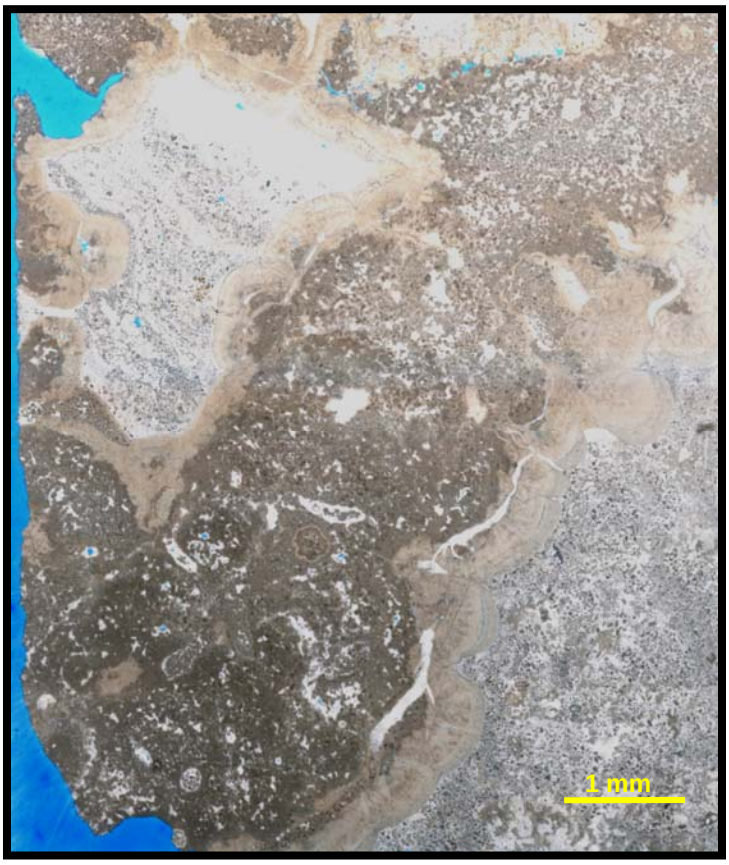

Figure C.26 – Photomicrograph - Burrowed thrombolite with irregular shape with peloids and clasts trapped in a clotted framework. The peloidal framework is coated by an early rim cement and internal sediment infill.